



<https://theses.gla.ac.uk/>

Theses Digitisation:

<https://www.gla.ac.uk/myglasgow/research/enlighten/theses/digitisation/>

This is a digitised version of the original print thesis.

Copyright and moral rights for this work are retained by the author

A copy can be downloaded for personal non-commercial research or study, without prior permission or charge

This work cannot be reproduced or quoted extensively from without first obtaining permission in writing from the author

The content must not be changed in any way or sold commercially in any format or medium without the formal permission of the author

When referring to this work, full bibliographic details including the author, title, awarding institution and date of the thesis must be given

Enlighten: Theses

<https://theses.gla.ac.uk/>
research-enlighten@glasgow.ac.uk

STUDIES ON THE THERMAL DEGRADATION OF SEVERAL
POLYMER-ADDITIVE AND COPOLYMER SYSTEMS

BY

JOHN JAMIESON LIGGAT

A THESIS FOR THE DEGREE OF
DOCTOR OF PHILOSOPHY

SUPERVISOR DR. I.C. McNEILL

CHEMISTRY DEPARTMENT

UNIVERSITY OF GLASGOW

DECEMBER 1987

© John Liggat 1987

ProQuest Number: 10997903

All rights reserved

INFORMATION TO ALL USERS

The quality of this reproduction is dependent upon the quality of the copy submitted.

In the unlikely event that the author did not send a complete manuscript and there are missing pages, these will be noted. Also, if material had to be removed, a note will indicate the deletion.



ProQuest 10997903

Published by ProQuest LLC (2018). Copyright of the Dissertation is held by the Author.

All rights reserved.

This work is protected against unauthorized copying under Title 17, United States Code
Microform Edition © ProQuest LLC.

ProQuest LLC.
789 East Eisenhower Parkway
P.O. Box 1346
Ann Arbor, MI 48106 – 1346

ACKNOWLEDGEMENTS

The work described in this thesis was carried out in the Department of Physical Chemistry at the University of Glasgow during the period October 1982 to December 1985. The Department is under the general supervision of Professor G.A. Sim.

I am indebted to the Science and Engineering Research Council for the award of a Research Studentship.

I wish to thank my supervisor, Dr. I.C. McNeill, for his encouragement, advice and patience during the period of this research. In addition, I acknowledge with gratitude the assistance provided on many occasions by the technical staff of the Chemistry Department - Mr. G. McCulloch and Mr. J. Gorman of the Polymer Group deserve special mention.

Finally I wish to thank all the colleagues and friends who have made my time at Glasgow so memorable. In particular I am grateful to Miss Caroline Johnston and Miss Edith Millan for their friendship and support.

IR and UV Spectra

Reactions of the Chelates with Acetic Acid
and Methyl Acetate

Thermal Decomposition of the Chelates

CONTENTS

	<u>Page</u>
SUMMARY	
CHAPTER 1 INTRODUCTION - TRANSITION METAL ACETYLACETONATE COMPLEXES AND THEIR ROLE IN POLYMER CHEMISTRY	
The Complexes - A General Introduction	1
The Use of Transition Metal Acetylacetonates as Polymerisation Initiators	3
Polymer - Additive Blends in General - Fundamental Interest	16
Objective of this Research	18
CHAPTER 2 EXPERIMENTAL TECHNIQUES OF POLYMER THERMAL DEGRADATION	
Introduction	19
Thermal Volatilization Analysis	19
Sub-Ambient Distillation	32
Thermogravimetry and other Thermal Analysis Techniques	40
Definition and Determination of T(onset) and T(max)	46
Comparison of Thermal Analysis Techniques	50
Other Experimental Techniques	51
CHAPTER 3 TRANSITION METAL ACETYLACETONATE CHELATES - PREPARATION, SPECTRA, THERMAL BEHAVIOUR	
Preparation of the chelates	57
IR and UV Spectra	60
Reactions of the Chelates with Acetic Acid and Methyl Acetate	84
Thermal Decomposition of the Chelates	93
Co(acac) ₃	93

Mn(acac) ₃	112
Co(acac) ₂	131
Mn(acac) ₂	135
Cu(acac) ₂	142
Blends of Polymers with Small Molecules	155
Compatibility of the Chelate - Polymer Blends	157
Solubility of the Chelates in Common Solvents	160

CHAPTER 4 THERMAL DEGRADATION OF POLYMERS

Introduction	161
Poly(methyl methacrylate)	166
Poly(vinyl acetate)	184
Poly(vinyl chloride)	190
Polystyrene	200
Poly(methacrylic acid)	202
1:59 Methacrylic Acid - Methyl Methacrylate Copolymer (Aldrich "Low Molecular Weight PMMA")	206

CHAPTER 5 BLENDS OF Co(acac)₃ AND Mn(acac)₃ WITH PMMA

Thermal Degradation of Co(acac) ₃ - PMMA Blends	222
TVA Behaviour	223
Structure of the Blends and Changes During Degradation	238
Formation of Co(acac) ₂	249
Mechanism of Double Bond Formation	252
Formation of Carboxylate Structures	253
Production of Anhydride Structures	254
Final Decomposition of Structures	255

	<u>Page</u>
Summary of Structural Changes	256
-196°C Condensible Products and CRF	258
Isothermal Degradation	265
Product Analysis by Mass Spectrometry	269
Conclusions on the Degradation of Co(acac) ₃ - PMMA Blends	270
Summary	284
Thermal Degradation of Mn(acac) ₃ - PMMA Blends	285
TVA Behaviour	285
Structure of the Blend and Changes During Degradation	292
-196°C Condensible Products and CRF	306
DSC Analysis	312
Conclusions on the Degradation of Mn(acac) ₃ - PMMA Blends	314
CHAPTER 6 BLENDS OF Co(acac) ₃ AND Mn(acac) ₃ WITH THE ^{31:59} MAA-MMA COPOLYMER	
Introduction	316
Degradation of Co(acac) ₃ - Copolymer Blends	316
TVA Behaviour	316
Structure of the Blend and Changes During Degradation	321
-196°C Condensible Products and CRF	333
Degradation of Mn(acac) ₃ - Copolymer Blends	333
TVA Behaviour	333
Structure of the Blend and Changes During Degradation	339
-196°C Condensible Products and CRF	347

	<u>Page</u>
Conclusions on the Degradation of Co(acac) ₃ and Mn(acac) ₃ Copolymer Blends	351
CHAPTER 7 BLENDS OF Co(acac) ₂ WITH PMMA AND THE 1:59 MAA-MMA COPOLYMER	
Introduction	353
Experimental	353
Co(acac) ₂ - PMMA Blend	354
TVA Behaviour	354
Structure of Undegraded and Partially Degraded Blend	357
-196°C Condensible Products and CRF	361
Co(acac) ₂ - Copolymer Blends	361
TVA Behaviour	361
Structure of Blend and Changes During Degradation	365
-196°C Condensible Products and CRF	372
Conclusions on the Degradation of Co(acac) ₂ -PMMA and Co(acac) ₂ - Copolymer Blends	372
CHAPTER 8 BLENDS OF Cu(acac) ₂ WITH PMMA AND 1:59 MAA-MMA COPOLYMER	
Introduction	376
Cu(acac) ₂ - PMMA Blends	376
TVA Behaviour	376
Structure of Blend and Changes During Degradation	383
-196°C Condensible Products and CRF	387
Discussion	389
Thermal Decomposition of PMMA in the Presence of Copper Powder	391

CHAPTER 10 BLENDS OF $\text{Co}(\text{acac})_3$, $\text{Mn}(\text{acac})_3$
AND $\text{Cu}(\text{acac})_2$ WITH POLYSTYRENE
AND PVC

Introduction	452
Chelate - PS Blends	452
TVA Behaviour	453
Conclusions	459
Chelate - PVC Blends	460
TVA Behaviour	460
Conclusions	466

CHAPTER 11 DEGRADATION OF STYRENE-METHACRYLIC
ACID COPOLYMERS

Introduction	467
Preparation of the Copolymers and Homopolymers	469
TVA and TG Behaviour of the Homopolymers	470
TVA Behaviour of the Copolymers	471
TG Behaviour of the Copolymers	478
Structure of Copolymers and Changes During Degradation	481
-196°C Condensable Products and CRF	485
Discussion	491
Summary	493

APPENDIX ONE

Gas Phase IR Spectra of Several Common Degradation Products	495
--	-----

APPENDIX TWO

IR and UV Spectra of PMMA

500

IR and UV Spectra of PVAc

502

REFERENCES

504

... of the transition metal and ... interact with electrophilic ... polymers ... their ... investigation.

Chapter 2 presents an ... analysis techniques employed in ... aspects on the comparative merits of ...

The preparation of the chelates is ... Chapter 3 and the nature of these ... ligand-donating compounds ... of the ... evidence. The thermal decompe ... is also discussed and a ... for the fragmentation of the chelate ... The thermal degradation of ... particularly those employed in this research ... subject of Chapter 4.

In Chapters 5, 6 and 7, the thermal de

SUMMARY

Transition metal chelates of acetylacetonone generally decompose in the first instance by a ligand scission mechanism with the release of acac· radicals. The ligand scission can be promoted by complexation with electron-donating species, and as described in Chapter 1, this has led to an interest in the use of the chelates as polymerisation initiators. Additional interest in the chelates comes from their use in modifying the degradation behaviour of polymers. The ability of the transition metal acetylacetonate chelates to interact with electron-donating sites within the polymers renders them particularly worthy of investigation.

Chapter 2 presents an introduction to the thermal analysis techniques employed in this research, with emphasis on the comparative merits of each system.

The preparation of the chelates is described in Chapter 3 and the nature of their interaction with electron-donating compounds considered on the basis of spectroscopic evidence. The thermal decomposition of the chelates is also discussed and a mechanism is proposed for the fragmentation of the chelates at high temperature. The thermal degradation of polymers (particularly those employed in this research) is the subject of Chapter 4.

In Chapters 5, 6 and 7, the thermal degradation

of blends of Co^{3+} , Co^{2+} and Mn^{3+} chelates with poly(methyl methacrylate) and a methyl methacrylate-methacrylic acid copolymer is described. Both polymers contain electron-donating structures (ester and acid side groups, unsaturated linkages) and these are found to promote the chelate ligand scission reaction in the manner of the low molecular analogues discussed in Chapters 1 and 3. The $\text{acac}\cdot$ radicals produced in the initial decomposition attack the polymer backbone and initiate depolymerisation, whilst small radicals produced in the advanced stages of chelate decomposition attack the substituent groups, inducing the formation of cyclic anhydride structures. The interaction of the chelates with the polymer side groups can promote scission of these groups from the polymer chain with the associated formation of unsaturated sites on the polymer backbone. Such modifications of the polymer block the usual depolymerisation reaction and leads to chain fragmentation.

The influence of $\text{Cu}(\text{acac})_2$ on the degradation behaviour of poly(methyl methacrylate) and the copolymer is discussed in Chapter 8. Although the $\text{Cu}(\text{acac})_2$ - PMMA blend behaves similarly to the blends of PMMA with the chelates considered earlier, the $\text{Cu}(\text{acac})_2$ - copolymer blend behaves in a markedly different fashion, with two new major unzipping processes and little fragmentation. Evidence is provided in this chapter which indicates that the different behaviour stems from

a copper catalysed decarboxylation process

In Chapter 9, the influence of the chelates on the thermal degradation of poly(vinyl acetate) is investigated. Interactions with the ester substituents are observed, similar to the case of the poly(methyl methacrylate) blends. Attack of $\text{acac}\cdot$ radicals on the poly(vinyl acetate) will not initiate depolymerisation as the polymer does not degrade by this mechanism but instead causes structural changes along the backbone. Structural changes are also expected to occur when $\text{acac}\cdot$ radicals attack polystyrene and poly(vinyl chloride) in the blends of these polymers with the chelates. The TVA behaviour of these blends is described in Chapter 10.

In the final chapter, Chapter 11, the thermal degradation of a series of styrene-methacrylic acid copolymers is described. It is found that anhydride ring structures, which block the unzipping of the styrene sequences, form between neighbouring methacrylic acid units. A slight overall stabilisation of the copolymer relative to polystyrene results.

CHAPTER 1

INTRODUCTION

TRANSITION METAL ACETYLACETONATE COMPLEXES AND THEIR ROLE IN POLYMER CHEMISTRY

THE COMPLEXES - A GENERAL INTRODUCTION

Acetylacetone (acacH), a β -diketone, is, like other ketones, capable of keto-enol tautomerism (Fig. 1.1).

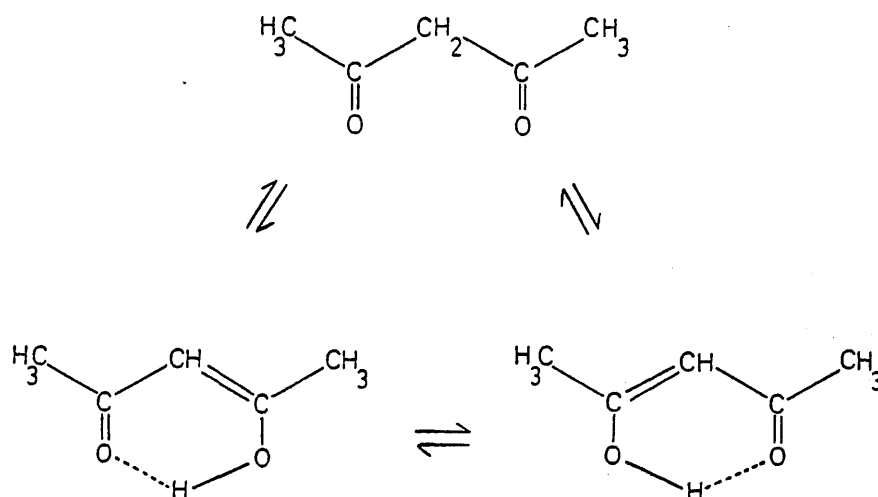


Fig. 1.1 Keto and Enol Forms of Acetylacetone

In the liquid phase, the enol tautomer predominates (81%).¹ The enolic hydrogen is easily displaced by metal ions to give bidentate chelate compounds, $\text{Me}(\text{acac})_n$ (Fig. 1.2).

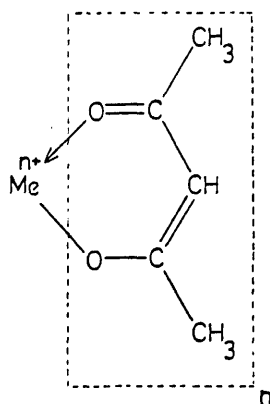
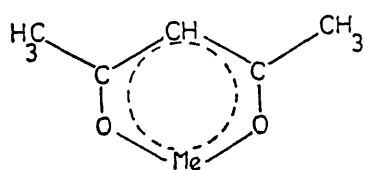


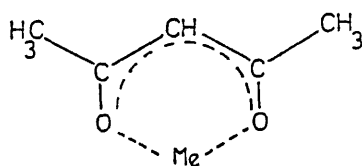
Fig. 1.2 Metal Acetylacetonate Chelate

Calvin and Wilson² first suggested the possibility of benzenoid resonance within the chelate ring to explain the anomalous stability of the chelates. Substantiating evidence for this theory comes from the observation that the metal acetylacetonates undergo electrophilic substitution at the C-3 position³⁻⁵. Spectroscopic evidence⁶⁻⁸ also indicates at least partial delocalisation, the exact extent dependent on the metal ion (Fig. 1.3).



complete delocalisation

e.g. Me = Cu²⁺



partial delocalisation

e.g. Me = Co²⁺, Zn²⁺

Fig. 1.3 Delocalisation in Metal Acetylacetonates

3

The structure of the chelates varies but, in general, the metal ion is six-coordinated. In the tris chelates the ligands arrange themselves in a roughly octahedral fashion; in $\text{Fe}(\text{acac})_3$, the arrangement is essentially a regular octahedron,⁹ whilst $\text{Mn}(\text{acac})_3$ displays the Jahn-Teller distortion expected of a high spin Mn^{3+} complex.¹⁰ The bischelates achieve six-fold coordination of the central ion by adduct formation (eg $\text{Co}(\text{acac})_2 \cdot 2\text{H}_2\text{O}$ ¹¹) or by polymerisation (e.g. $[\text{Co}(\text{acac})_2]_3$ ^{12,13}). However, as Cu^{2+} prefers four-fold coordination, $\text{Cu}(\text{acac})_2$ exists in an essentially square planar arrangement.¹⁴

The acetylacetonate chelates have physical properties more generally associated with organic compounds, and, for instance, tend to be soluble in organic solvents¹⁵ and volatile - the chelates tend to sublime on heating.¹⁶ Such properties have led to an interest in the use of the chelates in analytical chemistry.¹⁷⁻¹⁹

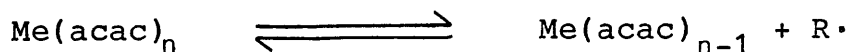
Details of the preparation, spectra, properties and decomposition of the specific chelates used in this research are contained in Chapter 3.

THE USE OF TRANSITION METAL ACETYLACETONATES AS POLYMERISATION INITIATORS

The use of metal containing systems, and transition metal compounds in particular, as initiators

for polymerisation reactions, both free-radical and ionic, has been the focus of much research.²¹ Systems range from the simple ferric ion - peroxide free-radical initiators to the complex vanadium and titanium containing Ziegler-Natta catalysts. Transition metal acetylacetonate chelates have received much attention as initiating agents for the free-radical polymerisation of unsaturated monomers since Arnett and Mendelsohn reported in their study of the autoxidation of such chelates that the chelates decomposed with the production of radical species.²²⁻²⁴

Arnett and Mendelsohn themselves performed a brief study of styrene polymerisation in the presence of the acetylacetonate chelates and found the Co(III), Mn(III) and Ce(IV) species to be the most active.²⁴ They proposed the mechanism:



where R· represents the acac· radical in one of its resonance forms (Fig. 1.4). The radical R· was then envisaged as the initiating species.

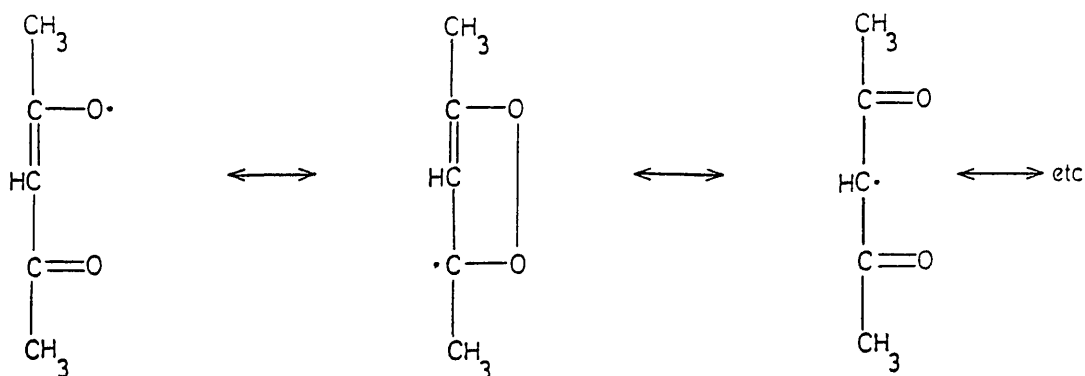


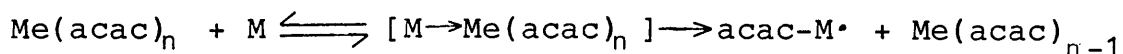
Fig. 1.4 Resonance Forms of acac· Radical

Kastning et al.²⁵ likewise found Co(III) and Mn(III) to be very reactive for the polymerization of styrene, acrylic and methacrylic esters, vinyl esters, ethylene and butadiene. Although emphasising that the mechanism was not fully understood, these authors inclined towards the opinion that the polymerisation followed a radical pathway. They were disinclined to believe that reduction of the central metal ion, as envisaged by Arnett and Mendelsohn, was necessarily involved, despite finding evidence for the incorporation of the ligand in the polymer molecule. Subsequent workers, however, found kinetic and spectroscopic evidence for an initiation mechanism occurring via homolysis of the chelate metal-oxygen bonds.^{26-30,37-40}

Otsu and co-workers in their study²⁶ of the activity of several acetylacetonate chelates for vinyl polymerisation found, in order of efficiency, Mn(III), Co(III), Mn(II), Cu(II) and Cr(III) acetylacetonates to

be effective initiators for methyl methacrylate polymerisation. This order could not be correlated with any obvious property of the chelates such as their thermal stability, stability constants, or central metal ion electronegativities or ionisation potentials. In general, though, a higher valence metal ion was more active than the lower valence ion. $\text{Mn}(\text{acac})_3$ was found to have an anomalously high initiating activity, ten times that of the other active chelates. The origin of this anomaly is unclear, although Otsu and his coworkers suggested that it could be related to the structural strain, believed at that time to exist within the $\text{Mn}(\text{acac})_3$ molecule. Recent re-evaluation of the structure negates this possibility. Otsu and coworkers, in common with Bamford and Lind,^{27,28} found the rate of polymerisation of methyl methacrylate to be proportional to the square root of initiator concentration which suggested an initiation reaction proceeding via a radical intermediate. An order with respect to methyl methacrylate concentration of 1.44, additionally suggested that initiation involved complexation of the monomer with the chelate. (A similar conclusion was reached tentatively by Riches²⁹ on the basis that strong radical inhibitors had no effect on the initiation of diene polymerisation.) Otsu and coworkers found polystyrene prepared by chelate initiation to contain ligand

residues and observed a colour change consistent with a reduction of the metal ion during a polymerisation initiated by $\text{Mn}(\text{acac})_3$ ²⁶. They thus proposed a mechanism of the type:-



where M represents monomer. Such a complex, by increasing the electron density on the metal ion, promotes the homolysis of the metal-oxygen bond and accounts for the considerable activity of the chelates at temperatures well below their normal decomposition temperatures. Thus other electron-donating agents could be expected to aid the decomposition process.

Just such behaviour is described by Bamford and coworkers^{27,29,30} who found solvents and other electron-donor additives to have an effect. Benzene, ethyl acetate and 1,2-diaminopropane, for instance, were found to promote the decomposition of $\text{Mn}(\text{acac})_3$.

Bamford and Ferrar³⁰ noted that the effectiveness of an additive or solvent in accelerating decomposition is dependent on its donor power. Commenting that an electron-donating compound (DC) would be expected to partially displace an acetylacetonate ligand, they proposed the following mechanism for the initiation of polymerisation by $\text{Mn}(\text{acac})_3$ in the presence of an electron donor which could, of course, be the monomer itself:-

polymerisation initiators, decomposing in solution in the range 60-130°C to produce either acac. or RCOO. radicals depending on the nature of R. Korshak et al.³⁵, although not isolating the mixed chelate, found acetic acid to have an accelerating influence on the Mn(acac)₃ initiated polymerisation of styrene and, interestingly in the context of this project, found poly(methacrylic acid) to have a similar influence.

The effect of the presence of halogenated additives on the initiating activity is less clear. Kastning et al.²⁵ observed an acceleration of the rate of polymerisation in the presence of halogenated compounds but Bamford and Lind²⁷, Riches²⁹ and Otsu et al.²⁶ were unable to reproduce these results. Dass³⁶ reports, however, that at low concentrations Cu(acac)₂ can form a charge transfer complex with CCl₄ to produce polymerisation initiating •CCl₃ radicals.

The exact nature of the complex between monomer and chelate was not discussed by Otsu²⁶ or by Bamford and coworkers,^{27,28,30} but Nandi and colleagues in a series of papers³⁷⁻³⁹ produced a description of its probable form. These workers recorded changes in the UV absorbance due to the $\pi-\pi^*$ transition of Fe(acac)₃ and the substituted acetylacetonate chelate Fe(DPM)₃ in the presence of styrene and methyl methacrylate.

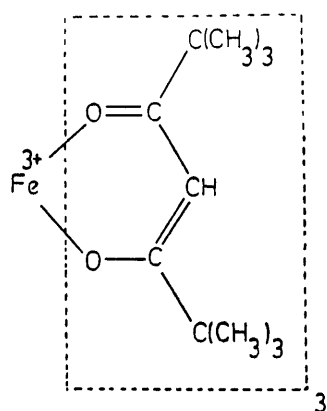
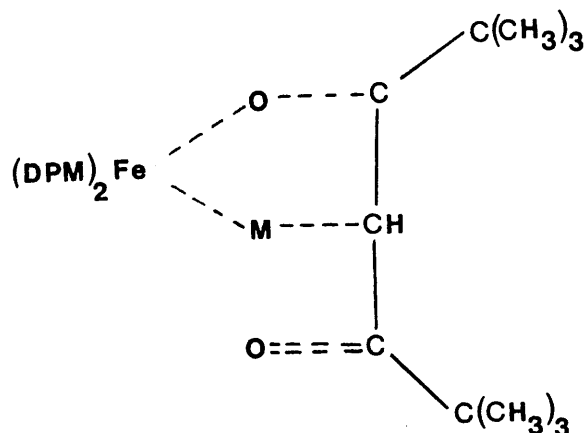


Fig. 1.5 Ferric Dipivaloylmethide ($\text{Fe}(\text{DPM})_3$)

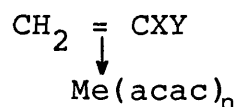
They also observed that the effectiveness of the chelate initiator was adversely affected by the electron-withdrawing nature of the substituents on the vinylic monomer; acrylonitrile, for instance, did not polymerise in the presence of $\text{Fe}(\text{DPM})_3$.

These results they interpreted as being due to the formation of a π -type complex between monomer and chelate which, as the ligand $\pi - \pi^*$ transition is shifted, must involve the ligand. They proposed a "displacement" type mechanism similar to that of Bamford and Lind²⁸:-



Although they took $\text{Fe}(\text{DPM})_3$ as the model, this mechanism can be equally well applied to $\text{Fe}(\text{acac})_n$ and the other $\text{Me}(\text{acac})_n$ complexes.

A similar conclusion regarding the nature of the $\text{Me}(\text{acac})_n$ - monomer complex was reached, on the basis of the polymerisability of variously substituted vinyl monomers, by Sahu et al,⁴⁰ who for convenience denoted the existence of such a π -type complex thus:-

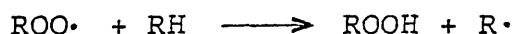


Recently there has been a resurgence of interest in the use of transition metal acetylacetonate chelates as polymerisation initiators, particularly for the graft polymerisation of methyl methacrylate onto natural and man-made fibres, a field in which Nayak, Lenka and coworkers have been particularly active.⁴¹⁻⁴³

USE OF TRANSITION METAL ACETYLACETONATES TO MODIFY POLYMER DEGRADATION

The transition metal acetylacetonates have been the subject of much interest, both academic and commercial, in relation to their application as stabilisers and destabilisers for polymer systems. Thus the patent literature lists such diverse uses for the chelates as synergistic flame retardents,⁴⁴ watertree prevention,⁴⁵ photothermography,⁴⁶ and anti-yellowing compositions for PVC.⁴⁷

Most interest in the application of the chelates is in relation to their influence on the thermo-oxidative and photo-oxidative degradation of polymers, particularly polyolefins. Key sites in the oxidation of polymers are structures such as carbonyl groups or unsaturated linkages which can act as chromophores for the absorption of incident light or as "weak links".⁴⁸ These structures can either be a regular part of the polymer or introduced during processing. Their effect is to produce macroradicals, $R\cdot$, within the polymer which can then react with ground state oxygen to produce hydroperoxide radicals $ROO\cdot$. These hydroperoxide radicals act as chain carriers for the oxidation chain reaction:-



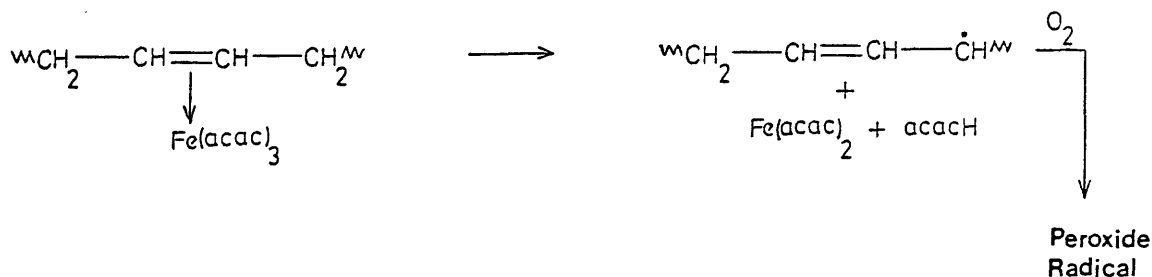
The acetylacetonate chelates can interact with carbonyl, unsaturated and hydroperoxide units and thus have an important role in polymer oxidation.

The use of the chelates as vinyl polymerisation initiators as already described gives some idea of the possible interaction with unsaturated and other electron donors. Nandi and Sasi,⁴⁹ following on from the earlier work of Nandi and coworkers³⁷⁻³⁹ on the use of $Fe(acac)_3$ and $Fe(DPM)_3$ as polymerisation initiators found spectroscopic evidence for a π -complex between the chelates and polystyrene. By analogy with the monomer-chelate interactions, they reasoned that such polymer-chelate interactions would

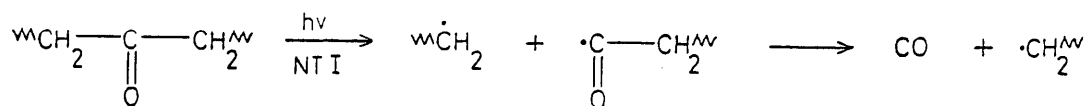
promote the decomposition of $\text{Fe}(\text{acac})_3$, producing $\text{Fe}(\text{acac})_2$, acacH and a macroradical $\text{R}\cdot$ which subsequently reacts with O_2 . This leads to the observed increase in the thermal oxidation of polystyrene in the presence of $\text{Fe}(\text{acac})_3$.

A similar mechanism was proposed by Ogiwara et al.⁵⁰ to explain, in part, the accelerating influence of $\text{Fe}(\text{acac})_3$ on the photo-oxidation of polyethylene (PE). These workers observed a shift in the UV spectrum of $\text{Fe}(\text{acac})_3$ in the presence of the 1,7 octadiene which they used as a model for a partly unsaturated PE.

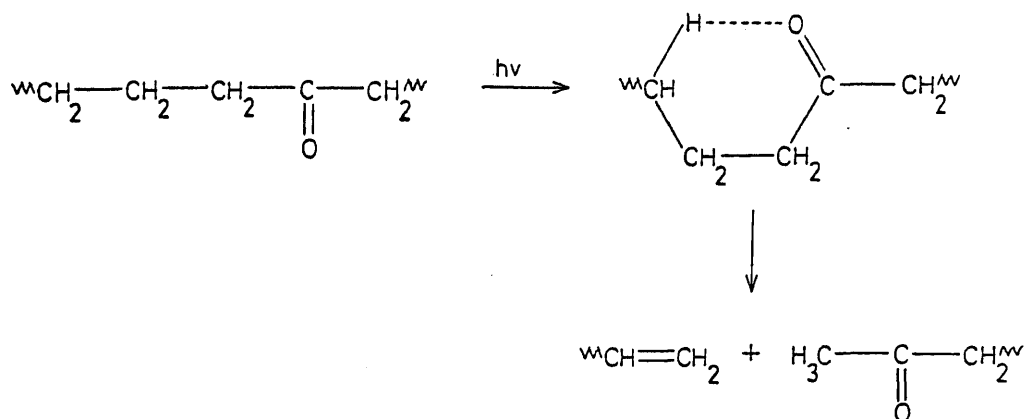
This suggested the formation of a π -complex between the two species and these workers proposed an analogous complex between $\text{Fe}(\text{acac})_3$ and PE which could accelerate photo-oxidation by the mechanism:-



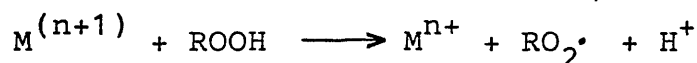
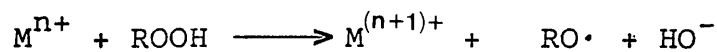
In addition, since a change in the UV spectrum of $\text{Fe}(\text{acac})_3$ in the presence of 2- and 3- octanone, was observed, these workers suggested that $\text{Fe}(\text{acac})_3$ may also interact with carbonyl groups introduced during processing. This, they proposed, would suppress the normal Norrish Type I decomposition pathway:-



and instead allow a Norrish Type II reaction.

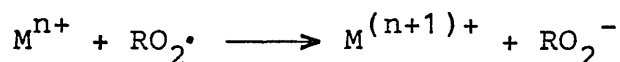


The accepted mechanism for the interaction of transition metal ions including those of the acetylacetonate chelates with hydroperoxides is⁵¹



where M^{n+} , $\text{M}^{(n+1)+}$ are two oxidation states of comparable stability e.g. $\text{Co}^{2+}/\text{Co}^{3+}$.

This has the effect of accelerating the oxidative degradation, yet the same metal ions can, at high concentration, inhibit the autoxidation:-



Thus, even on the basis of the hydroperoxide reactions above, it can be seen that whether a metal acetylacetonate is a pro- or anti-oxidant is finely balanced. Introduce the interaction with the

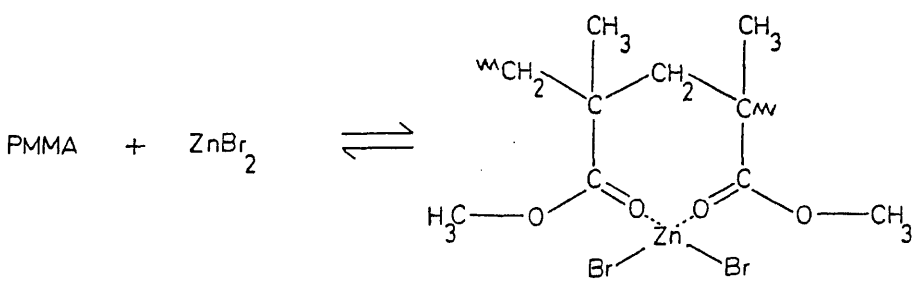
unsaturated and carbonyl units and the situation becomes very complex. Such complexity is reflected in the results of Amin and Scott⁵² who investigated the photo-oxidation of PE in the presence of a series of additives, including the Ni(II), Zn(II), Fe(III) and Co(III) acetylacetonates. $\text{Co}(\text{acac})_3$ and $\text{Fe}(\text{acac})_3$ were such strong pro-oxidants that the PE was badly oxidised during processing. $\text{Ni}(\text{acac})_2$ and $\text{Zn}(\text{acac})_2$ had no effect, although $\text{Ni}(\text{acac})_2$, by virtue of being a powerful triplet quencher was expected to act as stabiliser against photo-oxidation.

Fires provide an extreme example of thermal degradation and transition metal chelates have been considered as fire retardents and smoke suppressors, and have been the subject of many patents (see for instances refs.53-57). Kroenke⁵⁸ reviewed the use of transition metal compounds as smoke suppressors for PVC and reports that $\text{Cu}(\text{acac})_2$, $\text{Co}(\text{acac})_2$, $\text{Co}(\text{acac})_3$ and $\text{Cr}(\text{acac})_3$ are effective suppressors whilst $\text{Mn}(\text{acac})_2$ is not. The mode of action of these compounds remained unclear, the effectiveness varying with such factors as concentration, dispersion and particle size. The role of the oxidation state was ambiguous, $\text{Cr}(\text{acac})_3$ being effective whilst Cr_2O_3 was not. Kroenke suggested that the ability to undergo redox reactions may be important but in this context, the ineffectiveness of $\text{Mn}(\text{acac})_2$ is surprising. One role the chelates played was to act as char promoters

and Cullis and Hirschler⁵⁹, in a study of the influence of some metal acetylacetonates on the flammability of polypropylene noted a loose correlation between char formation and the pro-oxidant effect of the chelate. However, emphasising, the complexity of degradation processes, the antioxidant Ni(acac)₂ was also found to promote char formation.

POLYMER-ADDITIVE BLENDS IN
GENERAL - FUNDAMENTAL INTEREST

The study of the acetylacetonate chelates as degradation modifiers forms part of the wide ranging research into the effects of small molecule additives on polymer degradation. The effects of such additives on thermal degradation have recently been reviewed by McNeill⁶⁰ and much work on this field of research has been undertaken in these laboratories (ref. 60 and references therein). Of particular interest are those systems in which complexation can occur between the polymer and additive, for instance the metal halide-PMMA and PVAc systems studied by McNeill and McGuinness.⁶¹⁻⁶³ In these systems the metal halide complexes with the ester groups. For example, between ZnBr₂ and PMMA:-



OBJECTIVE OF THIS RESEARCH

There is much fundamental interest in the degradation of polymer-additive blends, particularly in those systems in which the small molecule additive can in some fashion complex with the polymer. From the previous sections of this introduction, it can be seen that transition metal acetylacetonates can interact with polymers in a number of ways and the subsequent possibilities of modifying the polymer degradation are manifold. It can also be seen that the complexity of the degradation processes leads to many confusing ambiguities. This complexity is further compounded by the degradations being performed in the presence of oxygen. To fully understand the degradation of a polymer in the presence of oxygen, it is first necessary to understand the processes occurring in the absence of oxygen. Consequently this research probes the influence of the more active acetylacetonates (Mn(II)/(III), Co(II)/(III), Cu(II)) on the in vacuo thermal degradation of a number of polymers with interest focussed on those polymers containing electron donor groups. Thermal degradation, more than photodegradation, allows a broad picture of the overall nature of the degradation behaviour to be obtained and as described in the following chapter, this laboratory is well equipped for the study of thermal degradation.

CHAPTER 2

EXPERIMENTAL TECHNIQUES OF POLYMER THERMAL DEGRADATION

INTRODUCTION

As subsequent chapters will demonstrate, the mechanisms of thermal degradation are complex and result in the formation of products with various characteristics. Products may be volatile enough to be non-condensable at liquid nitrogen temperatures (-196°C) or may be volatile only at the temperature of degradation and condense at room temperatures. Alternatively structural changes may occur within the polymers which produce no volatile material at all.

With such a range of mechanisms and products, it is generally unwise to rely solely on the results of one thermal analysis technique, particularly when there is no information on the nature of the products. This chapter describes the various techniques employed in this research. Particular emphasis is given to Thermal Volatilization Analysis which is the most versatile of the techniques described and allows study of all the products of degradation.

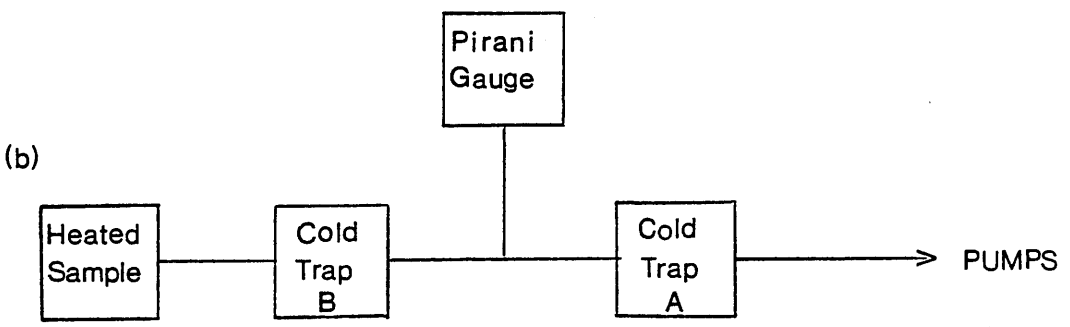
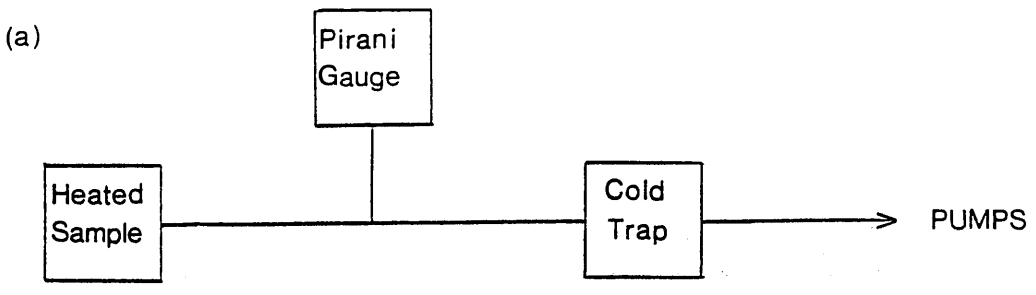
THERMAL VOLATILIZATION ANALYSIS

Thermal Volatilization Analysis (TVA) is a versatile thermoanalytical technique developed in this department by McNeill and co-workers and its development

is the subject of several publications.⁶⁴⁻⁶⁸

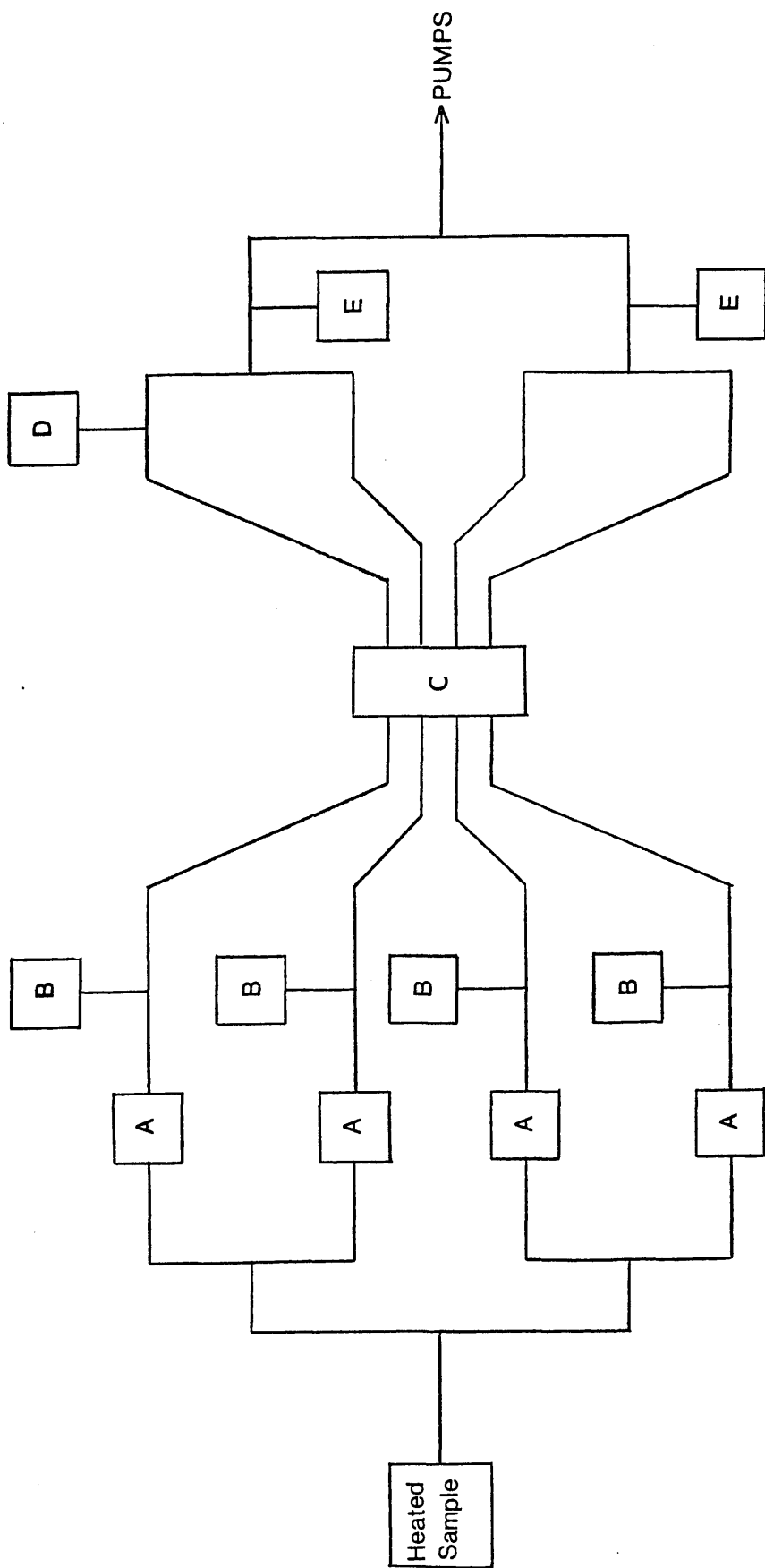
A polymer sample, commonly in the form of a powder or thin film, is heated in a continuously pumped high vacuum system. Gaseous degradation products will cause a small pressure increase as they distill from the sample to a cold trap placed some distance away. This pressure change, measured by a Pirani gauge and recorded as a function of time or temperature, gives a measure of the rate of volatilization of product. The system is depicted schematically in Fig. 2.1a.

A modification to the apparatus involves placing a second cold trap, B, at a temperature higher than that of the original trap, A, between the sample and Pirani gauge, Fig. 2.1b. Thus arises the possibility of differential condensation of the degradation products between the two traps. Consequently, this form of TVA is known as differential condensation TVA (DC-TVA). By undertaking a series of degradations each with trap B at a different temperature, valuable information on the nature of the degradation can be obtained. Such repetition is both tedious and time consuming, however, and the form of the apparatus currently used in this laboratory is that illustrated in Fig. 2.2, in which a number of limbs, each with an initial cold trap and a main -196°C trap, are joined in parallel. The temperature of the initial trap in each limb is different; in this laboratory temperatures of 0, -45, -75, -100°C are used. Pirani gauges placed after



$$T_B > T_A$$

Fig. 2.1 Schematic Representations of
(a) Basic TVA System,
(b) Differential Condensation TVA System.



A - 0° , -45° , -75° , -100° TRAPS

B, D - PIRANI GAUGES

C - -196° TRAP

E - SAMPLE TAKE-OFF POINTS

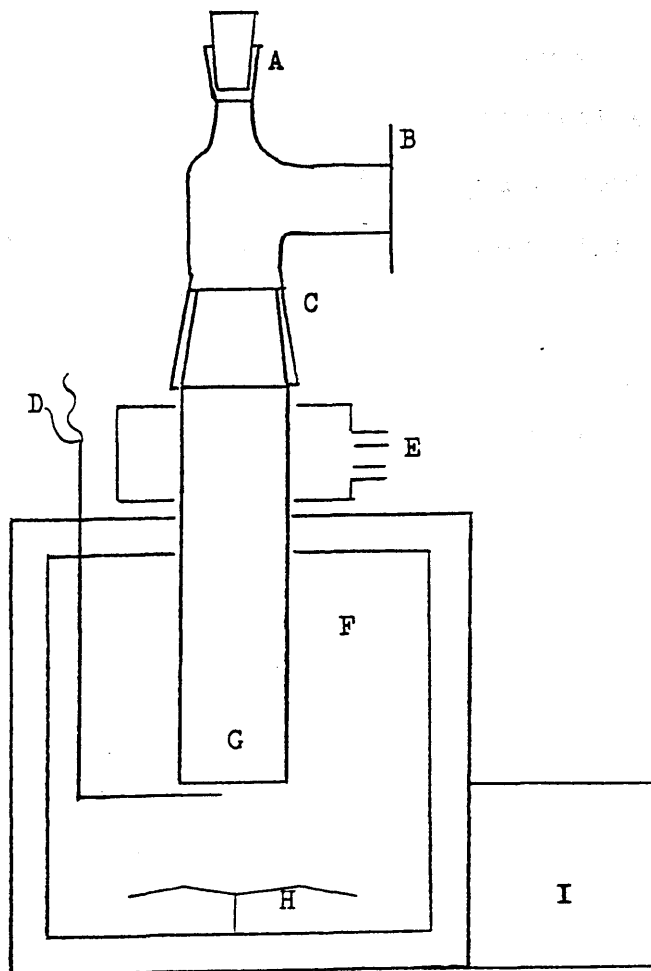
Fig. 2.2 Parallel Limb DC-TVA System

each initial trap monitor the passage of volatiles through the traps as in the basic DC-TVA arrangement; the addition of a Pirani gauge after the -196°C trap allows the detection of any non-condensable products which are lost to the pumps.

Provided care is taken to ensure that the pathlengths of each limb are equal, equal quantities of gaseous degradation products will enter each limb. Assuming the Pirani gauges to be matched (discussed below) any difference in output from the gauges can be ascribed to differential condensation of the products. Subsequent references in this thesis to "TVA" will be to this form of the technique.

TVA IN PRACTICE

Fig. 2.3 shows, diagrammatically, the oven and degradation tube assembly of a typical TVA line. The oven is a Perkin Elmer F11 gas chromatography oven, modified to take the tube assembly and to work to a maximum temperature of approximately 500°C . The oven can be used isothermally or, by using a programming module, can provide a linear temperature increase. In this research, the oven was used almost entirely in programmed mode, using a heating rate of $10^{\circ}\text{C min}^{-1}$. Oven temperatures were measured using a Type K thermocouple with 0°C reference and the millivolt output, along with that of the Pirani gauges, was recorded on a Leeds-Northrup Speedomax W multi-point



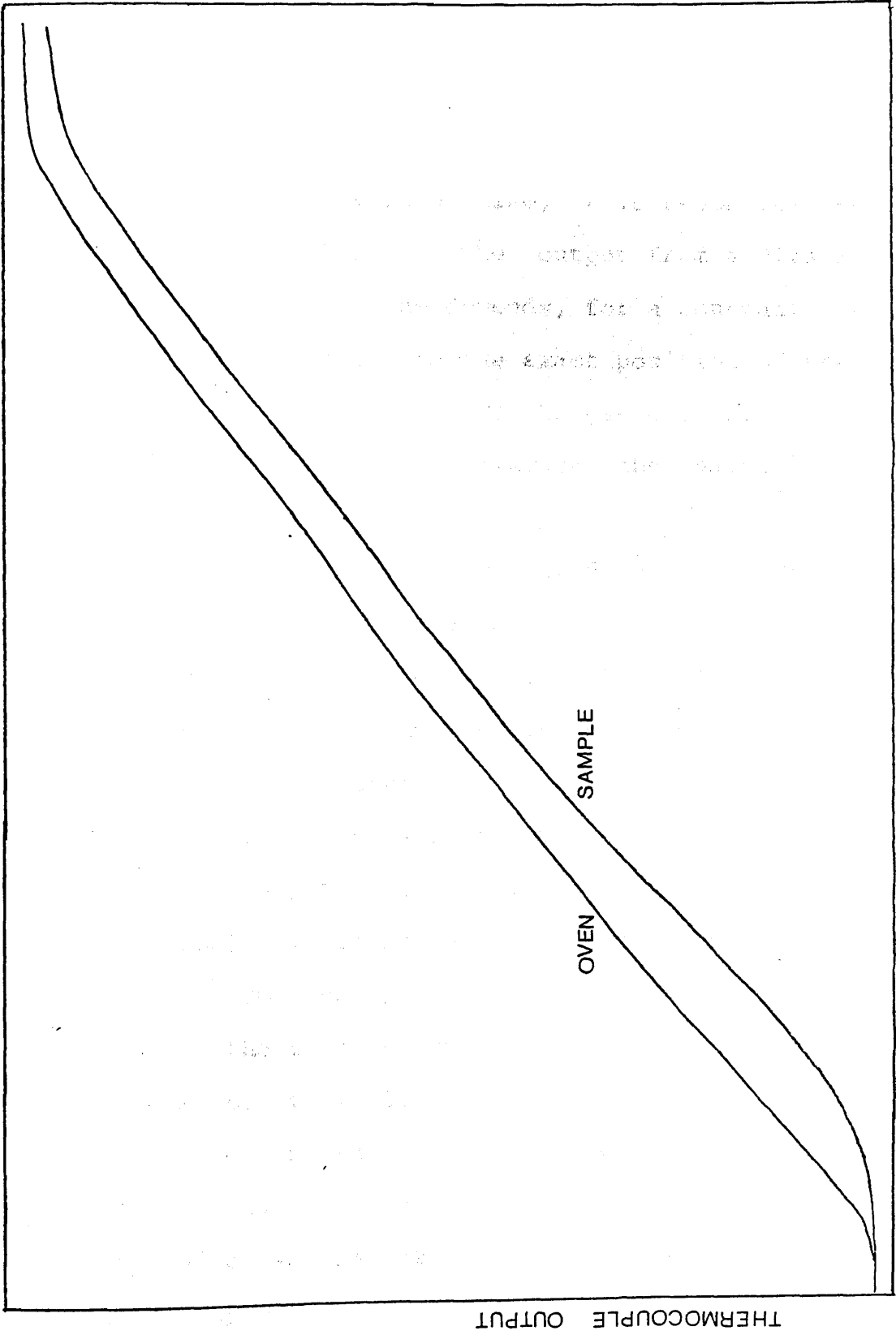
- A - B 19 SOCKET
- B - GROUND GLASS FLANGE JOINT
- C - B 40 GROUND GLASS JOINT
- D - TYPE K THERMOCOUPLE
- E - WATER COOLED JACKET "COLD RING"
- F - OVEN
- G - DEGRADATION TUBE
- H - FAN
- I - PROGRAMMING MODULE

Fig. 2.3 Degradation Tube and Oven Assembly

chart recorder. Millivolt readings were converted to temperatures using standard tables.

Due to a temperature differential across the tube base, sample temperatures are lower than the oven temperature, except in the case of isothermal heating when tube and oven have reached thermal equilibrium. Sample temperatures could be measured directly for each run but this is inconvenient and introduces the possibility of sample contamination. To overcome these difficulties, a temperature calibration curve is obtained for the degradation tube. A second Type K thermocouple is inserted through the socket A of Fig. 2.3 until the junction is in contact with the tube base. The system is evacuated and the oven heated in the normal fashion. Outputs from both oven and internal thermocouples are recorded to produce a chart similar to the one reproduced in Fig. 2.4. Using such a chart, the internal tube base temperature can be obtained for any given oven temperature. Due to the thinness of the polymer sample, the sample temperature can be taken as equal to that of the tube base. Such curves have to be obtained for each tube used and have to be repeated whenever an alteration in the position of the oven thermocouple or rewiring may alter the calibration.

The pumping system comprises an Edwards Speedivac EO1 Oil Diffusion Pump, backed by an Edwards Speedivac ED100 rotary pump. Using this system, pressures of 10^{-5} torr are obtainable.



TIME

Fig. 2.4 Tube Temperature Calibration Chart

Pressures were measured using Edwards GC5S2 Pirani gauge heads with Pirani 14 meter units. As TVA in the form used in this laboratory involves the comparison of the output of the five Pirani gauges attached to the vacuum line, it is essential that the outputs are matched. The output from a Pirani gauge attached to a TVA line depends, for a constant pressure and gas composition, on the exact position of the gauge and the characteristics of the gauge itself. Thus, it is necessary to cross-calibrate the gauges. This is done as follows.

First, the line is prepared as for a TVA run with all traps in place and pumped to high vacuum. The Pirani gauges are zeroed against the "sticky vacuum" of a Vacustat gauge. The line is isolated from the pumps, dry nitrogen is introduced and the line re-opened to the pumps until a Pirani output of approximately $1/2$ full scale output (the maximum usually achieved during a degradation) is recorded when the line is once again isolated from the pumps. The outputs from the Pirani gauges to the recorder are then brought into coincidence by means of variable resistances. The line is then pumped down in steps, the coincidence of the outputs being checked at each stage. A final check is made by degrading a sample of potassium permanganate. This evolves oxygen which at the reduced pressures in use is non-condensable at -196°C and thus passes through all five traps - the Pirani gauges should then all register

the same output.

Pirani gauge outputs are only linear over a range of 0-2 mv whilst the usual sample size (25-50mg), on degradation gives rise to an output of 4-5mv. Furthermore, the output is dependent on the nature of the gas as well as the absolute pressure and so the system is not suited to quantitative analysis of degradation products. Useful qualitative results and details of the degradation process can be obtained however. Fig. 2.5 reproduces a typical TVA curve, that of polystyrene, and the one step production of volatiles is clearly shown, with the onset temperature, $T(\text{onset})$, and the temperature of the maximum rate of production of volatiles, $T(\text{max})$, (the TVA trace is of an essentially "derivative" nature), easily obtainable. Additionally, the behaviour of the individual traces is typical of the production of styrene. A more complete interpretation of the TVA curve for polystyrene is given in Chapter 4.

TVA CURVES - DESIGNATION OF TRAP TRACES

When reproduced in this thesis, the following designation for the individual trap traces of TVA curves is employed as standard.

- _____ 0° (and colder traps if coincident)
- -45° "
- -75° "
- ==== -100° "
- ==== -196° "

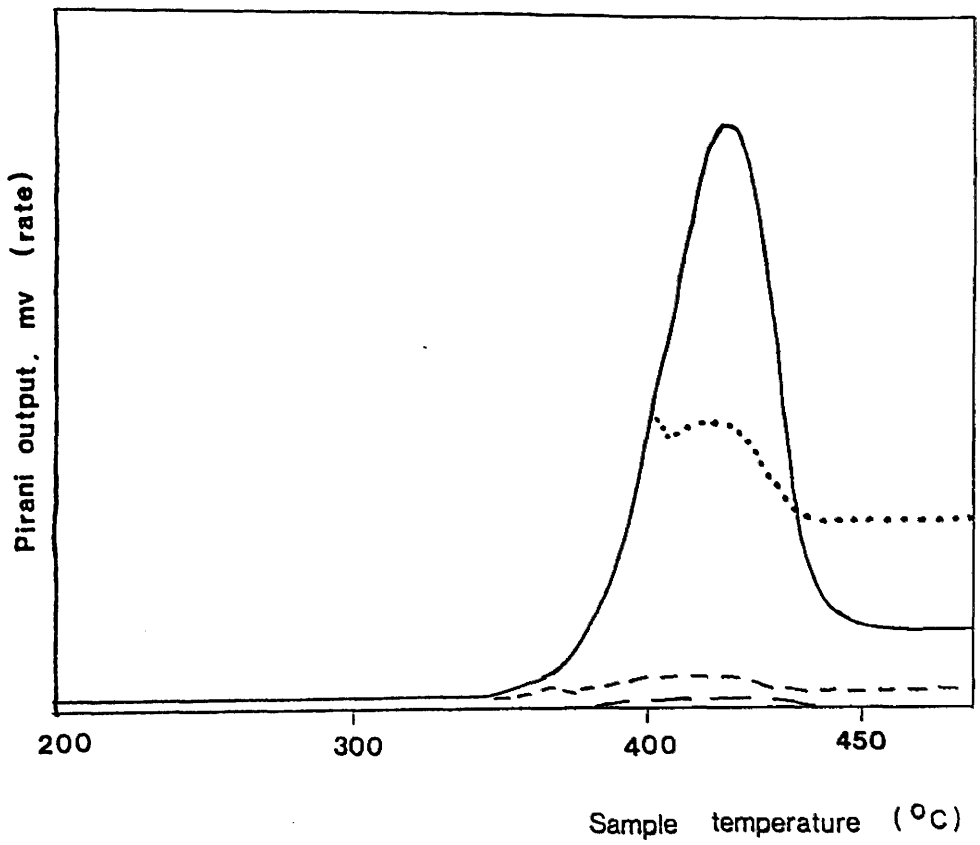


Figure 2.5 TVA curve for polystyrene

When only totally volatile products and total -196°C non-condensable products are recorded, the designation is as follows.

————— Total Volatile Products

— . — . — Total -196°C Non-Condensable Products

Any exception to this scheme will be noted where it occurs.

PRODUCT ANALYSIS FROM TVA

Degradation of a sample within the TVA apparatus gives two categories of products:-

- a) involatile residue
- b) volatile products

The volatile products can be further sub-divided into three classes:-

- 1 Products volatile at the degradation temperature but involatile at ambient temperature. These collect at the top of the degradation tube in the region cooled by the water jacket. Consequently this class of product is referred to as the cold ring fraction
- 2 Products volatile at degradation and ambient temperatures but condensable at -196°C - condensibles.
- 3 Products non-condensable at -196°C - non-condensibles.

The residue is removed, if possible, by

dissolution in suitable solvent. An infra-red spectrum can then be obtained either as a solution or as a film cast onto a NaCl plate. Insoluble residues may be analysed spectroscopically by first scraping some material from the tube base with a spatula and grinding the material to a fine powder prior to forming a KBr disc or Nujol mull. At advanced states of degradation it may be impossible to remove the residue from the tube base. To study the residues in such cases, a film can be cast directly onto a NaCl disc and this film degraded. The salt plate and associated residue can then be removed for subsequent IR analysis. Care must be taken, however, to account for any possible reaction between the NaCl disc and the degrading polymer.

Depending on its form, the coldring fraction can be removed for analysis either by scraping with a spatula or by swabbing with a tissue soaked in a suitable solvent.

Products condensable at -196°C can be distilled from the cold trap into a suitable collection vessel (attached at points E in Fig. 2.2) for analysis by infra-red spectroscopy, mass spectrometry or gas chromatography. For IR analysis, a gas cell similar to that depicted in Fig. 2.6 is used. A mixture of condensable products is usually first fractionated by means of sub-ambient distillation (q.v.).

Those materials (hydrogen, methane, oxygen, carbon monoxide) volatile at -196°C and thus not

trapped may be studied by carrying out a degradation in a sealed system similar to that illustrated in Fig. 2.7. The system is initially evacuated via stopcock A which is then closed prior to heating the sample. Condensable products are trapped in the -196°C trap whilst the non-condensibles diffuse through the system including the gas cell. At the end of the degradation, the gas cell can be removed and an IR spectrum obtained.

A more convenient method and that normally used in this laboratory, is to bleed the non-condensibles as they form into a mass spectrometer fitted on-line between the main trap and pumping system. Due to technical difficulties, this facility was unavailable for most of the duration of this project. However, as carbon monoxide and methane are the only commonly formed -196°C non-condensibles, this was not too serious a limitation.

SUB-AMBIENT DISTILLATION

This technique, developed independently by McNeill et al.⁶⁹ and Ackermann and McGill,⁷⁰⁻⁷² provides a simple method for separating the condensable products of a degradation, thus facilitating analysis. McNeill et al. called the technique sub-ambient thermal volatilization analysis (SATVA) whereas Ackermann and McGill prefer the term differential distillation. However, the name sub-ambient distillation (SAD) is considered more appropriate, and will be used throughout

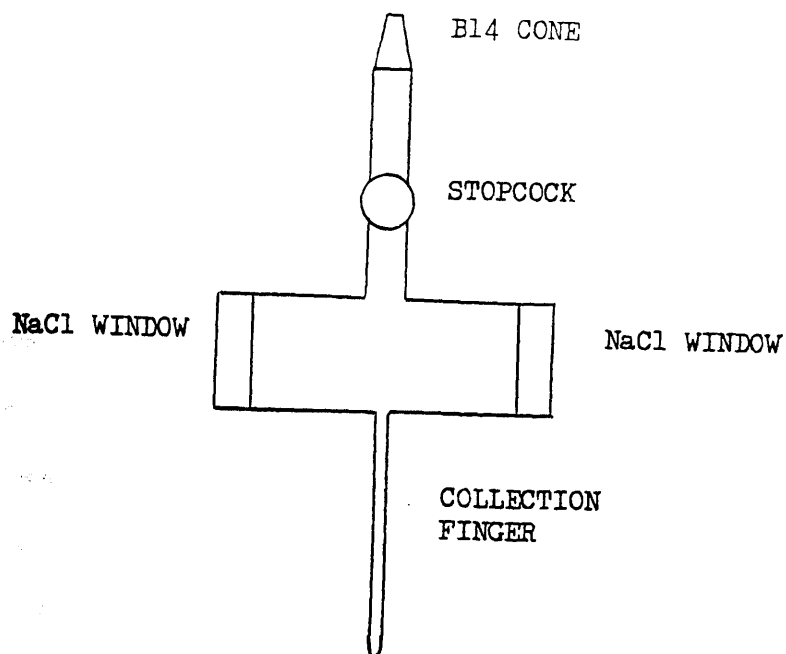
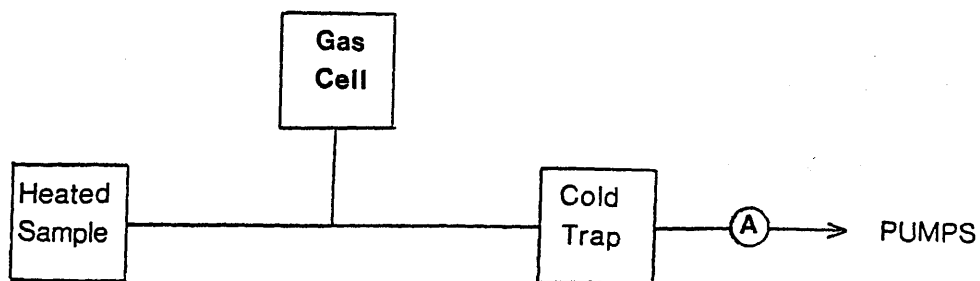


Fig. 2.6 Gas Cell For IR Analyses



A - Stopcock

Fig. 2.7

System for Analysis of -196°C Non-condensable Degradation Products

this thesis.

The principal features of a SAD system are shown in Fig. 2.8.

Degradation products from the heated sample are collected in the liquid nitrogen cooled trap A, the entire system being continually evacuated. The evolution of products from the sample can be monitored on Pirani 1, as in a TVA experiment, whilst Pirani 2 may be used to monitor those non-condensable products which pass through the trap and are thus lost to the pumps, unless bled off to a mass spectrometer.

Trap A, commonly called the sub-ambient trap, is depicted in detail in Fig. 2.9. The U-tube is surrounded by a Pyrex glass vessel containing glass beads. The glass vessel is itself surrounded by a Dewar flask containing liquid nitrogen. A thermocouple measures the temperature of the U-tube.

When the collection of products has been completed, stopcock S of Fig. 2.8 is closed and the liquid nitrogen removed from around the sub-ambient trap, A. The trap will now begin to warm up at a rate determined by the diameter of, and size of bead used in, the surrounding jacket. Although not quite linear, the heating rate is reproducible for any given jacket. As the trap warms, each of the condensed products will distill from the trap over a temperature range dependent on the volatility of the material concerned. The pressure changes associated with the distillation of the

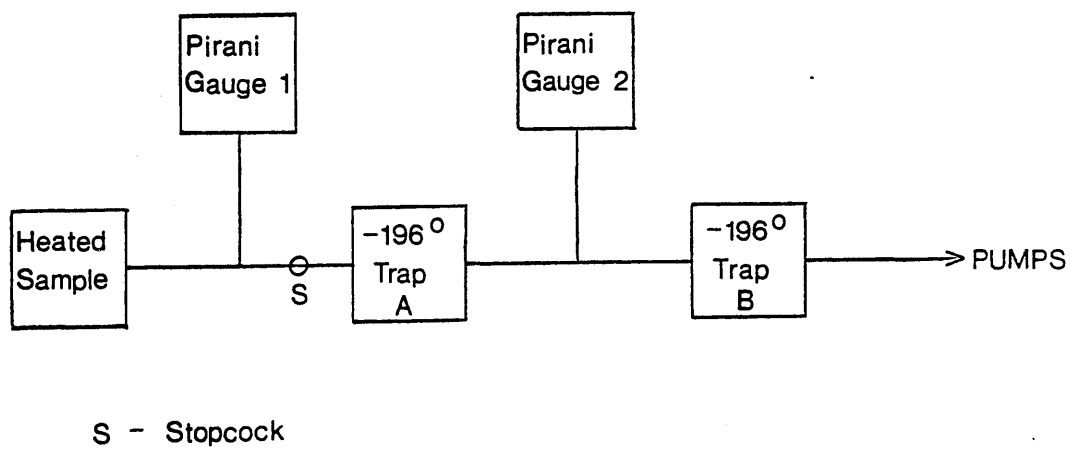
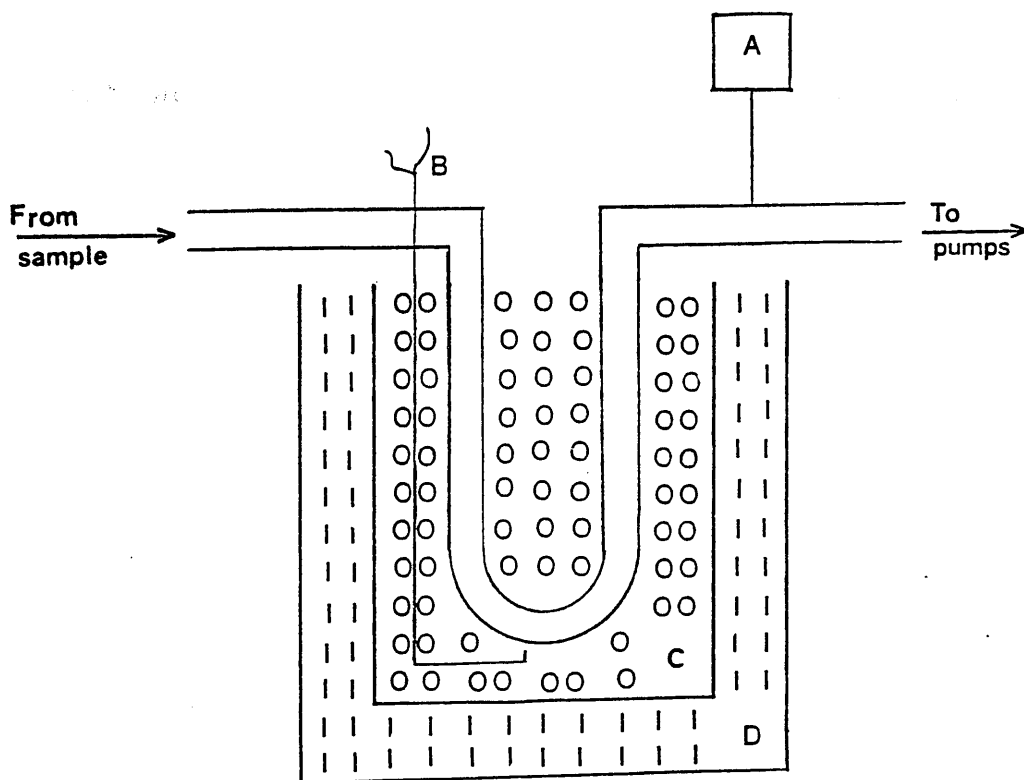


Fig. 2.8 Principal Features of a SAD System



- A - PIRANI GAUGE
- B - TYPE K THERMOCOUPLE
- C - 2.5 mm GLASS BEADS IN PYREX FLASK
- D - LIQUID NITROGEN

Fig. 2.9 Sub-ambient Trap

products from trap A to trap B are measured by Pirani 2. Both Pirani response and trap temperature are recorded as a function of time to give a trace similar to the typical example of Fig. 2.10. In general, longer warm up times enhance the resolution of the peaks although complete separation of products is seldom attained.

Isolation of the products giving rise to a specific SAD peak may be achieved by omitting trap B of Fig. 2.8 and linking SAD trap A directly to a system such as that illustrated in Fig. 2.11. Initially, taps b, c, d are closed and so any product distilling from B will pass down limb 1 and be condensed in the liquid nitrogen trap, A. When the peak corresponding to this product on the SAD trace has reached a minimum, tap b is opened and taps a and e closed (this specific order ensures that the SAD trap is always open to the pumps preventing spurious peaks on the SAD trace due to back pressures). Thus, the first peak product(s) are isolated in limb 1 whilst the second peak product(s) are collected in limb 2. Similarly, further products may be collected in limbs 3 and 4. Once the products have been isolated, they may be removed for analysis by distilling the material from the -196°C trap to an evacuated sample collection vessel, commonly a minimum volume gas cell, attached to the limb at the take-off points (marked B in Fig. 2.11). In this laboratory, the most commonly used analytical techniques are infra-red

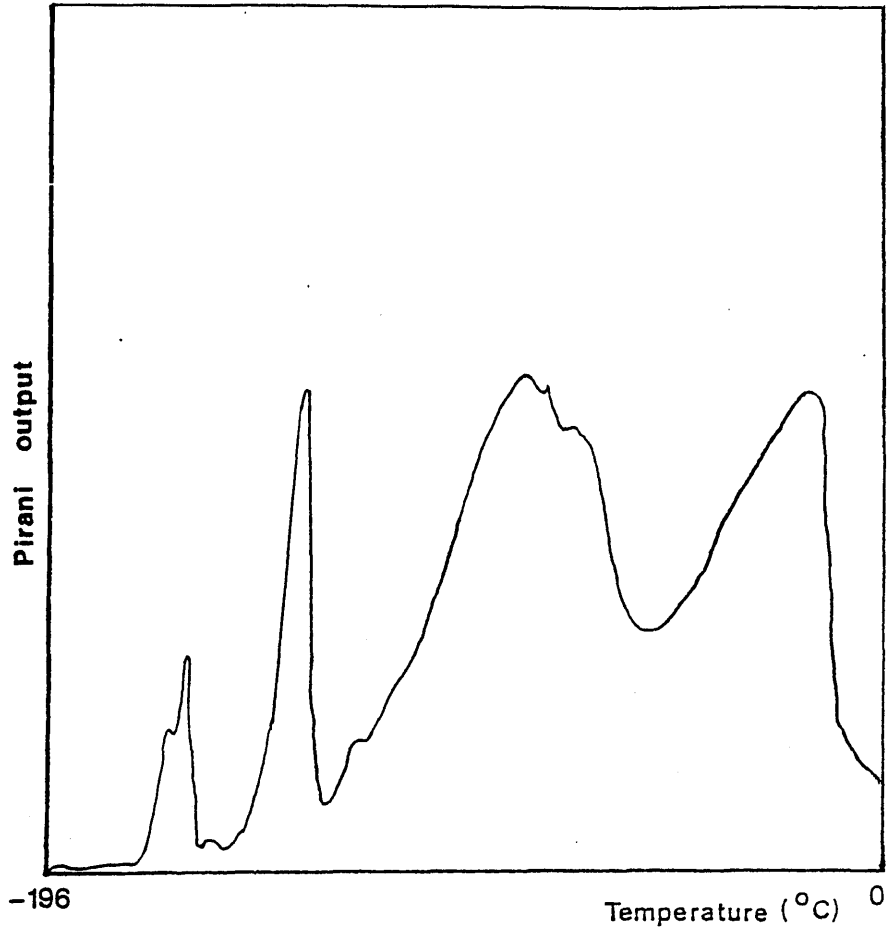


Fig. 2.10 Typical SAD Curve

... the measurement of the weight loss of a ...
 ... trap. This can be done as a function ...
 ... under programmed heating or as a function ...

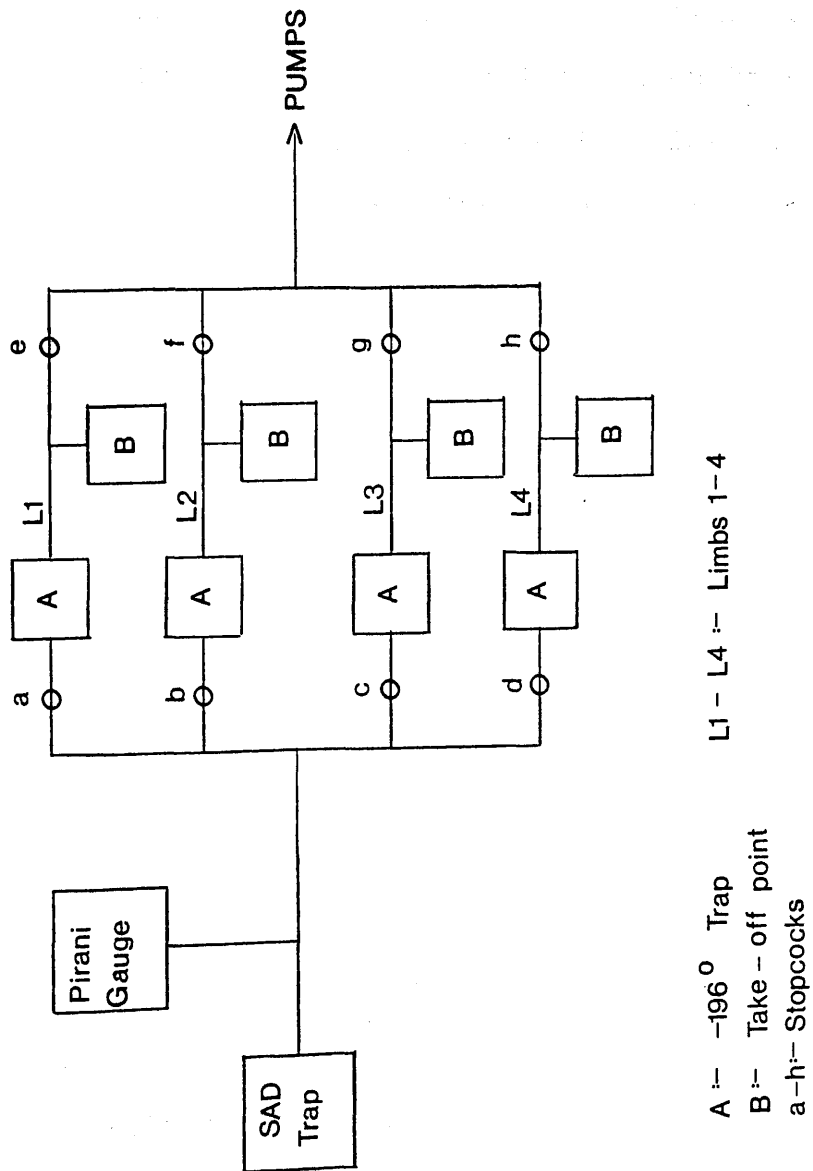


Fig. 2.11 System Employed for Isolation of Products via SAD

spectroscopy and mass spectrometry, gas chromatography also being used an occasion.

THERMOGRAVIMETRY

Thermogravimetry (TG) involves, as its name suggests, the measurement of the weight loss of a sample on heating. This can be done as a function of temperature under programmed heating or as a function of time under isothermal conditions. Unlike TVA which records only those products volatile enough to reach the Pirani gauge, TG will record the weight loss due to the evolution of any material from the sample pan. The sample may be heated under a variety of atmospheres or under vacuum.

For this work, a DuPont 951 Thermogravimetric Analyser coupled to a DuPont 990 Thermal Analyser was employed. Degradations were performed under a nitrogen flow of 50ml min^{-1} , with heating from ambient to 500°C at $10^{\circ}\text{C min}^{-1}$. Samples were of the order of 5-10mg and were in powder form (chelate compounds) or films cast directly into the sample pan from methylene chloride solution (polymers and polymer-chelate blends), except where noted otherwise.

The nature of TG curves is such that it is sometimes difficult to discern overlapping processes, and to facilitate interpretation it is helpful to have available the derivative trace of the weight-loss curve. This feature, known as differential thermogravimetric

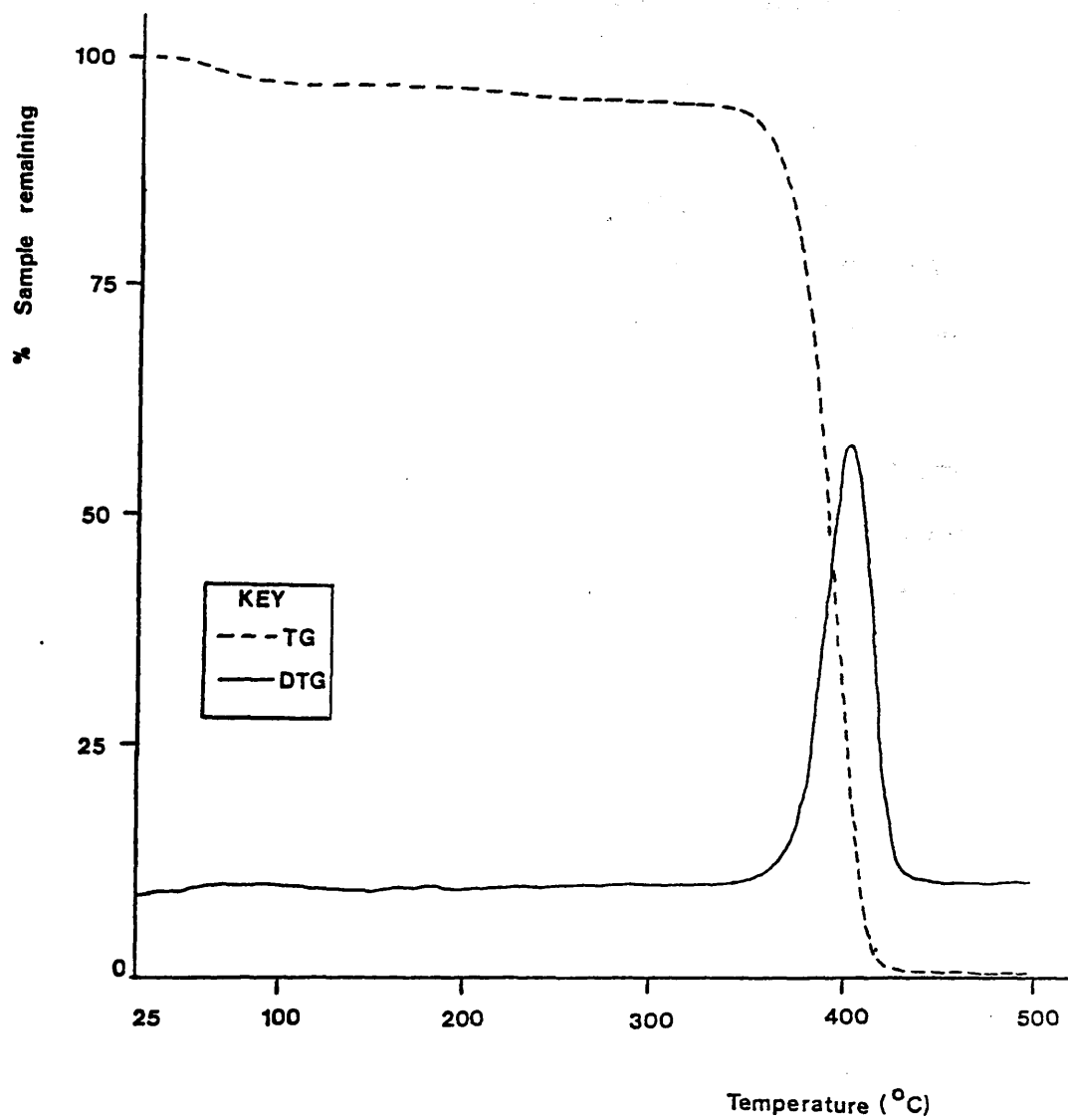


Fig. 2.12

TG (---) and DTG (—) Curves for Polystyrene (Nitrogen Atmosphere)

analysis (DTG), is available on the DuPont system and a DTG trace can be recorded simultaneously with the TG curve. The TG and DTG curves obtained for polystyrene are reproduced in Fig. 2.12 and can be compared with the TVA trace for polystyrene (Fig. 2.5). Note that unlike TVA, TG-DTG provides no information on the nature of the evolved material.

DIFFERENTIAL SCANNING CALORIMETRY (DSC)

In this technique, a sample and an inert reference are heated at a programmed rate. Any physical or chemical process involving a change in energy of the sample will result in a difference of temperature between sample and reference. An endothermic reaction, for instance, will cause the sample temperature, T_S , to lag behind that of the reference, T_R , whilst an exothermic reaction will cause T_S to rise above T_R . In the DSC apparatus, the sample and reference are maintained at the same programmed temperature by the addition of heat to one or other as required. The difference in power input required to equalise the sample and reference temperatures is recorded as a function of time. Thus is obtained a plot of dH/dT versus time, where H is the amount of energy transferred. The total amount of energy transferred is then proportional to the area under the curve. By convention, endotherms are depicted by a downwards deflection of the DSC curve, and exotherms by an upwards

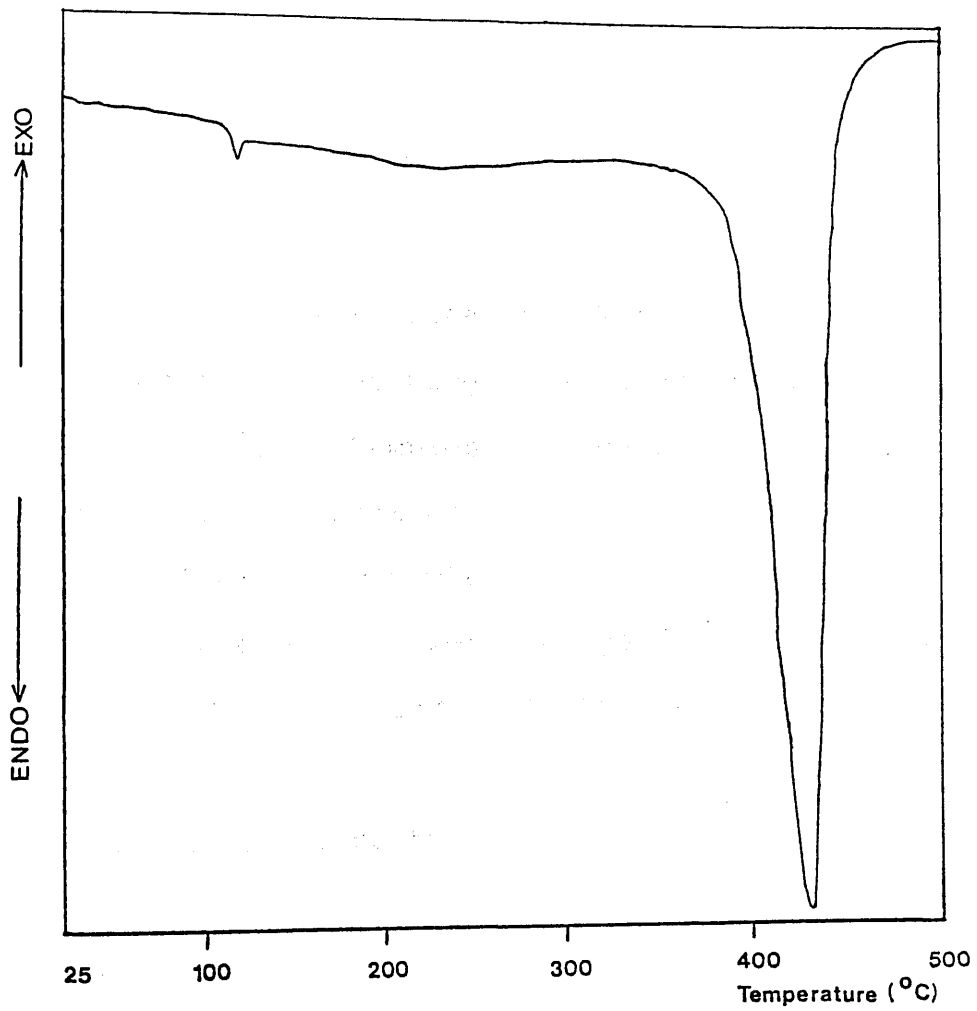


Fig. 2.13 DSC Curve for Polystyrene (Nitrogen Atmosphere)

displacement.

The equipment used in this study consisted of a DuPont 910 Differential Scanning Calorimeter in conjunction with a DuPont 990 Thermal Analyser.

All analyses were performed under a nitrogen atmosphere at a flow rate of 50ml min^{-1} except where stated otherwise. Heating was from ambient to 500°C at $10^{\circ}\text{C min}^{-1}$. Samples of polymers and polymer blends were in the form of films cast directly into the sample pan from a methylene chloride solution. The acetylacetonate complexes were analysed in powder form.

The DSC curve for polystyrene is reproduced in Fig. 2.13. The endotherm around 400°C corresponds to the weight loss observed by TVA and TG.

DIFFERENTIAL THERMAL ANALYSIS

Differential Thermal Analysis (DTA) is a technique similar to DSC and in several cases, depending on instrument availability, DTA curves, rather than DSC curves, were obtained for samples.

Whereas DSC involves measuring the varying energy input required to keep an inert reference and the sample at equal temperatures during a programmed heating regime, DTA involves the measurement of the temperature differences arising between sample and inert reference during programmed heating at a fixed energy input. Thus an endothermic reaction occurring within the sample is recorded by DSC in terms of the extra energy input to

the sample to keep it at the same temperature as the reference, whilst in DTA, no extra energy is added and instead the temperature lag is recorded. Conventionally sample temperature lags (endothermic reactions) are recorded by a downwards deflection of the DTA curve whilst temperature increases (exothermic reactions) are recorded by an upwards deflection. It can be seen therefore that both DTA and DSC record the same processes within the sample and DTA curves and DSC curves are in practice very similar. This is shown very clearly by a comparison of the DSC and DTA curves obtained for $\text{Mn}(\text{acac})_3$ (both at $10^\circ\text{C min}^{-1}$, dynamic nitrogen atmosphere) and reproduced in Fig. 2.14.

For this research, DTA analyses were performed on a DuPont 451 Thermal Analyser at a heating rate of $10^\circ\text{C min}^{-1}$ under a nitrogen flow of 50ml min^{-1} .

DEFINITIONS OF T(ONSET) AND T(MAX)

The most commonly quoted temperatures appertaining to TVA, DTA/DSC and TG-DTG curves are the peak onset and peak maxima, commonly referred to as T(onset) and T(max) respectively. Determination of T(max) is generally straightforward but there are several definitions of T(onset) and so it is important to be clear about how T(onset) and T(max) were determined in this research.

TVA Curves

Onset temperatures are defined as the temperature

the sample to keep it at the same temperature as the reference, whilst in DTA, no extra energy is added and instead the temperature lag is recorded. Conventionally sample temperature lags (endothermic reactions) are recorded by a downwards deflection of the DTA curve whilst temperature increases (exothermic reactions) are recorded by an upwards deflection. It can be seen therefore that both DTA and DSC record the same processes within the sample and DTA curves and DSC curves are in practice very similar. This is shown very clearly by a comparison of the DSC and DTA curves obtained for $\text{Mn}(\text{acac})_3$ (both at $10^\circ\text{C min}^{-1}$, dynamic nitrogen atmosphere) and reproduced in Fig. 2.14.

For this research, DTA analyses were performed on a DuPont 451 Thermal Analyser at a heating rate of $10^\circ\text{C min}^{-1}$ under a nitrogen flow of 50ml min^{-1} .

DEFINITIONS OF T(ONSET) AND T(MAX)

The most commonly quoted temperatures appertaining to TVA, DTA/DSC and TG-DTG curves are the peak onset and peak maxima, commonly referred to as T(onset) and T(max) respectively. Determination of T(max) is generally straightforward but there are several definitions of T(onset) and so it is important to be clear about how T(onset) and T(max) were determined in this research.

TVA Curves

Onset temperatures are defined as the temperature

at which the curve deviates from the base-line. Where two peaks overlap, the temperature of the turning point is taken as $T(\text{onset})$ although this may not represent the true onset temperature of the underlying decomposition process.

The determination of $T(\text{max})$, which in TVA represents the maximum rate of evolution of products, is straightforward.

The schematic diagram of a TVA curve, Fig. 2.15, illustrates these points.

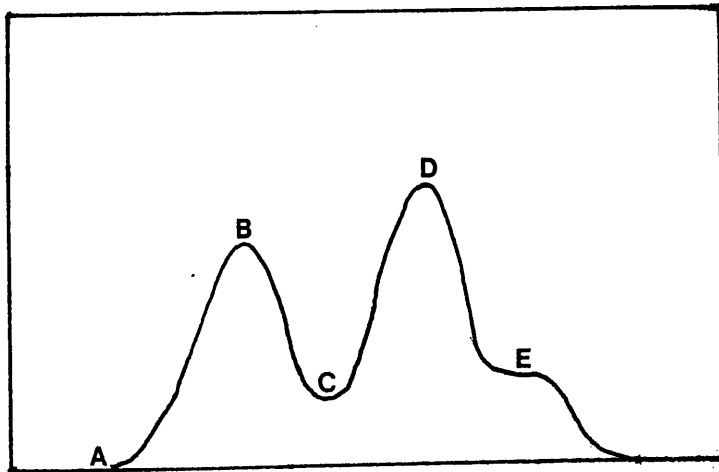


Fig. 2.15 Typical TVA Curve showing definitions of $T(\text{onset})$ and $T(\text{max})$.

A	$T(\text{onset})$	peak 1
B	$T(\text{max})$	peak 1
C	$T(\text{onset})$	peak 2
D	$T(\text{max})$	peak 2
E		shoulder to peak 2

DTA/DSC Curves

Again, the peak temperature is obtained without ambiguity. Various ways of deriving the onset temperatures are advocated⁷³ but the method employed here is simply to define T(onset) as the temperature at which the curve first deviates from the base-line. See Fig. 2.16.

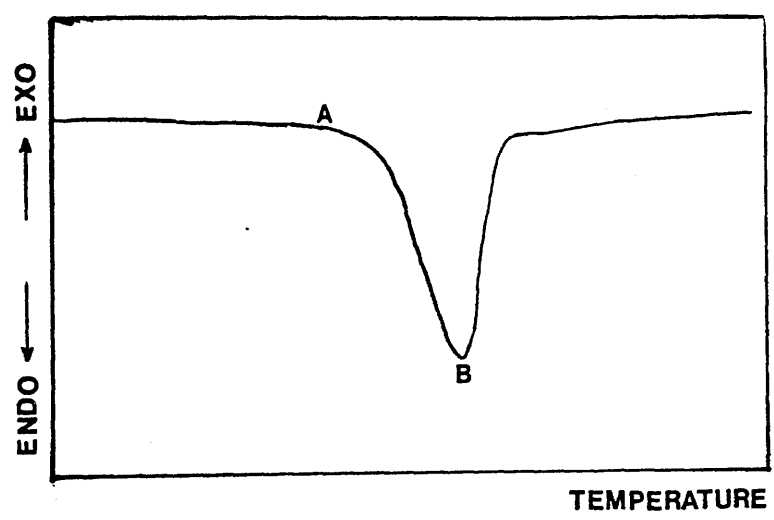


Fig. 2.16 Typical DTA/DSC curve showing definition of T(onset) and T(max).

A T(onset)

B T(max)

TG-DTG Curves

For TG, T(onset) is the temperature of the initiation of weight loss and T(max) is the temperature at which the rate of weight loss is at a maximum. T(onset) can be fairly easily determined from the weight loss curve but T(max) which corresponds to the point of maximum gradient of the weight loss vs. time curve is

less easy to pin-point accurately. It is however readily ascertained from the derivative of the weight loss curve. See Fig. 2.17.

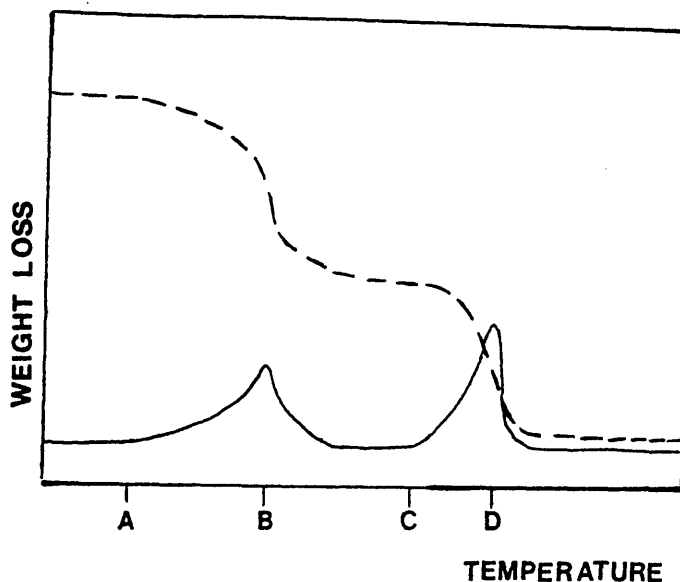


Fig 2.17 Typical TG curve (----) and associated DTG curve (—) showing definition of T(onset) and T(max)

- | | |
|---|-----------------------|
| A | T(onset) 1st wt. loss |
| B | T(max) " " " |
| C | T(onset) 2nd wt. loss |
| D | T(max) " " " |

ACCURACY OF THE DETERMINATION OF T(ONSET) AND T(MAX)

The nature of T(max) makes it very easy to determine accurately but T(onset), as defined above, can be difficult to determine with accuracy as the initial deflection of the curve can be very slight. Consequently, a change in T(onset), unless pronounced, should not alone be considered evidence for a modification of the degradation process.

TVA, TG, DSC - COMPARISON OF THE TECHNIQUES

Generally, no single thermal analysis technique is capable of supplying all the information required for a complete understanding of thermal degradation processes. Of the methods used in this research, TVA is the most versatile.

DSC analysis can indicate the occurrence within the sample of any process, chemical or physical, accompanied by an energy change. Thus it can detect processes which do not produce volatile material. To fully interpret a DSC curve, however, it is necessary to have additional information from TVA and TG.

Although TVA, unlike TG, is only semi-quantitative and is unable to record the evolution of those relatively involatile products which condense on the cold ring, it has several important advantages over TG. As well as providing valuable initial qualitative data, the form of the TVA apparatus and the use of a considerably larger sample facilitates further analysis of all products (solid residue, cold ring fraction, -196°C condensible and non-condensable gases and liquids), particularly when coupled with SAD.

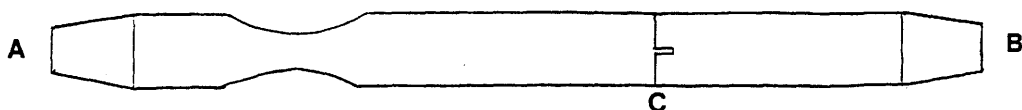
Continually evacuating the degradation zone aids the diffusion of volatile products from the sample and limits the possibility of secondary decomposition processes. Diffusion from the sample is also aided by the thinness of the film cast on the large area of the tube base - a 30mg sample will be less than 0.01cm

thick. The thinness of the film coupled with the large mass of the tube ensures that thermal effects due to the decomposition of the polymer and temperature differentials across the sample are minimised and thus, after calibration of the apparatus, accurate determination of the degradation temperatures can be made.

It is notoriously difficult to compare directly the temperatures of decomposition as recorded by different thermal analysis techniques due to the effects of sample sizes and forms, atmospheres and instrumental vagaries.⁷⁴ In this project TG and DSC determinations were performed under a nitrogen atmosphere and TVA determinations under high vacuum. Consequently, large discrepancies can occur. In general, a T(onset) or T(max) temperature obtained from TG under atmospheric pressure will be higher than that obtained from TVA due to the easier evolution of volatiles in the latter, high vacuum, technique.

DEGRADATIONS IN A SEALED TUBE

Some degradations of the chelates were performed in sealed tubes to prevent sublimation of the chelate from the heating zone. An example of a sealable tube is illustrated in Fig. 2.18.



A,B - B 14 Cone

C - Break-seal

Fig. 2.18 Sealable Tube

The volume of the sealable portion of the tube is approximately 5ml. The sample is introduced to this region by transferring, by pipette, a solution of the required amount of chelate (typically 10-25mg) in a volatile solvent such as methylene chloride, through the constriction. The solvent is then removed by applying gentle suction from a water pump followed by heating in a vacuum oven. This procedure avoids the possibility of material becoming caught in the constriction where it would be degraded on sealing.

The tube is sealed after first connecting to a vacuum line via cone A and evacuating to 5×10^{-3} - 10^{-4} torr. Care is taken to ensure the sample is not degraded during the sealing process.

The sealed tube is then clamped in the TVA oven such that the sample is positioned next to the oven thermocouple and the sample is then heated as required.

On completion of the degradation, the tube is

removed and small iron bar is inserted carefully through cone B. Taking care not to break the seal, the tube is connected via cone B to a SAD line (to socket D in Fig. 2.8). The tube is evacuated, the SAD trap cooled and, by means of a magnet the iron bar is used to break the break-seal. Volatile products then distill from the tube into the SAD trap, a process that can be monitored using Pirani 1 of Fig. 2.8 whilst Pirani 2 can monitor any material non-condensable at -196°C . After the distillation of products is completed, a normal SAD analysis can be performed.

INFRA-RED SPECTROSCOPY

Infra-red spectra were obtained on a Perkin Elmer 257 grating spectrophotometer. Solid samples were run as KBr discs or Nujol mulls. Spectra of polymers and polymer blends were acquired by first casting a film onto a sodium chloride disc. Gas cells of the type depicted in Fig. 2.6 were used to obtain spectra of those degradation products with an appreciable vapour pressure at ambient temperature.

INTERPRETATION OF INFRA-RED SPECTRA

The identification of degradation products from their IR spectra was performed by comparison with the spectra of authentic samples. Two valuable sources of reference gas phase spectra are the book by Welti⁷⁵ and the paper by Pierson, Fletcher and Gantz⁷⁶ whilst

the Aldrich⁷⁷ and Sadtler⁷⁸ catalogues of IR spectra provide extensive sources of liquid phase and solid state spectra.

Gas phase spectra, obtained in their research, of several common degradation products are reproduced in Appendix 1.

IDENTIFICATION OF KETENES BY IR SPECTROSCOPY

The gas phase IR spectra of the lower ketenes are very similar (compare for instance the spectra of ketene and dimethyl ketene shown in Fig. 2.19). Consequently, unambiguous assignment of absorptions in the region around 2150cm^{-1} cannot be made. Therefore, in this research, assignment of bands in this region is to "a ketene" and further evidence on the exact nature of the ketene(s) causing the absorption must come from mass spectrometry or consideration of the degradation mechanism.

MASS SPECTROMETRY

When available, a V.G. Micromass QX200 quadropole mass spectrometer was used coupled directly to the TVA-SAD system. Compounds with a molecular weight less than 150 a.m.u. could be analysed. Degradation products non-condensable at -196°C could be bled into the mass spectrometer during the degradation process. Condensable products were usually first fractionated using the SAD process, samples of each peak being admitted to the mass

spectrometer.

Occasionally, mass spectra were obtained on a Kratos MS12 machine.

ULTRA VIOLET SPECTROPHOTOMETRY

Spectra were obtained using a Pye Unicam SP 8-800 or Perkin Elmer 550 SE recording spectrophotometers. Data for the complexes were obtained for solutions in a suitable solvent, usually chloroform or methylene chloride. Spectra of blends before and after heating were obtained by first dissolving the material in a suitable solvent and casting a film onto a silica glass surface. The supported film could then be mounted in the machine.

(From refs. 77 and 80)

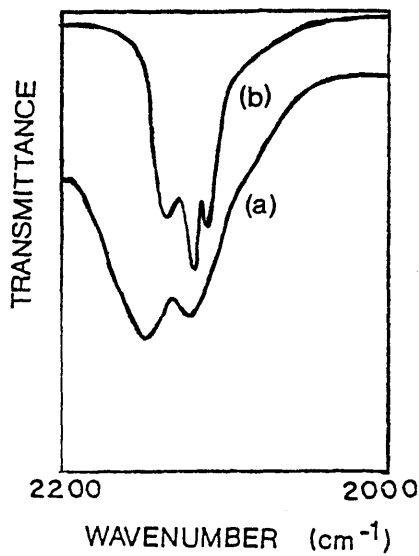


Fig. 2.19
IR Spectra of (a) Ketene, (b) Dimethyl ketene.
(From refs. 79 and 80)

CHAPTER 3

TRANSITION METAL ACETYLACETONATE CHELATES - PREPARATION, SPECTRA, THERMAL BEHAVIOUR

PREPARATION OF THE CHELATES

Reagents and Solvents

The reagents and solvents used in the preparation of the chelate compounds were, wherever possible, of analytical grade and were used without further purification. Acetylacetone was found to discolour with time and was distilled prior to use (b. pt. 138°C).

Tris Cobalt (III) Acetylacetonate ($\text{Co}(\text{acac})_3$)

Following the general method of Bryant and Fernelius,⁸¹ a slurry of basic cobalt (II) carbonate (16.50g equivalent to approx 0.13 moles Co^{2+}) in acetylacetone (120ml, 1.17 moles) was heated to 90°C . 180ml of 10% w/v hydrogen peroxide solution were added, with rapid stirring, over the period of one hour. The mixture was cooled in an ice-salt bath for several hours before filtering the product, obtained as very dark green lustrous crystals. After drying for seven hours at 110°C , the crude material was purified by dissolving in 150ml of hot toluene, hot filtering, and precipitating with 900ml of petroleum spirit. The precipitated material was filtered off, dried at the pump and the procedure repeated to yield the pure

$\text{Co}(\text{acac})_3$ as a green powder. Yield 33.22g, 74.0%.

Microanalysis

Found: C 50.39% H 5.71%

Calculated for $\text{Co}(\text{C}_5\text{H}_7\text{O}_2)_3$: C 50.57% H 5.94%

Melting range

Found: 197-199°C

Literature: 213°C,⁸¹ 240-241°C⁸²⁻⁸⁴

There is some discrepancy between the observed melting range and that recorded previously. Commenting on the difference between their observed melting range and that of earlier workers⁸²⁻⁸⁴ Bryant and Fernelius⁸¹ suggested that the variation could be due to the existence of more than one crystal form. A similar explanation is possible here, particularly as the compound is apparently pure by microanalysis and IR and UV spectroscopy (see subsequent section).

Tris Manganese (III) Acetylacetonate ($\text{Mn}(\text{acac})_3$)

By the method of Charles,⁸⁵ manganese (II) chloride tetrahydrate (32.59g, 0.17 moles) plus sodium acetate trihydrate (85g, 0.62 moles) were dissolved in water (1000ml) and acetylacetone (65ml, 0.63 moles) added with stirring. Potassium permanganate (16.5g, 0.04 moles) in water (300ml) was then added, followed after ten minutes by further sodium acetate trihydrate (85g, 0.62 moles) in water (300ml). The mixture was heated to

60°C for 10 minutes before chilling in ice. The product was then filtered from the mixture and washed with iced water and a small quantity of acetone. The crude product was purified by dissolution in warm toluene with precipitation by petroleum spirit 60°-80° followed by three recrystallisations from acetone, to give pure $\text{Mn}(\text{acac})_3$ as lustrous black crystals. Yield 34.33g, 57.33%.

Microanalysis

Found: C 50.9%, H 6.24%

Calculated for $\text{Mn}(\text{C}_5\text{H}_7\text{O}_2)_3$: C 51.1%, H 6.01%

Melting range

$\text{Mn}(\text{acac})_3$ decomposes above 150°C without melting (see subsequent sections).

Bis Copper (II) Acetylacetonate ($\text{Cu}(\text{acac})_2$)

The method of Jones⁸⁶ was followed. Cupric nitrate trihydrate (100.29g, 0.42 moles) was dissolved in 100ml of distilled water. To this solution was added 150ml of 0.88s.g. NH_3 solution followed by the addition with stirring, of acetylacetone (110ml, 1.07 moles). A light blue precipitate formed immediately; this precipitate was filtered off and washed with water until the washings were neutral. The material was allowed to air dry and was purified by recrystallisation

from chloroform (once) and methanol (twice) to yield blue, lustrous, needle-like crystals.

Yield 63.63g, 58.56%.

Microanalysis

Found: C 45.5%, H 5.03%

Calculated for $\text{Cu}(\text{C}_5\text{H}_7\text{O}_2)_2$: C 45.86%, H 5.39%

Melting range

$\text{Cu}(\text{acac})_2$ sublimes and decomposes without melting above 200°C (see subsequent sections).

Bis Cobalt (II) Acetylacetonate ($\text{Co}(\text{acac})_2$)

Bis Manganese (II) Acetylacetonate ($\text{Mn}(\text{acac})_2$)

These chelates were prepared, following published procedures, by Hazzard.⁸⁷

IR SPECTRA OF THE CHELATES

The IR spectra of $\text{Co}(\text{acac})_3$, $\text{Co}(\text{acac})_2$, $\text{Mn}(\text{acac})_3$, $\text{Mn}(\text{acac})_2$ and $\text{Cu}(\text{acac})_2$ are reproduced in Figs 3.1-3.5. For comparison both solution (in chloroform) and solid state (KBr disc) spectra are included. Differences between the spectra of the two forms are generally small. For instance, the absorption at 1555 cm^{-1} in the solution spectrum of $\text{Co}(\text{acac})_2$ is not observed when the sample is prepared as a KBr disc. All spectra agree well with those published in

the literature.^{6-8,73,88,89}

The assignment of the characteristic acetylacetonate chelate absorptions between 1500-1600 cm^{-1} was the subject of some debate due to the close similarity in bond order of C=C and C=O bonds in the chelate system. Bellamy et al.⁹⁰ for example, assigned the higher frequency bond to C=O stretching and the lower to C=C stretching whilst Nakamoto et al.⁶⁻⁸ assigned the absorptions in the reverse order. The matter was finally resolved when Pinchas et al.⁹¹ performed studies on ^{18}O labelled $\text{Cr}(\text{acac})_3$ and $\text{Mn}(\text{acac})_3$ and observed that the higher frequency band occurred some 12cm^{-1} lower for the ^{18}O labelled chelates, consistent with the assignment of the higher frequency band to a C=O stretch. The presence of an absorption band around 1550cm^{-1} in some chelates (eg $\text{Cu}(\text{acac})_2$) Pinchas et al.⁹¹ ascribed to the symmetrical stretch of the two C=O groups. In systems where this absorption is not evident (eg $\text{Co}(\text{acac})_3$) it probably merges with the higher frequency (approx. 1570cm^{-1}) asymmetrical stretching mode.

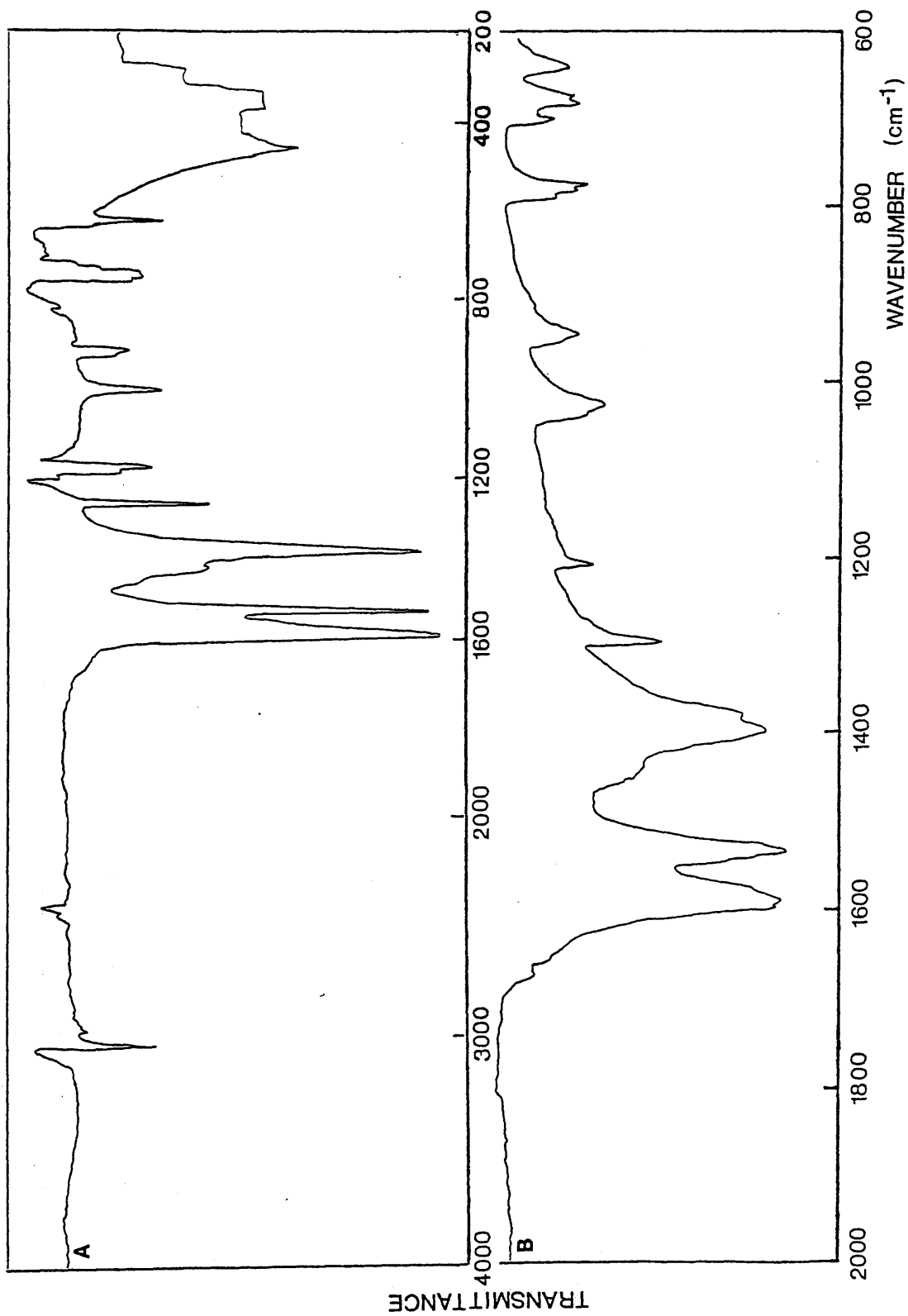


Figure 3.1 IR spectra of Co(acac)₃. CHCl₃ solution (A), KBr disc (B)

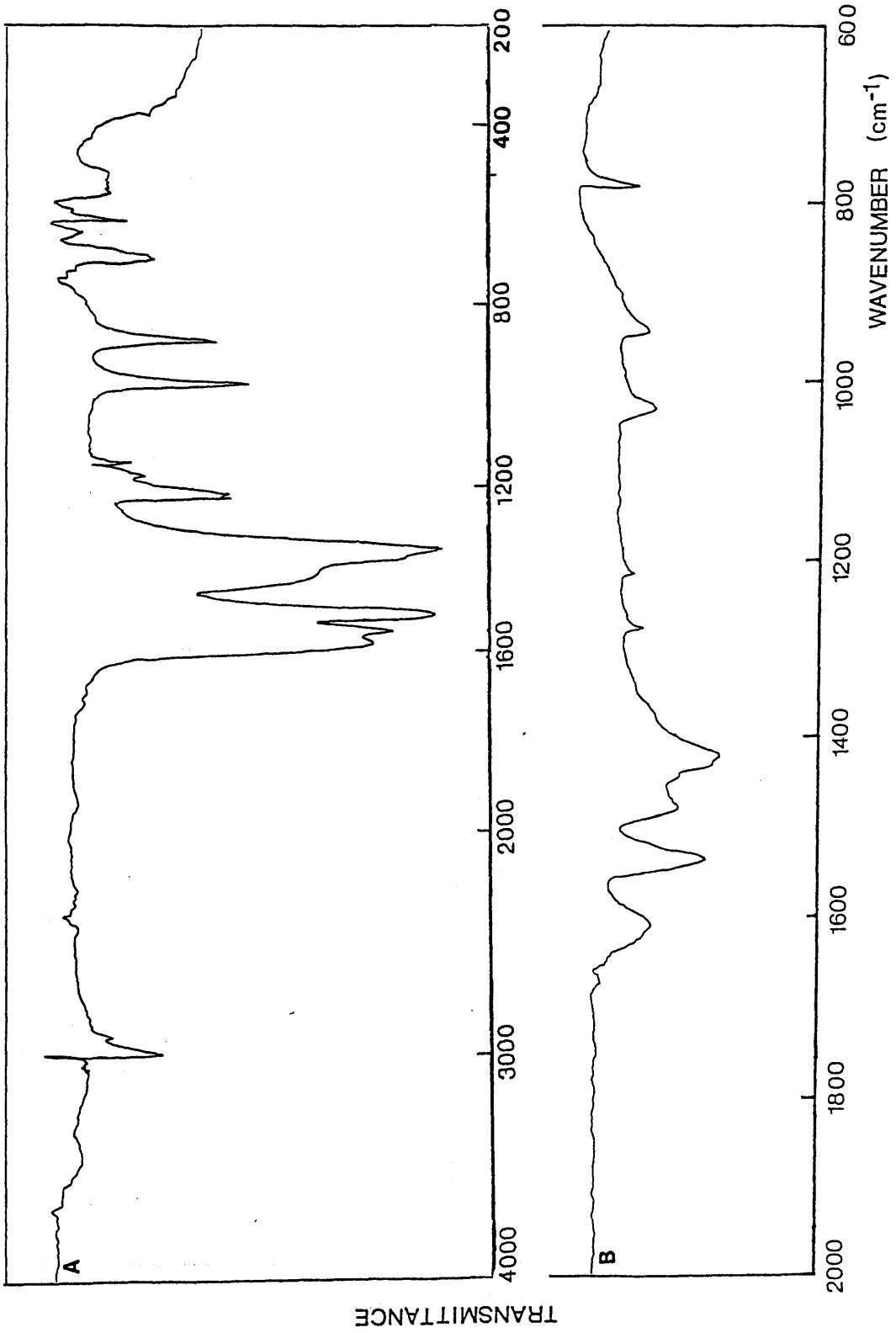


Figure 3.2 IR spectra of $\text{Co}(\text{acac})_2 \cdot \text{CHCl}_3$ solution (A), KBr disc (B)

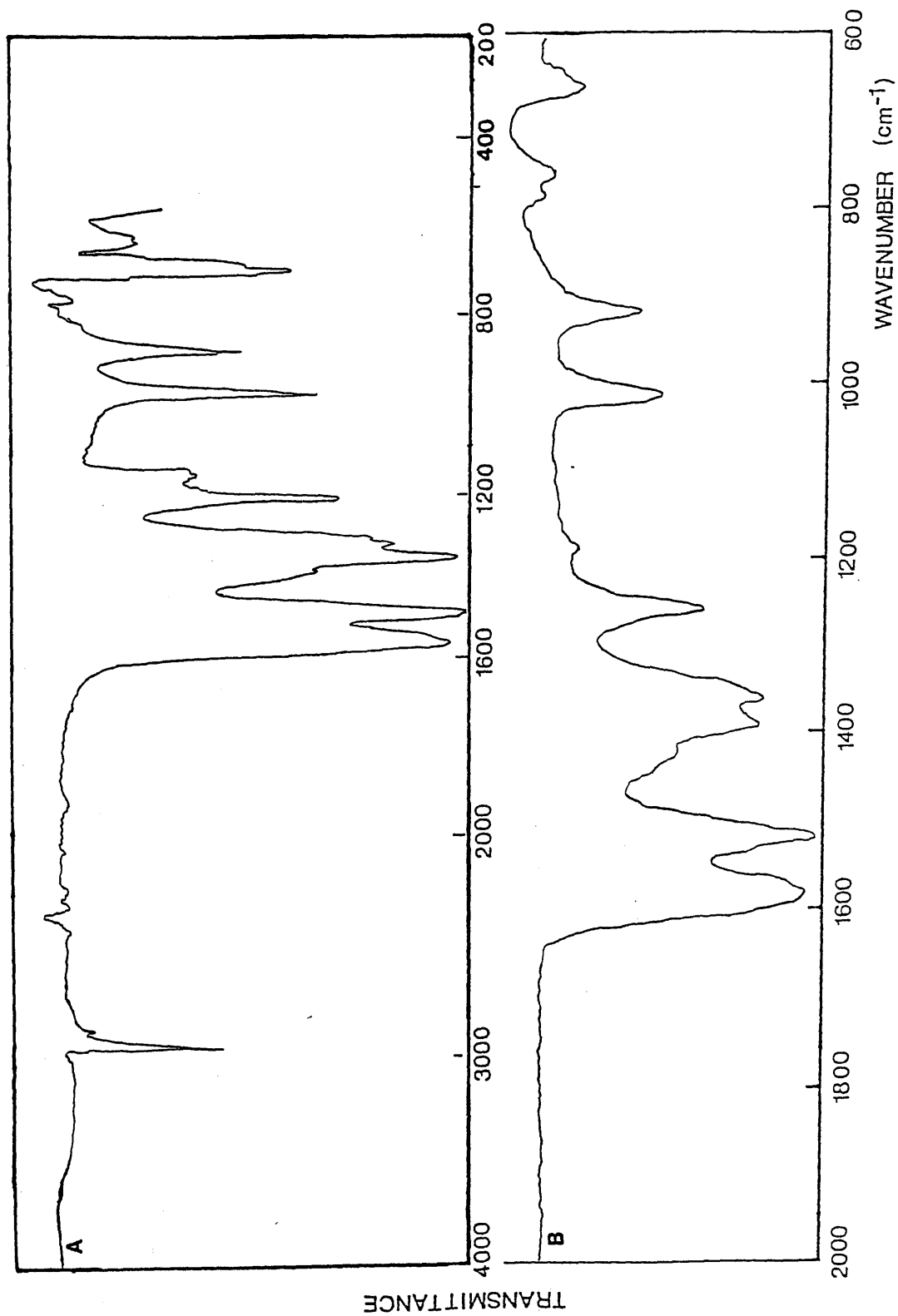


Figure 3.3 IR spectra of $\text{Mn}(\text{acac})_3$. CHCl_3 solution (A), KBr disc (B)

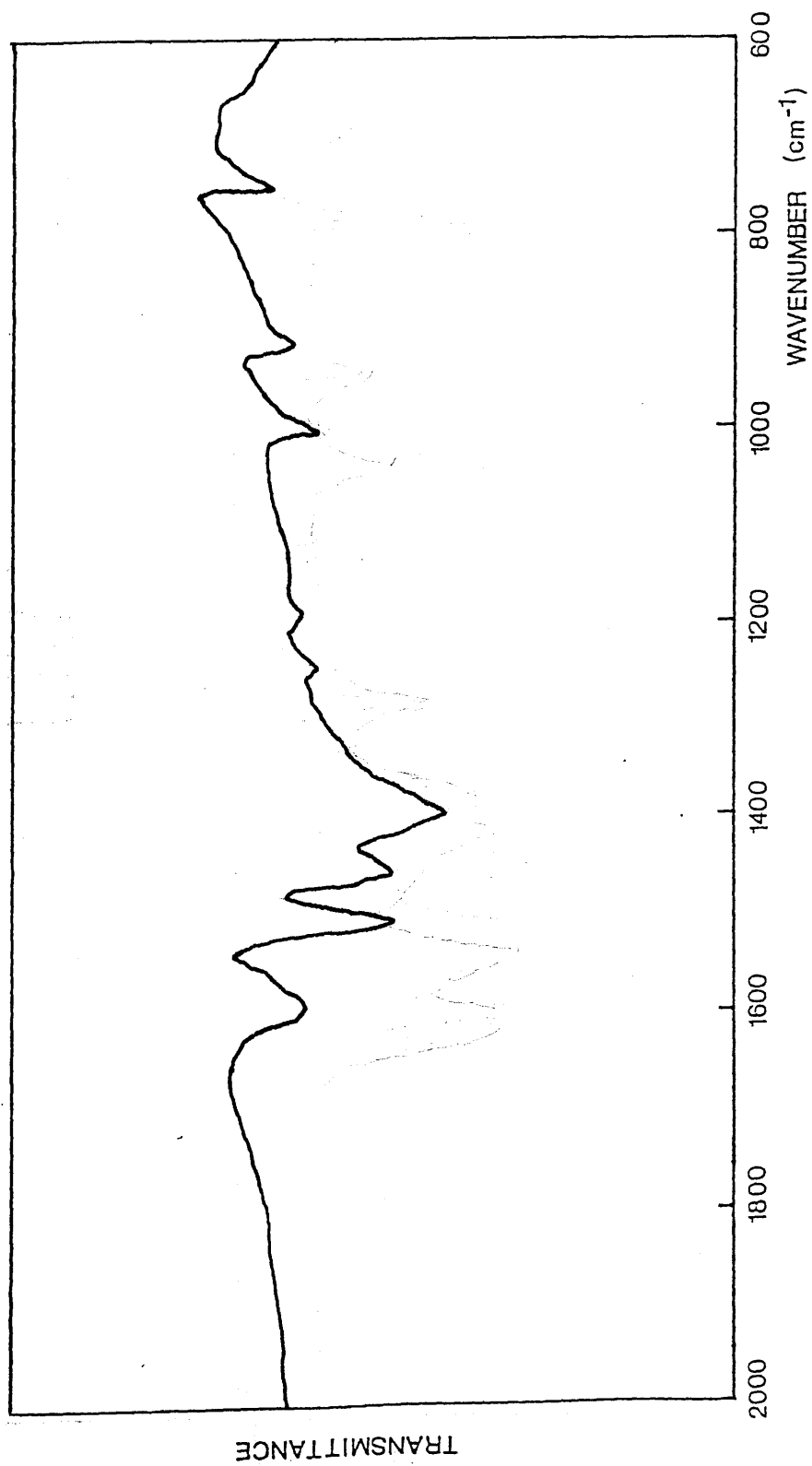


Figure 3.4 IR spectrum of $\text{Mn}(\text{acac})_2$ (KBr disc)

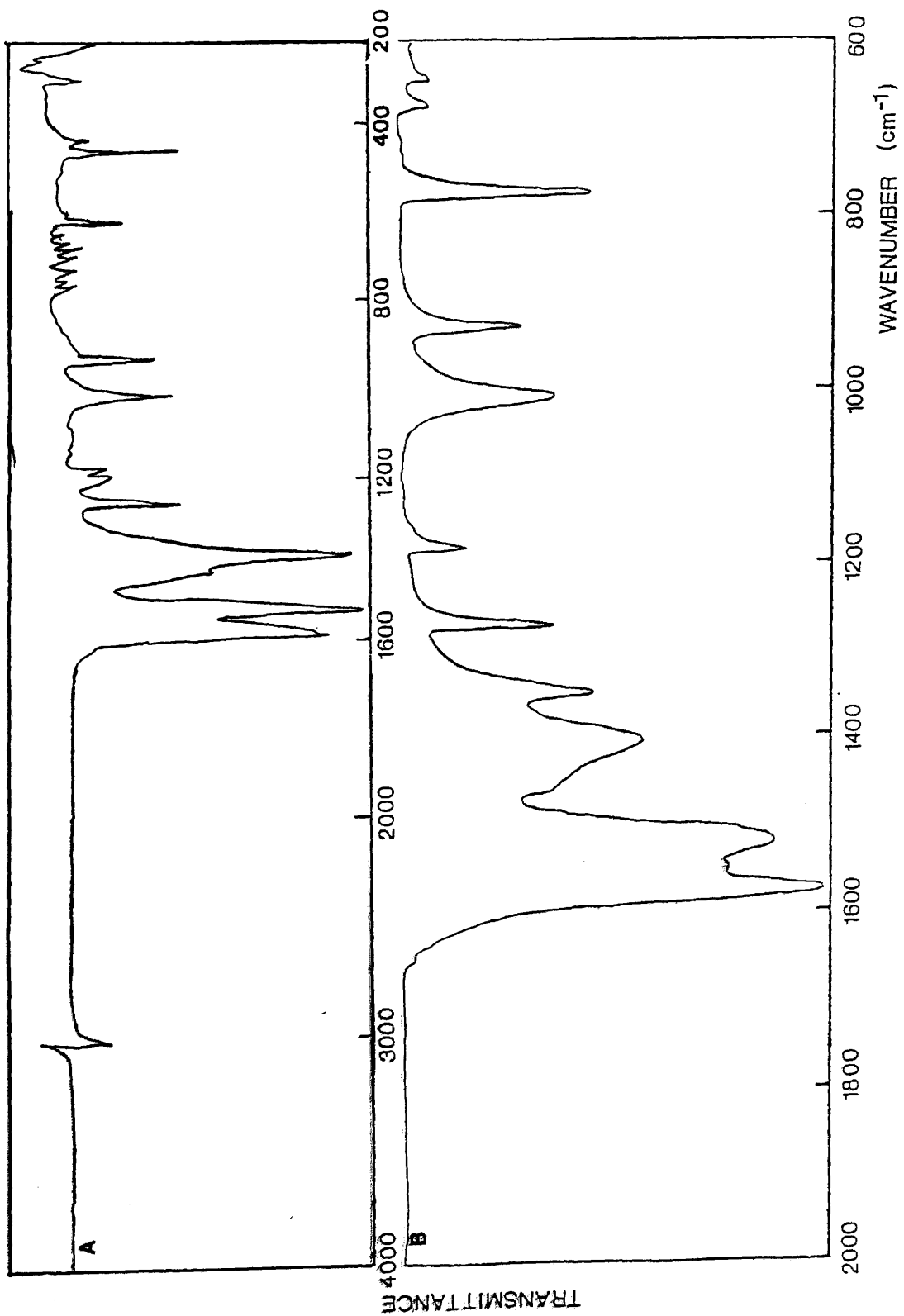


Figure 3.5 IR spectra of Cu(acac)₂. CHCl₃ solution (A), KBr disc (B)

UV SPECTRA OF THE CHELATES

The UV spectra of the chelates in chloroform or methylene chloride solution are illustrated in Figs.3.6-3.10 and detailed in Table 3.1. Literature values are also listed for comparison.

The values of $\lambda(\text{max})$ are in close agreement with the literature values for all the chelates but there is some discrepancy in the values of ϵ . The values for $\text{Cu}(\text{acac})_2$ lie within the range of published values but the experimentally obtained values for $\text{Mn}(\text{acac})_3$ are consistently high (the value in Table 3.1 is the average of six observations). The material is pure by microanalysis and the reason for the discrepancy is unknown.

INTERPRETATION OF THE UV SPECTRA

$\text{Co}(\text{acac})_3$

According to Barnum,⁹⁴⁻⁹⁶ the absorption with $\lambda(\text{max})$ 256nm can be ascribed to the $\pi_3-\pi_4$ ($\pi-\pi^*$) transition within the ligand, whilst the absorption at 320nm is due to a metal-ligand charge transfer. The strongest absorption in the UV region $\lambda(\text{max})$ 228nm is thought to be due to ligand-metal charge transfer (see $\text{Cu}(\text{acac})_2$).

$\text{Mn}(\text{acac})_3$

The absorption at 274nm has been attributed to

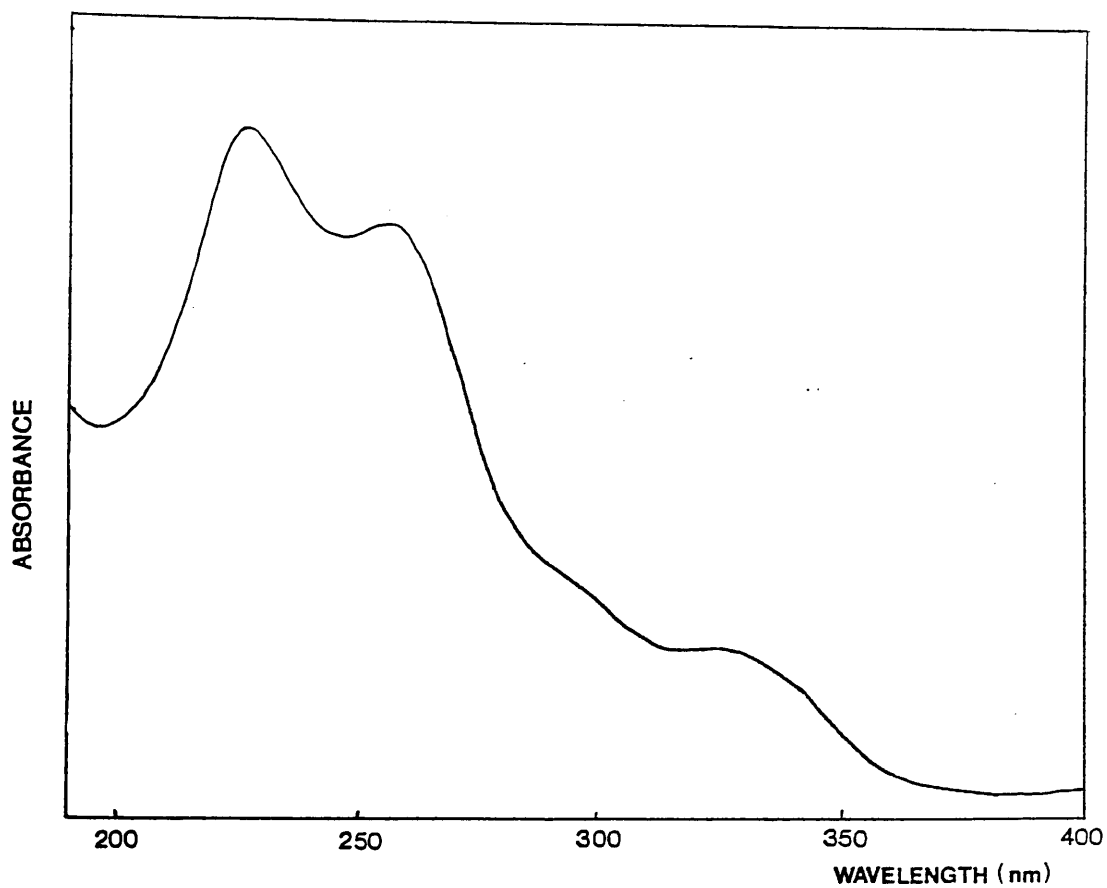


Figure 3.6 UV spectrum of $\text{Co}(\text{acac})_3$ (CH_2Cl_2 solution)

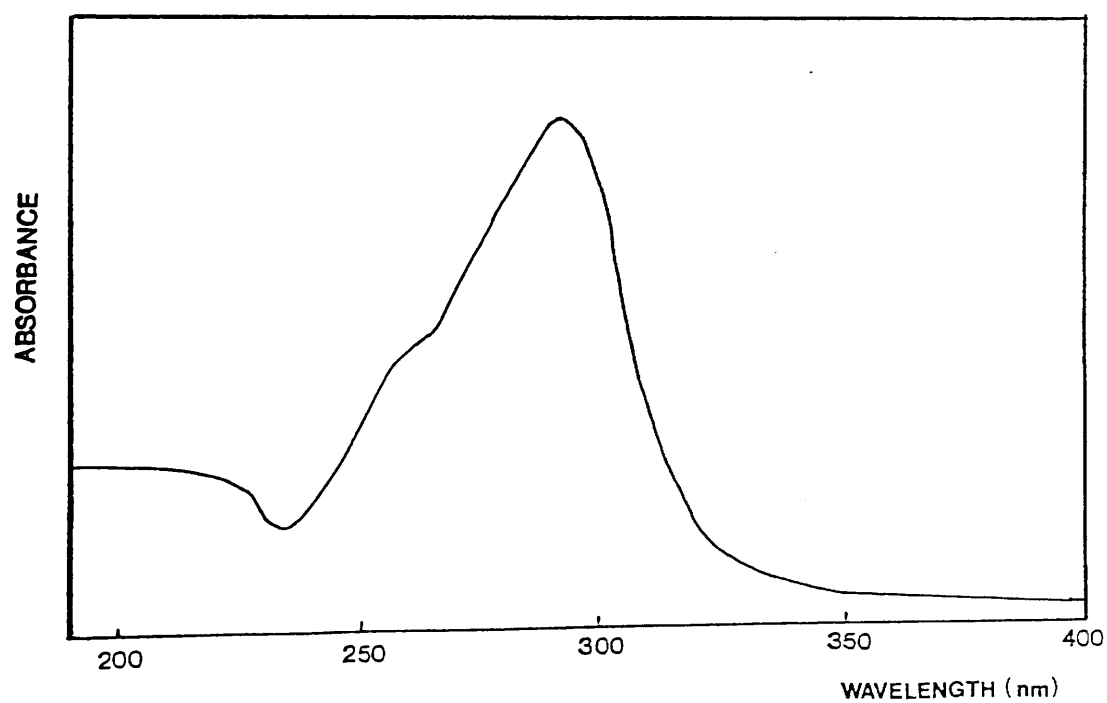


Figure 3.7 UV spectrum of $\text{Co}(\text{acac})_2$ (CH_2Cl_2 solution)

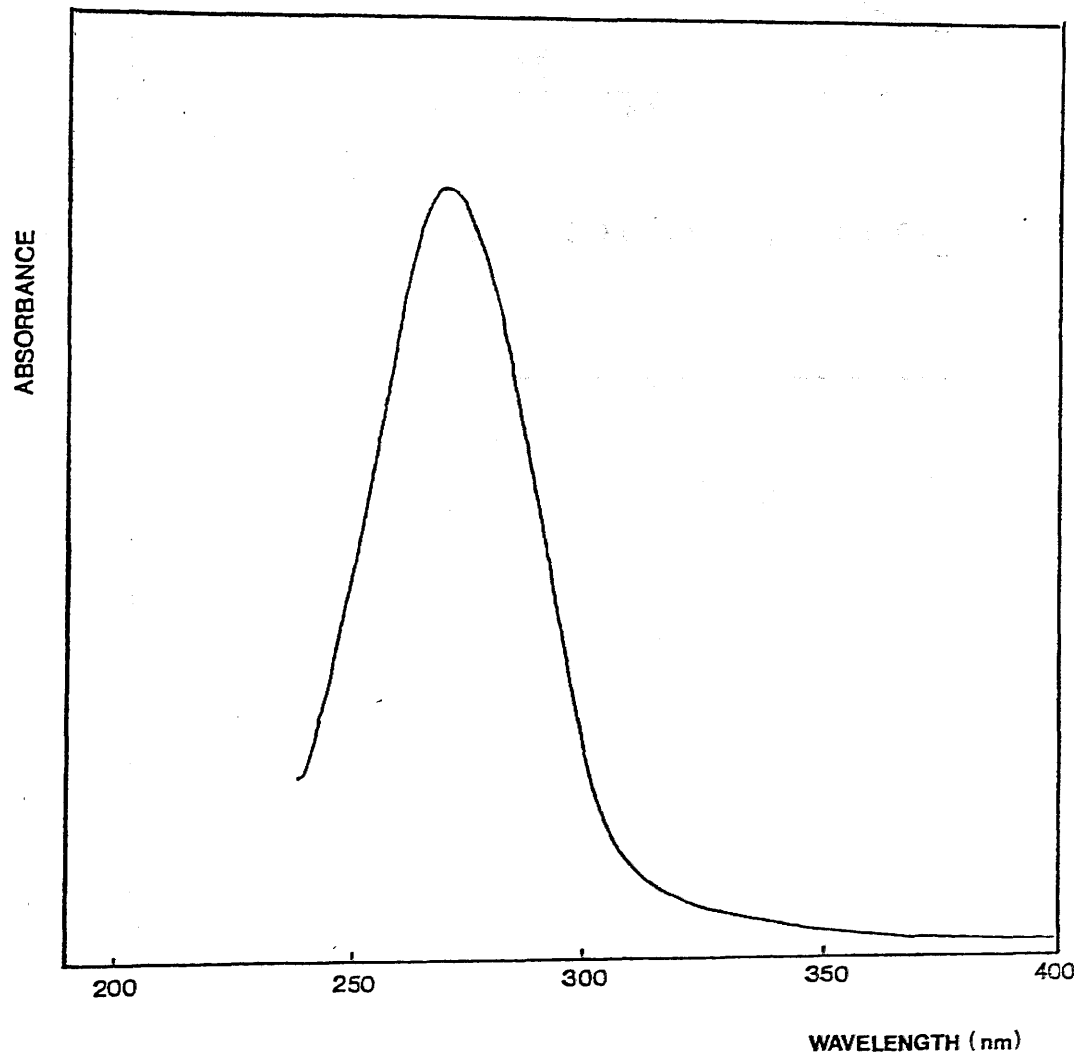


Figure 3.8 UV spectrum of Mn(acac)₃ (CHCl₃ solution)

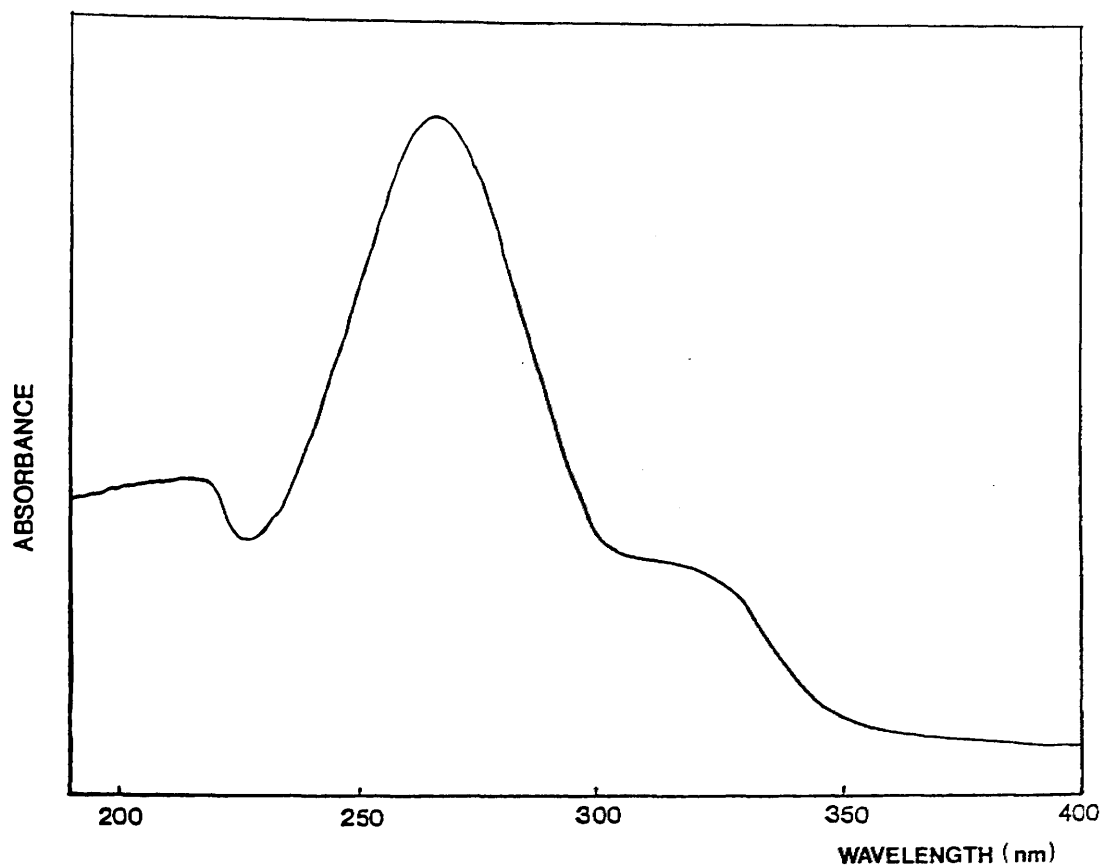


Figure 3.9 UV spectrum of Mn(acac)₂ (CH₂Cl₂ solution)

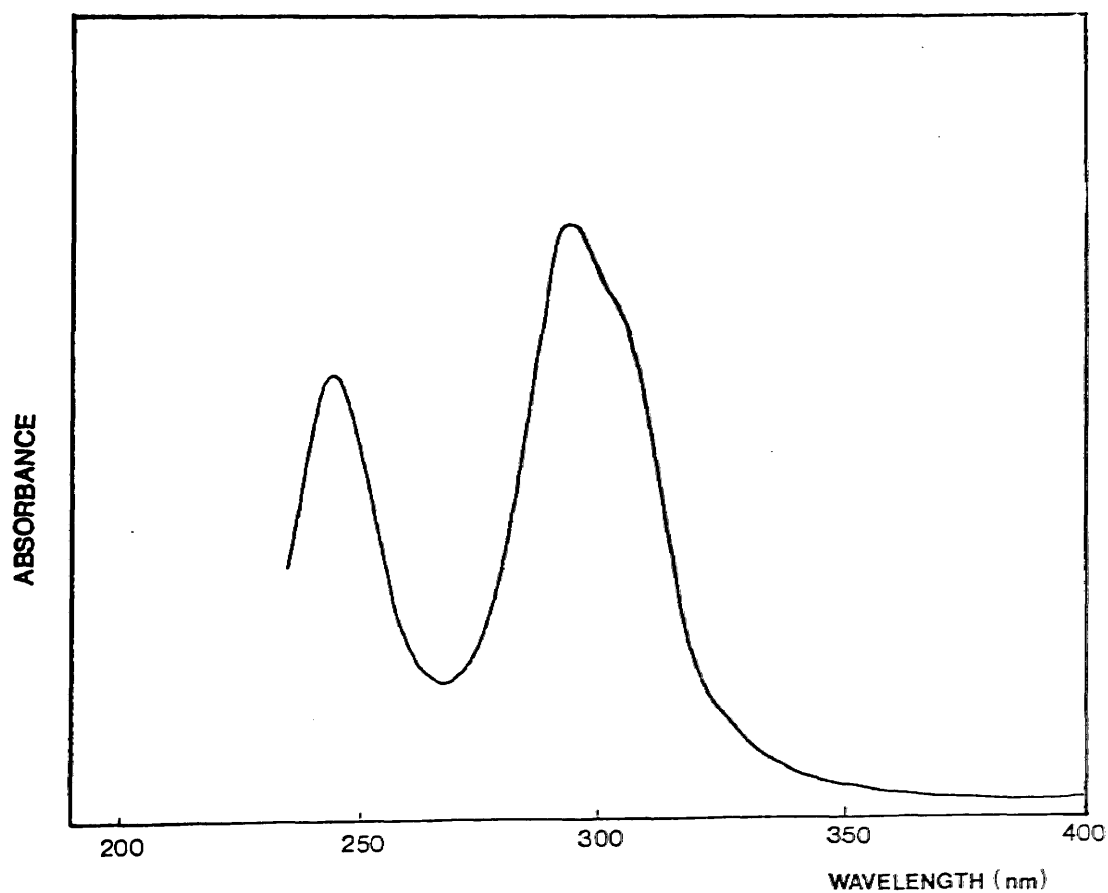


Figure 3.10 UV spectrum of Cu(acac)₂ (CHCl₃ solution)

CHELATE	OBSERVED VALUES		LITERATURE VALUES		REFERENCE	
	$\lambda(\text{max})$ nm	ϵ $\text{mol}^{-1} \text{cm}^{-1}$	$\lambda(\text{max})$ nm	ϵ $\text{mol}^{-1} \text{cm}^{-1}$		Solvent
Co(acac) ₃	258	33,200	258	34,000	CHCl ₃	92,93
	256	-----	257	34,700	CHCl ₃	94
	228	-----	227	34,000	C ₂ H ₅ OH	92
Mn(acac) ₃	274	30,000	274	24,000	CHCl ₃	92,93
			272	22,900	CHCl ₃	94
Cu(acac) ₂	296	23,600	296	24,600	CHCl ₃	92
	246	17,400	296	20,100	CHCl ₃	92
			296	26,000	CHCl ₃	95
			298	25,000	CHCl ₃	5
			245	20,100	CHCl ₃	92
Co(acac) ₂			246	15,800	CHCl ₃	95
			245	20,400	CHCl ₃	5
	291	-----	292	16,200	CHCl ₃	92
Mn(acac) ₂						
	273	-----	276	20,500	CHCl ₃	92

Table 3.1 UV Spectroscopic Data for the Acetylacetonate Chelates

the $\pi_3 - \pi_4$ transition by Barnum.⁹⁴⁻⁹⁶

Cu(acac)₂

Belford et al. assigned the λ (max) 296nm adsorption to a $\pi - \pi^*$ transition.⁹⁷ Fackler, Cotton and Barnum confirmed this interpretation, pin-pointing it as the $\pi_3 - \pi_4$ transition.⁹⁸ The band with (max) 246nm is analogous to the λ (max) 228nm absorption of Co(acac)_3 and although originally ascribed by Barnum⁹⁴ to the splitting of the transition by a configuration interaction it was later ascribed to a ligand-metal charge transfer.^{98,99} Subsequent observation of the reduction of Cu(acac)_2 on irradiating at that wavelength supports the revised interpretation.¹⁰⁰

Co(acac)₂, Mn(acac)₂

The absorptions λ (max) 291nm of Co(acac)_2 and that of Mn(acac)_2 with λ (max) 273nm are analogous to the 258nm absorption of Co(acac)_3 ⁹² and are due to the $\pi_3 - \pi_4$ transition.

UV SPECTRA OF THE CHELATES IN OTHER SOLVENTS

To provide information on the nature of the interaction between the chelates and the polymers studied here, UV spectra of the chelates were also obtained in methyl acetate, acetic acid and methyl methacrylate solution (see Figs. 3.11-3.13 and Table

3.2). These compounds serve as models for the polymer sites most likely to interact with the chelates:

1. ester substituents of PMMA and PVAc (methyl acetate)
2. acid substituents of methacrylic acid-methyl methacrylate copolymer (acetic acid)
3. unsaturated sites occurring at chain ends (methyl methacrylate).

Although the use of low molecular weight compounds to model polymer behaviour must be approached with caution, these compounds can provide a qualitative indication of possible interactions.

UV SPECTRA OF THE CHELATES IN METHYL ACETATE AND ACETIC ACID SOLUTIONS

Although the UV spectrum of $\text{Co}(\text{acac})_3$ is essentially unchanged in methyl acetate or acetic acid solutions, the spectra of the other chelates in these solvents all show some changes relative to the spectra in chloroform or methylene chloride.

In methyl acetate solution, the $\pi - \pi^*$ transition is shifted by a small degree to higher energy and in acetic acid solution the shift is if anything more pronounced.

This could be simply a polarity effect although if this were the case the transition would tend to move to lower energy, the more polar solvents stabilising the relatively polar orbitals of the ligand. Furthermore,

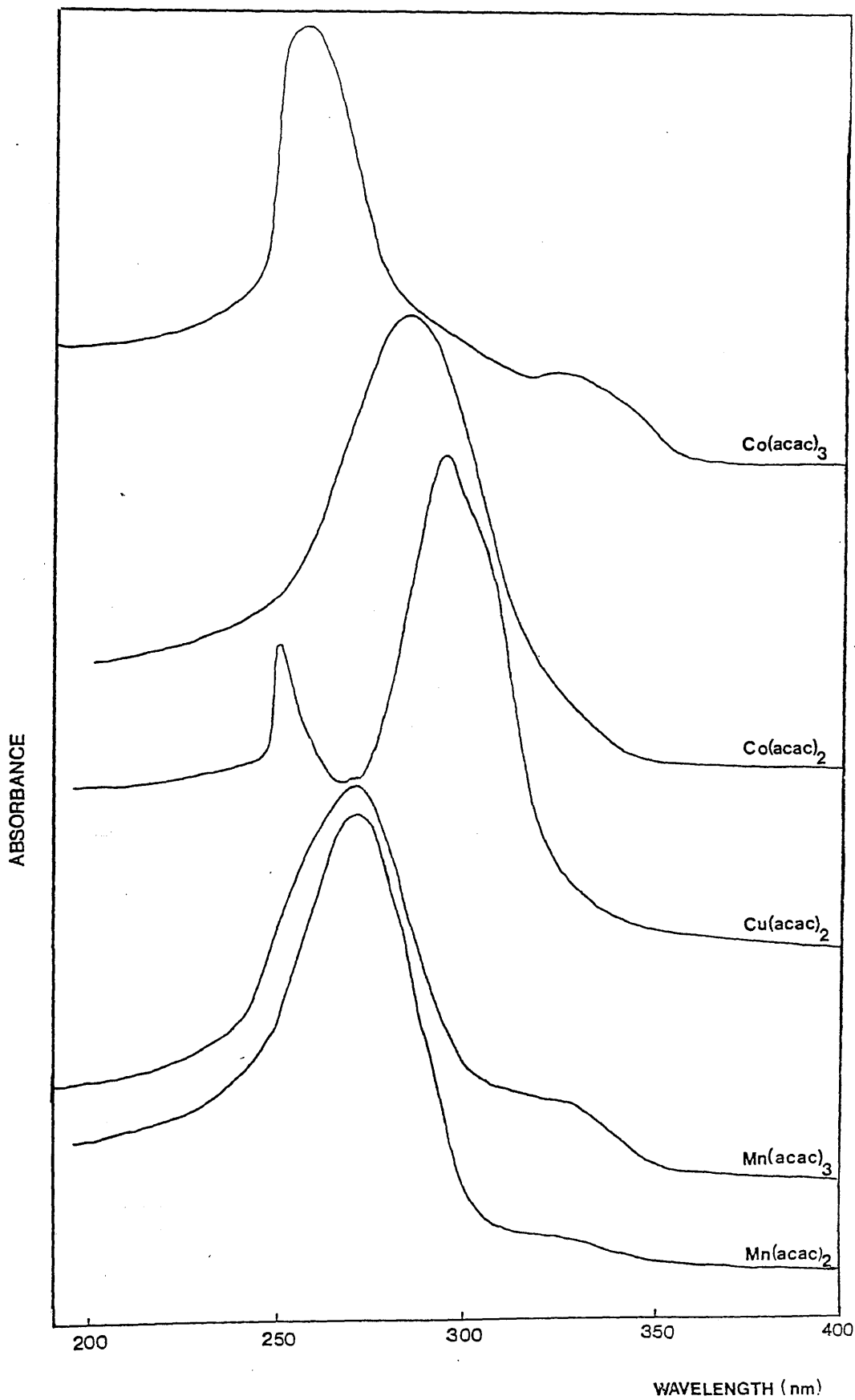


Figure 3.11
UV spectra of the chelates in methyl acetate solution

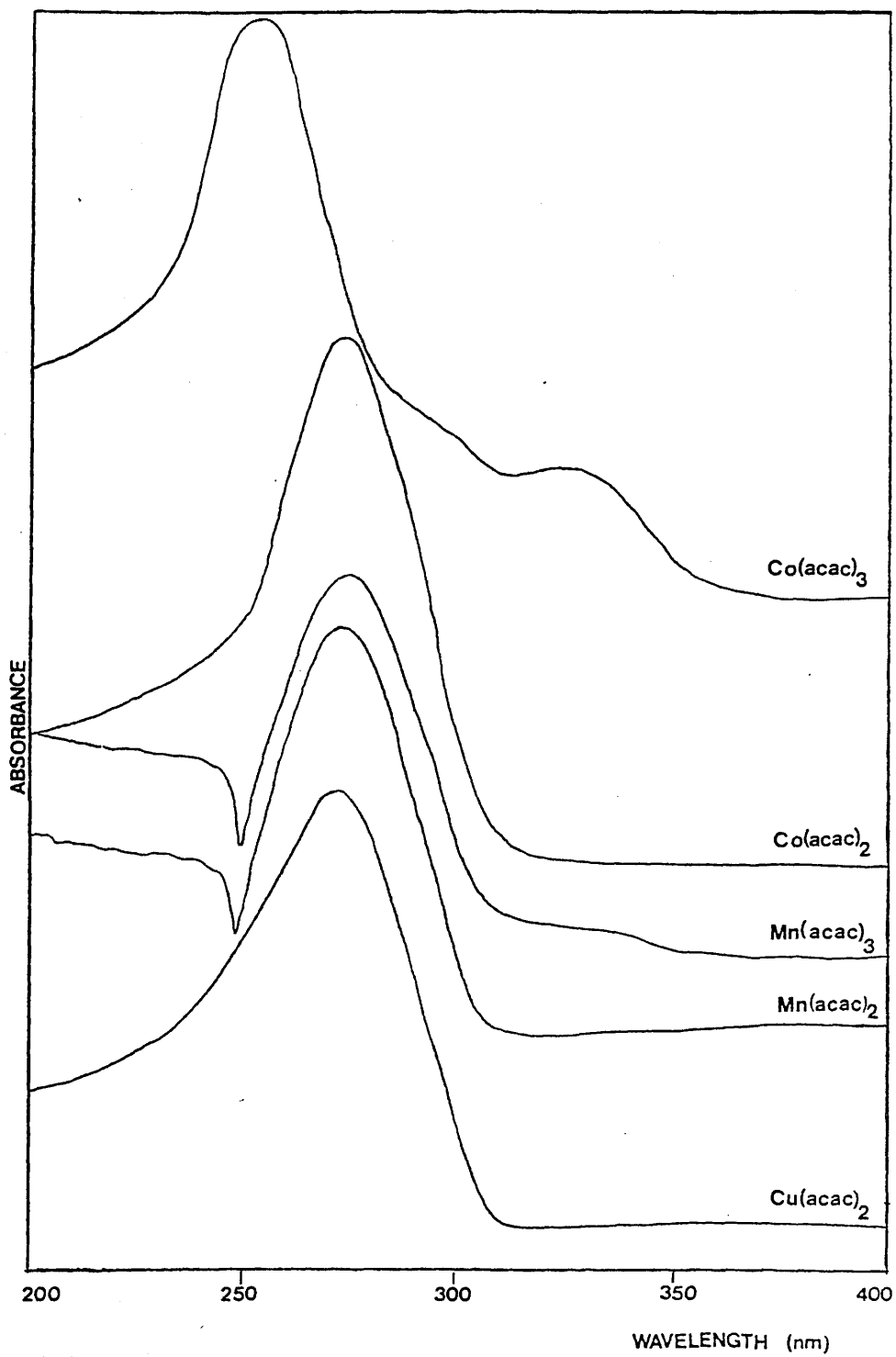


Figure 3.12

UV spectra of the chelates in acetic acid solution

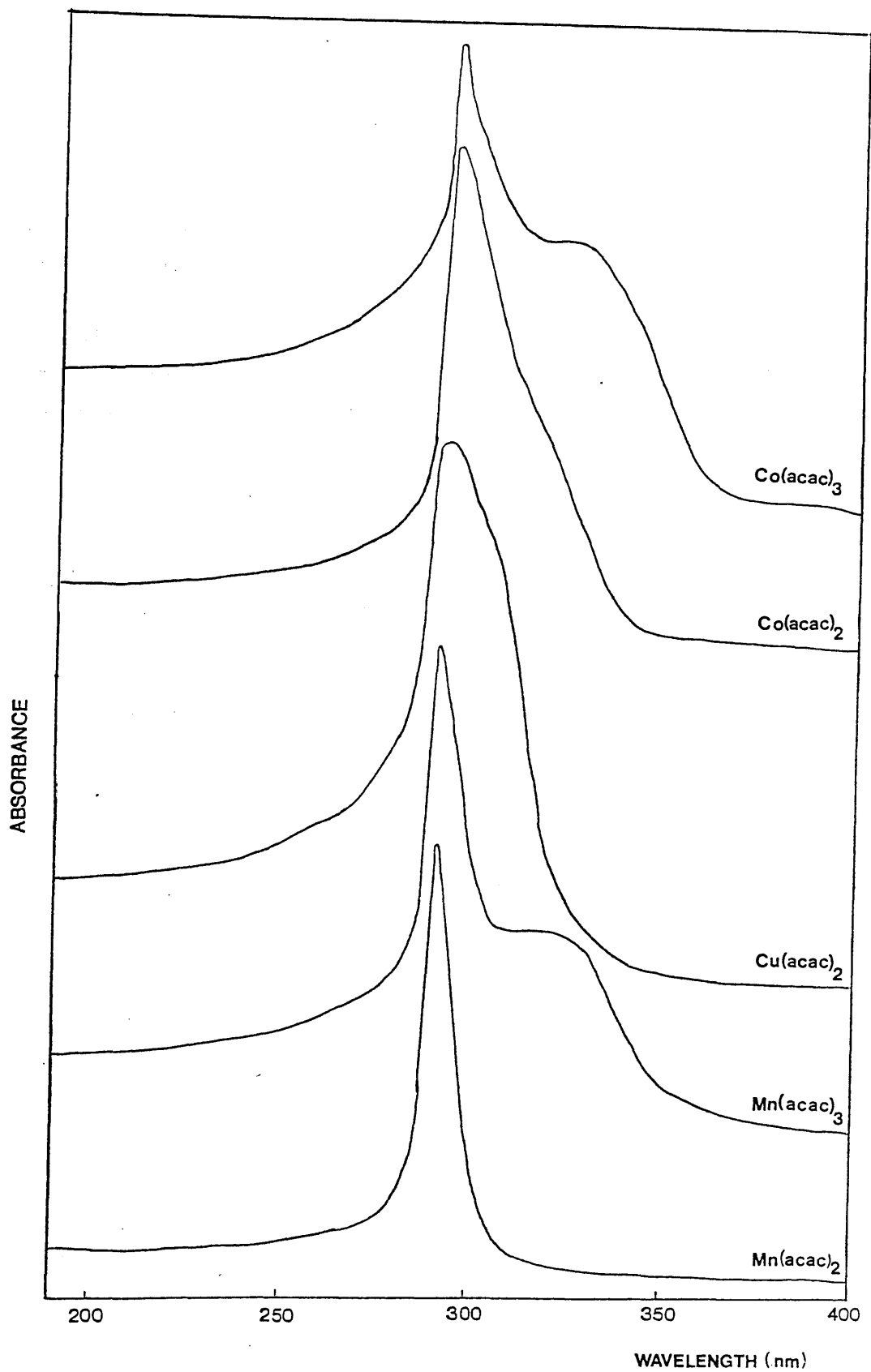


Figure 3.13 UV spectra of the chelates in methyl methacrylate solution

CHELATE	CHLOROFORM	SOLVENT		
		METHYL ACETATE $\lambda(\text{MAX})$ nm	ACETIC ACID	MMA
Co(acac) ₃	256 228 (CH ₂ Cl ₂)	257	256	293
Co(acac) ₂	291 (CH ₂ Cl ₂)	284	273	295
Mn(acac) ₃	274	270	272	290
Mn(acac) ₂	273 (CH ₂ Cl ₂)	270	272	290
Cu(acac) ₂	296 246	294 250	270	292

Table 3.2 Variation of $\lambda(\text{max})$ with solvent

the metal d -orbital and ligand p -orbital into e_g, t_{2g}, e_g with increasing d -orbital overlap. electron transfer becomes less probable and probable. As L-M bonding lowers the ligand π_g and $\pi_g \rightarrow \pi_g$ transition is thus moved to high (compare for example $\lambda(\text{max})$ Ti(acac)₃ 274nm, in ethanol or chloroform). Although it can be noted that $\lambda(\text{max})$ for i $\lambda(\text{max})$ 274nm. Thus the shift towards high observed for the Mn^{3+/2+}, Cu²⁺ and Co²⁺ can be attributed to an increase in electron density on the metal ion as a consequence of electron donation from the solvent promoting the L-M π -bonding.

such an effect influencing the ligands directly would be expected to be present for all the chelates. Rather, an association between chelate and solvent molecules is implied. Previous workers have reported^{28,30} that ethyl acetate destabilises $\text{Mn}(\text{acac})_3$ by acting as an electron donor, and the other chelates are believed to be influenced similarly, whilst $\text{Cu}(\text{acac})_2$ is reported to have acetic acid as axial ligands in acetic acid solution.¹⁰¹ The $\lambda(\text{max})$ shifts can be accounted for in terms of the effects of such interactions on the metal ligand-bonds.

Barnum's LCAO-MO calculations and subsequent work demonstrated that the $\pi - \pi^*$ transition of the acetylacetonate ligand was sensitive to the strength of the metal to ligand (M-L) and ligand to metal (L-M) metal d-orbital and ligand π -orbital interactions.^{94,96,102} With increasing 3d orbital population, M-L electron transfer becomes less probable and L-M more probable. As L-M bonding lowers the ligand π_3 orbital, the $\pi_3 - \pi_4$ transition is thus moved to higher energy (compare for example $\lambda(\text{max})$ $\text{Ti}(\text{acac})_3$ 308nm, $\text{Mn}(\text{acac})$, 274nm, in ethanol or chloroform solution, although it is to be noted that $\lambda(\text{max})$ for $\text{Fe}(\text{acac})_3$ is at 272nm). Thus the shift towards higher energy observed for the $\text{Mn}^{3+/2+}$, Cu^{2+} and Co^{2+} chelates can be attributed to an increase in electron density in the metal ion as a consequence of electron donation from the solvent promoting the L-M π -bonding. This

enhancement of the ligand to metal electron transfer in the presence of an electron-donating species increase the likelihood of reduction of the central ion with the production of an acac• radical and as discussed in Chapter 1, such behaviour is observed.

Consequently, it may be anticipated that at room temperature the Co^{2+} , $\text{Mn}^{2+/3+}$ and Cu^{2+} chelates may interact with the ester and acid side groups of PMMA and the MAA-MMA copolymer, interactions which would ultimately destabilise the chelate. Although there is no evidence for interaction with $\text{Co}(\text{acac})_3$ at room temperature, the literature evidence presented in Chapter 1 suggests that interaction with ester groups is also expected for this chelate at higher temperature.

acetylacetonate ligand can in fact be displaced as described later.

The acetate anion has been found to bind to the metal ion in the mixed complex of cobalt(II) and acetic acid and methyl acetate is suggested as acting similarly. Indeed, McLaughlin suggested⁶³ that the ester side groups of the polymer can act as bidentate ligands in competition with the polymer. However, it has been shown that acetylacetonate chelates do not interact with the

STRUCTURE OF THE METHYL ACETATE AND ACETIC ACID COMPLEXES OF THE CHELATES

For the bis chelates with vacant coordination sites it is easy to envisage the solvent molecules coordinating at these vacant positions. Thus acetic acid and methyl acetate could coordinate at the vacant axial positions of $\text{Co}(\text{acac})_2$ and $\text{Mn}(\text{acac})_2$ to give a six coordinated species. Mono and bis coordination of acetic acid at the axial sites of $\text{Cu}(\text{acac})_2$ has already been reported.¹⁰¹

With the tris chelates as noted in Chapter 1, coordination of the solvents requires displacement of an acetylacetonate ligand. Such displacement does not occur at room temperature for $\text{Co}(\text{acac})_3$ and so there is no shift in $\lambda(\text{max})$. $\text{Mn}(\text{acac})_3$, however, undergoes facile ligand displacement for reasons not fully understood and so the solvent molecules can coordinate to the chelate. (Under the correct conditions the acetylacetonate ligand can in fact be completely displaced as described later.)

The acetate anion has been found to act as a bidentate ligand in the mixed complex $\text{Mn}(\text{acac})_2(\text{OOCCH}_3)$ ³¹ and acetic acid and methyl acetate can be envisaged as acting similarly. Indeed, McNeill and McGuinness suggested⁶³ that the ester side chains of PMMA act as bidentate ligands in 1:1 blends of ZnBr_2 with the polymer. However in the case of the acetylacetonate chelates it is more likely that acetic

acid and methyl acetate will behave as monodentate ligands through the carbonyl group. This would more readily preserve the tendency of $\text{Co}(\text{acac})_2$ and $\text{Mn}(\text{acac})_2$ to form (pseudo)octahedral structures and similarly maintain the preferred geometry of $\text{Cu}(\text{acac})_2$ adducts. Adducts of $\text{Co}(\text{acac})_2$ with a monodentate carbonyl ligand have been observed previously.¹⁰³

... the... the metal-ligand bond...
 ... with a... complex with...
 ... in accord with the observed...
 ... 37-38 an...
 ... in Chapter 4.

... interactions occur with other...
 ... other... and acacetic...
 ... of $\text{Co}(\text{acac})_2$...
 ... similar...
 ... acidic...
 ... could be ex...
 ... complexes and...
 ... As well...
 ...

82

UV SPECTRA OF THE CHELATES IN METHYL METHACRYLATE SOLUTION

In methyl methacrylate solution, the spectra of the chelates are quite unlike those recorded for the chloroform, methylene chloride, acetic acid and methyl acetate solutions discussed above. The spectra of all the chelates are very similar, showing a very sharp absorption band around 290nm. This similarity, contrasting with the behaviour in methyl acetate and acetic acid solution, suggests that methyl methacrylate influences the $\pi-\pi^*$ absorption of the ligand directly rather than only via the metal-ligand bonds. Thus the chelates must form a π -type complex with methyl methacrylate in accord with the observations and conclusions of Nandi and co-workers³⁷⁻³⁹ and Sahu⁴⁰ as discussed in Chapter 1.

Such interactions occur with other π systems such as other vinylic monomers and aromatic systems. For example, the UV spectrum of $\text{Co}(\text{acac})_3$ in toluene solution is reproduced in Fig 3.14 and is similar to the spectrum of the methyl methacrylate solution of the chelate. Hence, such a complex could be expected to form between these chelate compounds and any unsaturated sites within a polymer matrix. As small molecule π -type complexes promote ligand scission (see Chapter 1) it is to be anticipated that chelate polymer complexes would likewise destabilise the chelate and, as discussed subsequently, such effects are observed.

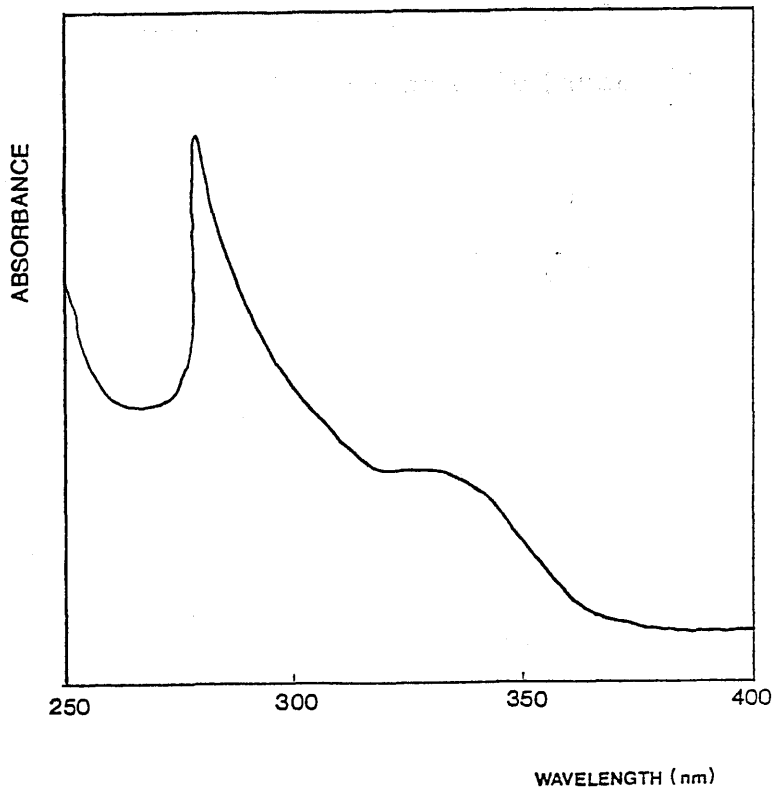


Figure 3.14
UV spectrum of $\text{Co}(\text{acac})_3$ in toluene solution

04

REACTIONS OF $Mn(acac)_3$ WITH ACETIC ACID AND METHYL ACETATE

As will be discussed subsequently, the UV spectra of the blends of $Mn(acac)_3$ with PMMA and with the methacrylic acid-methyl methacrylate copolymer showed features which could not be explained in terms of the spectra described above. It was thus decided to attempt to synthesise the mixed chelate $Mn(acac)_2(OOCCH_3)$ and obtain its UV and IR spectra for comparison purposes. As PMMA contains only ester groups, the reaction of $Mn(acac)_3$ with methyl acetate was also investigated.

REACTION OF $Mn(acac)_3$ WITH ACETIC ACID

Following Nikolaev et al.,³¹⁻³⁴ $Mn(acac)_3$ (3.70g 10.5 mmole) and acetic acid (0.66g, 11.1 mmole) were dissolved in 50ml of methylene chloride and allowed to stand overnight. The brown precipitate which formed was filtered off and washed with methylene chloride. The product was recrystallised from methanol and washed with methylene chloride to yield 0.46g.

The IR spectrum (KBr disc) and UV spectrum (methanol solution) were recorded and are reproduced in Figs 3.15 (curve A) and 3.16. The IR spectrum has a strong carboxylate absorbance at 1600cm^{-1} in addition to other 'acac-type' absorbances. The UV spectrum is broad and unstructured and considerably different from the spectra of $Mn(acac)_3$ or $Mn(acac)_2$ in acetic acid

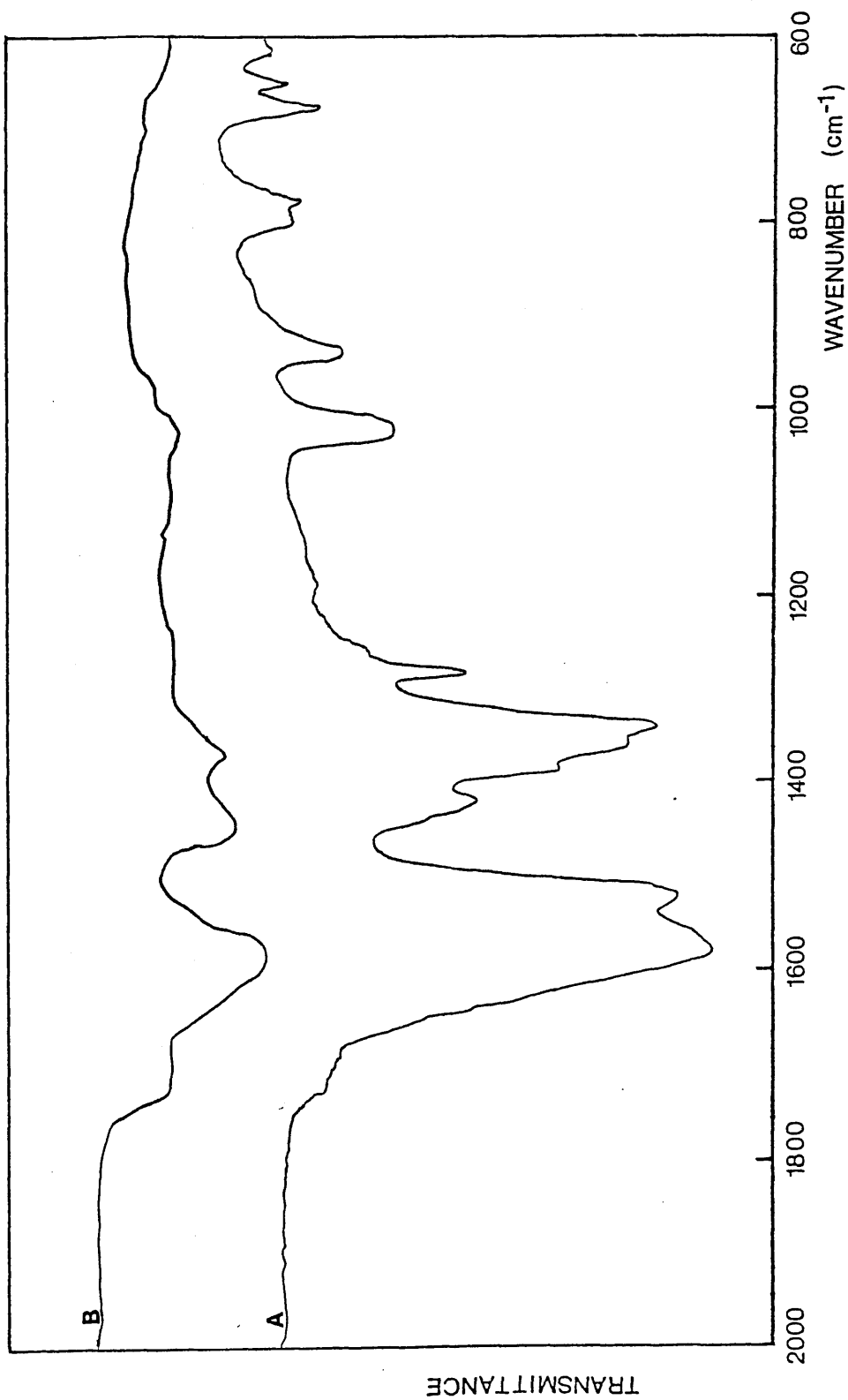


Figure 3.15 IR spectrum of product from reaction of $\text{Mn}(\text{acac})_3$ with acetic acid (curve A), and its decomposition product (curve B)

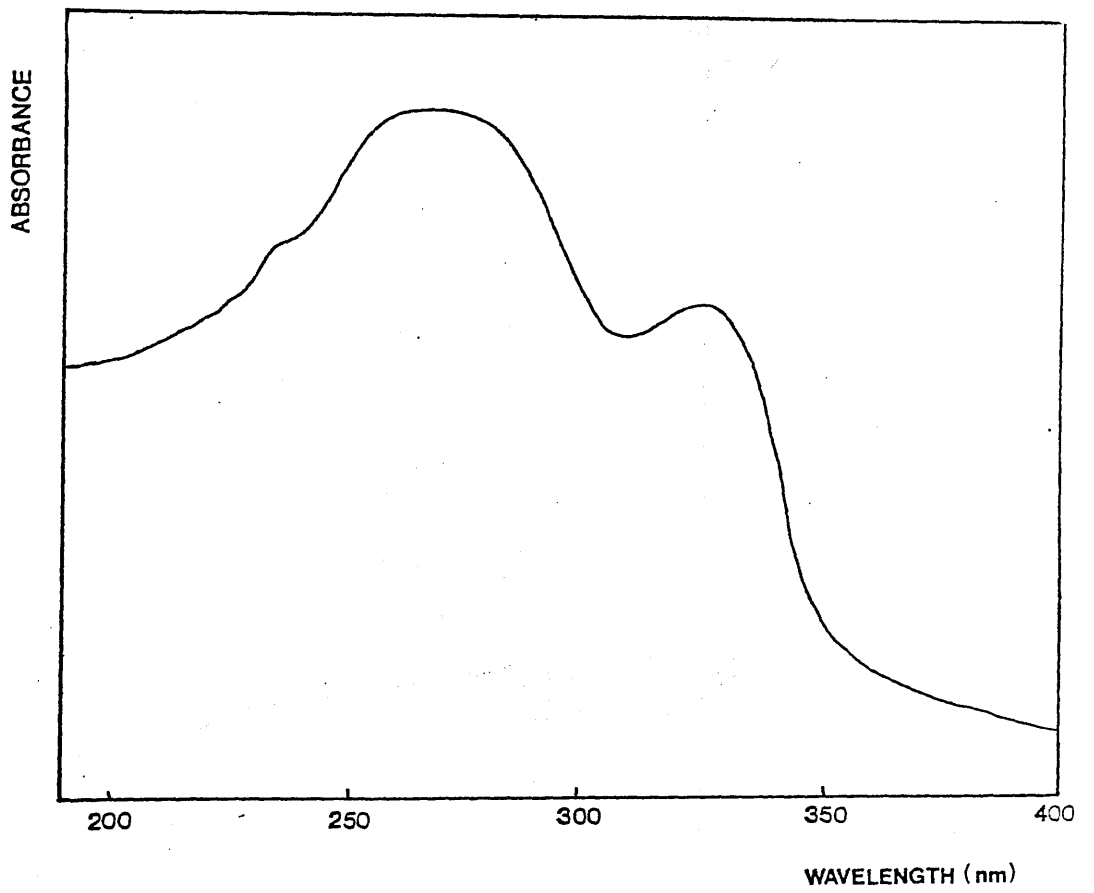


Figure 3.17 UV spectrum of product from reaction of $\text{Mn}(\text{acac})_3$ with methyl acetate

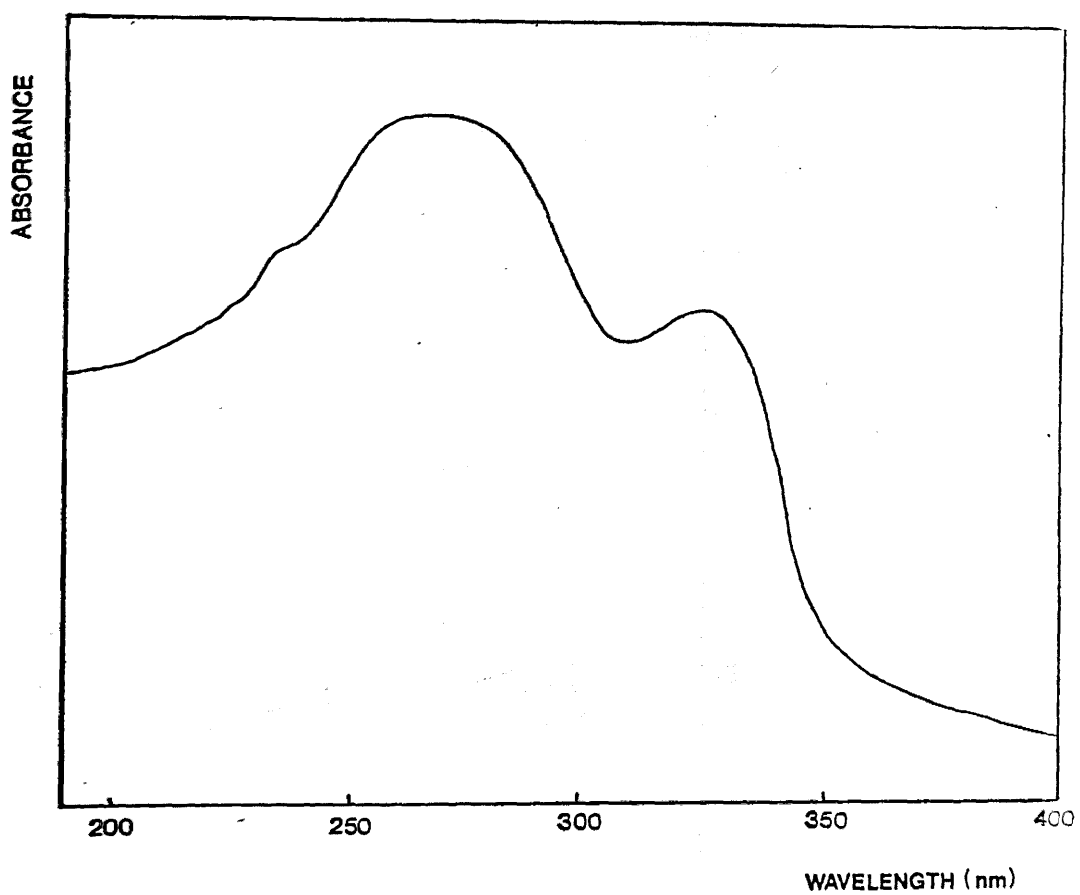


Figure 3.17 UV spectrum of product from reaction of $\text{Mn}(\text{acac})_3$ with methyl acetate

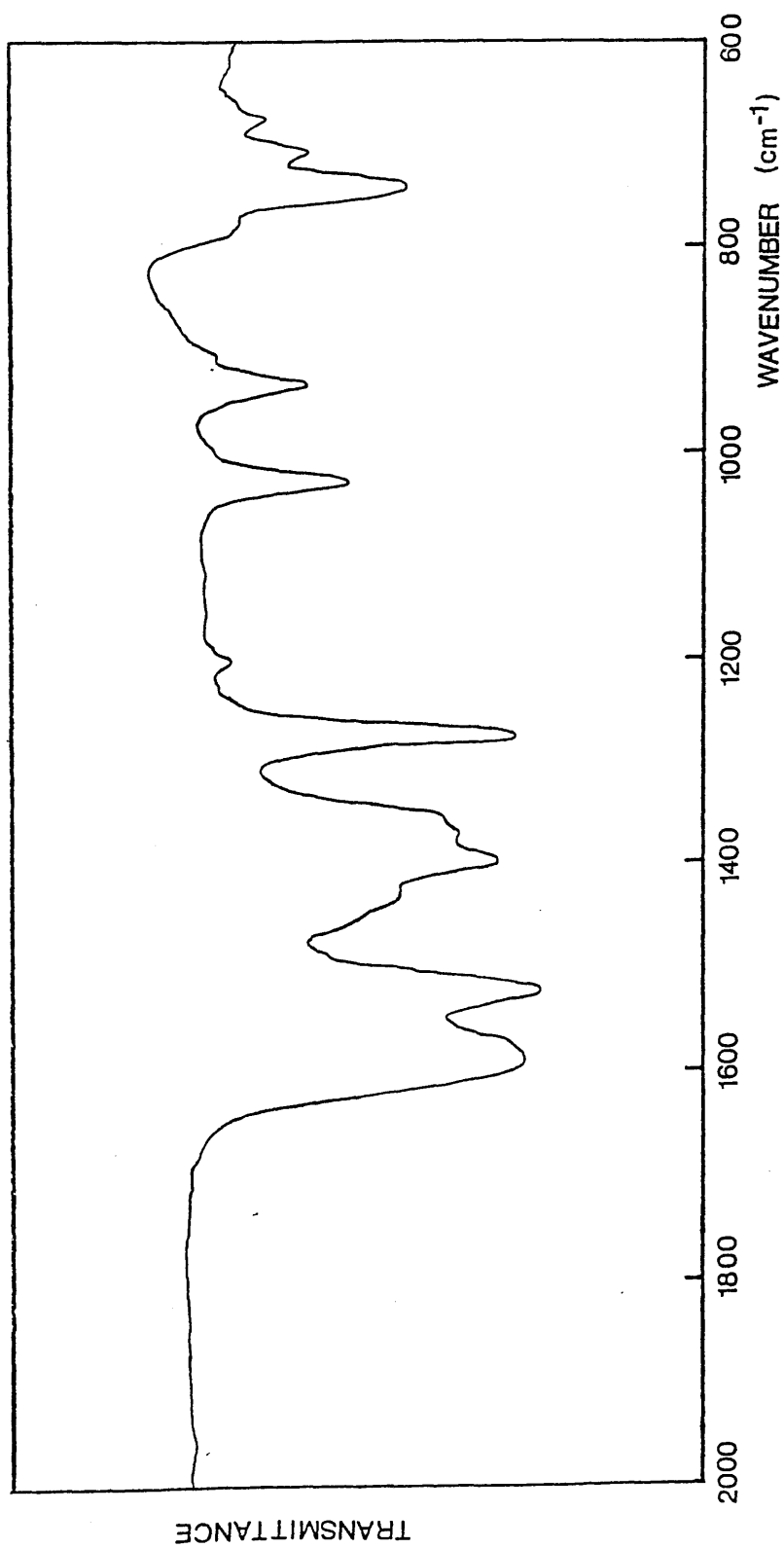


Figure 3.18 IR spectrum of product from reaction of $Mn(acac)_3$ with methyl acetate

changes relative to that of $\text{Mn}(\text{acac})_3$, with considerable broadening of the major peak to give a spectrum intermediate in character between the $\text{Mn}(\text{acac})_3$ and " $\text{Mn}(\text{acac})_2 (\text{OOCCH}_3)$ " spectra.

In the presence of acetic acid ligand substitution by the acetate anion is possible but ligand substitution in a similar manner by the methyl acetate would require the scission of the ester C-O bond which is unlikely at room temperature (in the PMMA - chelate blends carboxylate structures are formed by reaction with esters at higher temperatures). Thus, the compound isolated here is merely a solvate, albeit one in which the methyl acetate has partially displaced a ligand.

Co(acac)₃ AND Cu(acac)₂ PLUS ACETIC ACID

Under similar conditions to those outlined above no reaction between acetic acid and either Co(acac)₃ or Cu(acac)₂ was observed. In both cases the chelate was recovered unaltered.

REACTIONS OF THE CHELATES WITH METHYL ACETATE AND ACETIC ACID - CONCLUSIONS

The unusual lability of Mn(acac)₃ to ligand substitution is not well understood.³⁶ Whatever the reason, the effect is that Mn(acac)₃, unlike Co(acac)₃ and Cu(acac)₂, reacts at room temperature to form a mixed chelate with acetic acid. This variation in the stability of the chelate is reflected in the step-wise formation constants of the acetate and acetylacetonate complexes with the metal ions listed in Table 3.3. Whereas acetate displaces acetylacetonate from Mn(acac)₃, the reverse situation occurs with Cu²⁺¹⁰¹ and thus the lack of a reaction between Cu(acac)₂ and acetic acid is not unexpected although association, with acetic acid behaving as an electron donor, does occur.

The reason why there is no reaction between Mn(acac)₃ and neat acetic acid or methyl acetate is unclear but may be related to the stabilities of the mixed chelates in the neat solution. Comparison can be made with the mixed chelate Cu(acac)(OOCCH₃) which is reported to be stable in methanol but not stable enough

to exist in acetic acid.¹⁰¹

ION	LIGAND					
	ACETATE			ACETYLACETONATE		
	K ₁	K ₂	K ₃	K ₁	K ₂	K ₃
Co ²⁺	1.36			5.58	4.34	
Mn ²⁺	1.2			4.24	3.11	
Mn ³⁺						3.86
Cu ²⁺	2.16	1.04		8.31	6.85	

$$K_n = \frac{[Me^{n+} L_n]}{[Me^{(n-1)+} L_{(n-1)}][L]}$$

Table 3.3 Formation Constants for Acetate and Acetylacetonate Complexes.

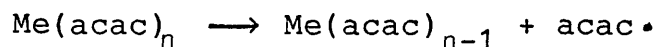
(From data in Ref 104. All values for 25°C and extrapolated to zero ionic strength.)

THERMAL DECOMPOSITION OF THE CHELATESCo(acac)₃LITERATURE REPORTS

In a study of the thermal degradation of several acetylacetonate complexes, Charles et al. found Co(acac)₃ to be one of the least stable of those investigated.¹⁰⁵ In a series of sealed tube experiments with the sample sealed under vacuum and heated isothermally for four hours, Co(acac)₃ was found to decompose above 150°C, yielding acetone and carbon dioxide as the major products. In this and a subsequent paper,¹⁰⁶ the authors concluded that the most probable route for the formation of the observed products is the loss from the chelate of acetylacetone which itself subsequently decomposes to give the observed products. An alternative mechanism involving the formation of cobalt acetate was considered but the behaviour of Mn(acac)₃ (discussed below) and the product distribution from some other chelates support the former interpretation.

As discussed in Chapter 1, work by Arnett et al.²²⁻²⁴ on the autoxidation of acetylacetonate chelates and by various workers^{26-30,37-40} on the use of the chelates as polymerisation initiators reinforced the theory that the initial step of the decomposition of

the chelates (particularly the tris chelates) was the loss of a ligand:-



Loss of acetylacetone from the chelate in the bulk phase was confirmed by Yoshida et al.¹⁰⁷ in their DTA study of several β -diketonate chelates.

The DTA curve for $\text{Co}(\text{acac})_3$ heated at 10°min^{-1} under nitrogen displayed an irreversible (i.e. not a phase transition) endotherm ($T(\text{max}) 220^\circ$) with a small shoulder to higher temperature. The residue produced on heating to the $T(\text{max})$ of the endotherm was similar in appearance to $\text{Co}(\text{acac})_2$ whilst the evolution of acetylacetone at this stage was confirmed by gas-liquid chromatography.

The authors concluded that these, and similar results obtained for $\text{Mn}(\text{acac})_3$ (discussed below) could be interpreted in terms of the homolytic scission of the metal-oxygen bond releasing the acac radical and producing the bis chelate. This endothermic process would account for the observed endotherm at $T(\text{max}) 220^\circ\text{C}$. Regeneration of the free ligand by H-abstraction or disproportionation would be expected to be exothermic and although an exotherm closely subsequent to the endotherm is observed for $\text{Mn}(\text{acac})_3$, this is not observed for $\text{Co}(\text{acac})_3$. This the authors attributed to the possible overlap of the endotherm-exotherm pair in this instance. The small endothermic shoulder to the main endotherm the authors

ascribe to the decomposition of the newly formed $\text{Co}(\text{acac})_2$ which is unstable at this temperature (see section on the decomposition of $\text{Co}(\text{acac})_2$).

Using the novel technique of Organic Particulate Analysis, Smith et al.¹⁰⁸ observed the onset of decomposition of $\text{Co}(\text{acac})_3$ at 150°C , under a flow of hydrogen at atmospheric pressure and at heating rate of 6°C min^{-1} . Acetylacetone was the only product detected by mass spectrometry.

Whilst Charles et al.¹⁰⁵ and Smith et al.¹⁰⁸ pinpoint the onset of decomposition as approximately 150°C , Yoshida et al.¹⁰⁷ report the onset as about 200°C . This discrepancy reflects the very great difficulties in correlating directly the results from different thermoanalytical methods.

THIS WORK

DTA AND TG-DTG OF $\text{Co}(\text{acac})_3$ UNDER NITROGEN

The DTA curve for $\text{Co}(\text{acac})_3$ obtained under similar conditions to those of Yoshida et al.¹⁰⁷ (ie $10^\circ\text{C min}^{-1}$ under nitrogen) is virtually identical to that obtained by these workers and is shown in Fig. 3.19. The shoulder to the major endotherm is not very pronounced but is nevertheless visible.

The TG-DTG curves obtained under similar conditions to the DTA curve show (Fig. 3.20) a large

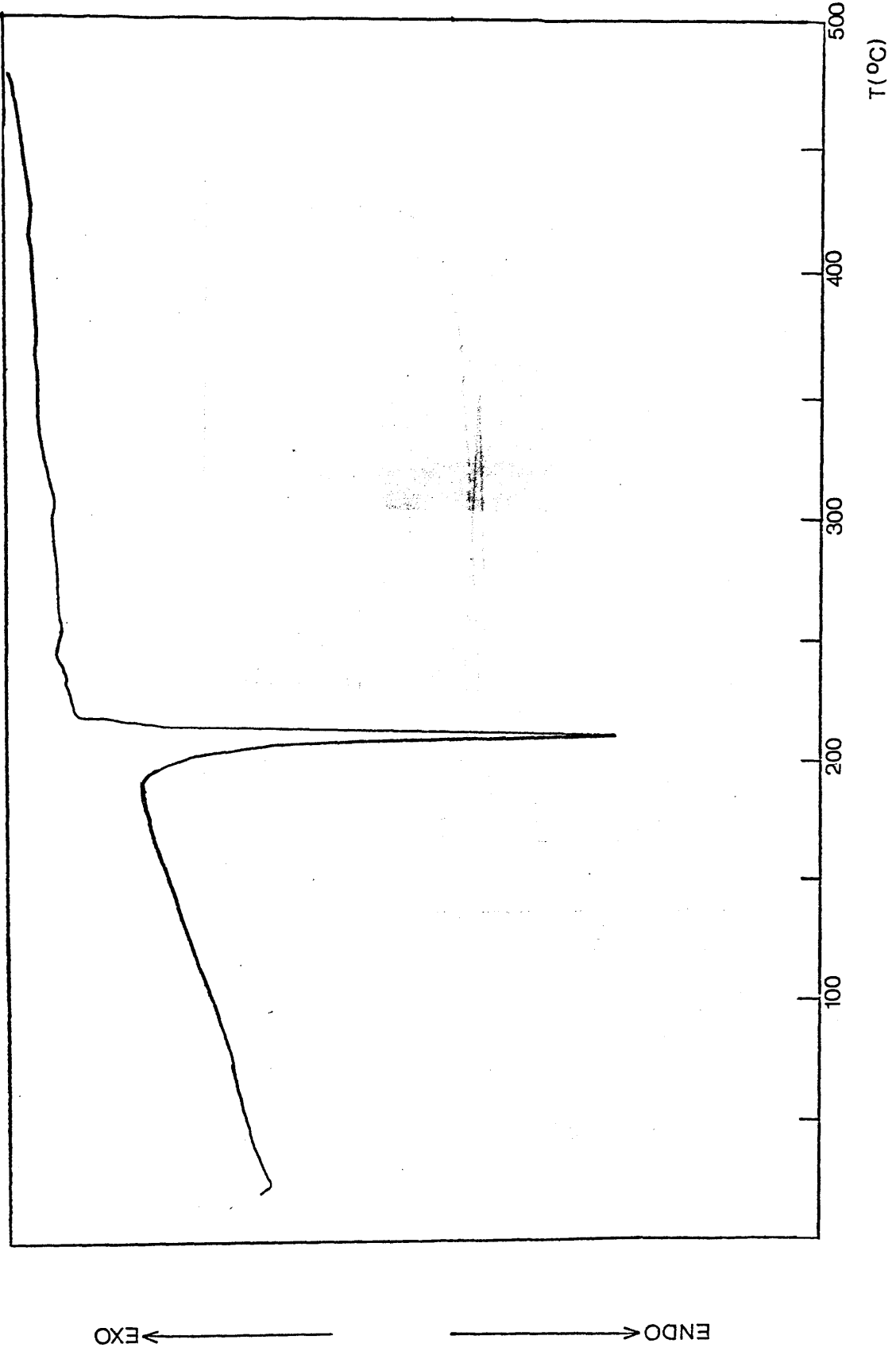


Figure 3.19 DTA curve for $\text{Co}(\text{acac})_3$ (N_2 atmosphere)

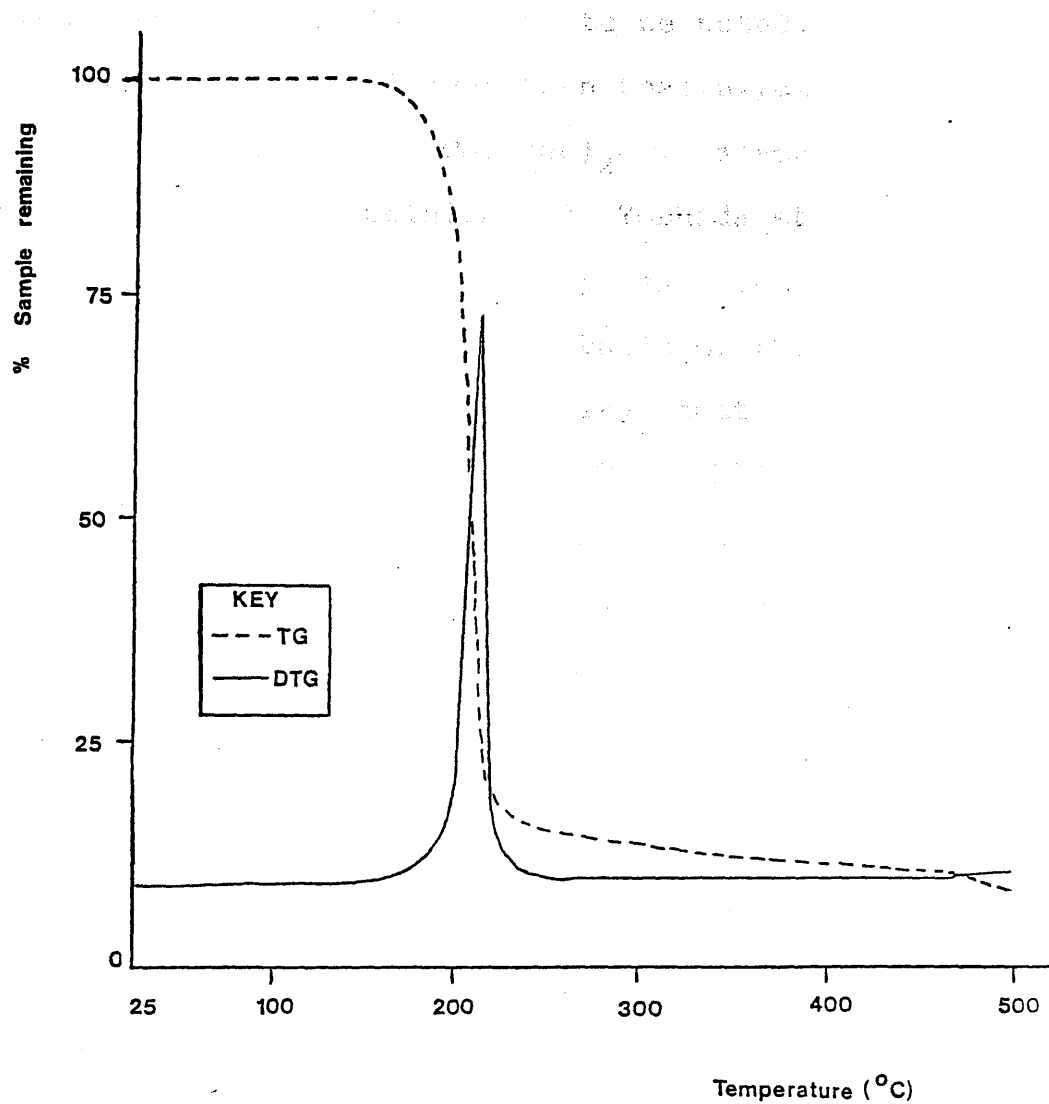


Figure 3.20 TG-DTG curves for $\text{Co}(\text{acac})_3$ (N_2 atmosphere)

initial single step weight loss (T(onset) 145°C, T(max) 221°C) which corresponds to the endotherm of the DTA curve (T(onset) 190°C, T(max) 210°C). The difference in degradation temperatures as measured by different techniques is again to be noted. The weight loss (80-85%) is much larger than that expected for the reduction $\text{Co}(\text{acac})_3 \rightarrow \text{Co}(\text{acac})_2 + \text{acacH}$. This is consistent with the opinion of Yoshida et al,¹⁰⁷ that the $\text{Co}(\text{acac})_2$ produced decomposes on formation. However, it is impossible on the basis of the TG results alone to exclude the possibility that material is subliming from the balance pan. The sublimate could be $\text{Co}(\text{acac})_3$ or $\text{Co}(\text{acac})_2$ or both. Results discussed below confirm that sublimation does indeed take place alongside the decomposition reactions.

DTA AND TG-DTG OF $\text{Co}(\text{acac})_3$ UNDER AIR

Degradations of $\text{Co}(\text{acac})_3$ under an atmosphere of air were performed for purposes of comparison with the results obtained under nitrogen. Curves are reproduced in Figs 3.21, 3.22.

The DTA curve is little changed. The major endotherm is essentially the same, including the small shoulder (T(onset) 190°C, T(max) 207°C, shoulder 215°C). There is however a broad exotherm just beyond the endotherm, not present under nitrogen. Similarly the TG-DTG curves show minor changes with the weight loss of the initial step reduced by ca. 10%, with an

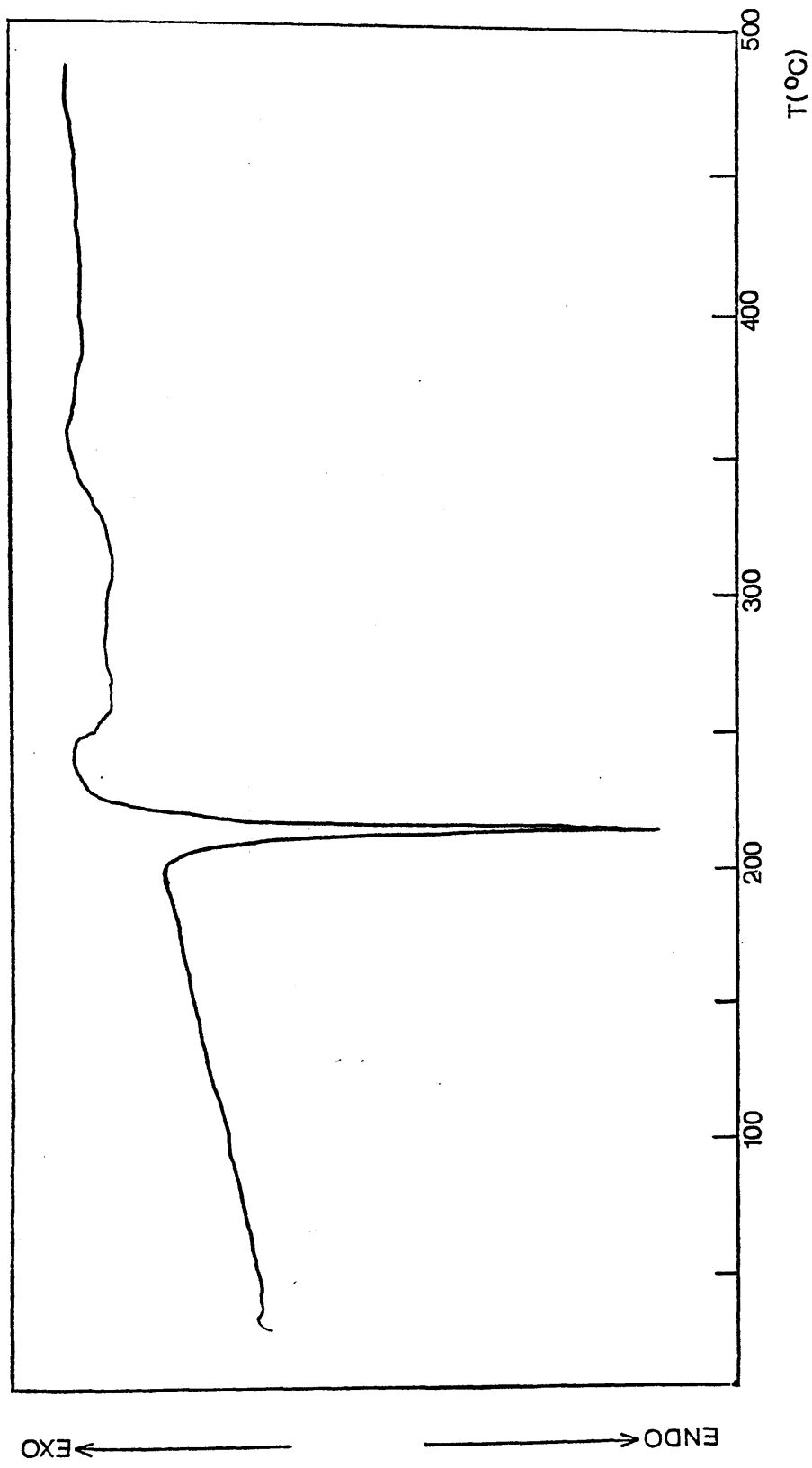


Figure 3.21 DTA curve for $\text{Co}(\text{acac})_3$ (air)

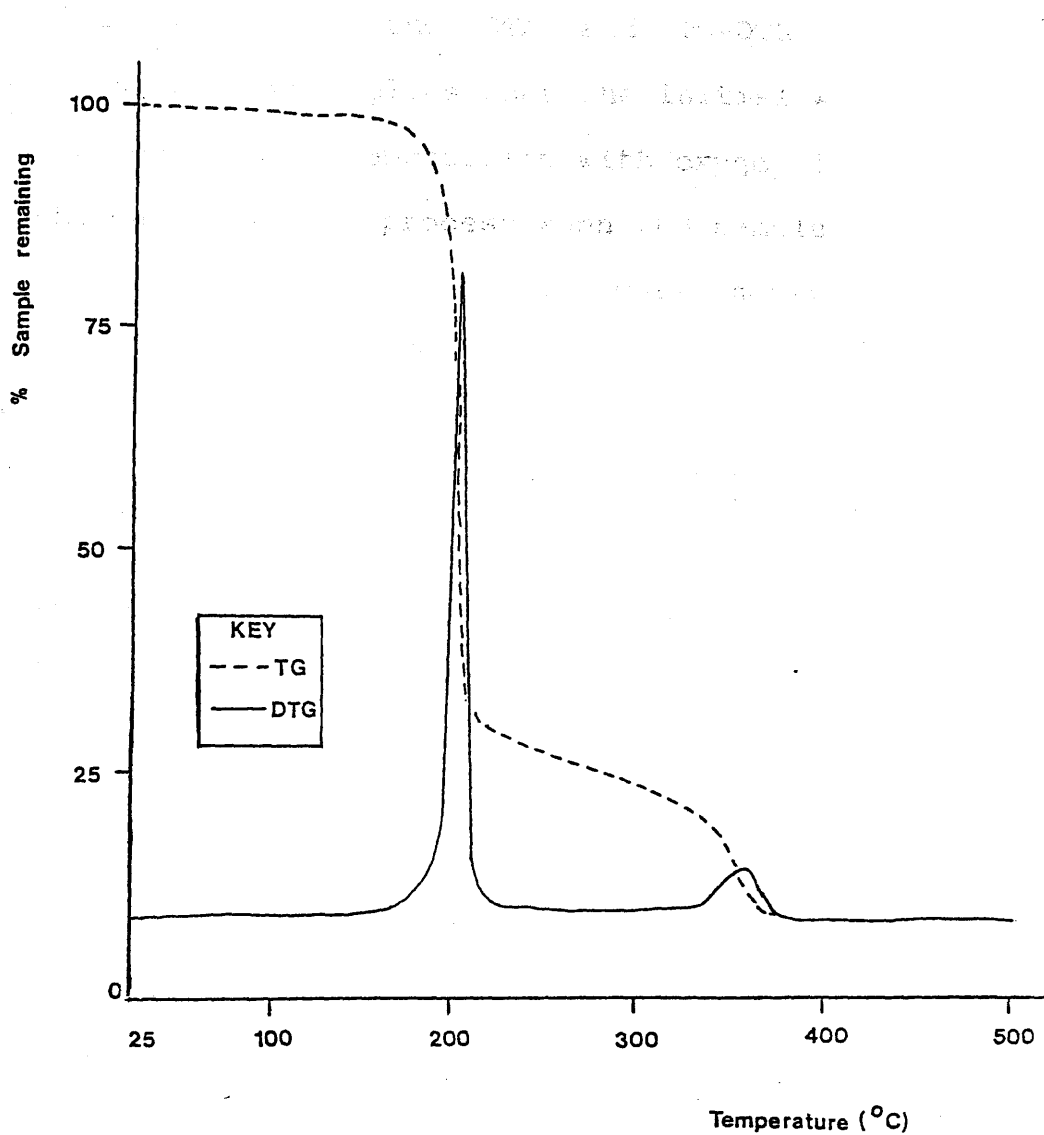


Figure 3.22 TG-DTG curves for $\text{Co}(\text{acac})_3$ (air)

additional weight loss around 350°C . $T(\text{onset})$ and $T(\text{max})$ of the initial weight loss (150°C and 212°C respectively) are little changed from those for the degradation under nitrogen.

The change in the DTA and TG-DTG curves on changing atmosphere implies that the initial weight loss does include some decomposition with oxygen interfering with the decomposition process when the sample is heated under air. Sublimation also occurs however. Its observation is described below.

DEGRADATION OF $\text{Co}(\text{acac})_3$ IN AN OPEN TVA TUBE

For this degradation, a 100mg sample of $\text{Co}(\text{acac})_3$ was placed in a TVA tube which was then inserted in a TVA oven as normal but without any connection to the remainder of the TVA system. The sample was then heated at $10^{\circ}\text{C min}^{-1}$ whilst the tube was watched for the evolution of volatile material.

Fumes were first observed at 137°C and rapidly became quite dense, peaking around 200°C . By 320°C there was no further visible indication of the production of volatile material. Some of the material condensed onto the cold ring zone and was identified as $\text{Co}(\text{acac})_3$ by UV spectroscopy. It would have been helpful to quantify the amount of sublimation, but the nature of the experiment meant that the bulk of the sublimate could not be collected. The distinctive odour of acetylacetone was noted at an early stage, indicating

that decomposition was also occurring.

TVA BEHAVIOUR OF Co(acac)₃

The TVA curve for a 60mg sample of Co(acac)₃ is reproduced in Fig 3.23 and shows an initial production of volatile material (T(onset) 80°C, T(max) 140°C) followed by a slow increase in volatile production before a more pronounced evolution of material (T(max) 388°C). However, this volatile production is due only to a small proportion of the sample as the cold ring fraction was found to account for 94% of the original sample mass. The green crystalline material deposited was identified as Co(acac)₃ sublimate by IR and UV spectroscopy and microanalysis. Sublimation was first observed at 83°C and subsequent experiments showed sublimation to be completed by 170°C. Subsequent experiments (below) showed that the initial production of volatile products, although in part due to the release of trapped solvent and precipitant from the purification process was also due to a decomposition process.

The final peak on the TVA curve (T(max) 388°C) is due largely to the production of -196°C non-condensable material which indicates the extensive fragmentation of the residual material.

PRODUCTS OF TVA DEGRADATION OF Co(acac)₃

Samples of Co(acac)₃ (50-100mg) were heated to

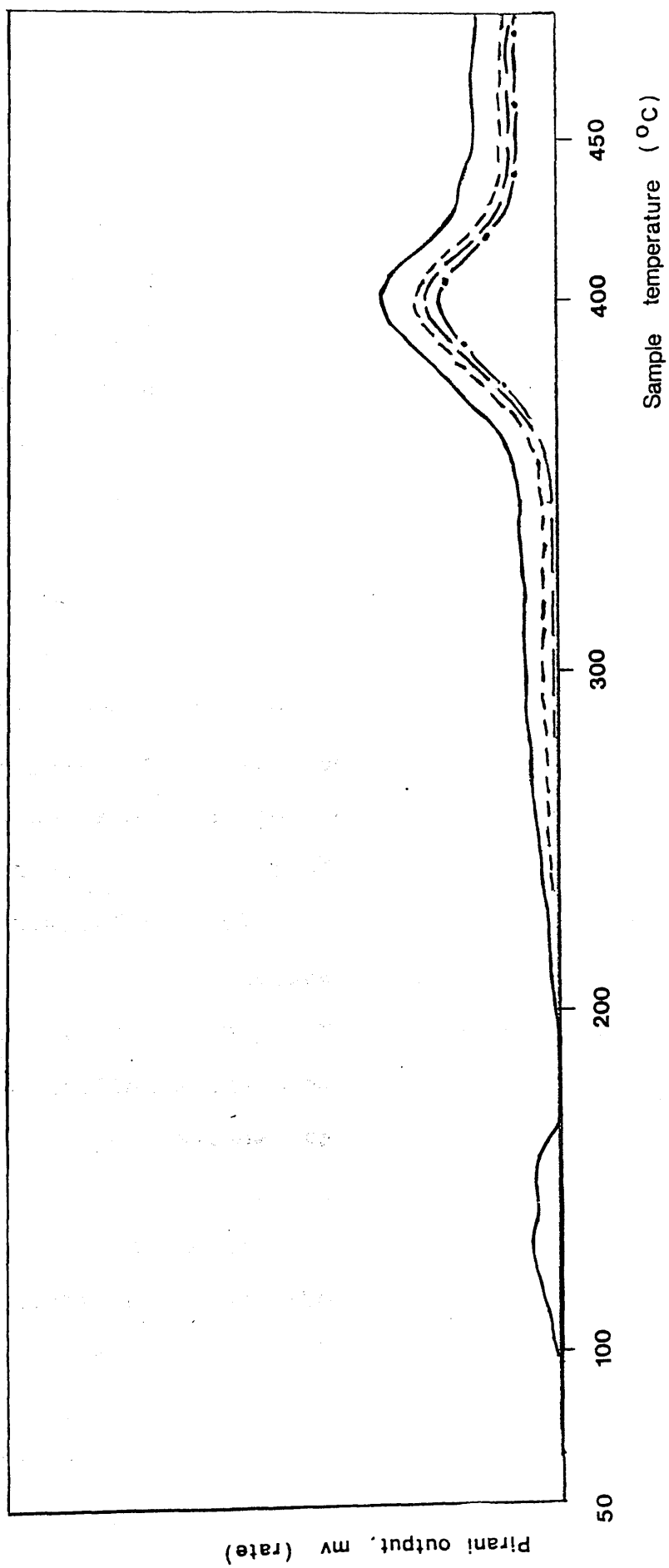


Figure 3.23 TVA curve for $\text{Co}(\text{acac})_3$

various temperatures at a rate of $10^{\circ}\text{C min}^{-1}$ under standard TVA conditions and the -196°C condensable gaseous products collected in the SAD trap. These were then separated by the standard SAD method and analysed by IR spectroscopy. Cold ring fraction and solid residue were also analysed by IR and UV spectroscopy and microanalysis. The results of these degradations are given in Table 3.4. See Figs. 3.24 and 3.25 for spectra of the residual material.

The identification of acetylacetone as a product associated with the first peak confirms that this peak is not due solely to the evolution of trapped solvent/precipitant on sublimation of the chelate. The occurrence of decomposition is also confirmed by analysis of the residue which shows a steady decrease in carbon and hydrogen content. The carbon and hydrogen content at 145°C is equivalent to a $\text{Co}(\text{acac})_3:\text{Co}(\text{acac})_2$ ratio of approximately 1.4:1 which is not consistent with a quantitative analysis of the UV spectrum. This indicates the formation of an unidentified solid product.

The residue formed by the end of the first process has a very low carbon and hydrogen content and remains unidentified. However, analysis of the volatile products produced above this temperature show it to decompose to acetylacetone, carbon dioxide, some acetone, a ketene (the exact nature of which is discussed at the end of this chapter) and a large

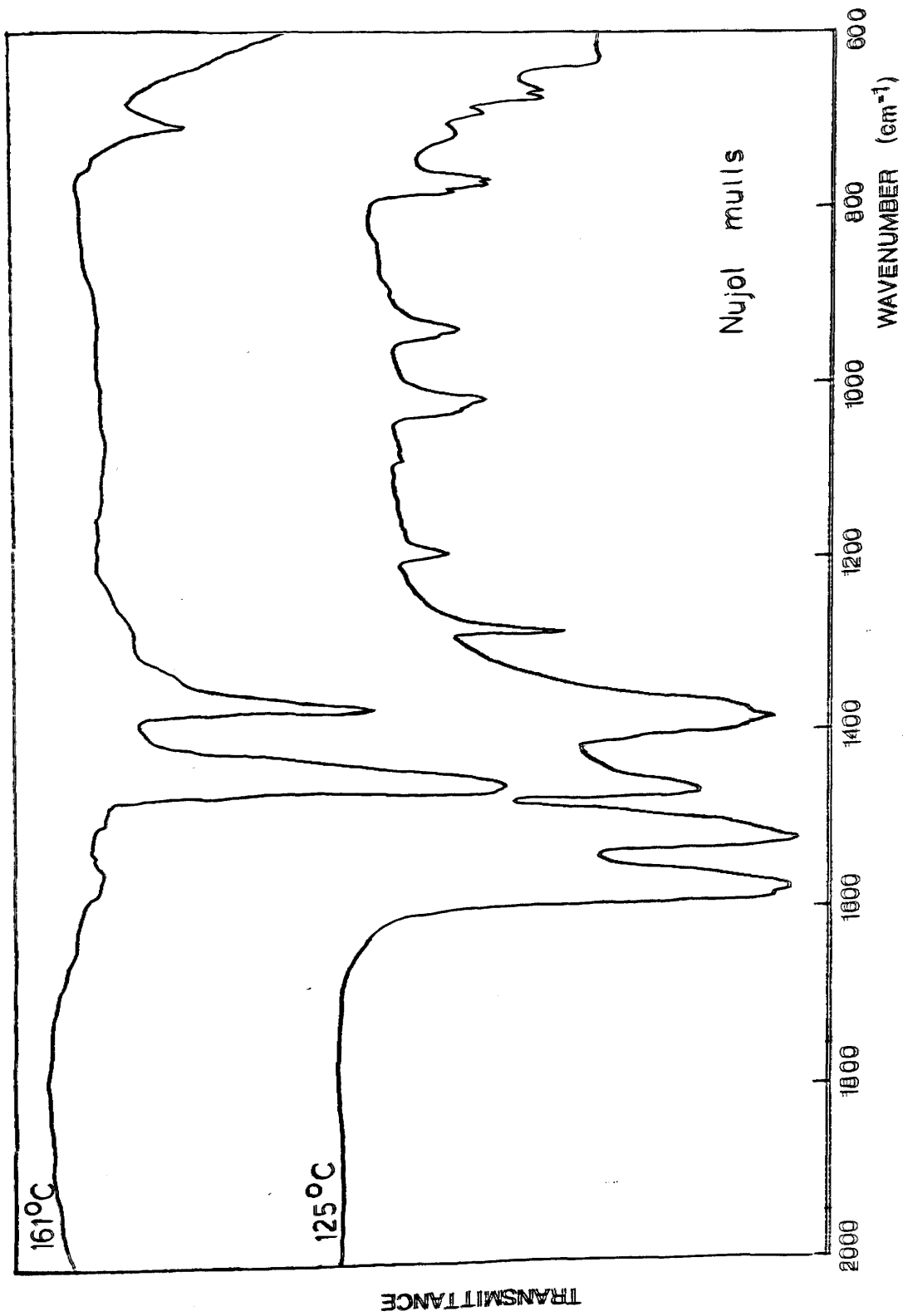


Figure 3.24 IR spectra of residues from TVA degradations of Co(acac)₃

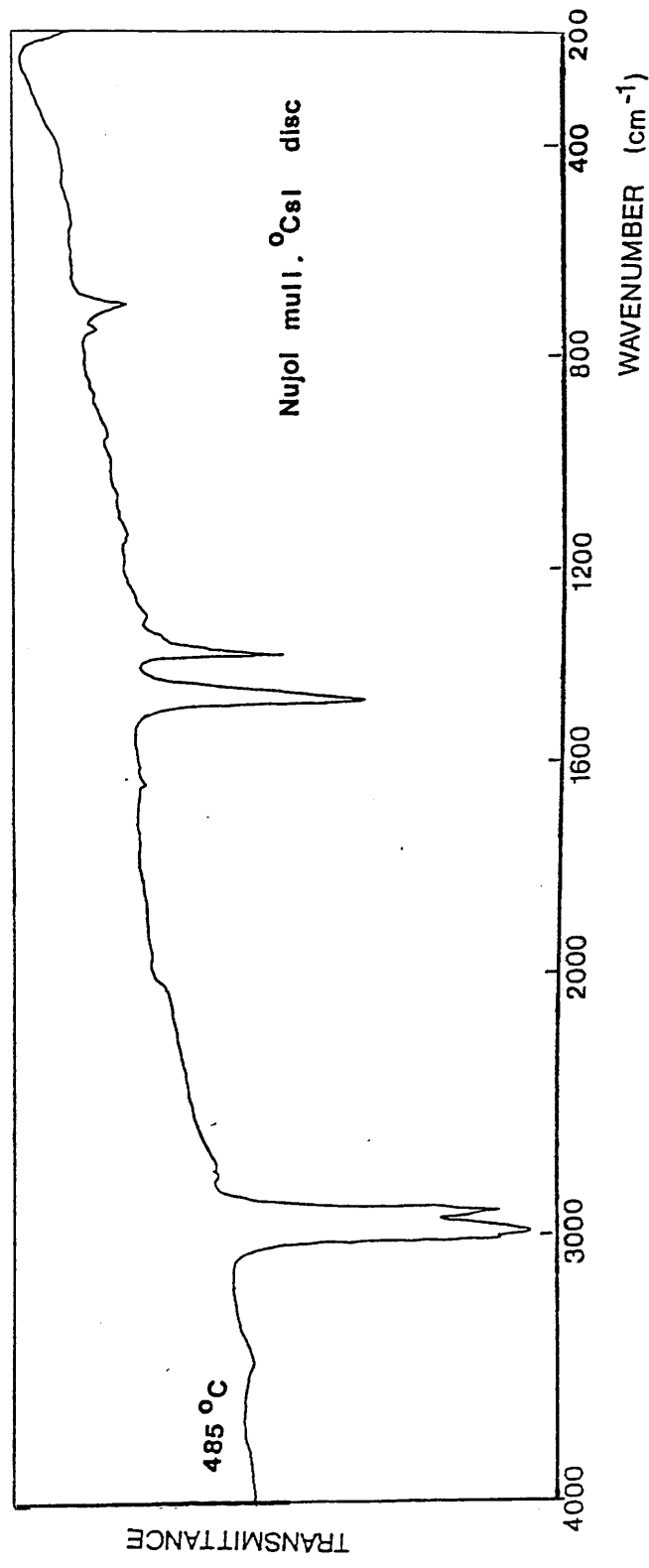


Figure 3.24 IR spectra of residues from TVA degradations of Co(acac)₃ (ctd.)

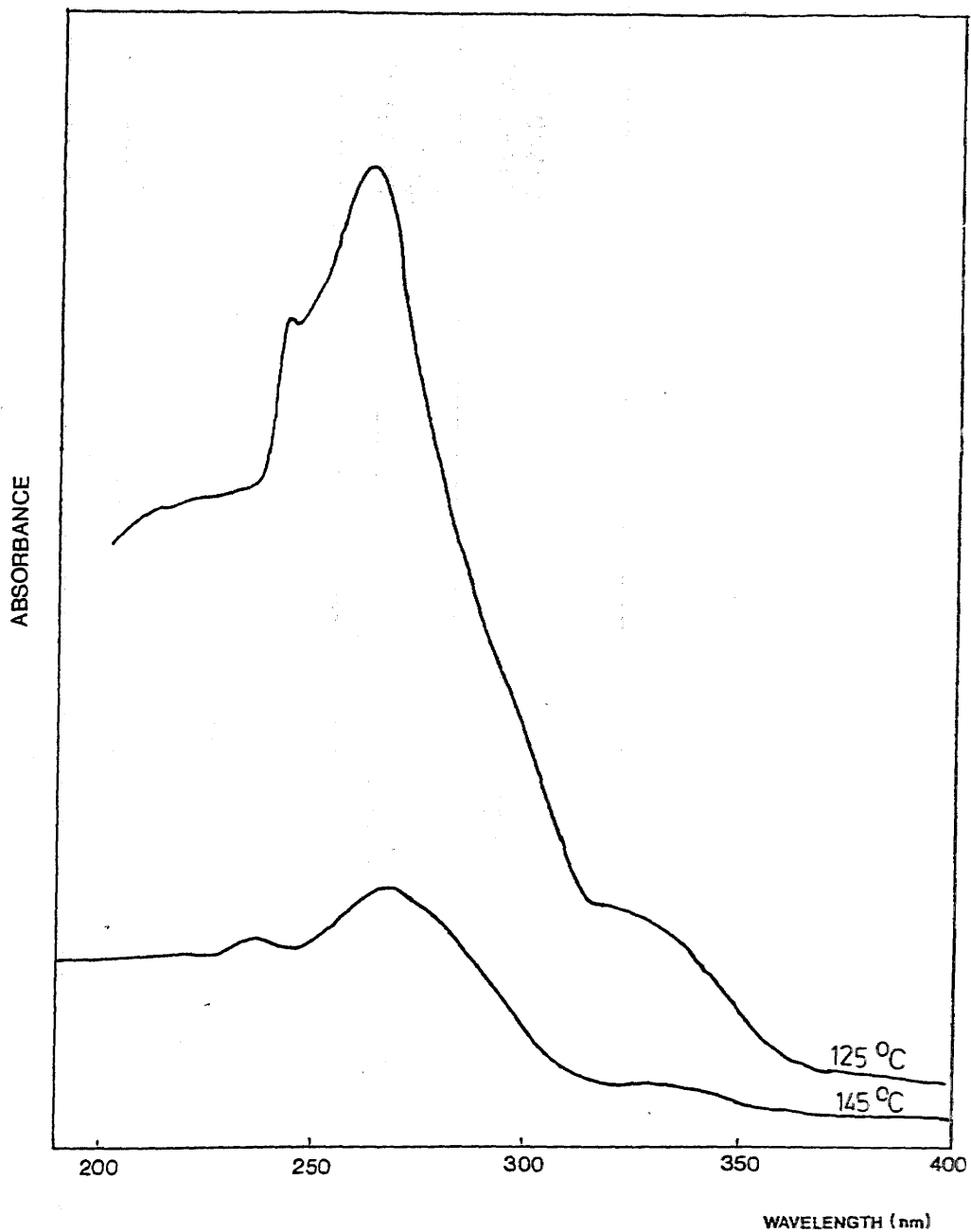


Figure 3.25
UV spectra of residues from TVA degradations
of $\text{Co}(\text{acac})_3$

EXTENT OF DEG-RADATION	-196°C CONDENSIBLE PRODUCTS	COLD RING FRACTION (% initial sample)	RESIDUE APPEARANCE	CH ₂ Cl ₂ SOLUBILITY	UV SPECTRUM	IR SPECTRUM	MICROANALYSIS
125°C	Some Acetyl-acetone	Sublimate	Unchanged	Yes - Green Solution	Co(acac) ₃	Co(acac) ₃	C 50.42% H 5.32%
145°C	-----	-----	Dark green	Yes - Green Solution	λ(max) 270nm => mix of Co(acac) ₂ and Co(acac) ₃	-----	C 47.46% H 5.58%
161°C	Acetyl acetone	Sublimate (94%)	Black powder	No	-----	Featureless 4000-625 cm	C 15.09% H 1.32%
485°C	Acetyl acetone, Carbon dioxide, a ketene	Sublimate (94%)	Black powder	No	-----	Featureless 4000-200 cm	-----

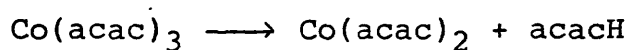
Table 3.4 Products from TVA Degradations of Co(acac)₃

proportion of -196°C non-condensable gases. The black residue obtained at the end of the degradation also remains unidentified but is most probably an oxide of cobalt.

That the small proportion of the sample which decomposes rather than sublimes was not merely an impurity was demonstrated by heating a freshly sublimed sample of $\text{Co}(\text{acac})_3$ and observing that its behaviour was the same as that outlined above.

CONCLUSIONS FROM THE TVA DATA

The production of acetylacetone and the shift in λ (max) of the UV spectrum of the residue is in accord with the occurrence of the reaction:-



Decomposition products are detected at 125°C , considerably lower than the onset of decomposition as observed by TG, DTA or organic particulate analysis. Such discrepancies between TVA results (high vacuum) and the other atmospheric pressure, observations are common and are due to the easier evolution of material under the high vacuum conditions and the very sensitive nature of the Pirani gauges. $T(\text{onset})$ of the first TVA peak is 80°C but as this is due partly to solvent and precipitant it would be unwise to correlate this with the onset of decomposition.

Beyond 125°C , the TVA behaviour is very similar to that of $\text{Co}(\text{acac})_2$ (Page 132).

DEGRADATION OF Co(acac)₃ IN A SEALED TUBE

To examine the behaviour of the chelate without most of the sample subliming from the degradation zone, two samples of Co(acac)₃ were degraded in sealed tubes using the technique described in Chapter 2.

Samples were 10-15mg and both the gaseous and solid products were examined spectroscopically. The results are listed in Table 3.5. In both cases solvent from the purification and sample introduction process were also released - these are not included in the table.

Heating a sample to 125°C for 60 mins produced a sample visibly no different from the starting material and similarly the UV spectrum was qualitatively unchanged. Quantitatively, however, the spectrum showed the sample to be only 72% Co(acac)₃, calculated on the assumption that the absorption at $\lambda(\text{max})$ 256nm could be treated as due solely to Co(acac)₃. That degradation had occurred was confirmed by the identification of acetylacetone as a gaseous product. The microanalysis of the residue produced results inconsistent with the residue being simply a mixture of Co(acac)₃ (72%) and Co(acac)₂ (28%). Nor could it be explained by the presence of a completely inorganic impurity such as broken glass. This indicates the presence of at least one other, unidentified, solid product. This is a similar conclusion to that reached for the TVA-type degradations.

EXTENT OF DEGRADATION	GASEOUS PRODUCTS IDENTIFIED	APPEARANCE OF RESIDUE	CH ₂ Cl ₂ SOLUBILITY	UV SPECTRUM	IR SPECTRUM	MICROANALYSIS
125°C 60 min	Acetylacetone	Unchanged	Yes	Qualitatively => Co(acac) ₃	-----	C 43.56% H 4.86%
200°C 120 min	Acetone, water (no acetyl- acetone)	Some pink material, remainder brown	Partly	Quantitatively => Co(acac) ₃ 72.3%	acac chelate absorptions at 1140 ₁ and 855 cm ⁻¹ un- identified	v. small peak

Table 3.5 Products from Sealed Tube Degradations of Co(acac)₃

On heating at 200°C for two hours, the identified products are fully consistent with the result of Charles et al.¹⁰⁵ The water identified by mass spectrometry, is most probably water absorbed on the tube and released during heating.

Mn(acac)₃

LITERATURE REPORTS

In their study, Charles et al.¹⁰⁵ found Mn(acac)₃ to be the least stable of the chelates studied. Heated isothermally for four hours in tubes sealed under vacuum, Mn(acac)₃ yielded acetylacetone as the sole gaseous product at temperatures between 150-175°C. The authors description of the residue at this stage is consistent with it being Mn(acac)₂. Above 175°C some carbon dioxide was produced, along with an increasing quantity of acetone and a decreasing quantity of acetylacetone. The inverse relationship between the production of acetone and acetylacetone suggested to the authors that the acetone was being produced as a decomposition product of acetylacetone, and in a subsequent paper¹⁰⁶ they demonstrated that acetone was indeed a decomposition product of acetylacetone, albeit at higher temperatures. (This discrepancy they suggested could be accounted for by the solid products of the Mn(acac)₃ decomposition catalysing the acetylacetone decomposition.)

Consequently the authors came to the conclusion that the initial step of the decomposition is the loss of ligand, although without comment on the nature of the mechanism. However, subsequent work, discussed in Chapter 1, demonstrated that in solution, in the presence of electron-donating additives, the initial ligand loss was by homolytic scission.^{26-30,37-40}

There has been little subsequent work on the decomposition of the bulk chelate. Glavas and Ribar¹⁰⁹ report the decomposition of $\text{Mn}(\text{acac})_3$ to involve the stepwise release of acetylacetone accompanied by the formation of stable intermediates. Yoshida et al.¹⁰⁷ examined by DTA the decomposition of the chelate under a nitrogen atmosphere and found two very similar irreversible endotherm-exotherm pairs in the regions $170\text{-}180^\circ\text{C}$ and $250\text{-}260^\circ\text{C}$. Formation of acetylacetone was observed in association with the first endotherm-exotherm pair and the residue obtained on heating to just beyond these peaks had an IR spectrum similar to $\text{Mn}(\text{acac})_2$. Furthermore, the peaks between $250\text{-}260^\circ\text{C}$ were very similar to those of the DTA curve of $\text{Mn}(\text{acac})_2$ which the authors also recorded. The authors' interpretation of the data was the same as that for $\text{Co}(\text{acac})_3$ with the initial ligand homolytic scission and subsequent regeneration of acetylacetone giving the endotherm-exotherm pair (clearly observed as such in contrast to $\text{Co}(\text{acac})_3$). Unlike $\text{Co}(\text{acac})_2$, $\text{Mn}(\text{acac})_2$ decomposes at a considerably higher

temperature than its tris chelate counterpart and its decomposition, presumably by essentially the same mechanism as $Mn(acac)_3$, produces the second endotherm-exotherm pair.

The Organic Particulate Analysis of Smith et al.¹⁰⁸ provides a value for $T(\text{onset})$ of the degradation of $132-133^\circ\text{C}$, a rather lower value than the others recorded for the bulk decomposition of the chelate and one which reflects the high sensitivity of this technique.

It is thought to occur:-



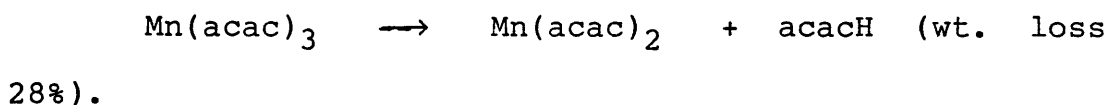
It is unlikely that any sublimation occurs under these conditions.

$Mn(acac)_2$ does not sublime under a vacuum at 10^{-4} and thus the second weight loss at 255°C can be identified as the decomposition of the bis chelate. The weight pair in the corresponding section of the TGA curve is associated with the decomposition of the bis chelate.

THIS WORKDTA AND TG-DTG OF Mn(acac)₃ UNDER NITROGEN

The DTA curve obtained for Mn(acac)₃ under a nitrogen atmosphere (50ml min⁻¹ and heated at 10°C min⁻¹) is reproduced in Fig. 3.26 and is in close agreement to that obtained by Yoshida et al,¹⁰⁷ with the peak temperatures of the two endotherm-exotherm pairs at 170, 175°C and 257, 260°C.

The TG-DTG curves obtained under similar conditions (Fig. 3.27) show a complex pattern of weight losses. The initial weight loss, T(onset) 145°, T(max) 177°C corresponds to the initial endotherm-exotherm pair of the DTA curve. The weight loss (24%) is in good agreement with that calculated for the process thought to occur:-



Thus it is unlikely that any sublimation of Mn(acac)₃ occurs under these conditions.

Mn(acac)₂ does not sublime under atmospheric pressure¹¹⁰ and thus the second weight loss, T(onset) 192°C, T(max) 255°C, can be identified with the decomposition of the bis chelate. The endotherm-exotherm pair in the corresponding region of the DTA curve suggests that Mn(acac)₂ decomposes by a ligand-loss reaction similar to Mn(acac)₃. The weight loss (40%) is not in accord with the simple scission of one

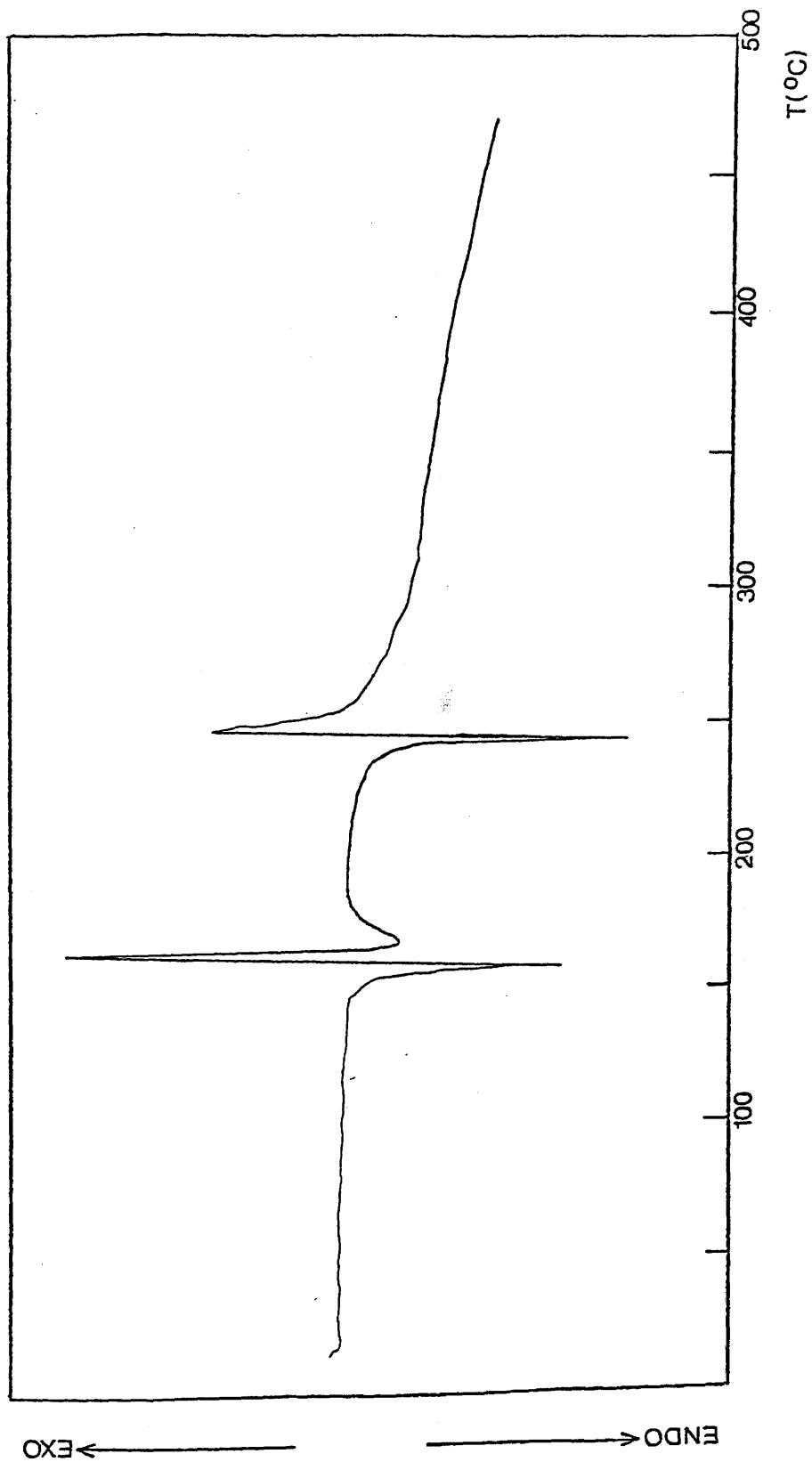


Figure 3.26 DTA curve for $\text{Mn}(\text{acac})_3$ (N_2 atmosphere)

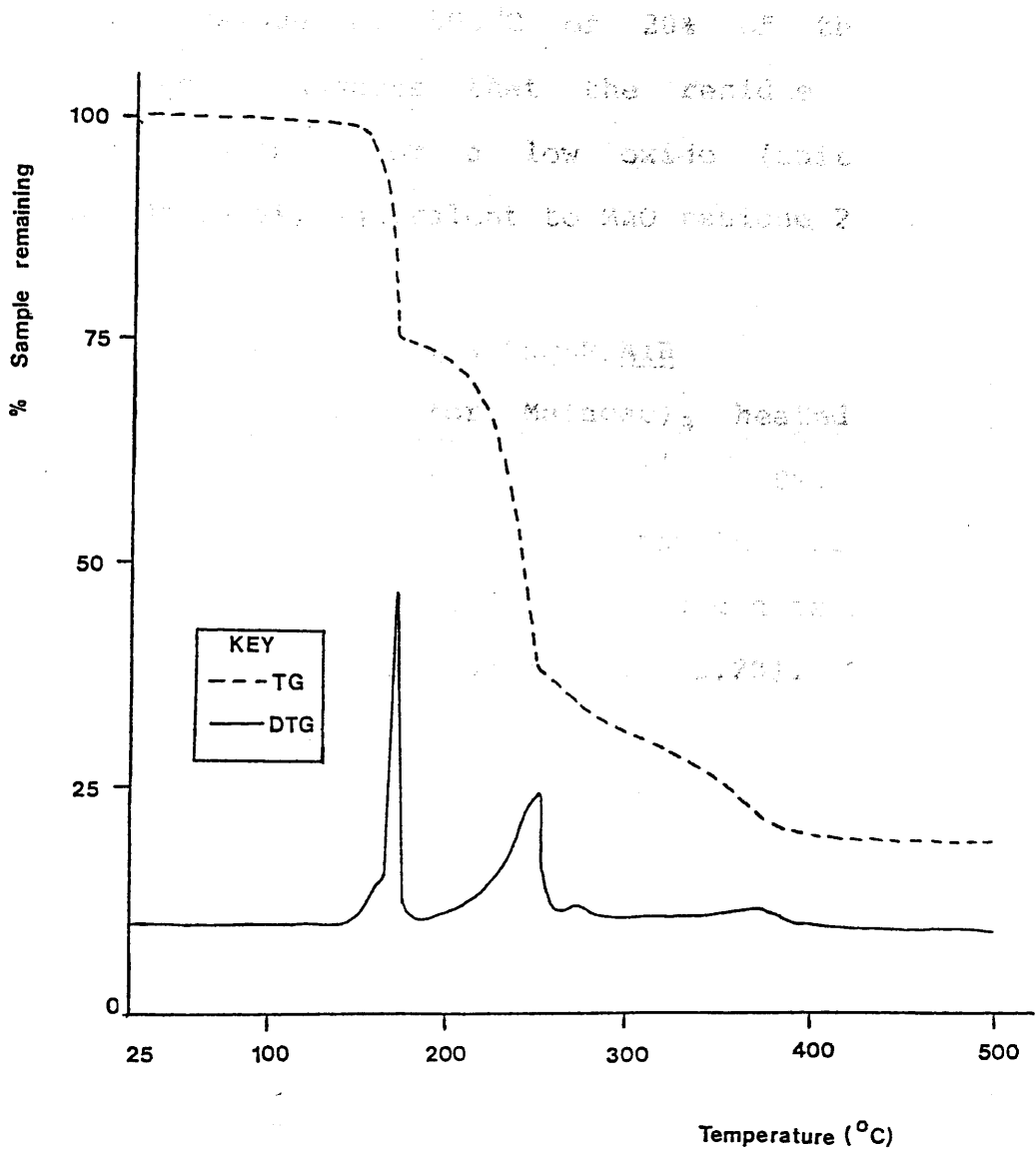


Figure 3.27 TG-DTG curves for $\text{Mn}(\text{acac})_3$ (N_2 atmosphere)

or both ligands and suggests that additional fragmentation reactions also occur. Further fragmentation of the residual material is indicated by the continued weight loss at higher temperatures.

A residue at 500°C of 20% of the original sample mass suggests that the residue is largely metallic manganese or a low oxide (initial sample contains Mn 15.6%, equivalent to MnO residue 20.1%).

DTA AND TG-DTG OF Mn(acac)₃ UNDER AIR

The DTA curve for Mn(acac)₃ heated under an atmosphere of air (10°C min⁻¹, 50ml min⁻¹ air flow) is rather more complex than the curve obtained under nitrogen, indicating that oxygen is interfering with the decomposition process (Fig. 3.28). The initial endotherm-exotherm-endotherm triplet occurs in the same temperature region as the endotherm-exotherm pair obtained under nitrogen and it can thus be assumed that the oxygen is reacting with the products of the initial decomposition. The curve is complex at higher temperatures, but a hint of the second exotherm-endotherm pair remains.

The corresponding TG-DTG curves are broadly similar to those obtained under nitrogen with additional process superimposed onto those occurring under nitrogen (Fig. 3.29). The initial weight loss is identical to that occurring under nitrogen, indicating that the initial loss of ligand is unaffected by the presence of

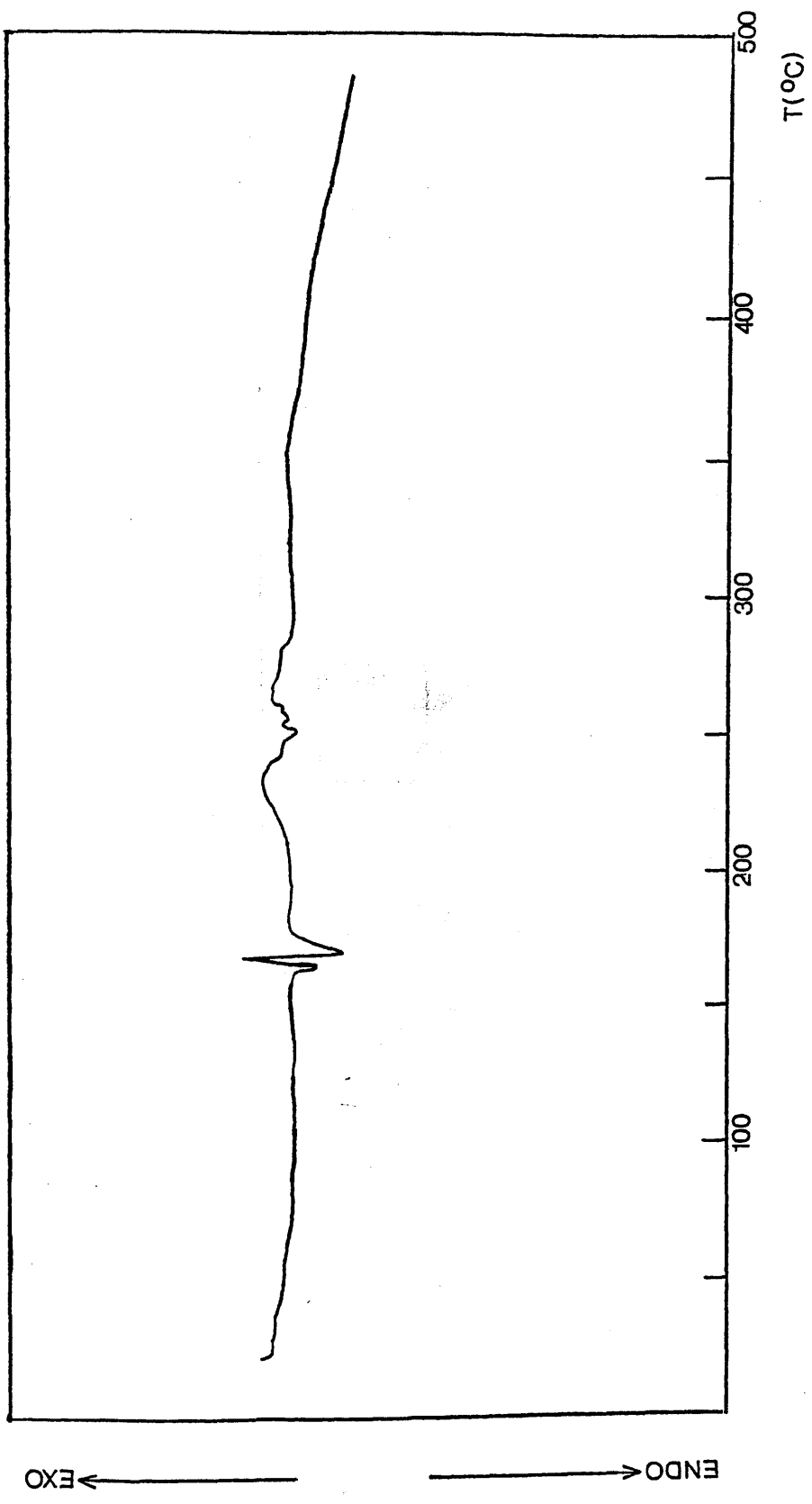


Figure 3.28 DTA curve for Mn(acac)₃ (air)

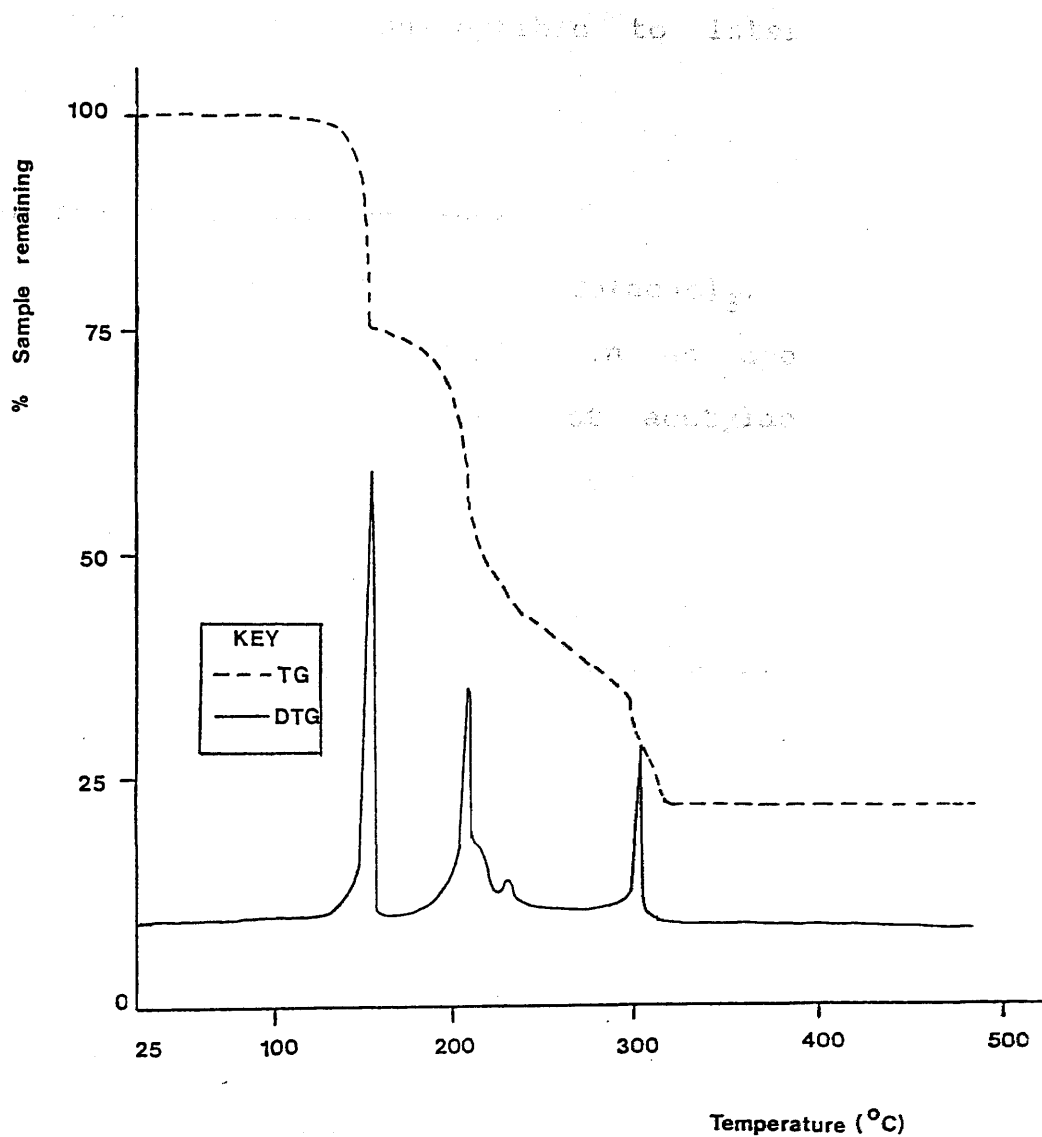


Figure 3.29 TG-DTG curves for $\text{Mn}(\text{acac})_3$ (air)

oxygen and that the change in the DTA curve is due to the reaction of oxygen with the acac radical. Small changes in the weight loss above 200°C reflect the more complex nature of the decomposition of $\text{Mn}(\text{acac})_2$ which make it more susceptible to interference by oxygen.

DEGRADATION IN AN OPEN TVA TUBE

In the same manner as $\text{Co}(\text{acac})_3$, a sample of $\text{Mn}(\text{acac})_3$ (100mg) was degraded in an open TVA tube. Fumes accompanied by a smell of acetylacetone were observed at 137°C. Visibly detectable evolution of material ceased by 260°C. A very small quantity of the fumes collected on the cold ring zone; the UV spectrum of this material (reproduced in Fig 3.30) indicates that if $\text{Mn}(\text{acac})_3$ or $\text{Mn}(\text{acac})_2$ sublimate is present then it is not the major component (no sublimate is expected). The remainder of the evolved material could not be collected.

The residue was a black powder soluble in cold concentrated nitric acid and a light bronzing of the tube walls below the cold ring zone suggests that secondary degradation of the evolved material occurred. This deposit was also soluble in cold concentrated nitric acid.

As with $\text{Co}(\text{acac})_3$, this method of degrading the sample provides evidence of decomposition occurring below the $T(\text{onset})$ observed by TG and DTA although it is

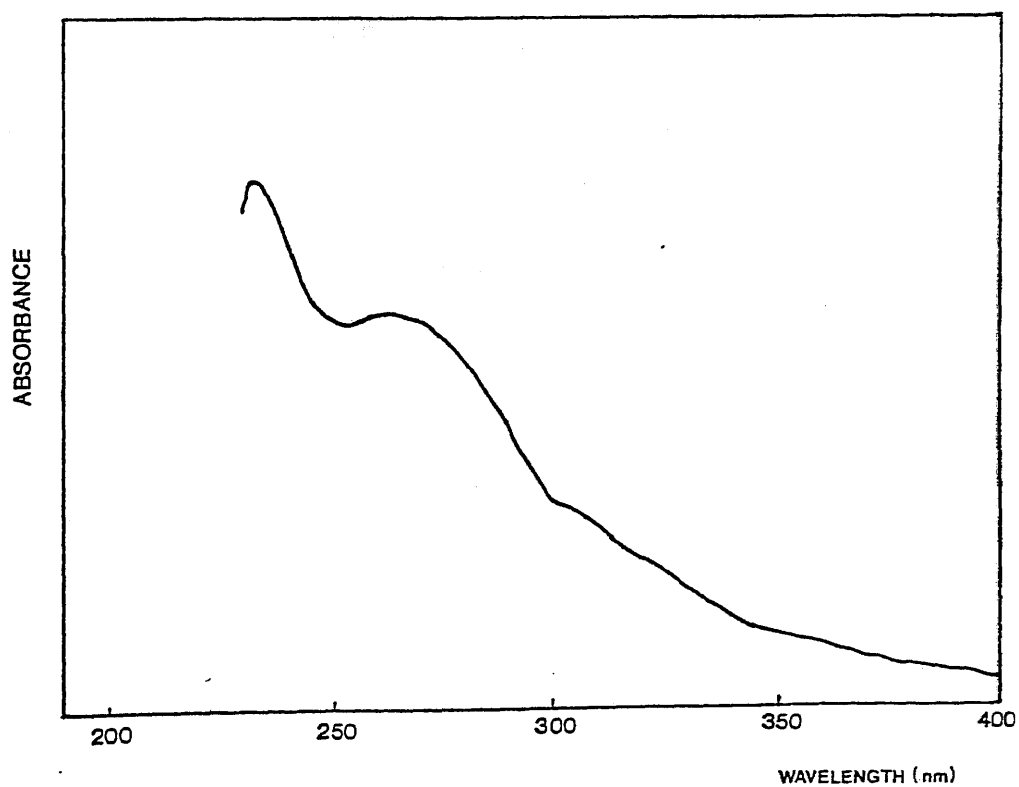


Figure 3.30
UV spectrum of CRF from "open-tube" degradation
of $\text{Mn}(\text{acac})_3$

in agreement with the results from the organic particulate analysis of Smith et al.¹⁰⁸

Such a curve for a 100°C material, is reproduced in Fig. 3.11.

The first peak extending from 60°C to 100°C has its onset similar to the appearance of sublimate. This peak has been purified by precipitation from a methylene chloride and subsequent analysis of this peak is due in part to the evolution of acetylacetone on sublimation of the chelate, a evolution of acetylacetone is also observed.

Second stage evolution of material starts with a stage around 100°C. An amount of 100°C non-condensable material (which is very small) points to from 100°C and at higher temperatures.

RESULTS FROM TVA DEGRADATIONS OF UO_2

Table 3.6 details the products of degradation at 700°C. Standard TVA conditions were used with sample sizes between 100 and 200 mg.

TVA BEHAVIOUR OF $\text{Mn}(\text{acac})_3$

$\text{Mn}(\text{acac})_3$, like $\text{Co}(\text{acac})_3$, mostly sublimes to the cold ring zone on heating under TVA conditions. This accounts for 90-95% of the material, and to obtain a significant deviation of the TVA curve from the base line it was necessary to use samples of at least 100mg and, in addition, record only the total volatile material and total -196°C non-condensable material production. Such a curve for a 134mg sample of $\text{Mn}(\text{acac})_3$ is reproduced in Fig 3.31.

The first peak extending from 68°C to 153°C with $T(\text{max})$ 128°C has its onset simultaneous with the first appearance of sublimate. This particular sample had been purified by precipitation from toluene into petroleum spirit and subsequent analysis confirms that this peak is due in part to the evolution of trapped precipitant on sublimation of the chelate, although the evolution of acetylacetone is also observed.

Beyond 153°C evolution of material is slow but steady with a slight hump around 400°C . An increasing amount of -196° non-condensable material (although always remaining very small) points to fragmentation of the residue at higher temperatures.

PRODUCTS FROM TVA DEGRADATIONS OF $\text{Mn}(\text{acac})_3$

Table 3.6 details the products of degradation to 200°C and 485°C . Standard TVA conditions were employed with sample sizes between 100 and 200mg and

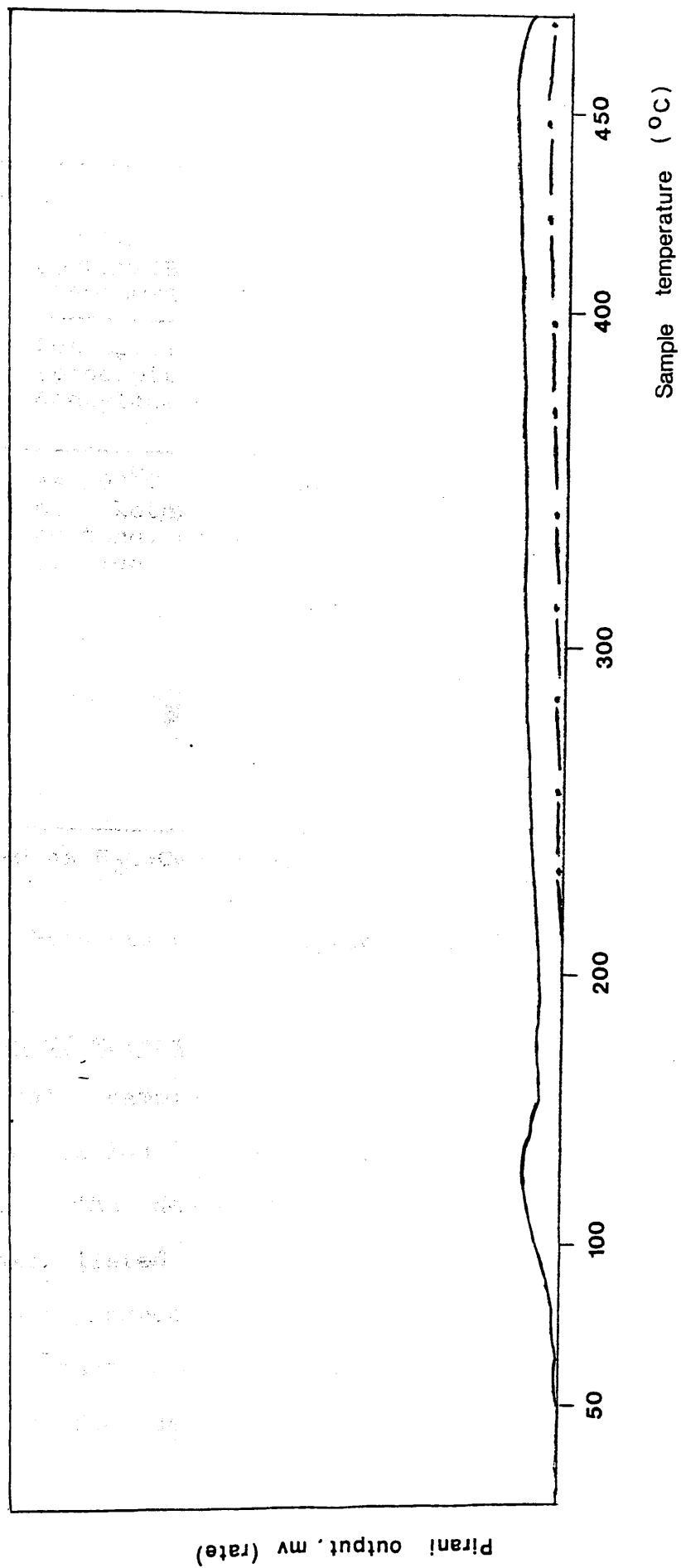


Figure 3.31 TVA curve for Mn(acac)₃

product analysis were performed by the methods described previously.

PRODUCTS			
TEMPERATURE	-196°C CONDENSIBLE PRODUCTS	CRF	RESIDUE
200°C	Pet spirit (precipitant) acetylacetone	Sublimate (pure by UV spec) amounts to 90-95% of initial sample	Black powder uniden- tified.
485°C	As 200°C plus ketene*, acetone, carbon dioxide,	As 200°C	Black powder soluble in cold conc. HNO ₃ . No signif- icant IR absorp- tion 4000-600 cm ⁻¹

* Identified as H₂C=C=O by mass spectrometry

Table 3.6 Products of TVA degradation of Mn(acac)₃

DEGRADATIONS OF Mn(acac)₃ IN A SEALED TUBE

Several samples of Mn(acac)₃ (10-15mg) were degraded in sealed tubes by the method described in Chapter 2. The degradation conditions and identified products are listed in Table 3.7. Spectra of the residues are reproduced in Figs. 3.32 and 3.33.

Note that the microanalysis results for the residue from the degradation at 159°C for 60 mins are

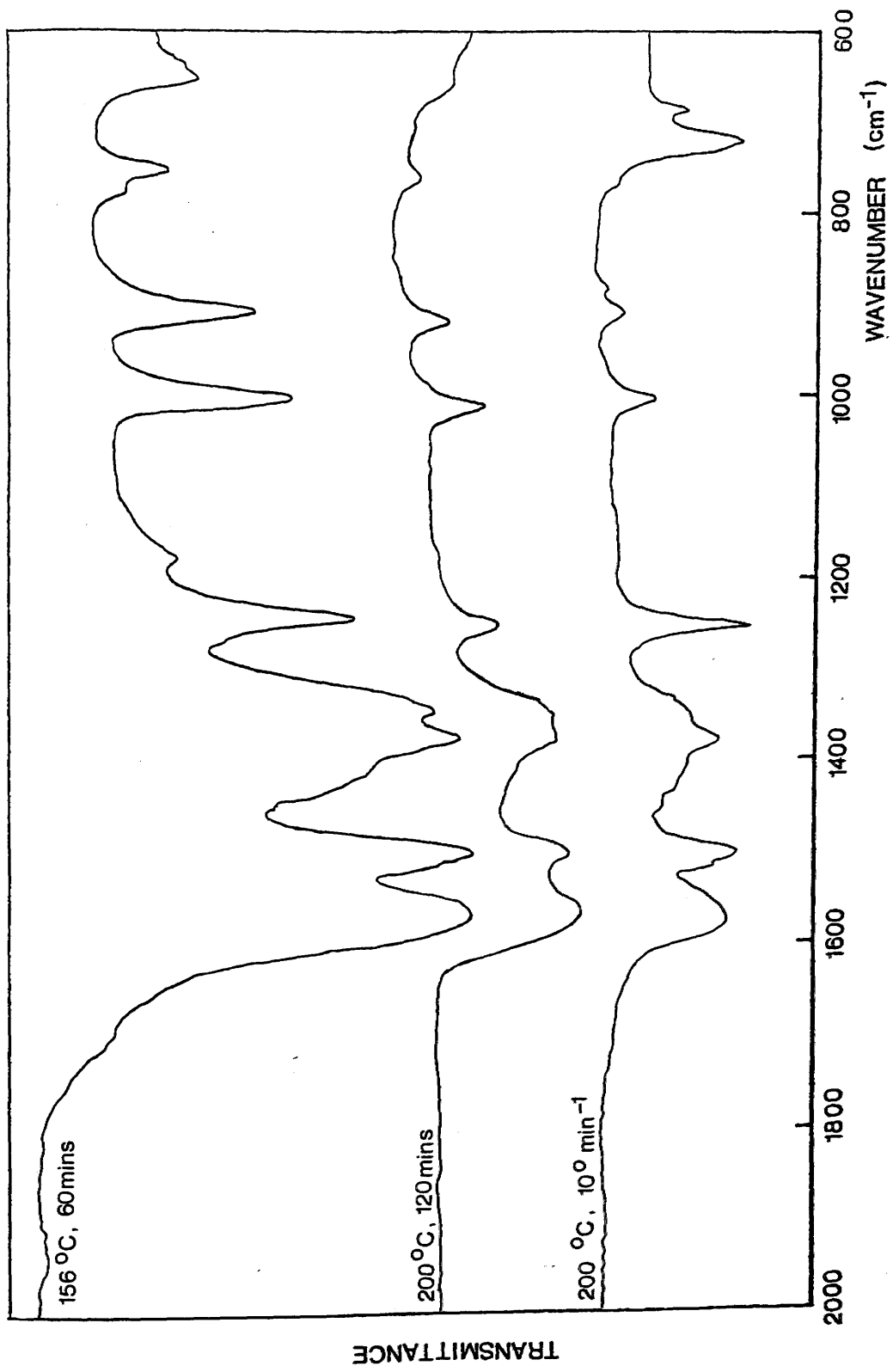


Figure 3.32 IR spectra of residues from sealed-tube degradations of Mn(acac)₃

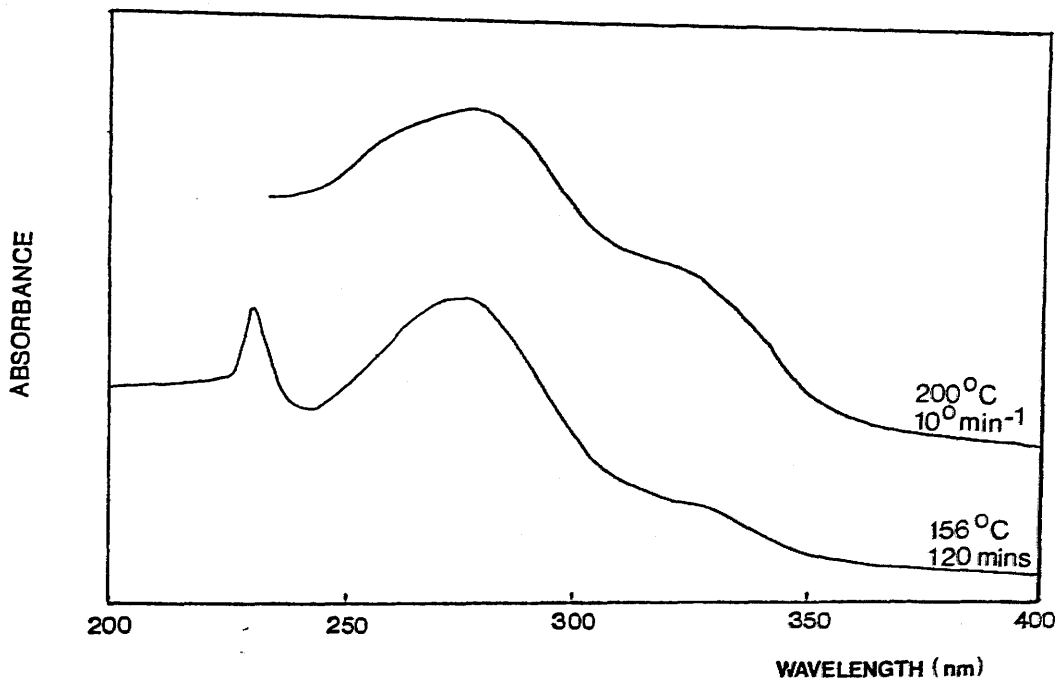


Figure 3.33 UV spectra of residues from sealed-tube degradations of $\text{Mn}(\text{acac})_3$

DEGRADATION CONDITIONS	RESIDUE		
	GASEOUS PRODUCTS IDENTIFIED	APPEARANCE OF RESIDUE	CH ₂ Cl ₂ SOLUBILITY
127°C 60 mins	None	Unchanged	Yes
159°C 60 mins	Acetylacetone	Brown	Yes
200°C 120 mins	Acetylacetone Carbon dioxide* carbon monoxide*	-----	--
200°C 10°C min ⁻¹	Acetylacetone	Fawn residue => Mn(acac) ₂	Yes

	RESIDUE		
	IR SPECTRUM	UV SPECTRUM (CH ₂ Cl ₂ SOLUTION)	MICROANALYSIS
127°C 60 mins	No change	No change	--
159°C 60 mins	Similar to Mn(acac) ₂ or Mn(acac) ₃	λ(max) 272 nm consistent with Mn(acac) ₂	C 34.56% H 4.07% SEE TEXT
200°C 120mins	Similar to Mn(acac) ₂ but intensification of 1575cm ⁻¹ peak	-----	--
200°C 10°C min ⁻¹	Consistent with Mn(acac) ₂	λ(max) 273nm breadth => not simply Mn(acac) ₂	

Table 3.7 Products from Sealed Tube Degradations of Mn(acac)₃

* Identified by mass spectrometry

possibly in error due to the presence of glass fragments - the observed C and H contents are lower than expected for $\text{Mn}(\text{acac})_2$ but the ratio C:H is in very close agreement to that calculated for $\text{Mn}(\text{acac})_2$:-

Observed C 34.56%, H 4.07% C:H = 8.49:1

Calculated for $\text{Mn}(\text{acac})_2$ C 47.44%, H 5.58%, C:H=8.50:1

Thus it is highly probable that the residue at this point is $\text{Mn}(\text{acac})_2$.

CONCLUSIONS FROM TVA AND SEALED TUBE DEGRADATIONS OF $\text{Mn}(\text{acac})_3$

The first peak of the TVA curve has its onset simultaneous with the onset of sublimation (68°C) which immediately suggests that the release of trapped solvent is involved, and petroleum spirit from the purification process is identified. Heating a sample of chelate at 125°C for 60 minutes produced no discernable degradation and thus the first TVA peak cannot be due, at least in its early stages, to decomposition.

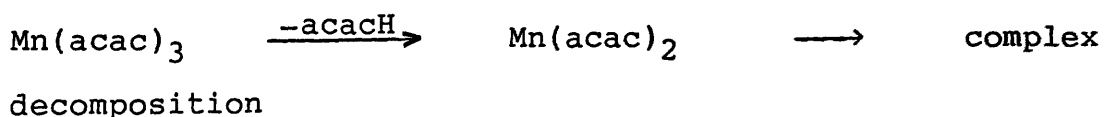
Decomposition is observed at 159°C and although the bis and tris chelates are virtually impossible to differentiate on the basis of their UV and IR spectra, the production of acetylacetone indicates that reduction does take place. Furthermore, assuming the microanalysis to be in error due to sample

contamination, the results can be taken as indicating the residue to be $\text{Mn}(\text{acac})_2$.

On heating to 200°C the residue remains largely $\text{Mn}(\text{acac})_2$, consistent with the interpretation of Yoshida et al.¹⁰⁷ Above 200°C the TVA behaviour and associated degradation products are consistent with $\text{Mn}(\text{acac})_2$ (see section on $\text{Mn}(\text{acac})_2$, below). Both the TVA curve and the TG curve already discussed show the degradation above 200°C to be more protracted than suggested by the DTA evidence but this probably reflects the difficulty in detecting shallow endotherms or exotherms from a DTA curve which can result in the "loss" of degradation processes.

SUMMARY

Overall the evidence presented suggests the following scheme, essentially that of Yoshida et al.¹⁰⁷



The decomposition of $\text{Mn}(\text{acac})_2$ is discussed subsequently.

$\text{Co}(\text{acac})_2$

LITERATURE REPORTS

Charles et al. found $\text{Co}(\text{acac})_2$ to decompose at temperatures above 150°C when heated for four hours in

a tube sealed under vacuum.¹⁰⁵ Between 150°C and 200°C acetone was the sole gaseous product, in increasing amounts. Above 200°C, carbon dioxide was produced in increasing amounts. This behaviour is very similar to that of $\text{Co}(\text{acac})_3$ under the same conditions. Both chelates show the first signs of decomposition around 150°C and thus any $\text{Co}(\text{acac})_2$ formed by the decomposition of $\text{Co}(\text{acac})_3$ would decompose almost immediately, hence the similarity in the products from $\text{Co}(\text{acac})_3$ and $\text{Co}(\text{acac})_2$ under these conditions.

Yoshida et al.¹¹¹ recorded the DTA curve for $\text{Co}(\text{acac})_2 \cdot 2\text{H}_2\text{O}$ under nitrogen and attributed to the endotherm $T(\text{max})$ 224°C to the pyrolytic decomposition of the dehydrated chelate. Thus the small endotherm shouldering the major endotherm of $T(\text{max})$ 210°C due to the reduction of $\text{Co}(\text{acac})_3$ in the DTA curve of that chelate was subsequently ascribed to $\text{Co}(\text{acac})_2$ decomposition.¹⁰⁷

THIS WORK (In association with A. Hazzard)

TVA BEHAVIOUR OF $\text{Co}(\text{acac})_2$

The TVA curve for an approximately 50mg sample of $\text{Co}(\text{acac})_2$ is reproduced in Figure 3.34. The behaviour of the individual trap traces during the small first peak is consistent with the evolution of water. This is

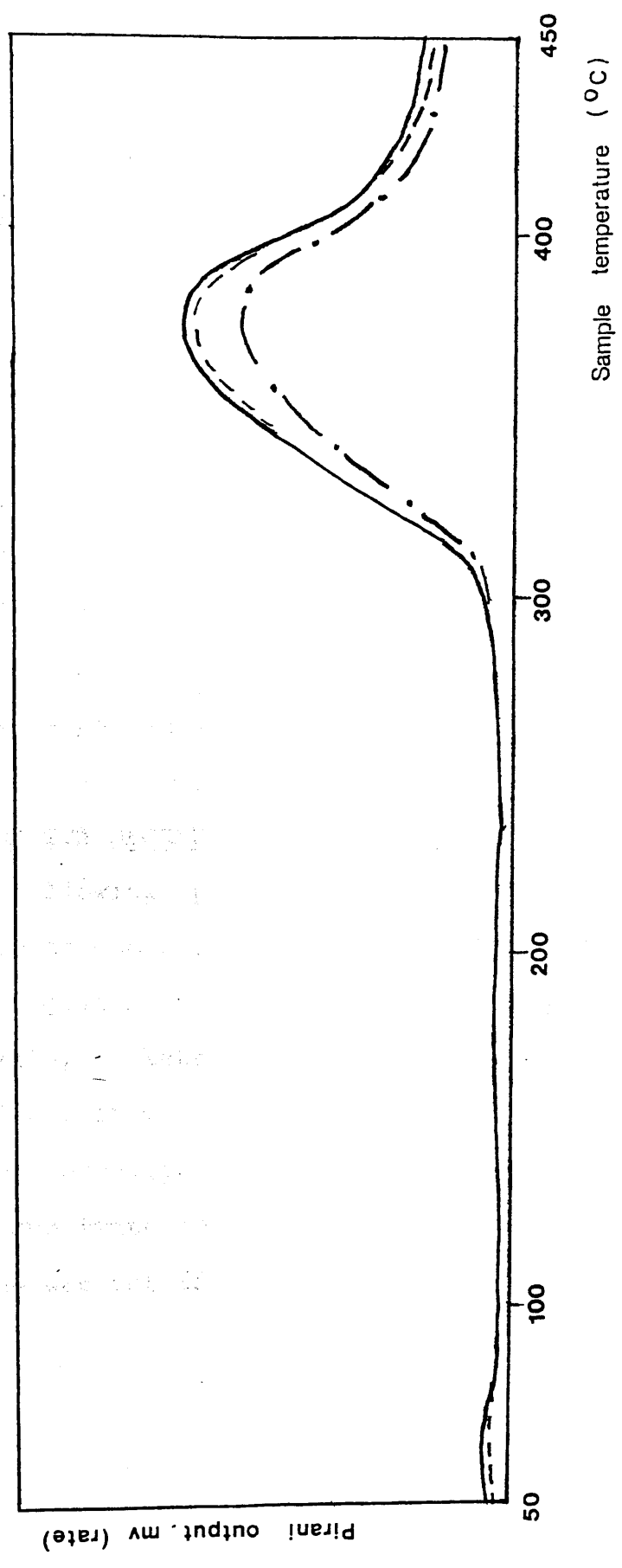


Figure 3.34 TVA curve for Co(acac)₂

probably the release of water of crystallisation, absorbed during the preparation of the sample (the sample was observed to gain mass whilst on the balance).

The remainder of the decomposition is reminiscent of the TVA behaviour of $\text{Co}(\text{acac})_3$ with prolonged evolution of small amounts of material culminating in the production of larger quantities of material, mostly non-condensable at -196°C , around 380°C . Again like $\text{Co}(\text{acac})_3$, this last peak is due to the degradation of only small quantities of chelate as the bulk of the sample sublimes from the degradation zone (sublimation first observed 87°C).

The similarities in TVA behaviour suggest that the later stages of the $\text{Co}(\text{acac})_3$ degradation involve $\text{Co}(\text{acac})_2$, as expected.

PRODUCTS FROM TVA DEGRADATION OF $\text{Co}(\text{acac})_2$

The following products were identified by gas - phase IR spectroscopy, after separating by SAD the products of degradation to 485°C of $\text{Co}(\text{acac})_2$:- carbon dioxide, a ketene, acetone, acetylacetone, water (of crystallisation).

These products are the same as those from $\text{Co}(\text{acac})_3$. Sublimate was identified in the CRF. The black residue was not identified.

Mn(acac)₂PREVIOUS WORK

The decomposition of this chelate has already been touched upon in relation to the decomposition of Mn(acac)₃ but will be described in more detail here.

Yoshida et al.¹⁰⁷ reported that the DTA curve of Mn(acac)₂ obtained for a sample heated under a nitrogen atmosphere displays a sharp endotherm-exotherm pair around 260°C. In relation to Mn(acac)₃ they describe such an endotherm pair as typical of homolytic cleavage of a ligand followed by hydrogen abstraction and the same interpretation seems likely to apply to Mn(acac)₂. This would be in agreement with the work of Glavas and Ribar¹⁰⁹ who report Mn(acac)₂ to decompose by the stepwise evolution of acetylacetone accompanied by the formation of a stable intermediate.

THIS WORK (In association with A. Hazzard)TVA BEHAVIOUR OF Mn(acac)₂

The TVA curve for an approximately 50mg sample of Mn(acac)₂ is reproduced in Fig 3.35. The protracted evolution of material at low temperatures is probably due to the release of trapped solvents and water absorbed by the hygroscopic Mn(acac)₂ during sample transfer. The peak with T(max) 215°C is due to decomposition of the chelate (see below) whilst the peak

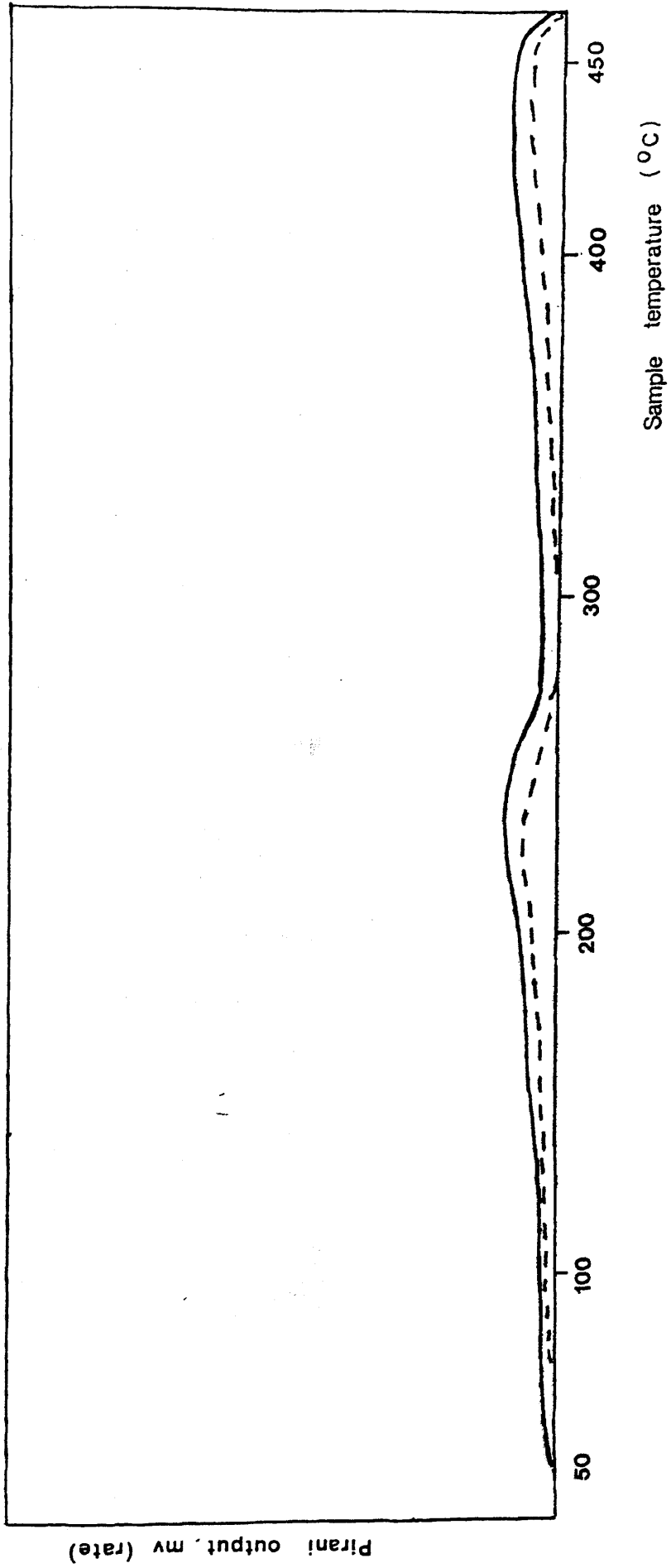


Figure 3.35 TVA curve for $\text{Mn}(\text{acac})_2$

above 400°C is due to fragmentation of the solid residue produced in the first step.

Thus the TVA trace for Mn(acac)₂ confirms the evidence from the decomposition of Mn(acac)₃ that the decomposition of Mn(acac)₂ is not a single step process.

[Faint, illegible text]

[Faint, illegible text]

[Faint, illegible text]

[Faint, illegible text]

[Faint, illegible text]

[Faint, illegible text]

[Faint, illegible text]

[Faint, illegible text]

[Faint, illegible text]

PRODUCTS FROM TVA DEGRADATION OF Mn(acac)₂

Products from a 100mg sample of Mn(acac)₂ degraded under standard TVA conditions were collected separately for heating in the ranges 25-230°C and 230-485°C and identified by IR spectroscopy. The results are presented below.

TEMPERATURE	-196°C CONDENSIBLE PRODUCTS	CRF	RESIDUE
To 230°C	Acetylacetone, acetone, water (of crystallisation)	-	-
Between 230-485°C	As above but less acetylacetone and no water	Mn(acac) ₂	Black powder not analysed

Table 3.8 Products from TVA Degradation of Mn(acac)₂

Excepting the presence of the water and the absence of ketene, these products are the same as those obtained in the advanced stages of the Mn(acac)₃ decomposition.

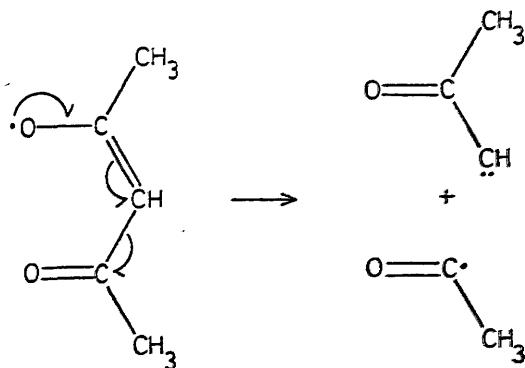
THE DECOMPOSITION MECHANISMS OF Co(acac)₂ AND Mn(acac)₂

The similarity of the degradation products of Co(acac)₂ and Mn(acac)₂ suggest that both decompositions occur in much the same manner and so both chelates will be discussed in this section.

Both chelates produce acetylacetone which indicates that some decomposition occurs by a simple ligand-scission mechanism similar to that which occurs in the tris chelates. This is reflected in the presence of the endotherm-exotherm pair in the DTA curve of $\text{Mn}(\text{acac})_2$.¹⁰⁷ On the other hand, production of a ketene, carbon dioxide, acetone, -196°C non-condensable material and what is apparently metal oxide indicates that more extensive fragmentation is also taking place.

FORMATION OF ACETONE, CARBON DIOXIDE, "KETENE" AND -196°C NON-CONDENSIBLE MATERIAL FROM $\text{Co}(\text{acac})_2$ AND $\text{Mn}(\text{acac})_2$

Regeneration of acetylacetone by H-abstraction is one route open to the $\text{acac}\cdot$ radical but fragmentation of the radical is also possible. The most probable fragmentation step is the loss of one acetyl group and formation of a ketocarbene.¹¹²

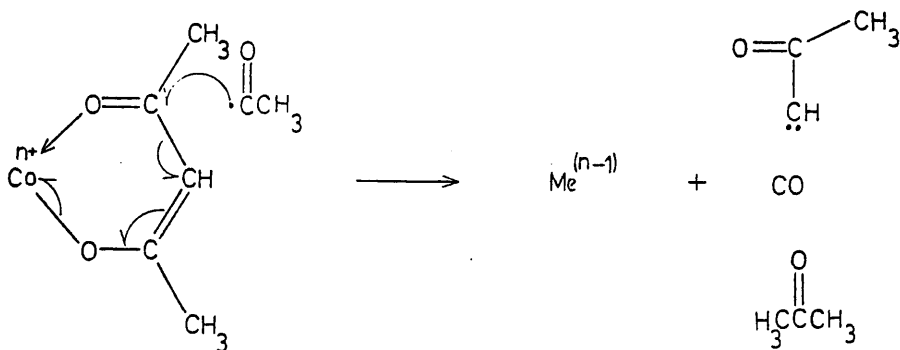


(This reaction could occur with the ligand in situ with the subsequent reduction of the metal ion and ketocarbene formation).

The ketocarbene undergoes a Wolff-type rearrangement to give methyl ketene¹¹²:-

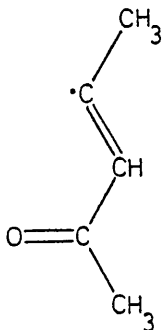


The acetyl radical can abstract a methyl radical from a neighbouring acac ligand or acac radical:-



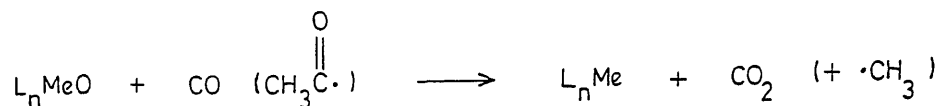
The ketocarbene will rearrange as before.

It is possible for the C-O bond to break rather than the Me-O bond. This produces a metal oxide, L_nMeO, where L_n represents any ligands remaining bound to the metal. The radical produced is:-



This radical will abstract a methyl group to produce mesityl oxide and although not identified in this research, mesityl oxide was identified by Charles et al.¹⁰⁵ as a minor product. The metal oxide could then react either with CO or H₃CC(=O)· to produce CO₂

(and $\cdot\text{CH}_3$ radicals in the case of the acetyl radical). This then explains the formation of CO_2 :-



The $\cdot\text{CH}_3$ radicals could combine with the acetyl or α, β unsaturated ketone radicals or abstract a proton to give methane.

Thus it can be seen that all the observed products can be accounted for.

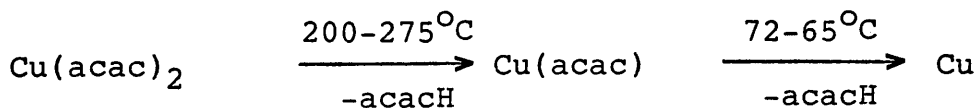
CONCLUSIONS FROM THE DEGRADATION OF $\text{Co}(\text{acac})_2$ AND $\text{Mn}(\text{acac})_2$

The similarities between the decomposition of the bis chelates and the later stages of the decomposition of the tris chelates is a further indication that the decomposition of the tris chelates proceeds via the bis species. Thus the elucidation of the decomposition mechanism of the bis chelates is necessary to fully describe the decomposition of the tris chelates and understand the action of the chelates in the polymers with which they are blended. The decomposition of the bis chelates is more complex than that of the tris chelates, producing small radical species which can react with the surrounding polymer more readily than the bulkier acac radicals.

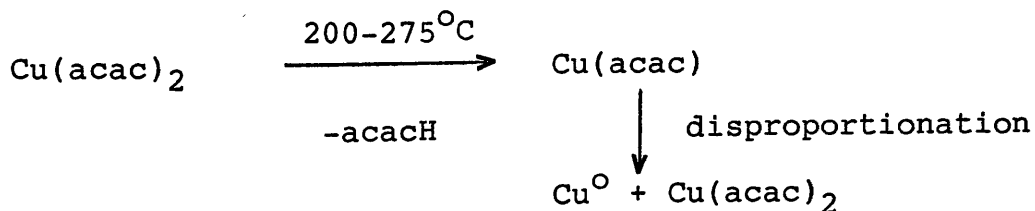
Cu(acac)₂LITERATURE REPORTS

Charles et al.¹⁰⁵ found that Cu(acac)₂ decomposed in a fashion similar to Mn(acac)₃ although it was rather more stable. Between 190-300°C acetylacetone was the sole gaseous product, increasing in quantity with increasing temperature. Above 300°C acetylacetone production decreased and there was a corresponding increase in the production of acetone. As with Mn(acac)₃ this suggests that the acetone is a secondary degradation product, from acetylacetone. At 250°C the residue was a black-brown crystalline material which Charles et al. do not identify but which matches the description of Cu(I)acac.¹¹³ Above 275°C metallic copper is produced.

The results of Charles et al. are consistent with the scheme



However, Cu(acac) is reported to be unstable and to disproportionate to Cu⁰ + Cu(acac)₂^{113,114} and so the mechanism below may also be involved.



Yoshida et al. obtained the DTA curve for $\text{Cu}(\text{acac})_2$ under atmospheres of nitrogen and air.¹¹¹ The curve obtained on heating the sample under nitrogen shows a single sharp irreversible endotherm $T(\text{onset})$ 250°C (estimated from their results), $T(\text{max})$ 283°C . In air, an exotherm pair was observed in the same region. The authors thus attributed the endotherm under nitrogen to the pyrolytic decomposition of the chelate and the exotherm pair to its oxidative decomposition. No mechanisms were proposed but the results of the decomposition under nitrogen suggests a sharper single step process than the results of Charles et al.¹⁰⁵ although this may be attributed to differences of technique (see conclusions below).

Differences of technique could also account for the discrepancies in the other reports of $\text{Cu}(\text{acac})_2$ decomposition. Glavas and Ribar¹⁰⁹ report that $\text{Cu}(\text{acac})_2$ sublimes and decomposes simultaneously (unknown atmosphere) above 100°C whilst Nair et al.¹¹⁵ in a TG study found $\text{Cu}(\text{acac})_2$ to decompose, under an atmosphere of air, between $190\text{-}265^\circ\text{C}$ in a single step with the formation of CuO . As with the other chelates, the OPA technique of Smith et al. produces the lowest $T(\text{onset})$ - $165\text{-}168^\circ\text{C}$.¹⁰⁸

The interpretation of these contradictory results is discussed subsequently in the light of results obtained in this study.

THIS WORK

TG-DTG AND DTA OF Cu(acac)₂ UNDER NITROGEN

The TG-DTG and DTA curves obtained on heating Cu(acac)₂ under a flow of nitrogen at 10°C min⁻¹ are reproduced in Figs 3.36 and 3.37.

The TG-DTG curves show a sharp single step weight loss (92%) with T(onset) 150°C and T(max) 240°C. Such a large weight loss occurring so sharply is almost certainly due to sublimation of the sample although in this temperature region some degradation is also expected. From TG it is impossible to state categorically that the weight loss is due to sublimation but degradation of a sample in an open TVA tube shows that sublimation does occur at this temperature under atmospheric pressure (see below).

The DTA curve is very similar to that of Yoshida et al.,¹¹¹ showing a single endotherm T(onset) 225°C T(max) 292°C and as such is at variance with the TG data obtained.

TG-DTG AND DTA OF Cu(acac)₂ UNDER AIR

The TG-DTG curves obtained for Cu(acac)₂ under an atmosphere of air (50ml min⁻¹ at 10°C min⁻¹) are shown in Fig 3.38 and are virtually identical to those obtained under nitrogen and thus in disagreement with the results of Nair et al..¹¹⁵

The DTA curve for Cu(acac)₂ obtained under a

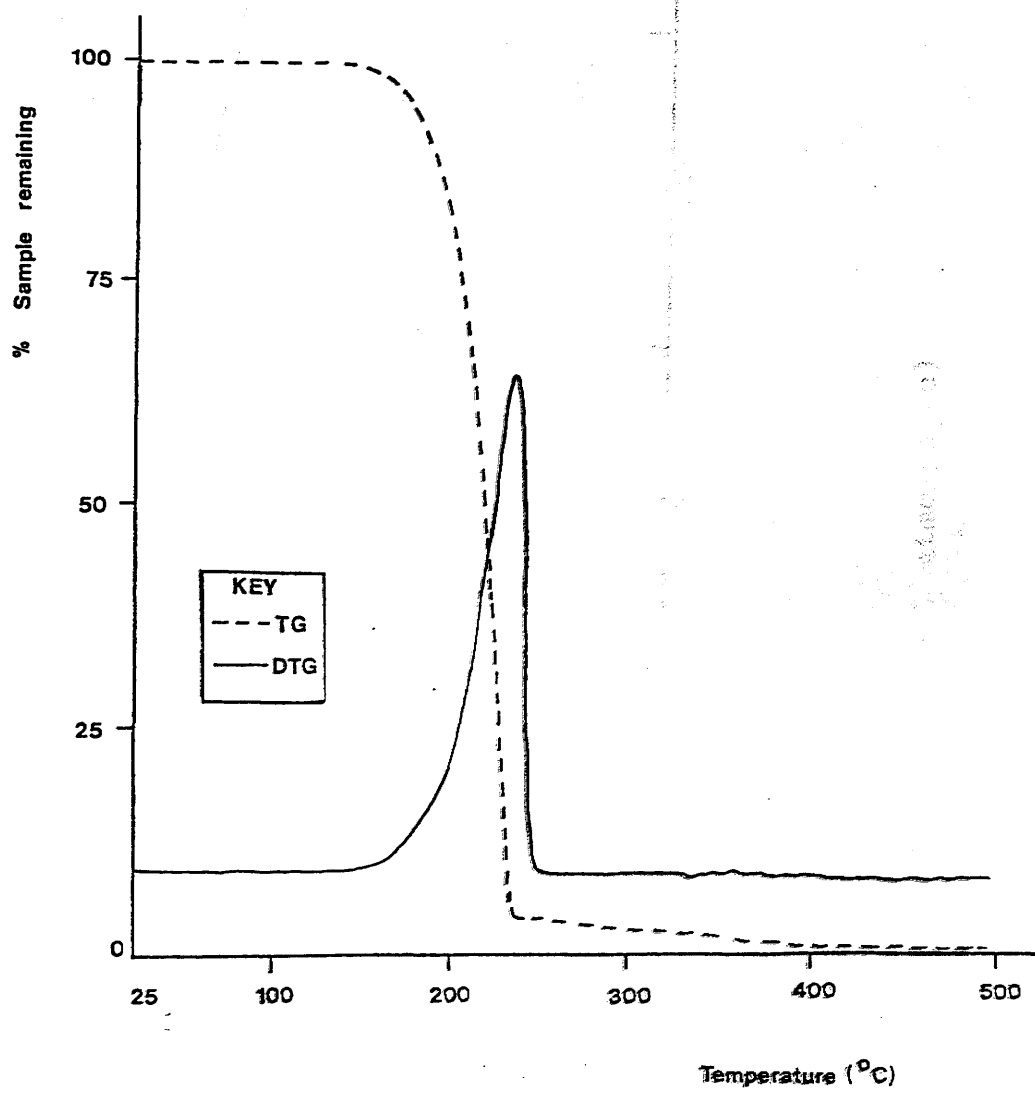


Figure 3.36 TG-DTG curves for $\text{Cu}(\text{acac})_2$ (N_2 atmosphere)

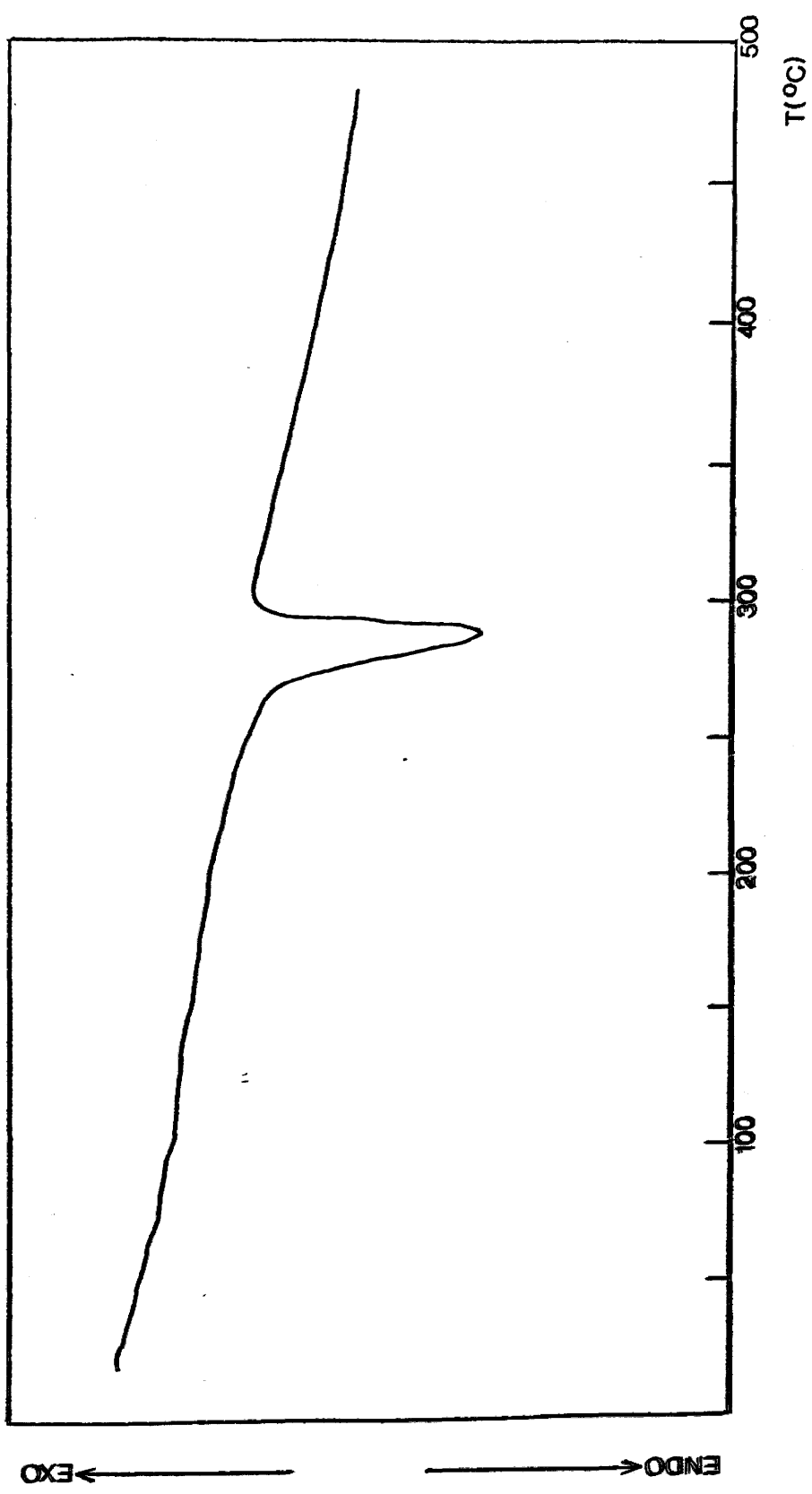


Figure 3.37 DTA curve for $\text{Cu}(\text{acac})_2$ (N_2 atmosphere)

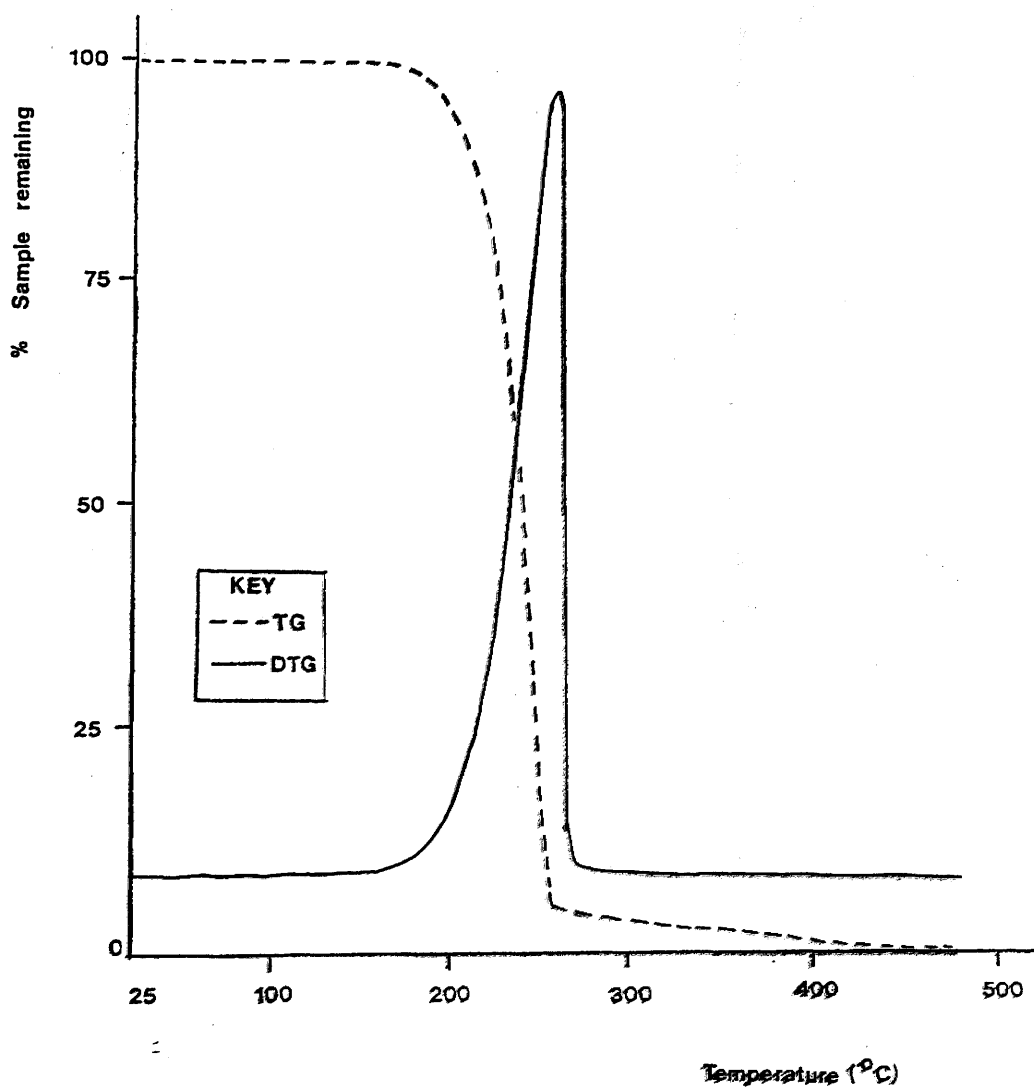


Figure 3.38 TG-DTG curves for $\text{Cu}(\text{acac})_2$ (air)

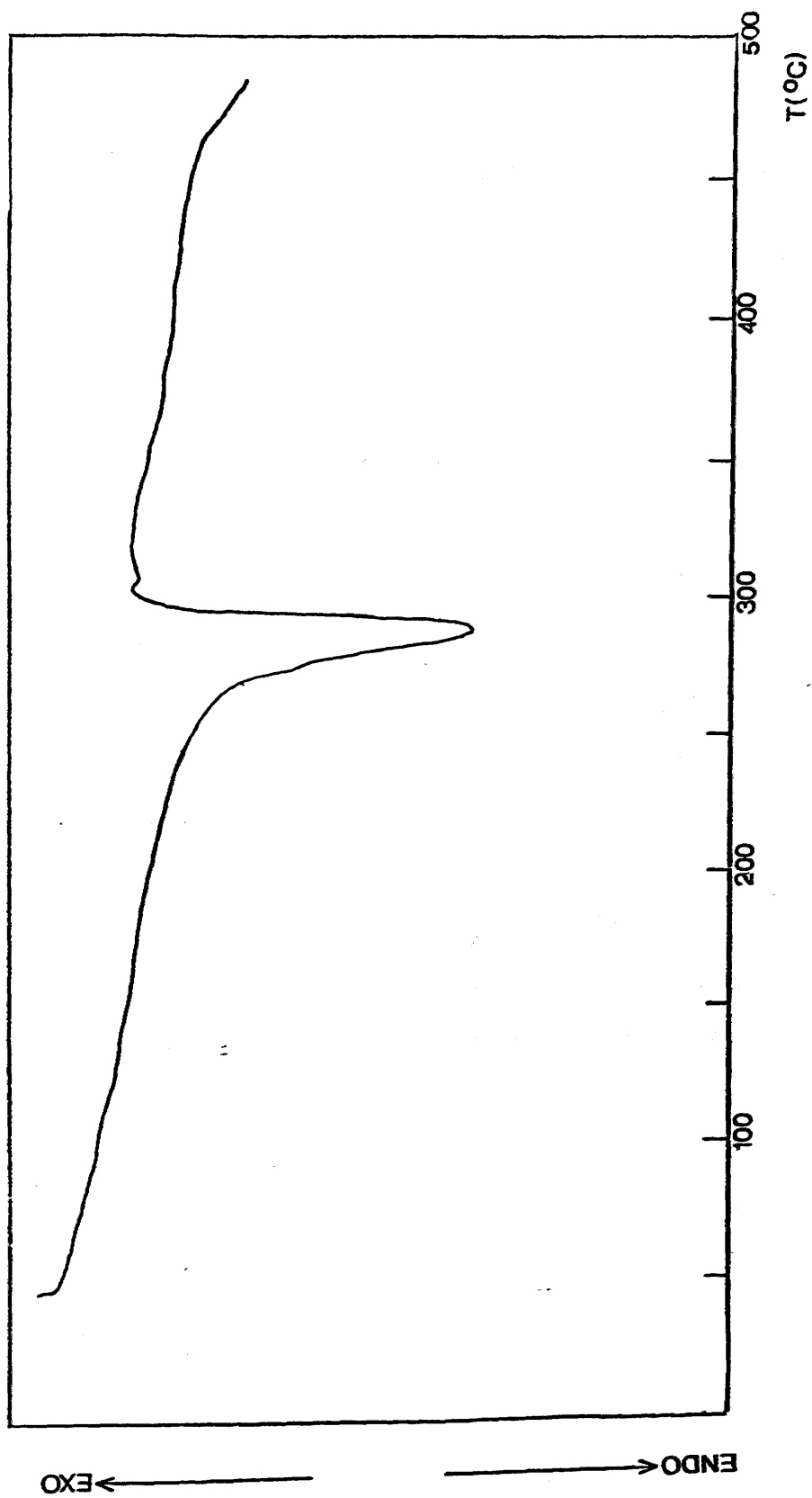


Figure 3.39 DTA curve for $\text{Cu}(\text{acac})_2$ (air)

flow of air (50ml min^{-1} , $10^{\circ}\text{C min}^{-1}$) is very similar to the DTA under nitrogen with a major endotherm with $T(\text{onset})$ 235°C and $T(\text{max})$ 290°C (Fig 3.39). The only difference is the presence of a small exotherm-endotherm pair after the main endotherm. This is in marked contrast to the exotherm pair recorded by Yoshida et al..¹¹¹

DEGRADATION OF $\text{Cu}(\text{acac})_2$ IN AN OPEN TVA TUBE

A sample of $\text{Cu}(\text{acac})_2$ (100mg) was heated in an open TVA tube in the manner described previously. Fumes were first observed at 154°C , rapidly becoming dense before ceasing by 406°C . Some material collected on the cold ring zone and this was identified by UV spectroscopy as $\text{Cu}(\text{acac})_2$. This supports the opinion that the initial weight loss recorded by TG is at least in part due to sublimation.

TVA BEHAVIOUR OF $\text{Cu}(\text{acac})_2$

Under TVA conditions $\text{Cu}(\text{acac})_2$ sublimes completely with sublimation first observed at 98°C . Microanalysis of the sublimate shows it to be pure $\text{Cu}(\text{acac})_2$. A very small peak (ca. 0.05mv) in the 0, -45, -75, -100 $^{\circ}\text{C}$ traces has $T(\text{onset})$ equal to $T(\text{sublimation})$ and is due to the evolution of trapped solvent.

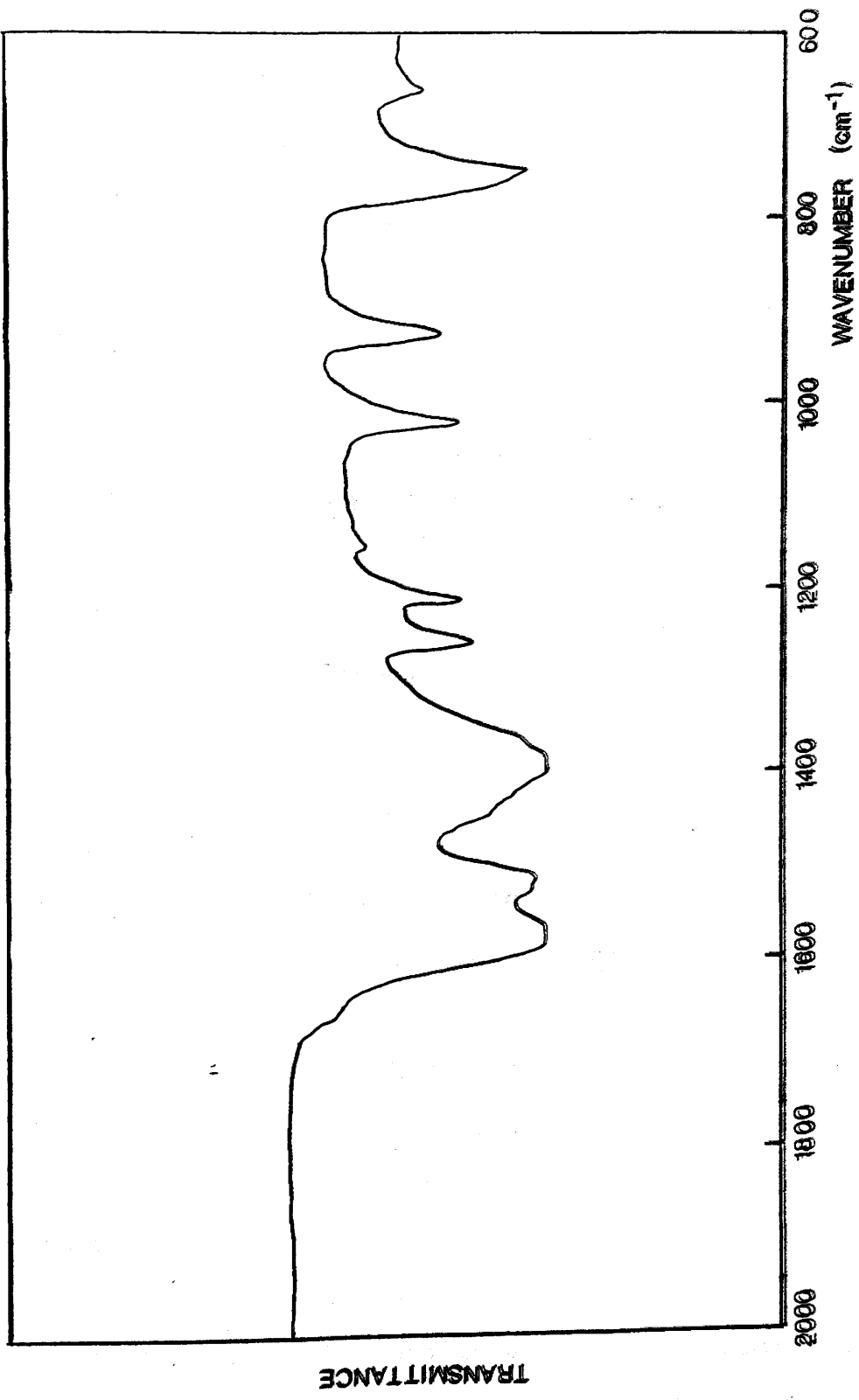


Figure 3.40 IR spectrum of residue from sealed-tube degradation of $\text{Cu}(\text{acac})_2$

DEGRADATION OF $\text{Cu}(\text{acac})_2$ IN A SEALED TUBE

Following the standard method, a 10mg sample of $\text{Cu}(\text{acac})_2$ was degraded in a tube sealed at 10^{-4} torr. Heating was at 262°C for 1 hour. Analysis of the volatile products by IR spectroscopy showed acetylacetone to be present. The solid residue consisted of metallic copper and maroon crystals. The IR spectrum of the crystalline material is reproduced in Fig. 3.40 and is similar to the IR spectrum of $\text{Cu}(\text{acac})_2$ (Fig. 3.5) although the latter lacks the broad absorption around 1100cm^{-1} .

INVESTIGATION OF $\text{Cu}(\text{acac})_2$ DECOMPOSITION - DISCUSSION

It has already been emphasised that the very nature of thermal degradation is such that the various thermal analysis techniques can provide not only complementary but also contradictory information. This is clearly demonstrated in the case of $\text{Cu}(\text{acac})_2$.

The DTA curves for degradation under nitrogen obtained by Yoshida et al.¹¹¹ and in this work are in close agreement, although that obtained in this work has a rather lower T(onset) and is thus more in accord with the results of Charles et al.¹⁰⁵ It is difficult to compare the prolonged isothermal technique of Charles et al. with the programmed heating DTA which is necessarily less sensitive to small amounts of decomposition, and thus some discrepancies, particularly in T(onset) are expected. The lack of sensitivity to protracted

degradation has already been described in relation to the decomposition of $\text{Mn}(\text{acac})_3$.

The discrepancy between the DTA results of Yoshida et al.¹¹¹ and of this work in relation to the decomposition under air is more difficult to explain. It may be due to an atmosphere effect in which the freshly released acetylacetone effectively excludes air from the immediate environment of the sample preventing oxidation of the residue. This is a known problem with some forms of TG and DTA equipment,¹¹⁶ and the design of the sample holder employed in this work - a small glass tube sealed at one end and of length 28mm and internal diameter 3mm - could well give rise to such an effect. That such an effect seems not to have influenced the DTA under air of the $\text{Mn}(\text{acac})_2$ produced from $\text{Mn}(\text{acac})_3$ may reflect both the nature of the gases evolved and the relative importance of the oxidation of the residue.

The design of the apparatus can also influence the sublimation behaviour of the sample. Nair et al.¹¹⁵ found no sublimation, and the endotherm system of the DTA curves seems to be due to decomposition rather than sublimation yet the open TVA tube experiment showed sublimation under atmospheric pressure to occur as low as 154°C , and this is paralleled by the size of the weight loss of onset 150°C , recorded by TG under both air and nitrogen atmospheres in this work. The isothermal sealed tube of Charles et al.¹⁰⁵ is the

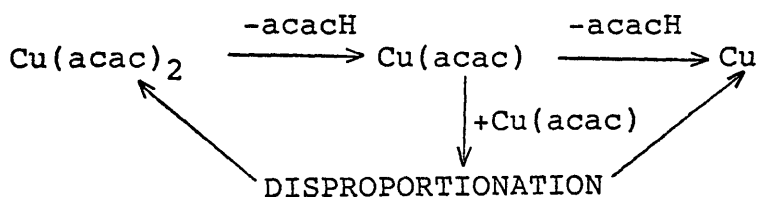
100

most sensitive of the techniques described here as regards detecting small amounts of degradation and as by this method only 2% of $\text{Cu}(\text{acac})_2$ was estimated to have decomposed after 50 hours at 191°C , it is unlikely that any of the weight loss below 190°C observed by TG is due to decomposition rather than sublimation. As the temperature increases above 190°C , decomposition will add increasingly to the weight loss.

Although Smith et al. did not identify sublimate,¹⁰⁸ in view of the evidence of the other techniques, it is possible that the T(onset) of degradation they quote is in fact the T(onset) of sublimation.

CONCLUSIONS

In the absence of sublimation, and in an inert atmosphere, $\text{Cu}(\text{acac})_2$ begins to lose acetylacetone above 190°C . This process continues until approximately 300°C with the final products being (in the absence of air) metallic copper and acetylacetone. By decomposing solely to the metal plus acetylacetone, $\text{Cu}(\text{acac})_2$ differs from the other chelates studied. The mechanism of the decomposition cannot be stated with any certainty on the basis of the data available but it is probable that both the simple stepwise release of the ligands and the slightly more complex disproportionation reaction are involved.



BLENDS OF POLYMERS WITH SMALL MOLECULES

The most important criterion to keep in mind when choosing a small molecule additive to modify the degradation behaviour of a polymer is its solubility in the polymer.⁶⁰ An additive which is soluble in the polymer at the required concentration will form a homogeneous one phase blend with the polymer. Such a blend is described as "compatible" and the additive is described as "compatible with the polymer". When an additive is not soluble in the polymer at the intended concentration the additive will not blend homogeneously with the polymer. Rather, a two phase system will result; the additive will dissolve in the polymer to the limit of its solubility - above this limit the excess additive may aggregate in discrete regions or may remain dispersed evenly, though heterogeneously, throughout the polymer matrix. In either case, the effectiveness of the additive will be diminished relative to the case where it is present in a homogeneous one phase system.

In general, an additive intended to alter the degradation properties of a polymer acts by interacting directly with the polymer chain or with the products of decomposition (eg small molecules, small radicals or macroradicals). In a heterogenous system, interaction with the chains will be prevented and any interaction with product species will be severely restricted by the need for the product to first diffuse across the phase boundary.

Thus, no matter how effective a modifier the additive may be, its usefulness will be limited by its ability to form a one-phase blend with the polymer. Indeed, an additive which forms non-compatible blends may in fact have an adverse effect on the polymer by reducing its physical integrity.

THEORY OF THE SOLUBILITY OF SMALL MOLECULES IN POLYMERS

Much work has been done on the sorption of gases and vapours by polymers, promoted in part by the increasing use of polymers for packaging and the hopes of using polymeric membranes for gas separation.^{117,118} Much less is known, however, about the solubility of solid additives in polymers, which possibly reflects the largely empirical methods employed in devising polymer-stabiliser combinations. Recently Billingham et al. have extended the Flory-Huggins theory of the mixing of liquids with polymers to encompass non-volatile solutes.¹¹⁹

For a small gaseous molecule the solubility in a polymer depends on the free energy of mixing ΔG_m . For a crystalline additive it is also necessary to take into account the free energy of fusion, ΔG_{fus} .

Now the Flory-Huggins theory¹²⁰ states that ΔG_m can be expressed by eqn. 1

$$\Delta G_m = RT [\ln \phi_1 + (1 - V_1/V_2) \phi_2 + \chi \phi_2^2] \quad (1)$$

where ϕ_1 , ϕ_2 are the volume fractions of additive and polymer respectively,

can be considered to be compatible. The presence of opaque or translucent regions is indication of phase separation.

Table 3.9 lists the compatibility of some of the blends studied. Blends with lower additive concentrations than those listed were also compatible. The precise limits of compatibility for the blends were not determined.

It would have been of interest to compare the relative incompatibility of $\text{Cu}(\text{acac})_2$ with respect to the other chelates in terms of ΔH_{fus} and T_m but as $\text{Cu}(\text{acac})_2$, in common with most of the other chelates, decomposes before melting, these values are not available. The compatibility of all the chelates with PMMA and PVAc is considerably less than that of CoBr_2 and ZnBr_2 which McNeill and McGuinness found to be compatible at salt:monomer unit ratios of 1:1.^{62,63}

Detailed analyses of blend structures are given in subsequent chapters.

CHELATE	PMMA		1:59 MAA-MMA		COPOLYMER		PVAC	
	COMPAT- IBLE	INCOMPAT- IBLE	COMPAT- IBLE	INCOMPAT- IBLE	COMPAT- IBLE	INCOMPAT- IBLE	COMPAT- IBLE	INCOMPAT- IBLE
Co(acac) ₃	1:50	1:10	1:50	1:10	1:50	1:10	1:50	1:10
Co(acac) ₂	1:50	1:10	1:50	1:10	1:50	1:10	1:50	N/A
Mn(acac) ₃	1:50	1:10	1:50	1:10	1:50	1:10	1:50	N/A
Mn(acac) ₂	1:50	1:10	1:50	1:10	1:50	1:10	N/A	N/A
Cu(acac) ₂	1:100	1:60	1:100	1:60	1:100	1:60	N/A	1:60

CHELATE	PS		PVC	
	COMPAT- IBLE	INCOMPAT- IBLE	COMPAT- IBLE	INCOMPAT- IBLE
Co(acac) ₃	1:50	N/A	1:50	N/A
Co(acac) ₂	1:50	N/A	1:50	N/A
Mn(acac) ₃	1:50	N/A	1:50	N/A
Mn(acac) ₂	N/A	N/A	N/A	N/A
Cu(acac) ₂	N/A	1:50	N/A	1:50

N/A - Not Ascertained

Table 3.9

Compatibility of Chelate - Polymer Blends

SOLUBILITY OF THE CHELATES IN COMMON SOLVENTS

One route to preparing additive-polymer blends and that followed here, is by the evaporation of a solution of the two components in a common solvent. It is thus of interest to have data on the solubility of the chelates in solvents which may be used in blend formation. Qualitative information on the solubility of $\text{Co}(\text{acac})_3$, $\text{Mn}(\text{acac})_3$ and $\text{Cu}(\text{acac})_2$ in a variety of solvents is included in Table 3.10.

SOLVENT	CHELATE		
	$\text{Co}(\text{acac})_3$	$\text{Mn}(\text{acac})_3$	$\text{Cu}(\text{acac})_2$
Acetone	Y	Y	Y
Chlorobenzene	Y	Y	OH
Chloroform	Y	Y	Y
Dichloromethane	Y	Y	Y
Diethyl Ether	Y	Y	N
Dimethylsulphoxide	Y	Y	Y
Ethanol	Y	Y	OH
Ethyl Acetate	Y	Y	N
Methanol	Y	Y	Y
Pet. Spirit (60°-80°)	N	N	N
Tetrahydrofuran	Y	Y	OH
Toluene	Y	Y	OH

Key Y = SOLUBLE
 OH = SOLUBLE ON HEATING
 N = INSOLUBLE

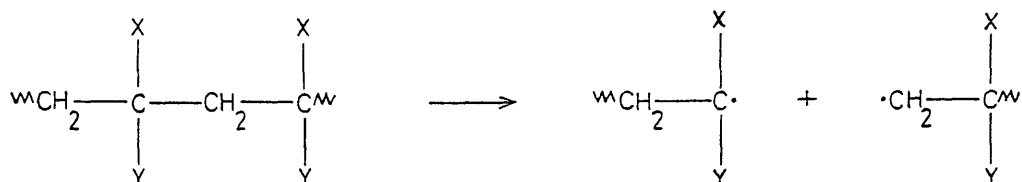
Table 3.10 Solubility of $\text{Co}(\text{acac})_3$, $\text{Mn}(\text{acac})_3$,
 $\text{Cu}(\text{acac})_2$ in Common Organic Solvents

CHAPTER 4

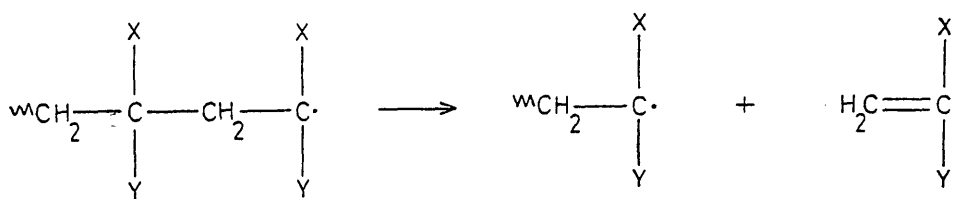
THERMAL DEGRADATION OF POLYMERS

INTRODUCTION

The thermal degradation of polymers in vacuo can be divided into two loose categories - main chain scission and substituent reactions.⁴⁸ Main chain scission, as the name suggests, involves the cleavage of a bond somewhere along the polymer backbone to produce macroradical species.



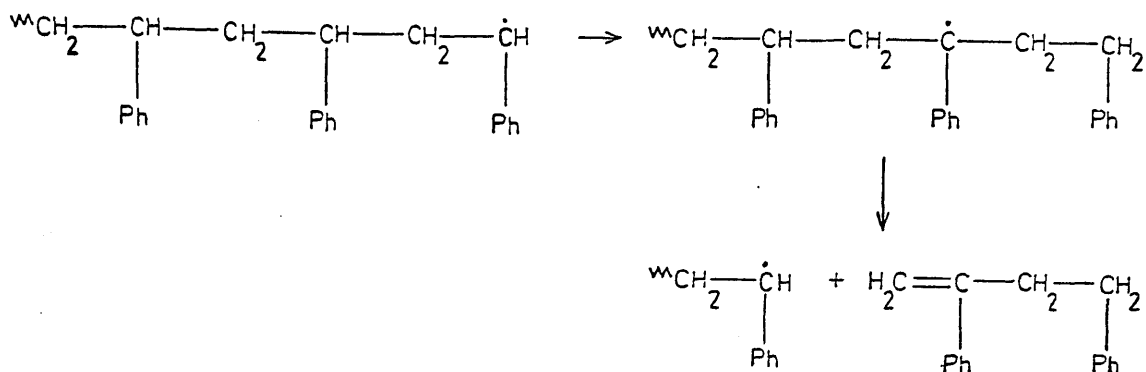
Once formed, a macroradical may react in a number of ways. Depolymerisation may occur with the stepwise regeneration of monomer.



This "unzipping" is favoured if the substituent groups X and Y stabilise the radical, either by an electron-withdrawing effect (e.g. polystyrene - X = H, Y = Ph) or by steric crowding (e.g. poly(methyl methacrylate) - X = CH₃, Y = COOCH₃). The presence

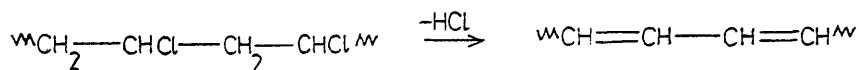
of an active α -hydrogen ($X = H$) allows hydrogen abstraction by a macroradical in a "backbiting" mechanism.

For instance, dimeric and trimeric products can be formed from polystyrene by this mechanism (see also later in this chapter).



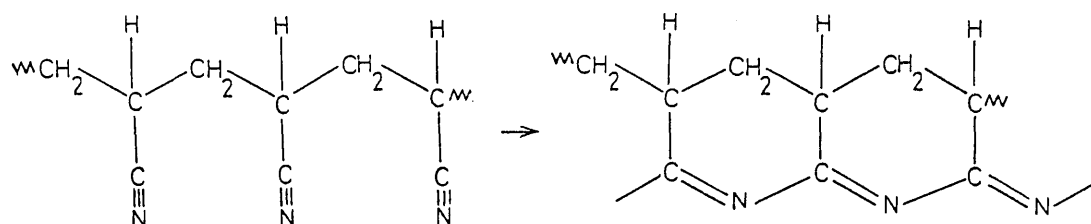
This reaction competes with the depolymerisation process and so the monomer yield from polystyrene is only about 40%. Eliminating the α -hydrogen as in poly(α -methyl styrene) increases the yield to almost 100%.⁴⁸

Reactions involving the side groups can be divided into three categories - elimination, cyclisation and decomposition. The archetypal example of an elimination reaction is the dehydrochlorination of poly(vinyl chloride).

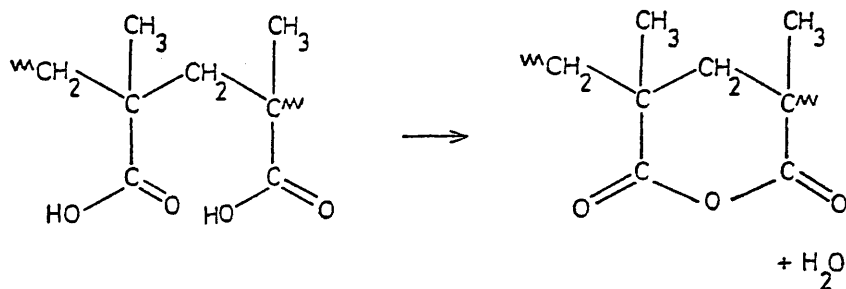


This reaction is discussed in more detail subsequently. Poly(acrylonitrile) provides the best known example of

substituent cyclisation reaction.¹²¹

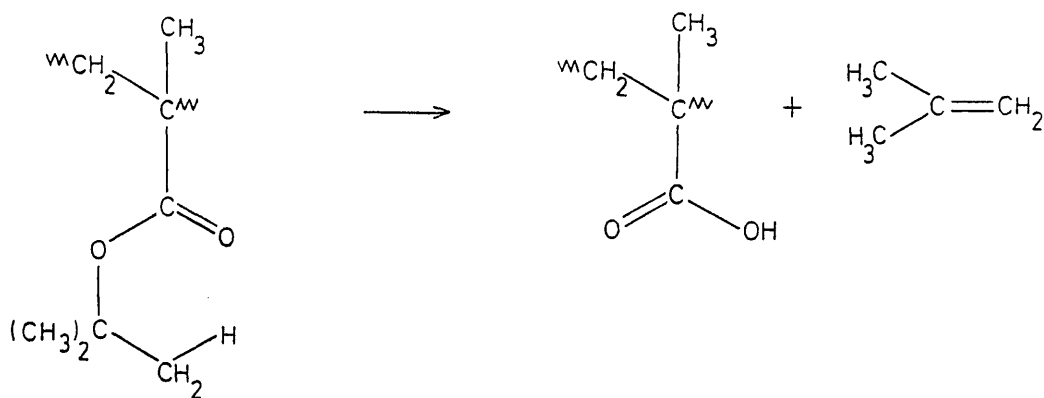


This reaction, which causes the discolouration of acrylic fibres is, however, of practical value, being of primary importance in the formation of carbon fibres. The cyclisation does not involve the release of volatile products but another cyclisation which does produce volatile material is that which occurs on the dehydration of poly(methacrylic acid), a reaction discussed in greater depth later in this chapter.



The corresponding intermolecular process causes cross-linking.

Decomposition of the side groups can occur, and an example is the ester decomposition of poly(*t*-butyl methacrylate)¹²²:-



Fragmentation of a polymer will occur at higher temperatures than the reactions just discussed and will produce a range of volatile products, from carbon monoxide and hydrogen to short sections of the polymer chain, with or without modification of the repeat structure. Fragments of polymer chain can also be evolved if the main chain scission occurs close enough to a chain end to produce a fragment short enough to be volatile at the degradation temperature.

It can thus be seen that the thermal degradation of polymers can produce a range of products. Structural changes may occur within the polymer with or without the release of volatile material. Volatile products may be volatile only at the degradation temperature or may be volatile at ambient temperature but not at reduced temperatures whilst some such as carbon monoxide, hydrogen and methane may be volatile even at liquid nitrogen temperature (-196°C). Successful elucidation of polymer degradation mechanisms demands experimental techniques that allow for the identification of products

of such different volatilities. It is also necessary to follow the course of the degradation by monitoring weight loss or evolution of volatiles or by following structural changes. It follows therefore that no single technique can provide all the necessary data. However, as described in the previous chapter, the most versatile technique and that most frequently used within this study is Thermal Volatilization Analysis (TVA). Consequently, in the following sections in which the thermal degradation of the various polymers used in this research is described, the TVA behaviour is also discussed.

... random throughout the length of ...
 ... specific weak links" introduces ...
 ... Consequently the exact nature of ...
 ... behaviour depends on the means of prep ...
 ... prepared PMMA which does not ...
 ... degrades, in vitro, in a single ...
 ... the depolymerisation process being initiated purely ...
 ... chain scission mechanism.¹¹⁴ ...
 ... prepared PMMA does contain ...
 ... its thermal stability. ...
 ...²³ found an additional depolymerisation ...
 ... some 100°C lower than the random ...
 ... process. Observing that the amount of po ...
 ... if this also varied with the initial volu

POLY(METHYL METHACRYLATE) PMMATHERMAL DEGRADATION OF PMMA

The thermal degradative behaviour of PMMA was first investigated several decades ago and the basic mechanism described by Grassie and Melville has since been supported by several workers. Grassie and Melville¹²³ demonstrated that PMMA degrades predominantly by a main chain process - depolymerisation. The polymer undergoes scission somewhere along its length to produce macroradicals which then "unzip" in a reaction the reverse of polymerisation. In this fashion almost 100% yields of methyl methacrylate are produced. The scission can occur either at random throughout the length of the chain or at specific "weak links" introduced during polymerisation. Consequently the exact nature of the degradation behaviour depends on the means of preparing the polymer. Anionically prepared PMMA which contains no irregularities degrades, in vacuo, in a single step, the depolymerisation process being initiated purely by a random chain scission mechanism.¹²⁴ However, radically prepared PMMA does contain "weak links" which influence its thermal stability. Grassie and Melville¹²³ found an additional depolymerisation step occurring some 100°C lower than the random-scission initiated process. Observing that the amount of polymer degrading in this step varied with the initial molecular

weight of the sample (proportionately more low molecular weight polymer unzipping in the low temperature step), they proposed that the additional step in the radically prepared PMMA was due to the presence of unsaturated chain ends formed in the disproportionation termination process.

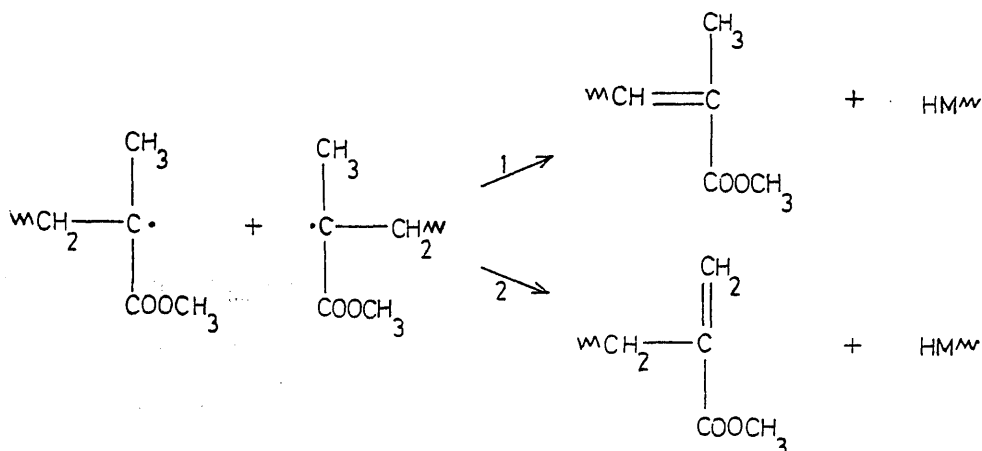


Fig. 4.1 Termination by Disproportionation of Growing PMMA Chains (Recent work¹²⁵ has shown route 2 to be the favoured path.)

The presence of an unsaturated linkage at the chain end results in the weakening (by approx. 80kJ mol⁻¹) of the C-C bond β to the double bond. This bond will thus cleave more readily than the other, unactivated, linkages and it is the cleavage of this weak link which initiates the lower temperature decomposition. As the molecular weight of the polymer increases, the relative number of chain ends (and weak links) decreases and this, combined with the tendency for the unzipping of the longer chains to terminated

before complete conversion of the chain to monomer, leads to the decreased importance of this process at high molecular weight. Although these mechanisms are sound, the effect of other possible weak links is ignored. Consequently, until recently the in vacuo thermal degradation of PMMA has been regarded as a two-step process, and although evolution of volatile material from PMMA had been observed at temperatures as low as 150°C , this had been attributed to the evolution of trapped precipitant.¹²⁴ In 1986, however, Kashiwagi et al., in a reinvestigation of the thermal behaviour of PMMA found evidence of an unzipping process occurring in just this temperature region.¹²⁶ They observed a weight loss occurring with $T(\text{onset})$ approx. 130°C , $T(\text{max})$ approx. 165°C , which, by analogy with oligomeric model compounds, they associated with unzipping initiated by the scission of weak links formed by the head-to-head combination of growing polymer chains during polymerisation. The weight loss for samples heated under a nitrogen atmosphere ranged from nil (anionically prepared sample) to 3% and 13% (radically prepared samples of m.wt. 176,000 and 44,600 respectively). Under an atmosphere of air the weight loss was nil due to an oxidative stabilisation mechanism. Samples prepared in the presence of a chain transfer agent (and thus having fewer such weak links¹²⁵) showed a reduction in the weight loss associated with this step. Although Kashiwagi et

al.¹²⁶ had no direct spectroscopic evidence for such head-to-head links, their results apparently provide strong support for their interpretation. A note of caution must be sounded in relation to the fact that these workers did not identify the evolved material, which they assumed to be methyl methacrylate. Although the absence of a weight loss in the presence of oxygen suggests that their samples were free from trapped volatiles, it is, in practice, very difficult to completely dry glassy polymers such as PMMA. As discussed below, this could influence their results. Further complications may arise from the fact that their samples were prepared at widely varying degrees of conversion, ranging from 7% to 79%. The high conversion polymers are particularly suspect. Polymerisation reactions at high degrees of polymerisation are complex and poorly understood; any number of abnormal structures (e.g. branching) may form and influence their results.

The TVA and TG curves obtained in the earlier stages of this project (see Figs. 4.5-4.7) were for PMMA samples cast as films from methylene chloride, in order to allow direct comparison with the blend films. Such curves show the evolution of considerable quantities of trapped solvent which limit their usefulness in the investigation of the possible head-head weak-link initiated depolymerisation. Thus, for comparison with the work of Kashiwagi et al. it was necessary to degrade PMMA in powder form and to take care in the

removal of any residual monomer, solvent or precipitant.

The PMMA samples (PMMA 1 and PMMA 2) were additionally reprecipitated from methylene chloride into petroleum spirit (60° - 80°) and dried for several days, at ambient temperatures, under vacuum. Finally, they were dried in the TVA apparatus at 10^{-4} torr at 80°C for 6 hours by which time no evolution of solvent or precipitant could be detected by the TVA Piranis. (Kashiwagi et al. dried their samples after purification by precipitation "in vacuo at 60°C "¹²⁶) Samples were then taken for TG and TVA as described below.

TVA DEGRADATION

Large samples (200 mg) of each polymer were degraded under TVA conditions to 180°C and the products collected for SAD analysis. For both PMMA 1 and PMMA 2 evolution of volatile material began between 90 - 100°C and was starting to tail off at 180°C (see Fig. 4.2). IR analysis of the SAD fractions showed that although methyl methacrylate was produced, much of the evolved material was petroleum spirit and some methylene chloride from the purification step, despite the lengthy drying process (see Fig. 4.3).

TG RESULTS

TG curves for the two samples (ca. 2.5 mg, $10^{\circ}\text{C min}^{-1}$, nitrogen atmosphere) are reproduced in Fig. 4.4. The % weight loss for PMMA 1 up to 200°C was

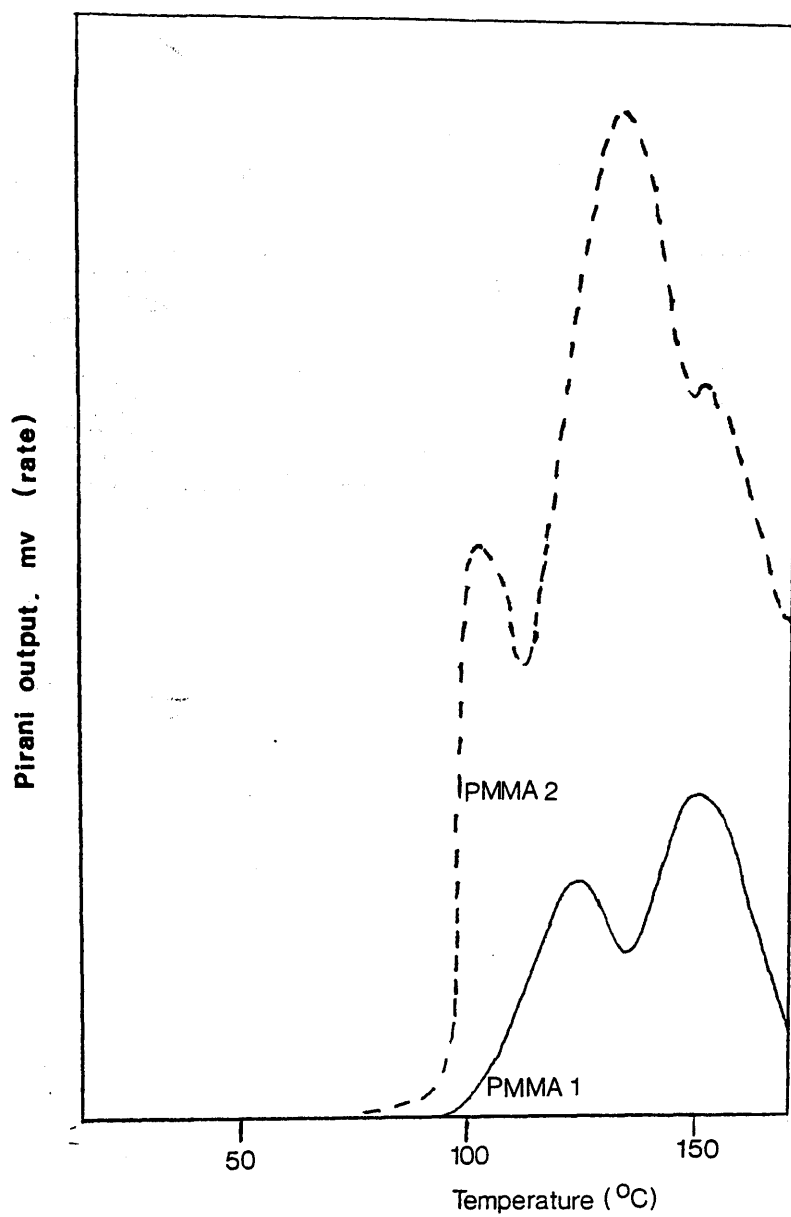


Figure 4.2
TVA curves (total products) for powder samples of
PMMA 1 and PMMA 2

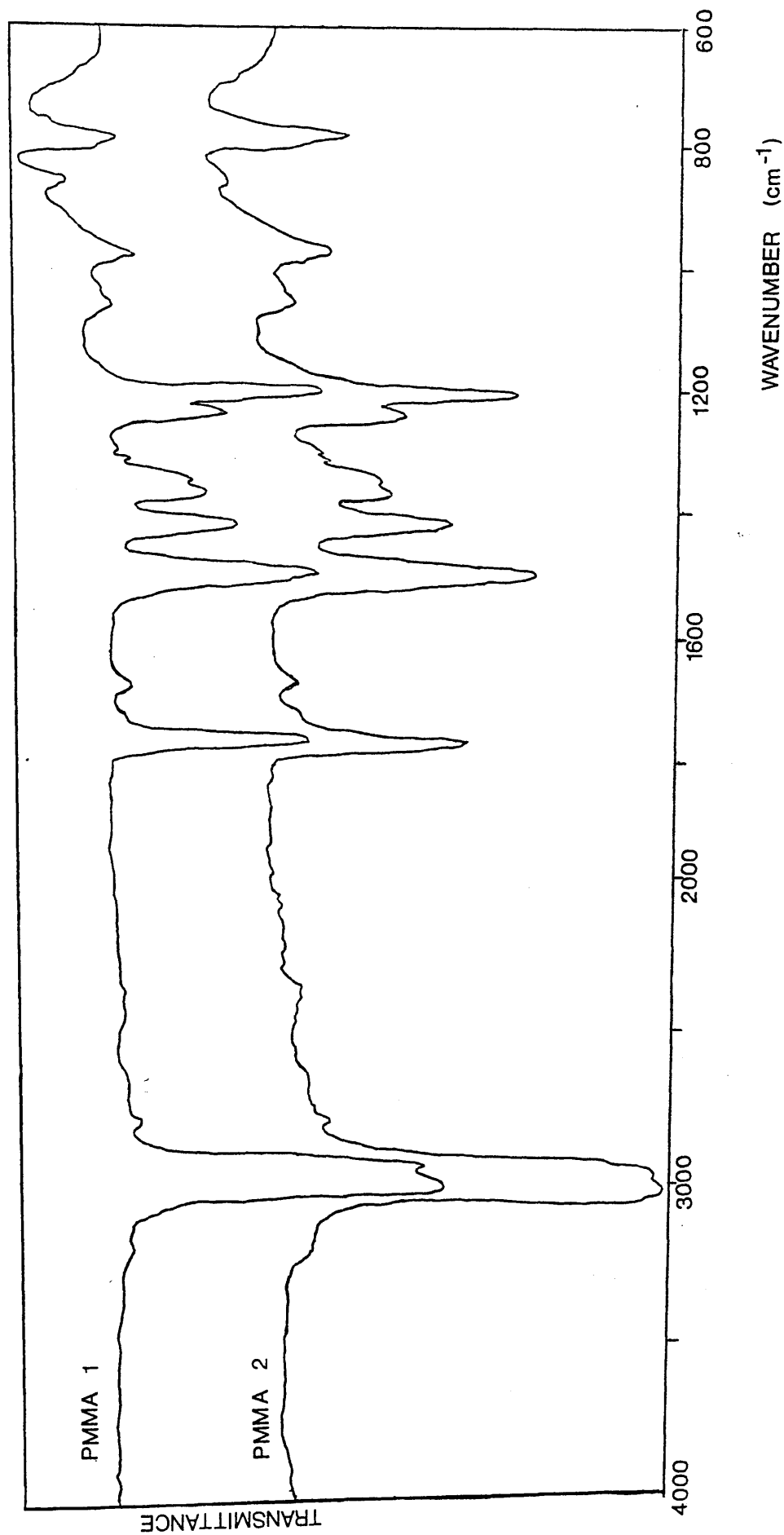


Figure 4.3 IR spectra of total products from PMMA 1 and PMMA 2 degraded to 180°C.

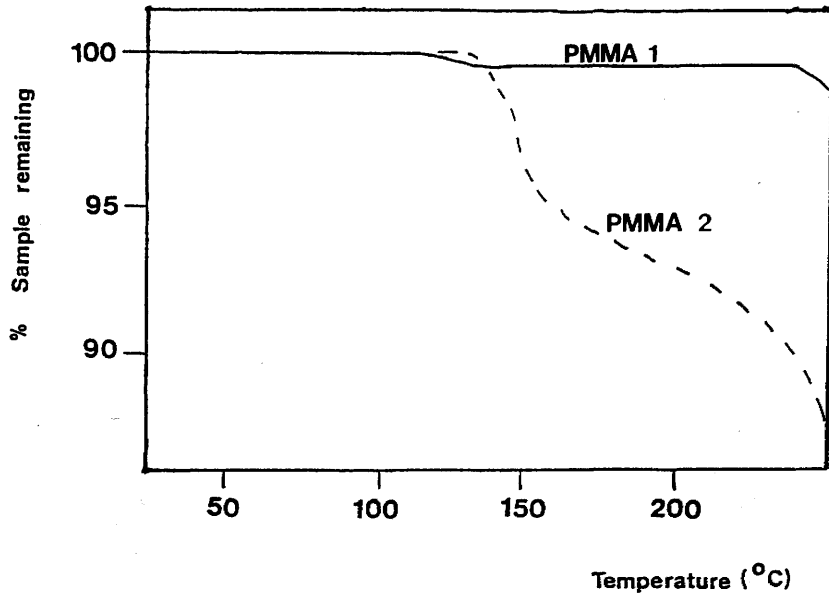


Figure 4.4
TG curves for PMMA 1 and PMMA 2 (N_2 atmosphere)

0.5%, and that for PMMA 2 to the same temperature 7%.

Kashawagi et al. recorded¹²⁶ a weight loss of 3% for a PMMA sample of approximately the same molecular weight as PMMA 2, the difference possibly being due to the presence of the petroleum spirit and methylene chloride in the sample of PMMA 2.

CONCLUSIONS

The identification of methyl methacrylate production below 180°C is consistent with the theory of Kashiwagi et al..¹²⁶ However, the presence of trapped petroleum spirit and methylene chloride from the purification step demonstrates the general difficulty in drying polymers, particularly below their glass transition temperatures. Although the evidence obtained here supports the theory of Kashiwagi et al. who themselves provide evidence for the existence of head-to-head weak links, it is perhaps significant that the weight losses, both observed here and reported by Kashiwagi et al., begin in the region of the glass transition temperature of PMMA, beyond which temperature evolution of trapped solvent and precipitant is facilitated. In the absence of identification by Kashiwagi et al. of the evolved material, it may be that the relative importance of the head-to-head initiated unzipping process (which almost certainly does occur to some extent) is exaggerated by the concurrent evolution of solvent and precipitant. This in fact demonstrates

nicely the point made in Chapter 2 that, when arriving at mechanisms of polymer degradation, it is unwise to rely solely on one thermal analysis technique.

PMMA SAMPLES USED IN THIS RESEARCH

TVA BEHAVIOUR

Figs. 4.5-4.7 illustrate the TVA curves obtained for the PMMA samples used in the study. Table 4.1 lists the origins of the three samples and Table 4.2 summarises the important features of the curves. All samples were degraded in the form of films cast from methylene chloride. The behaviour of the individual trap traces indicate that the initial peak is due mainly to the evolution of trapped solvent. Methylene chloride is non-condensable at -100°C but condensable at -196°C and the irregular shape of the peak is typical of the release of trapped solvent. It is in this region that the small weight-loss attributed¹²⁶ to depolymerisation initiated by the scission of head-to-head weak links occurs but the evolution of trapped solvent also occurs in the same region and masks any monomer evolution.

The effect of molecular weight on the degree of end-initiated depolymerisation is clearly reflected in the TVA behaviour, the decrease in height of the first degradation peak ($T(\text{max})$ $280\text{-}290^{\circ}\text{C}$) with increasing molecular weight being particularly noticeable. Both this peak and the final peak (due to the randomly

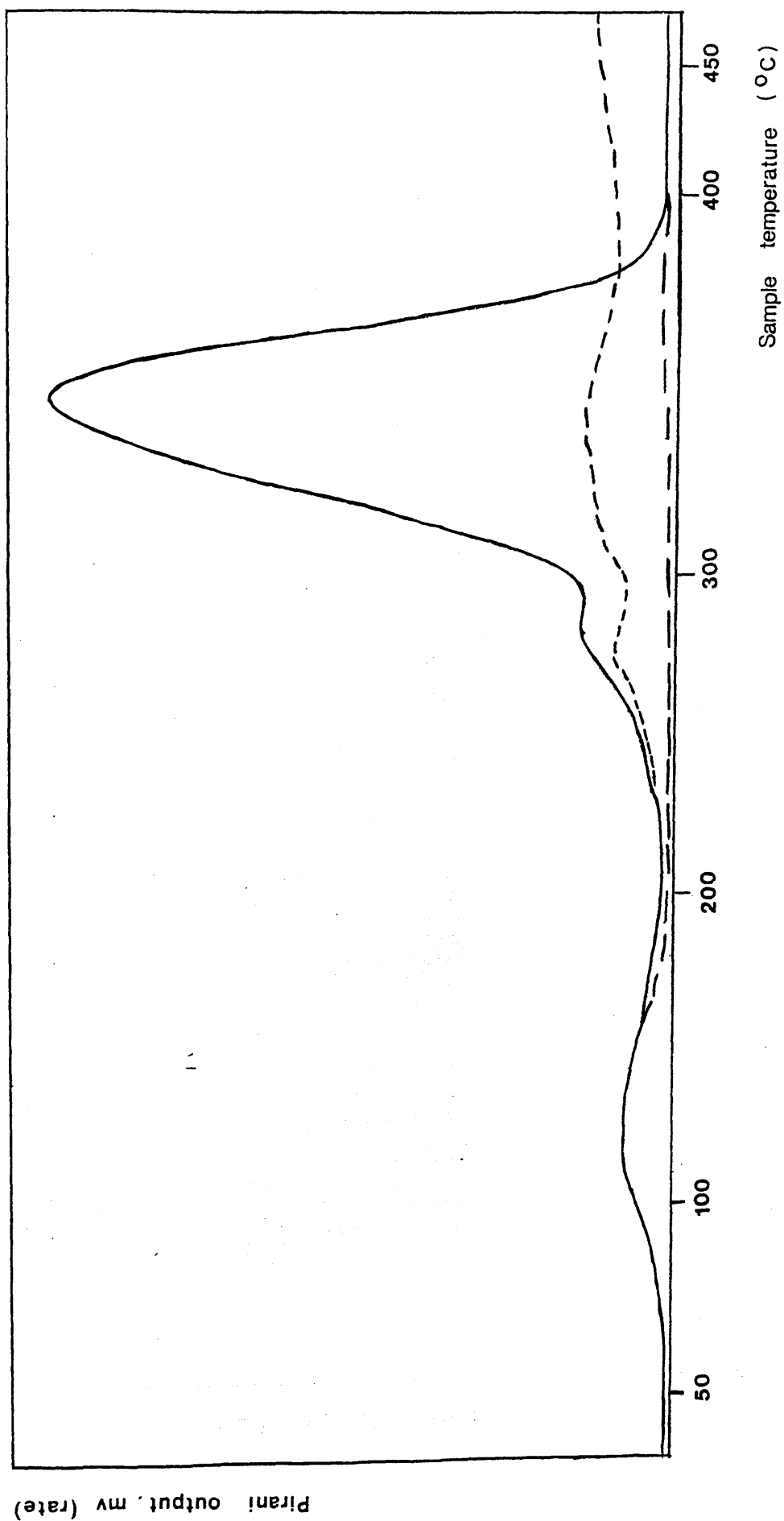


Figure 4.5 TVA curve for PMMA 1
(Film ex- CH_2Cl_2)

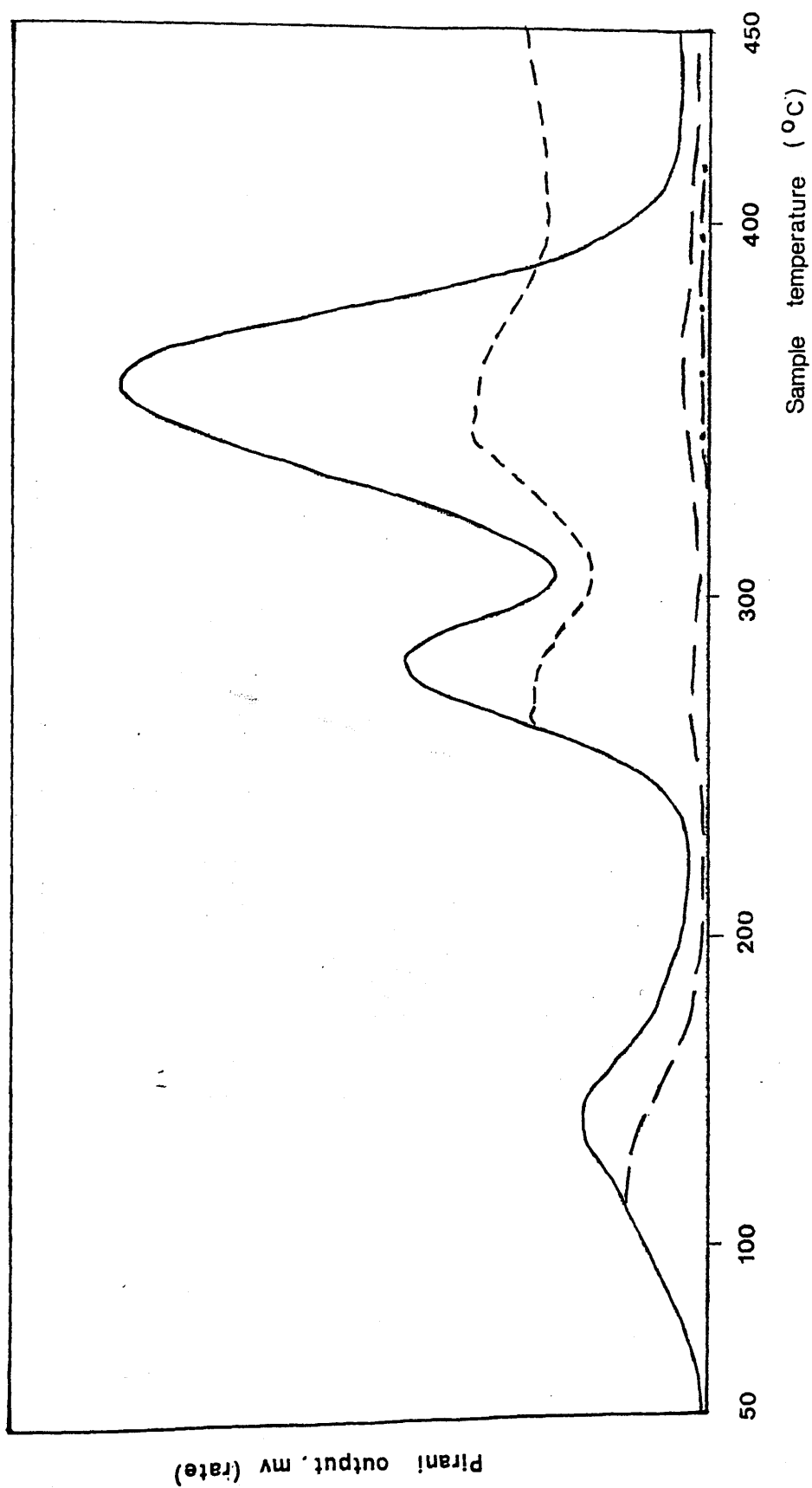


Figure 4.6 TVA curve for PMMA 2
(Film ex- CH_2Cl_2)

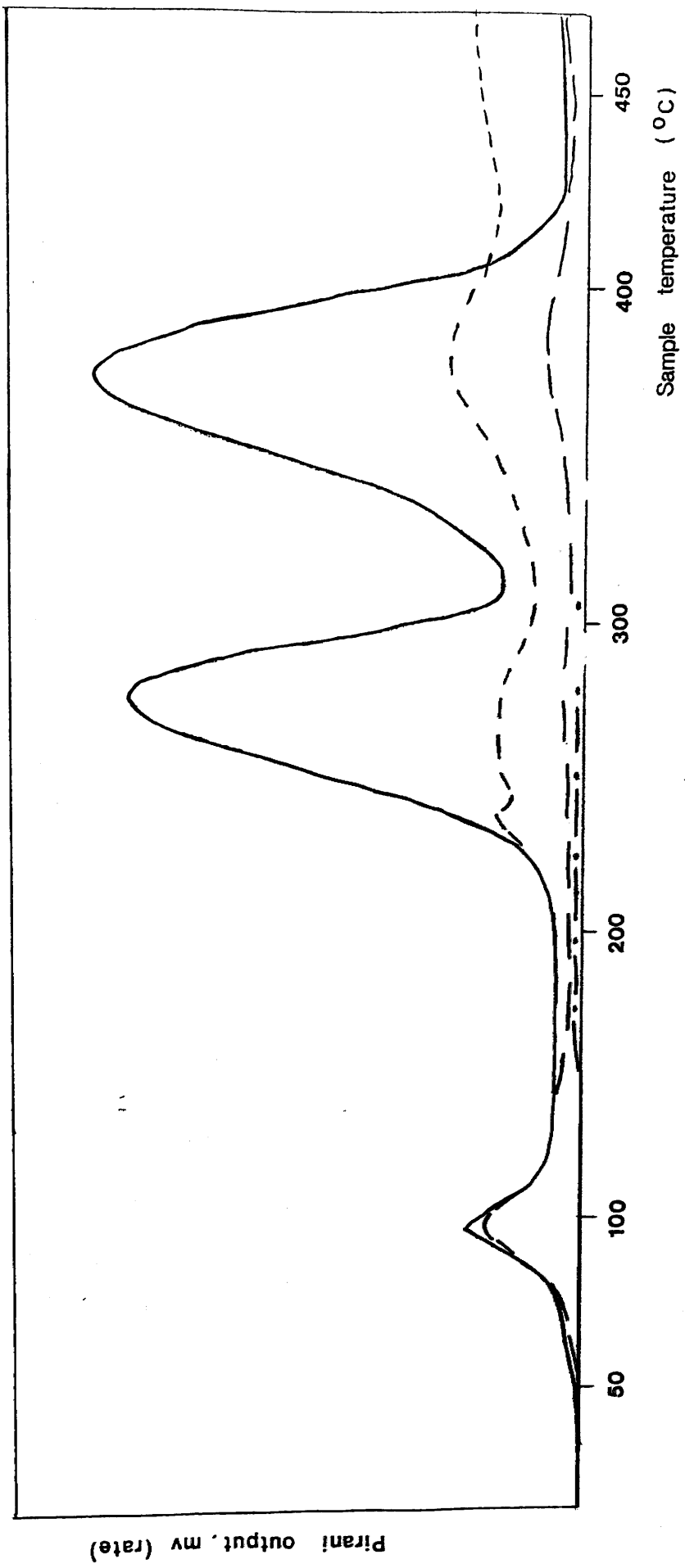


Figure 4.7 TVA curve for PMMA 3
(Film ex-CH₂Cl₂)

initiated depolymerisation of the polymer) demonstrate the "Limiting Rate Effect" on the -75°C trace. This behaviour, typical of methyl methacrylate,⁶⁸ is due to the fact that although methyl methacrylate condenses completely at -100°C and -196°C , at -75°C it condenses and redistills from the trap at a steady rate, keeping the -75°C trace at a constant height above the -100°C trace.

The behaviour of the -100°C and -196°C traces indicates that, as expected, production of high volatility, low molecular weight material is negligible.

TG AND DSC BEHAVIOUR

The TG curves for samples of PMMA 1 and PMMA 2 are shown in Figs. 4.8 and 4.9. The initial weight loss is due to the evolution of the solvent from which the films were cast (methylene chloride). Films rather than powder samples were employed to mimic the conditions under which the blends were prepared. Unfortunately, the weight loss due to solvent limits the usefulness of TG in this study.

The DSC curves for PMMA 1 and PMMA 2 are reproduced in Fig. 4.10. The initial endotherm is due to solvent evolution and later endotherm to the degradation processes. At this sensitivity, the second order glass transition cannot be detected.

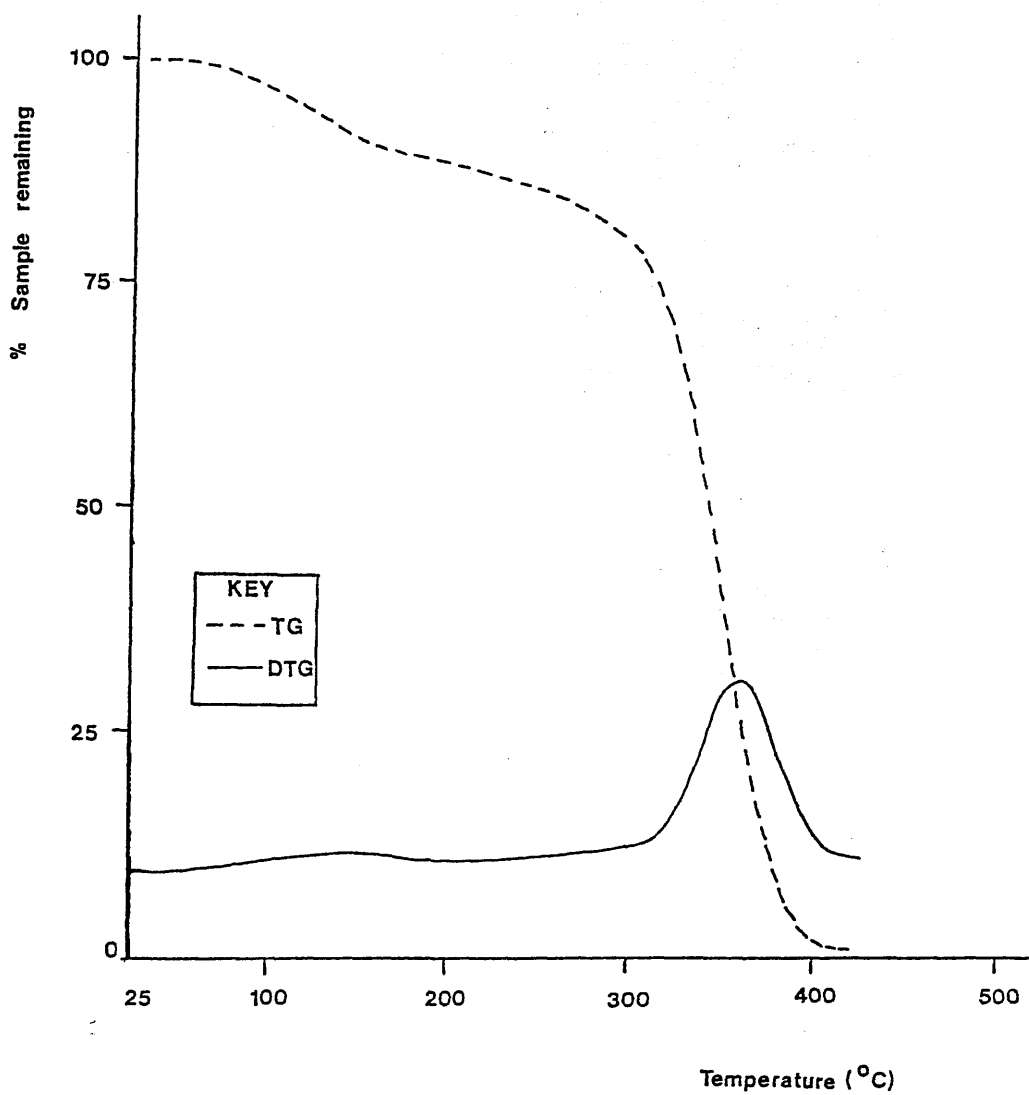


Figure 4.8 TG-DTG curves for PMMA 1, under nitrogen
(Film ex- CH_2Cl_2)

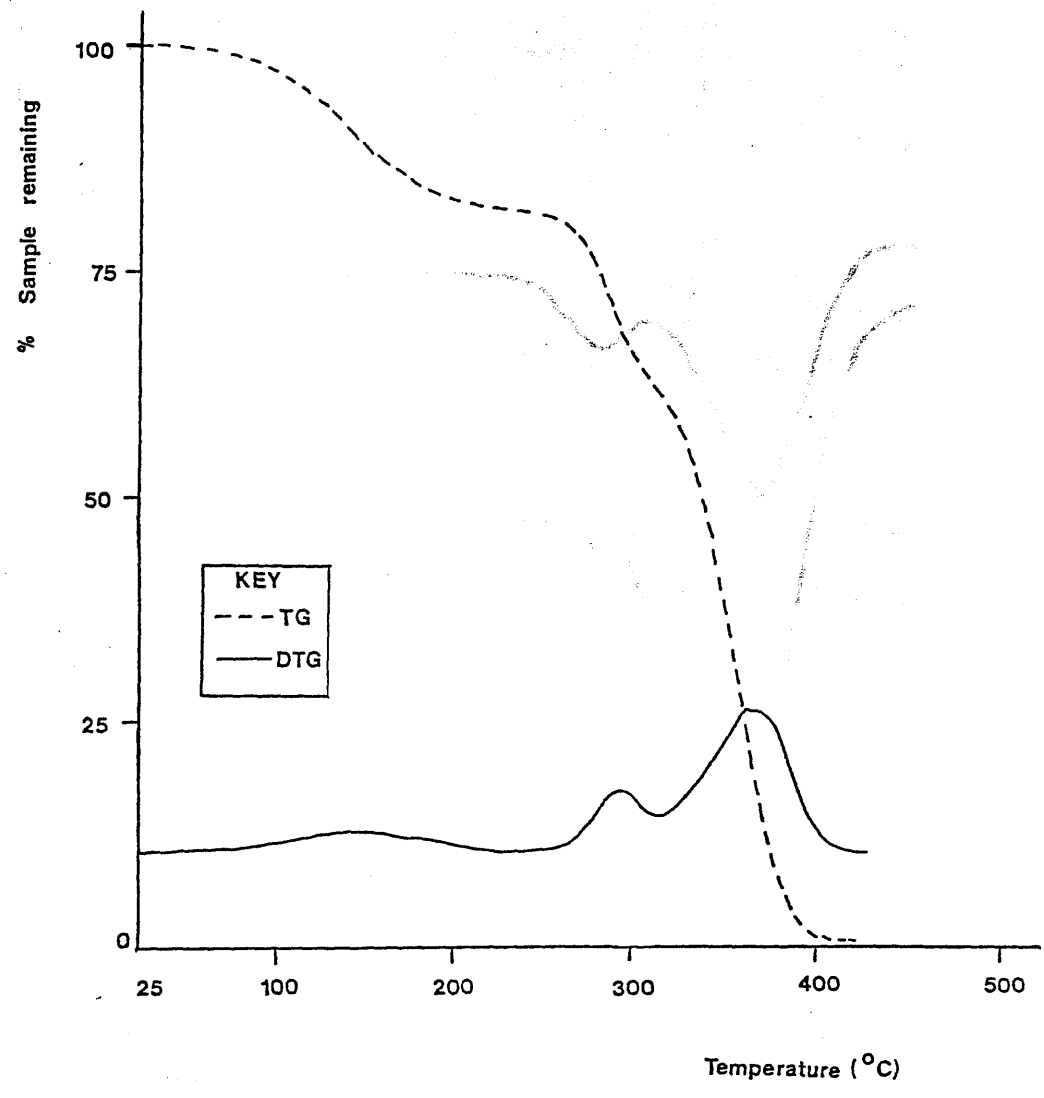


Figure 4.9 TG-DTG curves for PMMA 2, under nitrogen (Film ex-CH₂Cl₂)

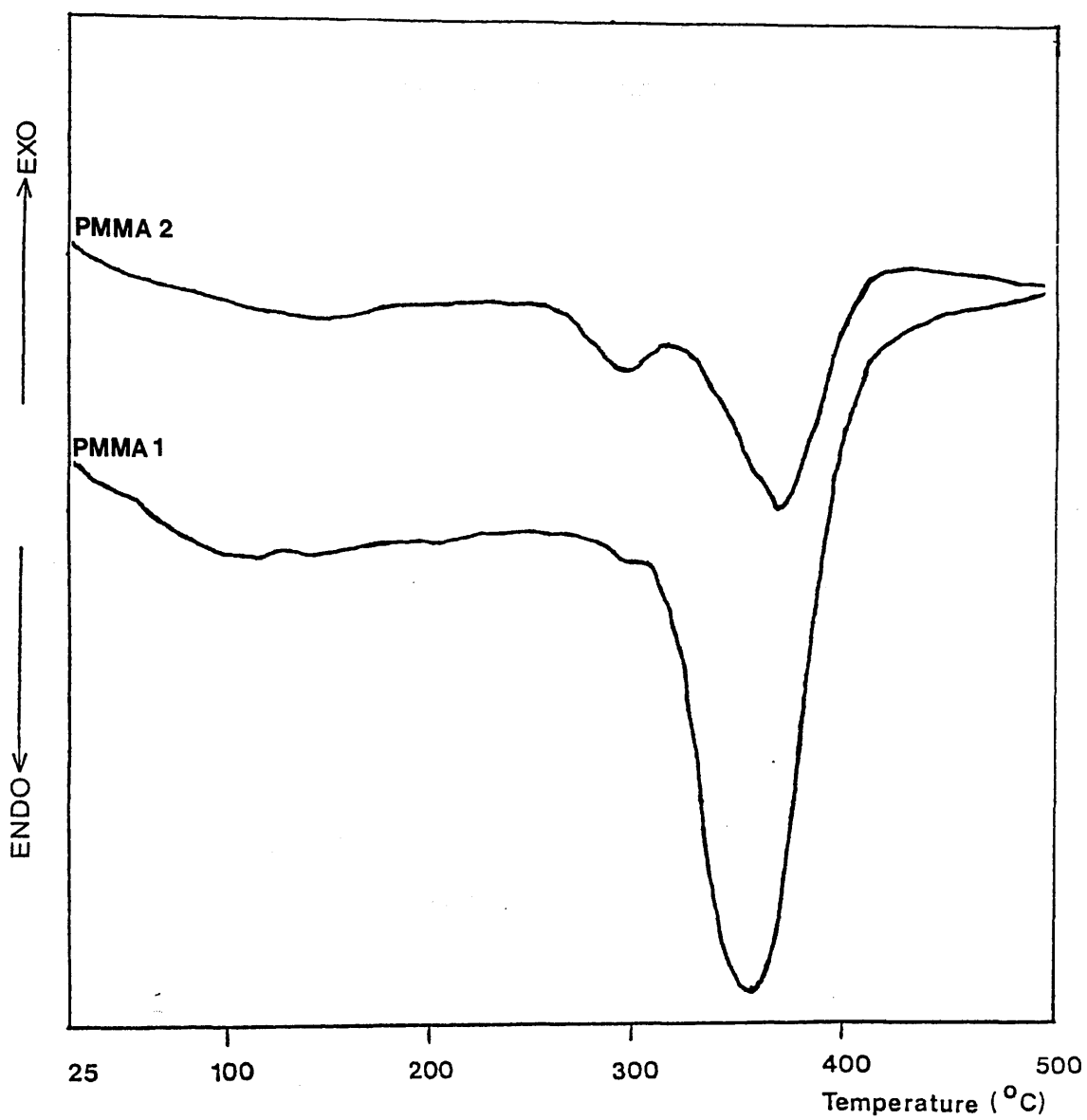


Figure 4.10

DSC curves for PMMA 1 and PMMA 2, under nitrogen
(Film ex- CH_2Cl_2)

<u>Sample</u>	<u>M.W.</u>	<u>Origin</u>	
PMMA 1	1,000,000	Bulk Polymerisation	*
PMMA 2	150,000	Aldrich High Molecular Weight	
PMMA 3	20,000	Bulk Polymerisation	**

* Prepared by Mr. G. McCulloch
 ** Prepared by Dr. M.J.A. Mohamad

Table 4.1 PMMA samples used in this research

<u>Feature</u>	<u>Sample</u>		
	PMMA 1	PMMA 2	PMMA 3
Initial Peak	50		200
	Largely solvent		
1st Degradation Peak			
T(onset)	208	217	246
T(max)	288	281	277
2nd Degradation Peak			
T(onset)	296	305	310
T(max)	353	356	373

Temperatures in °C.

Table 4.2 T(onset) and T(max) values from TVA curves of the PMMA samples used in this research

which irradiation was by the solution of 0.5% randomly along the chain. These bonds are weak C-C bonds and on heating it is found that

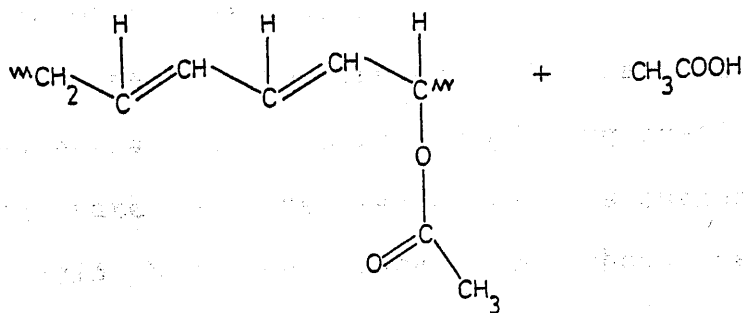
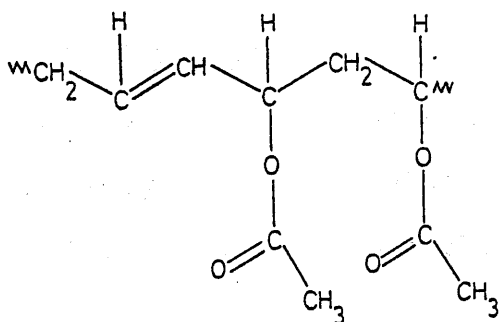
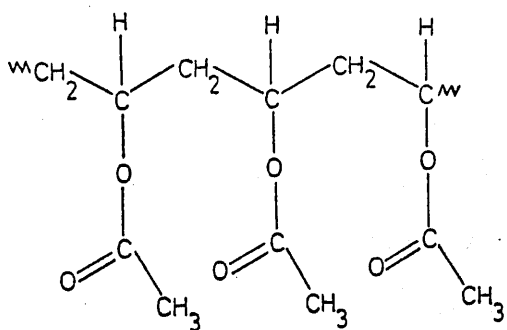
POLY(VINYL ACETATE), PVAcTHERMAL DEGRADATION OF PVAc

The thermal degradation of PVAc was first studied by Grassie^{127,128} in the 1950's, and although some aspects of his interpretation have been questioned by later workers, the general details are accepted.

The most important feature is the production of acetic acid in near quantitative yield, one acetic acid unit being produced from each monomer unit with formation of a double bond. Grassie viewed the reaction as being initiated at chain ends and propagating along the polymer molecule by allylic activation via a molecular mechanism. Grassie noted the formation of small amounts of other products - carbon dioxide, ketene, water - and although Servotte and Desraux failed to identify carbon dioxide or ketene,¹²⁹ Gardner and McNeill,¹³⁰ and Jamieson¹³¹ confirmed their presence in addition to carbon monoxide and methane, McNeill and Jamieson¹³² concluding that they were formed by decomposition of the acetate radical.

Servotte and Desraux¹²⁹ showed that the rate of deacetylation was independent of molecular weight, disproving Grassie's view that chain end initiation was involved. Madorsky¹³³ proposed a radical mechanism in which initiation was by the scission of C-O bonds randomly along the chain. These bonds are weaker than C-C bonds and on heating it is these bonds which break

first. This produces an acetate radical which then abstracts an H atom from the polymer backbone forming acetic acid and a double bond in the chain which activates the neighbouring ester unit.



Occasionally, abstraction may be from a neighbouring chain which can produce cross-linking. The conjugated polyene has been identified by Zimmerman¹³⁴ and by Gardener and McNeill¹³⁰ and Jamieson.¹³¹

Although Grassie had regarded the kinetic length of the elimination reactions to be equal to the degree of polymerisation, being stopped only by irregularities in the chain, Jamieson¹³¹ showed that the deacetylations continue only until the polyene sequences contains about twelve double bonds, beyond which the energy involved in the elimination of another acetic acid molecule outweighs the gain in energy associated with a more conjugated system.

TVA BEHAVIOUR OF PVAc

The TVA trace for PVAc (BDH Ltd), Mn 39,100, is shown in Fig. 4.11 and details summarised in Table 4.3. The sample, 27mg, was in the form of a film cast from methylene chloride.

The trace is similar to that obtained by McNeill⁶⁸; the low temperature peak is due to the evolution of trapped solvent.

Two peaks are present - the main peak is due to the deacetylation reaction producing acetic acid. The limiting rate on the -45°C trace is characteristic of acetic acid but the trace also shows that there are products non-condensable at -75° , -100° and -196°C . These are probably ketene, carbon dioxide,

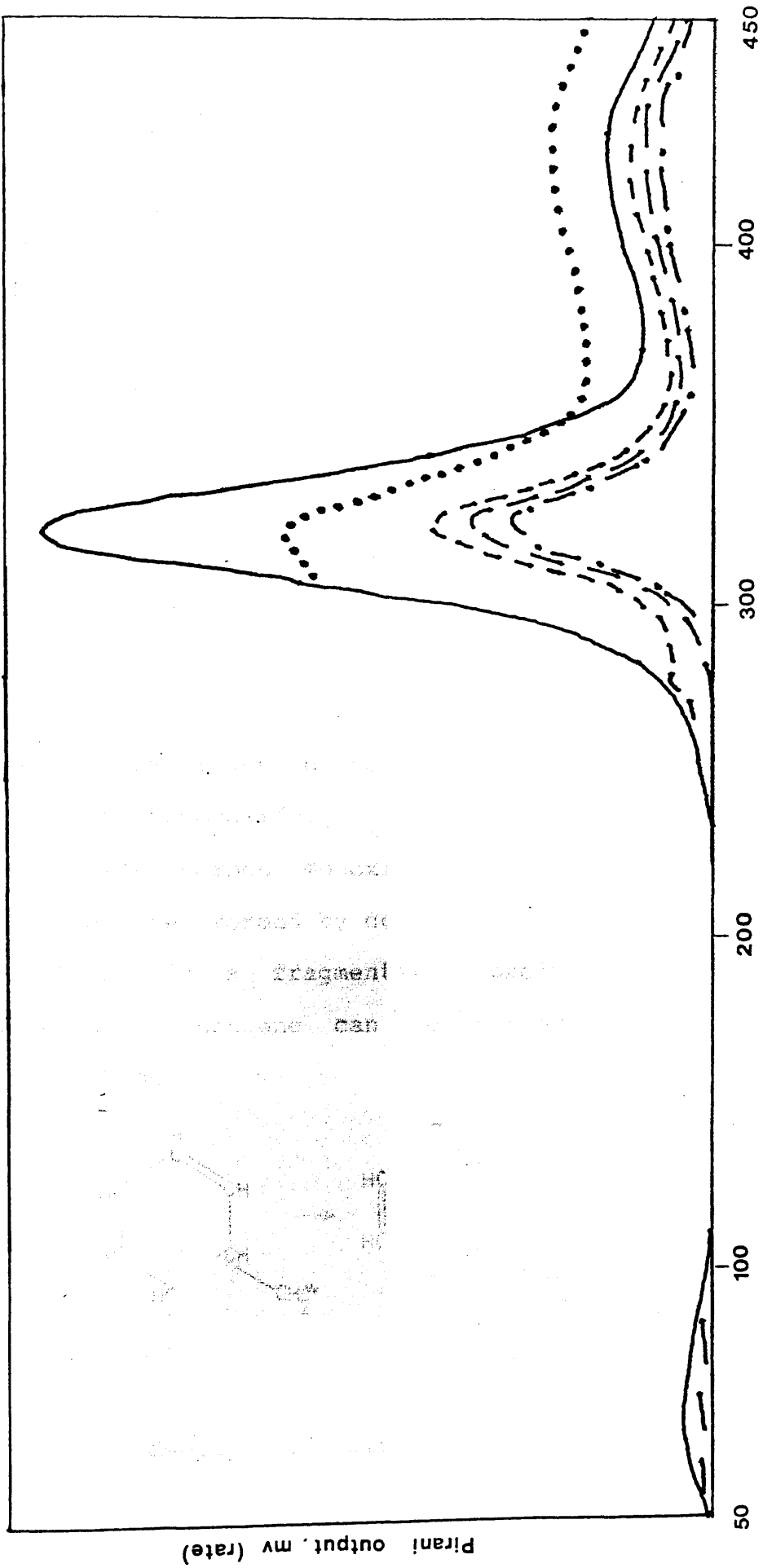


Figure 4.11 TVA curve for PVAC

water, methane and carbon monoxide.

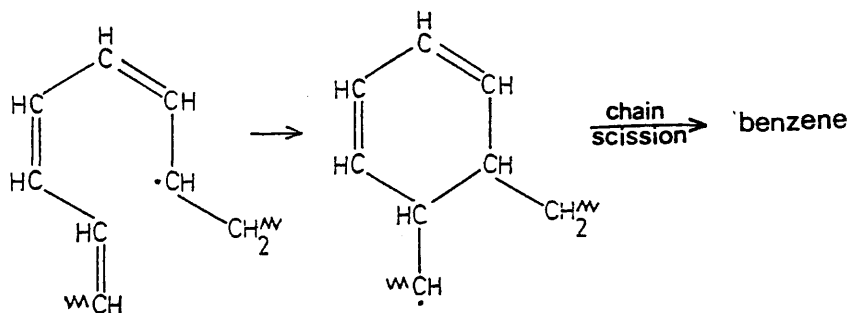
The second peak, due mostly to -196°C non-condensibles, is a result of fragmentation of the polymer backbone.

On completion of degradation, there was a highly coloured cold ring fraction and a carbonaceous residue.

PRODUCTS FROM TVA DEGRADATION OF PVAc

The -196°C condensible products were analysed by IR spectroscopy following separation by SAD. The major product was acetic acid, but ketene, carbon dioxide and benzene were also present. A trace quantity of but-1-ene was also identified. Although the -196°C non-condensibles were not analysed, previous work has shown this fraction to be predominantly methane with some carbon monoxide.

The carbon monoxide, carbon dioxide, ketene and methane are formed by decomposition of acetic acid, the but-1-ene is a fragmentation product of the conjugated backbone. Benzene can be formed by intramolecular cyclisation.



A deeply coloured orange CRF is also formed. An

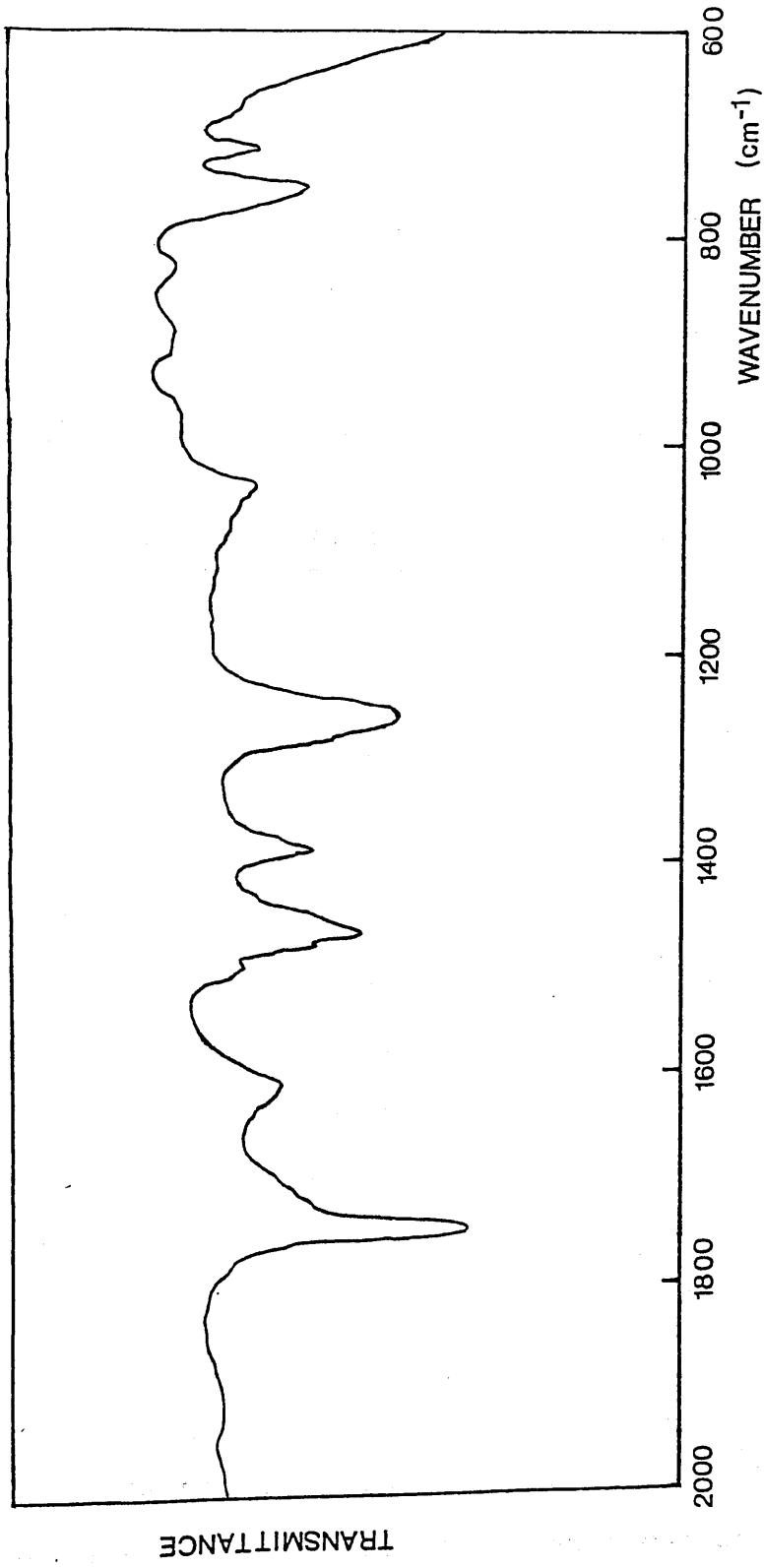


Figure 4.12 IR spectrum for CRF from PVAc

IR spectrum showed that it consists of chain fragments. A pronounced absorption at 1605cm^{-1} confirms the presence of unsaturation amongst the chain sequences (Fig 4.12).

The residue at 500°C is a carbonaceous char with no significant absorbances in the IR spectrum.

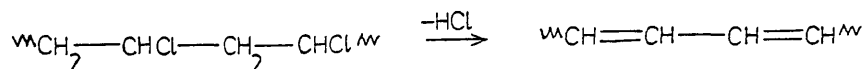
Deacetylation		Fragmentation	
T(onset)	T(max)	T(onset)	T(max)
221°C	328°C	375°C	435°C

Table 4.3 T(onset) and T(max) Data from TVA of PVAc

POLY(VINYL CHLORIDE), PVC

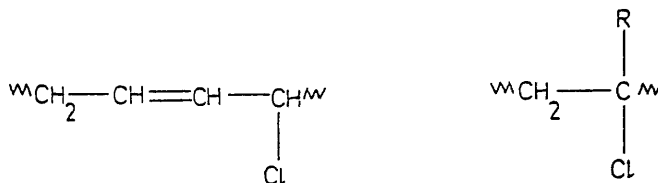
THERMAL DEGRADATION OF PVC

The thermal degradation of PVC occurs in two stages; the first step involves the dehydrochlorination of the chain:



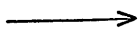
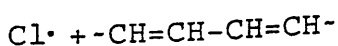
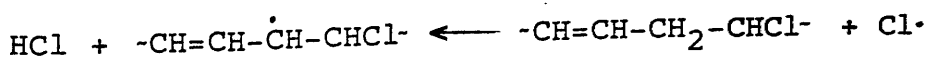
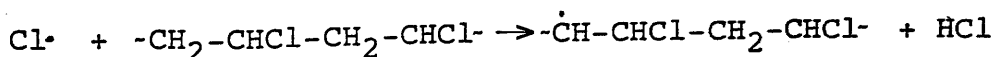
whilst at higher temperatures fragmentation of the highly unsaturated backbone occurs. Although the degradation of PVC has been the focus of considerable research,^{135,136} the mechanism of dehydrochlorination

has not been determined with any certainty, although there is a general consensus over the major features.⁴⁸ The dehydrochlorination reaction of PVC occurs at temperatures much lower than that of small model compounds and indeed occurs so readily that only the development of efficient stabilizers render PVC suitable for practical purposes. The ease of dehydrochlorination suggests that it is initiated at abnormal sites along the backbone. Several such structures have been suggested and on the basis of their low thermal stability and allylic and tertiary chlorines are among the favoured candidates:



Oxidised structures from reactions occurring during processing may also be significant.

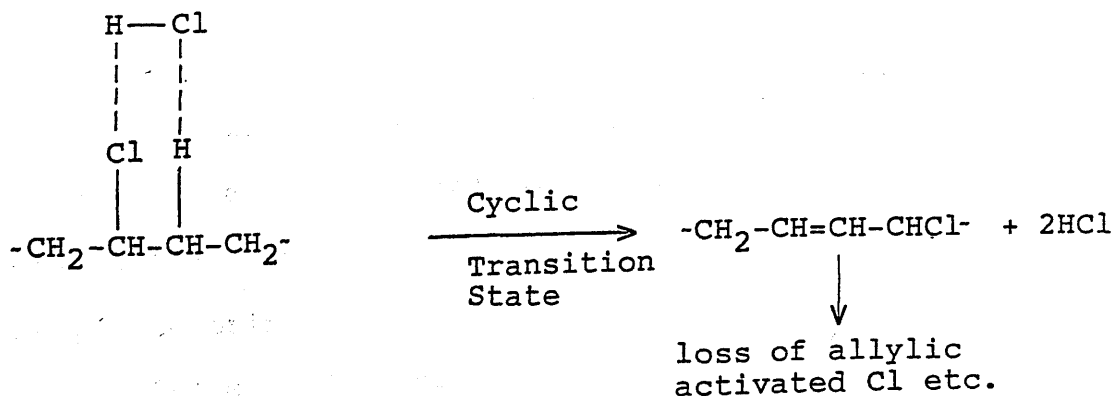
Initiation would involve the loss of a labile chlorine atom, $\text{Cl}\cdot$, which would proceed to abstract a hydrogen from the chain:



ETC.

The $\text{Cl}\cdot$ radicals react as they form with the neighbouring $-\text{CH}_2-$ unit, forming the conjugated sequences observed spectroscopically.

Although a radical mechanism is depicted above, molecular mechanisms have also been proposed, particularly as some features of the dehydrochlorination, such as its catalysis by HCl are not readily explained by a radical mechanism. Catalysis of the dehydrochlorination by HCl makes the process very dependent on sample form, for the easier it is for HCl to diffuse from the sample, the lower the amount of catalysis. This can affect even the very thin films used in TVA, a technique in which problems due to diffusion of product are usually minimal. Thus the catalysis by HCl lends another difficulty to the interpretation of the degradation. One molecular mechanism for the catalytic effect of HCl is shown below:



TVA BEHAVIOUR OF PVC

The TVA curves for four samples of PVC (British Geon's Breon 110, used as received) are reproduced in Fig. 4.13-4.16 and can be compared with that of Gardener and McNeill.¹³⁰ All samples were 25 mg and were cast from THF solution. THF is a poor solvent for TVA purposes, persisting in the film and outgassing until quite high temperatures, and the diffuse first peak of all the curves is due to the evolution of the solvent. The second peak, with coincident 0, -45, -75, -100°C traces is due to the evolution of the HCl associated with the dehydrochlorination process. Although all samples were the same size and cast in the same TVA tube, there are marked differences in the shape of this peak. This is presumably due to the catalytic effect of HCl and indicates that even very small changes in sample form can have a large effect on the overall dehydrochlorination. The final peak, due to the fragmentation of the backbone, has an associated -196°C non-condensable production, and does not vary from sample to sample.

Finally, there is shown in Fig. 4.17 the TVA curve of a 30 mg sample of Breon 110 in powder form to illustrate the effect of this sample form on the dehydrochlorination.

Table 4.4 lists the T(onset) and T(max) data for the major processes occurring in the first four samples. Due to the overlap of the solvent peak with the onset of the dehydrochlorination, T(onset) for this peak is determined from the -75°C trace.

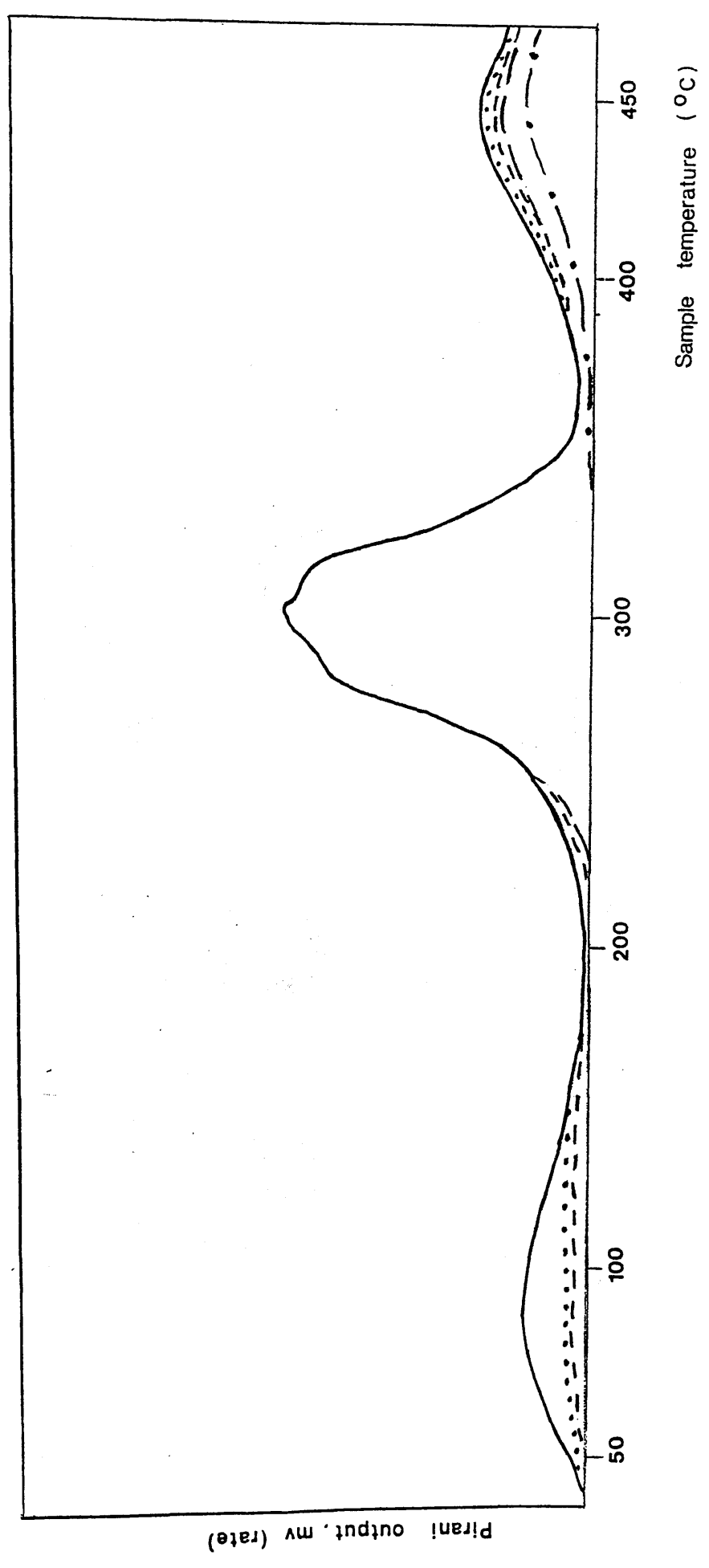


Figure 4.13 PVC sample 1

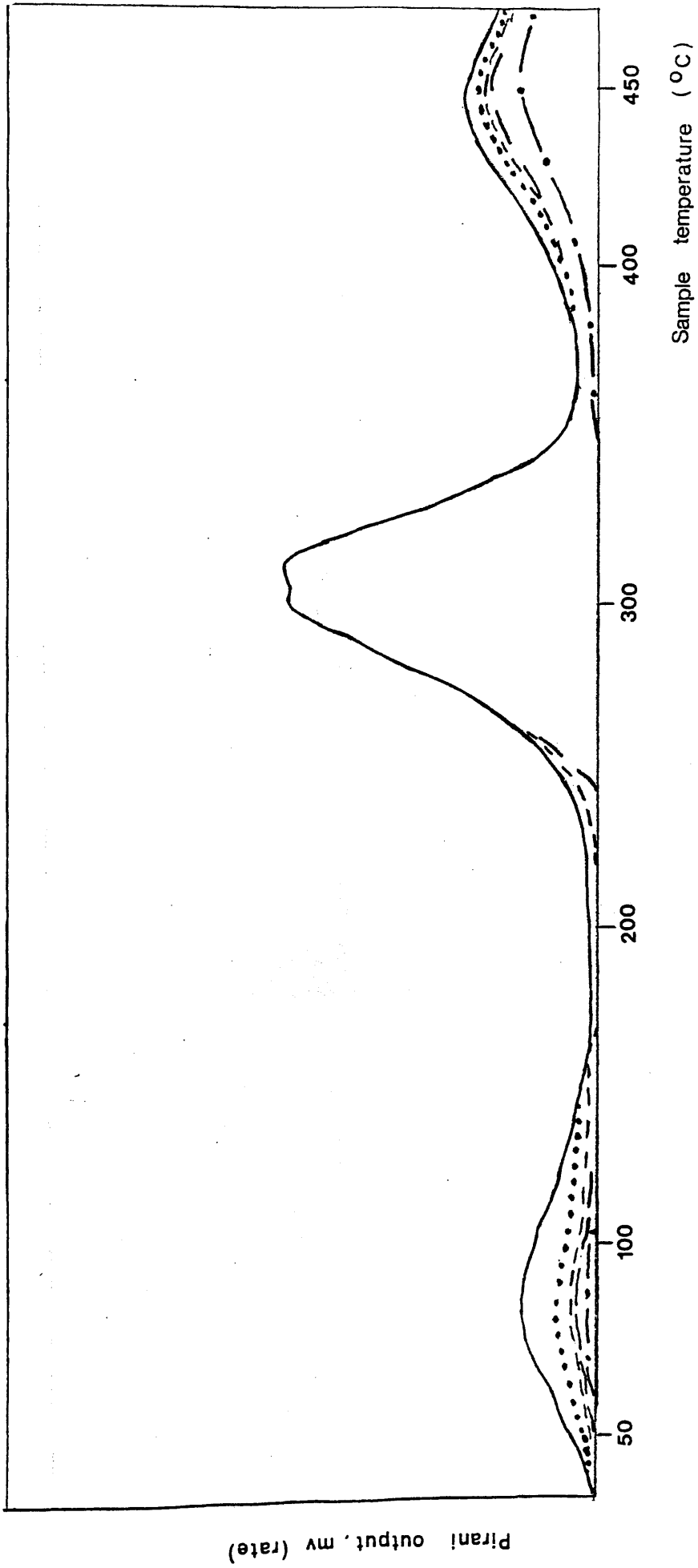


Figure 4.14 PVC sample 2

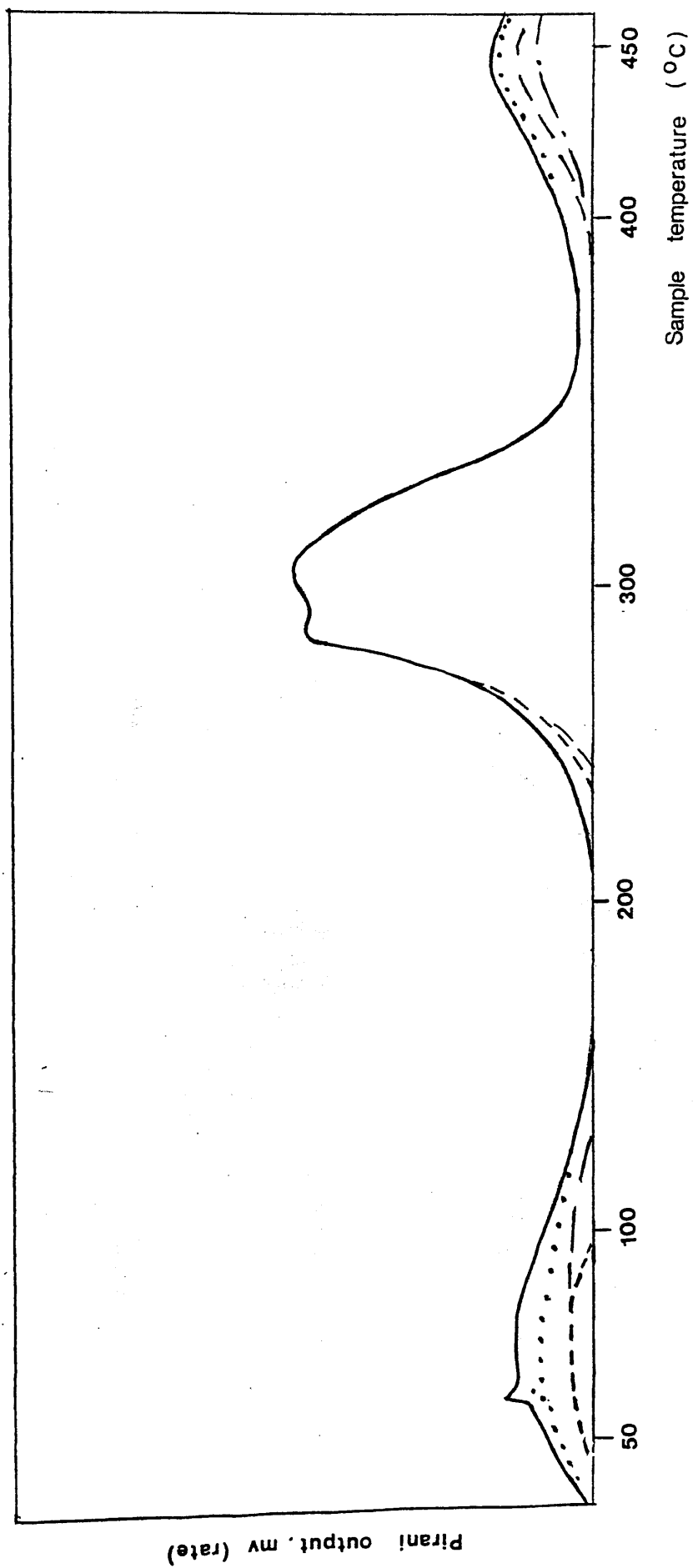


Figure 4.15 PVC sample 3

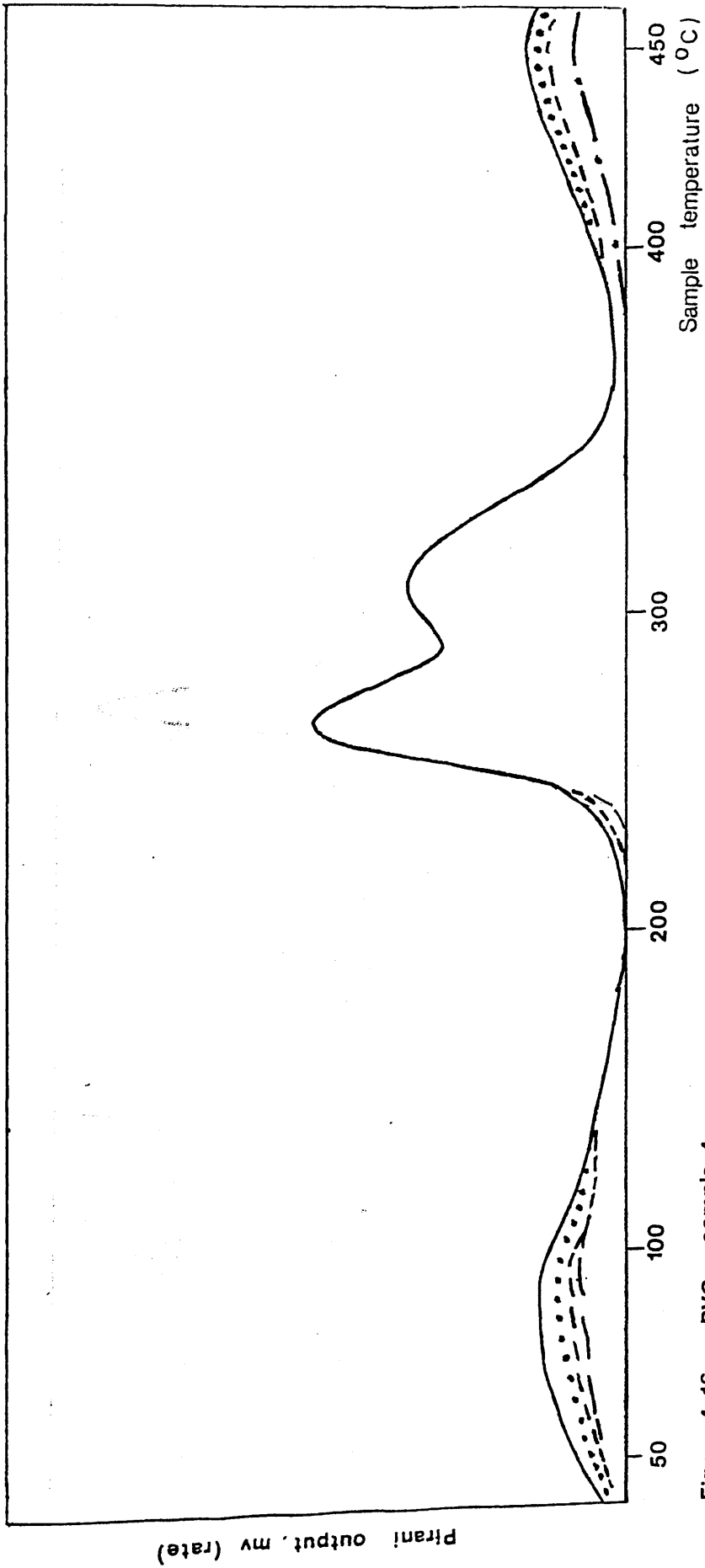


Figure 4.16 PVC sample 4

Figures 4.13 - 4.16 TVA curves for PVC
(Films ex-THF)

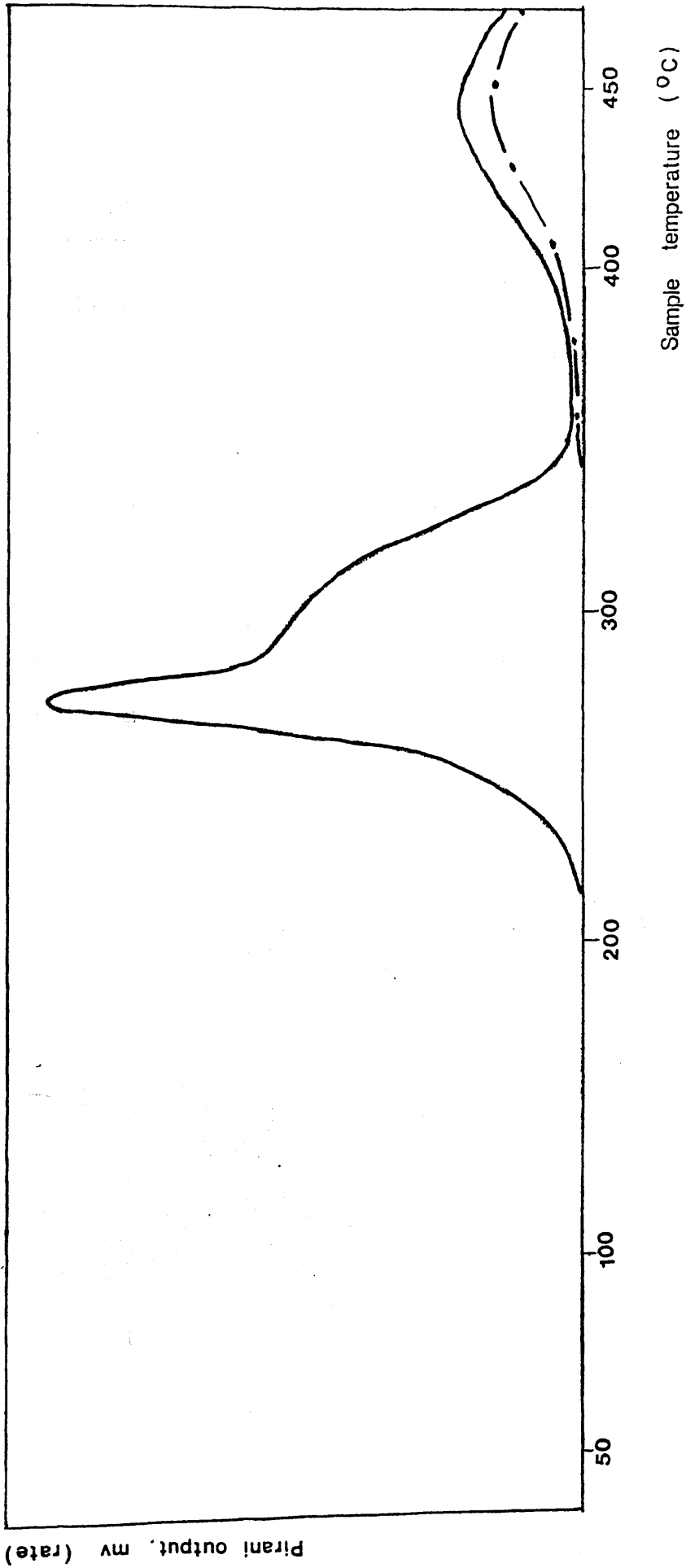


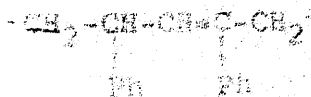
Figure 4.17 TVA curve for PVC (Powder sample)

PVC (Breon 110) Sample	Dehydrochlorination		Fragmentation	
	T(onset)	T(max) (°C)	T(onset)	T(max) (°C)
1	205	304	370	447
2	212	301-310	370	453
3	222	286, 307	374	444
4	215	268, 310	373	450

Table 4.4 T(onset) and T(max) Data for Breon 110 Film ex-THF

The residue from the degradation is a dark carbonaceous char and the cold ring fraction is a highly coloured resin, which IR analysis shows is highly unsaturated, resulting from fragmentation of the modified backbone.

and in this case the irregularities (due to results from oxidation.)

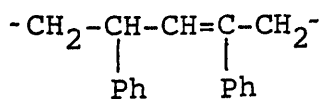


(I)

The higher temperature degradation involves the production of monomer by depolymerization. This unzipping is thought to be initiated

POLYSTYRENETHERMAL DEGRADATION OF POLYSTYRENE

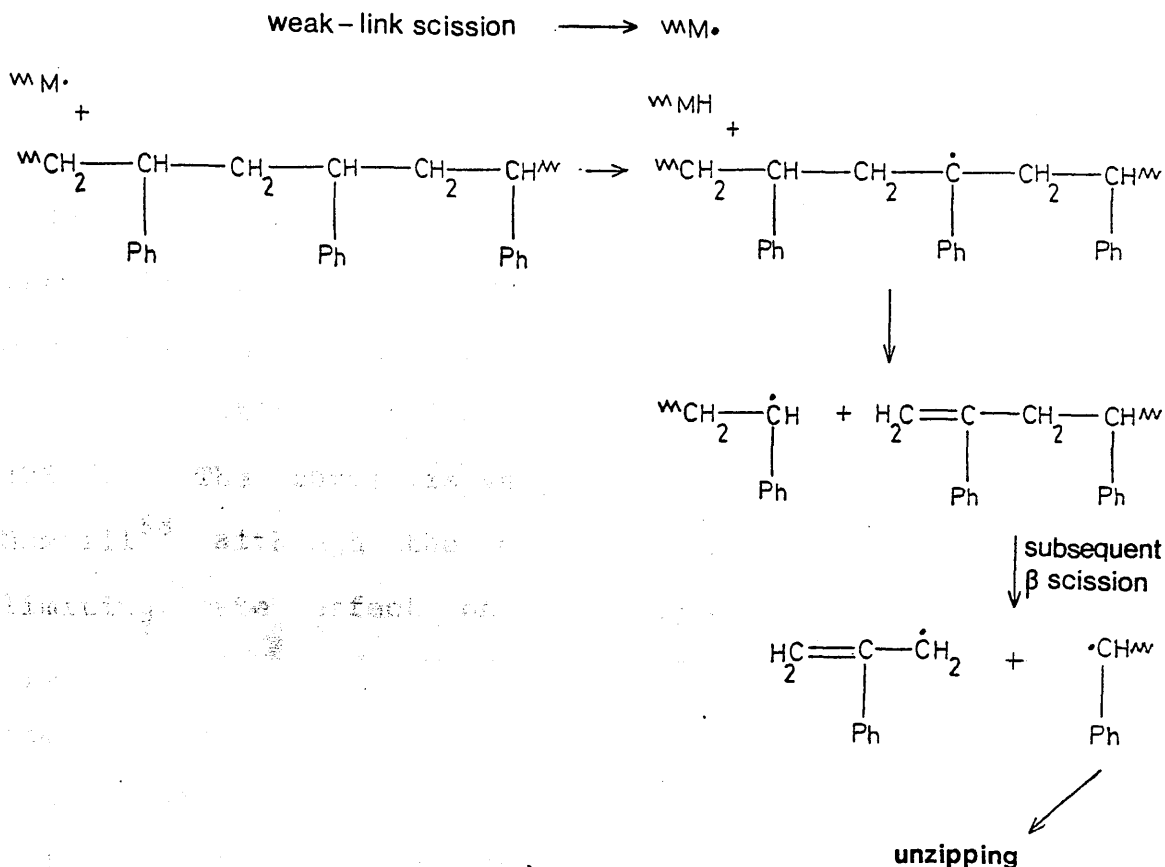
The degradation of polystyrene occurs in two stages, although only the second stage results in the formation of volatile products. The lower temperature process occurring between 200-280°C is a chain scission reaction which does not lead to volatilisation but only to a molecular weight decrease.^{137,138} As this step occurs only in radically prepared polystyrene and not in anionically prepared samples, the scission is believed to occur at irregular structures introduced in the polymerisation process. Although the exact nature of these irregularities is unclear, unsaturated structures such as (I) are expected to play a role.¹³⁸ (A recent paper¹³⁹ describes the detection of weak links in anionically prepared polystyrene. The samples were of commercial origin and unknown history however, and in this case the irregularities were thought to result from oxidation.)



(I)

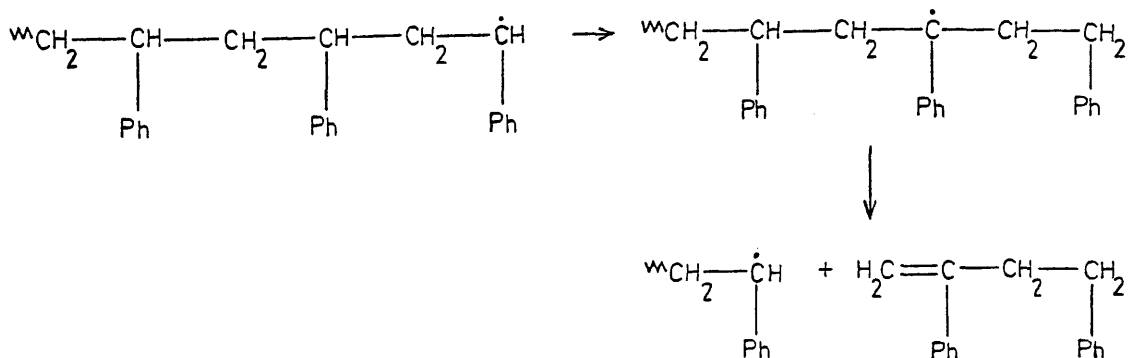
The higher temperature degradation reaction involves the production of monomer by depolymerisation. This unzipping is thought to be initiated almost

entirely by scission of chain end allylic links formed in the lower temperature "weak link" scission reaction and in the small amount of purely random chain scission which also occurs.^{140,141}



In terms of its initiation, therefore, the depolymerisation of polystyrene is similar to PMMA.

In addition to intermolecular transfer and unzipping reactions, intramolecular transfer is also important, with the active α -hydrogens allowing the formation of two to five membered oligomeric products via a "backbiting" reaction:-



TVA BEHAVIOUR OF POLYSTYRENE

A TVA curve for one of the polystyrene samples used in this research (Bextrene 161, British Xylenite Plastics Ltd., used without further purification) is reproduced in Fig. 4.18. The sample was approximately 27mg and was cast from chloroform solution. The first peak is due to evolution of trapped solvent, and it is interesting to observe that although PS and PMMA have very similar glass transition temperatures, PS traps much less solvent than PMMA. The onset of the evolution of degradation products is at 320°C with T(max) 423°C. The curve is very similar to that obtained by McNeill⁶⁸ although the curve obtained here shows a limiting rate effect on the -45°C trace. This is typical of styrene but is very dependent of the exact temperature of the "-45°C" trap. The TVA curve demonstrates clearly the "one-step" production of volatile material from polystyrene.

The cold ring fraction consisted of a small quantity of chain fragments and there was no residue.

POLY(METHACRYLIC ACID), PMAA

THERMAL DEGRADATION OF PMAA

The thermal degradation of poly(methacrylic acid) was first studied in depth by Grant and Grassie¹⁴² who found that the major process occurring was the formation

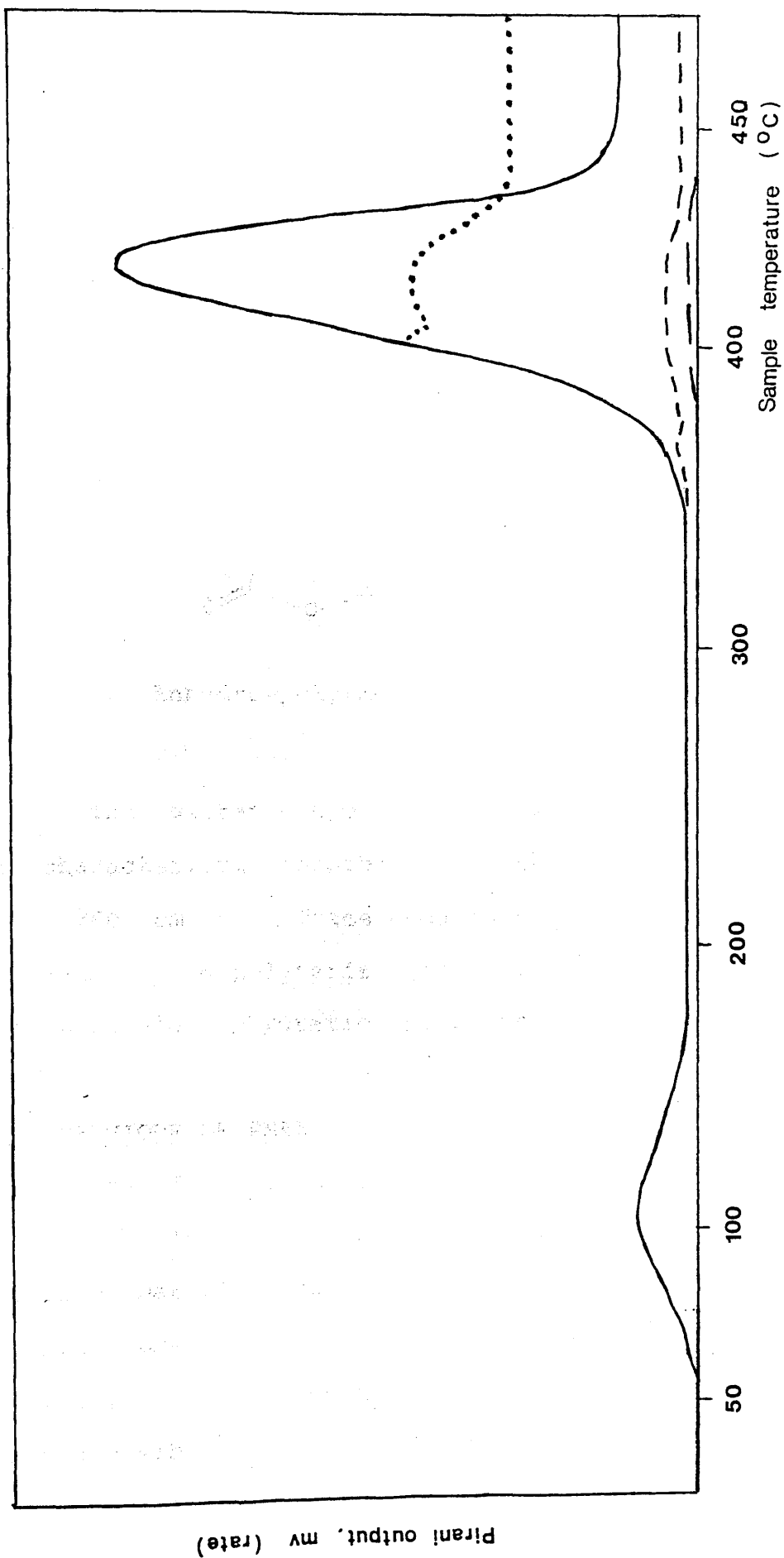
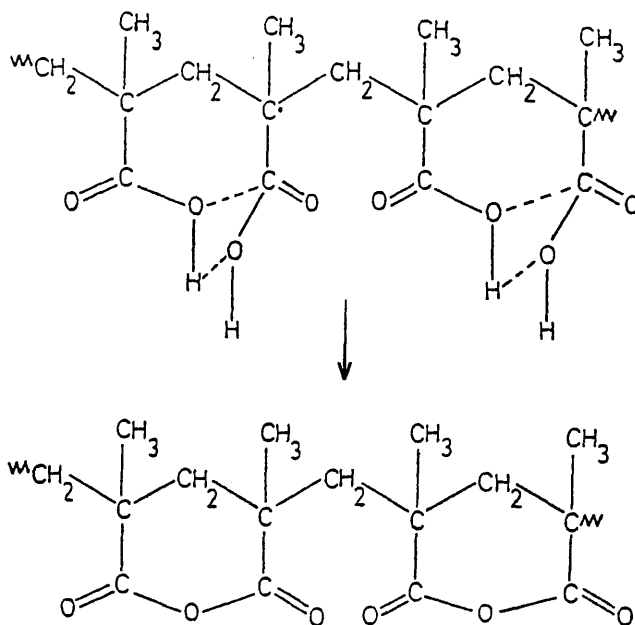


Figure 4.18 TVA curve for polystyrene (Bextrene 161)

between 200-300°C of anhydro-poly(methacrylic acid) by an intramolecular dehydration reaction:-



Anhydro-poly(methacrylic acid)

The glutaric-type anhydride structures give rise to characteristic absorbances in the IR spectrum at 1800 and 1760 cm^{-1} . Trace amounts of methacrylic acid are produced by depolymerisation whilst a small amount of intermolecular dehydration produces cross-links.

TVA BEHAVIOUR OF PMAA

The TVA curve of a sample of PMAA is reproduced in Fig. 4.19. The curve shows the production of volatile material around 225°C due to the evolution of trapped precipitant and water from the dehydration reaction. The production of material (mostly -196°C non-condensable) around 440°C is due to the

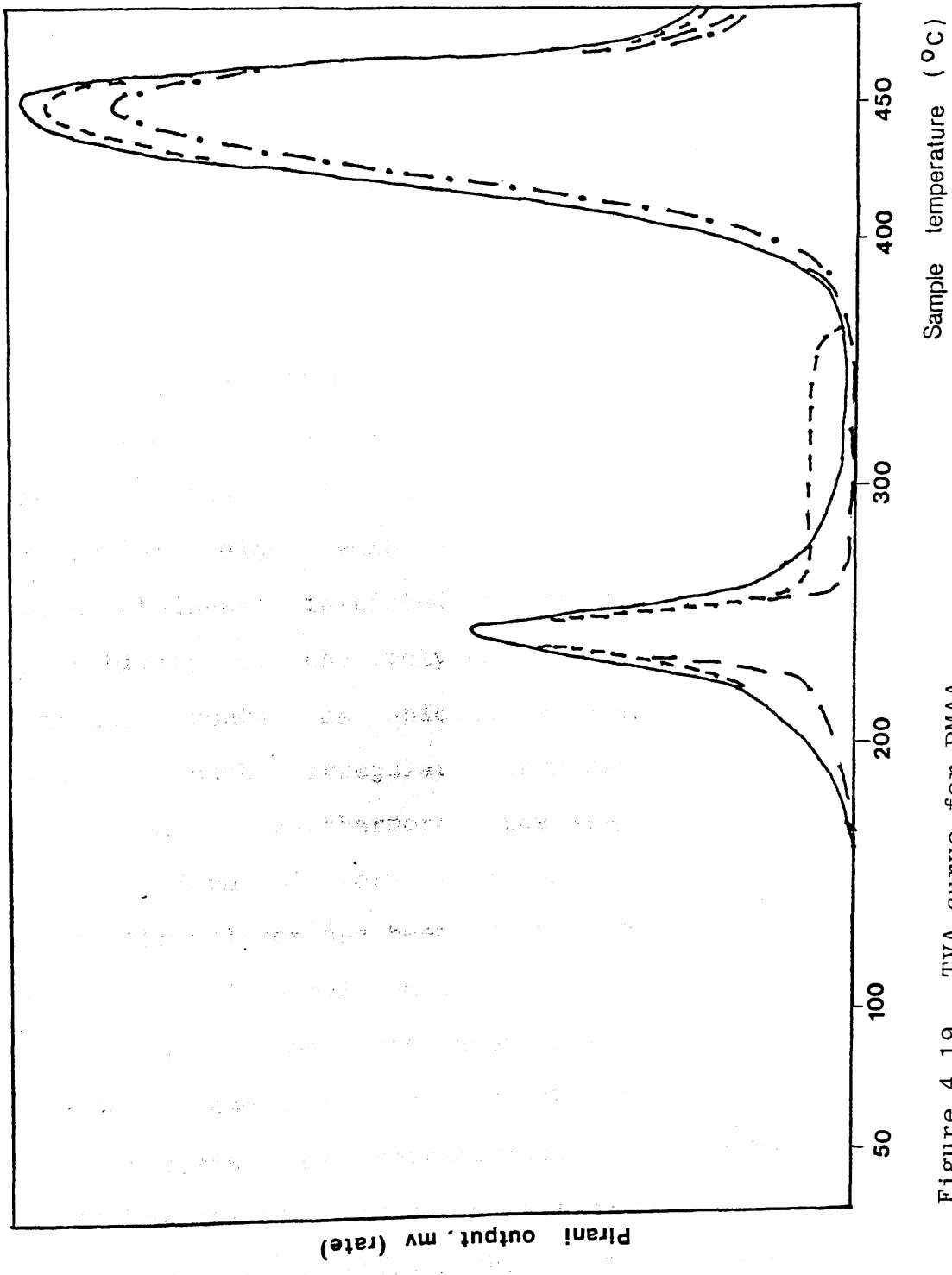


Figure 4.19 TVA curve for PMAA

fragmentation of the polymer. The curve is comparable to that of McNeill.⁶⁸ Further analysis of the degradation of PMAA is described in Chapter 11.

THERMAL DEGRADATION OF 1:59 MAA-MMA COPOLYMER (ALDRICH "LOW MOLECULAR WEIGHT PMMA")

The TVA curve obtained for this commercial "PMMA" is shown in Fig. 4.20 and summarised in Table 4.5. The anomalous nature of this polymer is immediately apparent. Despite having a molecular weight of approximately 20,000, the peak due to chain end initiated depolymerisation ($T(\max) 287^{\circ}\text{C}$) is much smaller than expected (compare with the similar molecular weight PMMA 3, Fig. 4.7). The existence of some chain-end initiated depolymerisation rules out the possibility of the polymer having been prepared by an anionic route, as anionic polymerisation would not produce such irregular structures as unsaturated chain-ends. Furthermore, the sample, as supplied, was in the form of very small spherical beads indicating that the polymer had been prepared by a suspension (i.e. radically initiated) route.

The polymer was apparently pure according to standard resolution ^1H NMR, IR and UV spectroscopy and microanalysis, and reprecipitating twice had no effect on either its analysis or thermal behaviour.

The possibility that the polymer had been

prepared using a chain transfer agent was considered. This would result in a decrease in the formation of unsaturated chain ends and hence a decrease in the chain-end initiated scission.¹²⁵ However, analysis of the degradation products of the polymer indicated that the anomalous behaviour was in fact due to the presence of a comonomer. In addition to the expected sole product, methyl methacrylate, methanol, carbon dioxide, a ketene, butene and isobutene and an unusual liquid product (discussed in the following section) were also identified. These products are consistent with those of a PMMA sample in which unzipping has been blocked,¹⁴³ thus allowing significant amounts of ester decomposition and fragmentation reactions to occur. The presence of a cold ring fraction and a carbonaceous residue are also in accord with this view. The IR spectrum of the cold ring fraction is shown in Fig. 4.21. The spectrum shows the CRF to consist of chain fragments. However, the peaks at 1800 cm^{-1} , and 1760 cm^{-1} are those typical of glutaric anhydride type structures¹⁴⁷ indicating the presence of these structures in the chain fragments.

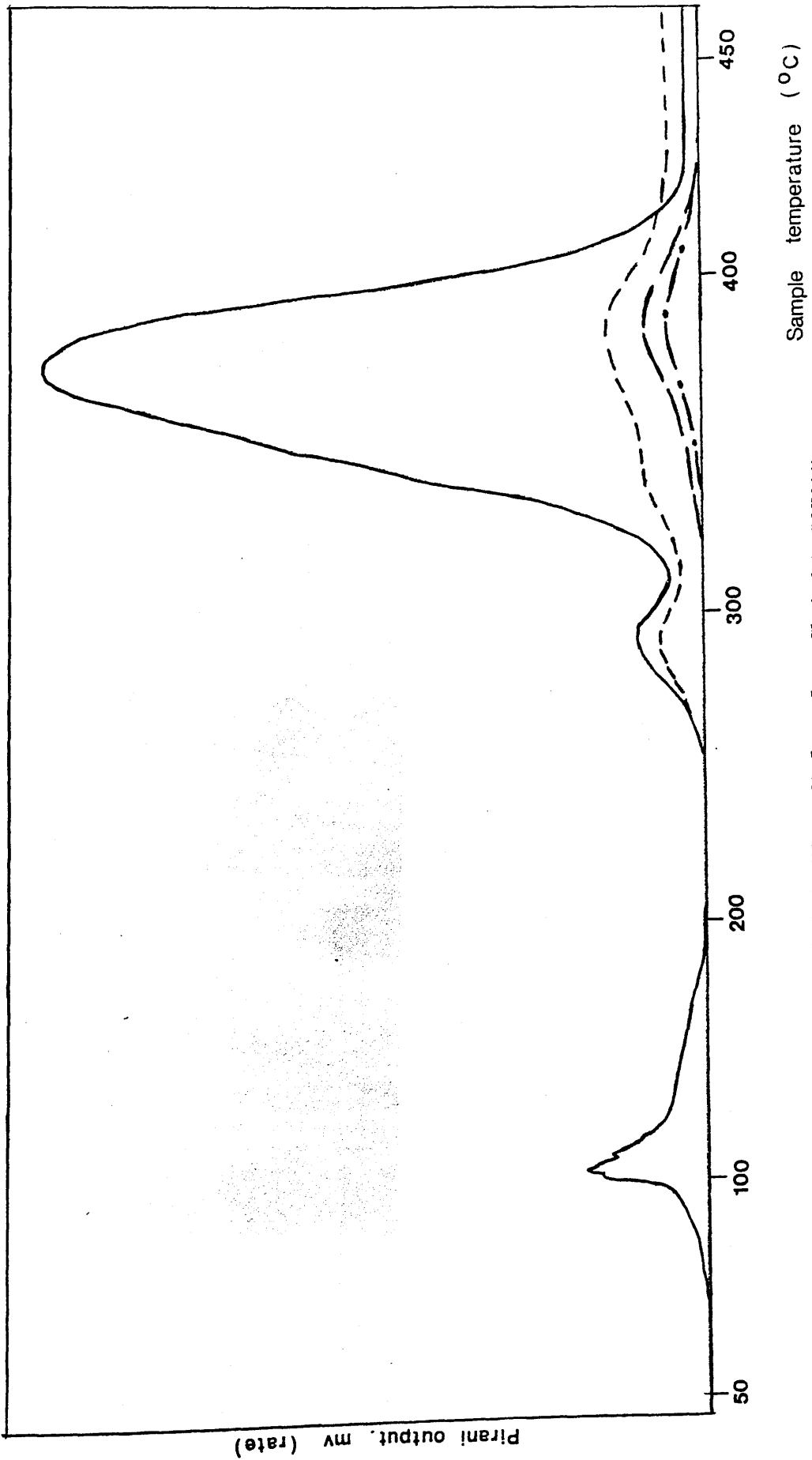
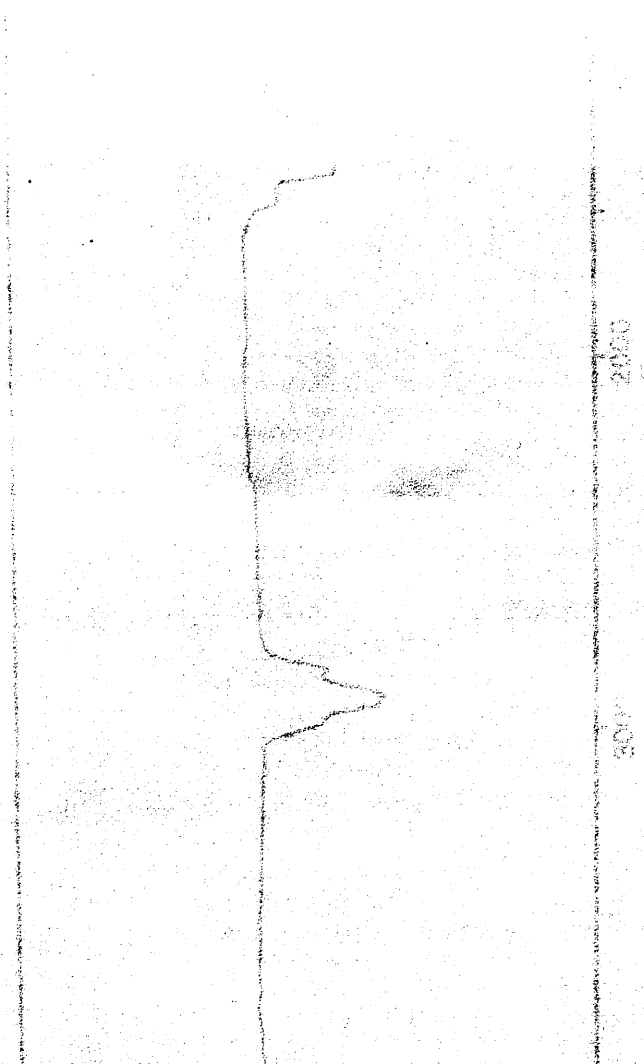


Figure 4.20 TVA curve for Aldrich "Low Molecular Weight PMMA"
(1:59 MAA-MMA copolymer)

<u>Feature</u>	<u>Temperature</u> °C
1st Peak	
T(onset)	224
T(max)	287
2nd Peak	
T(onset)	308
T(max)	376 (-196°C condensibles)
	386 (non-condensibles)

Table 4.5 T(onset) and T(max) values from TVA curve of 1:59 MAA-MMA copolymer



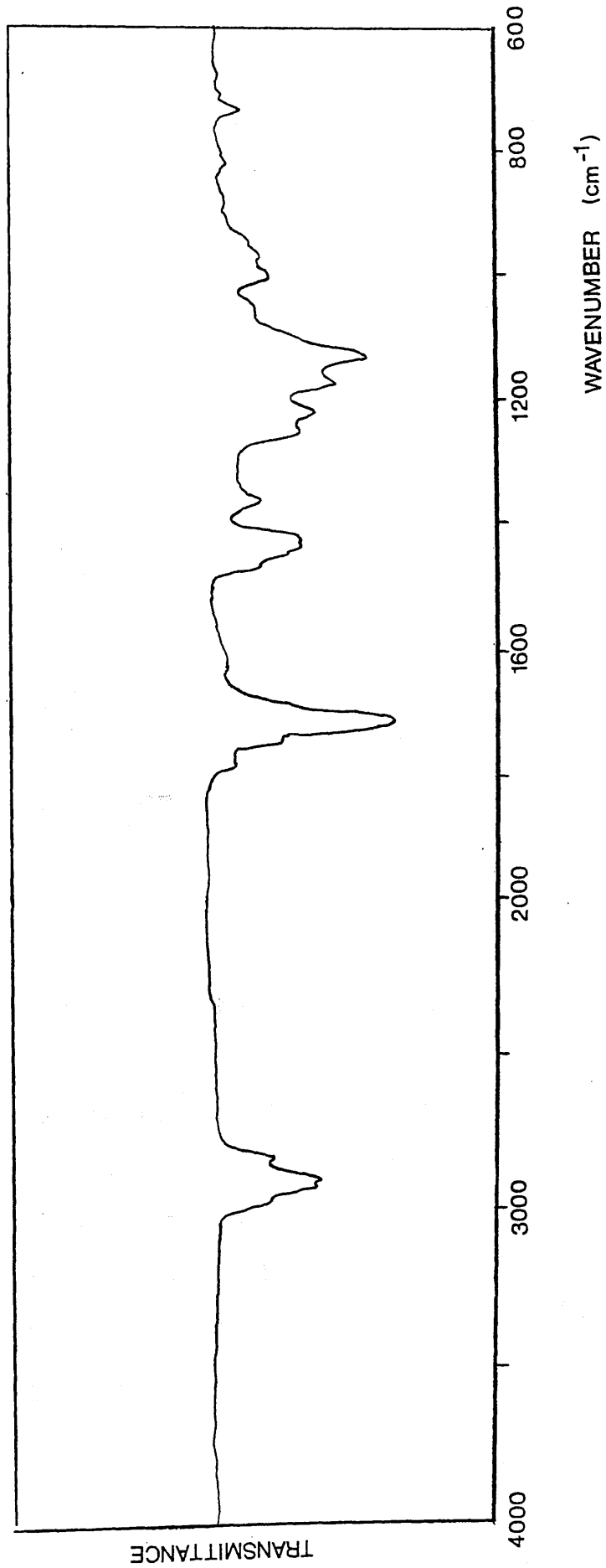


Figure 4.21 IR spectrum of CRF from 1:59 MAA-MMA copolymer

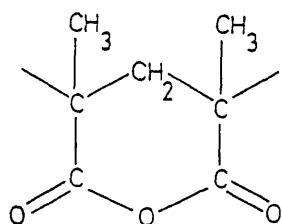
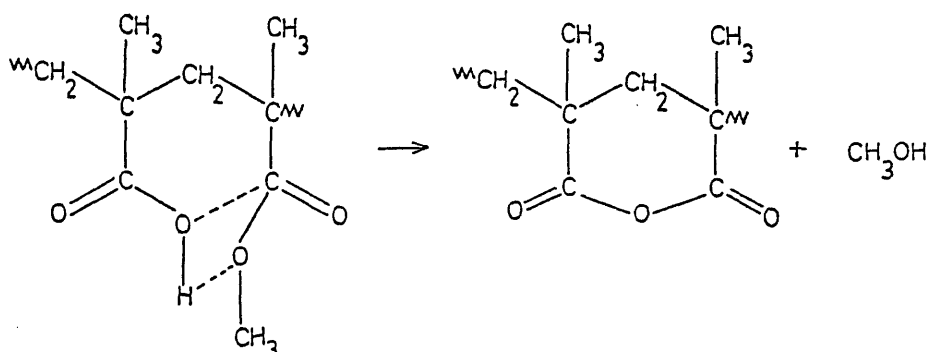


Fig. 4.22 Glutaric Anhydride Type Structure

Such structures have been observed by Jamieson and McNeill¹⁴² in the degradation of methyl methacrylate - methacrylic acid copolymers where they are formed by the reaction:-



These rings serve to block the unzipping of the MMA portions of the chains, with the subsequent formation of such fragmentation products as those obtained for this Aldrich sample.

Analysis of the residue at various stages of degradation showed that the anhydride structures form within the polymer in the region of the first degradation peak (Fig. 4.23). Thus the anomalously

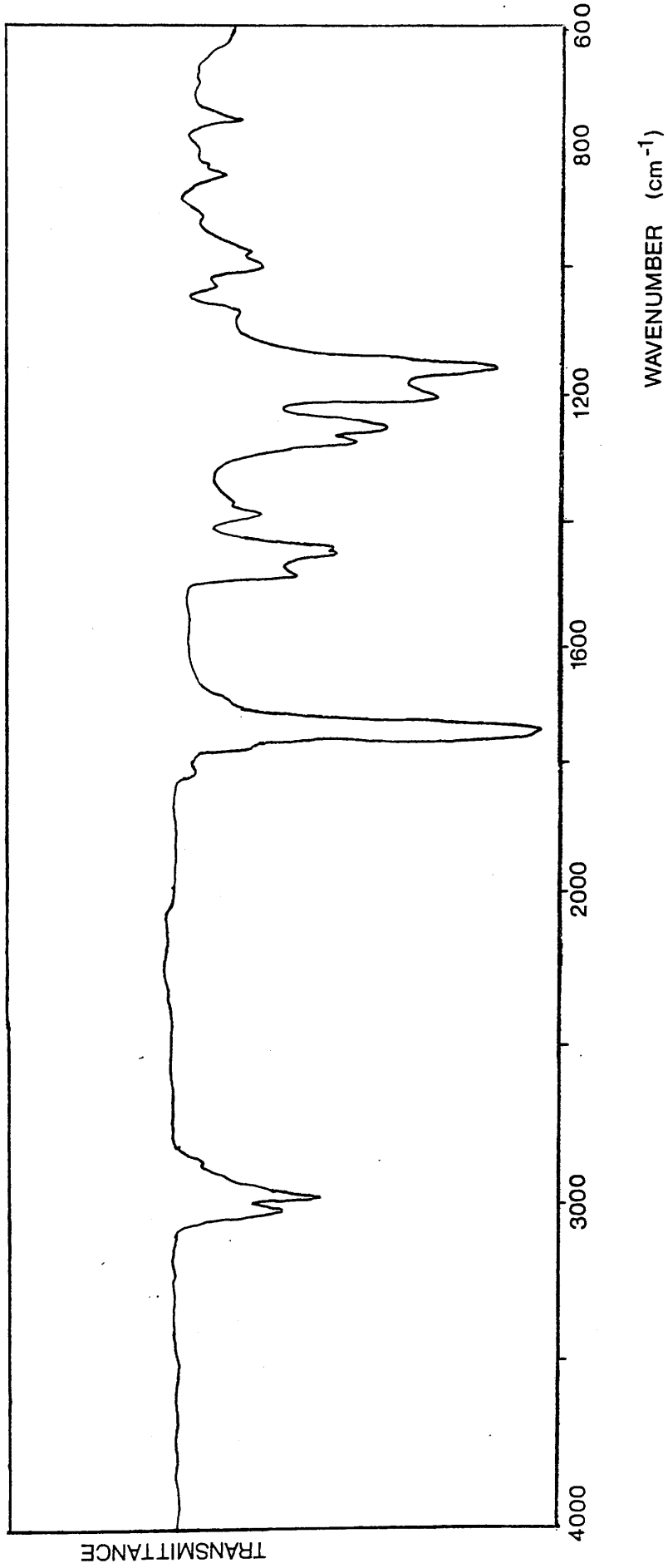


Figure 4.23 IR spectrum of 1:59 MAA-MMA copolymer after heating to 1st degradation peak (280°C)

small chain-end initiated depolymerisation peak may be explained by the blocking action of these anhydride structures.

Titration of an acetone solution of the polymer with aqueous sodium hydroxide showed the polymer to be acidic to the extent of one acid unit per fifty-nine methyl methacrylate units. This ratio, though small, significantly alters the behaviour of the additive blends of this 1:59 methacrylic acid - methyl methacrylate copolymer relative to the homopolymer.

Carboxylate structures ($= 1580 \text{ cm}^{-1}$ in Fig. 4.23) were also found in the residue at advanced states of degradation when the film had been degraded supported on a NaCl disc. These carboxylates result from the interaction of the polymer with Na^+ ions at high temperature and have been observed previously in a similar situation.¹⁴⁴ Rather unexpectedly, such carboxylate formation was also observed on degrading PMMA in the same manner, although to a lesser extent. As a consequence, the spectra of the residues of additive blends degraded in this fashion have to be interpreted with care.

THE NATURE OF THE LIQUID PRODUCT FROM THE 1:59 MAA-MMA COPOLYMER

As described in the previous section, along with the gaseous products was formed a liquid product. This low volatility material shows on the SAD trace as an

extended "tail" on the methyl methacrylate peak (Fig. 4.24). This material was collected in a cold finger and its mass and IR spectra obtained. The IR spectrum (Fig. 4.25) shows some methyl methacrylate absorptions but the features of interest are the absorptions at 1845 cm^{-1} and 1768 cm^{-1} which lie within the range expected for anhydride structures. The relative intensities of the two peaks suggest a cyclic structure and the relatively high frequency of the peaks suggests ring strain which, by analogy with other cyclic anhydrides, is most likely due to the structure being five-membered (See Table 4.6).

Of the compounds listed in Table 4.6 only citraconic anhydride is a liquid at room temperature but some derivatives of succinic anhydride (e.g. 1-decanylsuccinic anhydride) are also liquid under normal conditions. The mass spectrum (Table 4.7) is of little help in identifying the anhydride due to the large number of peaks. In fact, the "anhydride product" is most probably a range of variously substituted anhydride rings which can be expected given the complex nature of degradation reactions.

Given that six-membered cyclic anhydride structures are formed within the copolymer, as described in the previous section, the most likely source of the five-membered anhydrides is through some rearrangement of the larger rings. Five-membered anhydrides can also therefore be expected as degradation products of other

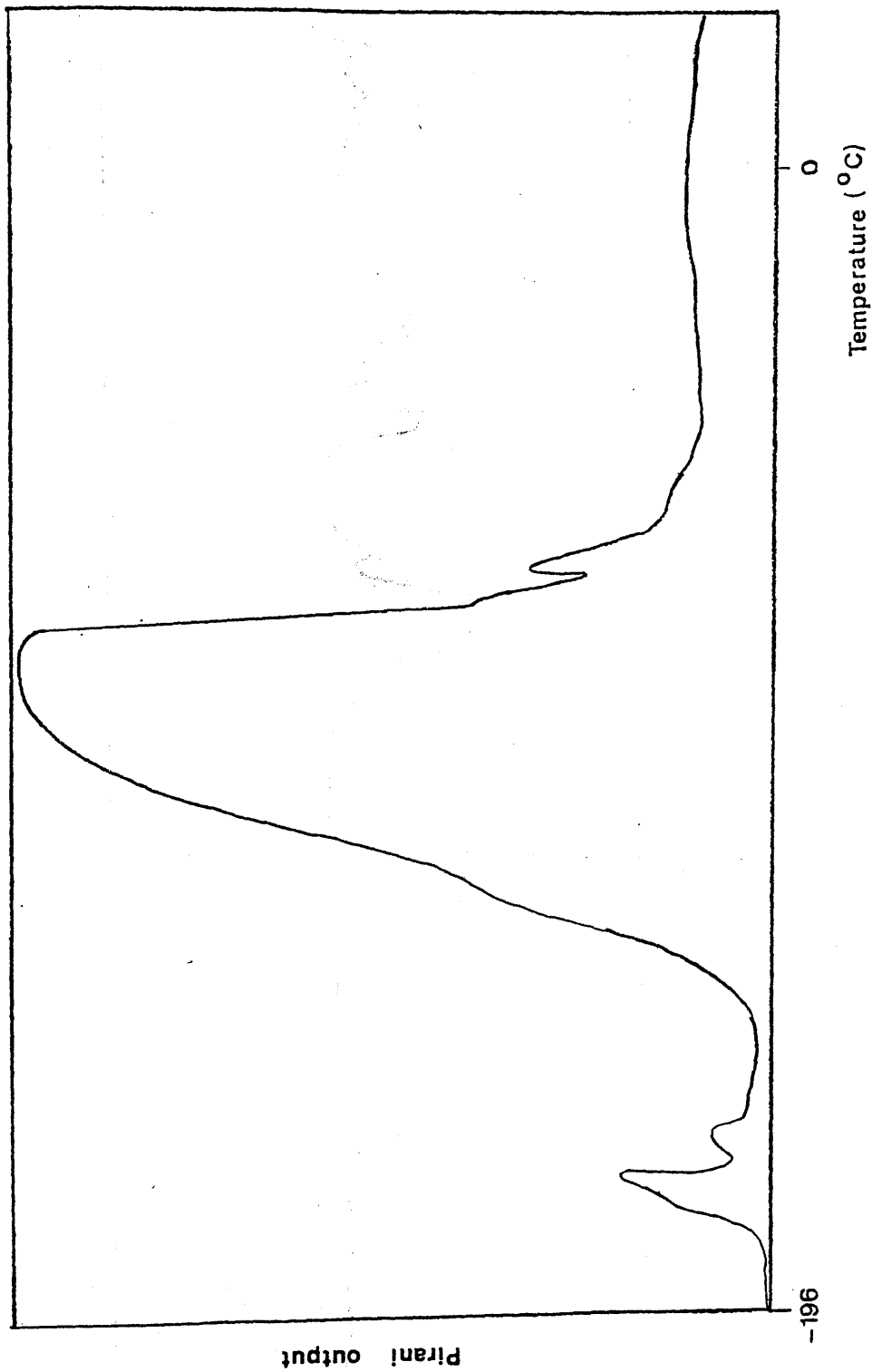


Figure 4.24 SAD curve for products of degradation to 485°C
of 1:59 MAA-MMA copolymer



Figure 4.25 IR spectrum of liquid fraction from SAD analysis of products of degradation of 1:59 MAA-MMA copolymer

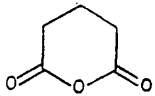
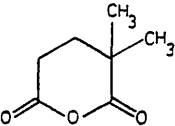
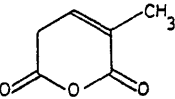
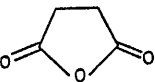
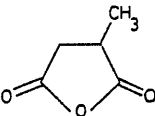

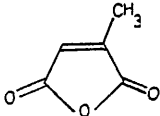
Anhydride	Structure	C=O Stretching Frequencies (cm^{-1})	
Glutaric		1800	1760
Di-methyl glutaric		1810	1765
γ -methyl glutaconic		1820	1760
Succinic		1865	1785
Methyl succinic		1850	1770
Maleic		1850	1770
Citraconic		1840	1760

Table 4.6 C=O Stretching Frequencies of Several Anhydrides

Mass	%AR. Base	Mass	%AR. Base
40.9	100.00	109.9	9.02
42.0	15.57	110.9	10.66
43.0	36.89	112.0	4.10
44.0	12.30	113.0	10.66
45.0	34.43	114.0	6.56
49.7	8.20	115.0	13.93
50.7	20.49	116.0	1.64
51.8	7.38	117.0	7.38
52.9	27.87	119.0	2.46
53.9	10.66	120.9	7.38
54.9	50.00	122.0	4.92
55.9	14.75	123.0	20.49
56.9	21.31	124.0	2.46
57.9	5.74	125.0	13.11
58.8	33.61	126.0	19.67
62.9	6.56	127.0	27.87
64.9	18.03	128.0	10.66
65.9	11.48	128.9	3.28
66.9	49.18	135.0	6.56
67.9	13.93	136.0	2.46
68.8	49.18	137.0	8.20
69.8	8.20	138.0	2.46
70.9	10.66	138.9	14.75
71.9	5.74	139.9	17.21
73.0	17.21	140.9	15.57
74.0	2.46	142.0	3.28
77.0	33.61	143.0	1.64
77.9	8.20	144.0	8.20
78.9	30.33	145.0	3.28
79.9	10.66	149.0	3.28
80.9	61.48	150.0	2.46
82.0	13.93	151.0	13.93
83.0	16.39	152.0	2.46
85.0	7.38	153.1	1.64
86.0	1.64	154.1	11.48
87.0	4.92	155.1	7.38
88.0	16.39	161.0	8.20
88.9	6.56	168.1	8.20
90.9	18.85	169.1	4.92
92.0	5.74	180.1	9.02
93.0	24.59	181.1	7.38
94.0	7.38	182.1	4.92
95.0	35.25	183.1	1.64
96.0	8.20	217.5	6.56
97.0	13.11	263.9	4.92
98.0	4.10		
98.9	24.59		
99.9	7.38		
100.9	9.02		
102.0	4.10		
103.0	3.28		
104.0	4.10		
105.0	8.20		
106.0	13.93		
107.0	13.11		
108.0	9.02		
109.0	35.25		

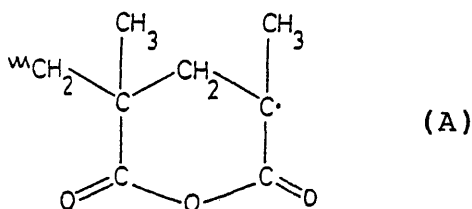
Table 4.7 Mass Spectrum of Liquid from 1:59 MAA-MMA Copolymer

systems which form the cyclic six-membered anhydride structure, and indeed, as described in subsequent chapters such structures are observed on degrading styrene-methacrylic copolymers and blends of $\text{Co}(\text{acac})_3$ and $\text{Mn}(\text{acac})_3$ with PMMA.

The five-membered structures have not been observed in earlier studies on MMA-MAA copolymers¹⁴³ or poly(methacrylic acid).¹⁴² However, those studies were not designed to identify products of such low volatility and so a sample of PMAA was degraded in the apparatus used for this project and the products separated by SAD. The fraction of comparable volatility to the liquid anhydride fraction from the 1:59 MAA-MMA copolymer was collected in a cold finger, and its IR spectrum obtained. This spectrum (Fig. 4.26) shows clearly the absorbances at 1845 cm^{-1} and 1765 cm^{-1} ascribed to the five-membered anhydride ring.

The rearrangement of the six-membered anhydride ring to the five-membered ring can occur when bond scission or depolymerisation produces the macroradical

(A):-



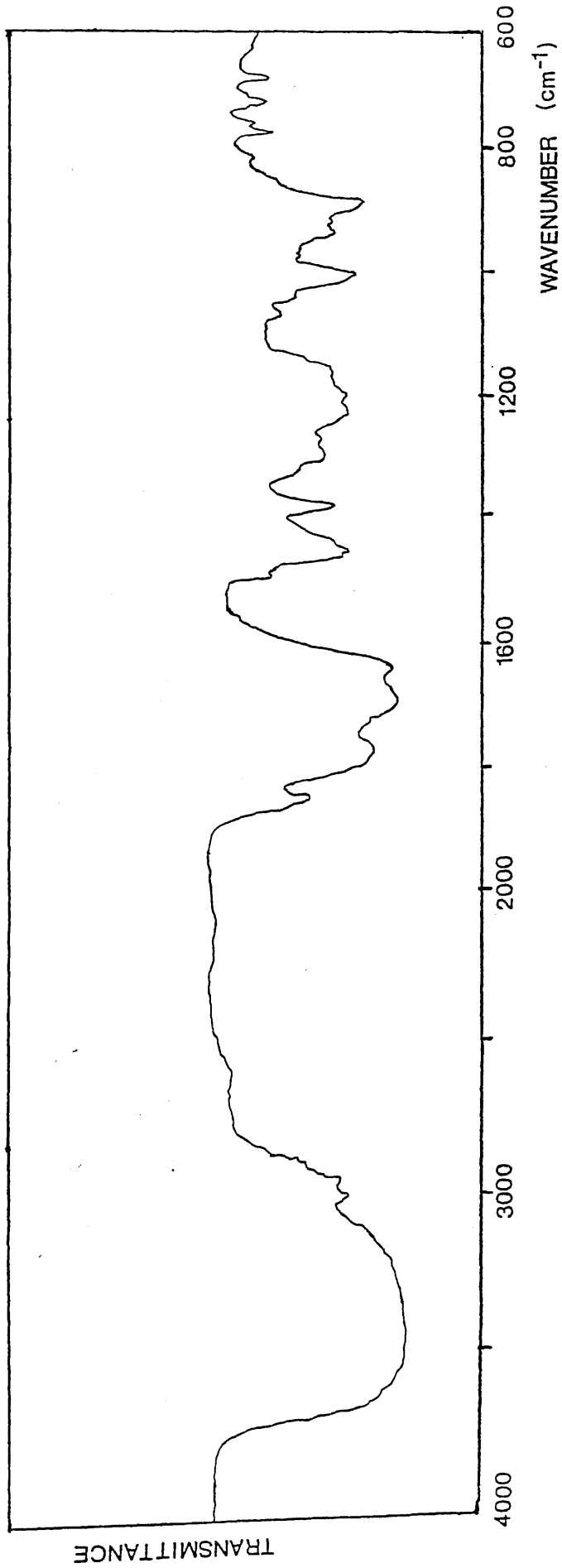
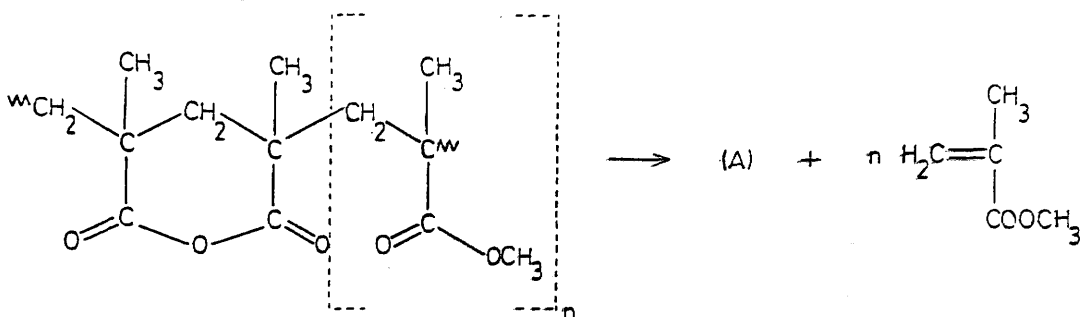


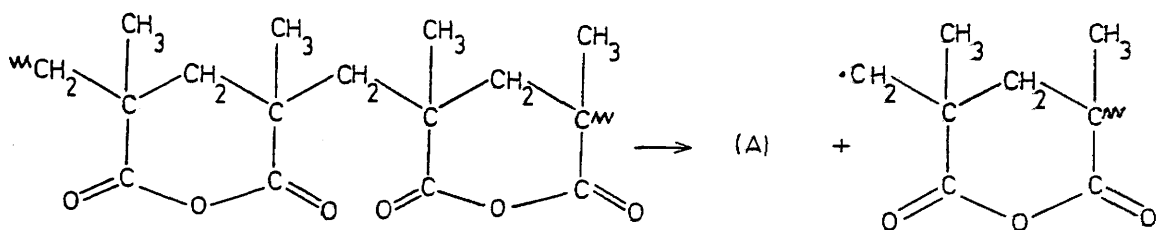
Figure 4.26 IR spectrum of liquid fraction from SAD analysis of products of degradation of PMAA.

For example

MMA-MAA copolymer

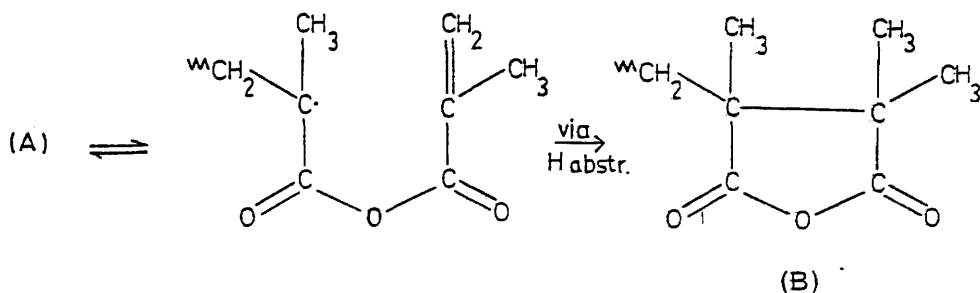


PMAA

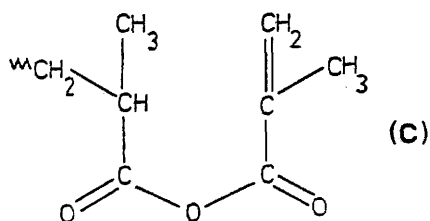


(A) can then rearrange to give the five-membered ring

(B) :-



Subsequent scissions and rearrangements will produce a variety of substituted succinic-type anhydrides. Alternatively, the unsaturated structure (C) can be found.



CHAPTER 5

BLENDS OF $\text{Co}(\text{acac})_3$ AND $\text{Mn}(\text{acac})_3$ WITH PMMA

INTRODUCTION

In this chapter the degradation of blends of PMMA with $\text{Co}(\text{acac})_3$ and $\text{Mn}(\text{acac})_3$, the two most active acetylacetonate chelates in terms of the initiation of methyl methacrylate polymerisation,²⁶ is considered. PMMA is of particular interest not only because it contains electron donors in the form of the ester side groups, but as it terminates mainly by disproportionation, the chain ends contain unsaturated sites which can also act as electron donors.

DEGRADATION BEHAVIOUR OF PMMA

The thermal degradation of PMMA has been discussed in Chapter 4 and TVA curves for the three PMMA samples used (PMMA 1, PMMA 2 and PMMA 3) are illustrated therein.

DECOMPOSITION OF $\text{Co}(\text{acac})_3$ AND $\text{Mn}(\text{acac})_3$

The thermal decomposition of the chelates is considered in Chapter 3.

THERMAL DEGRADATION OF Co(acac)₃ - PMMA BLENDS

THERMAL VOLATILIZATION ANALYSIS

TVA curves were obtained for blends of Co(acac)₃ with PMMA samples of low, medium and high molecular weight (PMMA samples 1, 2, 3) in the Co(acac)₃:MMA unit ratios of 1:10 and 1:50. Additionally, TVA curves were obtained for blends of the low molecular weight polymer (PMMA 3) at ratios of 1:200 and 1:400. These TVA curves are reproduced in Figures 5.1-5.8 and Table 5.1 summarises the important details.

All blends were prepared as films cast from methylene chloride and with the exception of the 1:10 blends were compatible. All were bottle green in colour. On completion of the heating programme (485°C), a brown charred residue remained in all cases and was most evident in the blends of highest Co(acac)₃ concentration. A cold ring fraction (CRF) was also obtained in all cases. The nature of these and other products is discussed later in this chapter.

COMMENT ON THE TVA CURVES

Peaks 1 and 2

In contrast to the TVA behaviour of PMMA alone, all the Co(acac)₃ - PMMA blends surveyed have two degradation steps below 200°C.

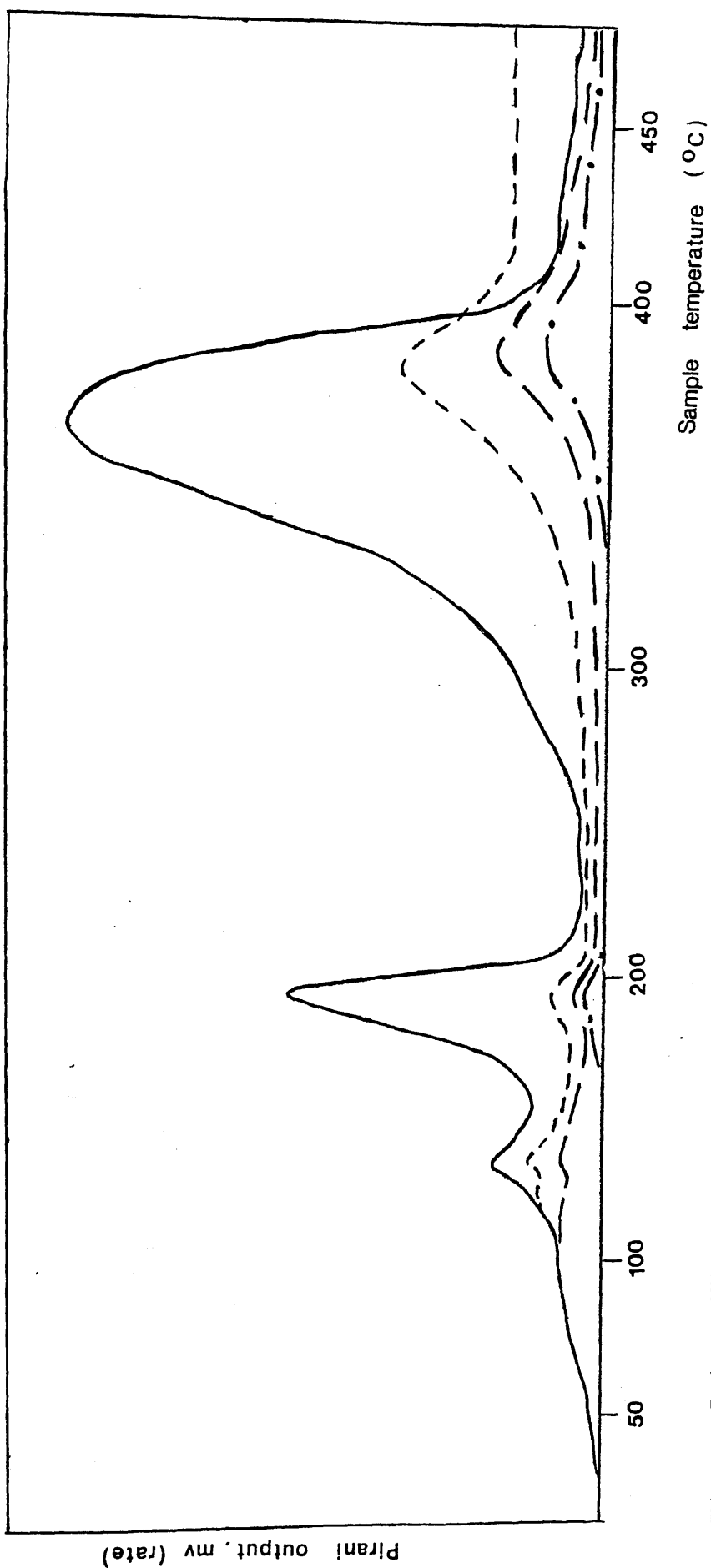


Figure 5.1 TVA curve for 1:10 $\text{Co}(\text{acac})_3$ - PMMA 1 blend

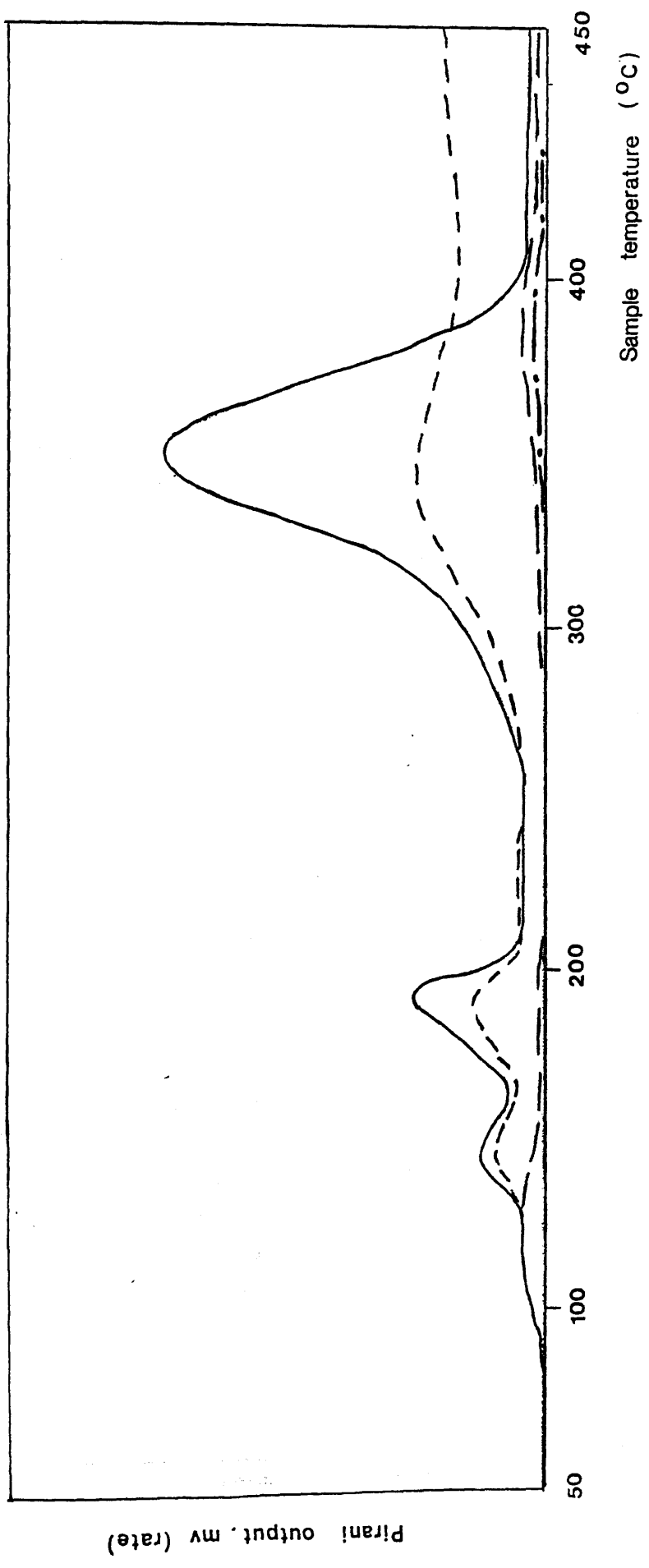


Figure 5.2 TVA curve for 1:50 Co(acac)₃ - PMMA 1 blend

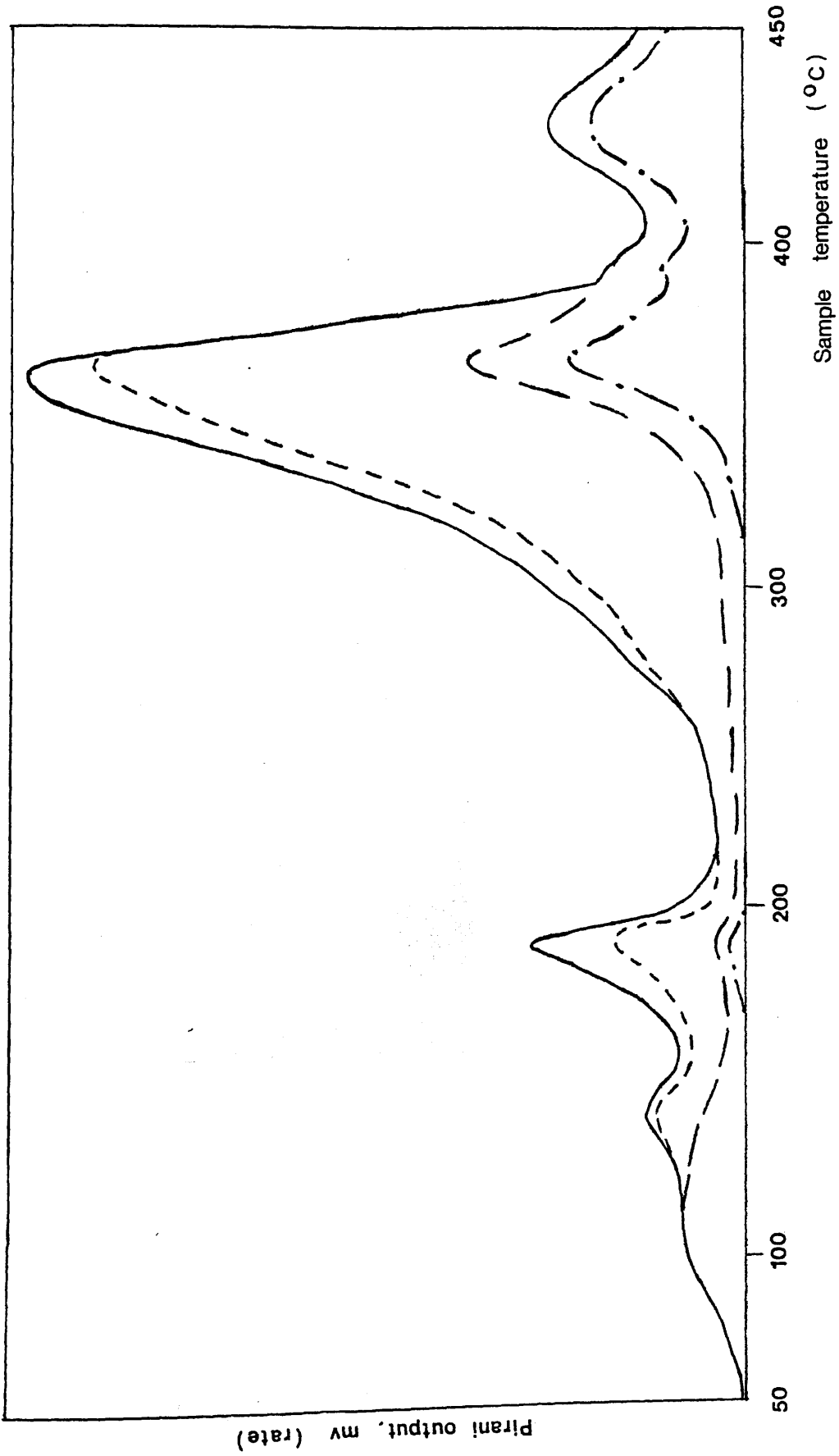


Figure 5.3 TVA curve for 1:10 Co(acac)₃ - PMMA 2 blend

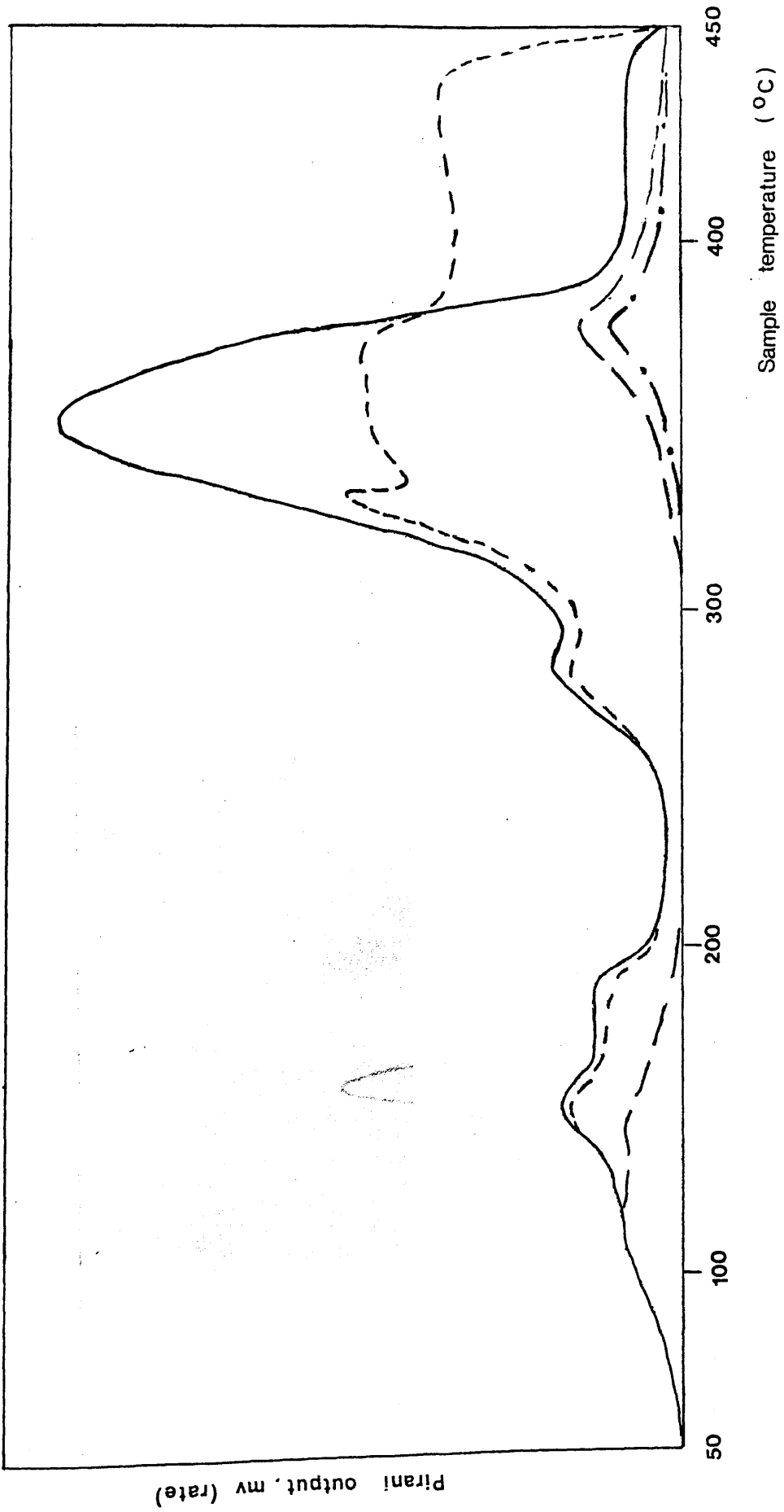


Figure 5.4 TVA curve for 1:50 Co(acac)₃ - PMMA 2 blend

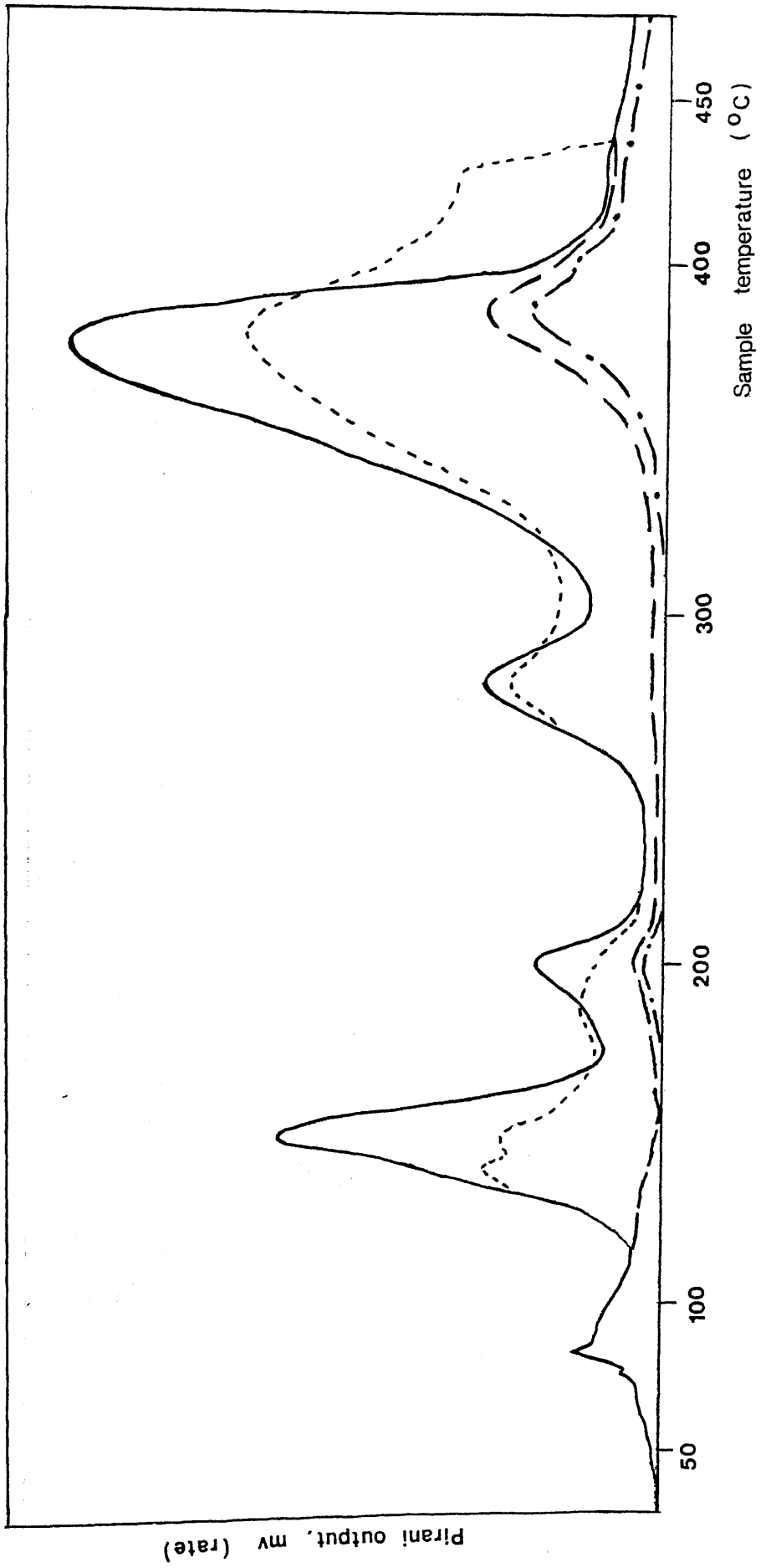


Figure 5.5 TVA curve for 1:10 Co(acac)₃ - PMMA 3 blend

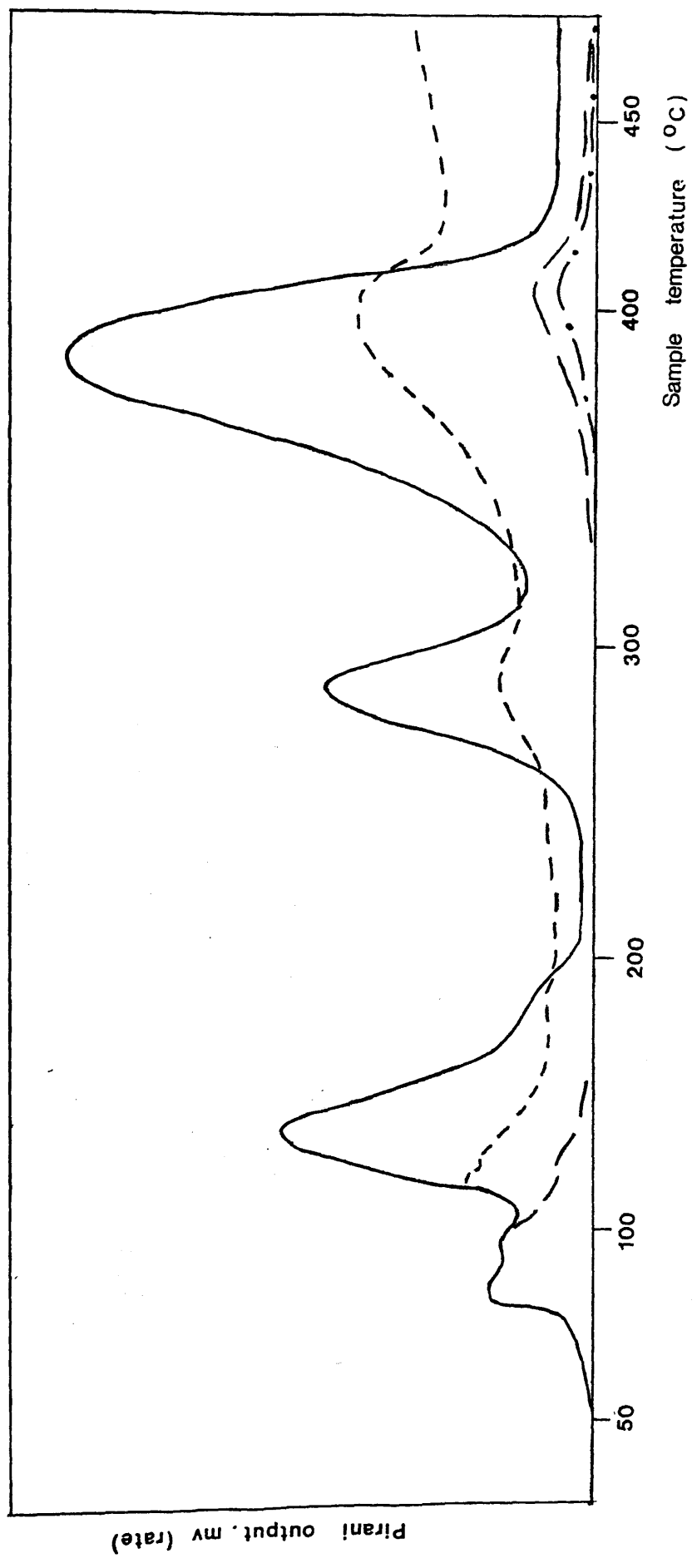


Figure 5.6 TVA curve for 1:50 Co(acac)₃ - PMMA 3 blend

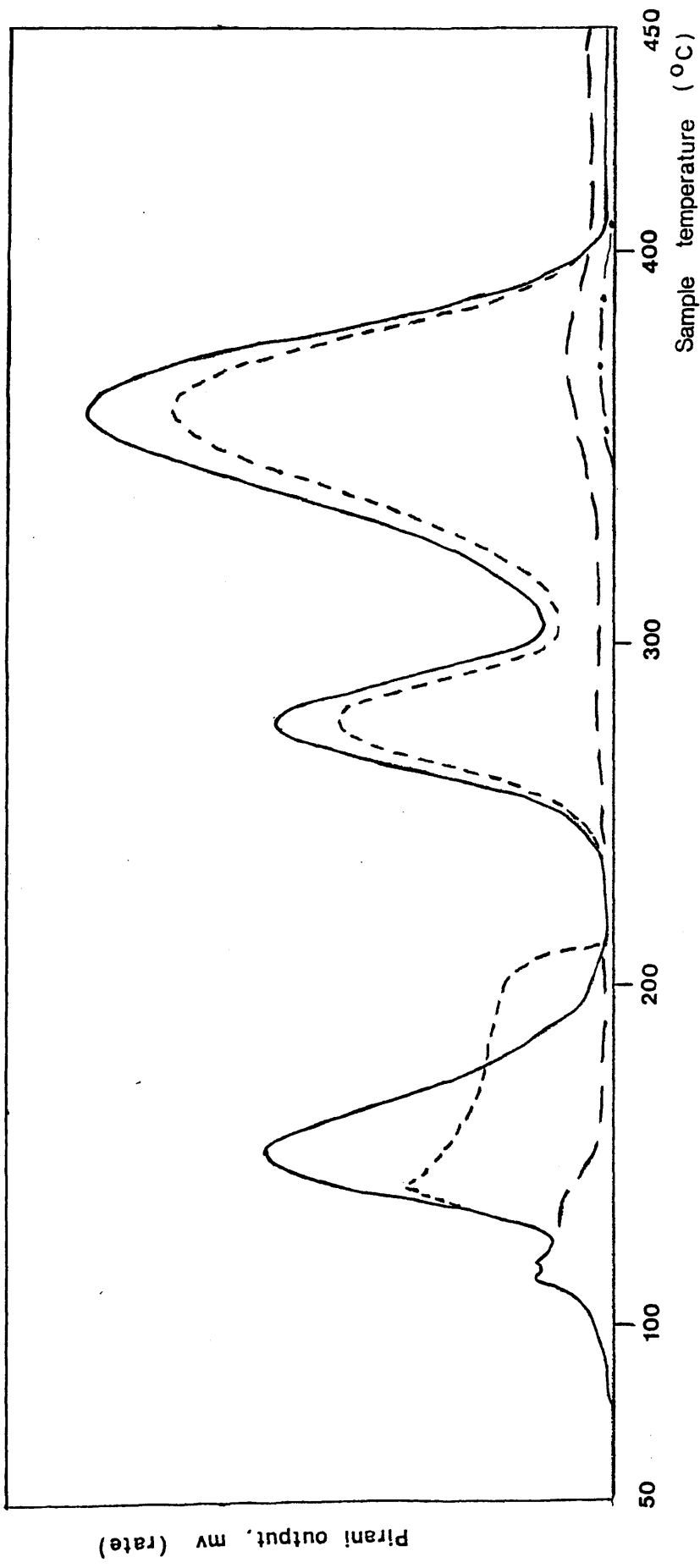


Figure 5.7 TVA curve for 1:200 Co(acac)₃ - PMMA 3 blend

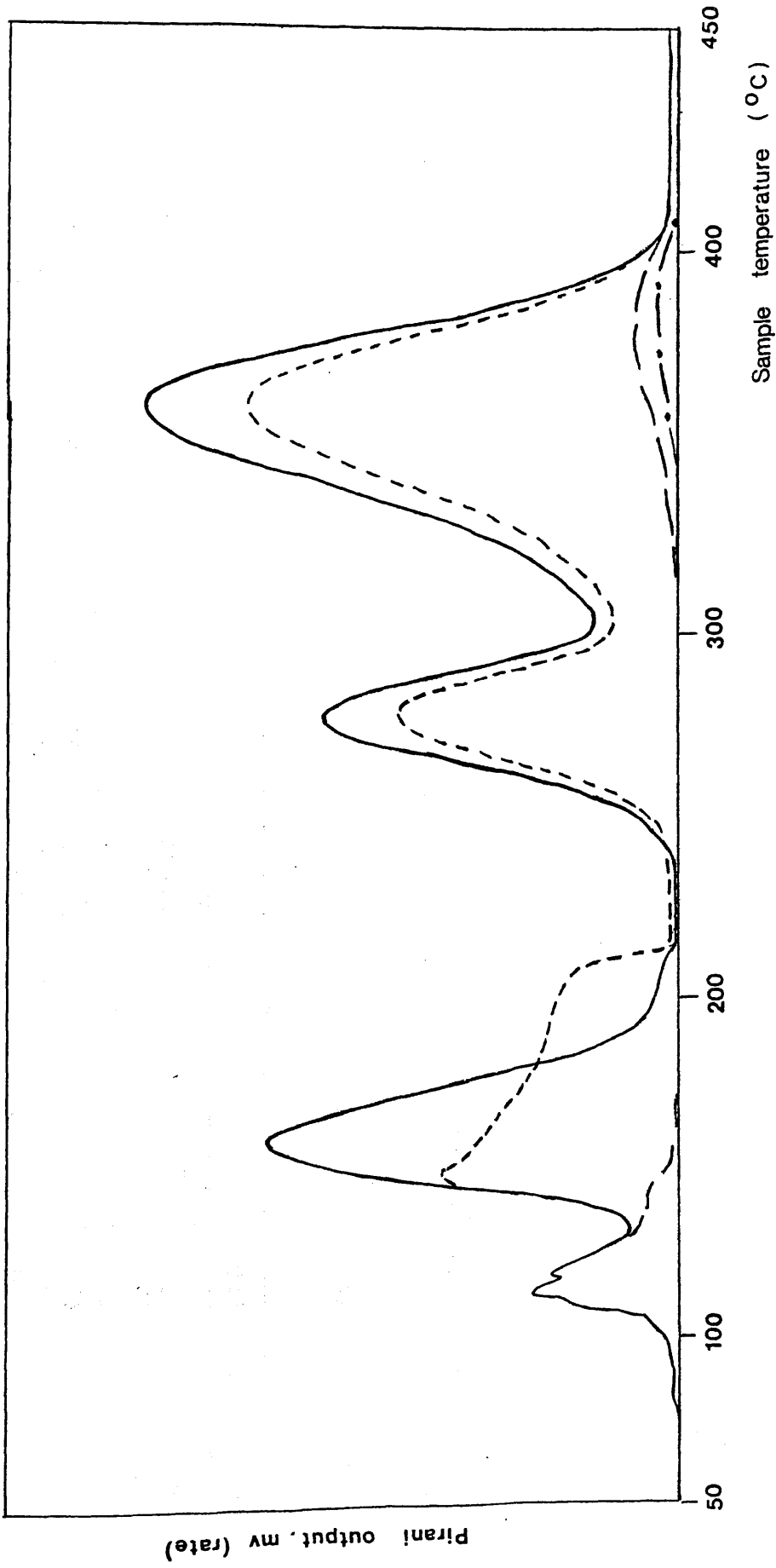


Figure 5.8 TVA curve for 1:400 Co(acac)₃ - PMMA 3 blend

BLEND PMMA SAMPLE AND Co(acac)₃ : MONOMER UNIT RATIO

FEATURE	PMMA 1 1:10	PMMA 1 1:50	PMMA 2 1:10	PMMA 2 1:50	PMMA 3 1:10	PMMA 3 1:50	PMMA 3 1:200	PMMA 3 1:400
Compatability	No	Yes	No	Yes	No	Yes	Yes	Yes
T (Sublimation)	92	Not observed but > 134°C (Table 8.5)	Not recorded	Not observed	108	Not observed	Not observed	Not observed
T(onset)*	101-110	120	116	107	116	125	127	131
1st Peak	134	135	137	134	151	153	150	158
2nd Peak	152	160	159	159	175	shoulder to 1st Peak to 175-206	shoulder to 1st Peak to 190-209	shoulder to 1st Peak to 197-206
T(max)	192	190	190	190	200	223	231	222
3rd Peak	Reduced to shoulder of 4th Peak	Reduced to shoulder of 4th Peak	Reduced to shoulder of 4th Peak	234	237	280	277	280
T(max)	232-295	246-297	229-278	286	283	280	277	280
4th Peak	295	297	278	298	307	307	304	310
T(max)	364	360	364	367	377	370	364	368
Condensibles	391	392	370	379	385	388	385	384
Non-condensibles								

Temperatures in °C

NOTES: *True T(onset) Peak 1 masked by solvent evolution

†Peaks 3 and 4 correspond to the chain end initiated and random scission initiated depolymerisations of the unblended PMMA

Table 5.1 TVA behaviour of some Co(acac)₃ - PMMA Blends

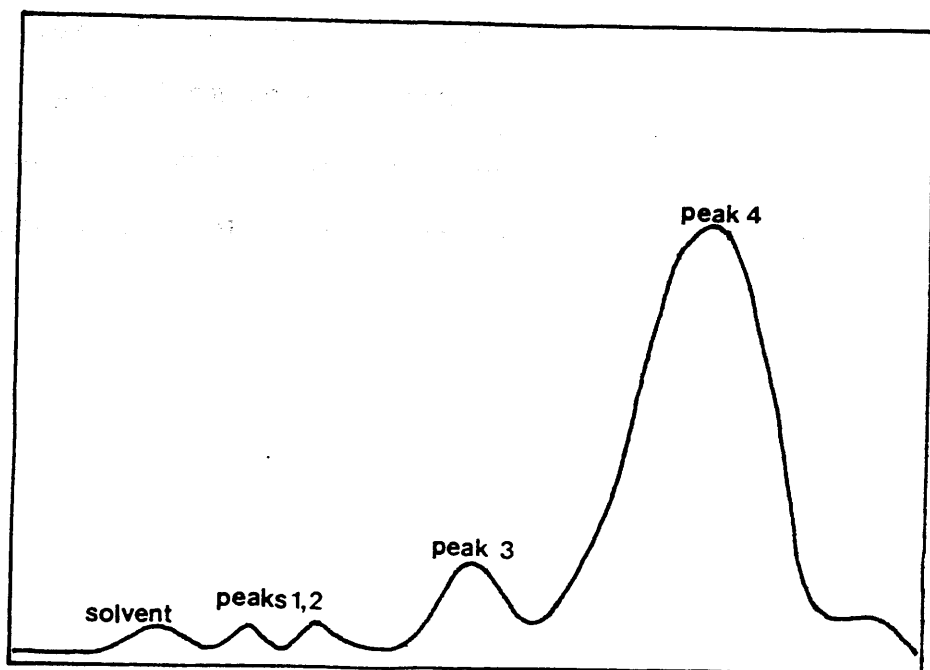


Fig 5.9 Representation of a typical TVA Curve for a $\text{Co}(\text{acac})_3$ - PMMA blend showing designation of peaks.

The lowest temperature peak ($T(\text{max})$ approx 135°C) varies in height with the molecular weight of the polymer, being most pronounced in the blends of the low molecular weight PMMA 3. Over the range of $\text{Co}(\text{acac})_3$ concentrations studied (1:10 - 1:400), this first peak is independent of $\text{Co}(\text{acac})_3$ concentration. This peak displays the Limiting Rate Effect on the -75°C trap trace typical of methyl methacrylate and can thus be assigned to a depolymerisation reaction.

The variation in peak height with molecular weight implies that the initiation of the depolymerisation occurs at the chain ends (cf. the chain end initiated depolymerisation of unblended PMMA). The initiation must stem from some interaction between the polymer and $\text{Co}(\text{acac})_3$, yet the process is independent of the concentration of $\text{Co}(\text{acac})_3$ in the blend over the range studied (1:400 - 1:10). This implies that the interaction between $\text{Co}(\text{acac})_3$ and the polymer cannot occur at every chain end since at a $\text{Co}(\text{acac})_3$:MMA unit ratio of 1:400 the blend of $\text{Co}(\text{acac})_3$ with PMMA 3 (m. wt. 20,000) has only one $\text{Co}(\text{acac})_3$ molecule per two chains and there would thus remain the possibility of increasing the number of interactions by increasing the concentration of $\text{Co}(\text{acac})_3$.

In fact, the most likely site for interaction is at those unsaturated chain ends formed in the disproportionation termination reaction, with which $\text{Co}(\text{acac})_3$ could form a π -type complex. Between 30-40% of the PMMA chains contain such a structure¹⁴⁵ and thus even at 1:400, every such active site could be involved in an interaction with a $\text{Co}(\text{acac})_3$ molecule, and so increasing the $\text{Co}(\text{acac})_3$ concentration would have no further effect on this process. It would have been of interest to prepare a blend with a $\text{Co}(\text{acac})_3$ concentration below the critical level and examine its behaviour. Unfortunately, lack of PMMA 3 prevented the preparation of a blend sample of a mass that would have

allowed direct comparison with the other blends. Investigation of the effect with the other, higher molecular weight samples would have involved $\text{Co}(\text{acac})_3$ concentrations so low as to be impractical.

The interaction at the chain ends is obviously favoured above any other interaction as evidenced by the observation that every chain end is apparently involved in an interaction with $\text{Co}(\text{acac})_3$ even when there is only one unsaturated site per four hundred monomer units and only one $\text{Co}(\text{acac})_3$ molecule.

Although there is apparently some process occurring at every chain end, peak 1 is always smaller than the chain-end initiated depolymerisation peak of the unblended PMMA which suggests that in this case the unzipping process is being terminated before the chains can completely depolymerise (indeed were it not for this termination, the height of peak 1 would be independent of molecular weight).

The second peak, also due to depolymerisation varies with both the molecular weight of the polymer and the $\text{Co}(\text{acac})_3$ concentration. Varying directly with $\text{Co}(\text{acac})_3$ concentration, the peak decreases in size with decreasing molecular weight to the extent that the peak is virtually non-existent for the 1:400 PMMA 3 blend. The former effect suggests that the process which causes this depolymerisation step is of a more general nature than that causing the previous step, whilst the latter is due simply to there being in the

lower molecular weight PMMA blends proportionately less $\text{Co}(\text{acac})_3$ available for the reaction pertaining to this second peak. This is because proportionately more $\text{Co}(\text{acac})_3$ is involved in chain-end interactions in the lower molecular weight samples.

The early production of non-condensable material in association with this peak at the highest $\text{Co}(\text{acac})_3$ concentration is to be noted.

Peaks 3 and 4

These two peaks correspond respectively to the unsaturated chain-end initiated and random scission initiated depolymerisation peaks in the TVA trace for PMMA (Chapter 4) and the same processes underlie the peaks described here.

Peak 3 (i.e. that due to chain-end initiation of the polymer itself) is reduced considerably in all the blends, the peak height decreasing with increasing $\text{Co}(\text{acac})_3$ concentration. This effect is most noticeable in the blends of PMMA 3 where the unsaturated chain-end initiated peak is normally most pronounced. With PMMA 1, the presence of $\text{Co}(\text{acac})_3$ reduces this peak to a weak shoulder of Peak 4, the chain-end initiated peak never being very pronounced in this, high molecular weight, sample.

The continued existence of a "normal" chain-end initiated depolymerisation process in the blend indicates the presence of unsaturated chain-end sites

despite the chain-end interaction which gives rise to Peak 1. Thus the Peak 1 process either does not completely remove the original sites, or new unsaturated chain-ends are generated as a consequence (e.g. in the termination reaction). In fact, both mechanisms are valid, as discussed subsequently. The decrease in peak height with increasing $\text{Co}(\text{acac})_3$ content can be attributed to the increased blocking of unzipping by an interaction of the chelate species with the polymer backbone.

Peak 4 (random scission initiated) is affected to only a small extent. There is an increase in the production of -196°C non-condensable material commensurate with the fragmentation of "blocked" chains.

Finally, in the 1:10 blends, there is a "tail" to the fourth peak due presumably to the fragmentation of structures formed in the earlier stages of degradation.

STRUCTURE OF BLENDS AND STRUCTURAL CHANGES DURING DEGRADATION

To study the structure of the blends of PMMA with $\text{Co}(\text{acac})_3$ and changes in structure during degradation, blends of $\text{Co}(\text{acac})_3$ with PMMA 1 in the ratio of 1:50 and 1:10 were prepared. Samples of the undegraded blends were cast from methylene chloride directly onto NaCl discs for IR spectroscopic analysis and onto a silica glass surface for UV spectroscopy, whilst other samples were prepared in the same way in TVA tubes for degradation. A fresh sample (ca. 30mg) was prepared for each degradation and wherever possible standard TVA procedure was followed, the film being cast directly onto the base of the TVA tube. The film was then degraded under standard TVA conditions and the residue formed at each stage of degradation dissolved from the tube base and recast onto a NaCl disc or silica glass surface prior to spectroscopic analysis. However, when the residue was not entirely soluble in methylene chloride, the initial blend was cast directly onto a NaCl disc and, thus supported, degraded. Alternatively, char residue, if removable from the tube base could be run as a KBr disc. In such cases, UV analysis was performed only on those portions of the blend which were soluble.

The spectra of the 1:50 blends are depicted in Figs. 5.10 and 5.11 and those of the 1:10 blends in Figs. 5.12 and 5.13. Tables 5.2 and 5.3 list the

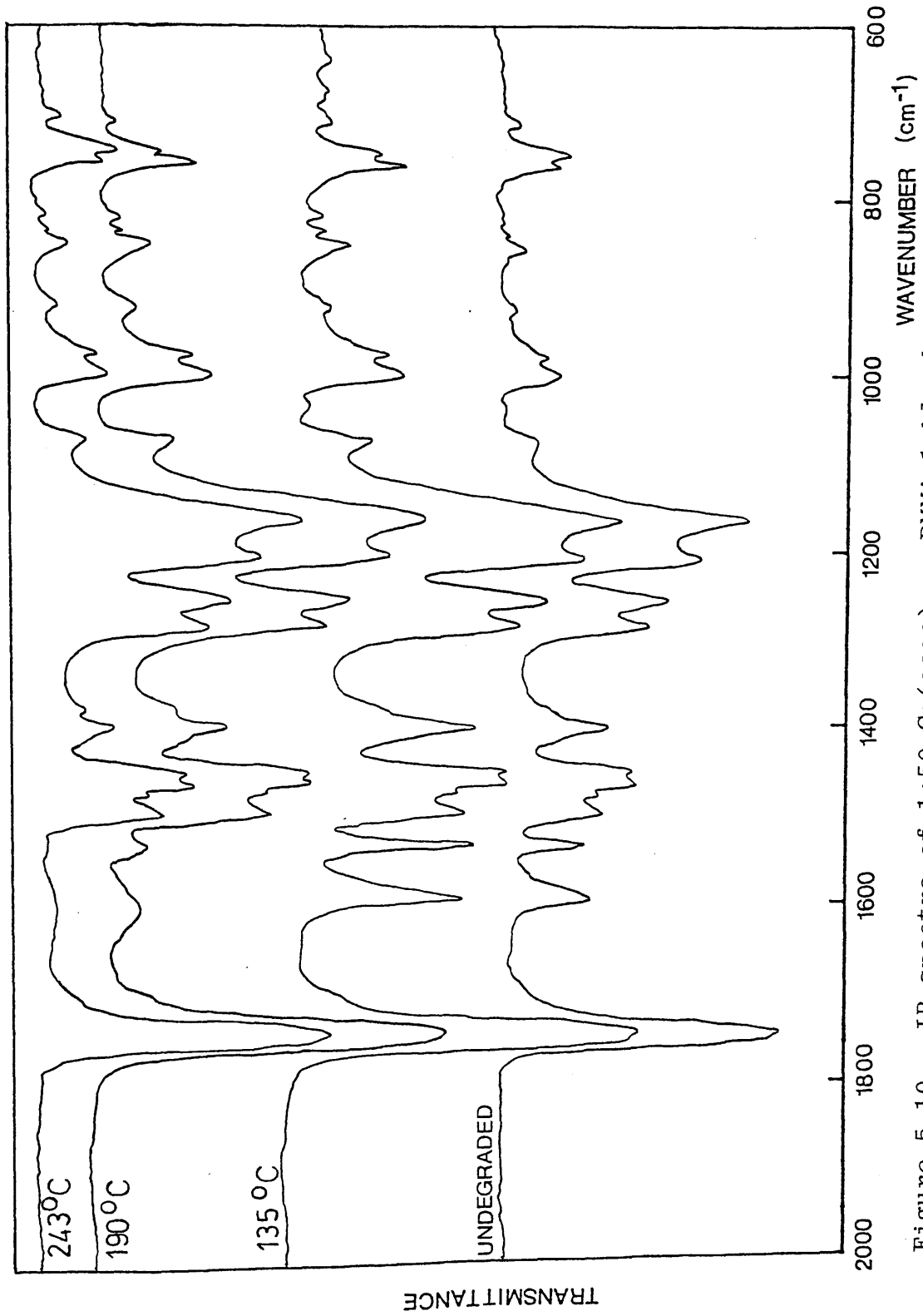


Figure 5.10 IR spectra of 1:50 Co(acac)₃ - PMMA 1 blend at various stages of degradation

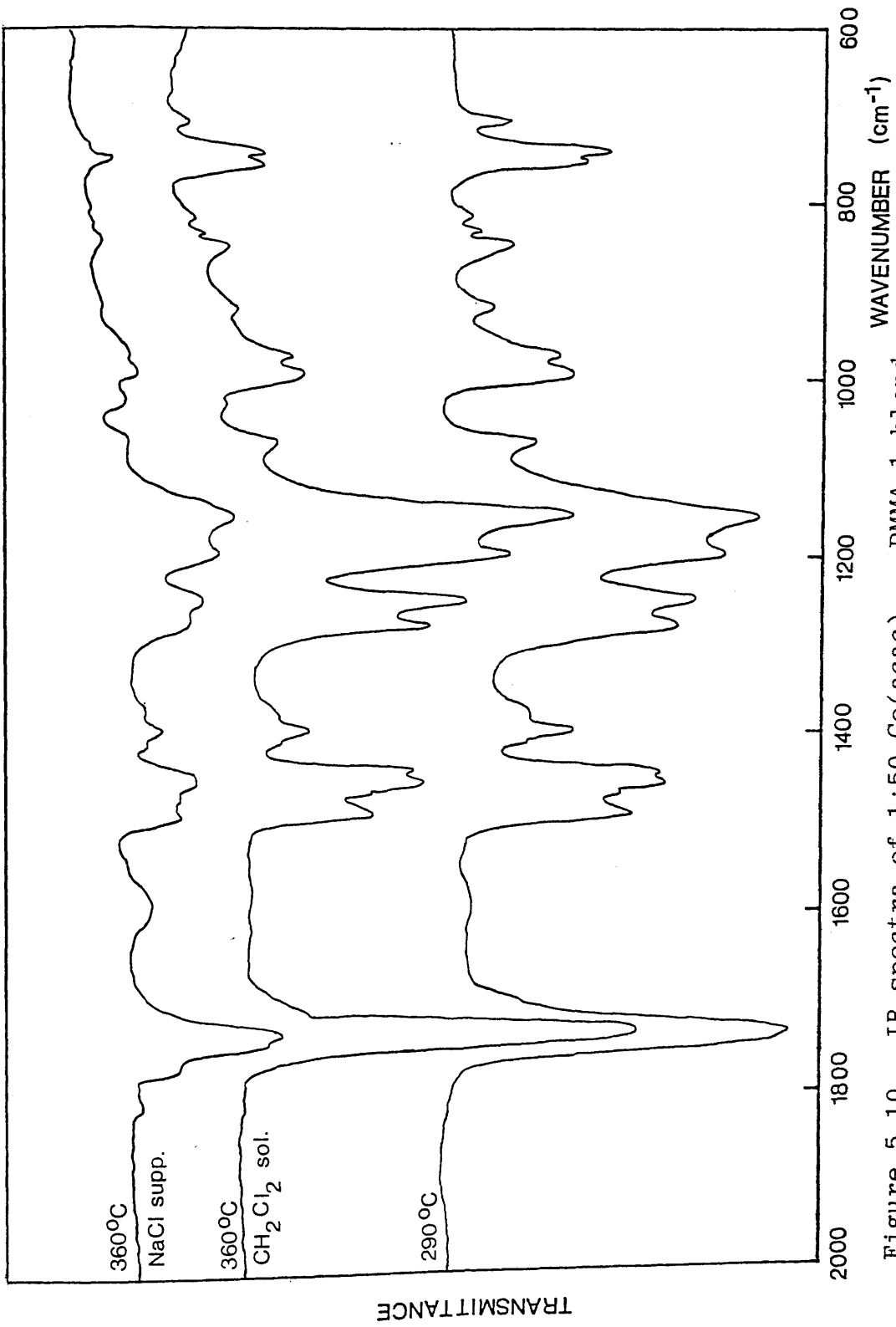


Figure 5.10 IR spectra of 1:50 Co(acac)₃ - PMMA 1 blend at various stages of degradation (ctd.)

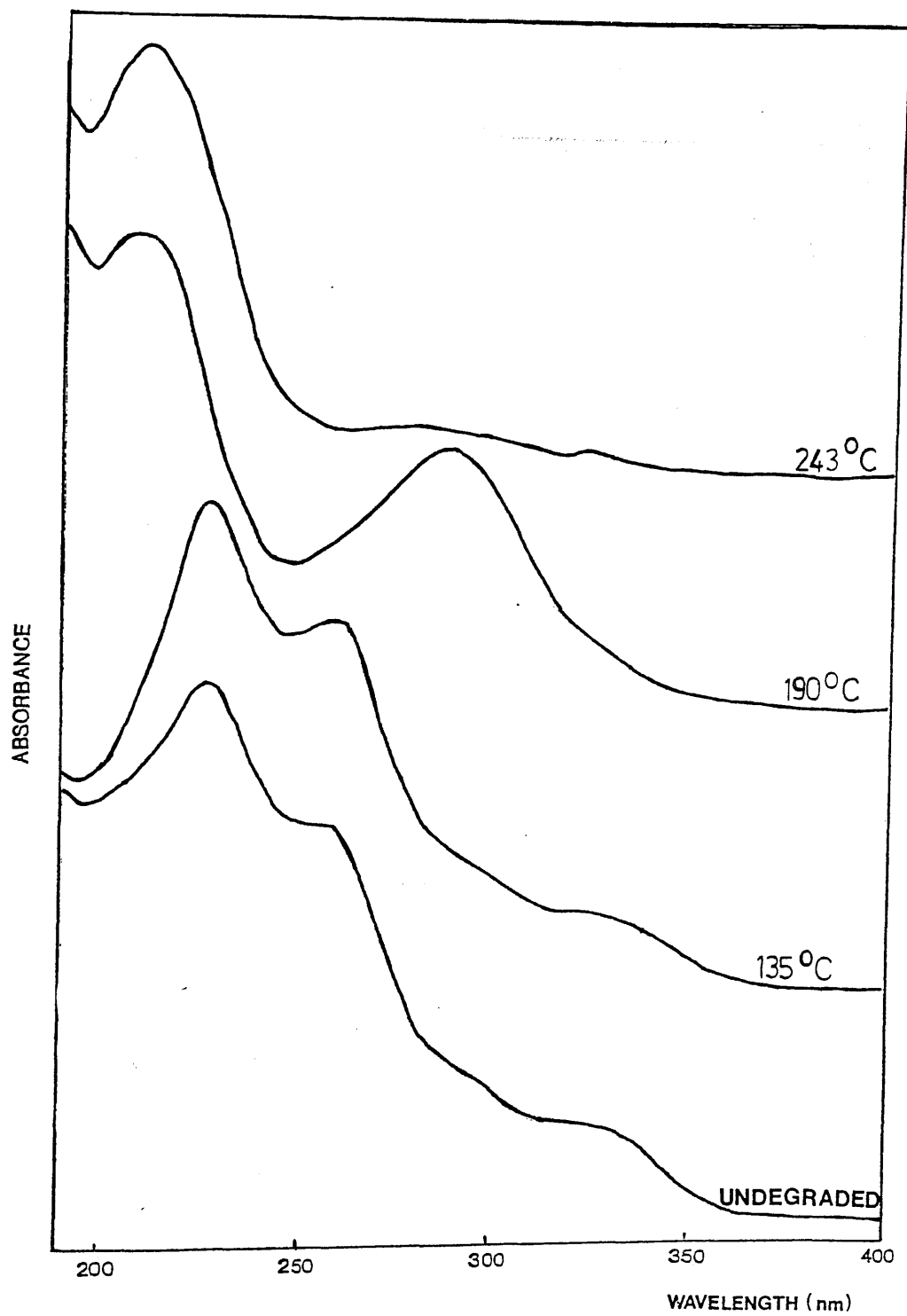


Figure 5.11 UV spectra of 1:50 Co(acac)₃ - PMMA 1 blend at various stages of degradation

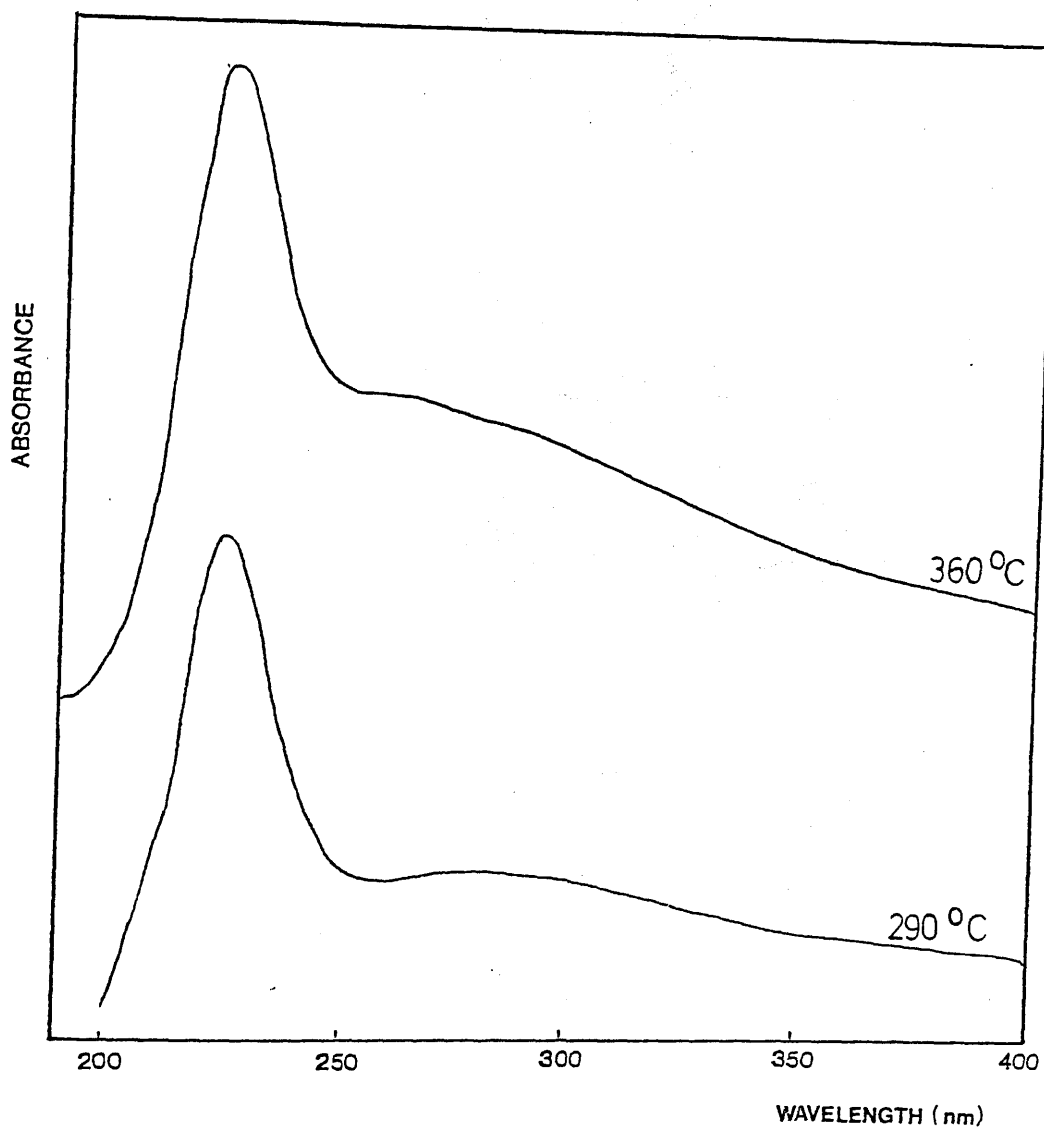


Figure 5.11 UV spectra of 1:50 Co(acac)₃ - PMMA 1 blend at various stages of degradation (ctd.)

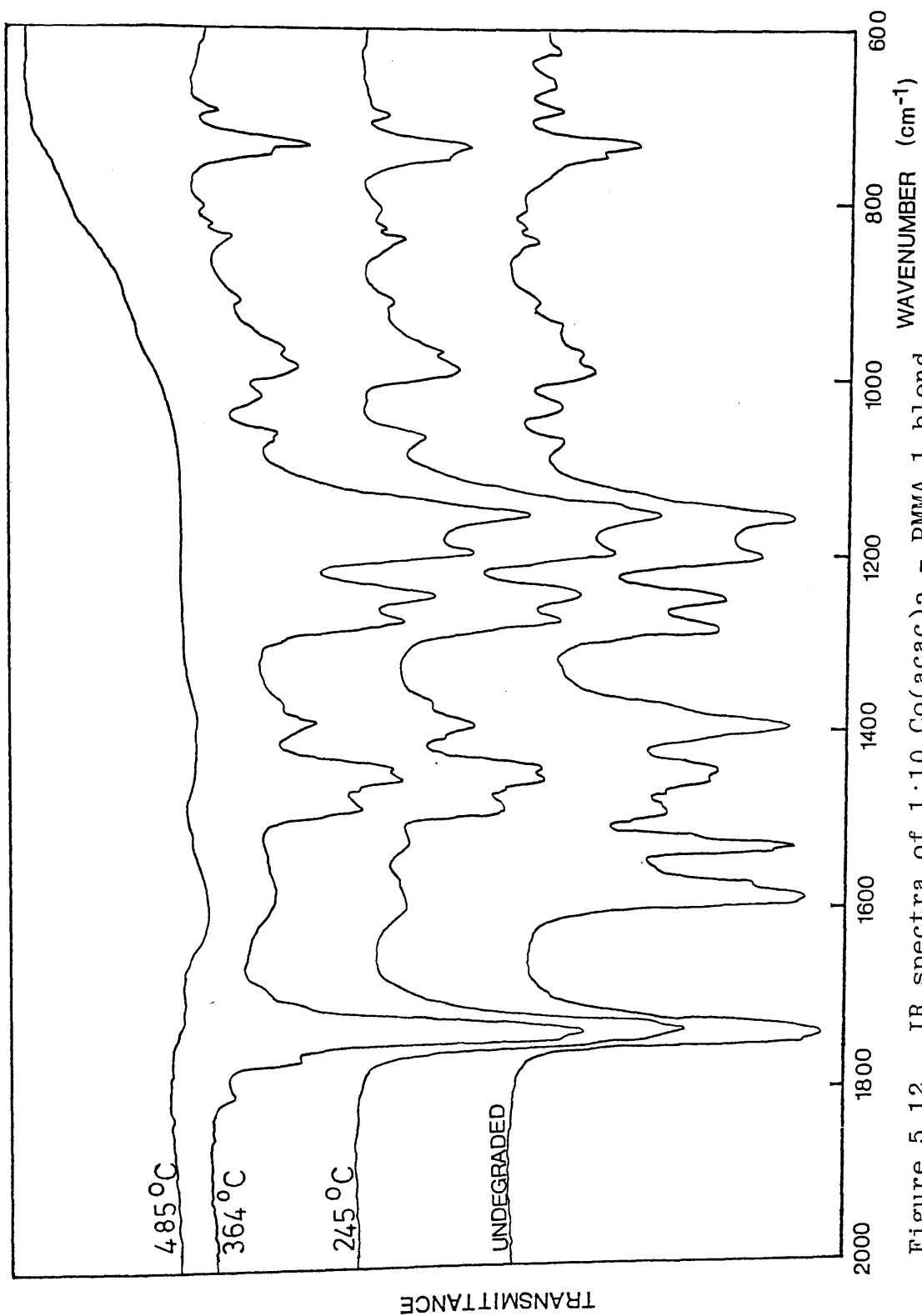


Figure 5.12 IR spectra of 1:10 Co(acac)₃ - PMMA 1 blend at various stages of degradation

TRANSMITTANCE

2000 1800 1600 1400 1200 1000 800 600
WAVENUMBER (cm⁻¹)

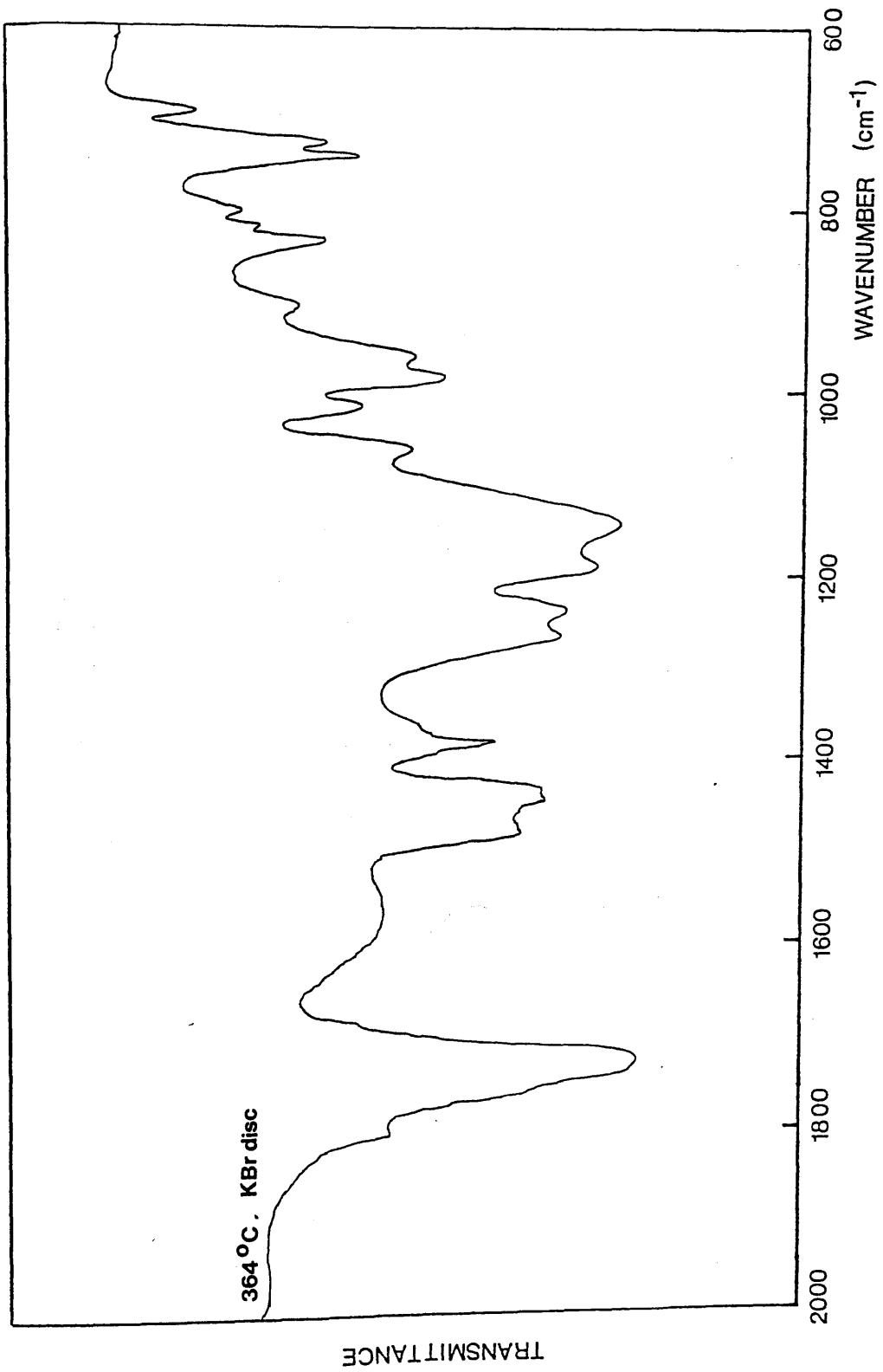


Figure 5.12 IR spectra of 1:10 Co(acac)₃ - PMMA 1 blend at various stages of degradation (ctd.)

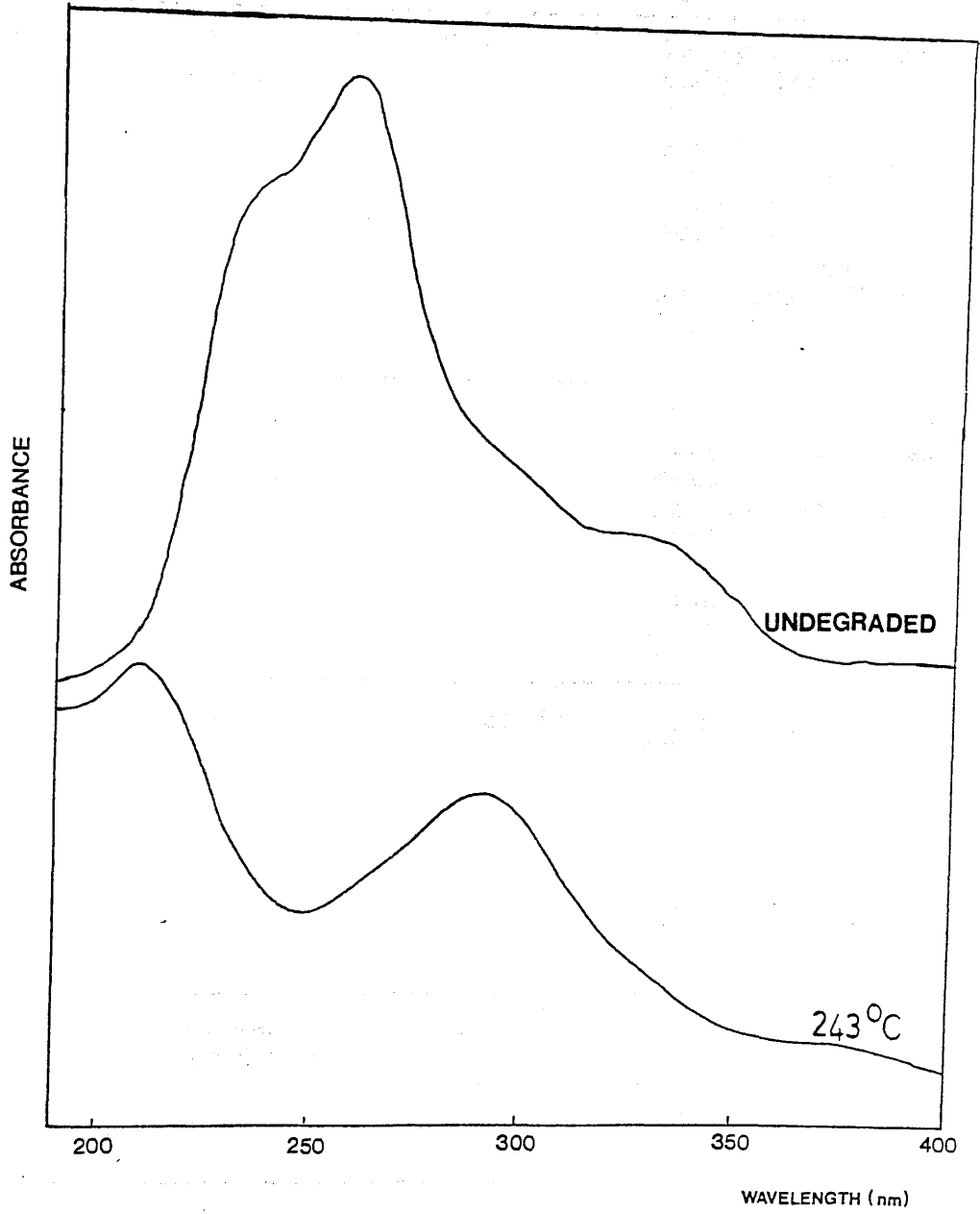


Figure 5.13 UV spectra of 1:10 Co(acac)₃ - PMMA 1 blend at various stages of degradation

Extent of Degradation	Visual Appearance	Solubility in CH ₂ Cl ₂	Other Comments
None	Green, transparent compatible	Yes	No spectroscopic evidence of polymer-chelate interactions.
135°C (A)	No change	Yes	No change in IR, UV spectra
190°C (B)	Transparent with pink colouration	Yes	IR spectrum shows reduction in quantity of chelate present. In UV spectrum $\lambda(\text{max})$ 292nm indicates chelate species in blend to be Co(acac) ₂ Absorption due to PMMA at 214nm now significant.
243°C (C)	Transparent with yellow colouration	Yes	IR spectrum shows very little chelate remains. Yellowing of film => double bond formation. UV spectrum shows PMMA absorption shifted to 228nm => unsaturation.
290°C (D)	No change	Partially	IR spectrum of CH ₂ Cl ₂ soluble portion similar to that at 243°C. Likewise, IR spectrum of film degraded on salt plate. UV spectrum similar to 243°C.
360°C (E)	Transparent Deep Orange	Yes	IR spectrum shows peaks at 1800, 1760 and 1015cm ⁻¹ => glutaric type anhydride rings
485°C (F)	Brown Char	No	Not analysed.

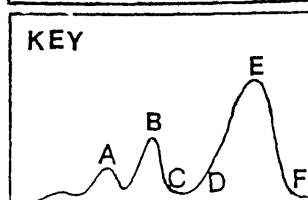


Table 5.2 Structural Changes in 1:50 Co(acac)₃-PMMA 1 Blend on Degradation

Extent of Degradation	Visual Appearance	Solubility in CH ₂ Cl ₂	Structural Features
None	Green, some opaque regions => incompatibility	Yes	No spectroscopic evidence for interaction.
245°C (A)	Transparent orange-yellow	Yes	IR spectrum shows chelate concentration reduced. UV spectrum shows this chelate to be Co(acac) ₂ . Discolouration => double bond formation.
364°C (B)	Orange-brown	Some insol. brown char Remainder soluble	IR spectrum shows absence of acac species. Pronounced 1800, 1760 and 1015 cm ⁻¹ peaks => glutaric-type anhydride structures Pronounced carboxylate absorption 1570cm ⁻¹
485°C (C)	Brown char	No	IR spectrum of char as KBr disc shows carboxylate absorption, centred on 1570cm ⁻¹

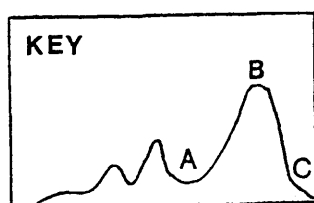
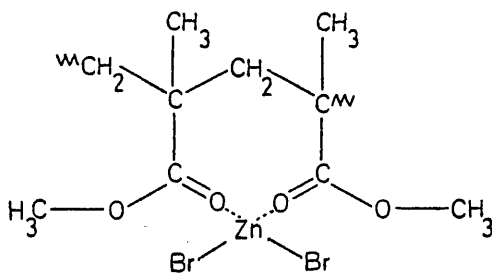


Table 5.3 Structural Changes in 1:10 Co(acac)₃ - PMMA 1 Blend

salient features.

STRUCTURE OF THE UNDEGRADED BLEND

McNeill and McGuinness^{62,63} in their study found that the presence of $ZnBr_2$ caused a broadening of the PMMA carbonyl absorption due to the carbonyl groups acting as donor ligands to the Zn^{2+} ion.



Further evidence for an association of this kind came from the visible spectrum of a model $CoBr_2$ -PMMA blend.

No such broadening of the PMMA carbonyl absorption in the $Co(acac)_3$ -PMMA blends is observed; nor is there any other change in the IR spectrum. Likewise, the UV spectrum shows only the absorptions expected of $Co(acac)_3$ (the PMMA absorption at 214nm is insignificant for the 1:10 and 1:50 blends). However, the lack of an interaction with the ester side chains at room temperature is not unexpected. $Co(acac)_3$ lacks the vacant coordination sites of $ZnBr_2$ and although the partial displacement of an acetylacetonate ligand is known to occur with some electron donors, the results

discussed in Chapter 3 suggest that the methyl ester is not effective for $\text{Co}(\text{acac})_3$ ligand displacement at room temperature.

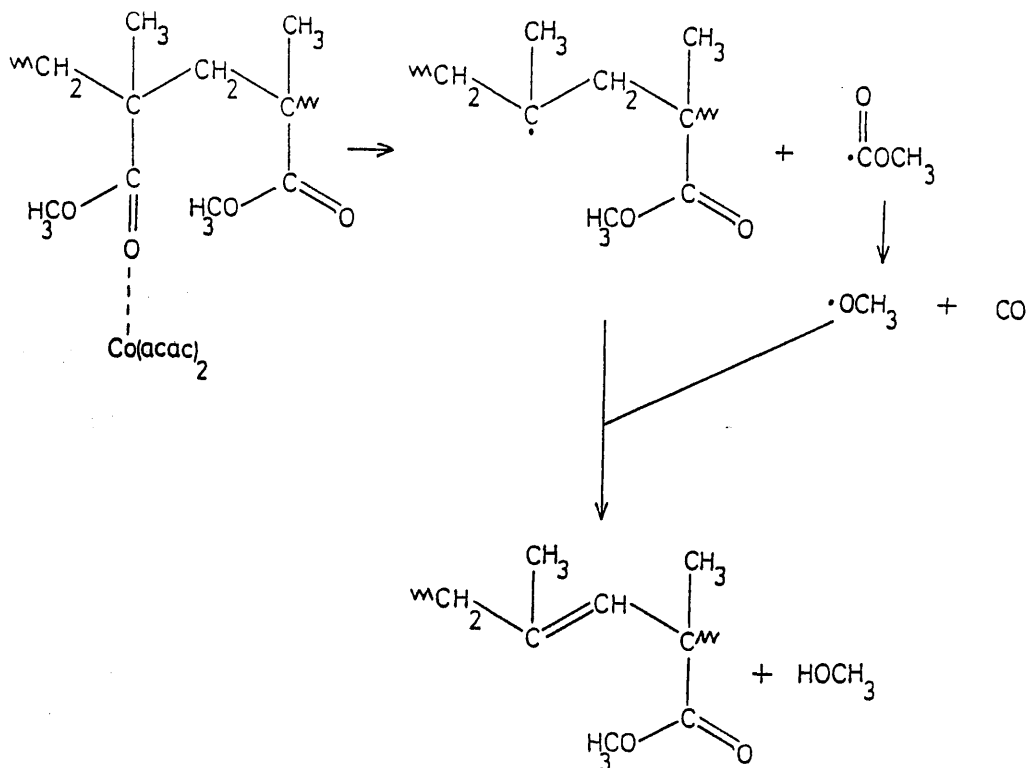
An interaction is expected to occur, however, at the unsaturated chain-ends. Such π -type complexes are observed between $\text{Co}(\text{acac})_3$ and several unsaturated monomers (see Chapters 1 and 3) and although occurring to too small an extent to be observed spectroscopically, the π -complex between $\text{Co}(\text{acac})_3$ and the unsaturated chain ends makes itself manifest by influencing the degradation of the blend (i.e. Peak 1).

CHANGES OF STRUCTURE DURING DEGRADATION

On comparing the structural changes in the 1:10 and 1:50 $\text{Co}(\text{acac})_3$ -PMMA blends, it can be seen that the only differences are essentially a matter of degree, the changes being more pronounced in the 1:10 blend. Consequently, the discussion below applies to both blends.

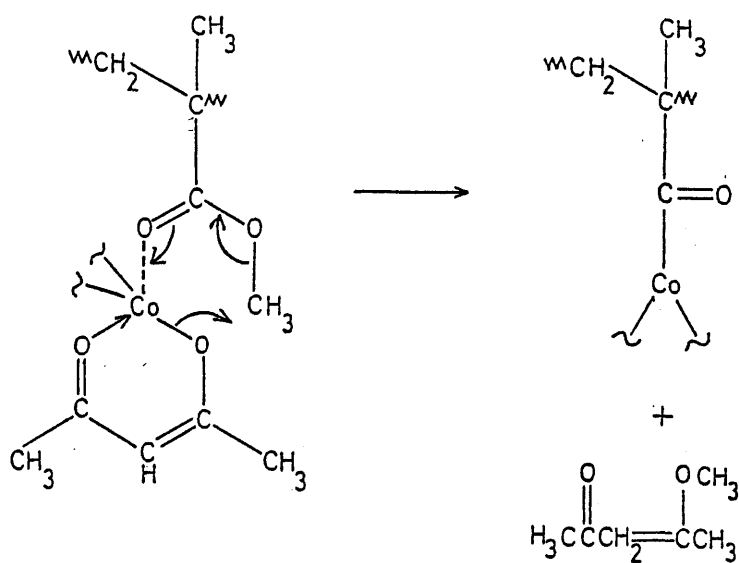
Formation of $\text{Co}(\text{acac})_2$

The first change in the blend observed spectroscopically is the formation of $\text{Co}(\text{acac})_2$. The concurrent formation of the $\text{acac}\cdot$ radical leads to the monomer production at the first two degradation peaks; the mechanism is dealt with later. The importance of $\text{Co}(\text{acac})_2$ in relation to the structure of the blend is that unlike $\text{Co}(\text{acac})_3$, $\text{Co}(\text{acac})_2$ will complex



Formation of Carboxylate Structures

An alternative process open to the polymer coordinated $\text{Co}(\text{acac})_2$ is the formation of polymer bound carboxylate structures by the reaction:-



readily with the ester side-chains. Although ZnBr_2 interacts with adjacent ester carbonyl groups to produce a pseudo-tetrahedral structure around the Zn^{2+} ion,⁶² the $\text{Co}(\text{acac})_2$ will prefer to maintain the square planer arrangement of acac ligands, the Lewis bases forming adducts in the axial position. This, for instance, is the structure of $\text{Co}(\text{acac})_2 \cdot 2\text{H}_2\text{O}$.¹¹

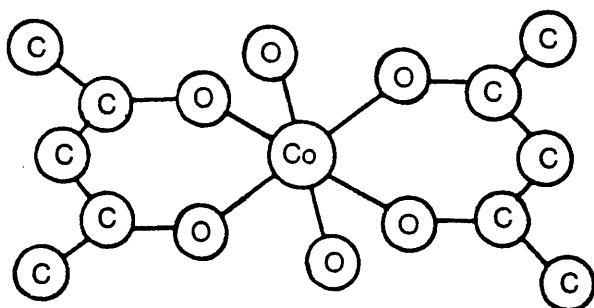
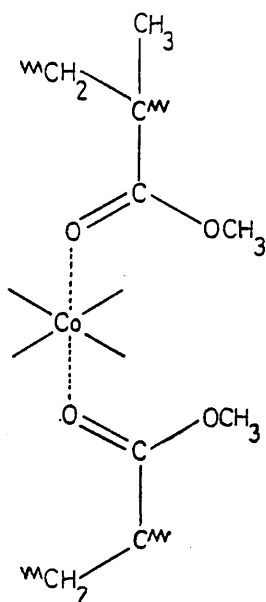


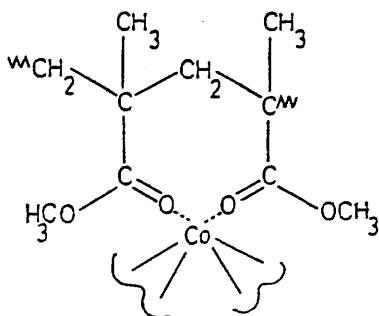
Fig. 5.14 Crystal Structure of $\text{Co}(\text{acac})_2 \cdot 2\text{H}_2\text{O}$
(Adapted from Ref. 11)

The analogous structure in the PMMA blend involving two chains,



is very similar to that expected to form in methyl acetate solution (Chapter 3) and the UV spectrum of the polymer residue at 190°C thus has $\lambda(\text{max})$ 287nm (cf. $\text{Co}(\text{acac})_2$ $\lambda(\text{max})$ 291nm, $\text{Co}(\text{acac})_2 \cdot 2\text{MeOAc}$ $\lambda(\text{max})$ 284nm).

Formation of a pseudo-octahedral structure with the $\text{Co}(\text{acac})_2$ complexing with neighbouring ester groups is conceivable but by requiring rearrangement of the ligands would be less favoured.

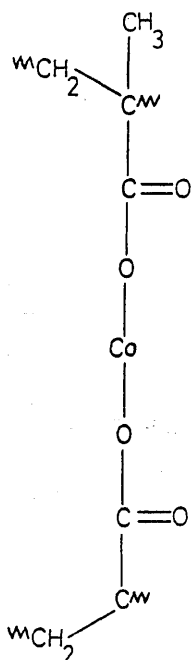


These complexes with the polymer, whose formation is reversible, can subsequently undergo irreversible reactions to form carboxylate and double bond structures as discussed below.

Mechanism Of Double Bond Formation

McNeill and McGuinness⁶³ found double bonds to be produced in the ZnBr_2 - PMMA system at temperatures below 200°C (i.e. in the same temperature region as those formed in the $\text{Co}(\text{acac})_3$ - PMMA blends). Their mechanism leads also to the formation of methanol and carbon monoxide. A small quantity of methanol and some -196°C non-condensable material are identified as products from the $\text{Co}(\text{acac})_3$ - PMMA blend in the same temperature zone as double bond formation and thus the mechanism operative in this system can be considered to be the direct analogy of that occurring in the ZnBr_2 - PMMA blend.

This process may, of course, be repeated to give two polymer chains linked by a dicarboxylate structure,

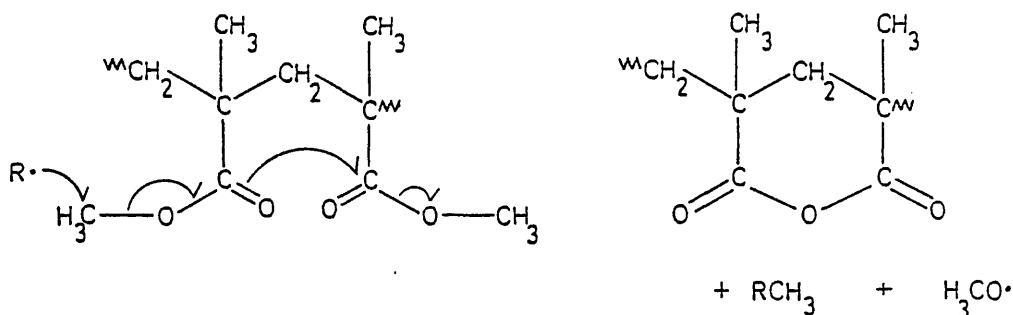


which is likely to be the process by which the polymer becomes partly insoluble in methylene chloride. No evidence for the presence of the 4-methoxy-3-penten -2-one expected to be produced in this carboxylate formation has been found in the IR spectra of the products but its similarity to acetylacetone would preclude separation by SAD and acetylacetone would mask the expected¹⁴⁶ IR spectrum absorptions at 1660 and 1632cm⁻¹.

Production of Anhydride Structures

The production of anhydride structures in poly(methacrylic acid) and methyl methacrylate-methacrylic acid copolymers has been discussed in

Chapter 4. The production of similar structures in the $\text{Co}(\text{acac})_3$ -PMMA blend, however, occurs by a different mechanism - that proposed by McNeill and McGuinness for the production of anhydride structures in ZnBr_2 - PMMA blends.⁶³

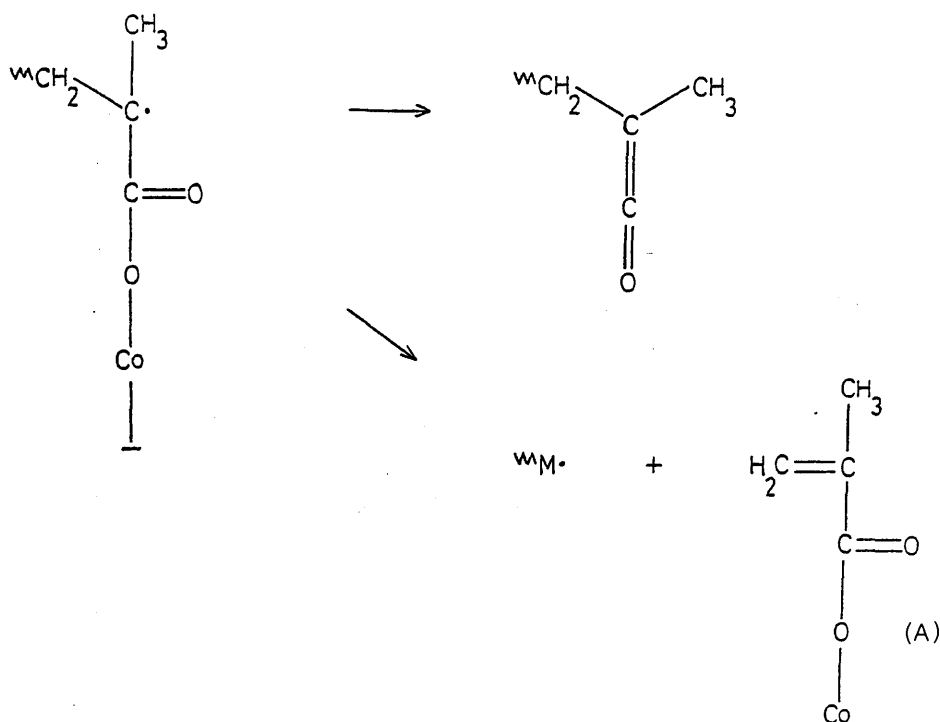


$\text{R}\cdot$ is probably a radical formed either by decomposition of $\text{Co}(\text{acac})_3$ or as a result of interaction between $\text{Co}(\text{acac})_3$ and polymer. The nature of $\text{R}\cdot$ will be discussed more fully in a later section.

Final Decomposition of Structures Formed

The final structural changes involve the decomposition of the structures formed previously with the evolution of gaseous products. The polymer chains depolymerise and fragment; the anhydride and carboxylate structures also fragment. Studies of metal polymethacrylates¹⁴⁷ similar to the cobalt carboxylate structure found in this blend have shown them to be thermally stable to approximately $400\text{-}450^\circ\text{C}$ and the cobalt carboxylate is also apparently thermally stable.

It survives until depolymerisation of the chain takes place.



Structures analogous to the cobalt methacrylate salt (A) are known to be thermally stable¹⁴⁸ and thus it will be this salt which persists at 485°C.

SUMMARY OF STRUCTURAL CHANGES

1. Decomposition of $\text{Co}(\text{acac})_3$ - chain-end complex with $\text{Co}(\text{acac})_2$ formation (not observed spectroscopically)
2. Thermal decomposition of $\text{Co}(\text{acac})_3$ with $\text{Co}(\text{acac})_2$ formation.
3. Complexing of $\text{Co}(\text{acac})_2$ to ester groups (reversible).

4. Formation of unsaturated and carboxylate structures.
5. Formation of anhydride structures.
6. Fragmentation of modified polymer chain.

The blends were cast as films from methanol and were of the order of 30-50mg. The films were subjected to standard TGA conditions to various temperatures; a fresh sample being prepared at 100°C condensable products were collected in a nitrogen trap before analysis by spectroscopy. Where necessary, the 196°C products were first reprecipitated by NaCl. IR is performed either in the gas or liquid phase to test reliability of the products.

The cold ring fraction (CRF) was seen as a white solid in a flask and was analysed by IR spectra. IR spectra were first cast into the CRF from solution into NaCl.

Table 5.4 & 5.7 list the composition of products from the 1:50 and 1:10 blends.

Blends of Colocast, with PMMA 2 at 1:50 and 1:10 were also degraded to IR products analysed. These were found to be those from the PMMA 1 blends.

-196°C CONDENSIBLE GAS AND LIQUID PRODUCTS AND COLD RING FRACTION OF Co(acac)₃ - PMMA BLENDS

To study the above products, blends of Co(acac)₃ and PMMA 1 were prepared at concentrations of 1:50 and 1:10. The blends were cast as films from methylene chloride and were of the order of 30-50mg. The blends were cast as films from methylene chloride and were of the order of 30-50mg. The films were heated under standard TVA conditions to a series of temperatures; a fresh sample being prepared for each run. -196°C condensible products were collected in a liquid nitrogen trap before analysis by IR spectroscopy. When necessary, the -196°C condensible products were first separated by SAD. IR analysis was performed either in the gas or liquid phase depending on the volatility of the products.

The cold ring fraction (CRF) was swabbed with a methylene chloride soaked tissue and UV analyses were performed on this solution. IR spectra were obtained by first casting the CRF from solution onto NaCl discs.

Tables 5.4 - 5.7 list the components of both types of products from the 1:50 and 1:10 blends.

Blends of Co(acac)₃ with PMMA 2 at the ratios of 1:50 and 1:10 were also degraded to 485°C and the products analysed - these were found to be the same as those from the PMMA 1 blends.

Extent of Degradation	Products
135°C (A)	Methylene chloride (solvent), methyl methacrylate
190°C (B)	As 135°C, plus acetylacetone
243°C (C)	As 190°C plus trace of methanol
290°C (D)	As 243°C
360°C (E)	As 243°C
485°C (F)	As 243°C plus methanol, a ketene, carbon dioxide, water(?), liquid cyclic anhydrides (See Fig. 5.15)

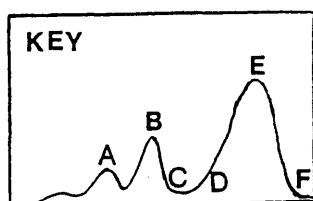


Table 5.4 Total -196°C Condensable Gases and Liquids from 1:50 Co(acac)₃ - PMMA 1 Blend at Various Stages of the Heating Programme

Extent of Degradation	Cold Ring Fraction
135°C (A)	No CRF detected.
190°C (B)	IR spectrum - chelate absorptions UV absorption λ (max) 290nm => Co(acac) ₂ is major component. Small quantity chain fragments.
243°C (C)	As 190°C.
290°C (D)	As 190°C.
360°C (E)	IR spectrum shows significant quantities of chain fragments including glutaric-type anhydride rings (1800 and 1760 cm ⁻¹) (Fig. 5.16).
485°C (F)	As 360°C.

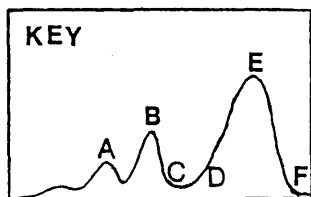


Table 5.5 Cold Ring Fraction from 1:50 Co(acac)₃-PMMA 1 Blend at Various Stages of the Heating Programme

Extent of Degradation	Products
245°C	Methyl methacrylate, acetylacetone, methanol, (acetone?)
485°C	Methyl methacrylate, acetylacetone, methanol, carbon dioxide, a ketene, acetone, methyl acetate, liquid cyclic anhydrides, butene (trace), isobutene (trace)

Table 5.6 Total -196°C Condensable Gases and Liquids from the 1:10 Co(acac)₃ - PMMA 1 Blend at Various Stages of the Heating Programme

Extent of Degradation	Products
245°C	Green sublimate. UV spectrum $\lambda(\text{max})$ 254nm confirms presence of Co(acac) ₃ as major component.
485°C	IR spectrum shows chain fragments including glutaric-type anhydride structures (Fig. 5.16).

Table 5.7 Cold ring fraction from the 1:10 Co(acac)₃ - PMMA 1 blend at various stages of the heating programme

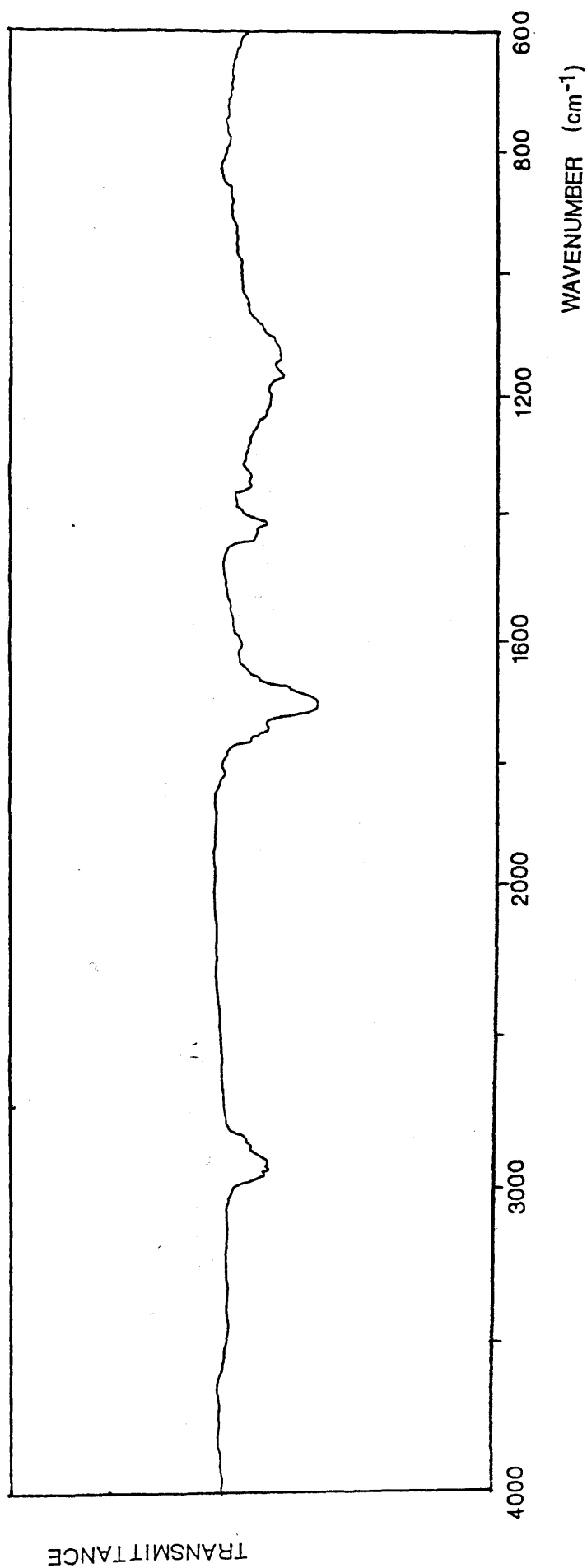


Figure 5.15 IR spectrum of liquid fraction from SAD analysis of products from degradation to 485°C of 1:10 Co(acac)₃ - PMMA 1 blend

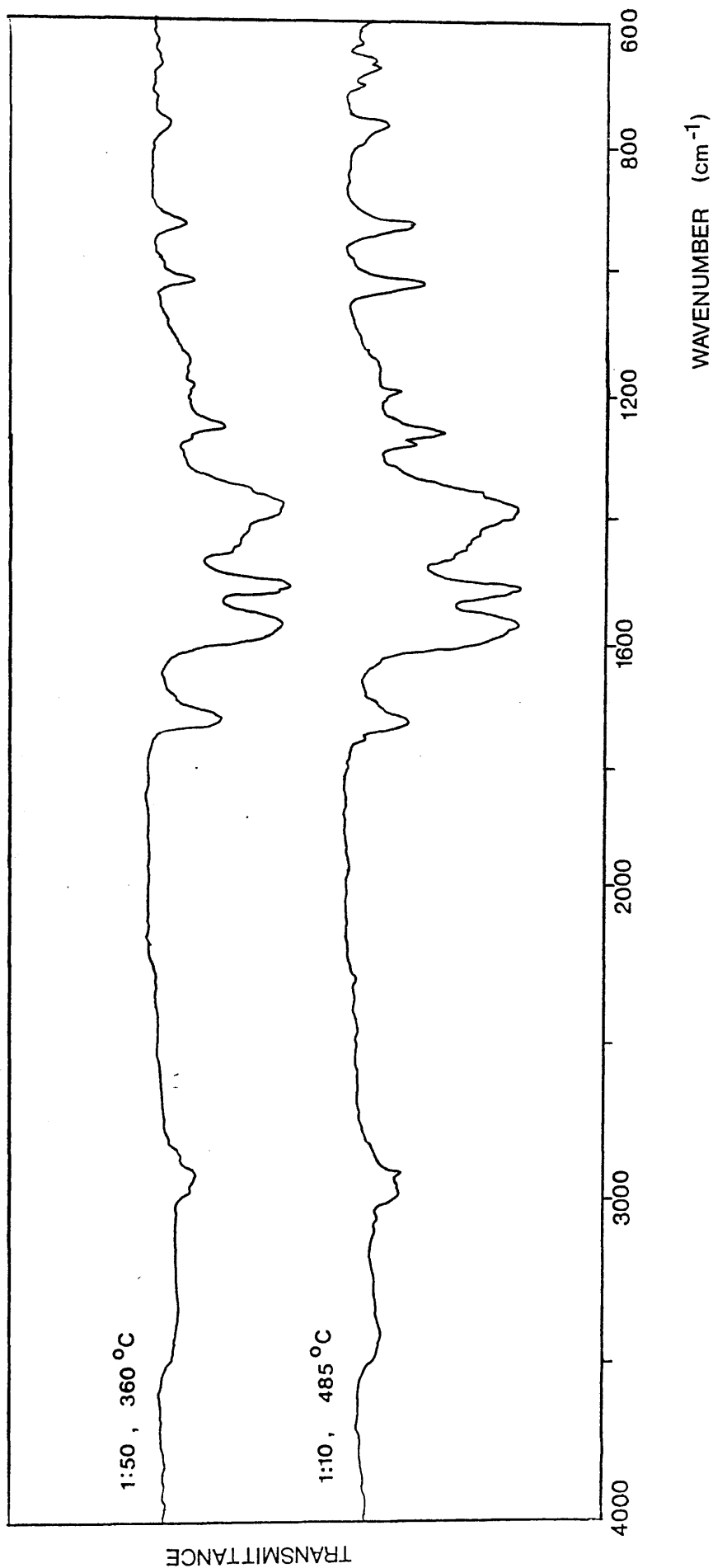


Figure 5.16 IR spectra of CRF from 1:50(1:10) Co(acac)₃ - PMMA 1 blend on degradation to 360°C (485°C)

COMMENTS ON THE -196°C CONDENSIBLE PRODUCTS AND COLD RING FRACTION

As is the case for structural changes, the differences between the 1:50 and 1:10 $\text{Co}(\text{acac})_3$ - PMMA 1 blends are of scale. The increased range and quantity of non-monomer products in the 1:10 blend is due to the greater amount of anhydride and carboxylate formation in this blend. Thus, the butene and isobutene observed as products from the 1:10 blend are, along with the carbon dioxide, "ketene" and some of the the methanol, fragmentation products of "blocked" PMMA and are not observed from the 1:50 blend simply because of the lower degree of fragmentation. Similarly, the methyl acetate and some of the methanol result from the production of anhydride rings. Acetone is a decomposition product of $\text{Co}(\text{acac})_3$ but can also be formed during the production of anhydride rings.

The acetylacetone produced in the region of 190°C results from the formation of the $\text{Co}(\text{acac})_2$ observed in the blend at their temperature, and the identification of the concurrent production of methyl methacrylate confirms the evidence from the TVA curves that the initial two degradation steps involve depolymerisation.

ISOTHERMAL DEGRADATION OF 1:50 Co(acac)₃ - PMMA 1 BLEND

To further elucidate the nature of the first two decomposition steps of the Co(acac)₃ - PMMA blends, isothermal degradations were performed on two samples of the 1:50 Co(acac)₃ - PMMA 1 blend. Samples (ca. 100mg) were cast for methylene chloride directly onto the base of a TVA tube and, with the exception of the isothermal heating, normal TVA conditions were applied. Samples were heated at 136°C and 197°C (approximately the T(max) of each of the first two peaks) and heating was continued until the cessation of volatile production (35 mins and 100 mins respectively). Analysis of products were performed in the same manner as for the programmed heating degradations.

Table 5.8 lists the nature of the products obtained. See also Fig. 5.17.

TRANSFORMED

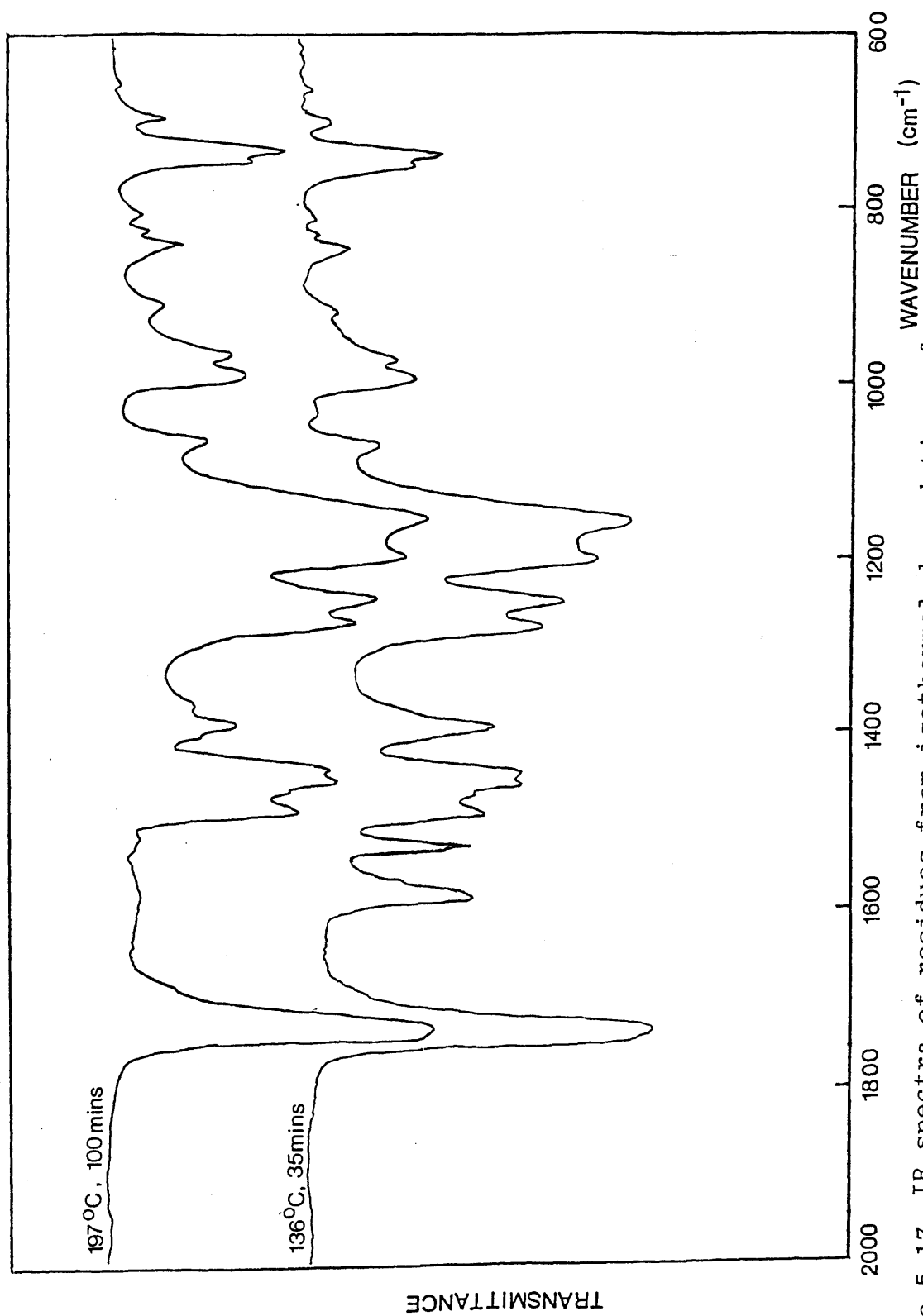


Figure 5.17 IR spectra of residues from isothermal degradations of 1:50 Co(acac)₃ - PMMA 1 blends.

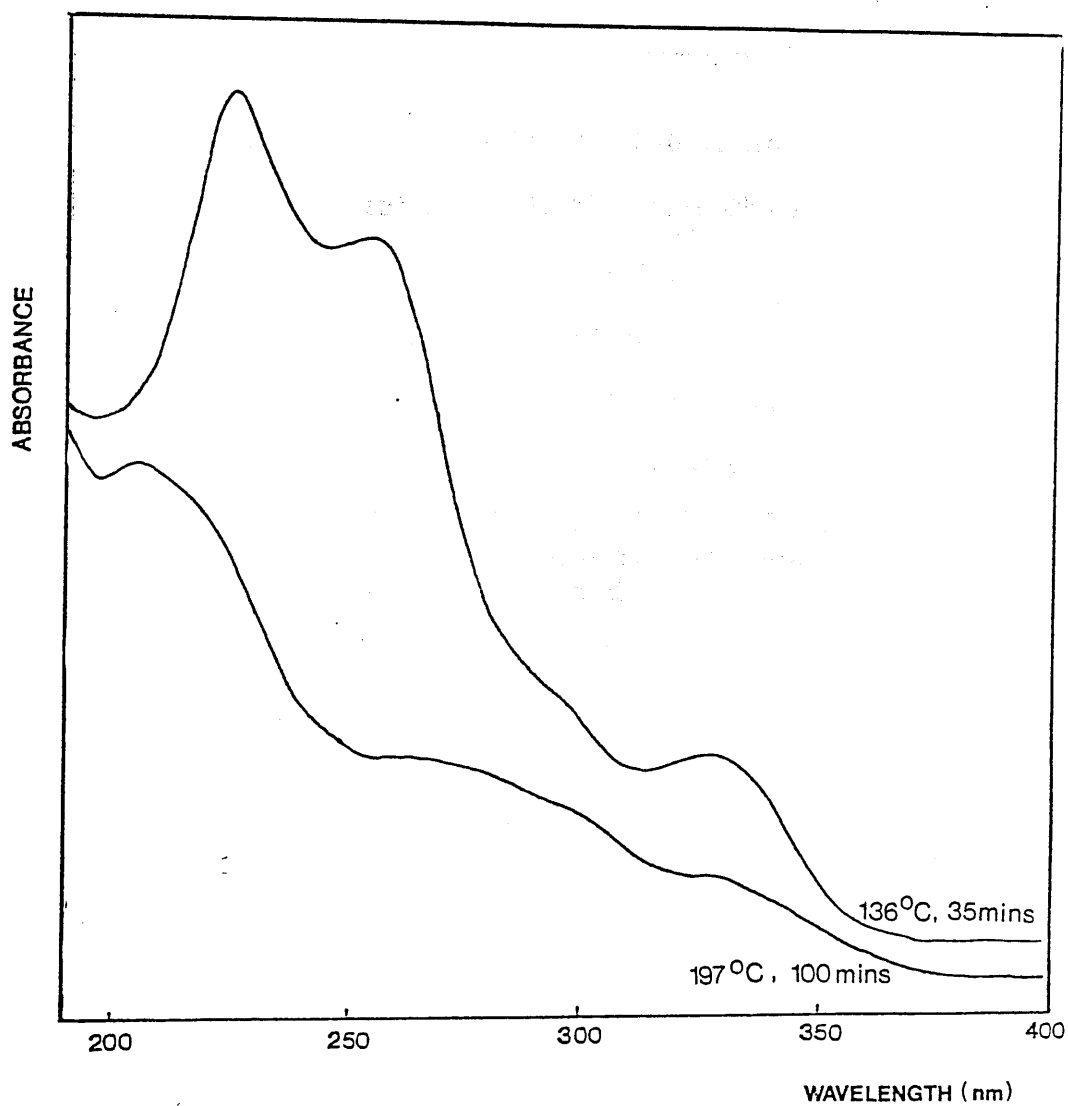


Figure 5.17a

UV spectra of residues from isothermal degradations of
1:50 Co(acac)₃ - PMMA 1 blends.

Co(acac) ₃ - PMMA 1 1:50 136°C 35 Mins	
-196°C Condensable Products	Methylene chloride (solvent), methyl methacrylate, acetylacetone
Cold Ring Fraction	None detected
Residue	Identical to undegraded blend
Co(acac) ₃ - PMMA 1 1:50 197°C 100 Mins	
-196°C Condensable Products	Methylene Chloride (solvent), Methyl methacrylate, acetylacetone, methanol (trace).
Cold Ring Fraction	Co(acac) ₃ , Co(acac) ₂
Residue	Yellow, CH ₂ Cl ₂ soluble.

Table 5.8 Products from isothermal degradations of 1:50 Co(acac)₃ - PMMA 1 Blend

Temperature (°C)

Fig. 5.18

samples were collected in gas cell analysis and analysed on a Kratos spectrometer. Due to a limitation on machine

IDENTIFICATION OF -196°C CONDENSIBLE PRODUCTS OF
DEGRADATION TO 485°C OF 1:10 Co(acac)₃ - PMMA 1
BLEND BY MASS SPECTROMETRY

The -196°C condensible products of degradation were analysed by mass spectrometry after separation by SAD. Fig. 5.18 illustrates the SAD trace and the separation of the fractions.

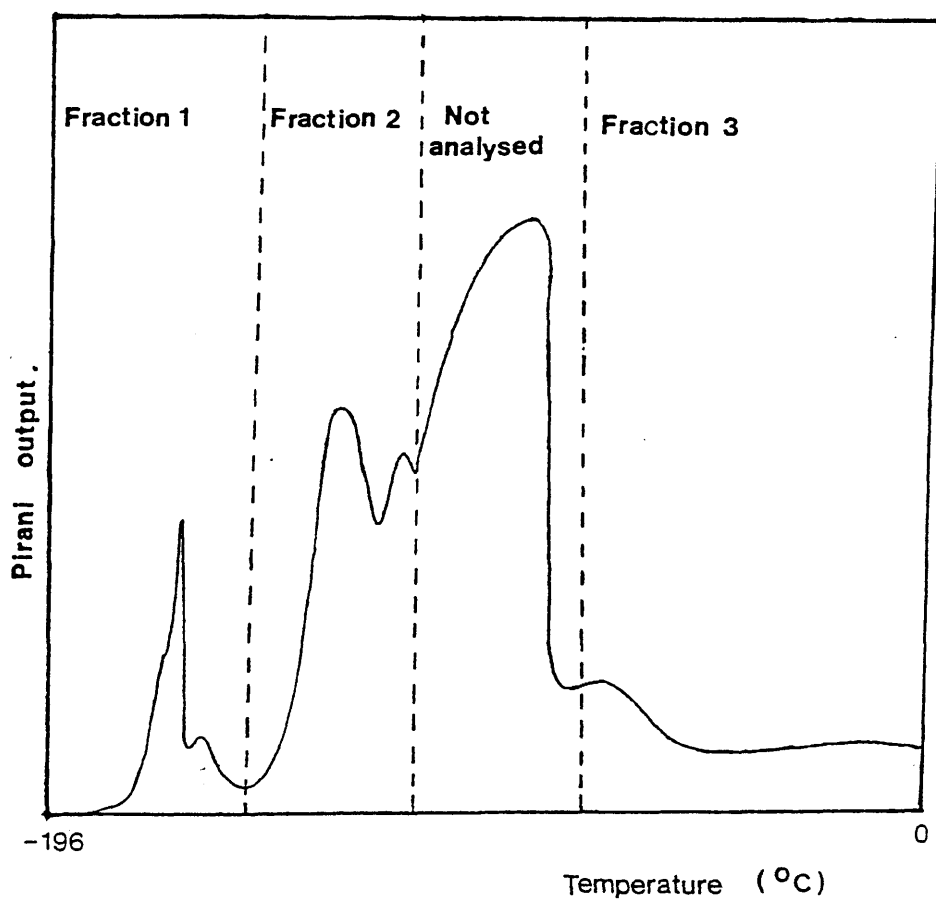


Fig. 5.18

Samples were collected in gas cells as for IR analysis and analysed on a Kratos MS12 mass spectrometer. Due to a limitation on machine time, the

fraction containing the major portion of the methyl methacrylate peak was not analysed. Table 5.9 lists the m/e - intensity data for the mass spectra of the fractions.

Interpretation of these mass spectra is difficult as each fraction contains a mixture of products, some of which have common fragment ions. Furthermore, the presence of methylene chloride in relatively large quantities significantly reduces the signals from the other components of the fraction.

The products identified by the mass spectra (Table 5.10) are mostly those already identified by IR spectroscopy. The appearance of a peak at m/e 70 in the first fraction suggests the presence of dimethyl ketene, whilst the peaks at m/e 45 and 46 could be attributed to dimethyl ether. Dimethyl ether was not identified by IR spectroscopy, but is a plausible product of the degradation. Dimethyl ether is observed by IR spectroscopy from the $\text{Co}(\text{acac})_3$ - copolymer systems in which anhydride formation and fragmentation are more emphasised (Chapter 6).

OVERALL CONCLUSIONS ON THE NATURE OF THE DECOMPOSITION OF THE $\text{Co}(\text{acac})_3$ - PMMA BLENDS

First Two Steps

Both the first two degradation processes occurring in the blend result from the initial

FRACTION 1		FRACTION 2		FRACTION 3	
Mass	% Ar. Base	Mass	% Ar. Base	Mass	% Ar. Base
22.1	0.74	24.8	0.39	24.8	0.37
24.8	0.12	25.5	0.37	26.3	0.32
25.3	0.74	26.3	1.00	27.3	0.61
26.3	2.78	27.3	1.59	28.1	2.62
27.3	7.67	28.1	2.52	29.0	1.24
28.1	13.18	29.0	4.40	29.8	0.13
29.0	4.76	29.8	0.59	30.9	0.90
29.8	0.74	30.9	3.66	32.1	1.11
30.9	0.80	32.1	1.90	35.2	15.51
32.0	1.24	33.2	0.32	36.2	3.09
35.2	13.12	35.2	18.10	37.1	4.97
36.2	2.60	36.2	3.79	38.1	1.14
37.1	4.27	37.1	5.98	39.0	3.57
38.1	5.45	38.1	3.10	39.9	0.71
39.0	24.88	39.0	17.51	41.1	7.32
39.9	6.00	39.9	3.54	42.0	1.82
41.0	34.59	41.0	27.89	43.1	3.01
42.1	8.17	42.1	1.88	44.1	0.24
43.2	1.30	43.1	2.83	45.2	0.16
44.1	100.00	44.2	0.27	47.1	24.15
45.2	3.28	45.2	0.61	48.0	10.62
46.2	2.04	47.1	29.52	49.0	100.00
47.1	19.80	48.0	13.04	49.9	4.25
48.0	8.66	49.0	100.00	50.9	31.61
49.0	79.21	49.9	5.03	52.0	0.37
49.9	4.52	50.9	36.43	53.1	0.18
50.9	24.57	52.0	0.44	55.2	0.29
52.0	0.87	53.1	0.61	56.2	0.21
53.1	1.24	54.2	0.37	58.1	0.13
54.2	0.62	55.2	1.20	59.0	0.40
55.2	4.15	56.2	1.07	69.0	2.70
56.2	5.01	57.1	0.39	69.9	0.79
57.2	0.37	58.1	0.49	72.0	0.55
58.1	0.06	59.0	2.17	82.0	0.90
59.0	1.24	59.9	0.05	83.0	2.22
67.1	0.19	67.0	0.07	84.1	62.68
68.1	0.06	68.1	0.29	85.1	2.09
69.0	8.23	69.0	14.24	86.1	40.06
70.0	1.24	69.9	1.61	87.0	0.66
72.0	0.43	71.1	0.22	88.0	6.47
82.0	1.18	72.0	0.88	89.0	0.03
83.0	1.92	73.1	0.20	99.1	0.42
84.1	49.69	74.1	0.27	100.0	1.98
85.1	1.98	81.1	0.15	101.1	0.13
86.1	31.00	82.0	1.29		
87.0	0.56	83.0	2.69		
88.0	4.83	84.1	74.33		
99.1	1.24	85.1	2.42		
100.0	3.77	86.1	47.42		
101.1	0.06	87.0	0.76		
		88.0	7.59		
		89.0	0.07		
		91.1	0.05		
		99.1	2.05		
		100.0	7.20		
		101.1	0.46		

Table 5.9 Mass Spectra of Products of Degradation of the 1:10
Co(acac)₃ - PMMA Blend After SAD Fraction

FRACTION	PRODUCTS IDENTIFIED
1	ketene, methyl ketene, dimethyl ketene dimethyl ether, carbon dioxide, butene/isobutene
2	acetone, methyl acetate, methylene chloride, methyl methacrylate
3	methylene chloride, methyl methacrylate

Table 5.10 Products from degradation to 485°C of 1:10 Co(acac)₃ - PMMA 1 blend, identified by mass spectrometry

decomposition of the chelate viz:-



Although under TVA conditions $\text{Co}(\text{acac})_3$ sublimes almost completely (94%), when blended with PMMA sublimation is inhibited as the chelate becomes trapped within the polymer matrix. Hence there is little sublimation of $\text{Co}(\text{acac})_3$ from the 1:50 blend although there is, of course, rather more from the incompatible 1:10 blend. Thus trapped, the chelate will undergo the type of decomposition observed in other systems in which sublimation from the reaction zone is inhibited (e.g. in sealed tubes or under an atmosphere of nitrogen).

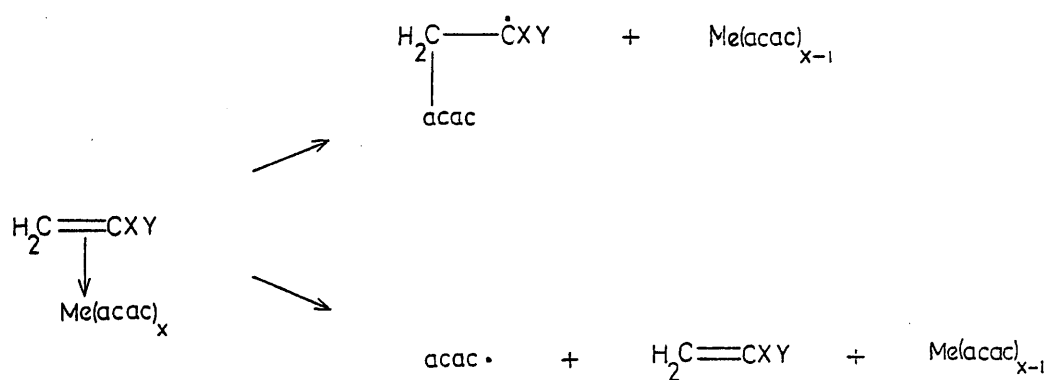
Step 1 (Peak 1 of Fig. 5.9)

The first degradation peak results from the decomposition of the π -type complex formed between $\text{Co}(\text{acac})_3$ and the unsaturated sites at the chain ends. Although there is no direct spectroscopic evidence for complex formation, such a complex is expected by analogy with the $\text{Co}(\text{acac})_3$ - methyl methacrylate system (Chapter 3). Furthermore, as already discussed, the TVA behaviour of this peak is consistent with it being due to an interaction at a limited number of chain ends.

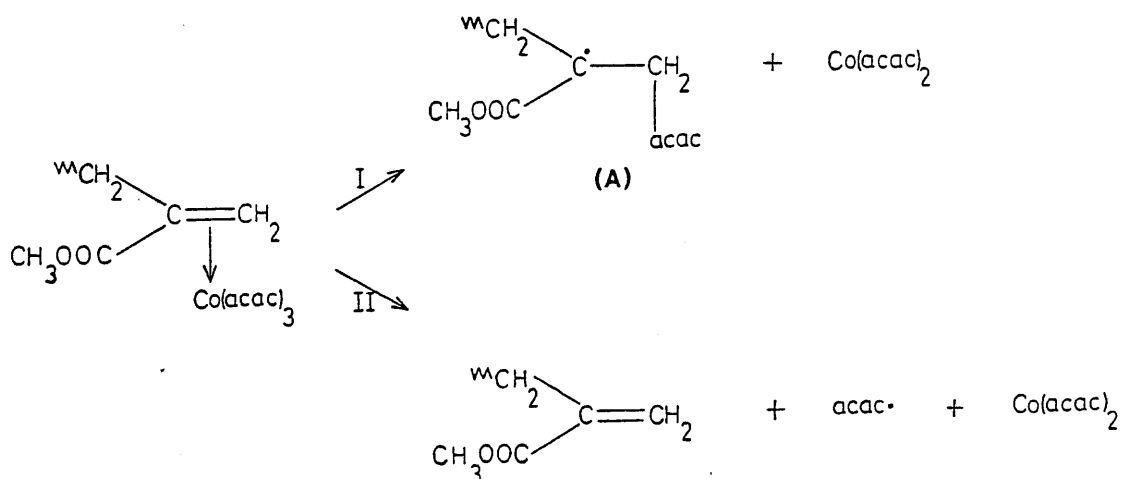
The π -complex weakens the chelate metal-ligand bonds and thus promotes ligand scission; this is the process exploited in the use of the metal acetylacetonates as polymerisation initiators (Chapter 1). Thus the $\text{Co}(\text{acac})_3$ complexed with the unsaturated

chain ends of the PMMA undergoes ligand scission at a lower temperature than the rest of the $\text{Co}(\text{acac})_3$ dispersed throughout the matrix. Although π -complex promoted ligand-scission in monomer solution is observed at temperatures as low as 60°C ,²⁶ such radical formation is not favoured in non-polar solvents¹⁴⁹ and thus in the polymer blend the ligand scission reaction occurs some $60\text{--}70^\circ\text{C}$ higher.

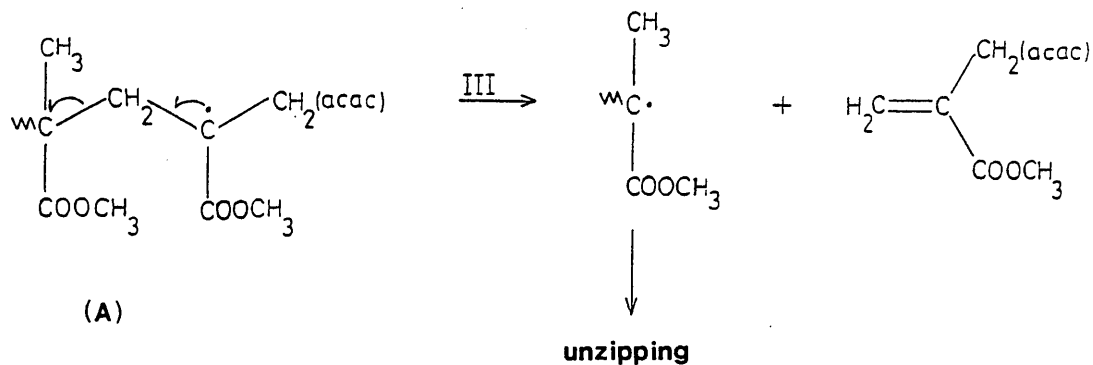
Two mechanisms have been proposed for the polymerisation initiation reaction:-



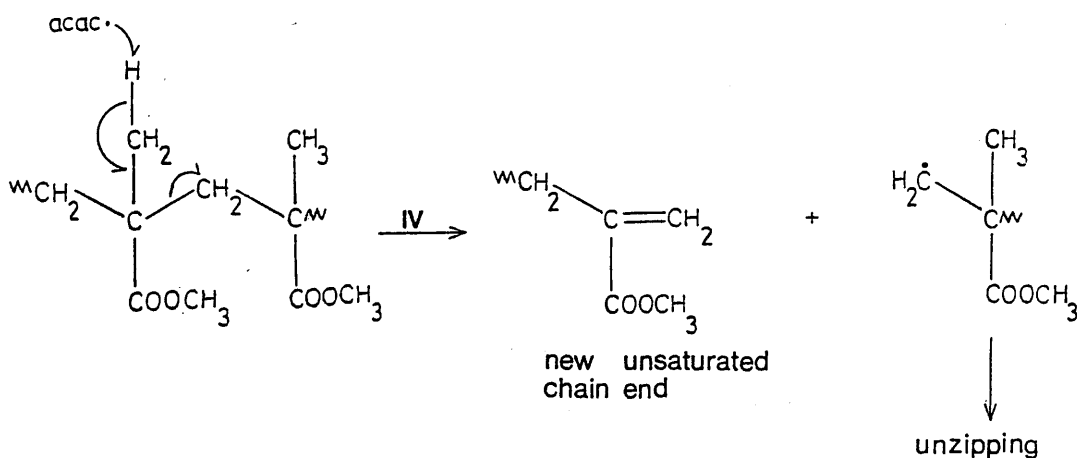
For the reaction of $\text{Co}(\text{acac})_3$ with the unsaturated sites of PMMA the analogous processes are:-



The macroradical (A) formed in reaction I would proceed to depolymerise:-



Thus reaction I leads to the loss of the unsaturated sites. On the other hand, the acac· radical formed in reaction II is free to attack the chain at any suitable site. It may, of course, add to the double bond to give structure (A) but it is also free to abstract an H atom from the polymer backbone to regenerate acetylacetonone. This latter process not only preserves the original unsaturated chain-ends but generates more in addition to forming depolymerisable macroradicals:

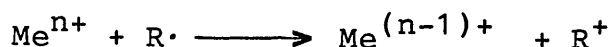


As in the disproportionation reaction of the growing polymer, the formation of vinylidene chain ends is favoured for steric reasons.

As described previously, evidence from the TVA curve indicates the continued presence of unsaturated chain-end sites, although in reduced concentration, which is consistent with the operation of both the above mechanisms. In addition, the occurrence of reactions II and IV accounts for the relatively small amounts of methyl methacrylate produced in association with Peak 1. Unzipping initiated at the chain ends, as occurring via reactions I and II, would lead to the complete unzipping of the chain, at least for the low molecular weight PMMA 3 (chain length for unzipping in this temperature region is ca. 200^{150}). Thus, if every chain end interaction led to initiation of depolymerisation by reactions I and III, every chain with an unsaturated end group would completely depolymerise and the height of Peak 1 would equal that of the chain end initiated unzipping peak of the corresponding unblended PMMA. This is not the case and can be accounted for by the observation that reaction IV leads to the unzipping of only a segment of the polymer chain. In addition, for PMMA 2 and particularly PMMA 1 (m.wt. 150,000 and $>1,000,000$) termination reactions, for example disproportionation and radical recombination, become important, although as such reactions become more probable with increasing

temperature, they would in fact serve to inhibit the chain end initiated unzipping of the unblended polymer more than this first decomposition step of the blend.

An alternative mechanism for the termination involves the newly formed $\text{Co}(\text{acac})_2$ species. Co^{2+} ions are readily oxidised to Co^{3+} and this process is involved in the inhibition of the autoxidation of polyolefins.⁵¹



This reaction could occur in the PMMA blends where $\text{R}\cdot$ is the depolymerising macroradical and would lead to the termination of the unzipping.

Step 2 (Peak 2 of Fig. 5.9)

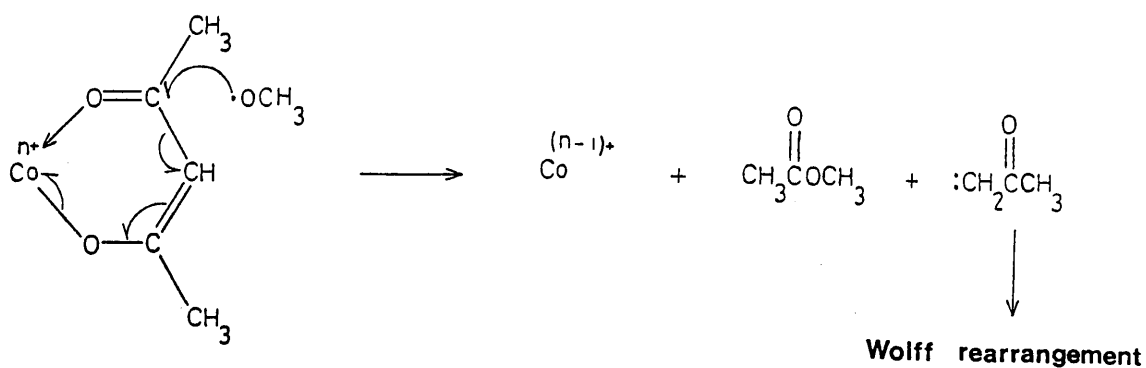
Although the first decomposition stage is caused by the decomposition of a π -type complex less stable than $\text{Co}(\text{acac})_3$ itself, the second stage is a consequence of the normal decomposition of the $\text{Co}(\text{acac})_3$ dispersed throughout the remainder of the polymer matrix. Thus trapped, the $\text{Co}(\text{acac})_3$ is expected to decompose in the same temperature range as observed for other systems in which sublimation is inhibited, and there is a close correspondence between the temperatures of decomposition of $\text{Co}(\text{acac})_3$ under nitrogen ($T(\text{onset})$ 150°C , $T(\text{max})$ 215°C) with that of Peak 2 ($T(\text{onset})$ 160°C , $T(\text{max})$ 190°).

The $\text{acac}\cdot$ radical produced by this decomposition is, of course, free to attack the polymer chain to

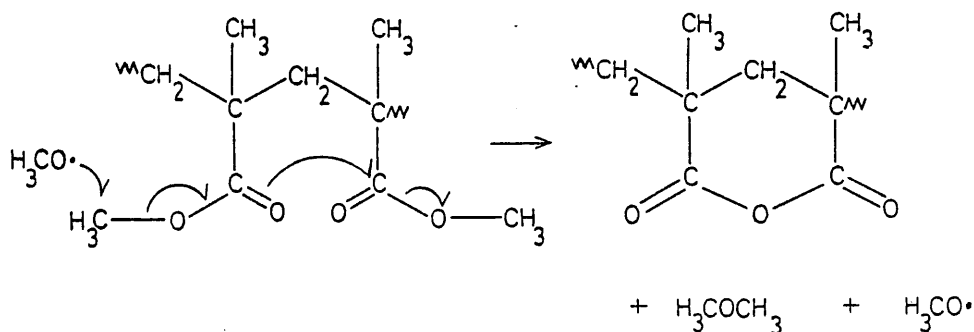
rings is more pronounced, gives rise to three products which can be considered as candidates for RCH_3 . These are acetone, methyl acetate and the dimethyl ether observed by mass spectrometry.

Acetone is formed as a degradation product of $\text{Co}(\text{acac})_3$ (or more properly $\text{Co}(\text{acac})_2$) via the production of $\text{CH}_3\overset{\text{O}}{\parallel}\text{C}\cdot$ radicals. In the blend, these radicals can attack the ester group, serving the role of R and producing the anhydride rings with acetone as the by-product.

Methyl acetate was found by McNeill and McGuinness in their study of ZnBr_2 - PMMA blends^{62,63} to be formed when $\text{CH}_3\overset{\text{O}}{\parallel}\text{C}\cdot$ radicals produced by the ZnBr_2 promoted scission of a side chain abstracted the ester methyl group from a neighbouring side chain to form an anhydride unit plus a methyl acetate molecule. However, this is a minor reaction of the $\text{CH}_3\overset{\text{O}}{\parallel}\text{C}\cdot$ radical, which normally dissociates to form CO and the $\text{CH}_3\text{O}\cdot$ radical, and although double bond formation occurs around 240°C anhydride and methyl acetate formation do not occur until a later stage. The methyl acetate is in fact produced by a reaction between the $\text{CH}_3\text{O}\cdot$ radical formed on anhydride formation and the remaining acetylacetonate units:-



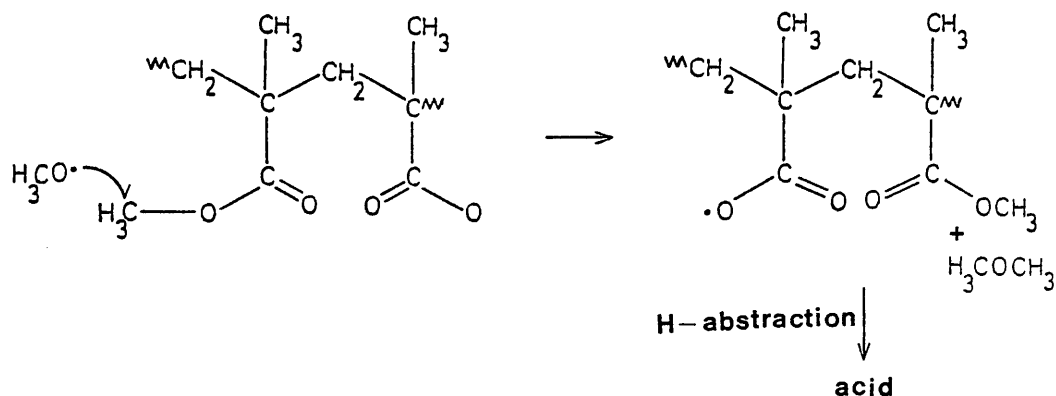
The dimethyl ether observed as a minor product is formed when the $\text{CH}_3\text{O}\cdot$ radical produced either in the formation of anhydride rings or in ester decomposition reactions reacts with a neighbouring side chain.



This is only a minor reaction of $\text{CH}_3\text{O}\cdot$, the radical preferentially abstracting a hydrogen atom to produce methanol. Consequently, the production of dimethyl ether occurs only when significant quantities of $\text{CH}_3\text{O}\cdot$ radicals are formed. In the case of these systems where there is greater production of dimethyl ether - the

$\text{Co}(\text{acac})_3$ - copolymer and $\text{Mn}(\text{acac})_3$ - PMMA/copolymer blends discussed later - there is a greater degree of anhydride ring formation and ester decomposition.

Attack of a $\text{CH}_3\text{O}\cdot$ radical on the ester methyl group can, in addition to the formation of anhydride rings, produce acid structures:-



This acid forming path will be favoured at temperatures above the decomposition temperature of the anhydride rings and although such acid formation is not observed in the $\text{Co}(\text{acac})_3$ - PMMA blends, it is observed with the $\text{Mn}(\text{acac})_3$ - PMMA blends, in which $\text{CH}_3\text{O}\cdot$ -producing fragmentation reactions are more significant.

Prior to the production of the anhydride units, the double-bond and carboxylate structures are formed, as discussed already. It is these structures which block the depolymerisation of the chains subsequent to its purely thermal initiation at the chain ends and results in the increased diminution of the corresponding TVA peak (Peak 3 in Fig. 5.9) at high $\text{Co}(\text{acac})_3$ concentrations (this mechanism operates in addition to

the mechanism by which unsaturated chain ends are lost by the interaction with $\text{Co}(\text{acac})_3$. At the higher temperatures of the random scission initiated depolymerisation, the anhydride structures have been formed and these also contribute to the the blocking of unzipping.

When unzipping is halted by a carboxylate unit two competing processes can occur. As described earlier, both involve the removal of the carboxylate units, one directly and one via the production of cobalt methacrylate, both routes producing ultimately dimethyl ketene and cobalt oxide.

The blockage by anhydride units, as outlined in Chapter 4, produces a macroradical which can react further to produce the 5-membered cyclic anhydride or unsaturated structures:



Finally, fragmentation of the polymer backbone occurs. In this way, chain fragments, some containing anhydride and unsaturated structures, are produced and condense on the cold ring. More complete fragmentation produces carbon dioxide, dimethyl ketene, methanol,

butene, isobutene and carbon monoxide; all except the latter being unambiguously identified as products from the 1:10 blend. The carbon monoxide is assumed to form the major proportion of the -196°C non-condensable material, although some methane is also expected. Small quantities of ethylene may be expected to be produced by fragmentation of the double bond sequences, but this was not detected.

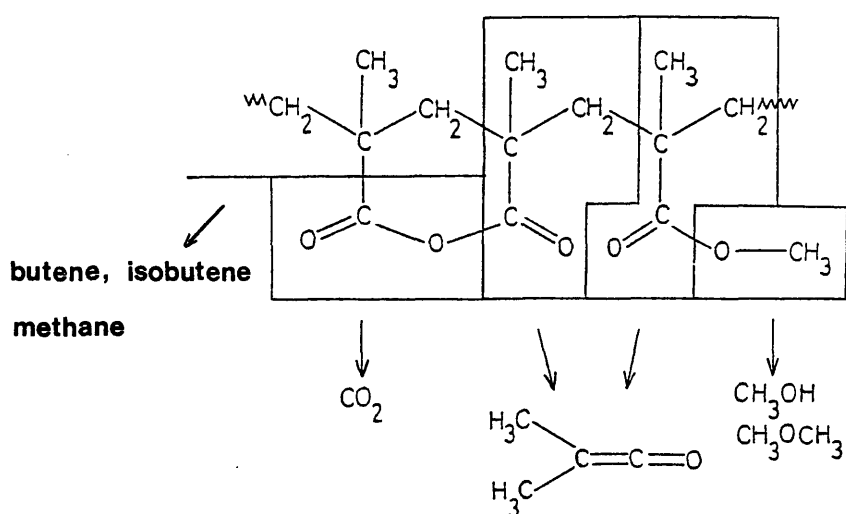
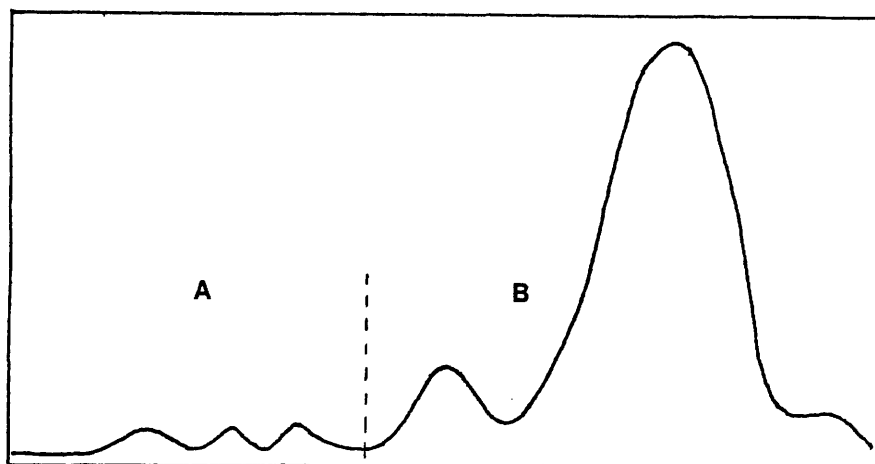


Fig. 5.19 Major Fragmentation Steps of the Polymer Backbone

SUMMARY OF DEGRADATION PROCESSES IN $\text{Co}(\text{acac})_3$ -PMMA BLENDS ON THE BASIS OF OBSERVATIONS FROM 1:10 AND 1:50 BLENDS



- A
1. Decomposition of π -complex at chain ends produces $\text{acac}\cdot$ radicals which initiate depolymerisation.
 2. Purely thermal decomposition of $\text{Co}(\text{acac})_3$ produces $\text{Co}(\text{acac})_2$ and $\text{acac}\cdot$ radicals. $\text{acac}\cdot$ initiates depolymerisation. $\text{Co}(\text{acac})_2$ complexes with ester groups and induces side chain scission and double bond formation.

- B
1. Formation of cobalt carboxylate structures and anhydride rings.
 2. Depolymerisation blocked by above structures.
 3. Fragmentation of above structures and remaining polymer chains.

Mn(acac)₃ - PMMA BLENDSTVA BEHAVIOUR

The TVA curves obtained for blends of Mn(acac)₃ with PMMA 1 and PMMA 2 at Mn(acac)₃:monomer unit ratios of 1:10 and 1:50 are reproduced in Fig. 5.20 - 5.23 and the details summarised in Table 5.11.

Samples were of the order of 30-40mg and were cast as films directly onto the base of a TVA tube from methylene chloride solution. The 1:50 blends were compatible, the films brown in colour but transparent. The 1:10 blends were similar but scattered small specks of Mn(acac)₃ showed the blend to be not completely compatible.

As expected, there are close similarities between the behaviour of the Mn(acac)₃ - PMMA blends and the Co(acac)₃ - PMMA blends. The reduction in the peak associated with the thermal chain-end initiated unzipping of PMMA (i.e. the peak with T(max) between 280-290°C) suggests the loss of unsaturated chain ends and the blocking of unzipping by alterations to the polymer structure. The production of -196°C non-condensable material also suggests blocked depolymerisation. However, the blocking, and consequently the fragmentation, is more pronounced in the Mn(acac)₃ - PMMA blends than in the Co(acac)₃ - PMMA blends. For instance, the 1:50 Mn(acac)₃-PMMA 1 blend shows approximately the same production of

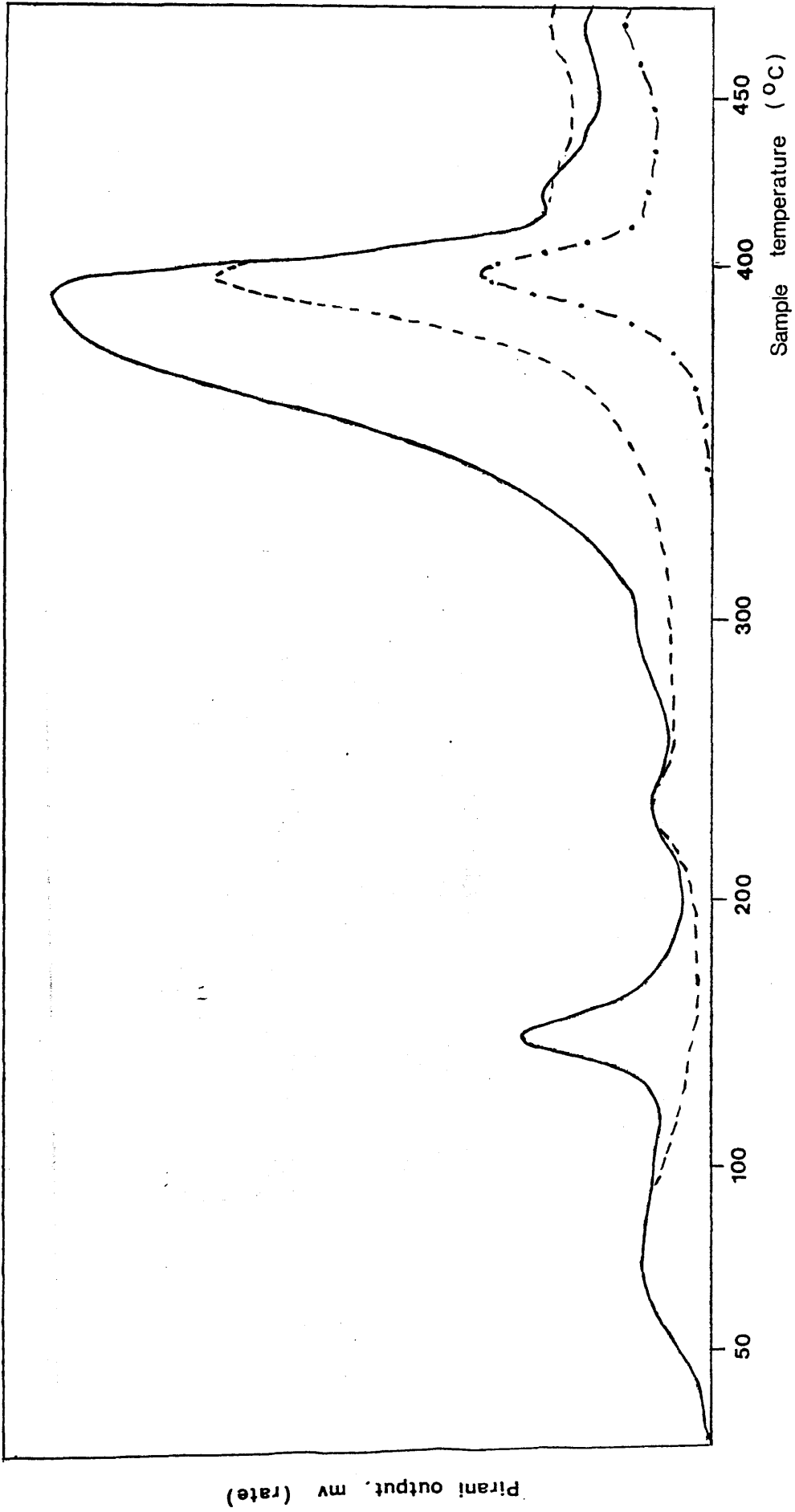


Figure 5.20 TVA curve of 1:10 Mn(acac)₃ - PMMA 1 blend

Pirani output, mv (rate)

Sample temperature (°C)

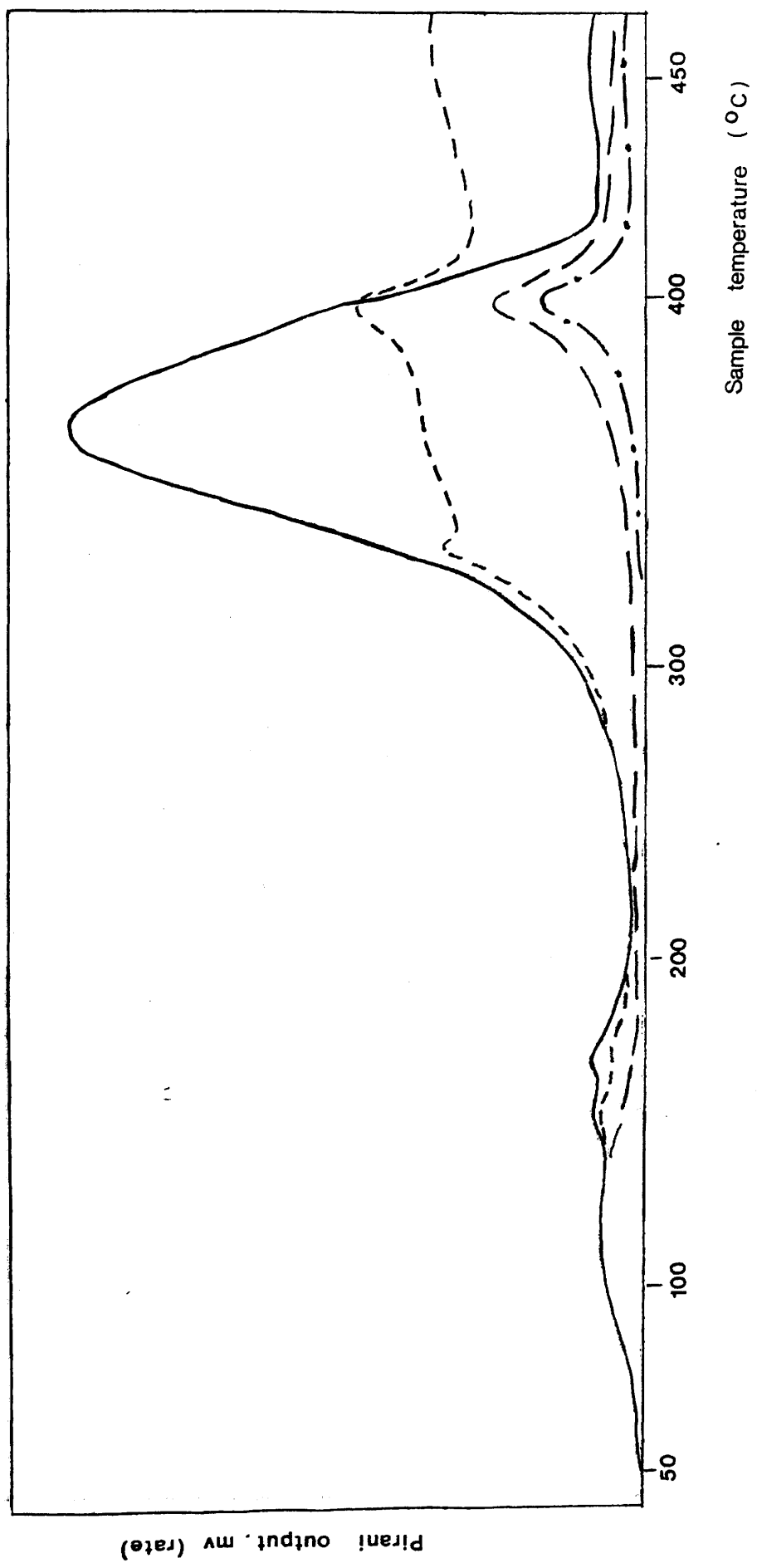
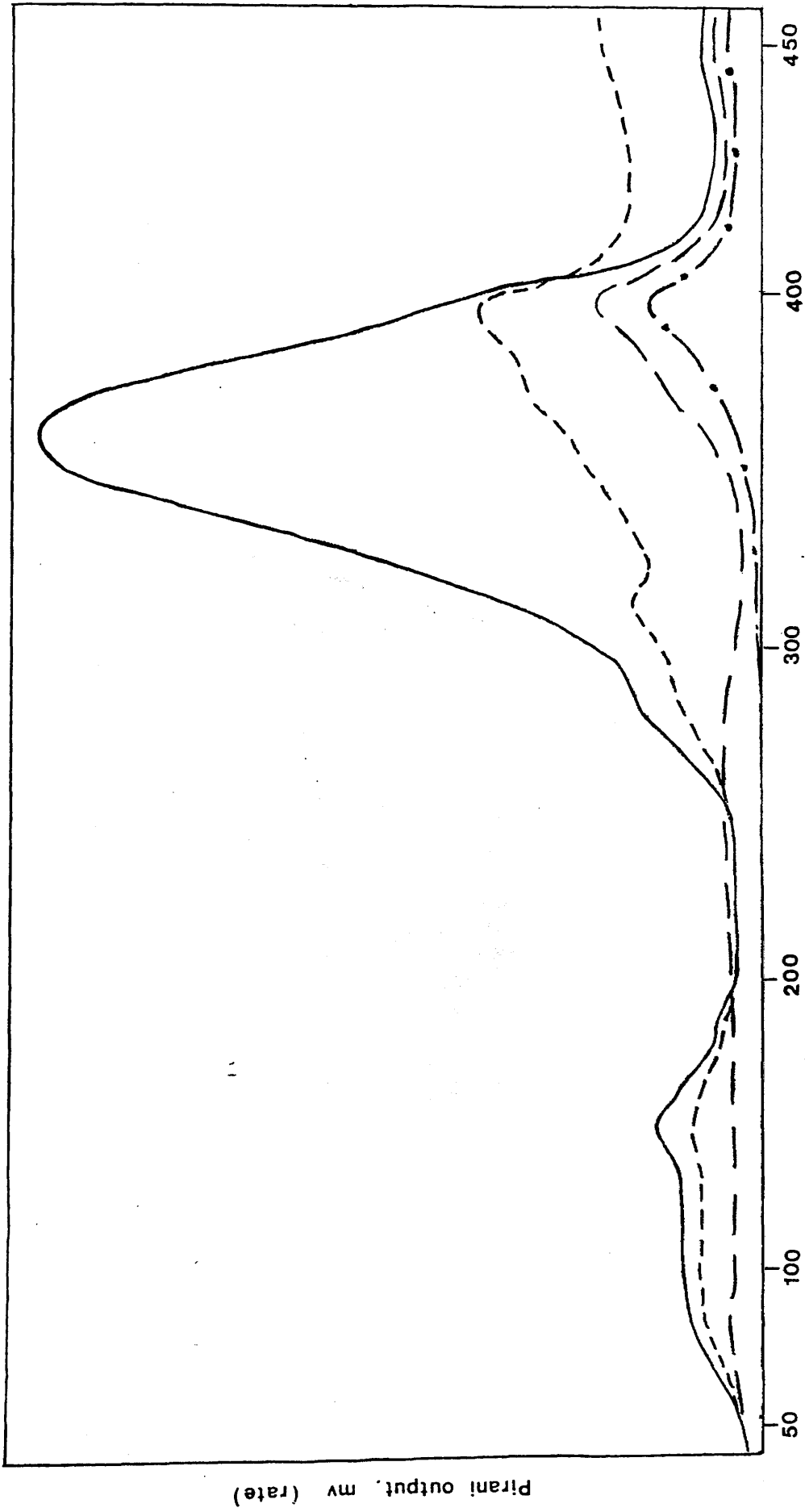


Figure 5.21 TVA curve of 1:50 Mn(acac)₃ - PMMA 1 blend



Sample temperature (°C)

Figure 5.22 TVA curve of 1:10 Mn(acac)₃ - PMMA 2 blend

Pirani output, mv (rate)

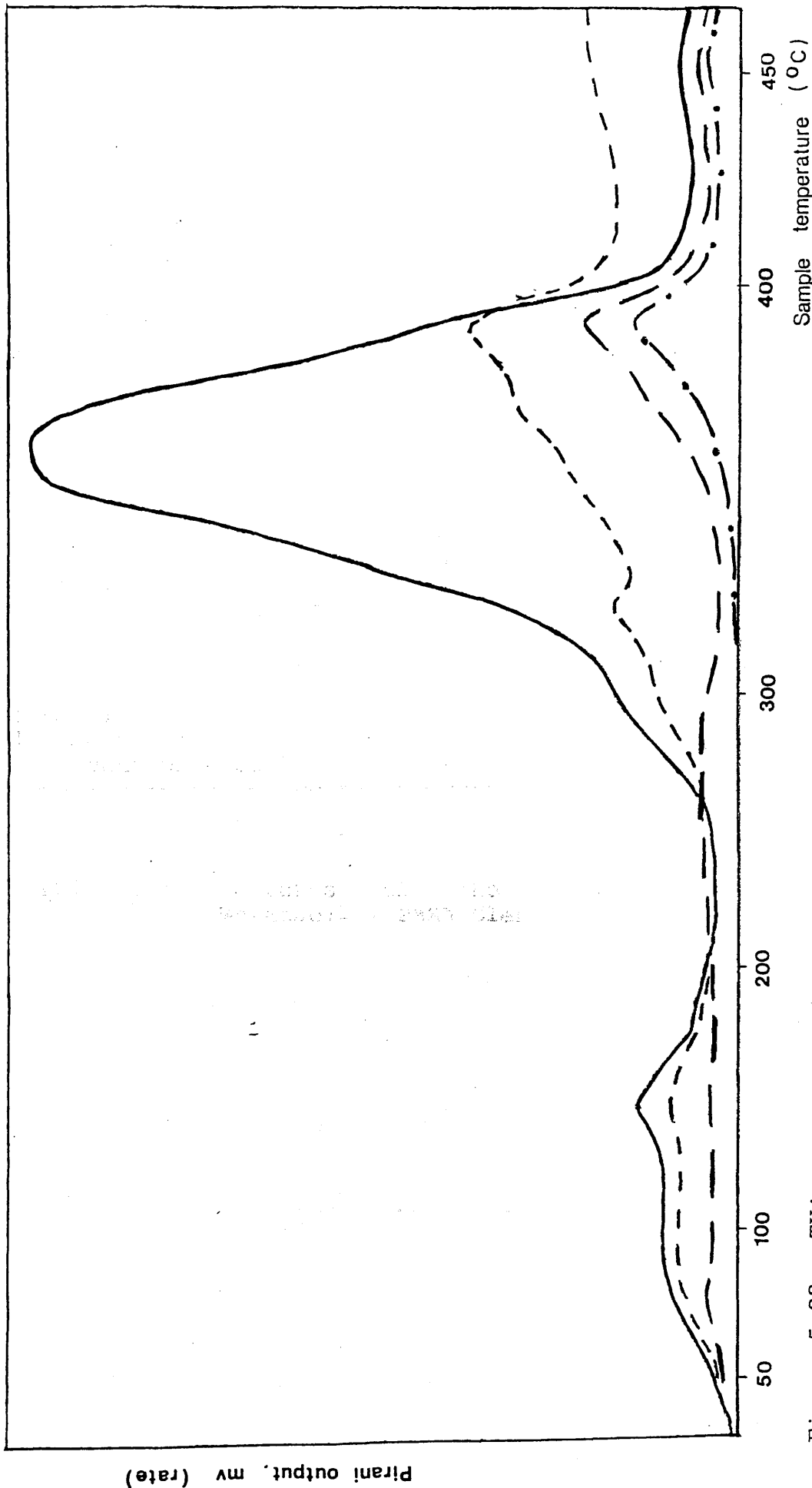


Figure 5.23 TVA curve of 1:50 Mn(acac)₃ - PMMA 2 blend

Pirani output, mv (rate)

Feature	BLEND			
	PMMA 1		PMMA 2	
	1:10	1:50	1:10	1:50
Compatibility	Not fully	Yes	Not fully	Yes
T(sublimation)	131	Not observable		Not observable
1st Peak				
T(onset)	127	129	128	128
T(max)	155	150	163	150
2nd Peak				
T(onset)	Masked by 1st peak	158	Masked by 1st Peak	Masked by 1st Peak
T(max)		165		
3rd Peak				
T(onset)	208	Not observed	221	Not observed
T(max)	233		244	
Main Peak				
Shoulder	258-304	220-293	267-299	231-292
T(max)				
Condensibles	399	365	401	367
Non-condensibles	"	396	"	400

Table 5.11 Features of the TVA Curves for Several Mn(acac)₃ - PMMA Blends

that directly analogous conclusions about the low temperature degradation processes

-196°C non-condensable material as the 1:10 Co(acac)₃ - PMMA 1 blend. The 1:10 Mn(acac)₃ blends show the distinct increase in T(max) of the major peak associated with considerable blocking of the unzipping process.

In common with the Co(acac)₃ - PMMA blends, the Mn(acac)₃ - PMMA blends display low temperature degradation steps (i.e. below 250°C). Unlike the Co(acac)₃ blends which have two such steps, the Mn(acac)₃ blends have three. The 1:50 Mn(acac)₃ - PMMA 1 blend shows two overlapping reactions with T(max) 150°C and 165°C. In the 1:10 Mn(acac)₃ - PMMA 1 blend, and both the 1:50 and 1:10 Mn(acac)₃ - PMMA 2 blends, the two peaks coalesce to give a single peak with T(max) ranging from 150-163°C depending, presumably, on which process dominates. Both of the 1:10 blends have an additional peak with T(max) around 240°C.

As will be described in a following section, Mn(acac)₃ can associate with both the unsaturated chain ends and the ester groups of the polymer at room temperature. This makes the situation rather more complicated than the Co(acac)₃ - PMMA blends where the Co(acac)₃ forms a complex as the blend forms at room temperature only with the unsaturated groups, and means that directly analogous conclusions about the nature of the low temperature degradation processes cannot be made.

STRUCTURE OF Mn(acac)₃ - PMMA BLENDS AND CHANGES DURING DEGRADATION

To study the structure of the Mn(acac)₃ - PMMA blends, samples of Mn(acac)₃ with PMMA 1 in the Mn(acac)₃:monomer unit ratios of 1:10 and 1:50 were prepared as described for the Co(acac)₃ - PMMA blends. Samples were heated under TVA conditions to various temperatures and structural changes followed spectroscopically using the same methods employed for the Co(acac)₃ - PMMA blends.

The spectra obtained for the 1:50 blends are reproduced in Figs. 5.24 and 5.25; those of the 1:10 blend in Figs. 5.26 and 5.27. Tables 5.12 and 5.13 summarise the important features.

STRUCTURE OF THE UNDEGRADED BLEND

The IR spectra of the 1:50 and 1:10 Mn(acac)₃ - PMMA 1 blends both show no evidence for an interaction between polymer and additive, being, in essence, superpositions of the Mn(acac)₃ and PMMA spectra. This is similar to the case of the Co(acac)₃ - PMMA blends. However, unlike those blends, which showed no evidence of an interaction in their UV spectra either, both the 1:10 and 1:50 Mn(acac)₃ - PMMA blends show major modifications to the Mn(acac)₃ spectrum expected in the absence of an interaction.

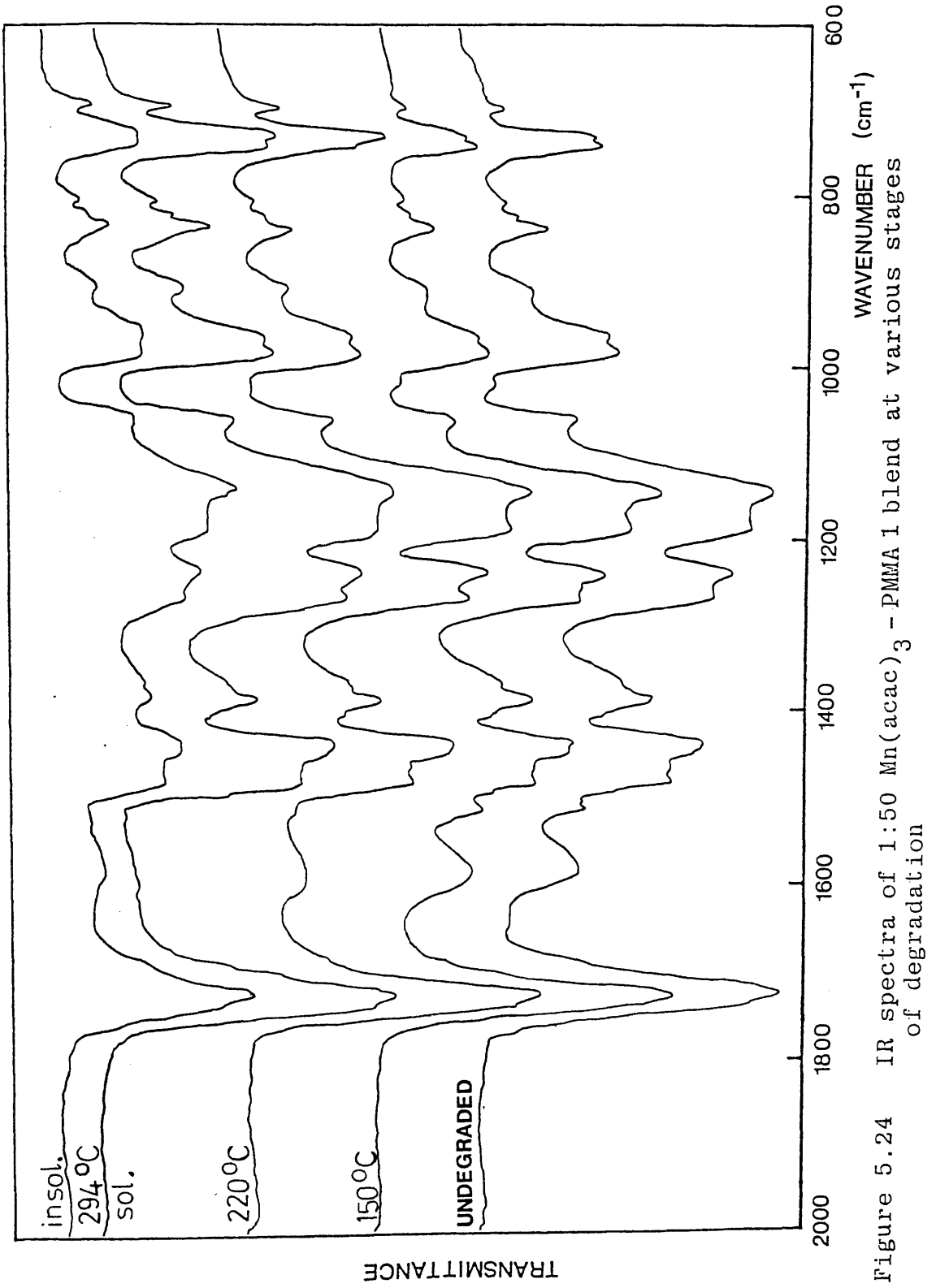


Figure 5.24 IR spectra of 1:50 Mn(acac)₃ - PMMA 1 blend at various stages of degradation

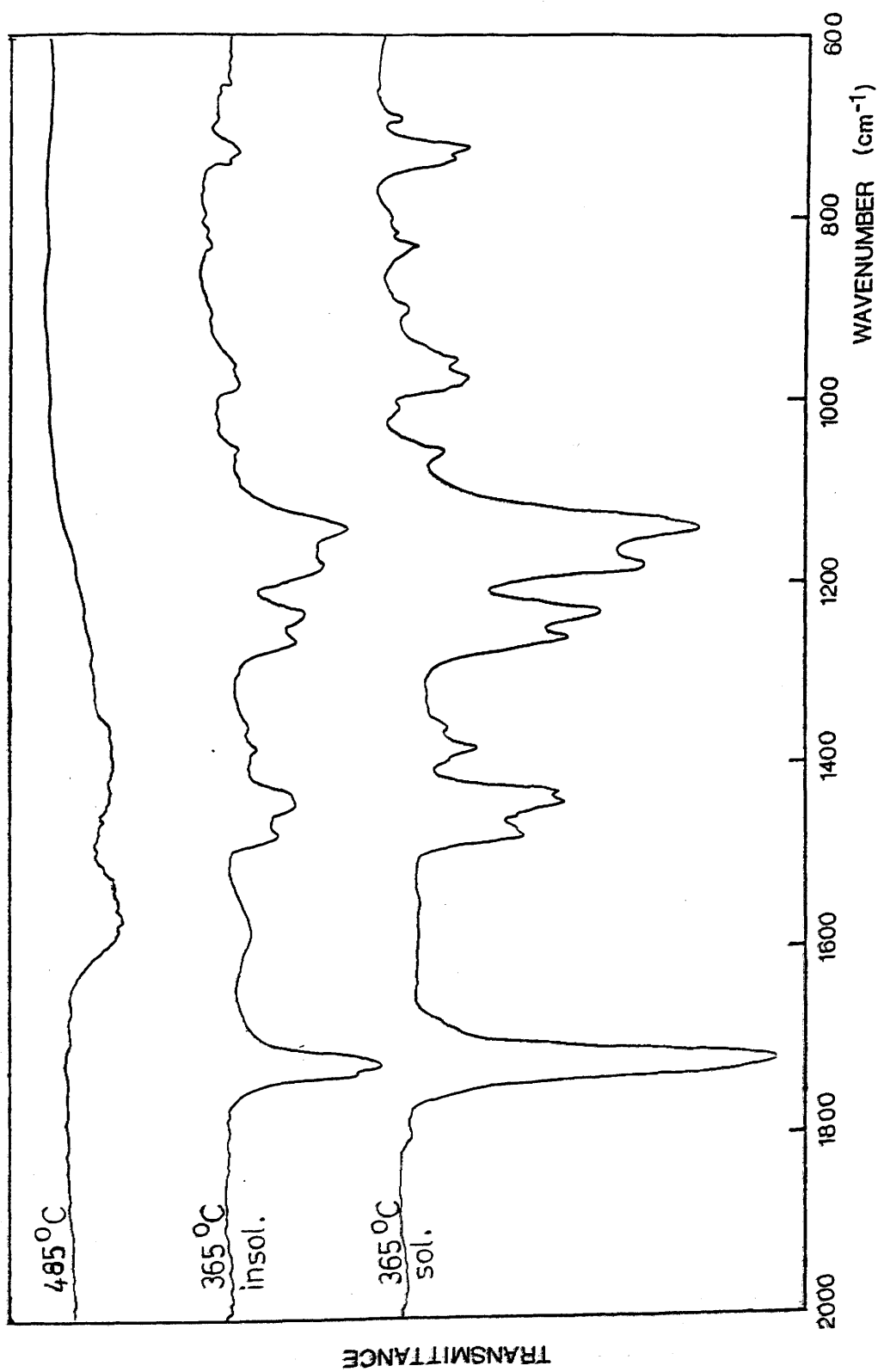


Figure 5.24 IR spectra of 1:50 Mn(acac)₃ - PMMA 1 blend at various stages of degradation (ctd)

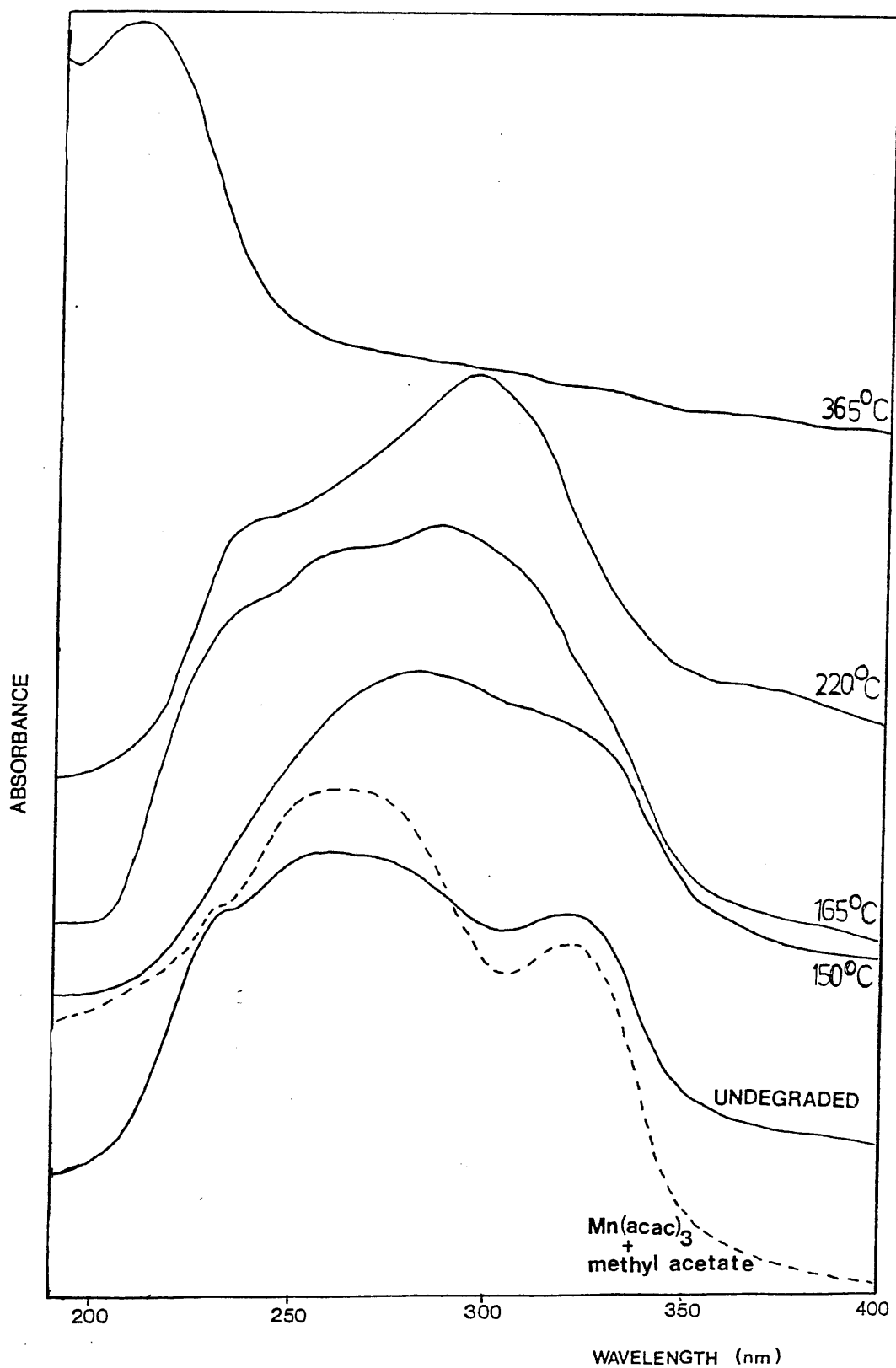


Figure 5.25 UV spectra of 1:50 Mn(acac)₃ - PMMA 1 blend at various stages of degradation

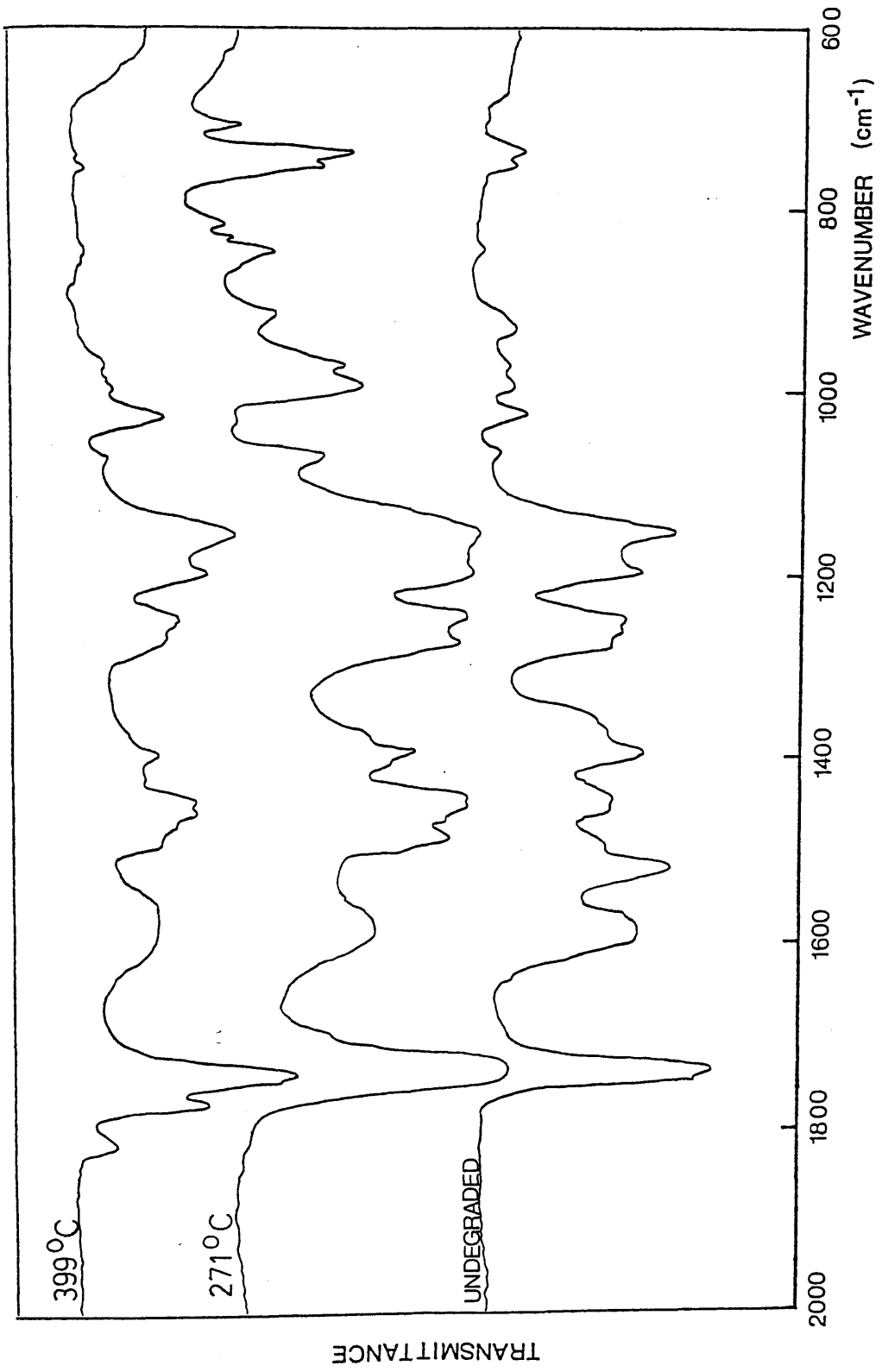


Figure 5.26 IR spectra of 1:10 Mn(acac)₃ - PMMA 1 blend at various stages of degradation

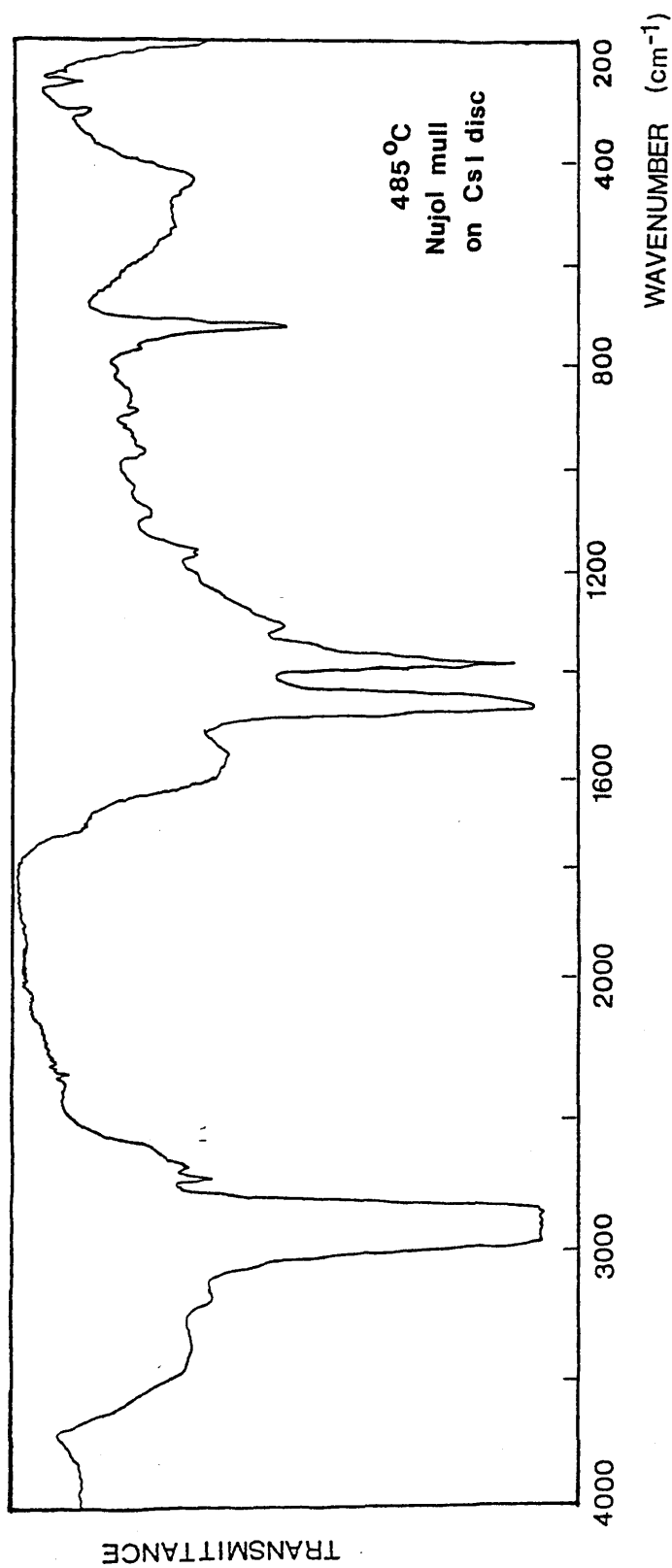


Figure 5.26 IR spectra of 1:10 Mn(acac)₃ - PMMA 1 blend at various stages of degradation (ctd.)³

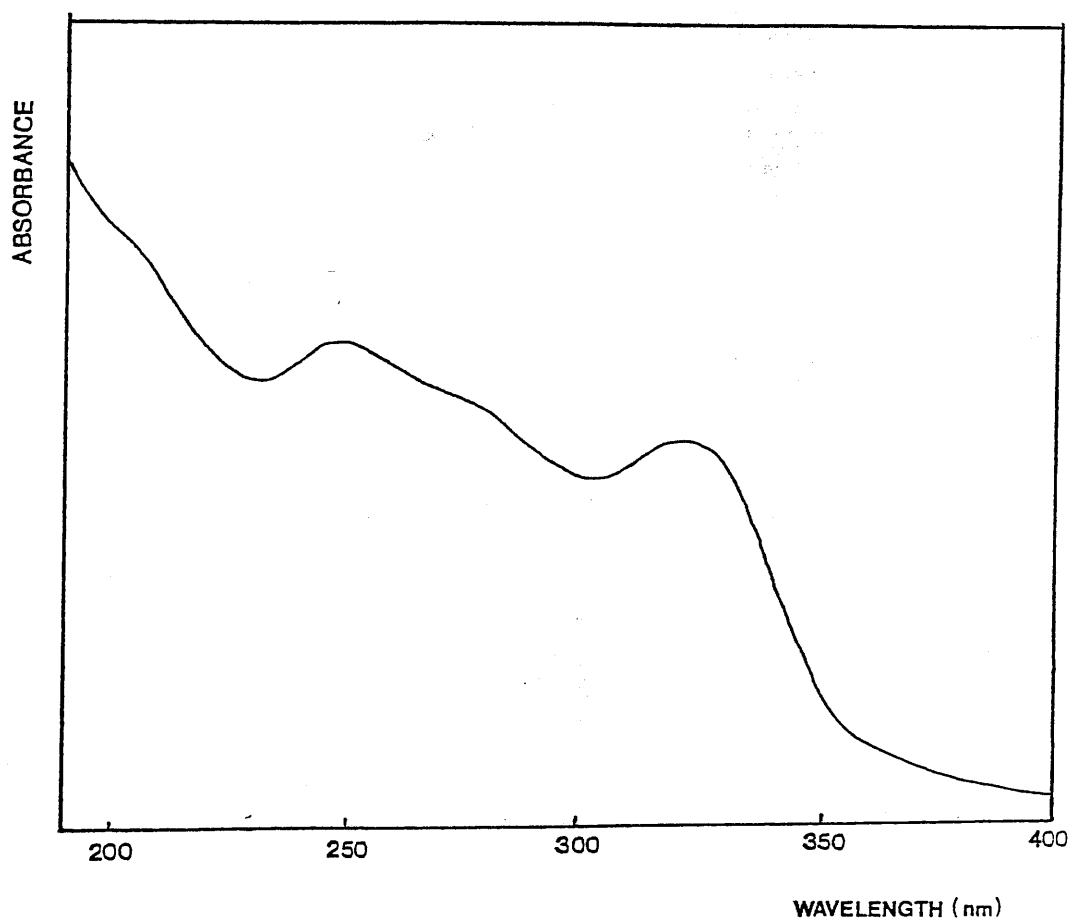


Figure 5.27 UV spectrum of 1:10 Mn(acac)₃ - PMMA 1 blend

Extent of Degradation	Visual Appearance	Solubility in CH_2Cl_2	Structural Features
None	Brown, transparent, compatible.	Yes	No evidence of interaction from IR spectrum. UV spectrum very similar to that of product from reaction of methyl acetate with $\text{Mn}(\text{acac})_3$.
150°C (A)	Similar to starting blend	Yes	IR spectrum - no change. UV spectrum still contains broad unstructured absorption.
165°C (B)	Similar to starting blend	Yes	IR spectrum - no change. UV spectrum - broad unstructured absorption.
220°C (C)	Similar to starting blend	With difficulty	IR spectrum - pronounced reduction in acac peaks. 1580cm^{-1} peak more intense than $1510\text{cm}^{-1} \Rightarrow$ underlying carboxylate absorption. UV spectrum - some structure regained with (max) 296nm.
294°C (D)	Similar to starting blend	Partially soluble to give yellow soln	Carboxylate absorption in IR spectrum of insoluble gel.
365°C (E)	Orange/brown	Mostly soluble	Insol. gel has IR spectrum similar to that of above. Some anhydride structures identified in IR spectrum of sol. portion. UV spectrum shows PMMA absorption as only identifiable feature.
485°C (F)	Brown char	Insoluble	Carboxylate structures identified in residue of film degraded on salt plate.

Table 5.12 Structure of $1:50 \text{ Mn}(\text{acac})_3$ - PMMA 1 Blend At Various Stages Of Degradation
(Key - page 307)

Extent of Degradation	Visual Appearance	Solubility in CH_2Cl_2	Structural Features
None	Brown, mostly transparent, some opacity	Yes	Visual appearance => not fully compatible. No evidence of interaction from IR spectrum.
271°C (A)	Entirely transparent, similar to above	Forms insoluble gel	Strong absorption 1575 cm^{-1} => carboxylate.
399°C (B)	Similar to above		Film degraded on NaCl disc. IR spec shows anhydride and carboxylate absorptions.
485°C (C)	Brown char	No	IR spectrum run as nujol mull on CsI disc carboxylate absorption remains, weak acid absorption present.

Table 5.13 Structure of 1:10 $\text{Mn}(\text{acac})_3$ - PMMA 1 Blend a
Various Stages of Degradation



THE NATURE OF THE INTERACTION BETWEEN $Mn(acac)_3$ AND PMMA

The UV spectra of the blends are virtually identical to the spectrum of the material obtained on reacting $Mn(acac)_3$ and methyl acetate at room temperature (Chapter 3) which is also reproduced in Fig. 5.25 for comparison. Thus, $Mn(acac)_3$ associates with the ester groups of the polymer in a manner directly analogous to its association with methyl acetate. This involves the partial displacement of a ligand and so it is anticipated that decomposition of $Mn(acac)_3$ via scission of an acetylacetonate ligand will be promoted in the blend as a result of this interaction.

The interaction with the ester groups of the polymer is reversible. This is clearly demonstrated by redissolving the blend in toluene and precipitating the polymer in methanol followed by a further dissolution and precipitation. The UV and IR spectra of the polymer thus obtained show only absorptions due to PMMA (Figs. 5.28 and 5.29).

A π -complex between $Mn(acac)_3$ and the unsaturated chain-end sites is also expected although as with the $Co(acac)_3$ - PMMA systems there is no spectroscopic evidence for it. In the $Co(acac)_3$ - PMMA blends, the only feasible sites for an interaction between chelate and polymer at room temperature are the unsaturated chain ends and thus every suitable site is involved in an interaction when the chelate

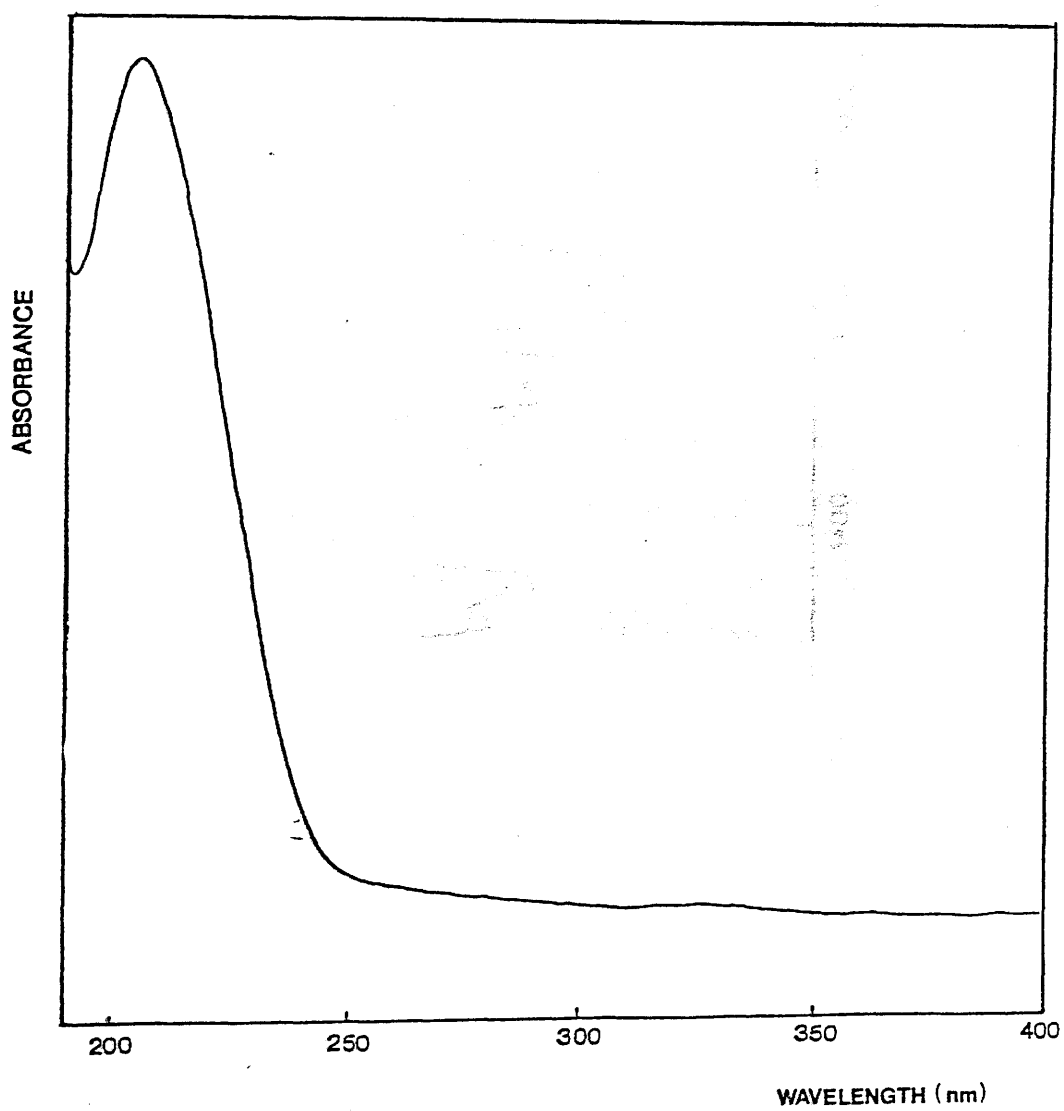


Figure 5.28 UV spectrum of 1:50 Mn(acac)₃ - PMMA 1 blend after precipitation

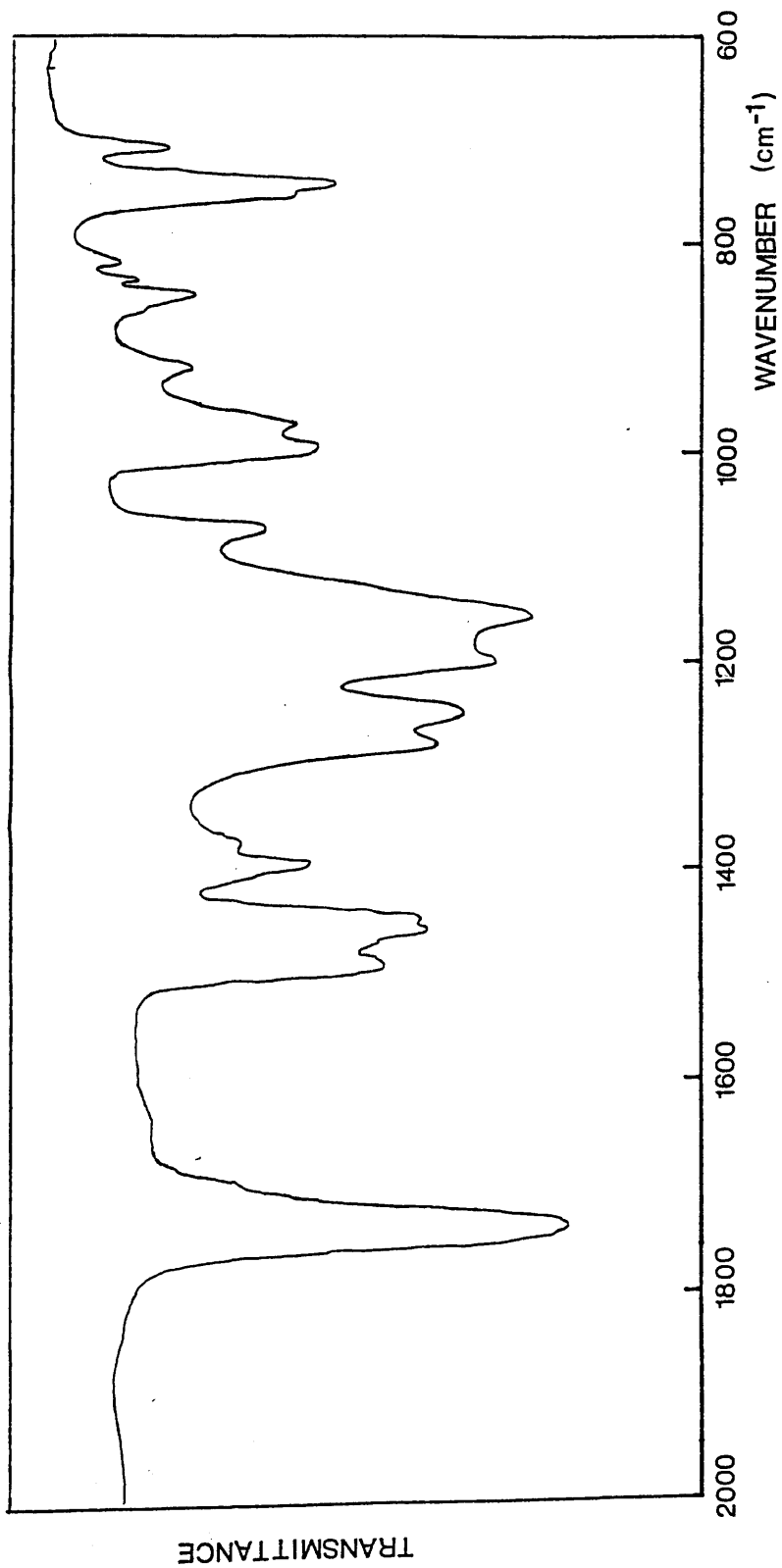


Figure 5:29 IR spectrum of 1:50 Mn(acac)₃ - PMMA 1 blend after precipitation

concentration exceeds that of the unsaturated sites. In the $\text{Mn}(\text{acac})_3$ - PMMA blends, however, the additional ester interaction means that there will be competition between the two sites. Depending on the relative strengths of the interactions, this may lead to the reduced importance of the chelate-unsaturated chain end site initiation process.

CHANGES OF STRUCTURE ON DEGRADATION

The $\text{Mn}(\text{acac})_3$ - PMMA blends have much in common with the $\text{Co}(\text{acac})_3$ - PMMA blends in terms of structural changes during degradation. Carboxylate and anhydride structures and cross-linking feature in both instances. In general, however, the changes are more pronounced in the $\text{Mn}(\text{acac})_3$ blends than the $\text{Co}(\text{acac})_3$ blends. This is due to the formation of the $\text{Mn}(\text{acac})_3$ -ester complex which serves to bind $\text{Mn}(\text{acac})_3$ to the polymer and prevent its sublimation. Although sublimation of cobalt chelate is inhibited by the polymer matrix, material does sublime, even from the compatible blends, particularly above the glass transition temperature of the polymer. In addition, the bulk of the $\text{Co}(\text{acac})_2$ is formed when it is itself volatile and unstable whilst $\text{Mn}(\text{acac})_2$, more thermally stable and less volatile will persist in the film to higher temperatures, even if not bound to the polymer. Compare for instance the IR spectra of the respective $\text{Co}(\text{acac})_3$ and $\text{Mn}(\text{acac})_3$ - PMMA 1 1:50 blends after

degradation to 220°C. The spectrum of the Mn(acac)₃ blend shows some chelate to be present - there is virtually no chelate species present in the Co(acac)₃ blend at this temperature.

These spectra also show the enhanced carboxylate production in the Mn(acac)₃ blend. This is the manganese analogue of the carboxylate salt formed in the Co(acac)₃ blend and its formation in the Mn(acac)₃ blend is favoured due to the stronger ester-chelate interaction.

The anhydride structures also form by the same mechanism as in the Co(acac)₃ - PMMA blends. With the greater amount of CH₃O• radical production in the Mn(acac)₃ - PMMA blends, some formation of acid units by the route described on page 281 is observed.

-196°C CONDENSIBLE GAS AND LIQUID PRODUCTS AND COLD RING FRACTION OF Mn(acac)₃ - PMMA BLENDS

The total -196°C condensible products and the CRF obtained for various stages of degradation of both the 1:50 and 1:10 blends of Mn(acac)₃ with PMMA 1 were studied. Film preparation, degradation and product collection and analyses were performed in the manner already described for the Co(acac)₃ - PMMA blends. Tables 5.14-5.17 list the products identified for each blend. Degradations of blends with PMMA 2 to 485°C produced a range of products identical to the degradation of the corresponding PMMA 1 blend.

The products obtained on degrading the Mn(acac)₃ - PMMA blends are similar to those of the Co(acac)₃ - PMMA blends, although, as expected from the TVA traces, there are greater quantities of, and additional, fragmentation products. For example, the dimethyl ether is produced in large enough quantity to be detected by IR spectroscopy whereas in the Co(acac)₃ - PMMA blends it was detectable only by mass spectrometry.

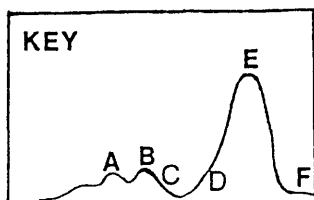
The production of significant quantities of acetylacetone in association with the first peak (T(max) 155°C) of the 1:50 blend TVA curve is important as this implies that the peak is associated with the decomposition of more Mn(acac)₃ than just that involved in the chain-end interactions.

Extent of Degradation	Products
150°C (A)	Acetylacetone, methyl methacrylate.
165°C (B)	As above.
220°C (C)	As above, plus trace of methanol.
290°C (D)	As 220°C plus acetone, methyl acetate and greater amount methanol.
365°C (E)	As 290°C plus anhydrides. (See Figure 5.30)
485°C (F)	As 365°C plus carbon dioxide, ketene, dimethyl ether, butene, isobutene, acetone.

Table 5.14 -196°C Condensable Gas and Liquid Products from 1:50 Mn(acac)₃ - PMMA 1 Blend at Various Stages of the Heating Programme.

Extent of Degradation	Products
150°C (A)	None.
165°C (B)	None.
220°C (C)	Small quantity, yellow solution in methylene chloride.
290°C (D)	As above.
365°C (E)	Small quantity of chain fragments present.
485°C (F)	Considerable brown CRF - mostly chain fragments which now include cyclic anhydride structures. (Fig. 5.31)

Table 5.15 Cold Ring Fraction From 1:50 Mn(acac)₃-PMMA blend at Various Stages of the Heating programme

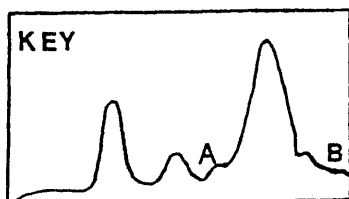


Extent of Degradation	Products
271°C (A)	Acetylacetone, methyl methacrylate, acetone, methyl acetate, methanol, carbon dioxide.
485°C (B)	As 271°C plus dimethyl ether, butene, isobutene, "ketene", anhydrides (See Fig. 5.30).

Table 5.16 -196°C Condensable Gas and Liquid Products from 1:10 Mn(acac)₃ - PMMA 1 Blend at Different Stages of the Heating Programme.

Extent of Degradation	Products
271°C (A)	Considerable quantity, UV and IR spectra consistent with Mn(acac) ₃ , 2.
485°C (B)	IR spectrum shows chain fragments including glutaric-type anhydrides, also some acid groups. See Fig. 5.31.

Table 5.17 Cold Ring Fraction from 1:10 Mn(acac)₃ - PMMA 1 Blend at Different Stages of the Heating Programme



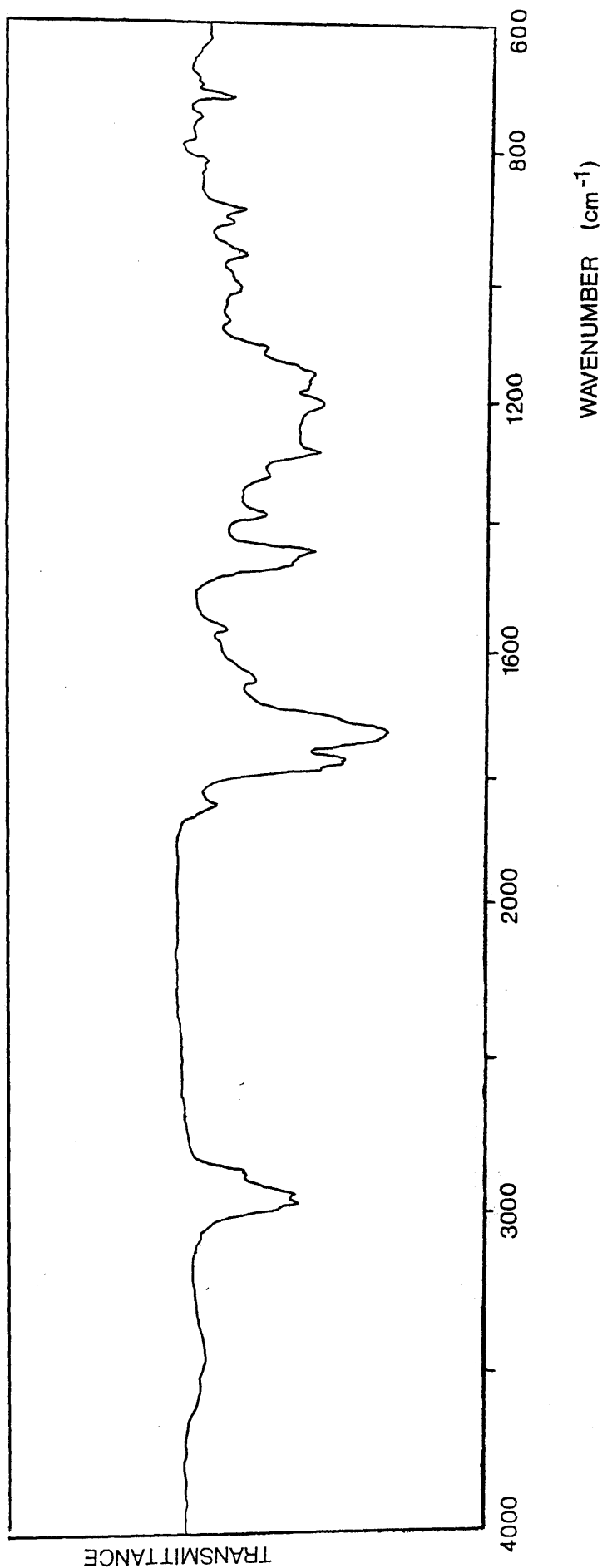


Figure 5.30 IR spectrum of liquid fraction from SAD analysis of products from degradation to 485°C of 1:50 Mn(acac)₃ - PMMA 1 blend

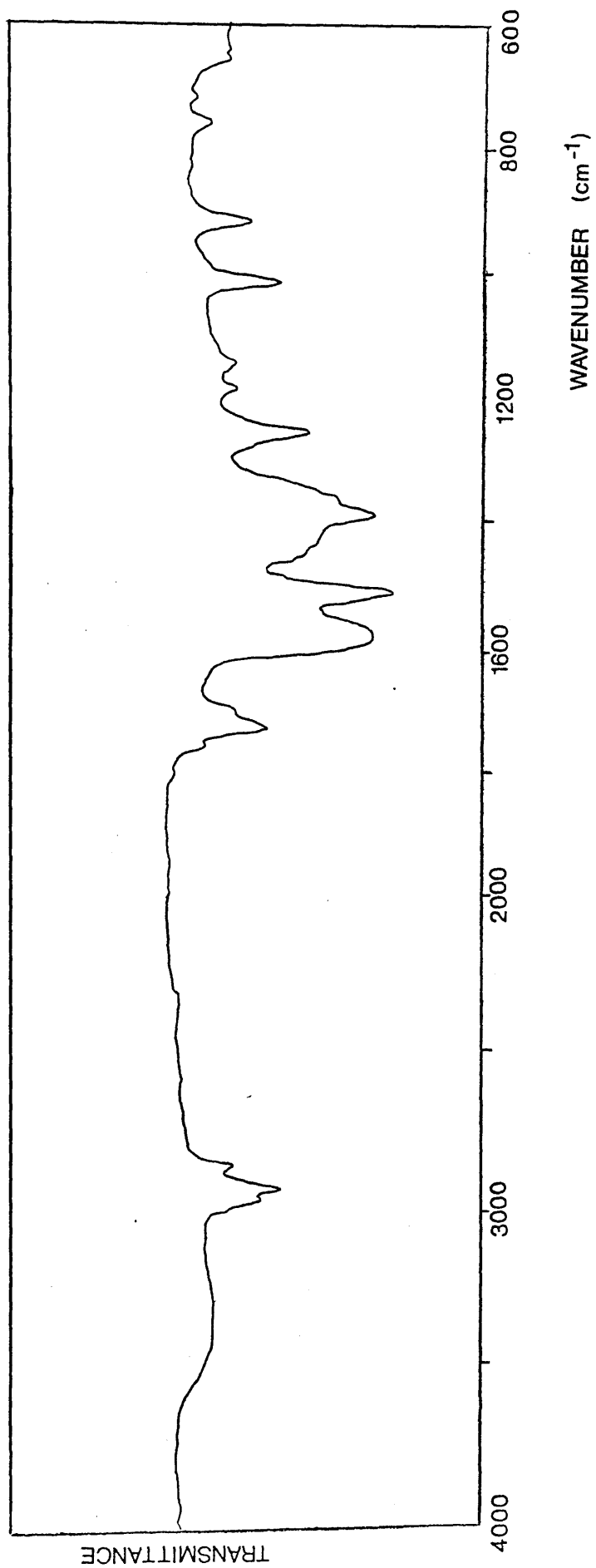


Figure 5.31 IR spectrum from CRF of 1:50 Mn(acac)₃ - PMMA 1 blend on degradation to 485°C

Production of acetone around 235°C is significant as $\text{Mn}(\text{acac})_2$ decomposes in this temperature region with the formation of acetone.

The similarities of the spectra of $\text{Mn}(\text{acac})_3$ and $\text{Mn}(\text{acac})_2$ make it difficult to identify unambiguously by this means any sublimate. However, as $\text{Mn}(\text{acac})_2$ does not sublime under TVA conditions until temperatures greater than 200°C , by which stage no $\text{Mn}(\text{acac})_3$ will remain undecomposed, the nature of any sublimate can be inferred from its temperature of formation. Note that unlike the $\text{Co}(\text{acac})_3$ blends, sublimate is observed below 200°C only for the non-compatible 1:10 $\text{Mn}(\text{acac})_3$ - PMMA blends.

At higher temperatures, the composition and quantity of the CRF mirror the effect of the considerable number of depolymerisation-blocking structures formed within the blend.

DSC ANALYSIS OF Mn(acac)₃ - PMMA 1 BLENDS

Examination of the DSC curves obtained for Mn(acac)₃ and its blends with PMMA 1 provides evidence that the early stages of degradation of the blend are associated with the decomposition of the Mn(acac)₃. Fig 5.32 compares the DSC curves obtained for the degradation under nitrogen of the 1:10 and 1:50 Mn(acac)₃ - PMMA 1 blends with that of Mn(acac)₃ alone.

As described in Chapter 3, the DSC curve of Mn(acac)₃ can be explained by the initial reduction of the complex with liberation of acetylacetone to produce Mn(acac)₂, which subsequently decomposes at higher temperatures. The sequence of endotherms and exotherms produced is very characteristic and significantly just such a sequence can be observed in the DSC curves obtained for the Mn(acac)₃ - PMMA blends. The pattern is much weaker - the quantity of Mn(acac)₃ in the blend samples is of course much smaller - but the peaks occur at almost exactly the same temperature.

In conjunction with the TVA and product analysis evidence (in particular, the identification of acetylacetone and acetone as products associated with the peaks T(max) 156°C and 235°C respectively), this provides strong support for the conclusion that the early degradation step, which produces acetylacetone and methyl methacrylate, is due to the initiation of

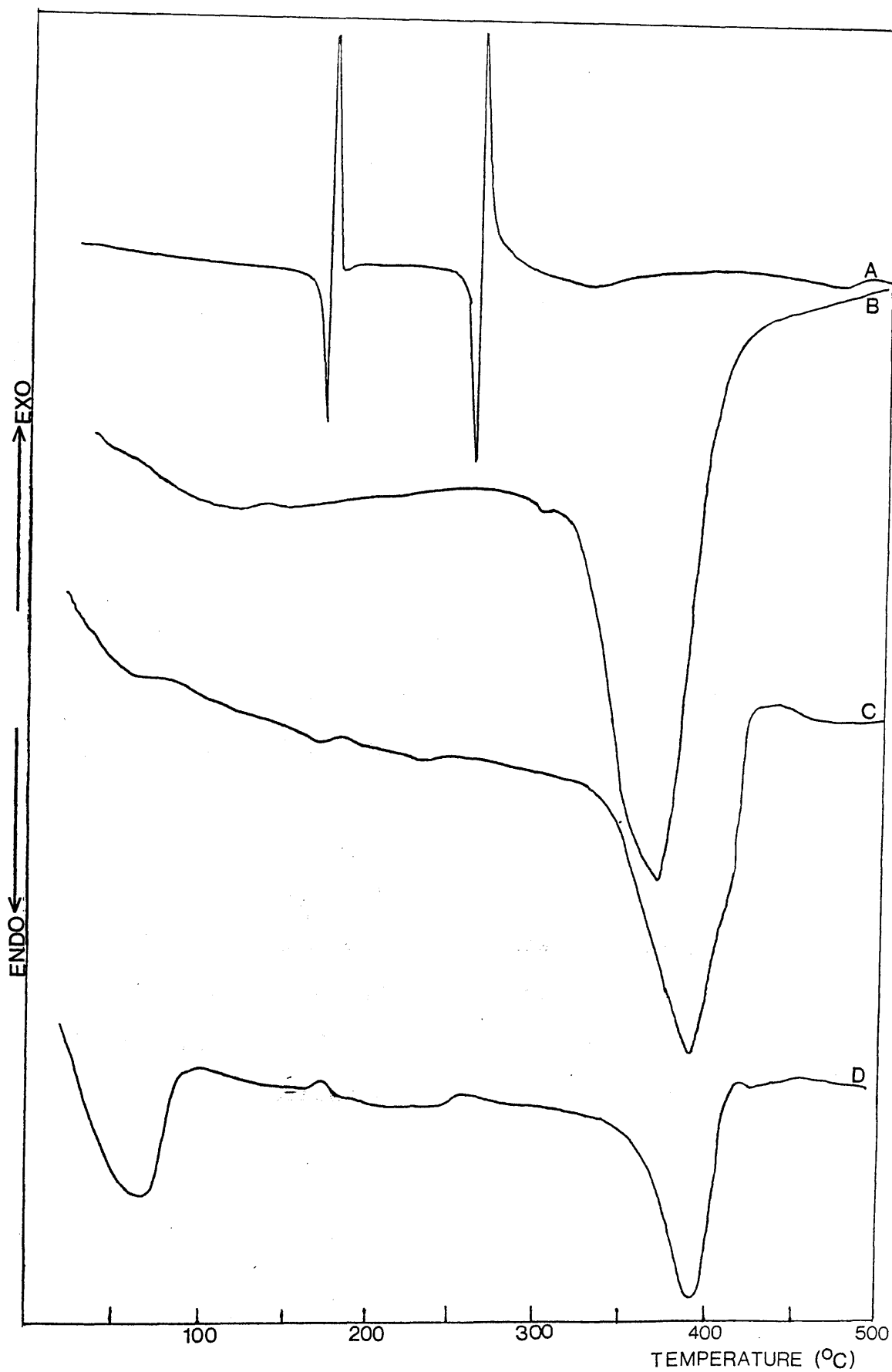


Figure 5.32 DSC curves (N_2 atmosphere) of $Mn(acac)_3$ (A), PMMA 1 (B), 1:50 $Mn(acac)_3$ - PMMA 1 (c), 1:10 $Mn(acac)_3$ - PMMA 1 (D)

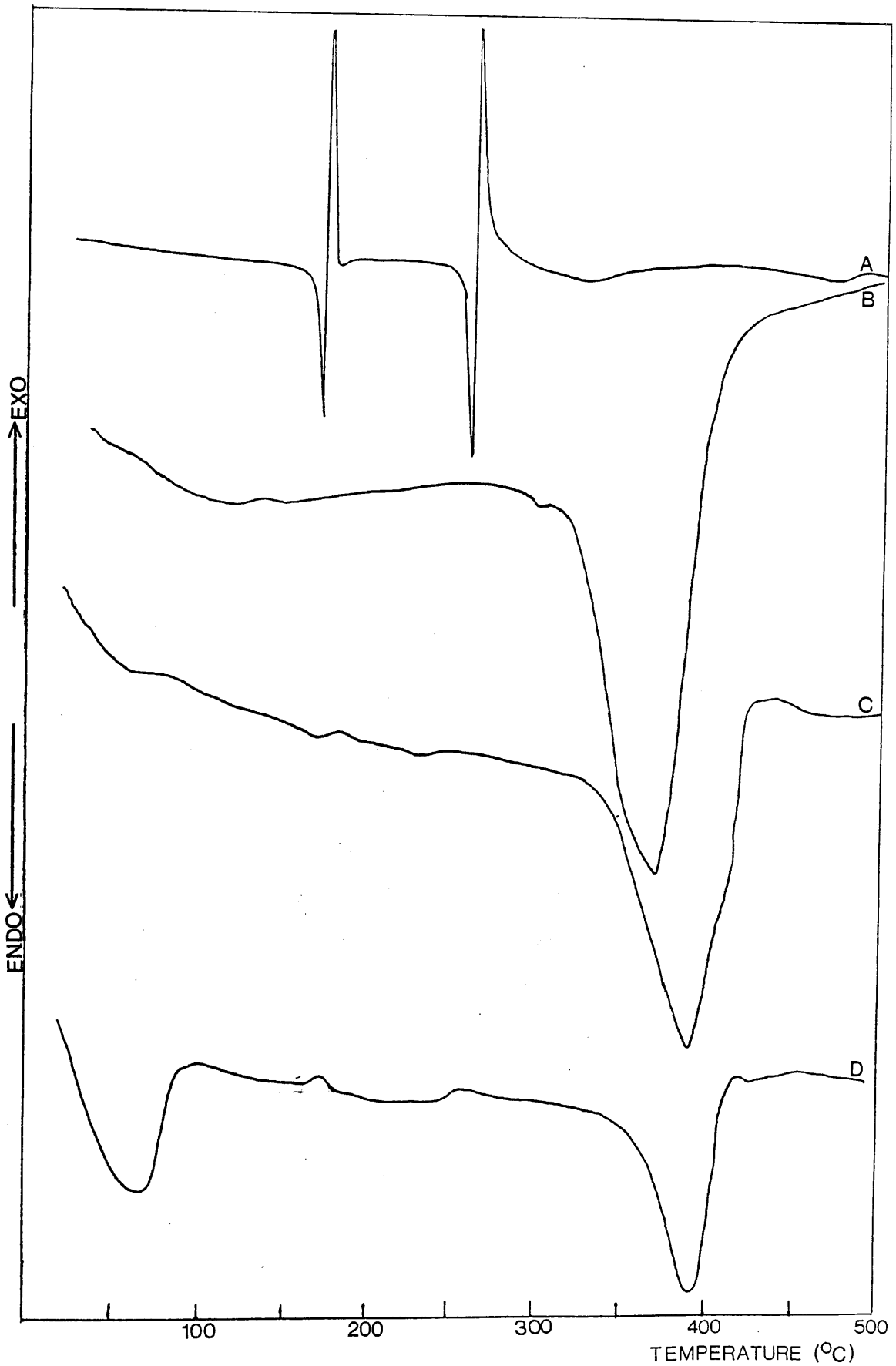


Figure 5.32 DSC curves (N_2 atmosphere) of $Mn(acac)_3$ (A), PMMA 1 (B), 1:50 $Mn(acac)_3$ - PMMA 1 (C), 1:10 $Mn(acac)_3$ - PMMA 1 (D)

depolymerisation by acac. radicals produced by the reaction



Similarly the peak with T(max) 235°C can be attributed to the decomposition of the bis chelate.

Note that the discrepancy of some 20°C in the T(max) temperature of the first decomposition step of the Mn(acac)₃ as recorded in the DSC and TVA curves for the blends was also found in the TG/DSC and TVA curves of Mn(acac)₃ alone and may be related to the different environment (atmospheric pressure or vacuum) in the two techniques.

CONCLUSIONS ON THE NATURE OF THE DEGRADATION OF Mn(acac)₃ - PMMA BLENDS

Degradation Processes Occurring Below 200°C

The first processes observed are those associated with the overlapping peaks between 150-165°C. The height of the coalesced peak varies with both the molecular weight of the polymer and the Mn(acac)₃ concentration, increasing with decreasing molecular weight and increasing Mn(acac)₃ concentration. The DSC evidence suggests that this decomposition is predominantly due to the normal thermal decomposition of Mn(acac)₃ to Mn(acac)₂. Decomposition promoted by interaction with the electron-donating unsaturated and ester groups of the polymer is expected to occur at a

considerably lower temperature than the purely thermal ligand scission reaction and could well be masked by the solvent peak. The partial dependence on molecular weight of the processes giving rise to the TVA peak between 150-163°C suggests that some chain-end interaction is taking place. This could be between the unsaturated chain ends and $\text{Mn}(\text{acac})_2$, $\text{Mn}(\text{acac})_2$ being more active in this respect than $\text{Co}(\text{acac})_2$.²⁶

It is conceivable that polymer bound carboxylates form by reaction of the ester bound $\text{Mn}(\text{acac})_3$ by a reaction directly analogous to that of the coordinated bis chelates to give a Mn(III) species. However this process requires C-O scission and is unlikely to be energetically feasible at the low temperatures of the electron donor promoted acac ligand scission.

Degradation Processes Occurring Above 200°C

The DSC analysis, dependence on $\text{Mn}(\text{acac})_3$ concentration, and the identification of acetone as an associated product point clearly to the TVA peak $T(\text{max})$ 235°C being due to the decomposition of the $\text{Mn}(\text{acac})_2$ formed earlier in the degradation.

Beyond this point, the degradation processes are much the same as those occurring in the $\text{Co}(\text{acac})_3$ blends although they are enhanced due to the greater degree of interaction of $\text{Mn}(\text{acac})_3$ (and $\text{Mn}(\text{acac})_2$) with the polymer in the earlier stages of the degradation.

CHAPTER 6BLENDS OF Co(acac)₃ AND Mn(acac)₃ WITH
THE 1:59 MAA-MMA COPOLYMERINTRODUCTION

Although the concentration of methacrylic acid units in the 1:59 MAA-MMA copolymer is very small, it is nevertheless similar to the concentration of chelates employed in the blends. Significant differences between the behaviour of the copolymer and PMMA blends are found and are discussed in this chapter.

THERMAL DEGRADATION BEHAVIOUR OF THE 1:59 MAA-MMA
COPOLYMER

This has already been discussed in Chapter 4.

DECOMPOSITION OF Co(acac)₃ AND Mn(acac)₃

The behaviour of Co(acac)₃ and Mn(acac)₃ on heating has been described in Chapter 3.

DEGRADATION OF Co(acac)₃ - COPOLYMER BLENDS, 1:10 AND
1:50TVA BEHAVIOUR

Figures 6.1 and 6.2 show the TVA curves obtained for the 1:10 and 1:50 Co(acac)₃ - copolymer blends. The blends were prepared in the normal TVA fashion by casting a film directly onto the base of a TVA tube from

a methylene chloride or chloroform solution.

As expected for a copolymer with a composition so similar to pure PMMA, the behaviour of the copolymer blends resembles that of the PMMA blends. In the lower temperature regions there are two peaks, the latter being $\text{Co}(\text{acac})_3$ concentration dependent and having a small degree of -196°C non-condensable material production associated with it at the higher $\text{Co}(\text{acac})_3$ concentration. The $T(\text{max})$ of this peak (159°C) is considerably lower than that of the corresponding peak in the PMMA blends (190°C). A similar phenomenon occurs also with the $\text{Mn}(\text{acac})_3$ - copolymer blends and its nature is discussed in the concluding section of this chapter.

Above 200°C the effect of the additive is rather more dramatic. The chain-end initiated depolymerisation of the unblended copolymer is reduced whilst the formation of larger amounts of non-monomeric fragmentation products than from the PMMA blend distorts slightly the shape of the major peak. Finally, above 400°C , there is a small peak due mostly to -196°C non-condensable material resulting presumably from the fragmentation of extra structures formed within the blend.

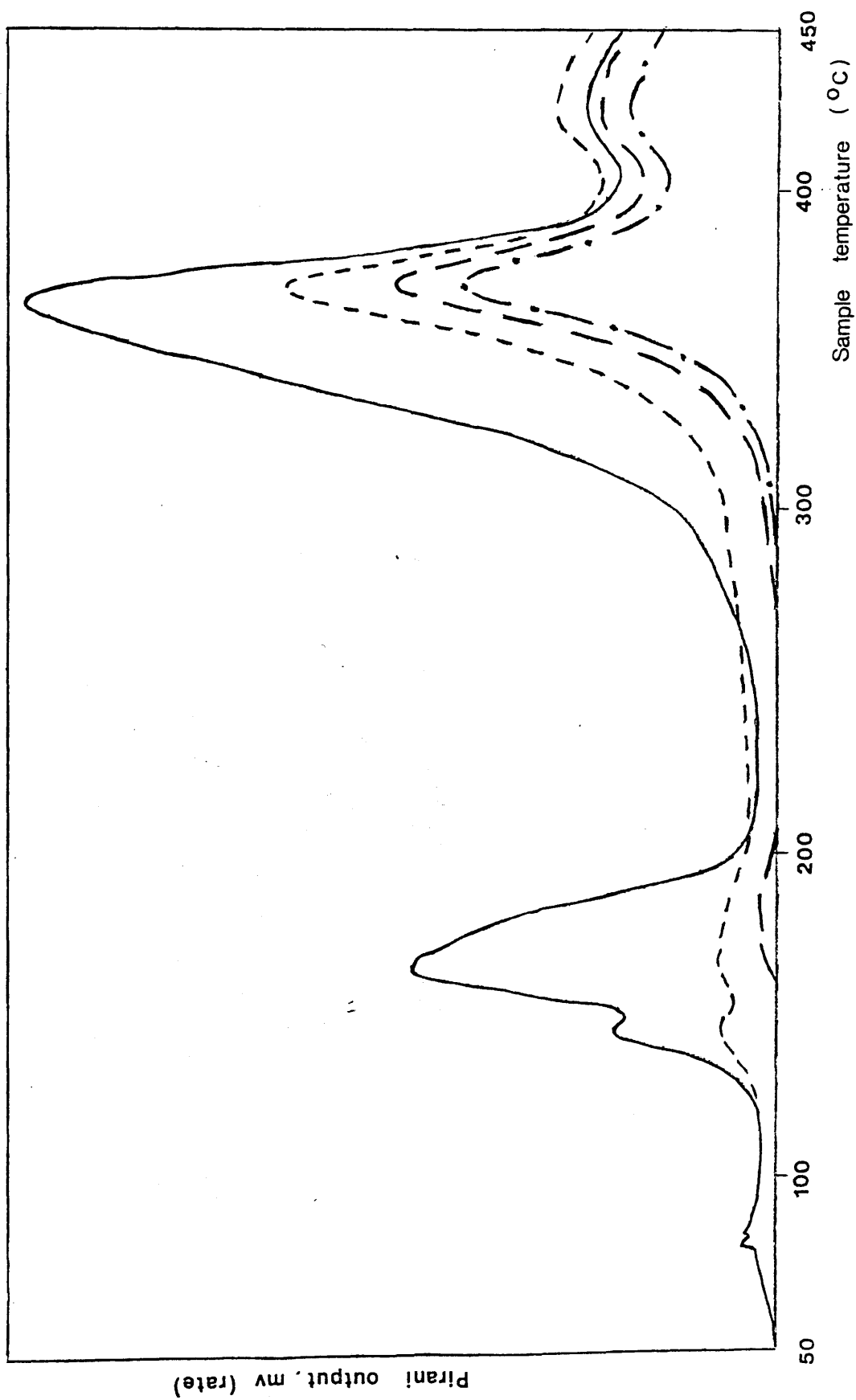


Figure 6.1 TVA curve for 1:10 Co(acac)₃ - copolymer blend

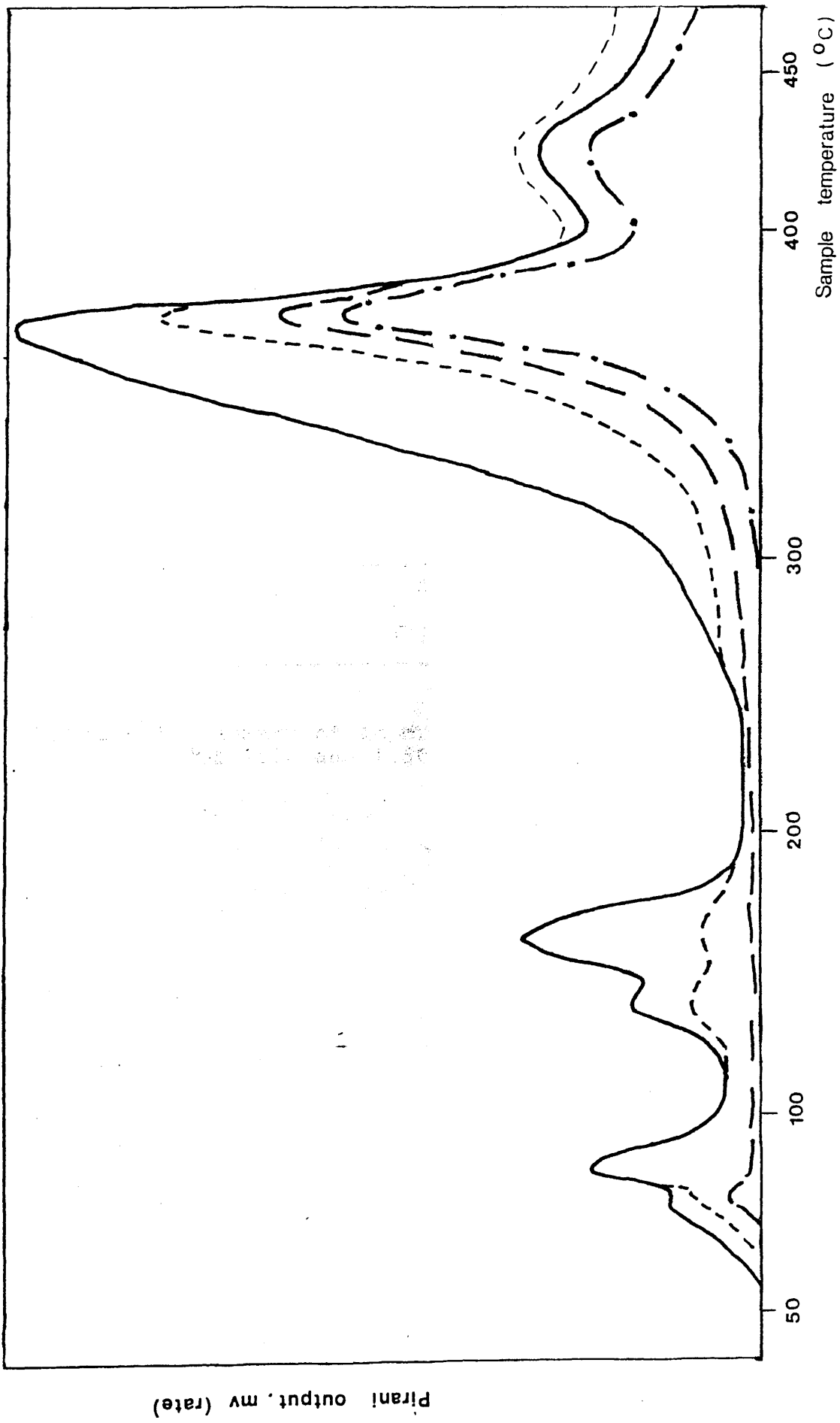


Figure 6.2 TVA curve for 1:50 Co(acac)₃ - copolymer blend

Feature	Co(acac) ₃ : Copolymer		
	1:10	1:50	
Compatibility	No	Yes	
T(sublimation)		>130	
1st Peak	T(onset)	104	114
	T(max)	125	133
2nd Peak	T(onset)	132	140
	T(max)	150	159
Shoulder on Main Peak	230-293	236-298	
Main Peak T(max)			
Condensibles	374	377	
Non-condensibles	379	383	
Final Peak	T(onset)	410	402
	T(max)	432	436

Table 6.1 Summary of Important Features from TVA traces of 1:10 and 1:50 Co(acac)₃ - Copolymer Blends

temperature interaction between Co(acac)₃ and
 acac ligand groups. This is also in accord
 and reference described in Chapter 1.

STRUCTURE OF Co(acac)₃ - COPOLYMER BLENDS AND CHANGES DURING DEGRADATION

The structure of the 1:50 and 1:10 Co(acac)₃ copolymer blends were examined by IR and UV spectroscopy. Films were prepared by the standard method and all degradations were performed under standard TVA conditions. The spectra obtained are illustrated in Figs. 6.3 - 6.6 and the details summarised in Tables 6.2 and 6.3.

STRUCTURE OF THE UNDEGRADED BLEND

As in the case of the Co(acac)₃ - PMMA blends, no interaction was detected in the undegraded blends by UV or IR spectroscopy. The π -type complex between Co(acac)₃ and the unsaturated chain ends is not observed spectroscopically, and as with the PMMA blends, the identification of this complex relies on the interpretation of the degradation behaviour. In accord with the behaviour discussed in Chapter 3, there was no evidence for a room temperature interaction of Co(acac)₃ with the ester side groups of PMMA (Chapter 5) and similarly there is no evidence here for a room temperature interaction between Co(acac)₃ and the ester or acid side groups. This is also in accord with the evidence described in Chapter 3.

CHANGES OF STRUCTURE ON DEGRADATION

The structural changes on degradation are similar

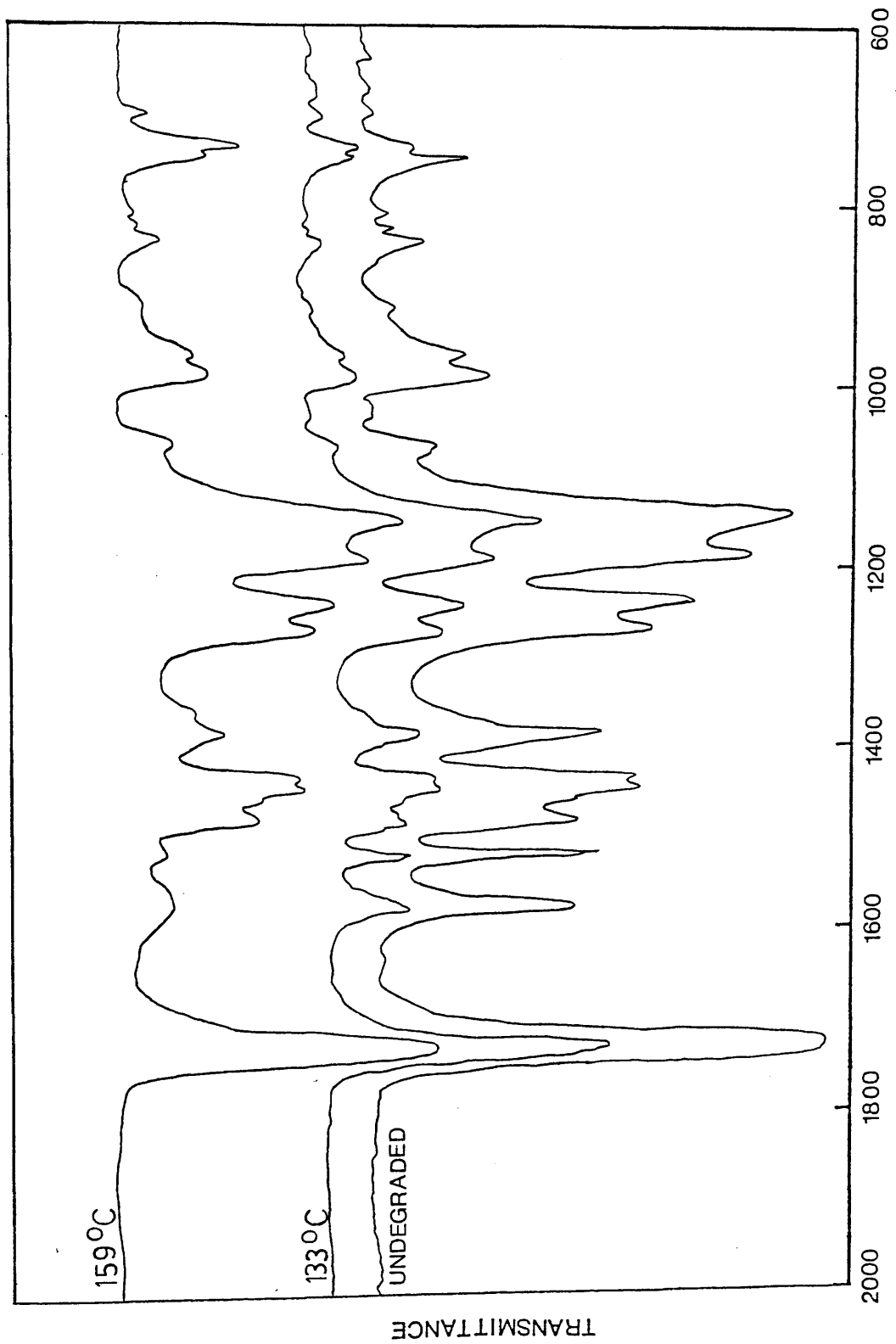


Figure 6.3 IR spectra of 1:50 Co(acac)₃ - copolymer blend at various stages of degradation

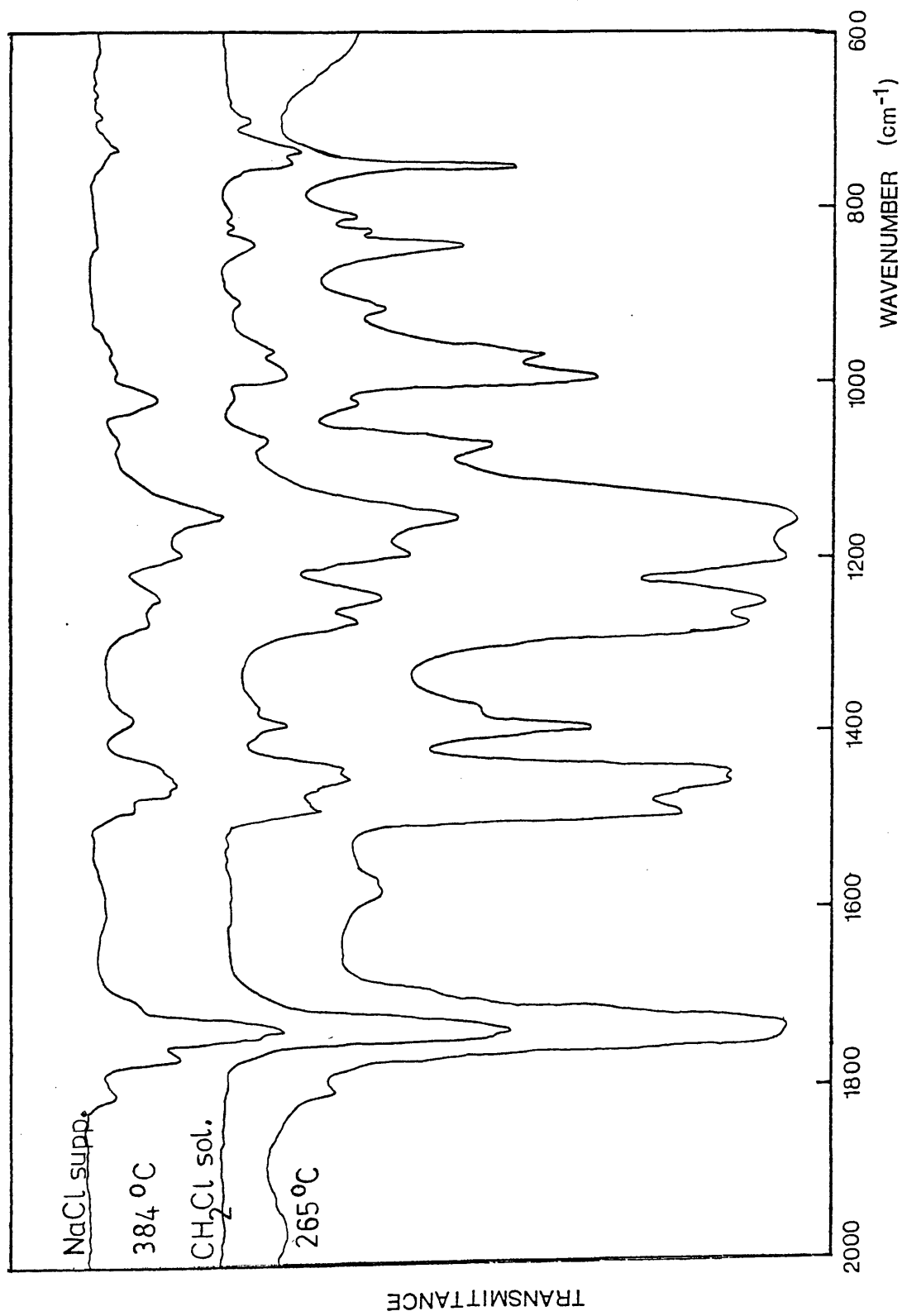


Figure 6.3 IR spectra of 1:50 Co(acac)₃ - copolymer blend at various stages of degradation (ctd.)³

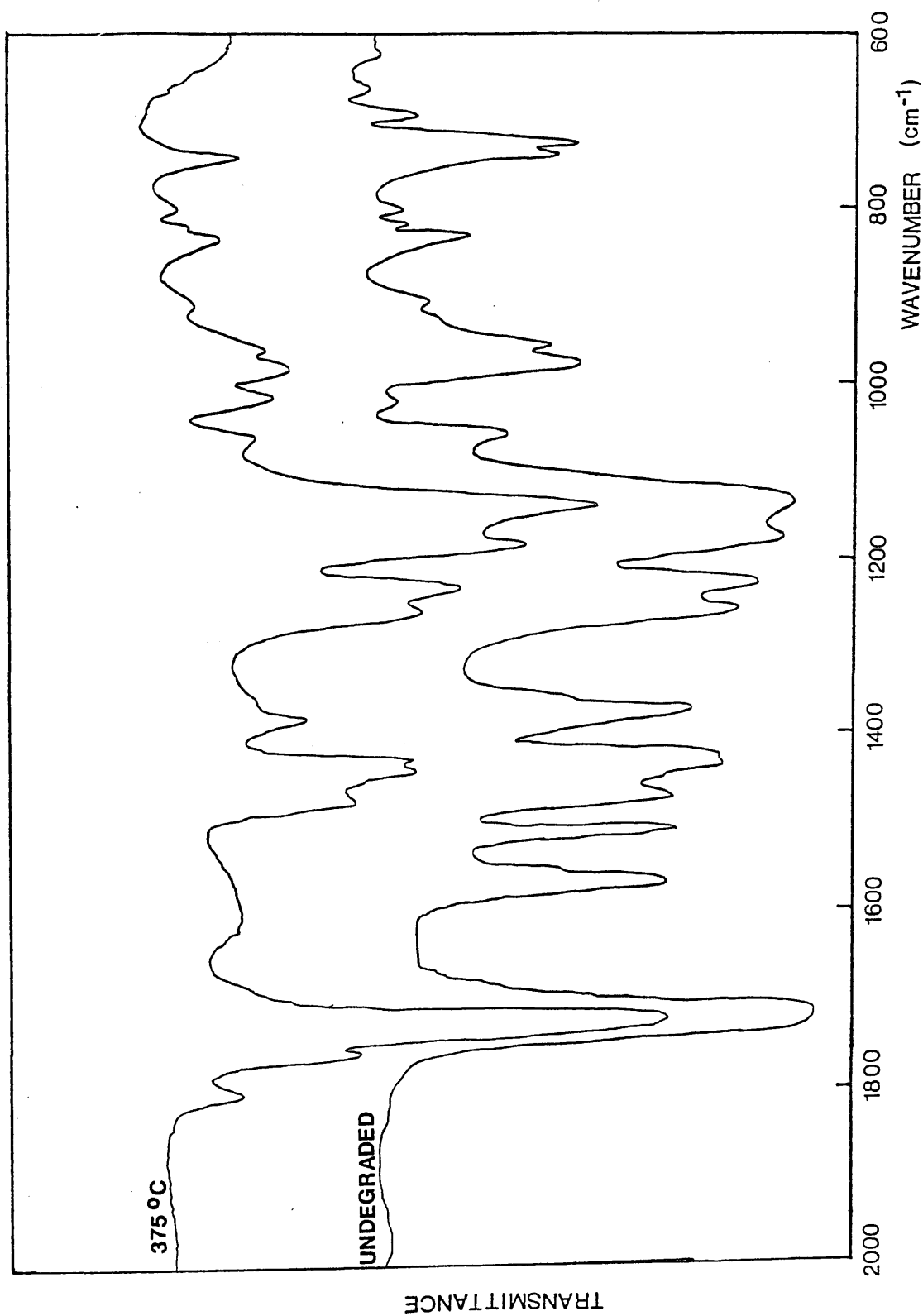


Figure 6.4 IR spectra of 1:10 Co(acac)₃ - copolymer blend at various stages of degradation

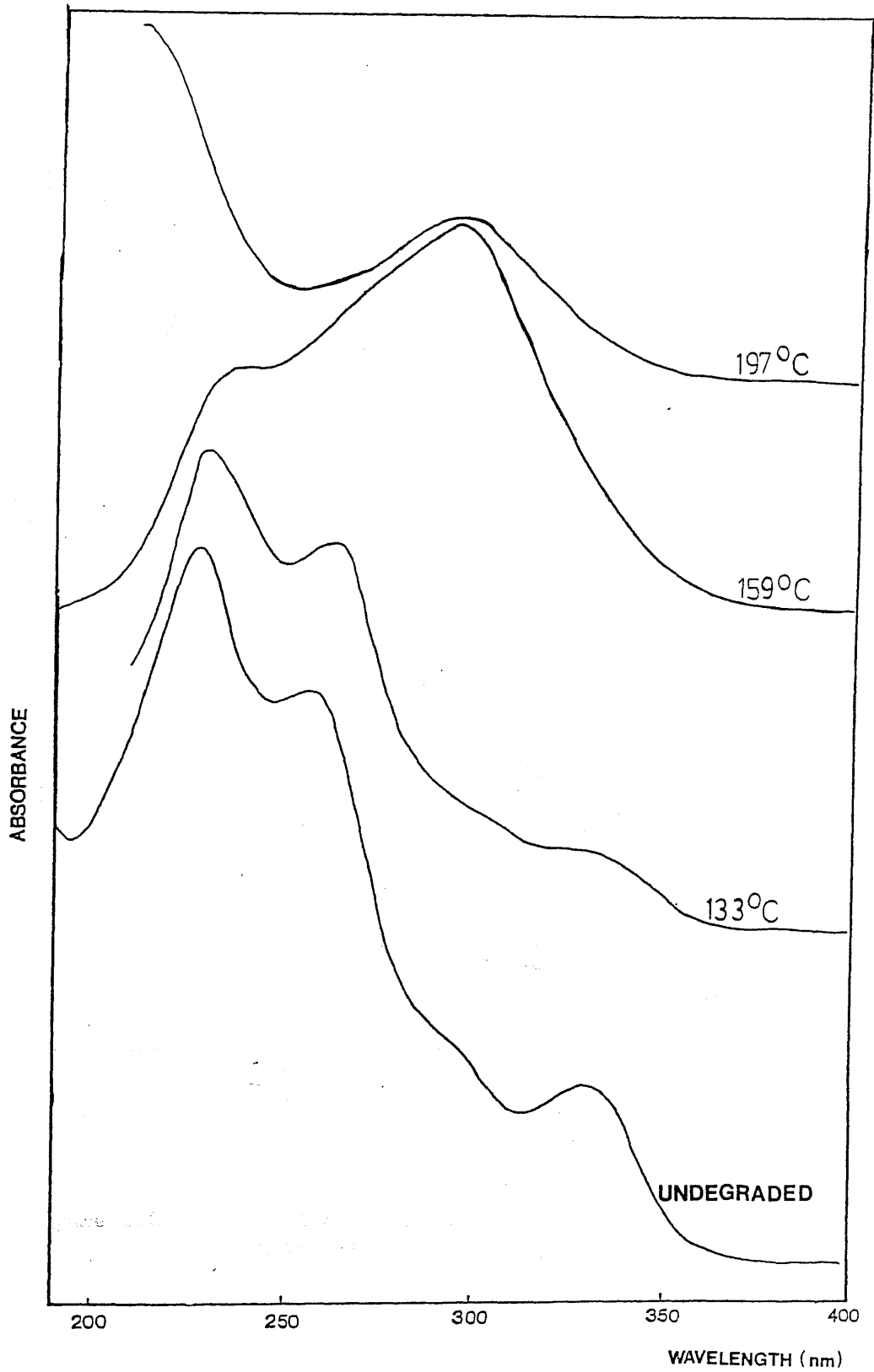


Figure 6.5

UV spectra of 1:50 Co(acac)₃ - copolymer blend at various stages of degradation

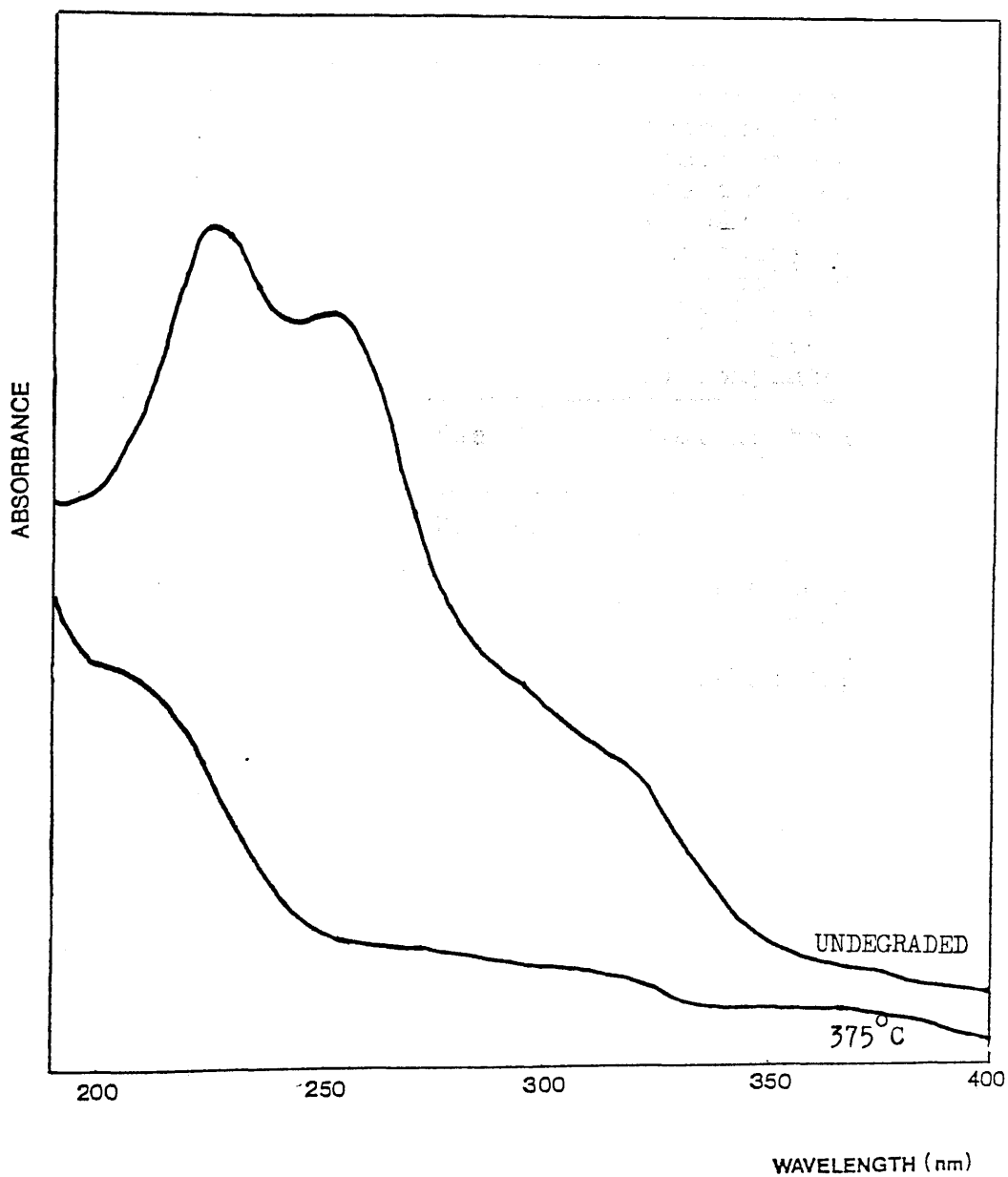


Figure 6.6 UV spectra of the 1:10 Co(acac)₃ - copolymer blend before and after degradation to 375°C

Extent of Degradation	Visual Appearance	CH ₂ Cl ₂ Soluble	Structure of Blend
None	Transparent bottle green	Yes	No evidence of interaction in UV, IR spectra
133°C (A)	No change	Yes	No detectable change
159°C (B)	Transparent, pink	Yes	Reduction in chelate concentration. UV spectrum shows chelate species to be Co(acac) ₂ (λ(max) 290 nm). IR - intensification of 1580 cm ⁻¹ absorption relative to that at 1510 cm ⁻¹ possible carboxylate formation
197°C (C)	Similar to 159°C	Yes	Similar to that at 159°C
265°C (D)	Transparent yellow	Partly	Film degraded on NaCl disc - IR absorption shows small amount anhydride and carboxylate absorption. CH ₂ Cl ₂ soluble portion of glass supported film similar
384°C (E)	Similar to 265°C	Partly	Soluble portion - IR spectrum shows pronounced anhydride absorption, also small amount carboxylate and acid absorption (1700 cm ⁻¹)
485°C (F)	Brown char	No	Spectrum of residue run as KBr disc shows only very weak carboxylate absorption

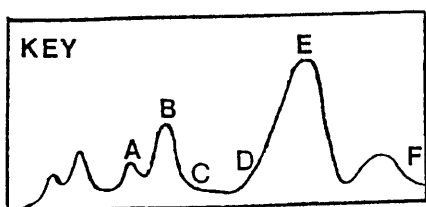


Table 6.2 Structure of 1:50 Co(acac)₃ - Copolymer Blend at Various Stages of the Heating Programme

Extent of Degradation	Visual Appearance	CH ₂ Cl ₂ Solubility	Structure of Blend
None	Green, opaque, incompatible	Yes	IR and UV spectra show no evidence of any interaction
375°C	Yellow/orange	Partly	Anhydride and carboxylate absorptions present in IR spectrum of NaCl supported film

Table 6.3 Structure of 1:10 Co(acac)₃ - Copolymer Blend Before and After Degradation to 375°C

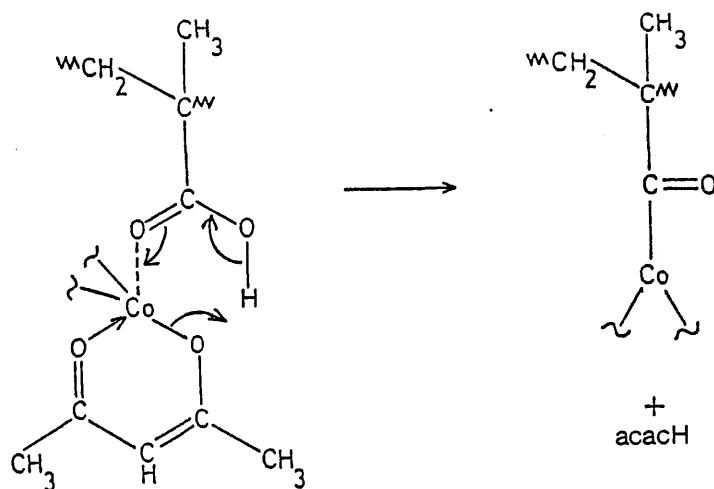
It is also conceivable that a cobalt(III) carboxylate forms by the direct reaction of Co(acac)₃ with the acid groups. Such a mixture would be expected to show a characteristic IR spectrum.

The IR spectrum of the blend

is shown in Figure 6.3.

to those of the $\text{Co}(\text{acac})_3$ - PMMA blends. The formation of $\text{Co}(\text{acac})_2$, carboxylate structures and their subsequent decomposition are common to both systems. Like the PMMA blends, the first structural change, the decomposition of the π -complex is not detected spectroscopically but is associated with the first TVA peak.

The 1:50 $\text{Co}(\text{acac})_3$ - copolymer blend shows more carboxylate production than the 1:50 $\text{Co}(\text{acac})_3$ - PMMA blend. This is due to the reaction between the newly formed $\text{Co}(\text{acac})_2$ and methacrylic acid subunits which is analogous to that with the ester side groups but is favoured for steric reasons.



It is also conceivable that a cobalt(III) polymer bound carboxylate forms by the direct reaction of $\text{Co}(\text{acac})_3$ with the acid groups. Such a mixed chelate forms with $\text{Mn}(\text{acac})_3$ at room temperature as described subsequently. However, there is no indication that $\text{Co}(\text{acac})_3$ associates with the methacrylic acid units

of the chain at room temperature and at higher temperatures below T_g the extent of any reaction would be limited by the slow migration of $\text{Co}(\text{acac})_3$ to the acid sites. At temperatures above T_g , the mixed chelate, by analogy with the manganese(III) example would be unstable. Nevertheless, it is possible that some of the polymer bound cobalt(II) mixed chelate could be formed by direct substitution of $\text{Co}(\text{acac})_3$ by an acid group followed by the immediate reduction to $\text{Co}(\text{II})$ with the loss of another acac ligand rather than by the reaction with $\text{Co}(\text{acac})_2$ described above.

Anhydride ring structures are formed in this blend both by the intermolecular cyclisation of the acid and ester side groups found to occur in the unblended copolymer, and by the mechanisms outlined in relation to the $\text{Co}(\text{acac})_3$ - PMMA blends. The production of anhydride rings by acid-ester reaction occurs at a lower temperature (ca. 280°C) than the chelate induced cyclisations ($>300^\circ\text{C}$).

In all other respects the structural changes parallel those of the PMMA blends. As degradations to 377°C and 485°C were performed on NaCl discs, it is impossible to differentiate between Co^{2+} and Na^+ methacrylate salts. However, the degradation studies of the PMMA blends indicate that the cobalt salt will persist at elevated temperatures.

Extent of Degradation	Total Products Identified
133°C (A)	Methyl methacrylate, methylene chloride
159°C (B)	As 133°C + acetylacetone
197°C (C)	As 159°C + trace methanol
265°C (D)	As 159°C + methanol, methyl acetate
*384°C (E)	As 290°C + carbon dioxide, "ketene", dimethyl ether, butene, isobutene
*485°C (F)	As 377°C

* Although not collected in a form suitable for analysis an extended tail fraction on the SAD curve obtained for the products of degradation at 384°C and 485°C suggests that the 5-membered cyclic anhydride product may also be present.

Table 6.4 Condensable Products from 1:50 Co(acac)₃ - Copolymer Blend

Extent of Degradation	Cold Ring Fraction
133°C (A)	Very small amount; gives green solution; IR spectrum indicates acac chelate to be present - most likely Co(acac) ₃ but not confirmed in absence of UV spectrum
159°C (B)	As 133°C
197°C (C)	IR spectrum shows some chain fragments to be present
265°C (D)	Only sample for which UV spectrum obtained - indicates presence of Co(acac) ₂ and Co(acac) ₃
377°C (E)	Heavy, brown. IR spectrum shows chain fragments including anhydride and unsaturated structures (Fig. 6.7)
485°C (F)	As 377°C

Table 6.5 Cold Ring Fraction from 1:50 Co(acac)₃ - Copolymer Blend for Various Stages of Degradation

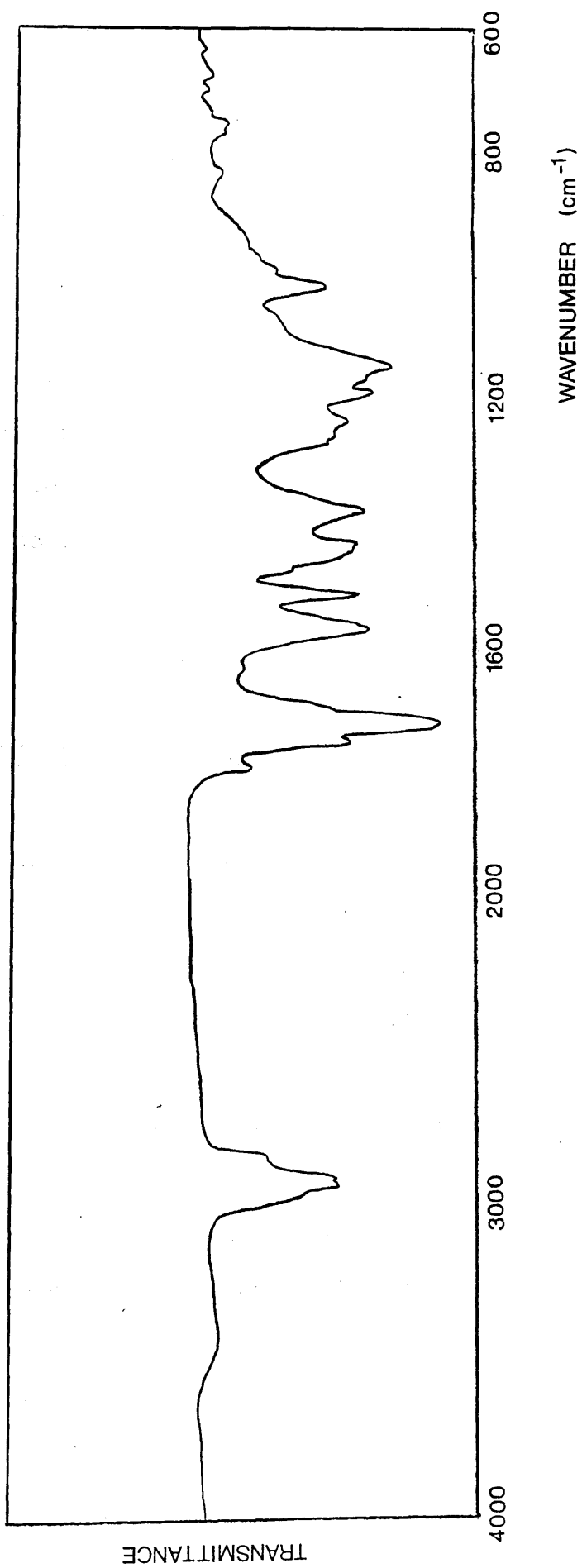


Figure 6.7 IR spectrum of CRF from 1:50 Co(acac)₃ - copolymer blend on degradation to 485°C

-196°C CONDENSIBLE PRODUCTS AND COLD RING FRACTION
FROM 1:50 AND 1:10 Co(acac)₃ - COPOLYMER BLENDS

Investigations of the -196°C condensible products and cold ring fraction formed for various stages of degradation were performed by the usual methods. Tables 6.4 and 6.5 list, respectively, the total -196°C condensible products and CRF identified at each stage.

The products from the 1:10 blend were analysed only for degradation to 485°C and were found to be the same as those obtained from the 1:50 blend although with the enhanced production of fragmentation products and sublimate.

DEGRADATION OF Mn(acac)₃ - COPOLYMER BLENDS, 1:10 AND
1:50

TVA BEHAVIOUR

TVA curves of the 1:10 and 1:50 blends of Mn(acac)₃ with the copolymer are shown in Figs. 6.8 and 6.9 and the important features are summarised in Table 6.6.

Unlike the Co(acac)₃ - copolymer blends which produce little change in the T(max) of the major degradation peak, the Mn(acac)₃ - copolymer blends show a considerable increase in the value for T(max) relative to that of the copolymer alone. This shift (ca. 25°C) indicates that more extensive blocking of the unzipping occurs in the Mn(acac)₃ - copolymer

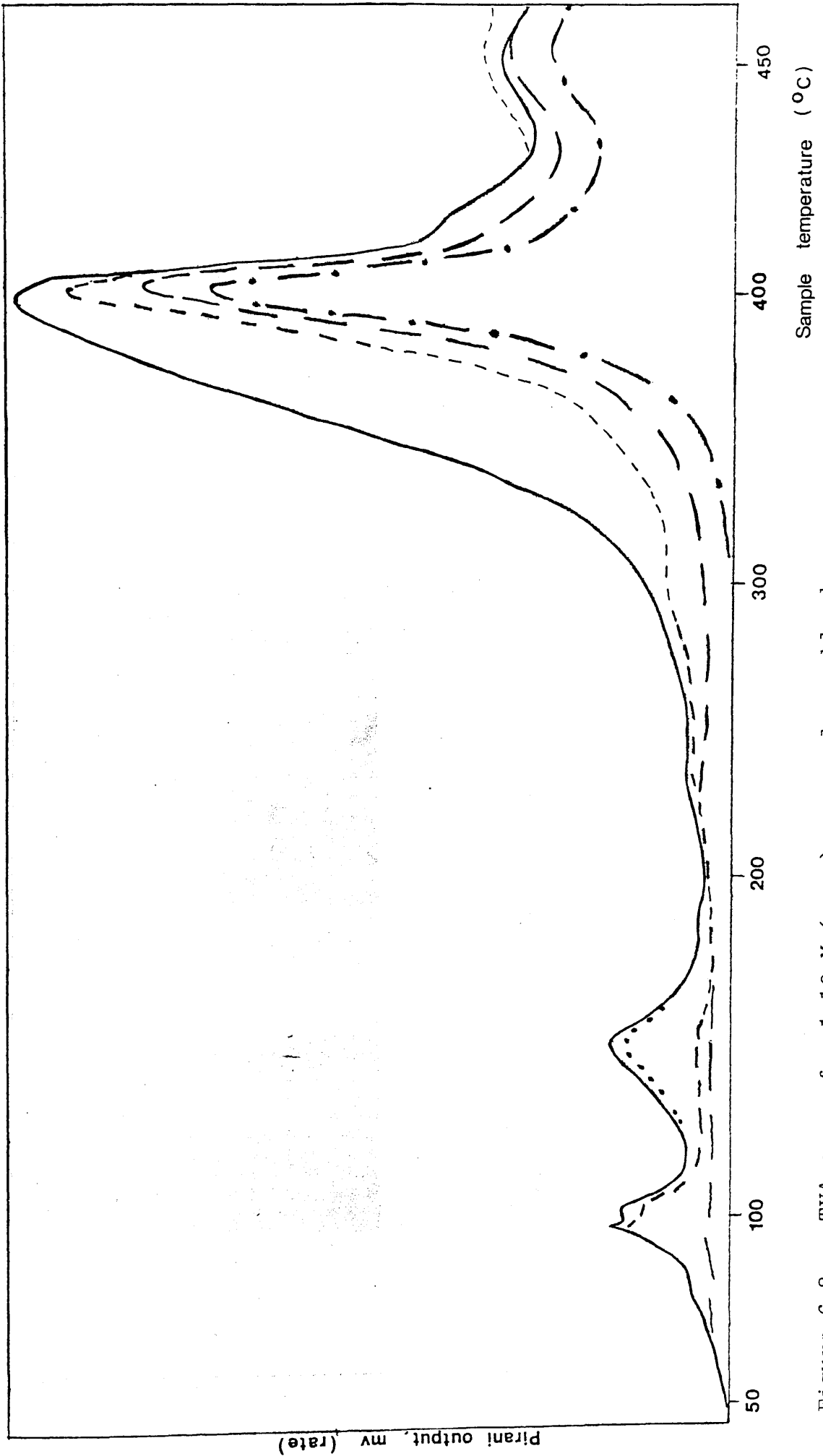


Figure 6.8 TVA curve for 1:10 Mn(acac)₃ - copolymer blend

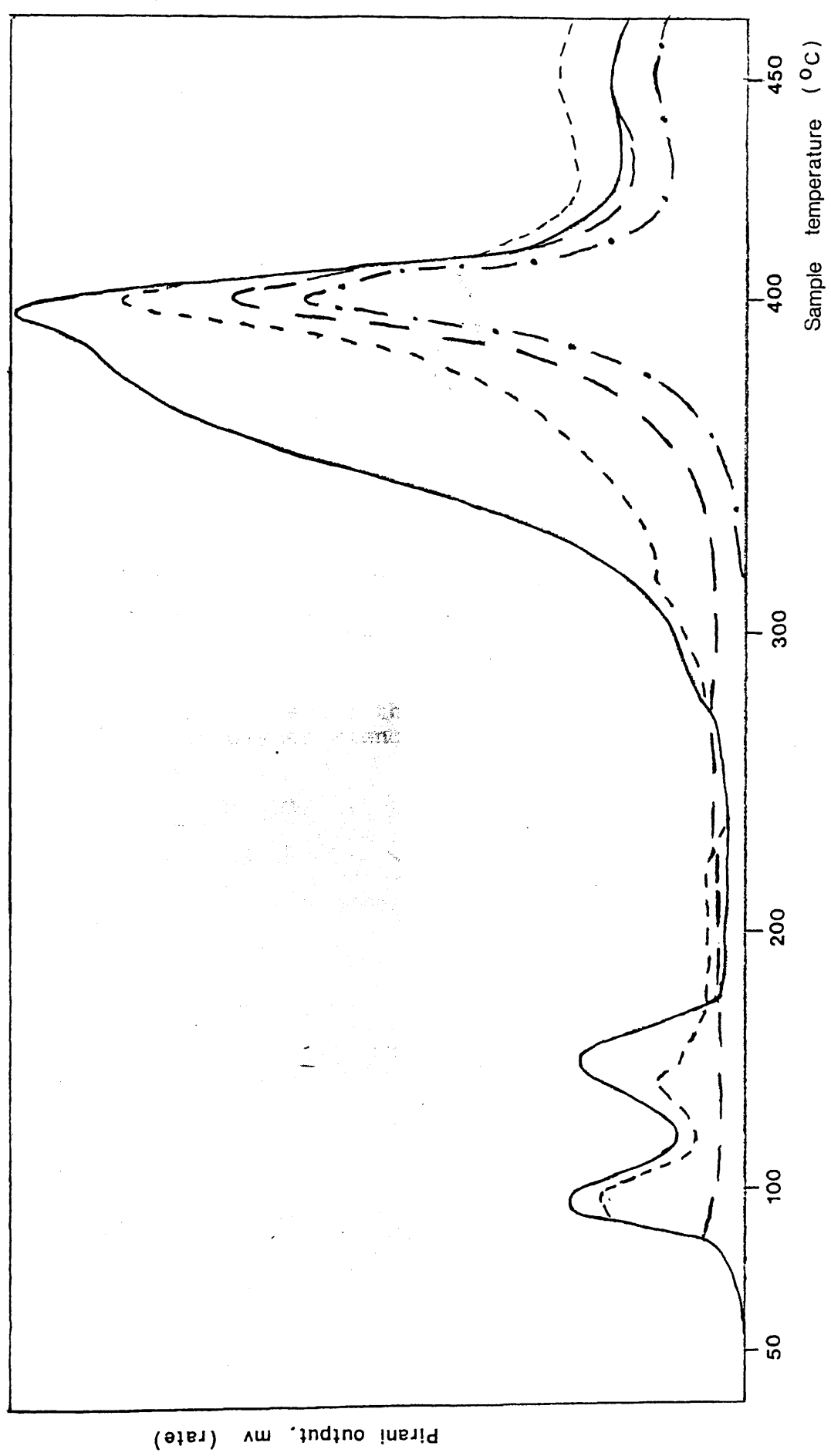


Figure 6.9 TVA curve for 1:50 Mn(acac)₃ - copolymer blend

Feature	Mn(acac) ₃ : Copolymer	
	1:10	1:50
Compatibility	Not Fully	Yes
T(sublimation)	Not recorded	Not observed
1st Peak T(max)	96	98
2nd Peak T(onset)	ca. 116	ca. 117
2nd Peak T(max)	145	146
Shoulder on Main Peak	218-294	232-294
Main Peak T(max)	400	347
Final Peak T(onset)	441	429
Final Peak T(max)	457	455

Temps. in °C

Table 6.6 TVA Data for the 1:10 and 1:50 Mn(acac)₃ - Copolymer Blends

blends than in those of $\text{Co}(\text{acac})_3$. This parallels the behaviour of the PMMA blends of these complexes.

Although occurring in the same region as the evolution of trapped solvent, there is, what its size and regular shape implies is a degradation peak with $T(\text{max})$ $96-98^\circ\text{C}$. Occurring at a temperature well below that of any degradation process identified for $\text{Mn}(\text{acac})_3$, the copolymer alone, or the $\text{Mn}(\text{acac})_3$ - PMMA blends, this peak can only be attributed to a reaction dependent in the presence of the acid side groups. Also, the peak attributed for the $\text{Mn}(\text{acac})_3$ - PMMA blends to the $\text{Mn}(\text{acac})_3$ decomposition initiated unzipping occurs some $6-7^\circ\text{C}$ lower in the copolymer blends. A similar effect also occurs in the $\text{Co}(\text{acac})_3$ - copolymer blend and will be discussed at the end of this chapter.

The peak $T(\text{max})$ 233°C , due to the degradation of the $\text{Mn}(\text{acac})_2$ produced by the decomposition of $\text{Mn}(\text{acac})_3$, noticeable in the 1:10 PMMA blend, appears in the copolymer blend TVA curve as a basal shoulder at the onset of the major degradation peak and the chain end initiated unzipping of the copolymer ($T(\text{max})$ 287°C) is reduced to near nil in both the 1:50 and 1:10 blends.

Finally, as in the case of the $\text{Co}(\text{acac})_3$ - copolymer blend, there is in the 1:10 and 1:50 $\text{Mn}(\text{acac})_3$ - copolymer blends a pronounced peak $T(\text{max})$ $455-457^\circ\text{C}$ not observed with the PMMA blends and which

is probably associated with the more extensive alterations to the copolymer chain backbone.

The IR spectrum of the copolymer is very similar to that of PMMA film, with the characteristic absorption bands which are associated with the polymer. In the IR spectrum only a few bands are very prominent. The presence of the carbonyl group introduced the possibility of an ester linkage in the copolymer (see Chapter 10). The IR spectrum of the copolymer was recorded after the copolymer was prepared by the procedure described in Chapter 10. The IR spectrum of the copolymer is shown in Figure 10. The IR spectrum of the copolymer is very similar to that of PMMA film, with the characteristic absorption bands which are associated with the polymer. In the IR spectrum only a few bands are very prominent. The presence of the carbonyl group introduced the possibility of an ester linkage in the copolymer (see Chapter 10). The IR spectrum of the copolymer was recorded after the copolymer was prepared by the procedure described in Chapter 10. The IR spectrum of the copolymer is shown in Figure 10.

STRUCTURE OF THE $Mn(acac)_3$ - COPOLYMER BLEND AND CHANGES ON DEGRADATION

Figs. 6.10-6.11 illustrate the IR and UV spectra of the 1:50 $Mn(acac)_3$ - copolymer blend at various stages of degradation and the salient features are summarised in Table 6.7. Samples were prepared, degraded and analysed in the standard manner.

STRUCTURE OF THE UNDEGRADED BLEND

The UV spectrum of the undegraded 1:50 $Mn(acac)_3$ - copolymer blend is very similar to that of the $Mn(acac)_3$ - PMMA blend, with the same broad, complicated absorbance, which indicates interaction of the chelate with the polymer. In the PMMA blend in which only ester side groups are present the complexation was shown to be reversible at room temperature. The presence of the methacrylic acid groups introduces the possibility of an irreversible ligand substitution reaction (see Chapter 3) and the occurrence of just such a reaction was demonstrated by dissolving a sample of the 1:50 $Mn(acac)_3$ - copolymer blend in methylene chloride and precipitating in methanol. The process was repeated three times and although the IR spectrum of the precipitated material is essentially that of the copolymer, the UV spectrum shows the persistence of an absorption at 240 nm, intense enough to mask the absorption at 214 nm due to the copolymer alone (see Figs. 6.12 and 6.13). This implies

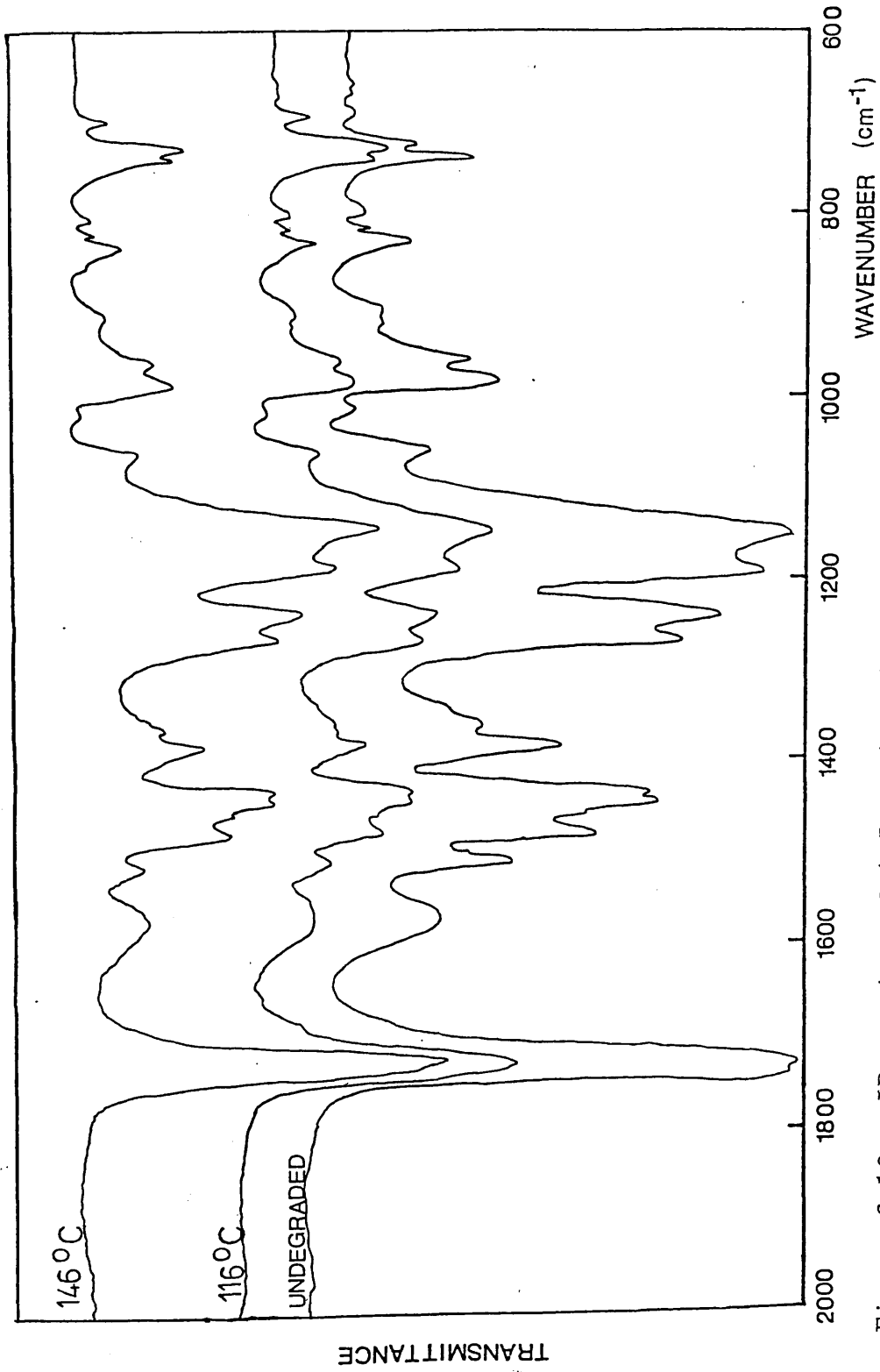


Figure 6.10 IR spectra of 1:50 Mn(acac)₃ - copolymer blend at various stages of the heating programme

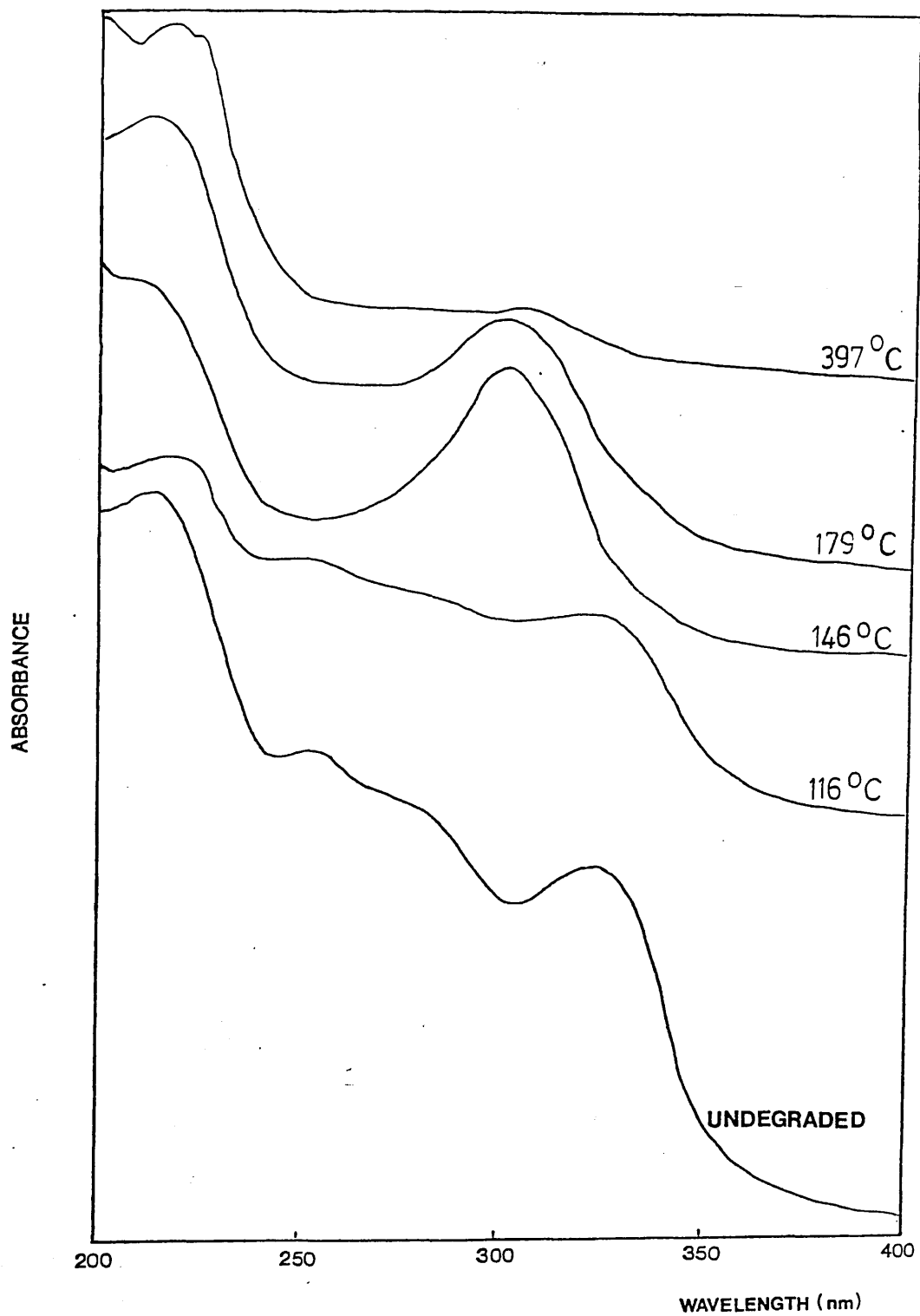


Figure 6.11 UV spectra of 1:50 Mn(acac)₃ - copolymer blend at various stages of the heating programme

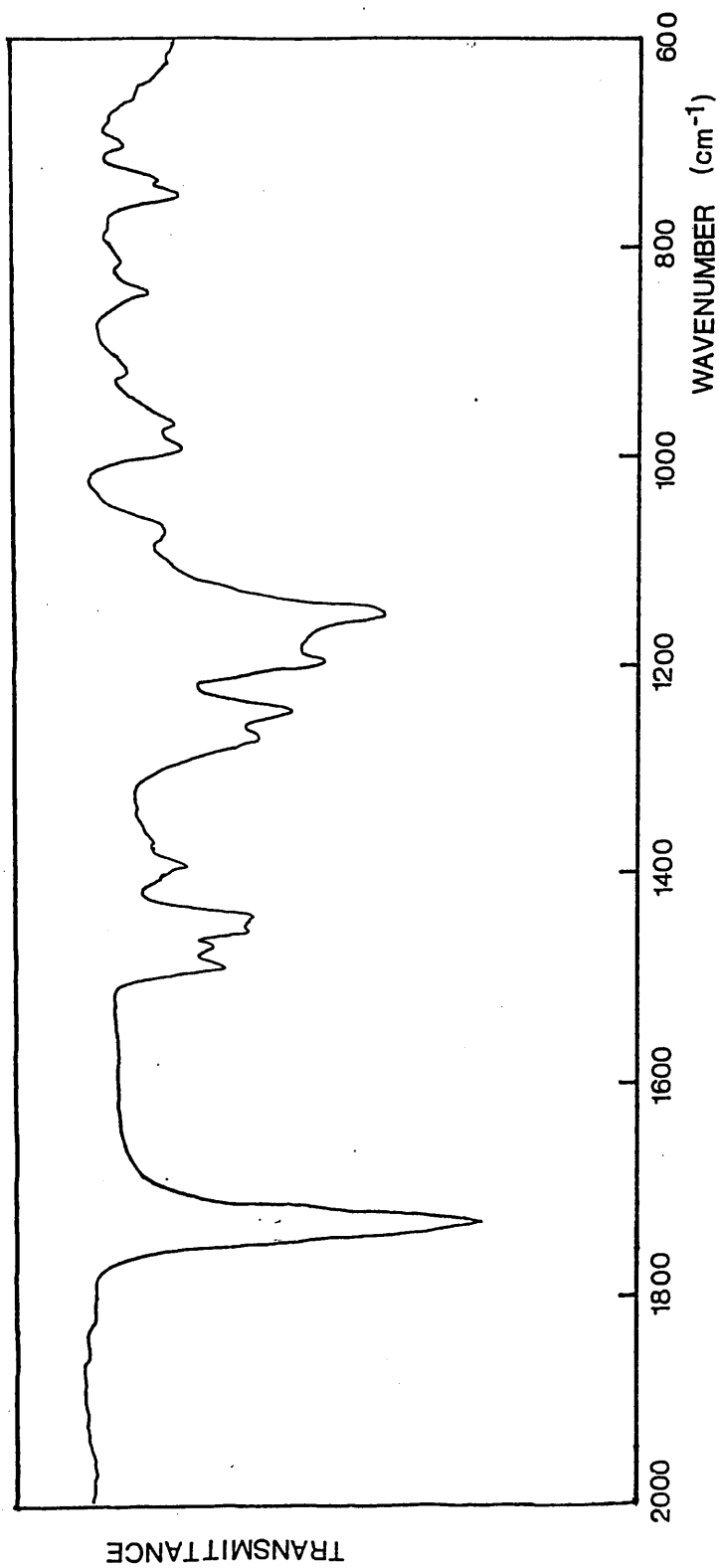


Figure 6.12 IR spectrum of 1:50 Mn(acac)₃ - copolymer blend after precipitation

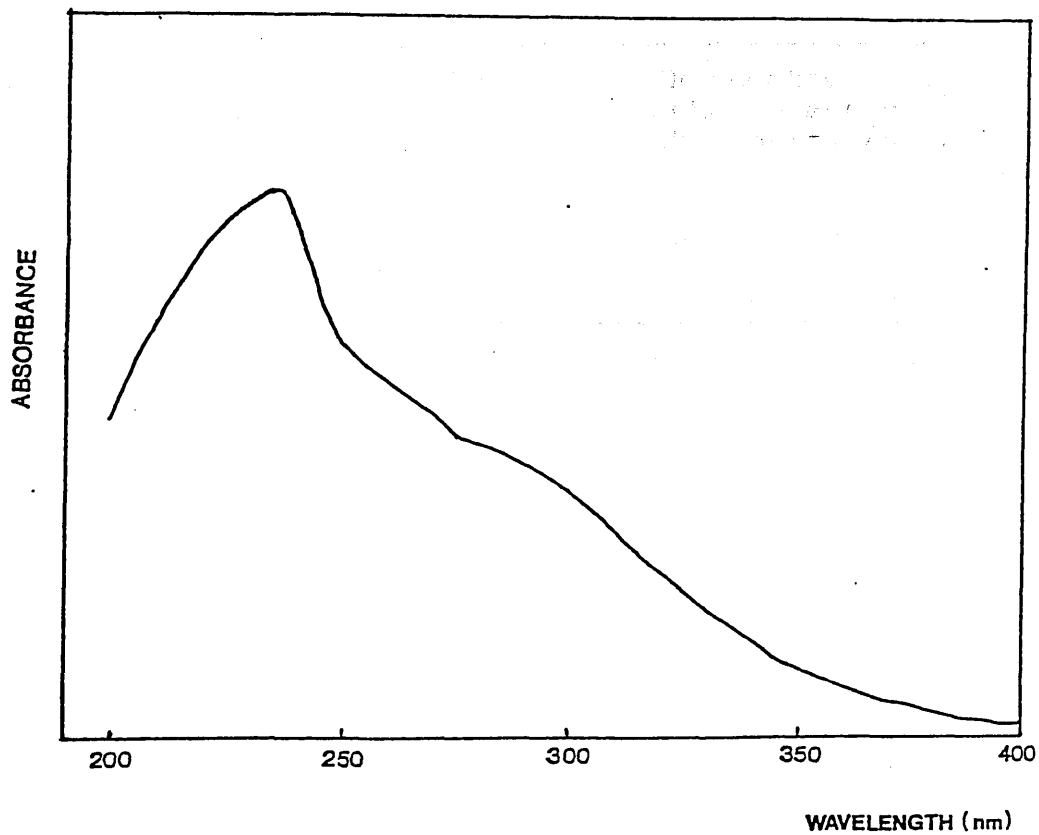
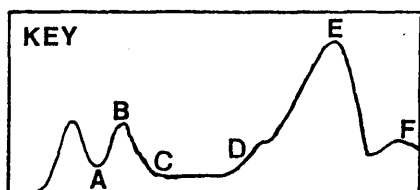


Figure 6.13
UV spectrum of 1:50 Mn(acac)₃ - copolymer blend
after precipitation

Extent Of Degradation	Visual Appearance	CH ₂ Cl ₂ Solubility	Structural Features
None	Transparent with brown colouration, compatible	Yes	No interaction detectable from IR spectrum. UV spectrum shows features very similar to those observed in Mn(acac) ₃ - PMMA blends.
116°C (A)	No change	Yes	No change.
146°C (B)	Film now has yellow cast	Yes	IR spectrum - slight enhancement of 1575 cm ⁻¹ absorption relative to 1515 cm ⁻¹ peak => underlying carboxylate absorption. UV spectrum shows distinct absorbance at 300 nm. Colour => unsaturation.
179°C (C)	As 146°C	Yes	Much reduction in chelate concentration. Enhancement of 1575 cm ⁻¹ absorption pronounced.
290°C (D)	Film now has orange cast	Partly	No chelate absorptions in IR spectrum and peak at 1575 cm ⁻¹ unequivocally attributed to the carboxylate absorption. Small amount anhydride absorption.
397°C (E)	As 290°C	Partly	Film degraded on NaCl disc shows anhydride and acid absorptions. Carboxylate absorption cannot be unambiguously assigned in presence of possible polymer - disc interaction.
485°C (F)	Brown char	No	Film degraded on NaCl disc - only acid and carboxylate absorptions persist.

Table 6.7 Structure of 1:50 Mn(acac)₃-Copolymer Blend at Various Stages of Degradation



that some chelate has become polymer bound, by a reaction between the chelate and acid side groups analogous to that between $\text{Mn}(\text{acac})_3$ and acetic acid. This reaction must occur in the methylene chloride solution from which the blend is cast.

It is possible that the carboxylate acts as a bidentate ligand,³¹ but there is no evidence here to confirm this.

Association with the ester groups will, of course, also occur in competition with the acid group reaction as will formation of the $\text{Mn}(\text{acac})_3$ - unsaturated chain end complex.

CHANGES OF STRUCTURE ON DEGRADATION

The changes of structure recorded spectroscopically parallel those which occur in the PMMA blend. Carboxylate structures are detected by IR spectroscopy at an earlier stage of degradation - some will be those formed by the route outlined above, and others will be produced at higher temperatures by reaction of $\text{Mn}(\text{acac})_2$ with the ester and acid groups. The formation and the decomposition of the π -complex is, as before, not observed spectroscopically. The chain bound manganese(III) carboxylate - acetylacetonate mixed chelate is expected to be unstable, by analogy with the mixed chelates described by Nikolaev et al.³¹⁻³⁴ but its decomposition does not observably affect the UV spectrum due to the continued presence of

the $Mn(acac)_3$ -ester complex absorption. The decomposition does, however, affect the TVA behaviour as discussed later.

The anhydride structures observed in the residue at $290^\circ C$ are formed by the acid-ester cyclisation of the copolymer; the chelate induced cyclisations occurring at higher temperatures.

Overall, the structural changes are very similar to those occurring in the $Mn(acac)_3$ - PMMA blends.

-196°C CONDENSIBLE PRODUCTS FROM 1:50 AND 1:10
Mn(acac)₃ - COPOLYMER BLENDS

Table 6.8 lists the total -196°C condensible products identified at various stages of degradation of the 1:50 Mn(acac)₃ - copolymer blend. Degradations of films of approximately 30mg were performed under standard TVA conditions and all products were identified by gas phase IR spectroscopy.

For the 1:10 blend only the products of complete degradation were analysed. These were found to be the same as those obtained from the corresponding degradation of the 1:50 blend although with greater production of fragmentation products.

COLD RING FRACTION FROM 1:50 AND 1:10 Mn(acac)₃ -
COPOLYMER BLEND

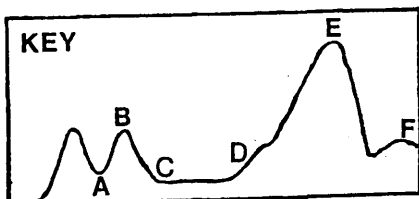
Table 6.9 lists the CRF obtained at various stages of degradation of the 1:50 Mn(acac)₃ - copolymer blend. The CRF was removed by the standard procedure; all identifications were by IR spectroscopy.

Very little CRF was obtained in the early stages and observation of the cold ring during degradation failed to pinpoint its first appearance. However, tests showed there to be no sublimation prior to the onset of degradation. Only the CRF from the complete degradation of the 1:10 blend was analysed, the constituents being the same as those of the CRF from the 1:50 blend at the same stage of degradation.

Extent Of Degradation	Total -196° Condensable Products
116°C (A)	Methyl methacrylate, acetylacetone
146°C (B)	As 116°C
179°C (C)	As 146°C plus trace amounts of methanol and methyl formate
290°C (D)	As 146°C plus methanol trace amount of methyl acetate, acetone
*397°C (E)	As 290°C plus methyl acetate, carbon dioxide, "ketene", isobutene, acetone
*485°C (F)	As 397°C

* Although not collected in a form suitable form for analysis, a prolonged tail fraction can be ascribed to the presence of 5-membered cyclic anhydrides

Table 6.8 -196°C Condensable Products from 1:50 Mn(acac)₃ - Copolymer Blend at Various Stages of Degradation



Extent Of Degradation	Cold Ring Fraction
116°C (A)	None
146°C (B)	Very small quantity of chain fragments evident in IR spectrum
179°C (C)	As 146°C
290°C (D)	IR absorptions due to acac complex, either Mn(acac) ₃ or Mn(acac) ₂
397°C (E)	Considerable brown CRF IR spectrum now indicates in addition to material present at 290°C, chain fragments containing anhydride, acid, some unsaturated structures
485°C (F)	As 397°C (Fig. 6.14)

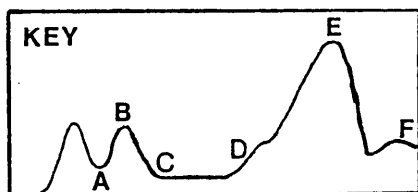
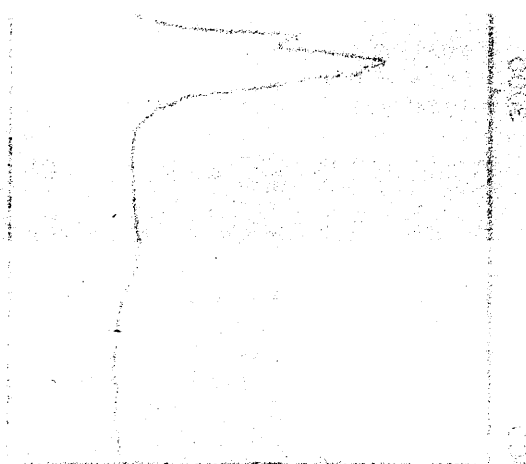


Table 6.9 Cold Ring Fraction from 1:50 Mn(acac)₃ - Copolymer Blend at Various Stages of Degradation



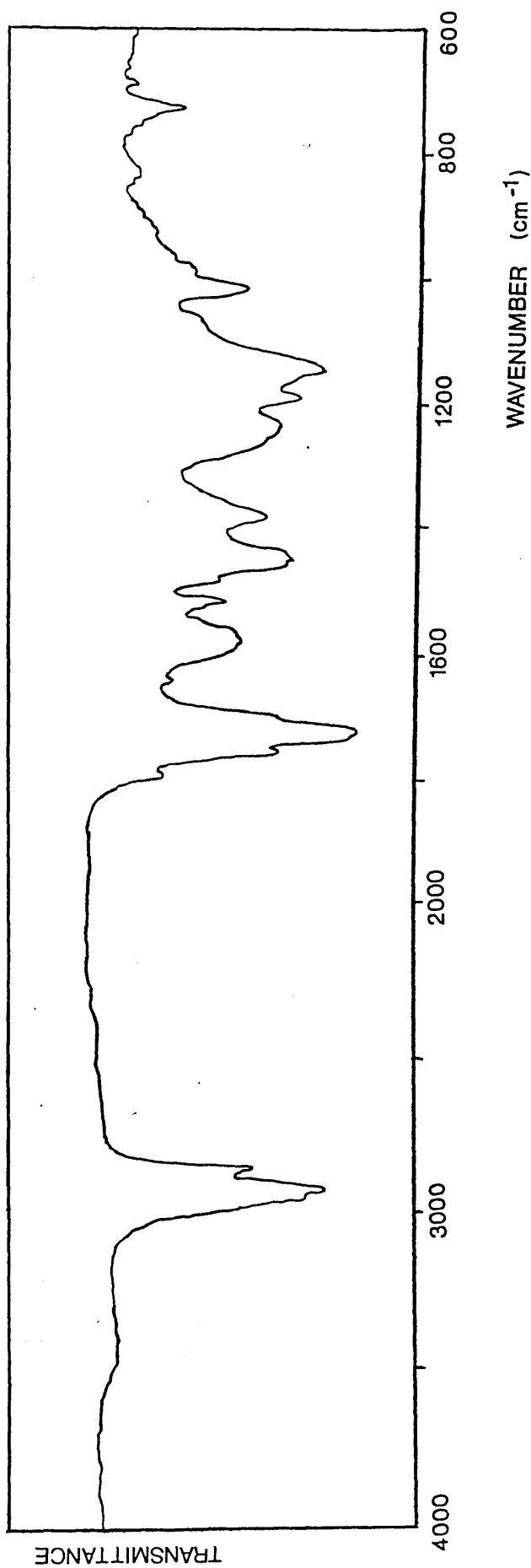


Figure 6.14 IR spectrum of CRF from 1:50 Mn(acac)₃ - copolymer blend on degradation to 485°C

CONCLUSIONS ON THE NATURE OF THE DEGRADATION OF
Co(acac)₃ AND Mn(acac)₃ - COPOLYMER BLENDS

The behaviour of the copolymer blends is broadly similar to that of the PMMA blends, as expected for a copolymer with a composition so similar to that of PMMA. However, the presence of methacrylic acid units in the chain does have important consequences. For steric reasons, the interaction with the methacrylic acid units is stronger than that with the ester groups and accordingly the ligand scission reactions occur at lower temperature in the copolymer blends than in those with PMMA. For instance, T(max) of the unzipping initiated by the decomposition step



drops from 190°C in the PMMA blend to 159°C in the copolymer blend. In the Mn(acac)₃ blend, the interaction with the acid groups is strong enough to lead to ligand substitution at room temperature. Consequently there is in the Mn(acac)₃ - copolymer blend a degradation reaction around 90°C due to the decomposition of the Mn(III) mixed ligand chelate.

The stronger interaction of the bis chelates with the acid structures inhibits sublimation and encourages further formation of depolymerisation blocking structures, thus enhancing the effect of the chelates on the later stages of degradation which are otherwise much the same as those of the PMMA blends.

The methyl formate produced at high temperatures

results from a minor fragmentation reaction of the polymer - the scission of an ester side chain followed by H-abstraction. The formation of methyl formate at temperatures as low as 150°C presumably stems from the decomposition of the $\text{CH}_3\text{OC}^{\cdot}\text{H}$ radicals produced by side-chain scission although there is no non-condensable (carbon monoxide) production detected at this point.

... are described in this chapter. This work was done, in part, in association with A. Hartzell on a 4th year thesis project.⁵⁷

EXPERIMENTAL

TGA curves and data on the nature of product structural changes were obtained by the standard method in earlier chapters, with the exception due to the hygroscopic nature of $\text{Co}(\text{acac})_3$, film was under a flow of nitrogen and handling elsewhere kept to a minimum. The degradation behavior of the unlabeled EMA and copolymer and of $\text{Co}(\text{acac})_3$ are described in earlier chapters.

CHAPTER 7BLENDS OF Co(acac)₂ WITH PMMA AND THE MAA-MMA COPOLYMERINTRODUCTION

The studies of the Co(acac)₃ blends with both PMMA and 1:59 MAA-MMA copolymer demonstrate the important part that Co(acac)₂ plays in the degradation process. It is of interest therefore to investigate the behaviour of Co(acac)₂ blends. The results of a brief study of blends of Co(acac)₂ with PMMA and the copolymer are described in this chapter. This work was undertaken, in part, in association with A. Hazzard as part of a 4th year thesis project.⁸⁷

EXPERIMENTAL

TVA curves and data on the nature of products and structural changes were obtained by the standard methods outlined in earlier chapters, with the exception that, due to the hygroscopic nature of Co(acac)₂, films were cast under a flow of nitrogen and handling in the atmosphere kept to a minimum. The degradation behaviour of the unblended PMMA and copolymer and of Co(acac)₂ has been described in earlier chapters.

Co(acac)₂ - PMMA 1 BLENDTVA BEHAVIOUR

The TVA curve for a 30mg sample of the 1:50 Co(acac)₂ - PMMA 1 blend is shown in Fig 7.1. Unfortunately, the evolution of a large quantity of trapped solvent masks the earlier peaks. However, the TVA curve for another sample with less trapped solvent is shown in Fig 7.2 - this records only the total evolved products. Table 7.1 summarises the features of the TVA curves.

FEATURE	TEMPERATURE (°C)
Compatibility	Yes
T(sublimation)	113
Plateau	156-214 (onset 122)
Main Peak	
Shoulder	246-295
T(max)	
Condensibles	365
Non-condensibles	398

Table 7.1 Summary of TVA Curve of 1:50 Co(acac)₂ - PMMA 1 Blend

The Co(acac)₂ has little effect on the TVA behaviour of the PMMA. There is a slight increase in the production of -196°C non-condensibile material and an associated slight increase in T(max) of the main peak which indicate a small amount of blockage of the

unzipping process. This and the nature of the process causing volatilization at low temperatures are discussed subsequently.

STRUCTURE OF THE UNDEGRADED BLEND

Figs 7.3 and 7.4 reproduce the IR and UV spectra of the undegraded 1:50 $\text{Co}(\text{acac})_2$ - PMMA 1 blend. This blend was compatible, the film a transparent pink. The IR spectrum is simply a superposition of the $\text{Co}(\text{acac})_2$ and PMMA absorptions. However the UV spectrum shows the $\text{Co}(\text{acac})_2$ absorption to be shifted from its position in methylene chloride solution ($\lambda(\text{max})$ 291nm) to $\lambda(\text{max})$ 288nm). Such a shift is observed in methyl acetate solution and also for the $\text{Co}(\text{acac})_2$ formed in the decomposition of the $\text{Co}(\text{acac})_3$ - PMMA blends and indicates the association of chelate and ester groups.

Like $\text{Co}(\text{acac})_3$, $\text{Co}(\text{acac})_2$ forms π -complexes with unsaturated linkages and is expected to form such complexes with the unsaturated chain ends of the polymers. Unlike $\text{Co}(\text{acac})_3$, however, the interaction does not significantly promote decomposition of $\text{Co}(\text{acac})_2$,²⁶ and thus the chain end interaction does not influence the degradation of the blend.

STRUCTURE OF THE BLEND AT 215°C

On heating to 215°C, the residual film shows only the absorption bands expected for PMMA (Fig 7.3).

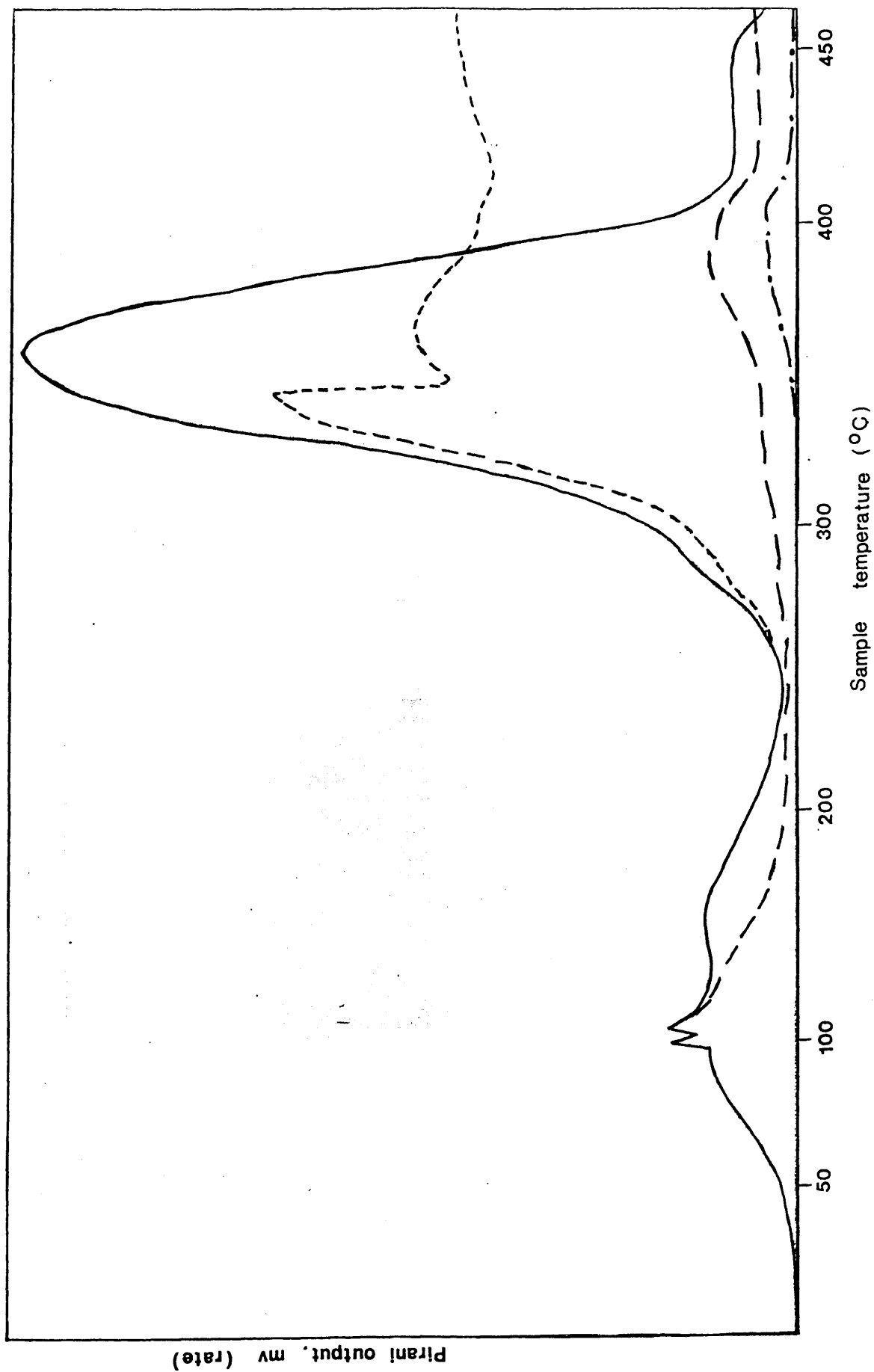


Figure 7.1 TVA curve for 1:50 Co(acac)₂ - PMMA 1 blend

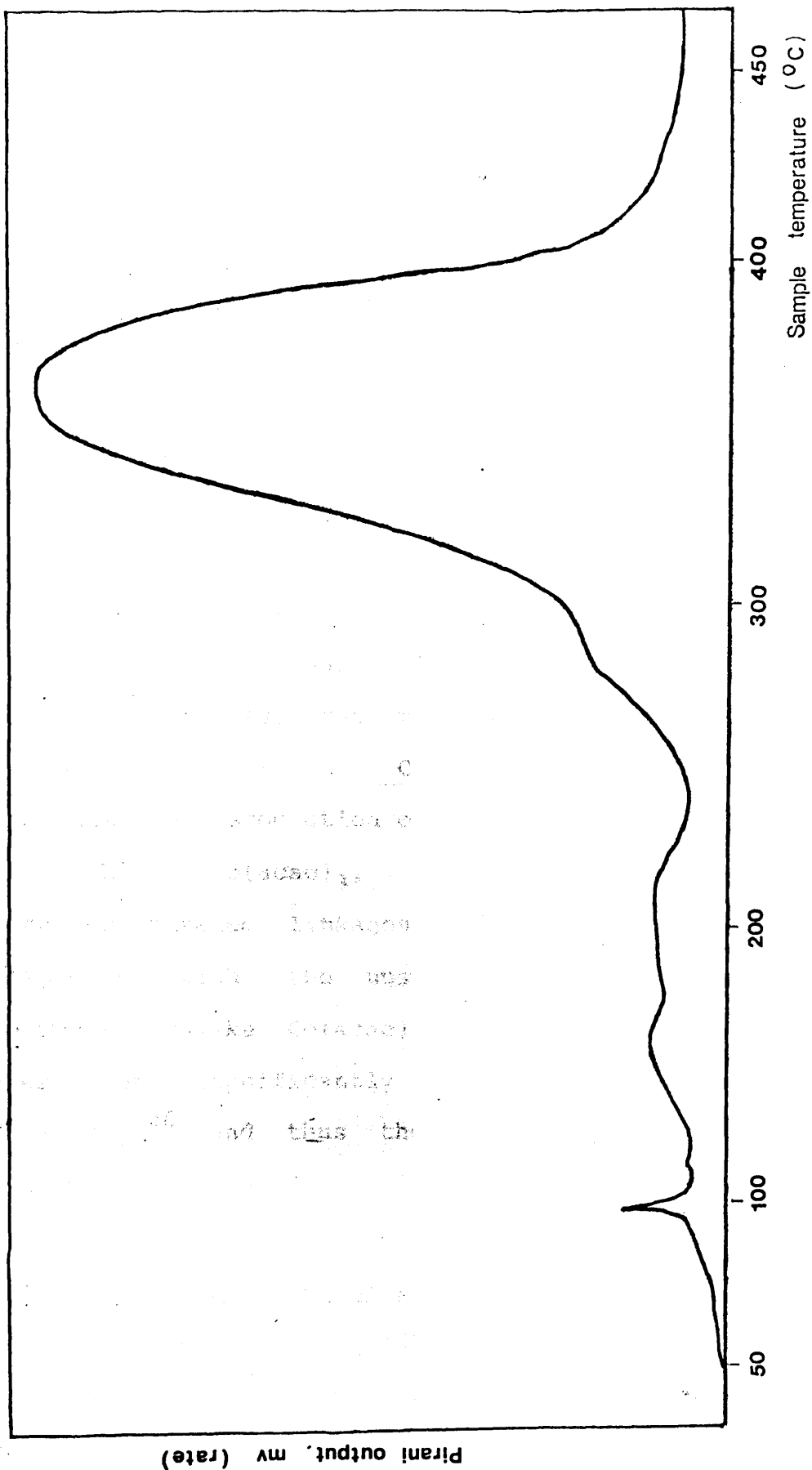


Figure 7.2 Total products TVA curve for 1:50 Co(acac)₂ - PMMA 1 blend

unzipping process. This and the nature of the process causing volatilization at low temperatures are discussed subsequently.

STRUCTURE OF THE UNDEGRADED BLEND

Figs 7.3 and 7.4 reproduce the IR and UV spectra of the undegraded 1:50 $\text{Co}(\text{acac})_2$ - PMMA 1 blend. This blend was compatible, the film a transparent pink. The IR spectrum is simply a superposition of the $\text{Co}(\text{acac})_2$ and PMMA absorptions. However the UV spectrum shows the $\text{Co}(\text{acac})_2$ absorption to be shifted from its position in methylene chloride solution ($\lambda(\text{max})$ 291nm) to $\lambda(\text{max})$ 288nm). Such a shift is observed in methyl acetate solution and also for the $\text{Co}(\text{acac})_2$ formed in the decomposition of the $\text{Co}(\text{acac})_3$ - PMMA blends and indicates the association of chelate and ester groups.

Like $\text{Co}(\text{acac})_3$, $\text{Co}(\text{acac})_2$ forms π -complexes with unsaturated linkages and is expected to form such complexes with the unsaturated chain ends of the polymers. Unlike $\text{Co}(\text{acac})_3$, however, the interaction does not significantly promote decomposition of $\text{Co}(\text{acac})_2$,²⁶ and thus the chain end interaction does not influence the degradation of the blend.

STRUCTURE OF THE BLEND AT 215°C

On heating to 215°C, the residual film shows only the absorption bands expected for PMMA (Fig 7.3).

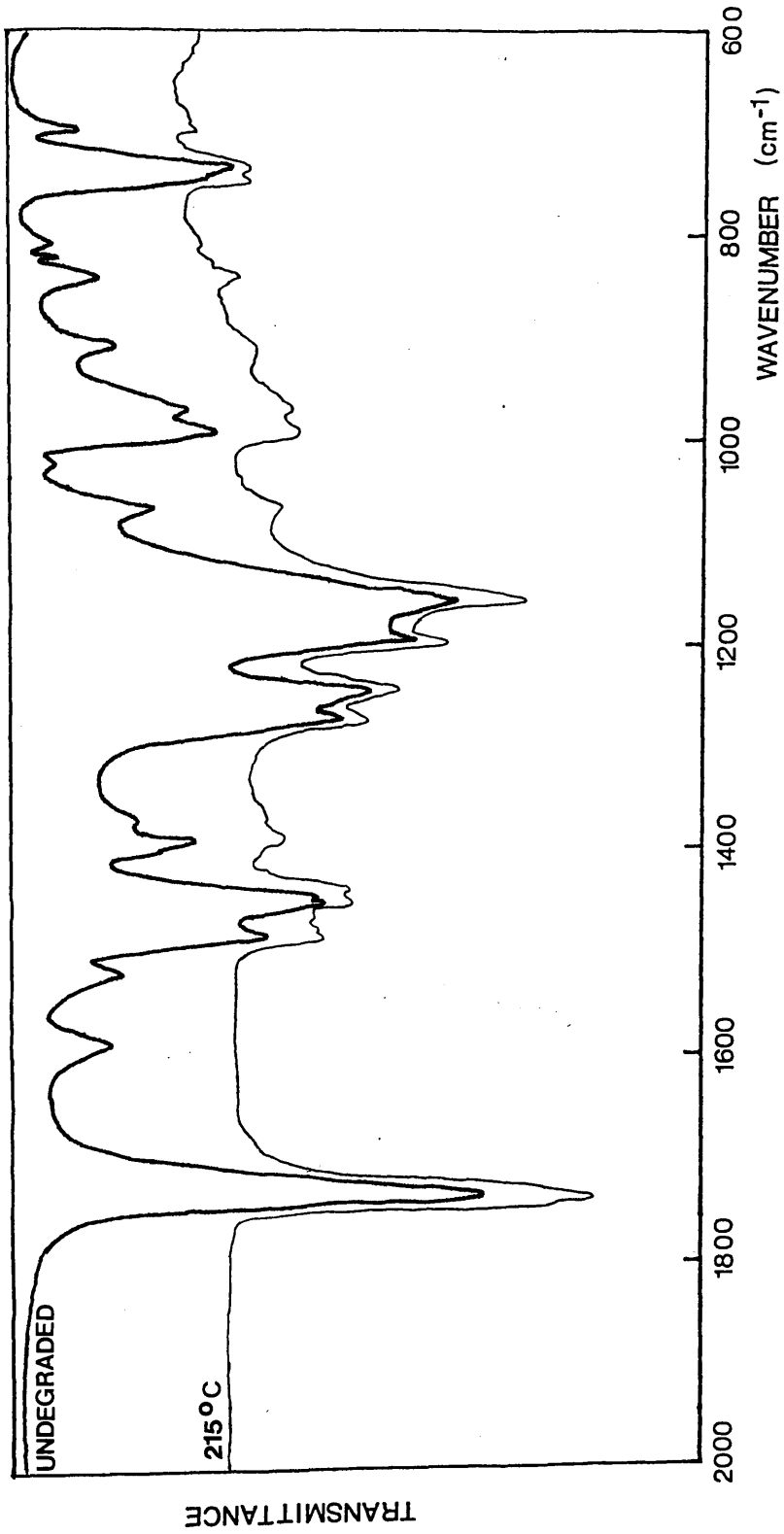


Figure 7.3 IR spectrum of 1:50 Co(acac)₂ - PMMA 1 blend before and after degradation to 2150°C.

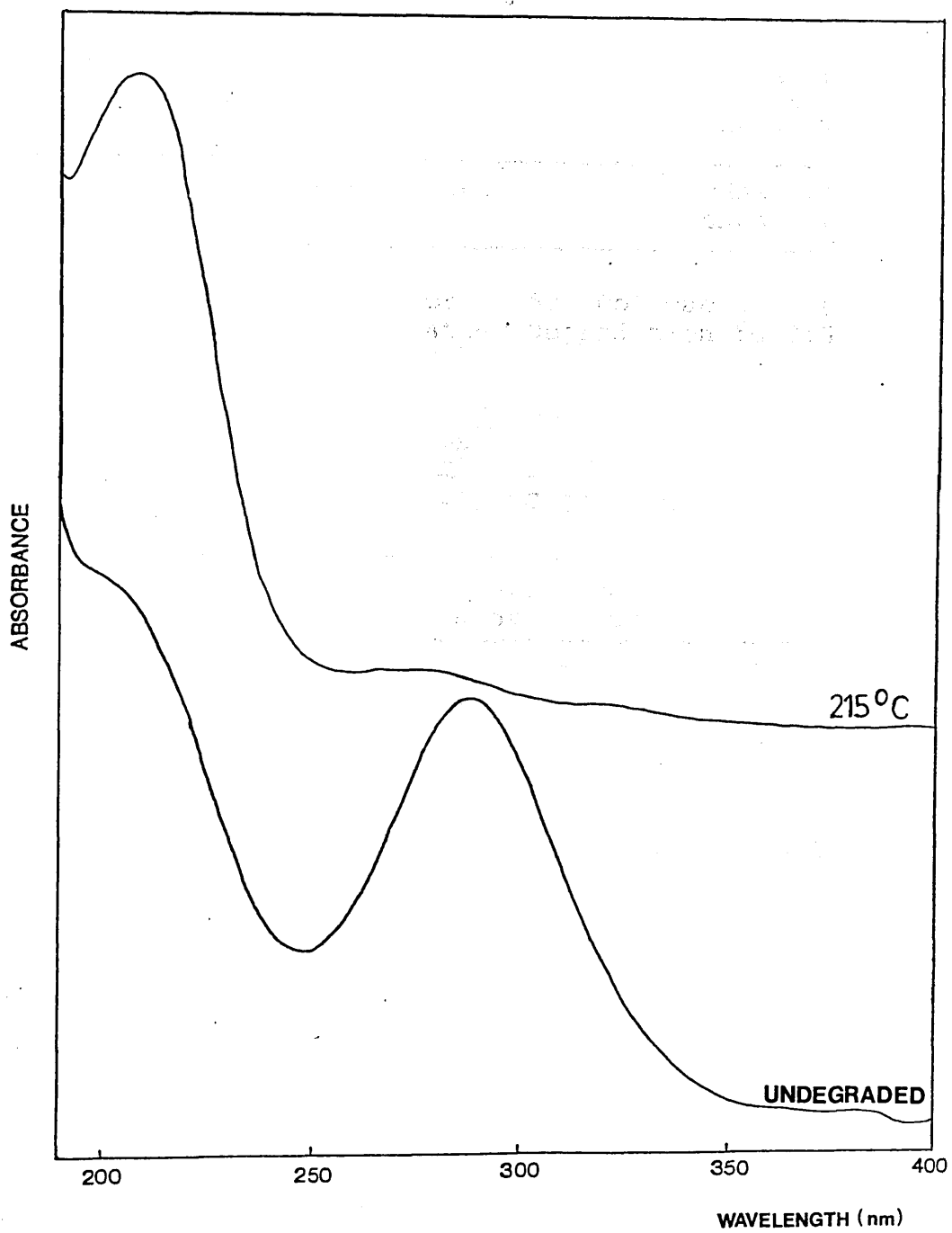


Figure 7.4
UV spectrum of 1:50 $\text{Co}(\text{acac})_2$ - PMMA 1 blend before and after degradation to 215°C

EXTENT OF DEGRADATION	VISUAL APPEARANCE	SOLUBILITY IN CH ₂ Cl ₂	SPECTROSCOPIC FEATURES
None	Pink, compatible	Yes	IR spectrum - superposition of Co(acac) ₂ + PMMA bands. UV spectrum λ(max) 288nm => interaction.
215°C	Colourless	Yes	PMMA absorption bands only.

Table 7.2 Structure of 1:50 Co(acac)₂ - PMMA 1 Blend Before and After Degradation to 215°C.

EXTENT OF DEGRADATION	-196°C CONDENSIBLE PRODUCTS
215°C	Methyl methacrylate, methylene chloride (solvent).
485°C	As 215°C plus carbon dioxide, methanol, a ketene.
	COLD RING FRACTION
485°C	Co(acac) ₂ , some chain fragments.

Table 7.3 -196°C Condensable Products and Cold Ring Fraction from the 1:50 Co(acac)₂ - PMMA 1 Blend

The curve for the 1:50 blend shows the
 amount of total gaseous products and
 condensable material. There is some doubt

-196°C CONDENSIBLE PRODUCTS AND COLD RING FRACTION
FROM THE 1:50 Co(acac)₂ - PMMA 1 BLEND

The identity of the products of degradation to 215°C and 485°C are listed in Table 7.3.

No acetylacetone is detected by 215°C and this implies that if the depolymerisation step below this temperature is initiated by acac· radicals, only a very small number of such radicals can be involved.

No acetylacetone is detected, either, on degradation to 485°C but at this extent of the degradation the large quantities of methyl methacrylate produced could easily mask, both in the SAD separation and IR spectrum, any acetylacetone present, as also occurred with the Co(acac)₃ and Mn(acac)₃ blends.

Overall, the -196°C condensible products and CRF including the small quantities of fragmentation products (carbon dioxide, methanol, a ketene and the short chain fragments in the CRF) are similar to those identified from the Co(acac)₃ - PMMA blends in which only a small amount of chain blockage was present.

Co(acac)₂ - COPOLYMER BLENDS

TVA BEHAVIOUR

TVA curves for both the 1:50 and 1:10 blends are illustrated in Figs 7.5 and 7.6 and summarised in Table 7.4. The curve for the 1:10 blend shows only the evolution of total gaseous products and -196°C non-condensable material and there is some doubt about

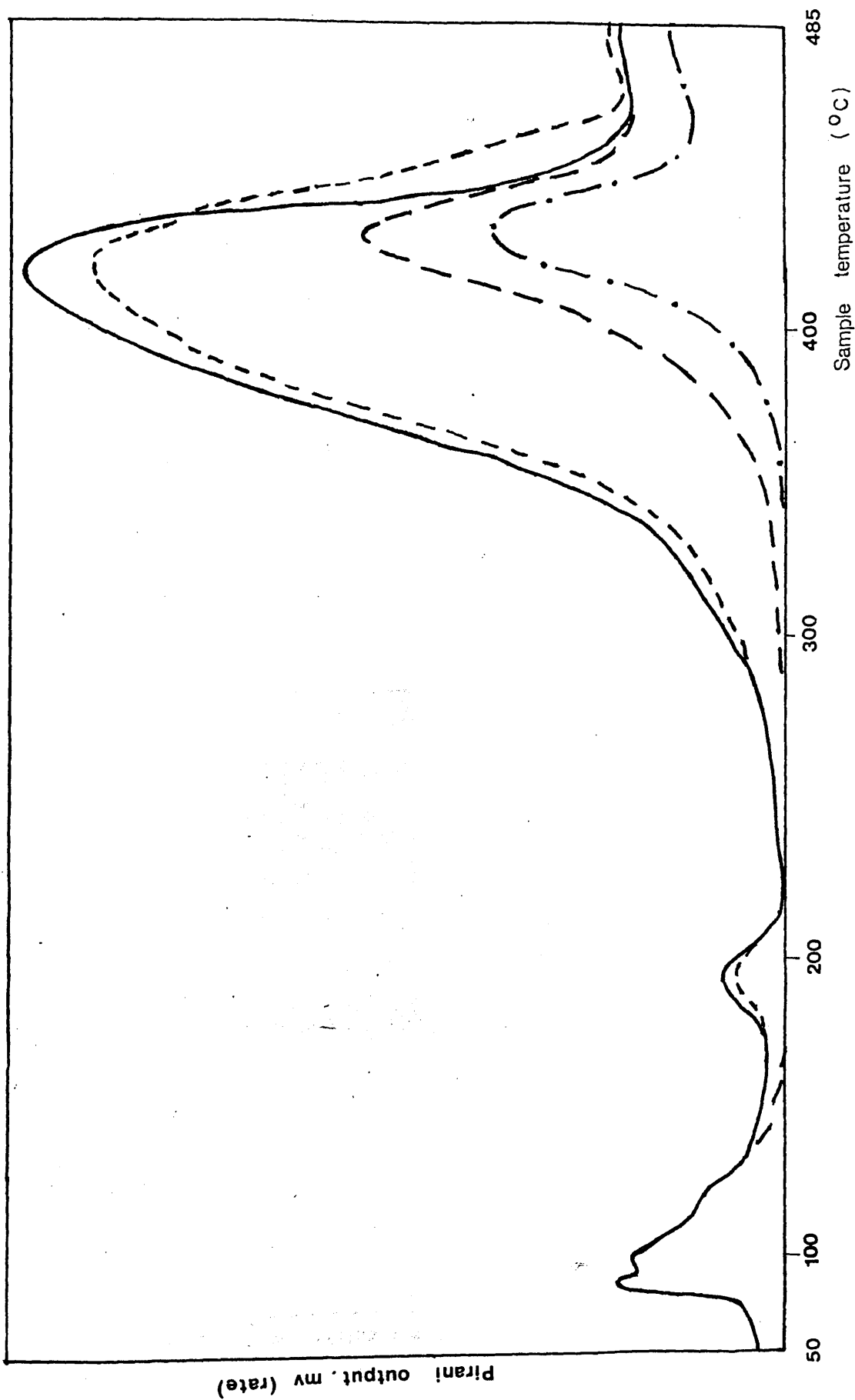


Figure 7.5 TVA curve for 1:50 Co(acac)₂ - copolymer blend

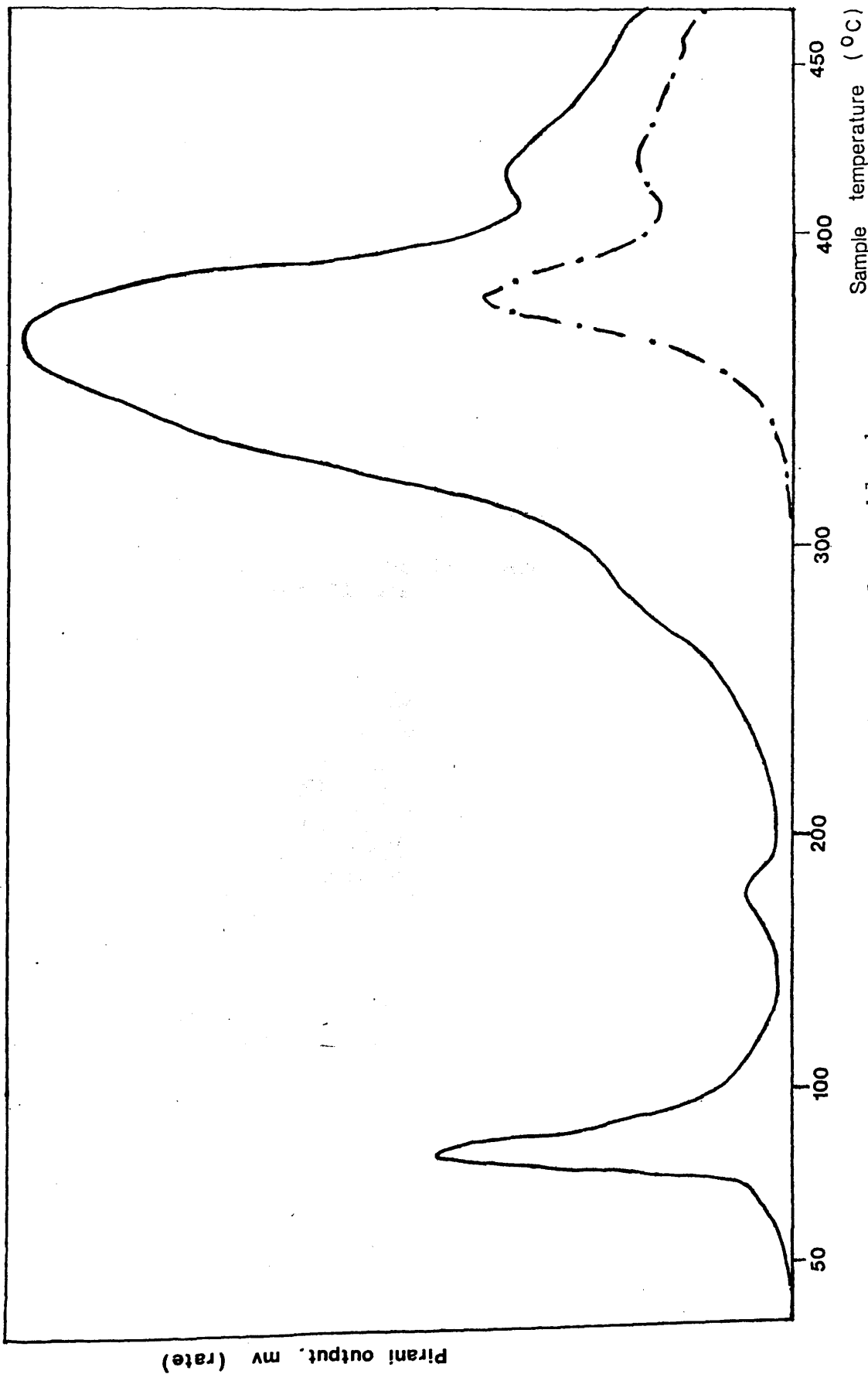


Figure 7.6 TVA curve for 1:10 Co(acac)₂ - copolymer blend

FEATURE	BLEND	
	1:10	1:50
Compatibility	No	Yes
T(sublimination)	Not recorded	125°C
1st Peak		
T(onset)	145°C	ca. 166°C
T(max)	178°C	197°C
Main Peak		
Shoulder	197-289°C	215-242°C
T(max)		
Condensibles	373°C	378°C
Non-condensibles	382°C	385°C
Final Peak		
T(max)	420°C	486°C

Table 7.4 TVA Data for the 1:10 and 1:50 Co(acac)₂ - Copolymer Blends

STRUCTURE OF THE COPOLYMER BLENDS

The structure of the blends of Co(acac)₂ and copolymer is similar to that of the PMMA blend which is influenced by the presence of the methacryli component. The IR spectra of the 1:10 and 1:50 are simple superpositions of the spectra of the components, but the UV spectra show the shift in the Co(acac)₂ absorption typical of the copolymer.

the temperature calibration associated with the curve for the 1:50 blend, but the overall shape of the curves is the critical factor in their analysis.

Both blends have a degradation process occurring below 200°C ($T(\text{max})$ 178°C for the 1:10 blend), rather more sharply defined than in the PMMA blend. At both concentrations of chelate, the chain-end initiated depolymerisation occurring with $T(\text{max})$ 287°C in the unblended copolymer is quenched almost completely as happens also in the $\text{Co}(\text{acac})_3$ - copolymer blends. Likewise the increased production of -196°C non-condensable material in association with the main degradation peak and the presence of a peak at higher temperature mirror the behaviour of the $\text{Co}(\text{acac})_3$ - copolymer blend and reflects the presence of the methacrylic acid units in the copolymer.

STRUCTURE OF THE 1:10 AND 1:50 $\text{Co}(\text{acac})_2$ - COPOLYMER BLENDS AND CHANGES ON DEGRADATION

STRUCTURE OF THE UNDEGRADED BLENDS

The structure of the blends of $\text{Co}(\text{acac})_2$ with the copolymer is similar to that of the PMMA blends, but it is influenced by the presence of the methacrylic acid component. The IR spectra of the 1:10 and 1:50 blends are simple superpositions of the spectra of the components, but the UV spectra show the shift in $\lambda(\text{max})$ of the $\text{Co}(\text{acac})_2$ absorption typical of the coordinated

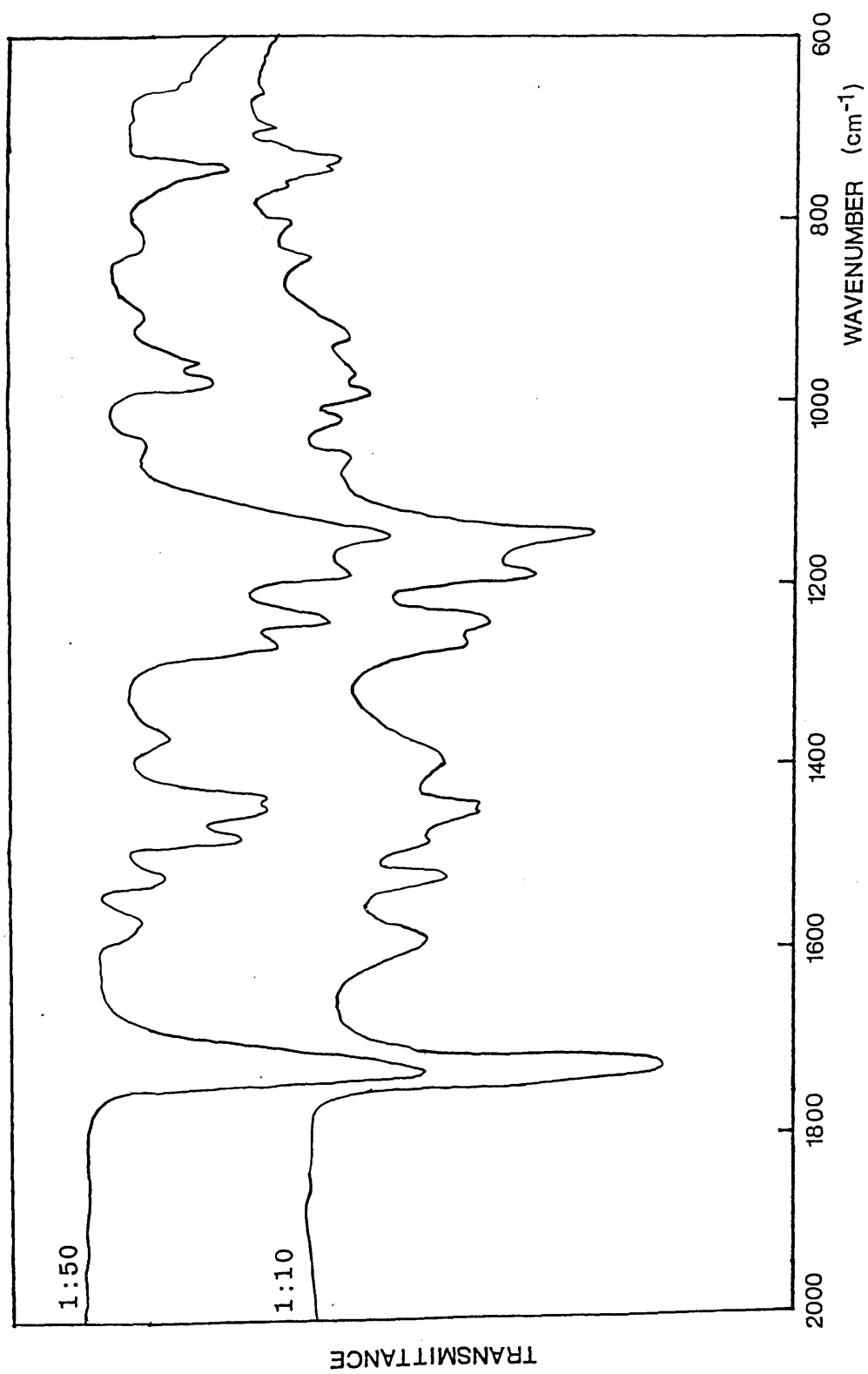


Figure 7.7 IR spectra of 1:50 and 1:10 $\text{Co}(\text{acac})_2$ - copolymer blends

chelate. The shift from 291nm in methylene chloride solution to 283nm in the copolymer blend is greater than the shift for the PMMA blend and is a consequence of the stronger interaction of the chelate with the methacrylic acid units. The UV spectrum of the 1:50 blend is reproduced in Fig 7.8 (the spectrum of the 1:10 blend is identical).

CHANGES OF STRUCTURE ON DEGRADATION

On degradation to 220°C, the concentration of $\text{Co}(\text{acac})_2$ is reduced, due both to sublimation and decomposition, and carboxylate structures are formed (see Fig 7.9, 7.10). The production of these is expected to be by the ligand displacement reactions described on pages 253 and 329 although acetylacetone is not observed as a volatile product (see below).

Figure 7.8

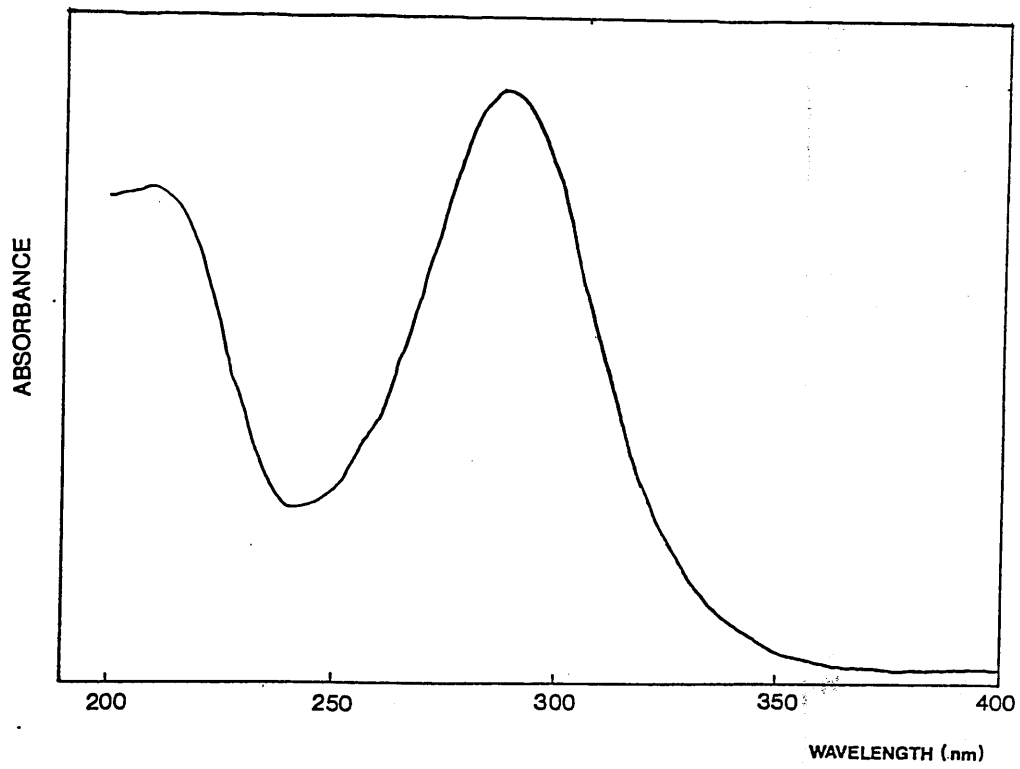


Figure 7.8
UV spectrum of 1:50 Co(acac)₂ - copolymer blend

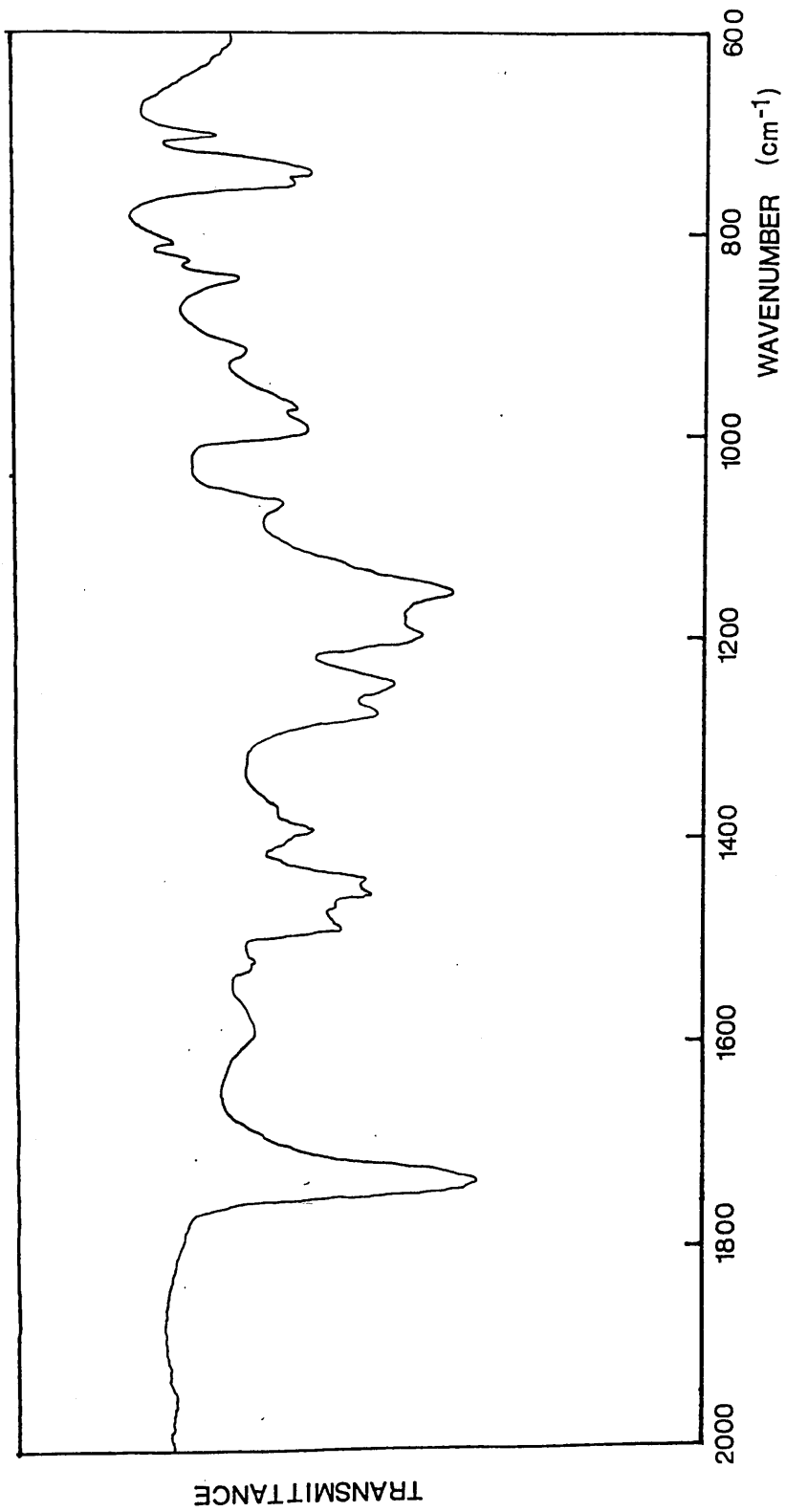


Figure 7.9 IR spectrum of 1:50 Co(acac)₂ - copolymer blend after degradation to 220°C

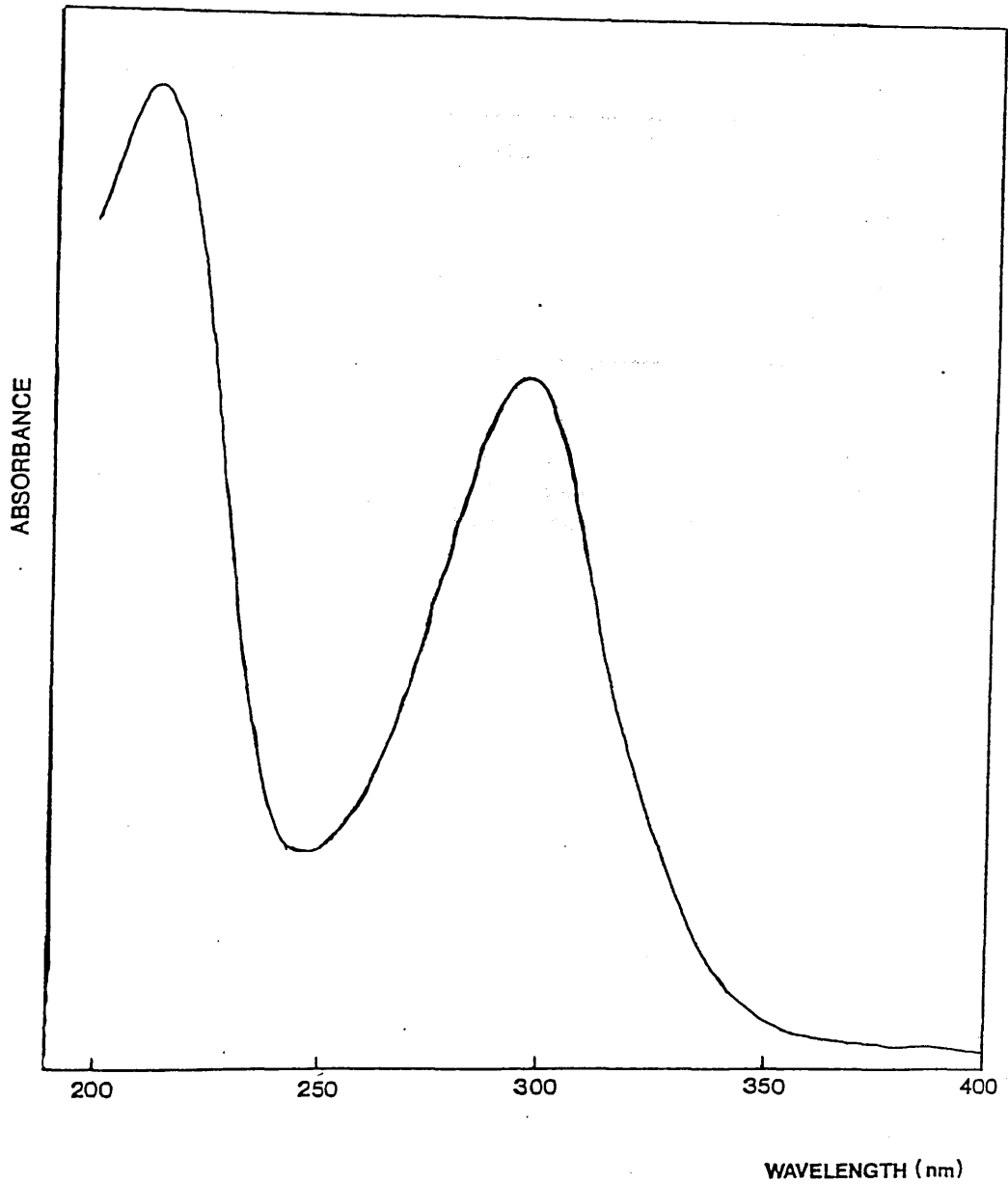


Figure 7.10
UV spectrum of 1:10 Co(acac)₂ - copolymer blend
after degradation to 220°C

EXTENT OF DEGRADATION	VISUAL APPEARANCE	SOLUBILITY IN CH ₂ Cl ₂	SPECTROSCOPIC FEATURES
None	Pink compatible (1:50 blend)	Yes	IR spectrum superposition of Co(acac) ₂ + PMMA absorptions. UV- (max) 283nm => interaction
200°C		No	Chelate concentration much decreased. IR band at 1580 cm ⁻¹ => carboxylate formation (1:10 blend)

Table 7.5 Structure of Co(acac)₂ - Copolymer Blend Before and after Degradation to 220°C

DEPENDENCE ON THE NATURE OF THE THERMAL DEGRADATION

OF PMMA AND Co(acac)₂ - COPOLYMER BLENDS

The degradation behaviour of Co(acac)₂ blends is very similar to that of PMMA blends.

-196°C CONDENSIBLE PRODUCTS AND COLD RING FRACTION
FROM 1:50 AND 1:10 Co(acac)₂ - COPOLYMER BLENDS

Table 7.6 lists the -196°C condensible products and CRF from 30mg samples of the 1:50 Co(acac)₂ - copolymer blend at various stages of degradation. With the exception of the absence of methyl acetate and acetylacetone which may have been missed here through inefficient SAD separation, the products are the same as those identified on degradation of the 1:50 Co(acac)₃ - copolymer blend. Similarly, the CRF contains the same types of polymer fragments or that from the Co(acac)₃ blend. The chelate sublimate is in this case, of course, Co(acac)₂.

The products from the 1:10 blend on degradation to 485°C are listed in Table 7.7. Although methyl formate was not identified as a product from the Co(acac)₃ blend, it was identified as a product from the Mn(acac)₃ - copolymer blend in which it was formed by a side chain scission mechanism and will have a similar origin here.

CONCLUSIONS ON THE NATURE OF THE DEGRADATION OF THE
Co(acac)₂ - PMMA AND Co(acac)₂ - COPOLYMER BLENDS

Overall the degradation behaviour of the Co(acac)₂ blends is very similar to that of the corresponding Co(acac)₃ blends.

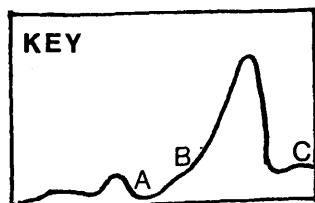
The Co(acac)₂ associates with the ester and acid groups of the polymers at room temperature as

EXTENT OF DEGRADATION	-196°C CONDENSIBLE PRODUCTS
220°C (A)	Methyl methacrylate, methylene chloride
320°C (B)	As A + some methanol
485°C (C)	As B + carbon dioxide, "ketene", dimethyl ether, butene, isobutene, liquid anhydrides
485°C (C)	COLD RING FRACTION Co(acac) ₂ , chain fragments containing anhydride and acid structures

Table 7.6 -196°C Condensible Products and Cold Ring Fraction from 1:50 Co(acac)₂ - Copolymer Blend

EXTENT OF DEGRADATION	TOTAL -196°C CONDENSIBLES
485°C (c)	Methyl methacrylate, methanol, carbon dioxide, "ketene", dimethyl ether, methyl acetate, butene, isobutene, liquid anhydrides.
485°C (c)	COLD RING FRACTION Co(acac) ₂ , chain fragments including anhydride and acid structures.

Table 7.7 -196°C Condensible Products and Cold Ring Fraction from 1:10 Co(acac)₂ - Copolymer Blend



predicted by the behaviour of $\text{Co}(\text{acac})_2$ with methyl acetate and acetic acid (Chapter 3). The $\text{Co}(\text{acac})_2$ interacts more strongly with the acid groups of the copolymer for steric reasons and this produces a disparity between the effects of $\text{Co}(\text{acac})_2$ on PMMA and the copolymer similar to that observed for the $\text{Co}(\text{acac})_3$ blends. The similarity between degradation behaviour of the $\text{Co}(\text{acac})_3$ and $\text{Co}(\text{acac})_2$ systems shows that the influence of $\text{Co}(\text{acac})_2$ on the degradation process is the same whether it is introduced before degradation or produced in situ from $\text{Co}(\text{acac})_3$.

Below 200°C , the degradation of the $\text{Co}(\text{acac})_2$ blends differ from those of $\text{Co}(\text{acac})_3$ due to the different decomposition behaviour of the two complexes. The decomposition of $\text{Co}(\text{acac})_2$ is not so readily promoted by electron donors (i.e. the unsaturated units and ester and acid groups) as that of $\text{Co}(\text{acac})_3$,²⁶ and there is thus not the sharp distinction in the temperatures of the promoted and the purely thermal decomposition of $\text{Co}(\text{acac})_2$ that there is for $\text{Co}(\text{acac})_3$. Consequently the depolymerisation initiated by the acac. radicals produced in the decomposition of the chelate occurs over a greater temperature range and hence there is a plateau on the TVA curve of the $\text{Co}(\text{acac})_2$ - PMMA blend between $156\text{-}214^\circ\text{C}$ rather than a sharp peak. The acid groups of the copolymer are rather more effective in promoting ligand scission and the copolymer blends show a more

sharply defined peak.

The other difference is the identification of methyl formate. Although not detected from the $\text{Co}(\text{acac})_3$ blends its identification here, as in the $\text{Mn}(\text{acac})_3$ - copolymer blends, merely reflects the occurrence of an amount of side chain scission. Here, it is simply a concentration effect; the interaction of $\text{Co}(\text{acac})_2$ with the polymer substituents inhibits sublimation of the chelate. There is thus a higher concentration of $\text{Co}(\text{acac})_2$ in the blend at elevated temperatures than in the $\text{Co}(\text{acac})_3$ blend of identical initial chelate concentration in which sublimation of $\text{Co}(\text{acac})_3$ is not inhibited. The mechanism of the methyl formate formation is analogous to that on page 352.

This has been discussed in Chapter 2.

PMMA BLENDS

The TGA curves obtained for blends of Co
and different chelate concentration

CHAPTER EIGHTBLENDS OF $\text{Cu}(\text{acac})_2$ WITH PMMA AND 1:59 MAA-MMA
COPOLYMERINTRODUCTION

In this chapter the effect of $\text{Cu}(\text{acac})_2$ on the thermal degradation of PMMA and the 1:59 MAA-MMA copolymer is investigated. It is found that although the $\text{Cu}(\text{acac})_2$ - PMMA blends behave similarly to the chelate - PMMA blends already considered, there are major changes in the degradation of the $\text{Cu}(\text{acac})_2$ - copolymer blend.

DEGRADATION OF THE UNBLENDED POLYMERS

The degradation behaviour of the polymers employed (PMMA 1, PMMA 2, PMMA 3 and the 1:59 MAA-MMA copolymer) has been discussed in Chapter 4.

DEGRADATION BEHAVIOUR OF $\text{Cu}(\text{acac})_2$

This has been discussed in Chapter 3.

 $\text{Cu}(\text{acac})_2$ - PMMA BLENDSTVA BEHAVIOUR

The TVA curves obtained for blends of $\text{Cu}(\text{acac})_2$ with PMMA at different $\text{Cu}(\text{acac})_2$ concentrations and for various polymer molecular weights are reproduced in Figs. 8.1 - 8.4. Table 8.1 summarises the details of

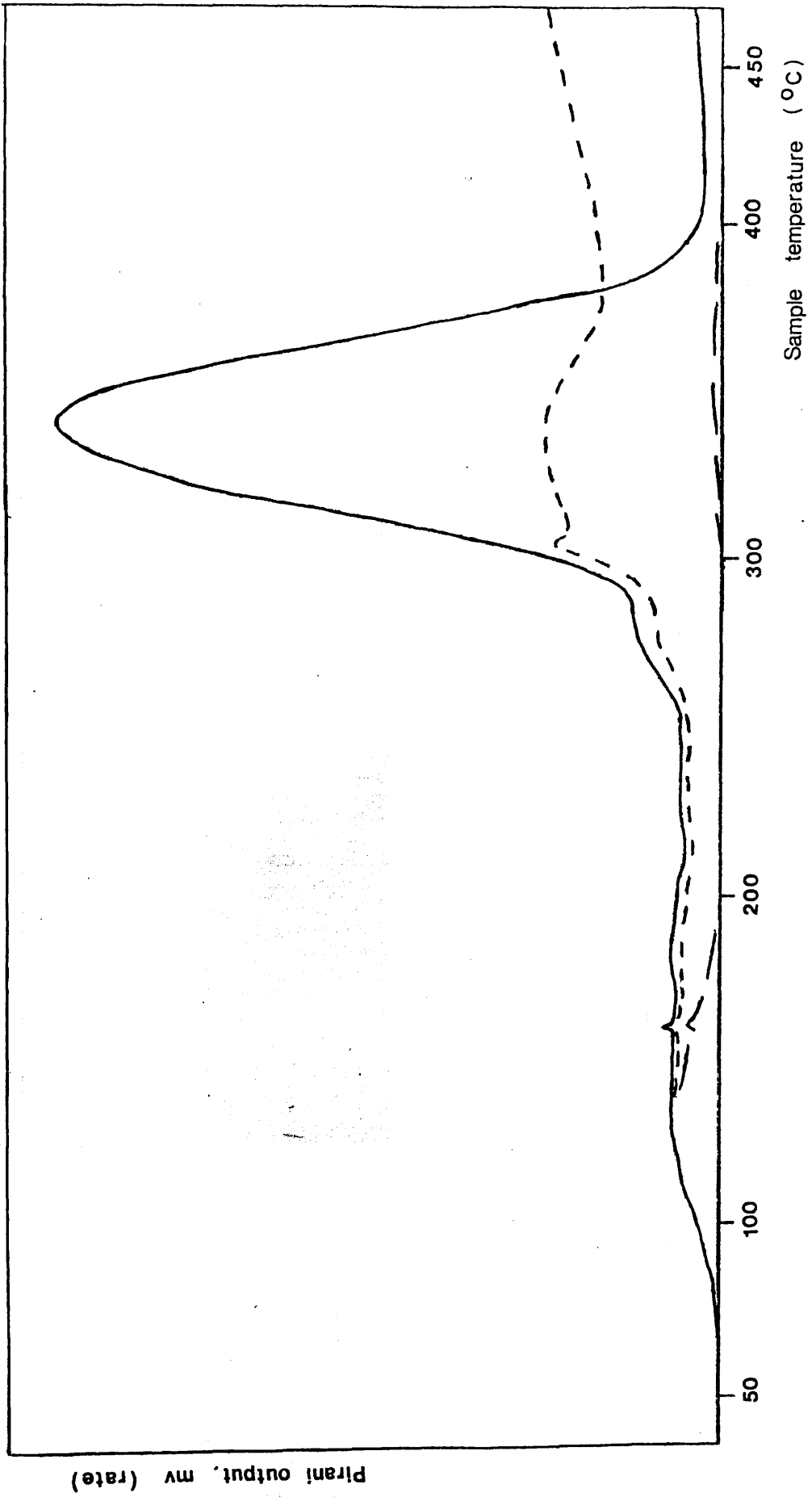


Figure 8.1 TVA curve for 1:100 $\text{Cu}(\text{acac})_2$ - PMMA 1 blend

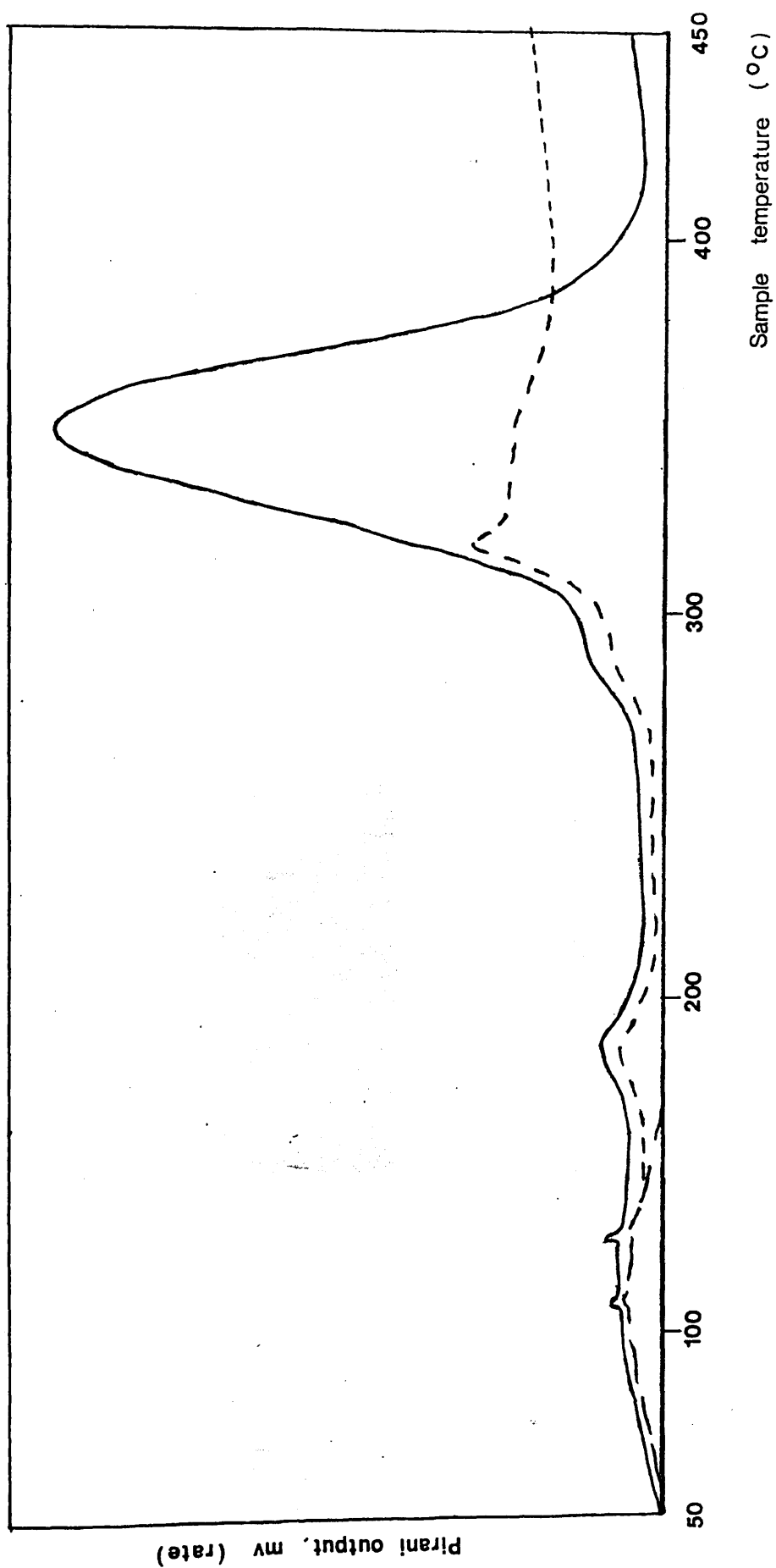


Figure 8.2 TVA curve for 1:50 $\text{Cu}(\text{acac})_2$ - PMMA 1 blend

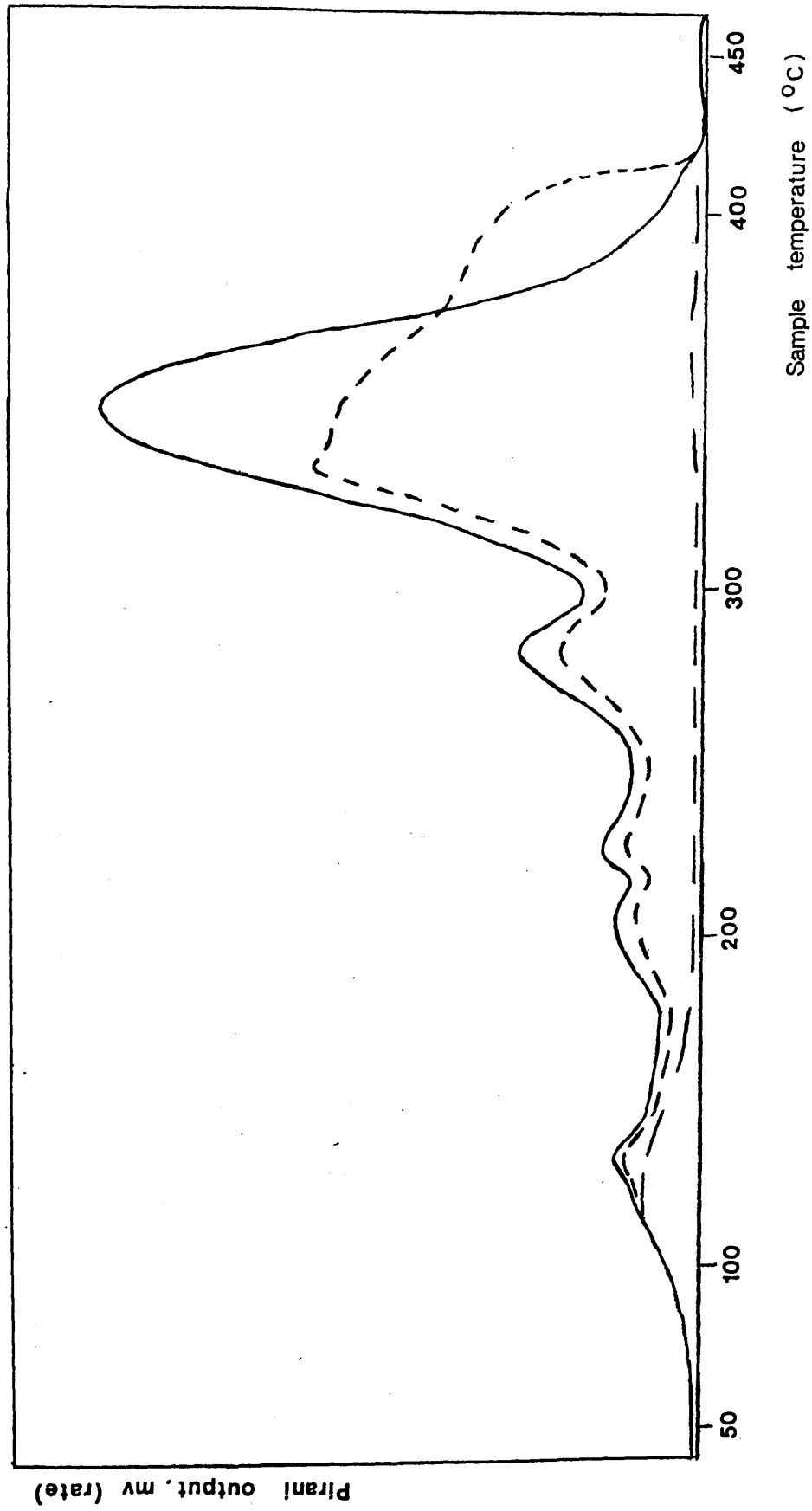


Figure 8.3 TVA curve for 1:50 Cu(acac)₂ - PMMA 2 blend

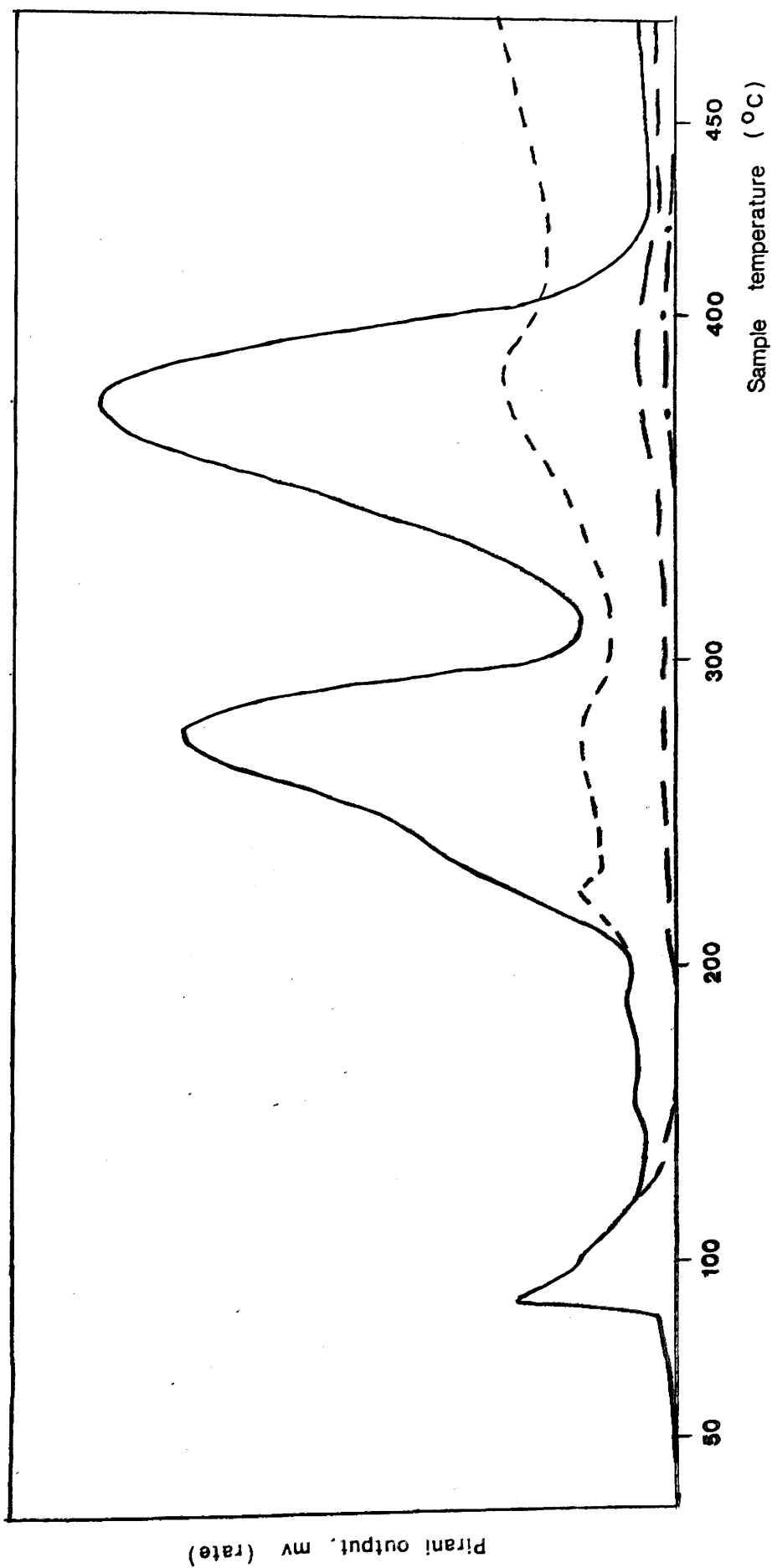


Figure 8.4 TVA curve for 1:50 $\text{Cu}(\text{acac})_2$ - PMMA 3 blend

BLEND				
	PMMA 1	PMMA 1	PMMA 2	PMMA 3
FEATURE	1:100	1:50	1:50	1:50
Compatibility	Yes	No	No	No
T(Sublimation)	Not observed	131°C	117°C	104°C
1st Peak	Steady evolution of volatiles to 253°C	Onset masked by solvent at ca. 153°C T(max) 194°C	Onset masked by solvent at ca. 150°C T(max) 203°C with overlapping peak T(max) 222°C	Steady rise to 200°C
2nd Peak	Shoulder to main peak 253-290°C	Shoulder to main peak 255-294°C	T(onset) 251°C T(max) 283°C	T(onset) 200°C Shouldered to 250°C T(max) 277°C
3rd Peak	T(max) 346°C	T(max) 352°C	T(onset) 301°C T(max) 352°C	T(onset) 320°C T(max) 373°C

Table 8.1 TVA Behaviour of $\text{Cu}(\text{acac})_2$ - PMMA Blends

these curves. All samples were of the order of 30mg and were cast as films from methylene chloride or chloroform, and the first peak in all the curves is due to evolution of very small amount of trapped solvent. The 1:50 blends had a frosted appearance indicating non-compatibility but the 1:100 blend was compatible.

The presence of $\text{Cu}(\text{acac})_2$ has a minor effect on the TVA behaviour of PMMA. The behaviour of the 1:100 $\text{Cu}(\text{acac})_2$ - PMMA 1 blend is little changed from that of the unblended polymer. A small peak with $T(\text{max})$ around 200°C is seen most clearly in the TVA curves for the 1:50 PMMA 1 and PMMA 2 blends, whilst the 1:50 PMMA 2 blend has a second, additional peak overlapping the first with $T(\text{max})$ 222°C . In the PMMA 3 blend there is no clearly defined peak around 200°C and the process occurring around 220°C overlaps with the early stages of the chain-end initiated unzipping of PMMA, resulting in the formation of a shoulder to the "chain end" peak. The height of the "chain end" peak (i.e. that with $T(\text{max})$ around 280°C) of the PMMA 2 and PMMA 3 blends is reduced slightly but not as much as in the $\text{Co}(\text{acac})_3$ - PMMA blends which implies that the chelate-chain end π -complex does not play as significant a role in the $\text{Cu}(\text{acac})_2$ blends.

The behaviour of the individual trap traces suggests that methyl methacrylate is the major product from each process. It is difficult to determine from these TVA curves any relationship between the newly

introduced degradation processes and the concentration of chelate or molecular weight of the polymer, although the peak around 220°C may be molecular weight dependent.

STUDY OF VOLATILE AND NON-VOLATILE PRODUCTS FROM THE $\text{Cu}(\text{acac})_2$ - PMMA BLENDS

As with the $\text{Co}(\text{acac})_3$ and $\text{Mn}(\text{acac})_3$ blends with PMMA, the study of the products of degradation was concentrated on the PMMA 1 blend, at a 1:50 $\text{Cu}(\text{acac})_2$:MMA unit ratio. Analyses of residues, cold ring fraction and -196°C condensible products were performed by the methods described in earlier chapters.

STRUCTURE OF THE UNDEGRADED BLEND AND CHANGES ON DEGRADATION

The IR and UV spectra of the blend before degradation and after various stages of degradation are reproduced in Figs. 8.5 and 8.6. Salient points are listed in Table 8.2.

The UV spectrum of the undegraded blend is in fact of the 1:100 blend which is compatible and thus not complicated by the presence of $\text{Cu}(\text{acac})_2$ in the solid state. The UV spectrum is unchanged from that of $\text{Cu}(\text{acac})_2$ in methylene chloride and does not show the shift of $\lambda(\text{max})$ present in methyl acetate solution. This suggests that most of the chelate is dispersed throughout the matrix rather than involved in an

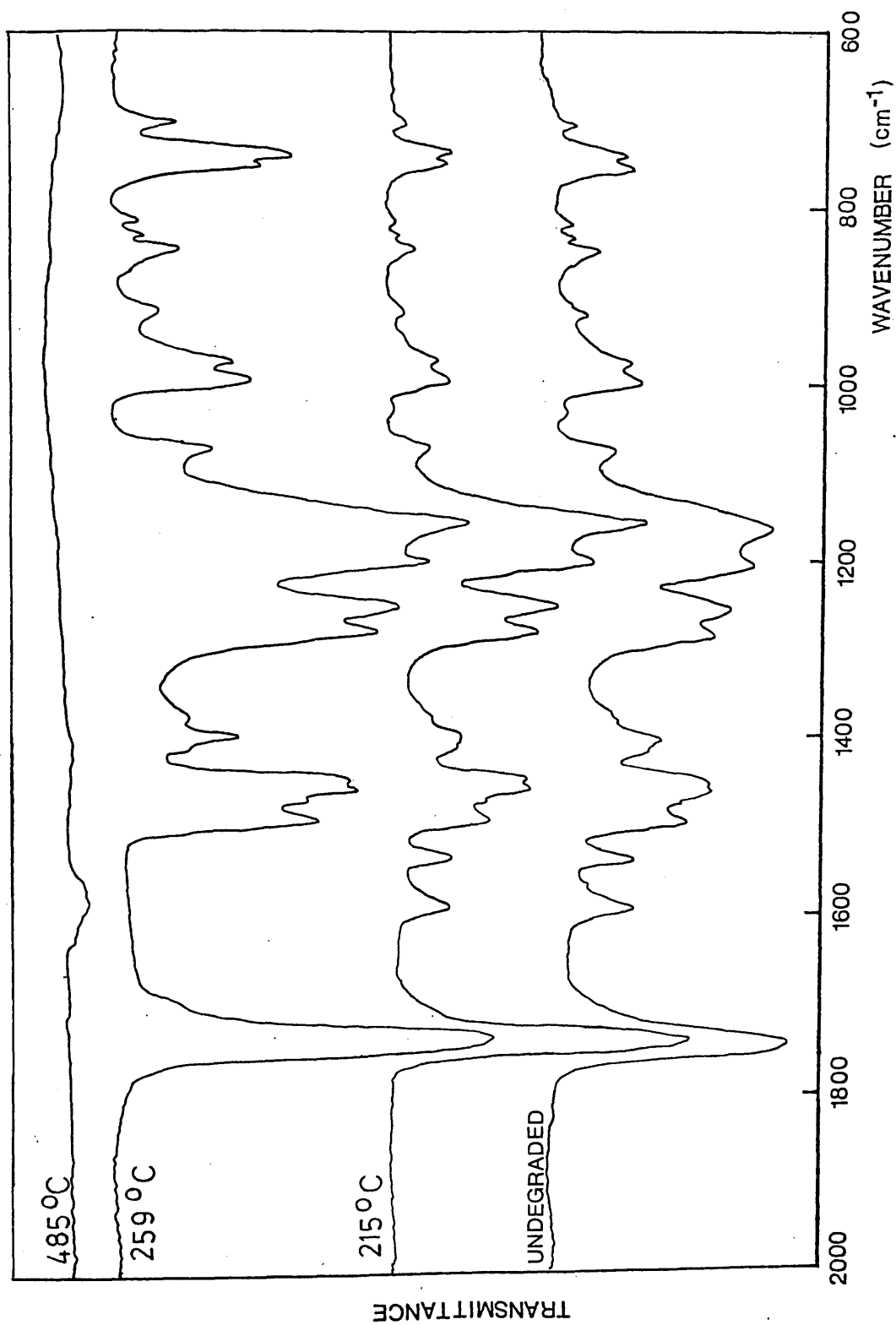


Figure 8.5 IR spectra of 1:50 Cu(acac)₂ - PMMA 1 blend at various stages of degradation

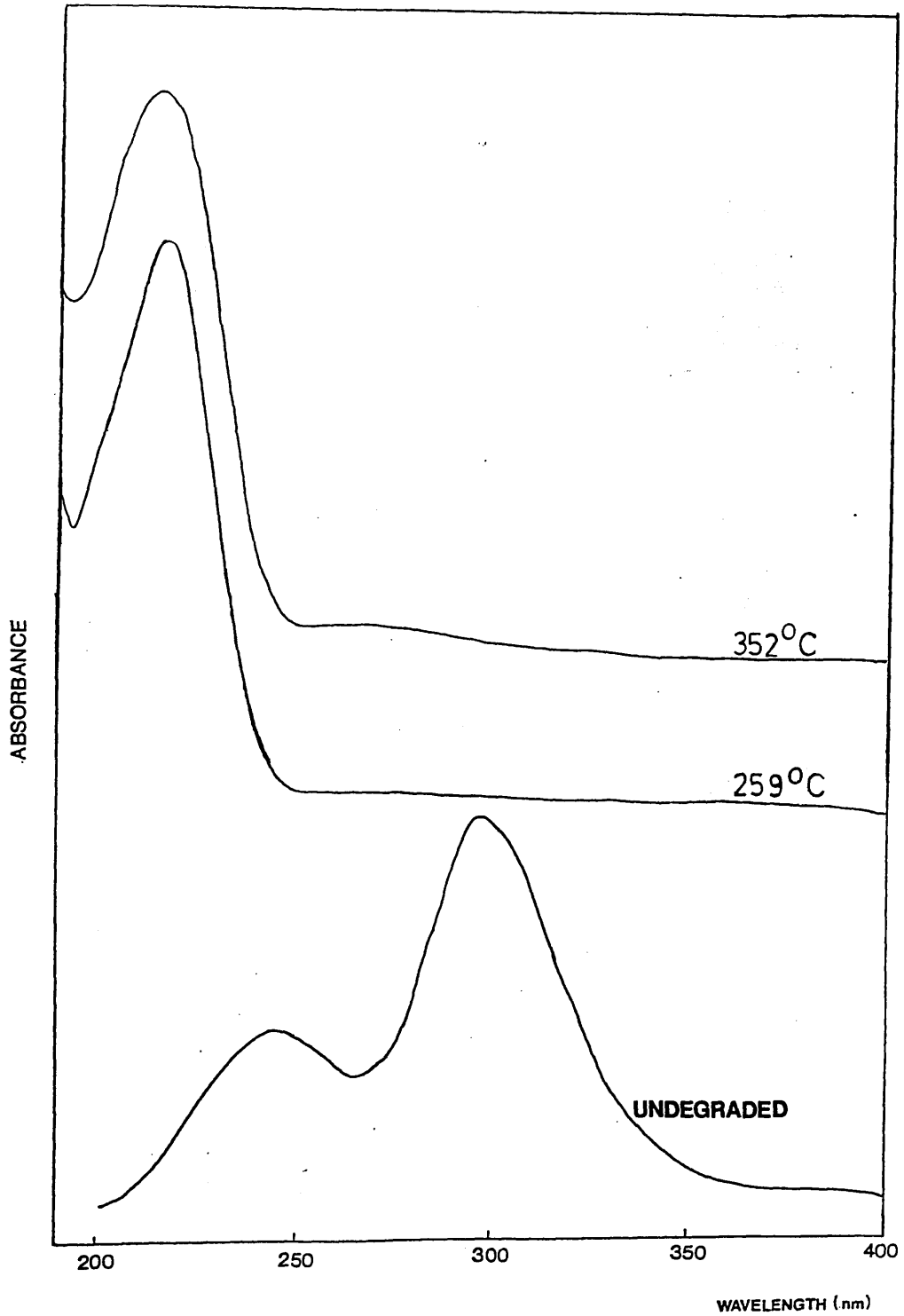
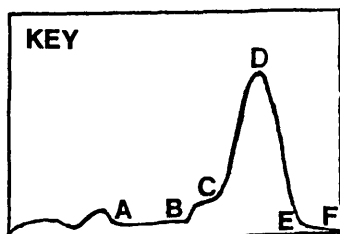


Figure 8.6
UV spectra of 1:50 (1:100) Cu(acac)₂ - PMMA 1 blend
at various stages of degradation

Extent of Degradation	Visual Appearance	CH ₂ Cl ₂ Solubility	Structural Features
None	Blue, frosted, incompatible	Yes	IR spectrum is superposition of spectra of PMMA and Cu(acac) ₂ (solid state). UV spectrum of 1:100 blend shows no evidence of interaction.
215°C (A)	Homogeneous, very slight blue colour	Yes	Cu(acac) ₂ still present, in reduced amount.
259°C (B)	Colourless	Yes	Only PMMA absorptions in both UV and IR spectra.
298°C (C)	Colourless	Yes	As 259°C
352°C (D)	Colourless	Yes	As 259°C
485°C (F)	Black char (v. small quantity)	No	IR spectrum of sample degraded on NaCl disc shows only carboxylate absorption, probably due to reaction with disc.

Table 8.2 Structural Features of 1:50 Cu(acac)₂ - PMMA 1 Blend at Various Stages in the Heating Programme



interaction with the ester groups, although this will occur to some extent. Although not observed spectroscopically, an interaction between the chelate and unsaturated chain ends is expected.

It is to be noted that on degradation the blend does not become detectably unsaturated or cross-linked in the manner of the $\text{Co}(\text{acac})_3$ and $\text{Mn}(\text{acac})_3$ blends, and remains colourless and soluble until high temperatures.

-196°C CONDENSIBLE GASEOUS PRODUCTS

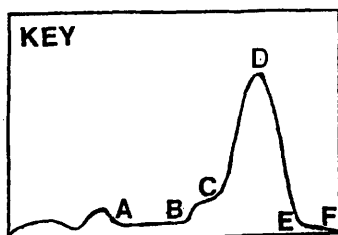
Analysis of the -196°C condensible gases confirmed the indication from the TVA trace that methyl methacrylate is almost the sole product (see Table 8.3). The only other product identified was acetylacetone, first detected on degrading the blend to 215°C. This is at the lower end of the decomposition range of $\text{Cu}(\text{acac})_2$ and the production of enough acetylacetone to be detected by IR spectroscopy suggests that the decomposition of the chelate is being promoted by some interaction with the polymer.

COLD RING FRACTION

The CRF which was produced in small quantity was largely $\text{Cu}(\text{acac})_2$ sublimate. At the later stages of degradation (379°C and above) trace quantities of chain fragments were also observed (see Table 8.3).

Extent of Degradation	Cold Ring Fraction	-196°C Condensable Gases
215°C (A)	Cu(acac) ₂	Methyl methacrylate, acetylacetone
259°C (B) 298°C (C) 352°C (D)	As 215°C	As 215°C
379°C (E) 485°C (F)	As above plus trace of chain fragments	As above plus trace of methanol

Table 8.3 Cold Ring Fraction and -196°C Condensible Products from the 1:50 Cu(acac)₂ - PMMA 1 Blend



DEGRADATION OF THE $\text{Cu}(\text{acac})_2$ - PMMA BLENDS -DISCUSSION

The evidence presented in Chapter 3 suggests that $\text{Cu}(\text{acac})_2$ interacts at room temperature with ester groups rather more strongly than $\text{Co}(\text{acac})_3$ but not as readily as $\text{Mn}(\text{acac})_3$ and, as the spectrum of the undegraded 1:100 $\text{Cu}(\text{acac})_2$ - PMMA 1 blend indicates, most of the chelate is dispersed at random throughout the polymer matrix as the blend forms from solution. A $\text{Cu}(\text{acac})_2$ π -complex is expected to form at unsaturated chain-ends but from the TVA evidence this does not greatly affect the chain-end initiated unzipping of the polymer and thus the decomposition of $\text{Cu}(\text{acac})_2$ promoted by π -complexation cannot be very significant in this blend. The reason for this is unclear, particularly as $\text{Cu}(\text{acac})_2$ is reported²⁶ to be almost as active as $\text{Co}(\text{acac})_3$ as a polymerisation initiator for methyl methacrylate.

The ester interaction can also promote decomposition and this underlies the detected production of acetylacetone at 215°C. At this temperature significant quantities of acetylacetone would not be expected from the purely thermal decomposition of $\text{Cu}(\text{acac})_2$ (Charles et al. found only ca. 10% decomposition of $\text{Cu}(\text{acac})_2$ after four hours at 215°C¹⁰⁵), and decomposition of the π -complex would also only produce a small quantity overall. Reflecting the fact that not all of the chelate is involved in the

ester interaction, the IR spectrum of the residue at 215°C shows that a considerable quantity of chelate remains (contrast with the Cu(acac)₂ - copolymer blend discussed subsequently).

The acac. radicals produced by chelate decomposition will initiate depolymerisation (methyl methacrylate is the other product identified at 215°C) by the same mechanism as already discussed for the Co(acac)₃ blends on page 259. Termination of unzipping by metal ion deactivation of the depropagating radical is expected to be greater in the Cu(acac)₂ blend than in the Co(acac)₃ blend as the reaction



is particularly favoured for Cu²⁺.⁵¹

The depolymerisation occurring around 220°C may be due to the small amount of decomposition of the π -complex (the associated peak seems to be molecular weight dependent) but increasingly, the purely thermal decomposition of Cu(acac)₂ will become important at these temperatures.

Carboxylates are not observed spectroscopically, although this does not preclude their formation since carboxylates were also undetected in the spectra of the 1:50 Co(acac)₃ - PMMA blend simply because the concentration was too low.

Cu(I)acac, which is formed as an intermediate in the decomposition of the chelate, is known to disproportionate to copper metal plus Cu(acac)₂ in the

absence of stabilising ligands.^{113,114} The ester groups may stabilise Cu(I)acac but there is no evidence here to confirm this.

The ultimate fate of the $\text{Cu}(\text{acac})_2$ in the blend is to decompose to copper metal plus two mole equivalents of acac·radicals. This is in contrast to the other chelates studied which produce small radicals which can promote the formation of anhydride rings between the polymer substituents. Furthermore, since there is no formation of unsaturated sites along the backbone, the presence of $\text{Cu}(\text{acac})_2$ does not lead to fragmentation of the polymer. Although metallic copper is well known for its catalytic properties in polymer degradation¹⁵¹, its production in the PMMA blend has little, if any, effect. The lack of influence of copper on PMMA degradation is clearly demonstrated by degrading PMMA in the presence of copper powder as described in the following section.

Thus, the influence of $\text{Cu}(\text{acac})_2$ on PMMA is limited to acac·radical initiated decomposition.

THERMAL DECOMPOSITION OF PMMA IN PRESENCE OF COPPER POWDER

The degradation of PMMA in the presence of copper powder was examined by TVA. 3g of copper powder were spread evenly across the bottom of a TVA tube to give a layer approximately 1mm deep. The PMMA sample (30mg of PMMA 1) was then cast onto the bottom of the TVA tube

from a methylene chloride solution in the usual manner. This resulted in a PMMA film with an even, though heterogeneous, copper content. The TVA curve was obtained in the usual fashion and is reproduced in Fig. 8.7 from which it can be seen that the behaviour of the polymer is essentially unchanged compared with the behaviour of the polymer in the absence of copper (Fig. 4.5). This is not unexpected as Grassie and Melville in the first investigation of the degradation of PMMA,¹²³ degraded the sample in a copper tray covered with copper powder to ensure even heat distribution and found the copper to have no effect.

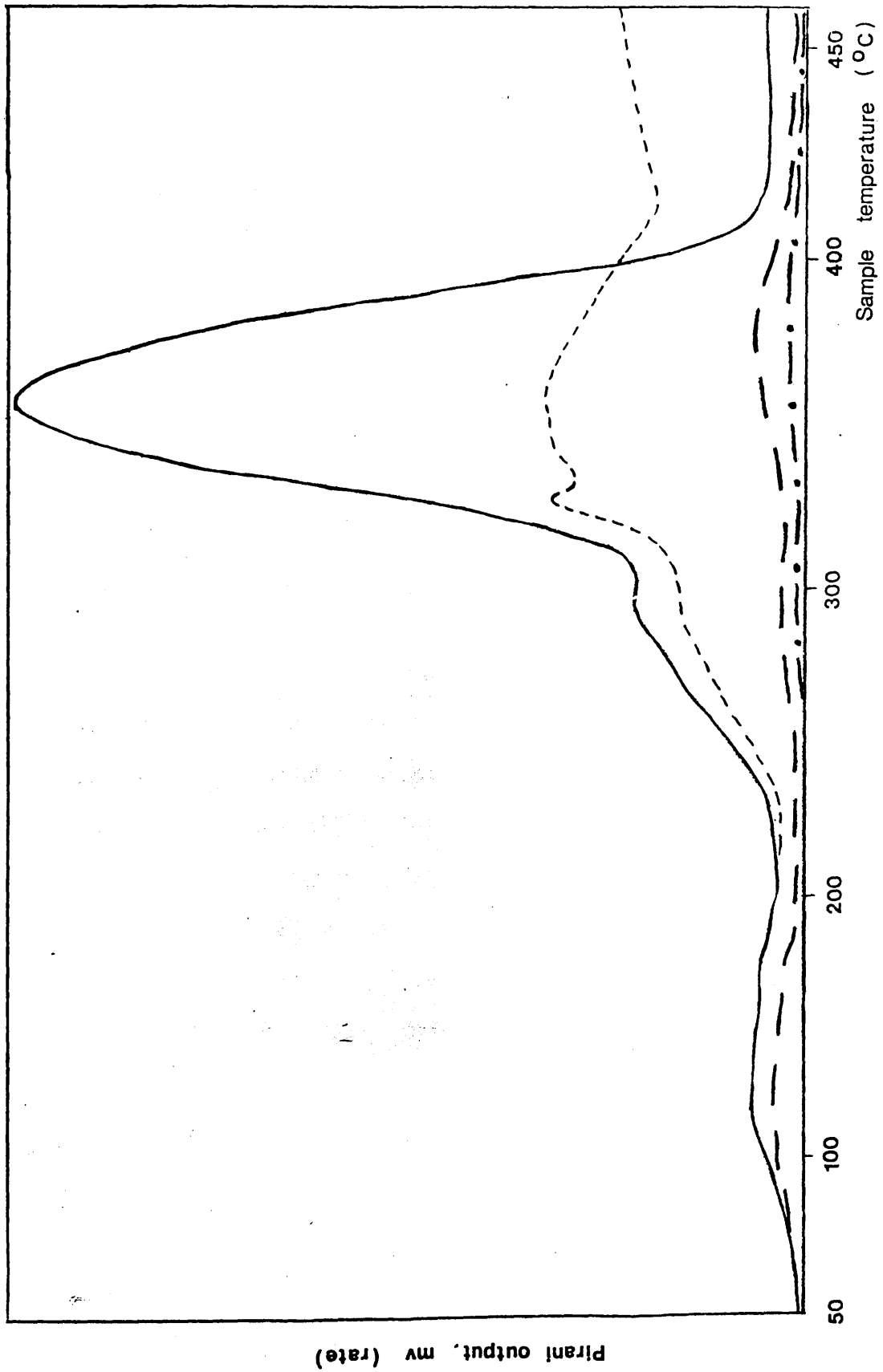


Figure 8.7 TVA curve for PMMA 1 degraded in the presence of copper powder

BLEND S OF $\text{Cu}(\text{acac})_2$ WITH THE 1:59 MAA-MMA COPOLYMERTVA BEHAVIOUR

In contrast to the minor influence $\text{Cu}(\text{acac})_2$ has on the thermal degradation of PMMA, the chelate has a marked effect on the degradation behaviour of the copolymer. This is demonstrated clearly by the TVA curves obtained for the $\text{Cu}(\text{acac})_2$ - copolymer blends at various concentrations of $\text{Cu}(\text{acac})_2$ which are reproduced in Figs. 8.8-8.10. The samples, cast from methylene chloride solution, were of the order of 30mg. The 1:50 blend was frosted and incompatible, the 1:10 and 1:220 blends were compatible.

Relative to the TVA curve of the copolymer, there are two additional major peaks with $T(\text{max})$ in the ranges $190-204^\circ\text{C}$ and $267-280^\circ\text{C}$ respectively and an overlapping peak between $300-360^\circ\text{C}$. The final peak can be associated with the normal random scission initiated unzipping of the polymers. Although no peak corresponds directly to the chain-end initiated depolymerisation of the unblended polymer (normally $T(\text{max})$ 287°C), the shift in $T(\text{max})$ of the second peak from 267°C to 280°C with decreasing chelate concentration suggests that the chain-end initiated unzipping underlies this peak. The increase in $T(\text{max})$ of the first peak with increasing $\text{Cu}(\text{acac})_2$ concentration suggests that two processes occur in this temperature region and the TVA curve of the 1:65

$\text{Cu}(\text{acac})_2$ - copolymer blend, reproduced in Fig. 8.11, shows, rather fortuitously, that there are in fact two overlapping peaks with $T(\text{max})$ 189°C and 202°C respectively.

From the behaviour of the individual trap traces, methyl methacrylate is seen to be almost the sole volatile product of the complete degradation. There is some deviation of the -100°C trace under the second peak and of the -100°C and -196°C trace under the final peak although to only a very small extent. This is in sharp contrast to the $\text{Co}(\text{acac})_3$ and $\text{Mn}(\text{acac})_3$ blends with the copolymer in which considerable quantities of -196°C non-condensable material and other non-monomer species were produced, and suggests that the mechanism of interaction of $\text{Cu}(\text{acac})_2$ with the copolymer differs from that of the other chelates. Comparing the behaviour of the $\text{Cu}(\text{acac})_2$ - PMMA and $\text{Cu}(\text{acac})_2$ - copolymer blends suggests that the presence of methacrylic acid units considerably enhances the effect of $\text{Cu}(\text{acac})_2$.

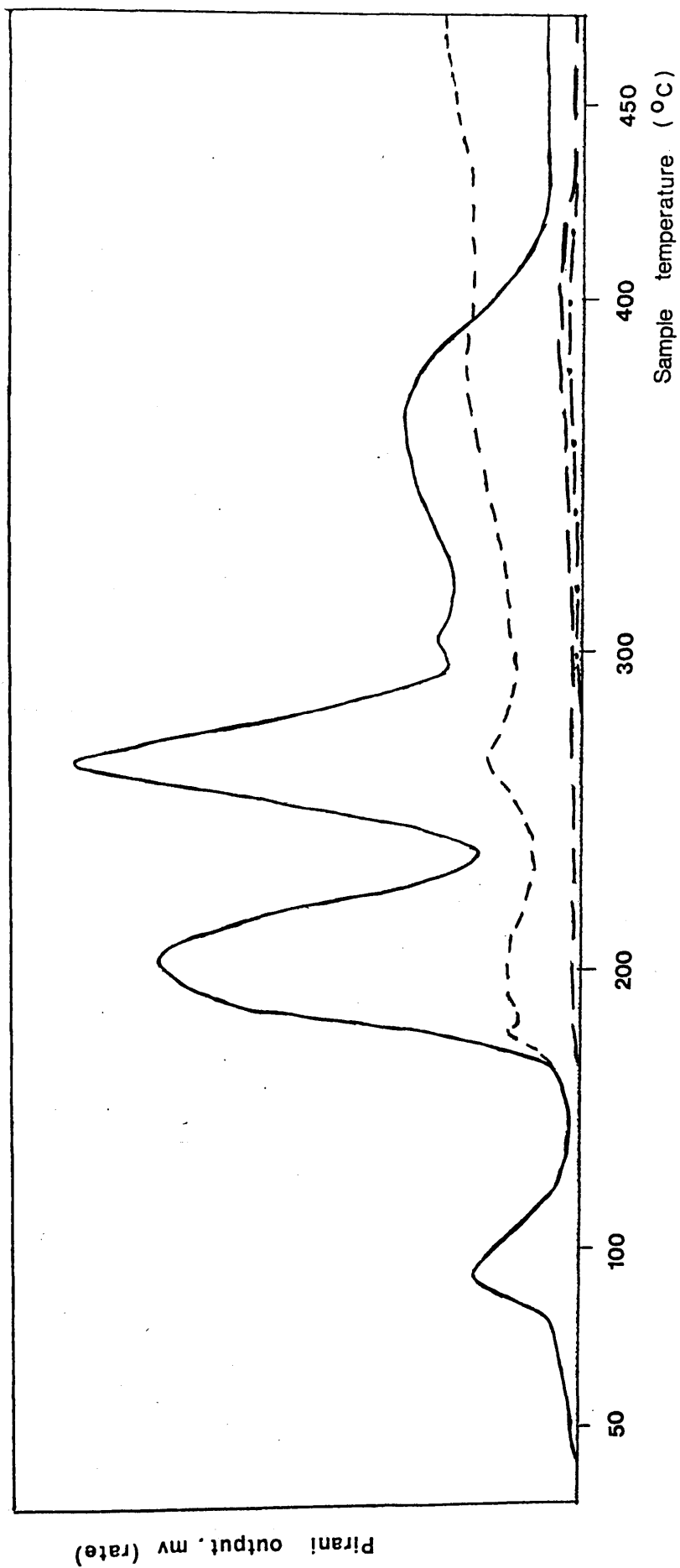


Figure 8.8 TVA curve for 1:50 $\text{Cu}(\text{acac})_2$ - copolymer blend

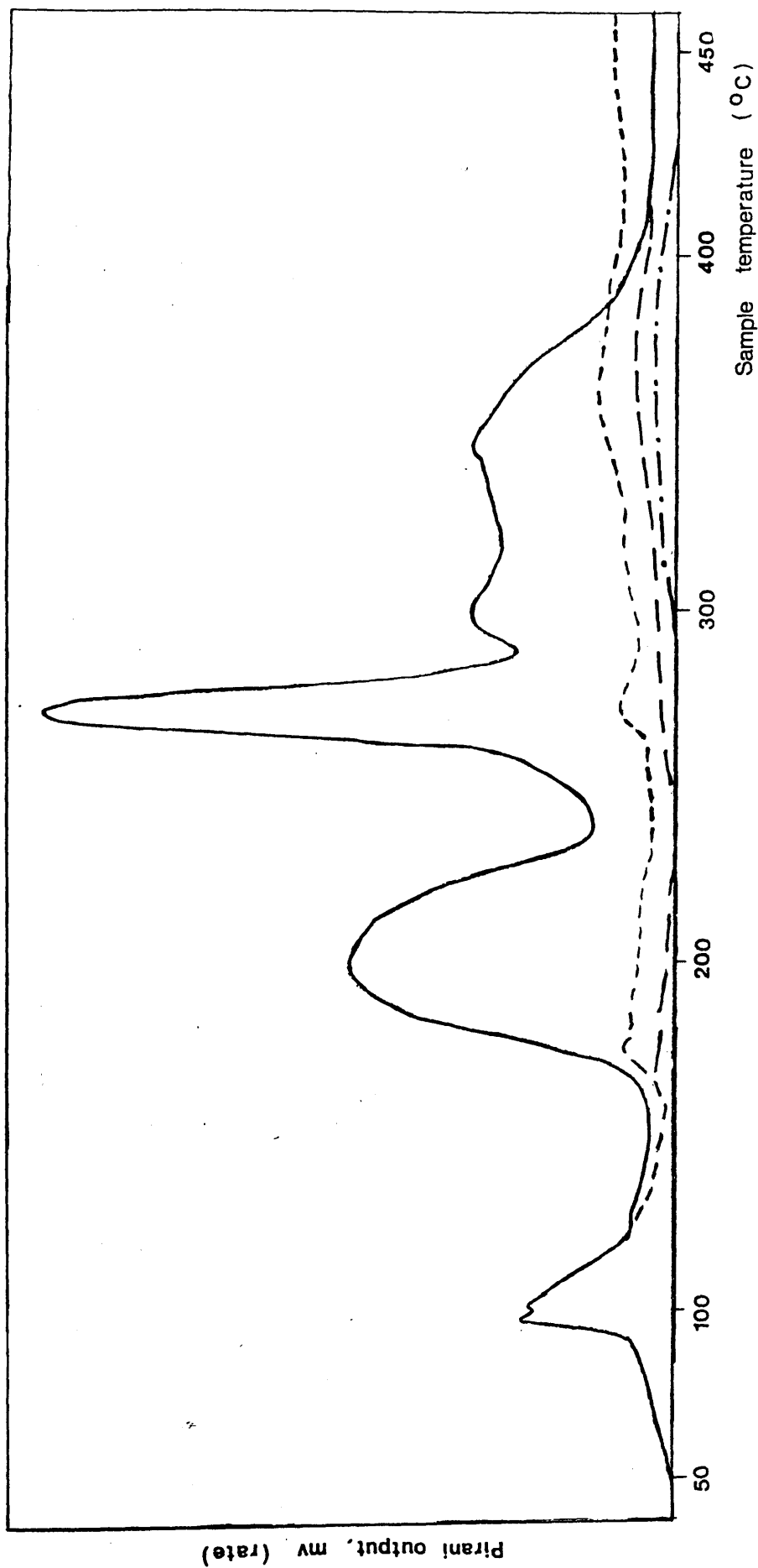


Figure 8.9 TVA curve for 1:110 Cu(acac)₂ - copolymer blend

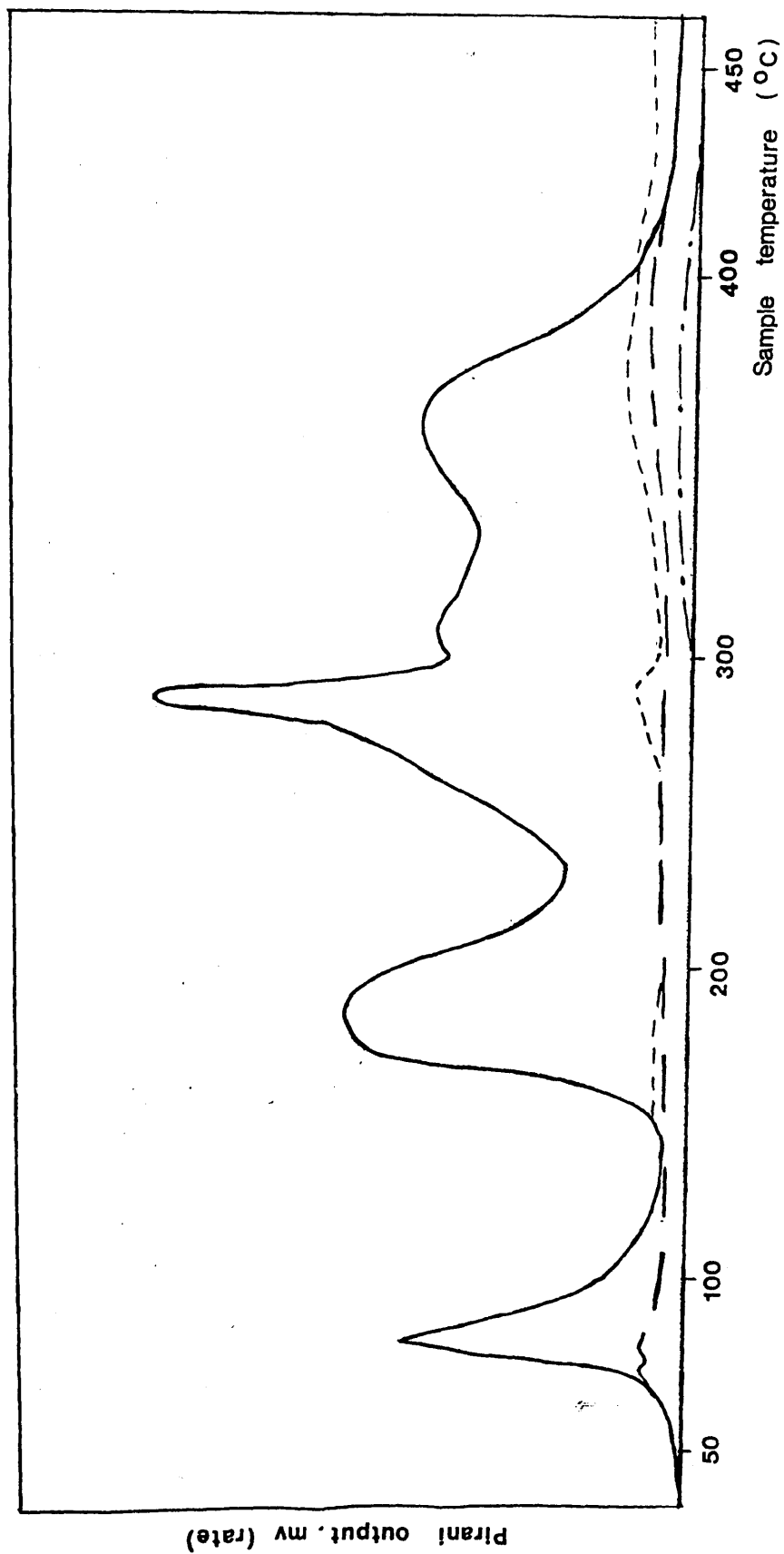


Figure 8.10 TVA curve for 1:220 $\text{Cu}(\text{acac})_2$ - copolymer blend

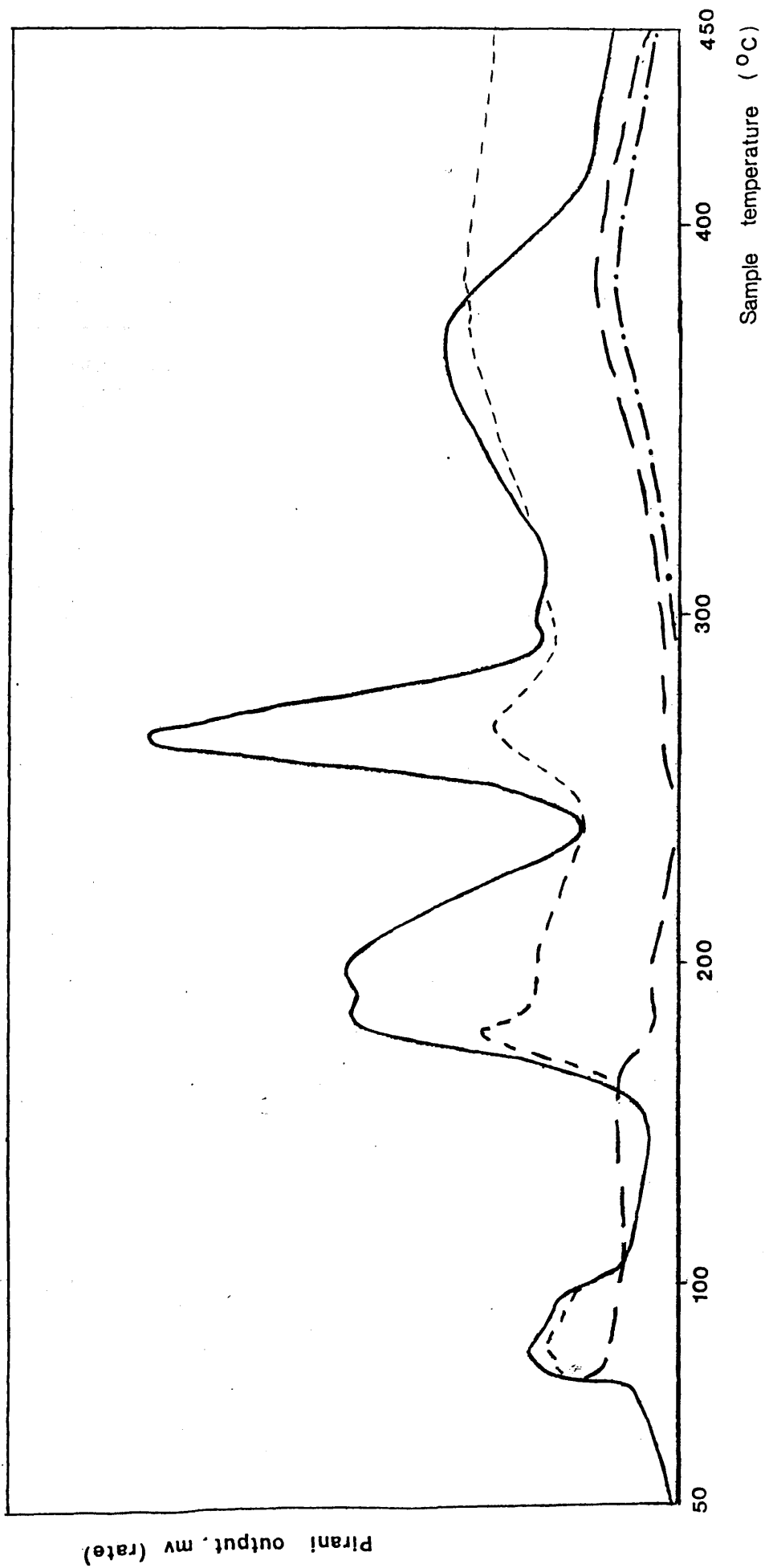


Figure 8.11 TVA curve for 1:65 $\text{Cu}(\text{acac})_2$ - copolymer blend

Feature	Blend		
	1:50	1:10	1:220
T(sublimation)	104	165	Not observed
1st Peak			
T(onset)	152	156	150
T(max)	204	197	190
2nd Peak			
T(onset)	240	237	237
T(max)	268	271	280
3rd Peak			
T(onset)	293	289	295
T(max)	302	300	306
4th Peak			
T(onset)	315	321	336
T(max)	367	350	358

Temperatures in °C

Table 8.4 Features of TVA Curves of $\text{Cu}(\text{acac})_2$ - 1:59 MAA-MMA Copolymer Blends

ANALYSIS OF PRODUCTS, VOLATILE AND INVOLATILE, FROM 1:50
Cu(acac)₂ - COPOLYMER BLEND AT VARIOUS STAGES OF THE
HEATING PROGRAMME

The nature of the -196°C condensible products and the structure of the cold ring fraction and residual film were investigated at various extents of degradation by the standard methods previously described.

STRUCTURE OF THE UNDEGRADED BLEND AND CHANGES ON
DEGRADATION

Figs. 8.12 and 8.13 show the UV and IR spectra of the blend at various stages of the heating programme; the UV spectrum of the undegraded blend is of the compatible 1:100 blend rather than the incompatible 1:50 blend.

In contrast to the Cu(acac)₂ - PMMA blend, the Cu(acac)₂ - copolymer blend shows a broadening of the absorption centred on 295nm. This is the only overt indication of an interaction between polymer and chelate and is due to association of Cu(acac)₂ with the acid groups of the copolymer.

On degradation there are several features which differentiate the Cu(acac)₂ - copolymer blend from the Cu(acac)₂ - PMMA blend. These are the earlier decomposition of Cu(acac)₂ (only trace quantities remain at 206°C - compare with the situation for the 1:50 PMMA blend at 215°C), the appearance of carboxylate structures (detected by their IR absorption,

the UV absorption at λ (max) 199nm may also be due to such structures but it is difficult to assign UV absorptions unequivocally) and the development of a green colour. It is to be noted that both the green colour and 199nm absorption persist when the carboxylate absorption is no longer present in the IR spectrum.

The origin of the green colour is unclear. Samples of the polymer were heated to 280°C at which point the residue is dark green. One sample was dissolved in methylene chloride and shaken with water. The aqueous layer remained colourless and the organic layer retained its colour. The second sample was dissolved in acetone (completely soluble) and precipitated in methanol. This resulted in only a slight reduction of the green colour. These results suggest that the species giving rise to the green colour may be polymer bound.

-196°C CONDENSIBLE PRODUCTS AND COLD RING FRACTION

Tables 8.6 and 8.7 list the products identified at various stages of the heating programme.

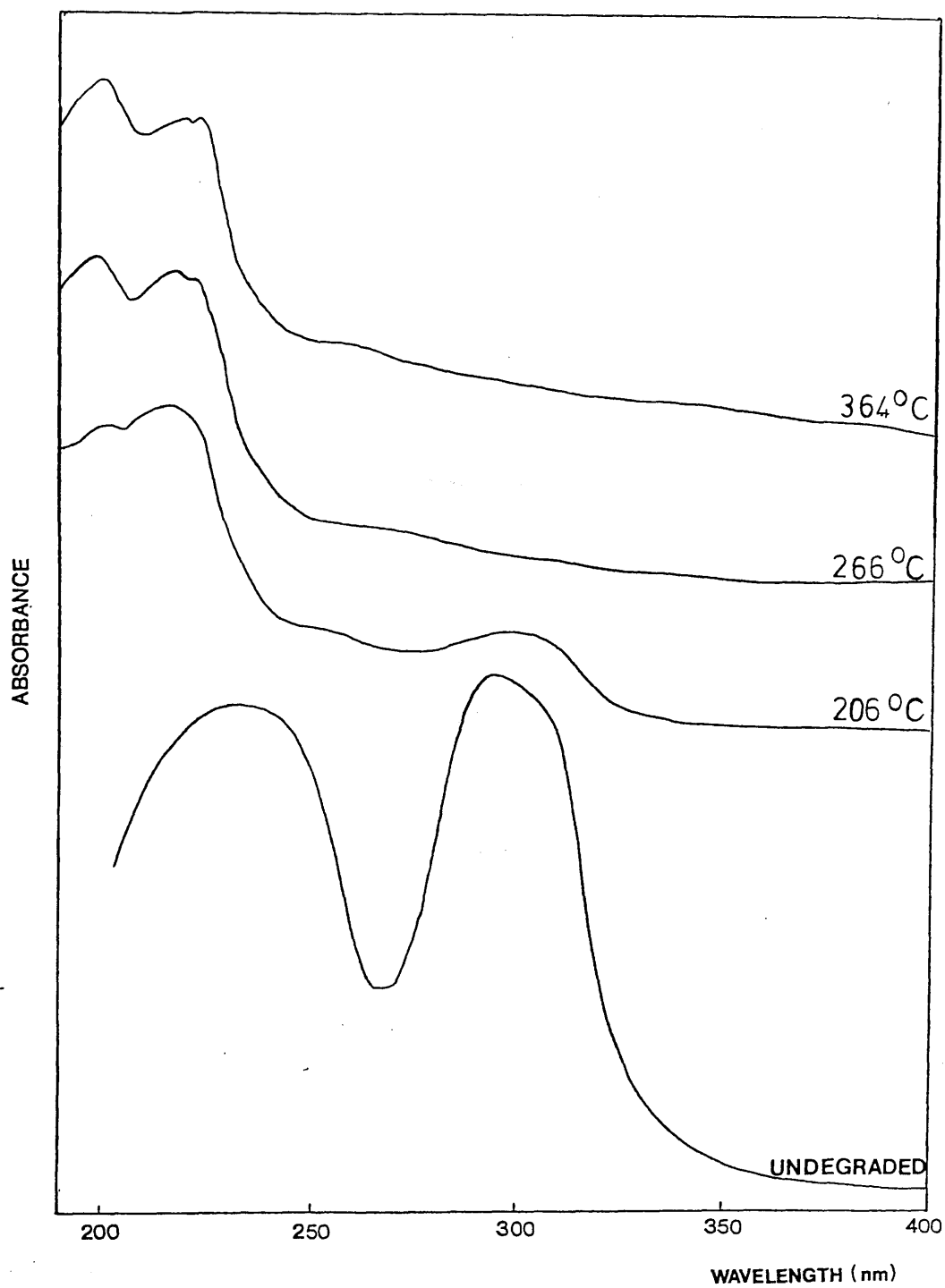


Figure 8.12

UV spectra of 1:50 (1:100) Cu(acac)₂ - copolymer
blend at various stages of the heating programme

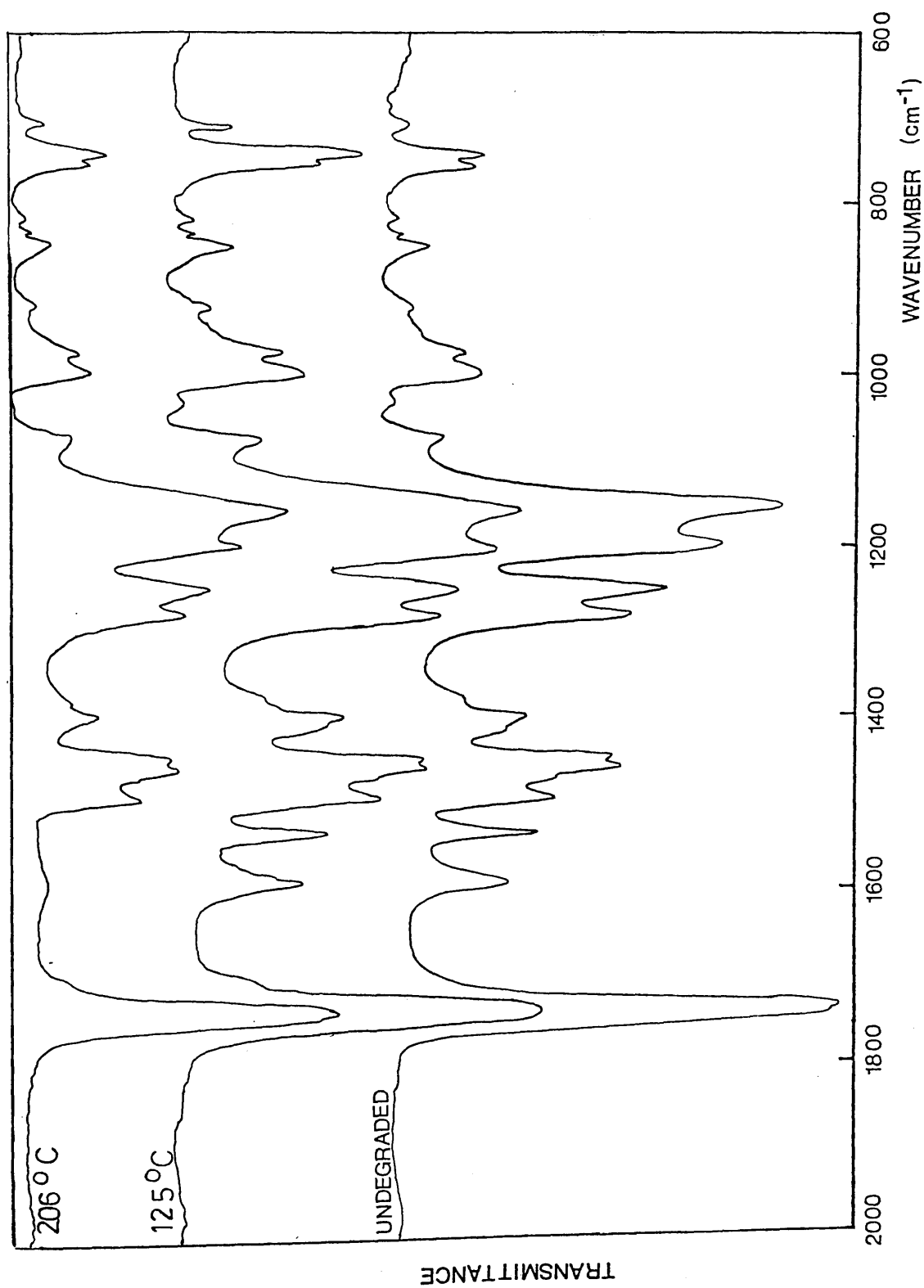


Figure 8.13 IR spectra of 1:50 Cu(acac)₂ - copolymer blend at various stages of the heating programme

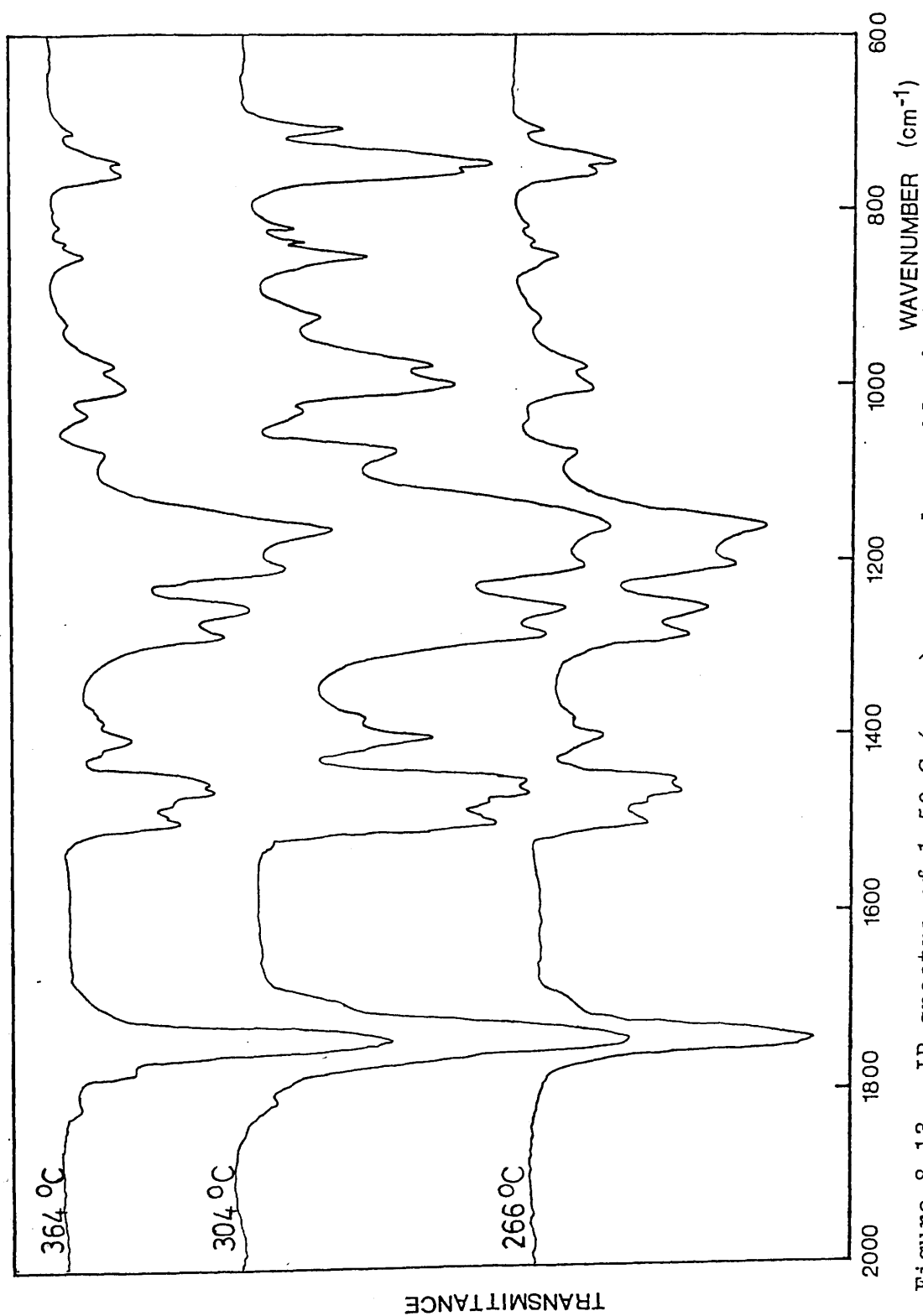


Figure 8.13 IR spectra of 1:50 Cu(acac)₂ - copolymer blend at various stages of the heating programme (ctd.)

Extent of Degradation	Visual Appearance	CH ₂ Cl ₂ Solubility	Comments
None	Blue, "frosted", incompatible	Yes	IR spectrum shows no interaction, chelate peaks 1500-1600 cm ⁻¹ reflect fact that some chelate present in solid state. Minor changes in UV spectrum.
125°C (A)	Homogeneous	Yes	Reduction of chelate absorptions due to sublimation from film. Relative intensities of 1500-1600cm ⁻¹ peaks => remaining chelate in polymer solution.
206°C (B)	V. faint green colour	Yes	IR spectrum => little or no chelate; 1580cm ⁻¹ absorption => some carboxylate. UV spectrum => little or no chelate; absorption λ(max) 200nm => carboxylate (?), 214nm => PMMA.
266°C (C)	Dark green	Yes	Some carboxylate absorption present in IR spectrum. Carboxylate (?) absorption still present in UV spectrum.
304°C (D)	Dark green	Yes	IR spectrum - peaks at 1800, 1020 cm ⁻¹ => glutaric type anhydrides Carboxylates (?) still present in UV spectrum.
364°C (E)	Dark green	Yes	Similar to 304°C.
485°C (F)	Brown char	No	Not analysed.

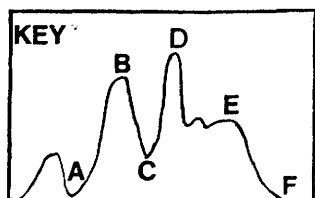
Table 8.5 Structure of Cu(acac)₂ - 1:59 MAA-MMA Copolymer blend at various stages of degradation

Extent of Degradation °C	Components of CRF
125 (A)	Cu(acac) ₂
206 (B)	Cu(acac) ₂
266 (C) 304 (D) 364 (E)	Cu(acac) ₂ + chain fragments
485 (F)	Chain fragments now include glutaric type anhydride structures.

Table 8.6 -196°C Condensable Products from Cu(acac)₂ - 1:59 MAA-MMA Copolymer Blend at Various Stages of the Heating Programme.

Extent of Degradation °C	-196°C Condensable Products
206 (B)	Methyl methacrylate, acetylacetone
266 (C)	As 206°C plus trace methanol
304 (D)	As 206°C
364 (E)	As 266°C plus significant quantity methanol, trace of carbon dioxide and "ketene".
485 (F)	As 304°C, rather more carbon dioxide and "ketene". Liquid anhydride product.

Table 8.7 Cold Ring fraction from Cu(acac)₂ - 1:59 MAA-MMA Copolymer Blend at Various Stages of the Heating Programme.



DEGRADATION OF 1:59 MAA-MMA COPOLYMER IN THE PRESENCE OF COPPER POWDER

An even dispersion of copper powder in a film of the copolymer was prepared in a TVA tube as described earlier for the PMMA homopolymer, and the TVA curve obtained in the usual manner. The curve is reproduced in Fig. 8.14 and demonstrates that the presence of copper has a significant effect on the thermal degradation of the copolymer, in contrast to its influence on PMMA. There is a strong resemblance between this curve and that of the $\text{Cu}(\text{acac})_2$ -copolymer blends with a peak at 298°C (strongly shouldered at 274°C) a smaller, overlapped peak at 316°C and the random scission peak, slightly reduced in importance but otherwise unchanged at 368°C . The behaviour of the individual trap traces suggests that methyl methacrylate is the major product. A very small amount of -196°C non-condensable material is produced and the deviation of the -100°C trace indicates the production of an additional condensable product. Thus, the effect of introducing copper to the copolymer is to initiate, directly or indirectly, depolymerisation. Since the copper induces depolymerisation only in the presence of the methacrylic acid units, these acid groupings must also play a role. Copper is known as a catalyst for the thermal decarboxylation of carboxylic acids,¹⁵²⁻¹⁵⁴ and although the mode of action is not well understood, the catalysis is believed to proceed

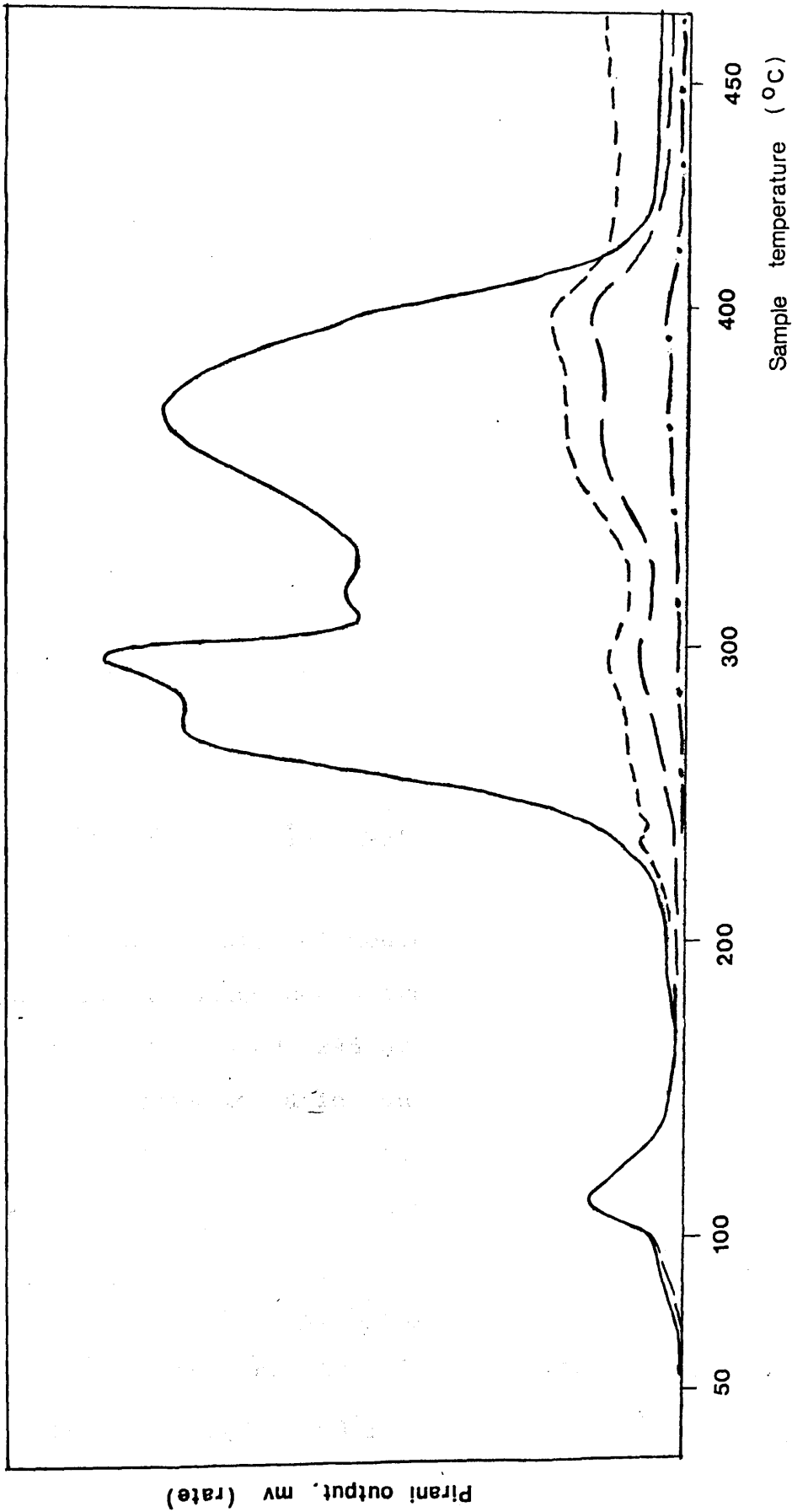


Figure 8.14 TVA curve for 1:59 MAA - MMA copolymer degraded in the presence of copper powder

via a radical mechanism and involve the formation of Cu-C bonds. Hence, it is likely that the initial depolymerisation of the copolymer is initiated by radical species produced in the copper catalysed decarboxylation of the acid side groups. Of course, carbon dioxide would also be produced, although in small amount relative to the methyl methacrylate evolved, and this would account for the early deviation of the -100°C trace. Decarboxylation of non-aromatic carboxylic acids catalysed by copper does not occur "cleanly" and thus there will be produced within the polymer a number of irregular structures which themselves could act as initiating sites for depolymerisation, hence the peak $T(\text{max})$ 316°C .

DEGRADATION OF 1:50 $\text{Cu}(\text{acac})_2$ - 1:59 MAA-MMA COPOLYMER
- DISCUSSION

The only evidence of an interaction in the undegraded blend comes from a broadening of the major UV absorption around 295 nm and is due to association with the methacrylic acid units. To a lesser extent, some association with the ester groups is expected and there will also be the unsaturated chain end π -complex.

THE NATURE OF THE DEGRADATION BELOW 210°C

On heating to 206°C , (i.e. beyond the first degradation peak) only trace quantities of $\text{Cu}(\text{acac})_2$

remain, in contrast to the $\text{Cu}(\text{acac})_2$ - PMMA blend. $\text{Cu}(\text{acac})_2$ will not sublime any more readily from the copolymer blend than from the PMMA blend and thus the greater loss of $\text{Cu}(\text{acac})_2$ from the former can be ascribed to decomposition. Hence, as expected by analogy with the $\text{Co}(\text{acac})_3$ and $\text{Mn}(\text{acac})_3$ systems studied earlier, the acid groups promote the decomposition of the chelate more than do the ester groups. The interaction is the same as that with the other chelates and the decomposition produces $\text{acac}\cdot$ radicals which initiate depolymerisation by the mechanism already considered. Ester promoted decomposition would also occur at the same temperature as in the PMMA blend. However, attributing the first peak solely to the acid and ester side group induced decomposition of the chelate does not account for the relative independence of the peak height from $\text{Cu}(\text{acac})_2$ concentration or the increase of $T(\text{max})$ with increasing $\text{Cu}(\text{acac})_2$ concentration. Independence from chelate concentration usually implies a chain-end interaction but why one should occur in the copolymer blend and not in the PMMA blend is not clear.

The peak height is also considerably greater than that associated with any of the chelate induced unzipping processes in the PMMA blend but this can be accounted for not only by more chelate decomposing at once but also by the reduction of the chelate over a narrower temperature range restricting the amount of

deactivation of radicals by Cu^{2+} .

Although $\text{Cu}(\text{acac})_2$ is expected to be more stable to ligand substitution than the cobalt and manganese chelates, (See Table 3.3) some carboxylate formation does take place in the blend. This will occur by the cyclic mechanism shown on page 329. The data in Table 3.3 suggests that substitution will occur more readily for the reduced complex, $\text{Cu}(\text{I})\text{acac}$, than for $\text{Cu}(\text{acac})_2$. In either event, the polymer remains soluble and cross-linking via carboxylate bridges cannot be extensive.

When not involved in carboxylate formation the $\text{Cu}(\text{I})\text{acac}$ decomposes, either by disproportionation or directly to copper metal plus $\text{acac}\cdot$.

THE NATURE OF THE DEGRADATION ABOVE 210°C

Above 210°C , the TVA behaviour is very similar to that of the copolymer degraded in the presence of copper metal, and the same interpretation of the degradation can be invoked. The peak with $T(\text{max})$ ca. 270°C , due largely to methyl methacrylate, can thus be assigned to depolymerisation consequent upon initiation by radicals produced in the decarboxylation process, and the peak with $T(\text{max})$ ca. 300°C , also due to methyl methacrylate, assigned to depolymerisation initiated at weak links formed in the decarboxylation process. In the case of the $\text{Cu}(\text{acac})_2$ blend, the copper metal catalysing the decarboxylation is produced in situ by

the decomposition of the $\text{Cu}(\text{acac})_2$. The green colour develops in parallel with the decarboxylation and may be due to some structure formed in this process. Alternatively it could result from oxidation of the polymer bound carboxylate.

The decarboxylation occurs in the same temperature region as the anhydride formation by side chain cyclisation and some anhydrides form despite the decarboxylation.

The $\text{Cu}(\text{acac})_2$ - copolymer blends differ from those of $\text{Co}(\text{acac})_3$ and $\text{Mn}(\text{acac})_3$ by producing little fragmentation. A number of factors are involved in this. There will be fewer carboxylate structures formed and those that are do not persist to such high temperatures as the cobalt and manganese compounds. Side chain scission does not appear to be significant (no yellowing of the blend at moderate temperatures) and the decomposition of $\text{Cu}(\text{acac})_2$ produces no small radical species which could induce anhydride formation, and indeed the decarboxylation process leads to a reduction in the copolymer anhydride formation. The lack of modified structures along the chain means that unzipping progresses relatively unhindered and thus yields of monomer from the decarboxylation-initiated depolymerisation are high. The thermal chain-end scission initiated unzipping occurs in the same region as the decarboxylation and being blocked by fewer anhydrides will be more important in the blend than in

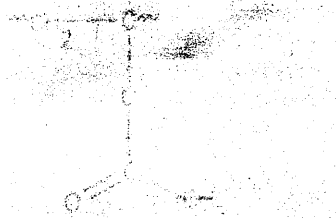
the unblended polymer. With enhanced monomer production in the early stages, the final random scission process becomes less significant.

CONCLUSIONS

$\text{Cu}(\text{acac})_2$ modifies the degradation of the copolymer in two ways. First, the decomposition of the chelate (promoted by interactions with the polymer) produces $\text{acac}\cdot$ radicals which initiate depolymerisation. Second, the copper metal produced in the above stage catalyses the decarboxylation of the polymer, producing radicals which initiate depolymerisation. Newly created "weak links" in the polymer act as sites for the initiation of further unzipping.



PVAc



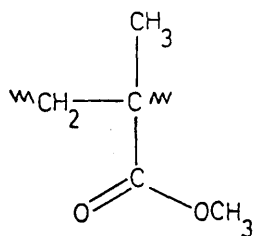
PVAc

CHAPTER 9

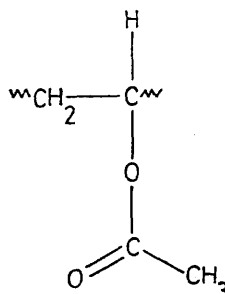
THERMAL DEGRADATION OF BLENDS OF POLY(VINYL ACETATE) WITH TRANSITION METAL ACETYLACETONATESINTRODUCTION

In the previous chapters it has been shown that blending transition metal acetylacetonates with PMMA modifies its thermal behaviour. The two principal sites for interaction of the chelates with the polymer are the unsaturated end groups and the ester side groups.

As poly(vinyl acetate) (PVAc) also contains ester side groups it is of interest to investigate the influence of the chelates on the thermal degradation of this polymer particularly as the ester groups of PVAc are linked to the backbone via the ester oxygen rather than via a C-C bond and the degradation behaviour is markedly different from that of PMMA.



PMMA



PVAc

DEGRADATION OF PVAc

This was discussed in Chapter 4.

DEGRADATION OF THE ACETYLACETONATE CHELATES

The decomposition behaviour of the chelates was described in Chapter 3.

BLENDS OF PVAc WITH Co(acac)₃, Mn(acac)₃, Co(acac)₂, Cu(acac)₂TVA BEHAVIOUR

The TVA behaviour of several chelate-PVAc blends was investigated and the TVA curves obtained are reproduced in Figs. 9.1-9.5 with the relevant details summarised in Table 9.1 (data for PVAc is included for comparison). Blends were prepared in the chelate: monomer unit ratio of 1:50 (a 1:10 Co(acac)₃ - PVAc blend was also investigated) and were cast as films from methylene chloride solution. Samples of around 30mg were used and the TVA curves were obtained in the standard manner.

The effect of the chelates on PVAc is slight. Co(acac)₃ and Cu(acac)₂ have no effect on the deacetylation process but both Mn(acac)₃ and Co(acac)₂ reduce the T(onset) of the deacetylation peak. Mn(acac)₃ and Co(acac)₃ each introduce a minor low temperature degradation step, T(onset) 145°C and 184-190°C respectively, which in this temperature

region, is almost certainly due to the decomposition of the chelates.

The easier sublimation of chelate from the PVAc blends than from the PMMA blends is to be noted. PVAc has T_g 28°C , some 100°C lower than PMMA and thus does not provide such a hindrance to sublimation (no $\text{Co}(\text{acac})_3$ sublimed from the compatible PMMA blends at less than 130°C). For $\text{Mn}(\text{acac})_3$, whose sublimation from the PMMA blends was hindered by its interaction with the ester groups, its sublimation from PVAc suggests that it does not bind so strongly to the acetate side chains.

As no change was observed in the TVA behaviour of the $\text{Cu}(\text{acac})_2$ blend, a more detailed analysis was not undertaken. The other blends were looked at in more detail and the results are described in the following sections.

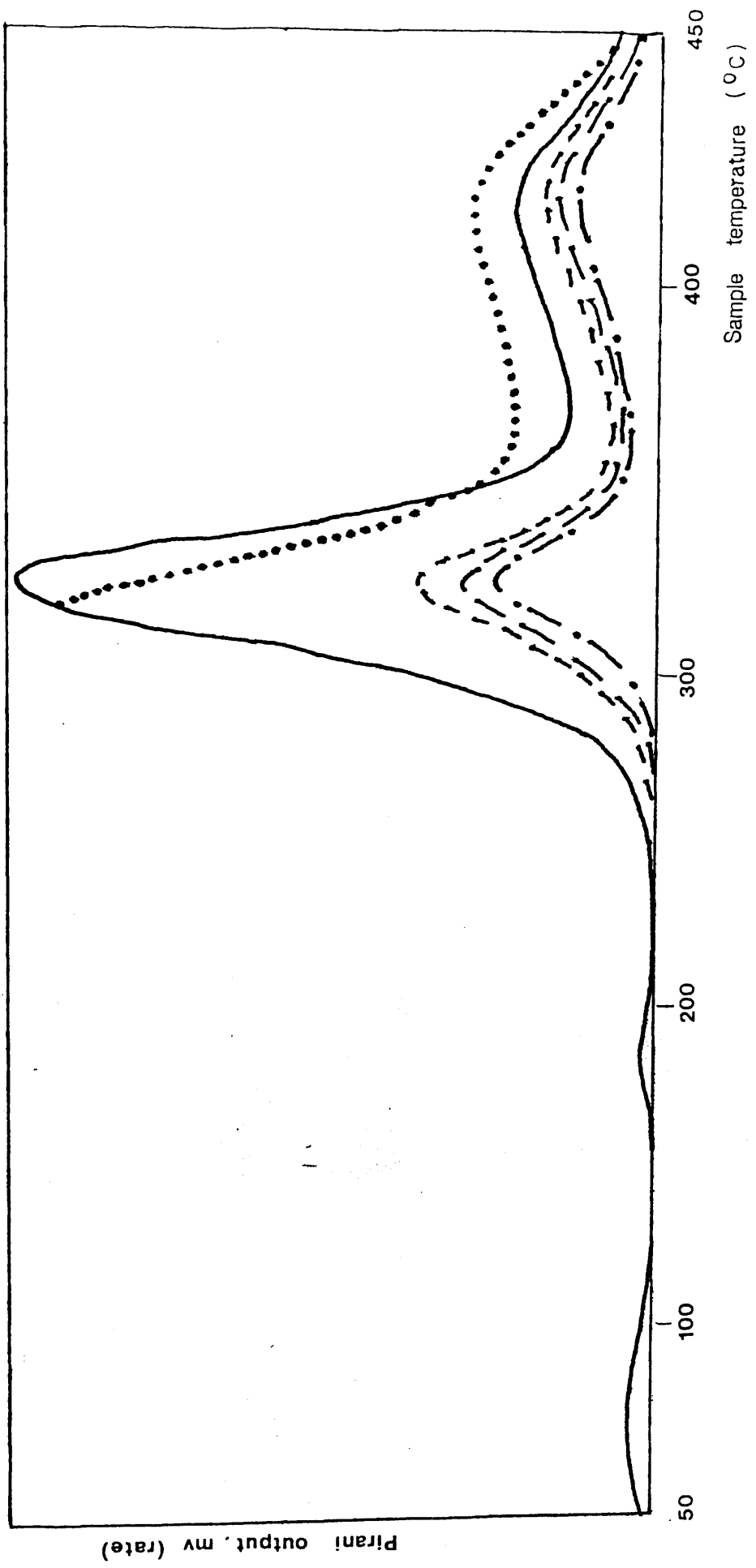


Figure 9.1 TVA curve for 1:50 Co(acac)₃ - PVAc blend

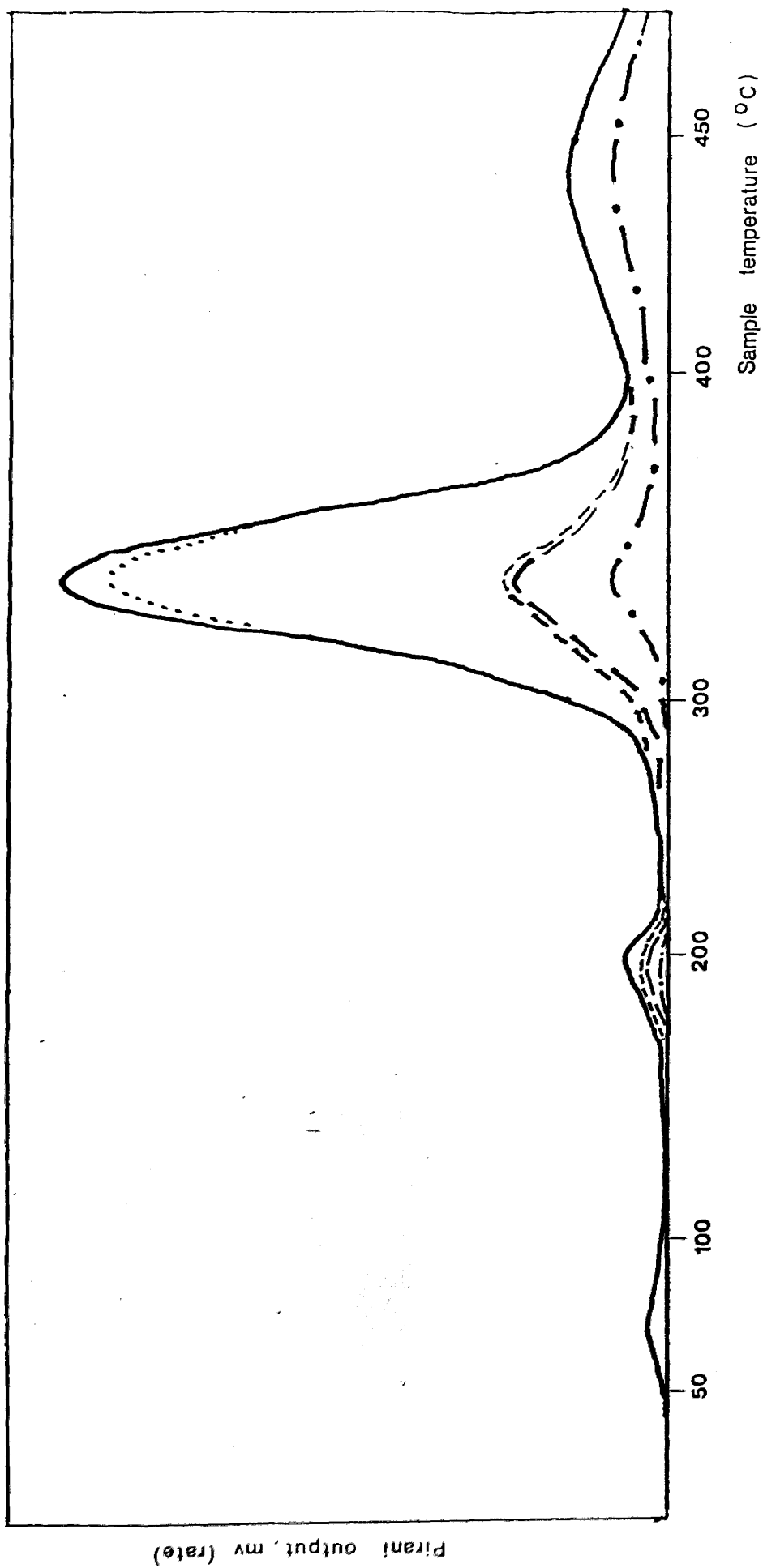


Figure 9.2 TVA curve for 1:10 Co(acac)₃ - PVAc blend

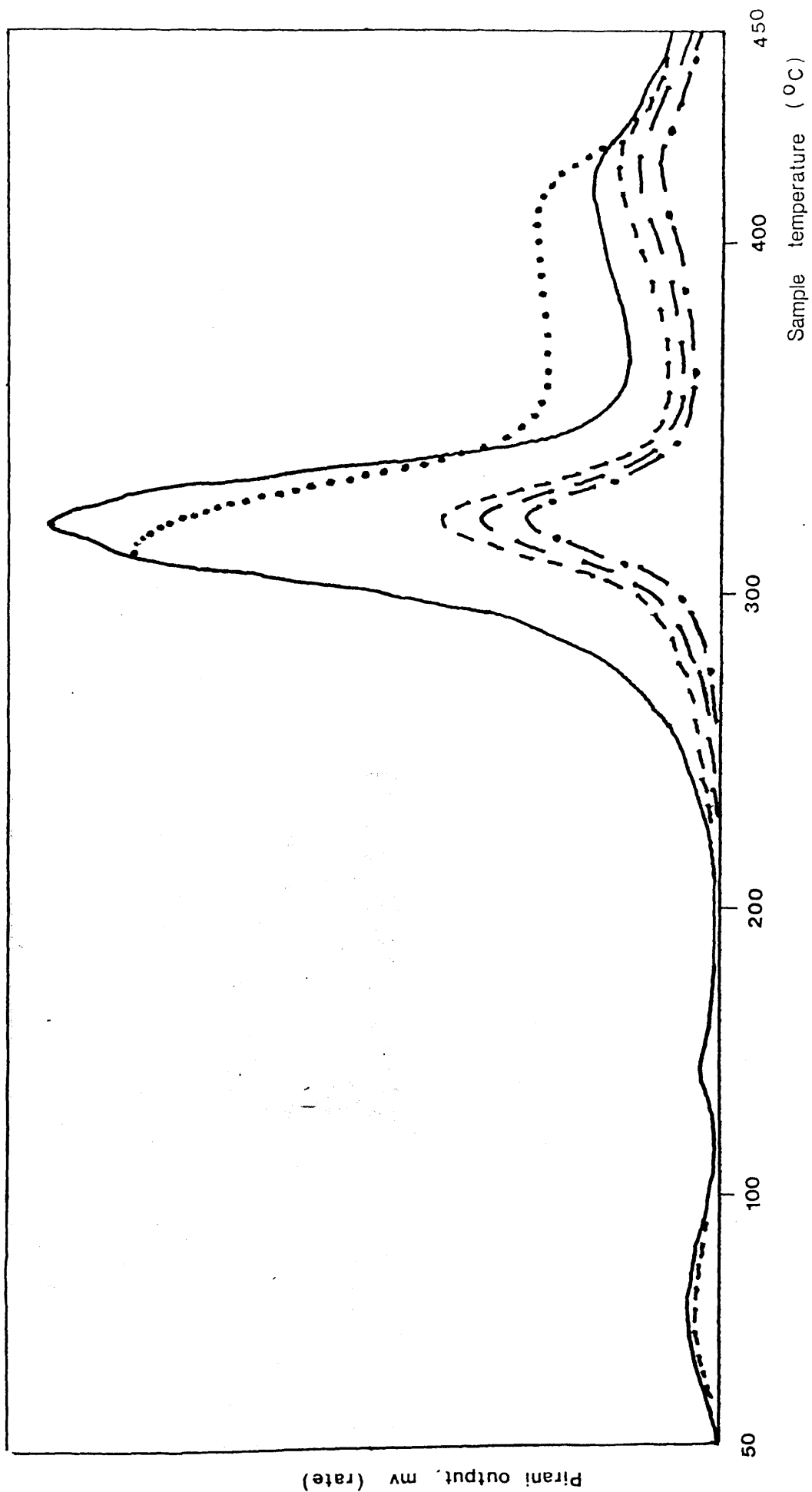


Figure 9.3 TVA curve for 1:50 Mn(acac)₃ - PVAc blend

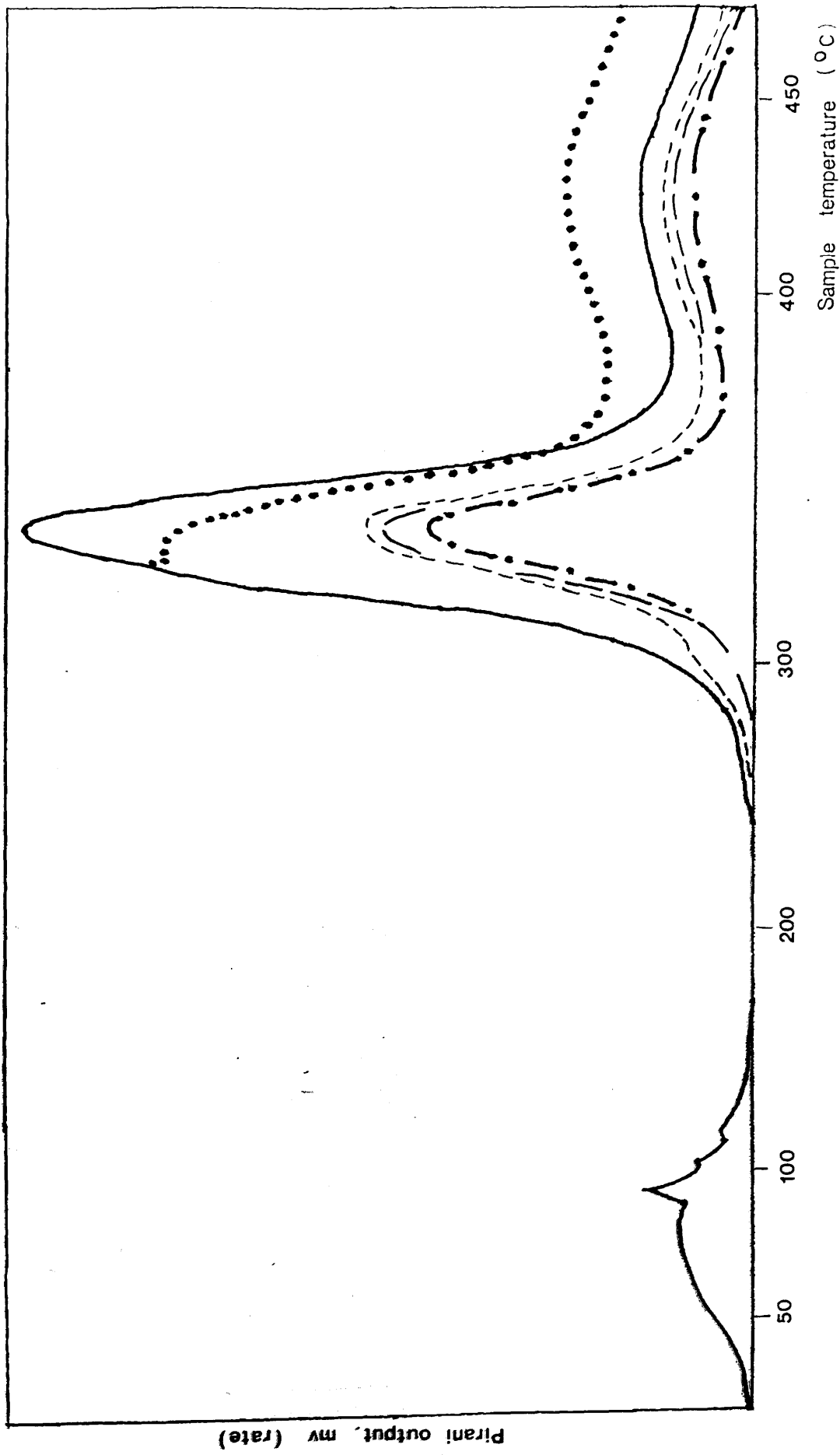


Figure 9.4 TVA curve for 1:50 Cu(acac)₂ - PVAc blend

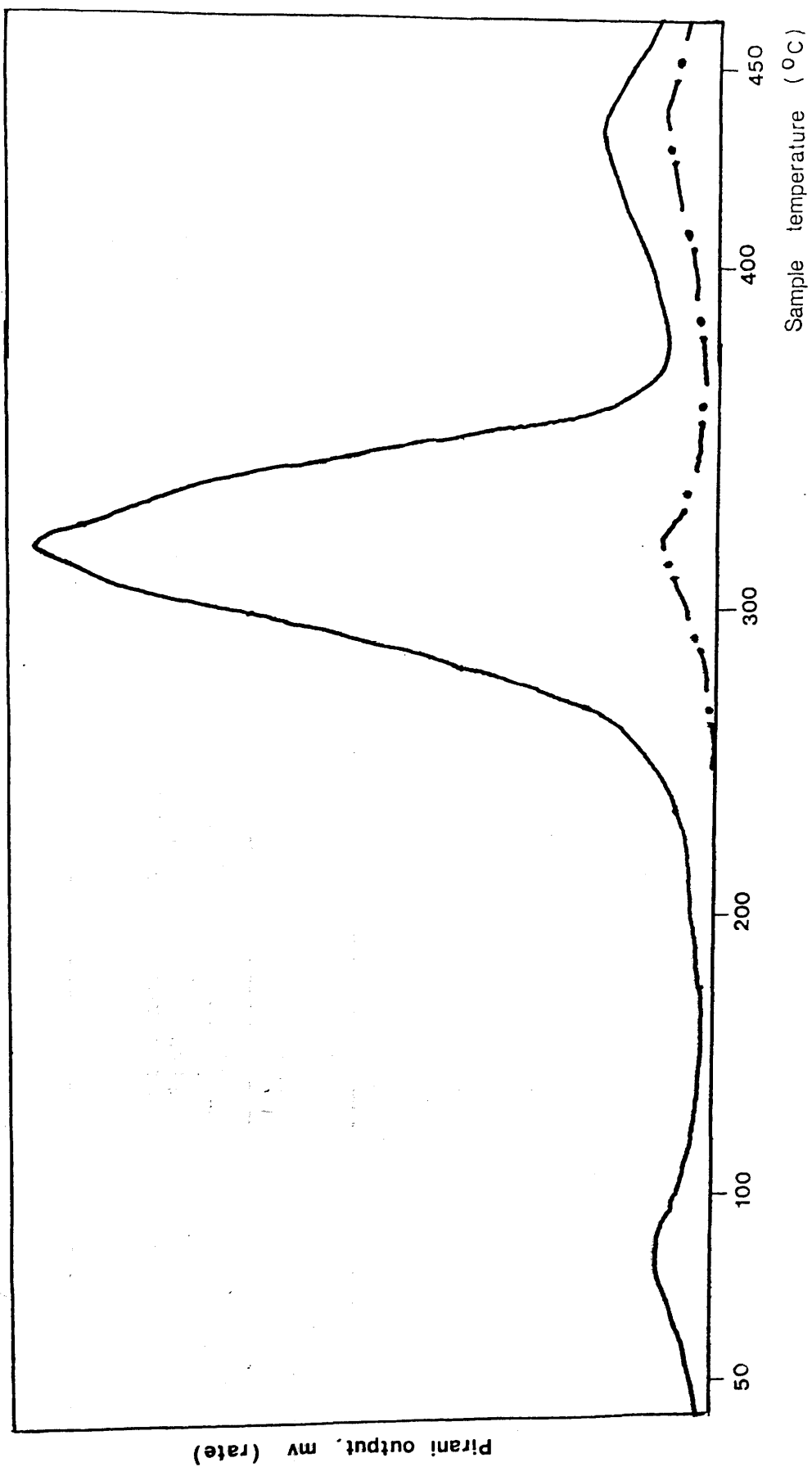


Figure 9.5 TVA curve for 1:50 $\text{Co}(\text{acac})_2$ - PVAc blend

FEATURE	PVAc UNBLEND-ED		Co(acac) ₃ 1:50		Co(acac) ₃ 1:10		Mn(acac) ₃ 1:50		Co(acac) ₂ 1:50		Cu(acac) ₂ 1:50	
Sublimation	-	95	95	86	95	Not recorded	95	Not recorded	95			
T(onset)	-	145	145	138	138	Masked by solvent	-	-	-	-	-	-
1ST PEAK	-	184	184	190	190	145	-	-	-	-	-	-
T(max)	-	225	225	224	224	200	190	221				
2ND PEAK	328	322	322	328	328	320	325	328				
T(max)	375	379	379	379	379	380	382	363				
3RD PEAK	435	433	433	441	441	424	444	433				
T(max)												

Temperatures in °C

Table 9.1 Features of TVA Curves of Several Chelate PVAc Blends

ANALYSIS OF PRODUCTS FROM BLENDS OF Co(acac)₃, Mn(acac)₃ AND Co(acac)₂ WITH PVAc AT VARIOUS STAGES OF THE HEATING PROGRAMME

The analysis of -196°C condensible gas and liquid products, cold ring fraction and solid residues from the Co(acac)₃ and Mn(acac)₃ - PVAc blends (1:50 chelate: monomer unit) were performed using the standard procedures outlined in earlier chapters. The -196°C non-condensable products from the degradation to 485°C of the 1:50 Co(acac)₂ - PVAc blend were also analysed. No attempts were made to identify non-condensable products. All samples were around 50mg and were cast from methylene chloride.

1:50 Co(acac)₃ - PVAc BLEND

STRUCTURE AND CHANGES ON DEGRADATION

The IR spectra of the undegraded blend and the residue on degradation to 225°C, 328°C and 485°C are reproduced in Fig. 9.6. The UV spectra of the undegraded blend and the residue at 225°C are shown in Fig. 9.7. The important structural features are listed in Table 9.2.

STRUCTURE OF THE UNDEGRADED BLEND

The blend is completely compatible, being transparent with a green tint. Neither UV nor IR spectra show any evidence of an interaction between the polymer

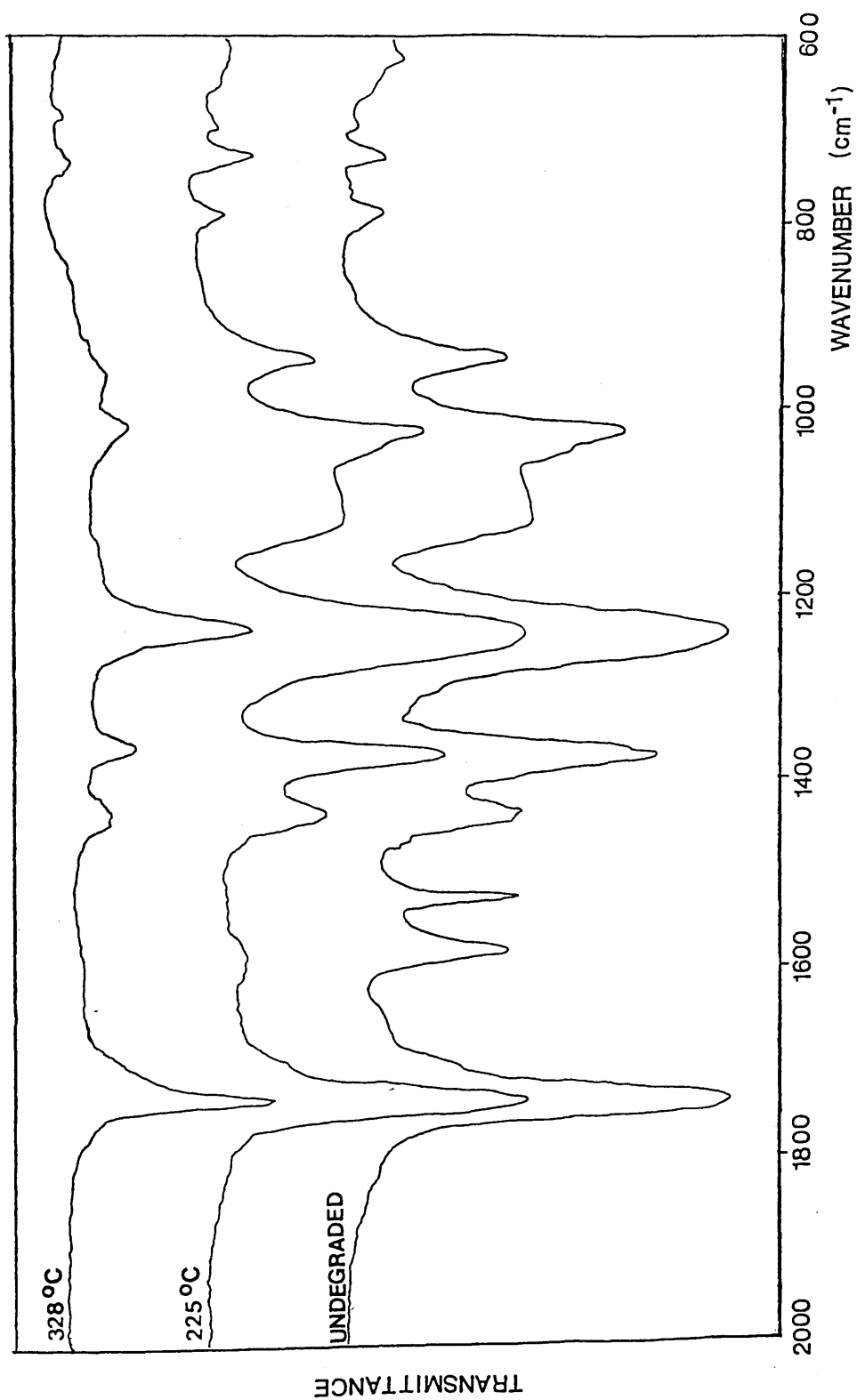


Figure 9.6 IR spectra of 1:50 Co(acac)₃ - PVAc blend at various stages of degradation

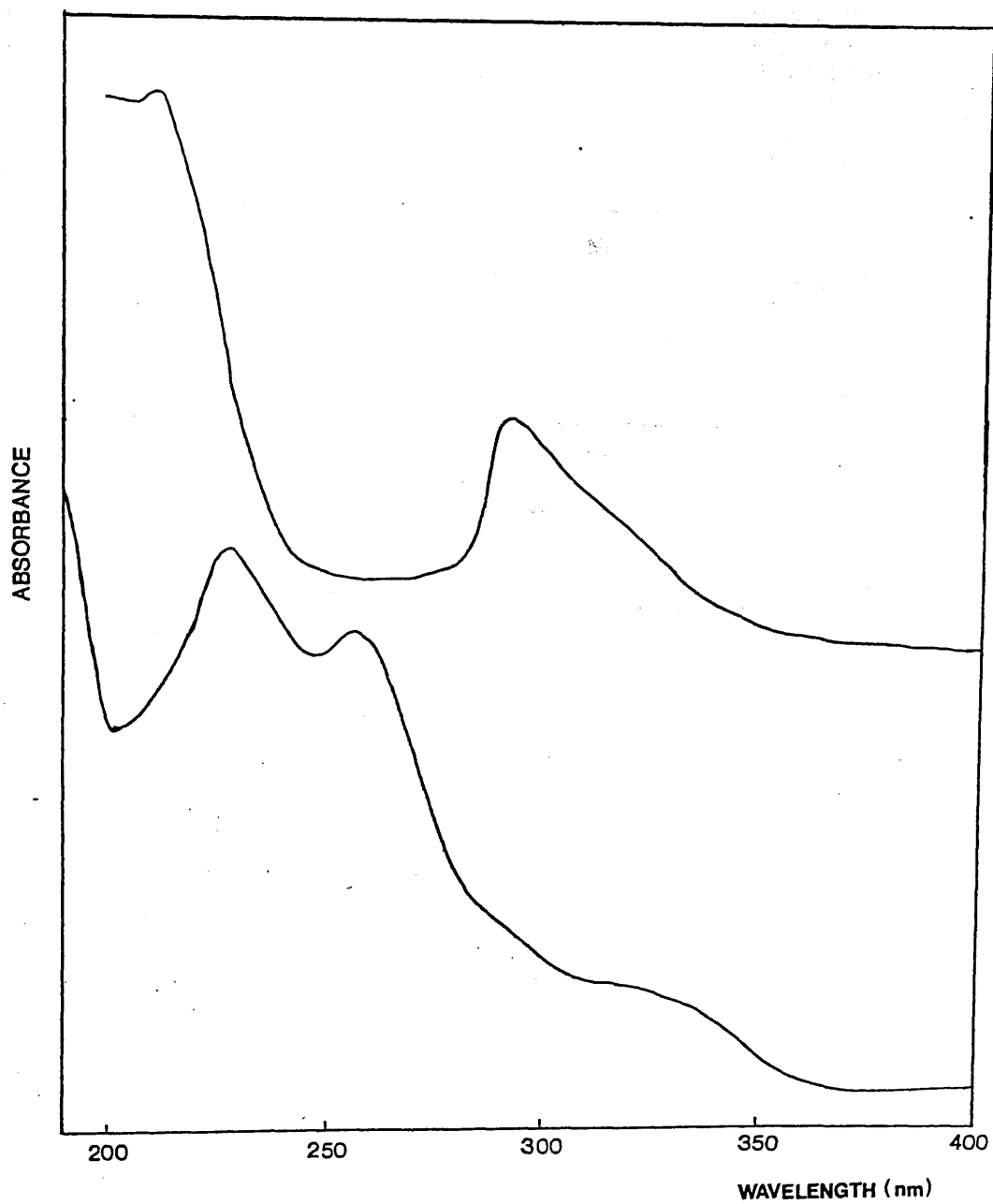
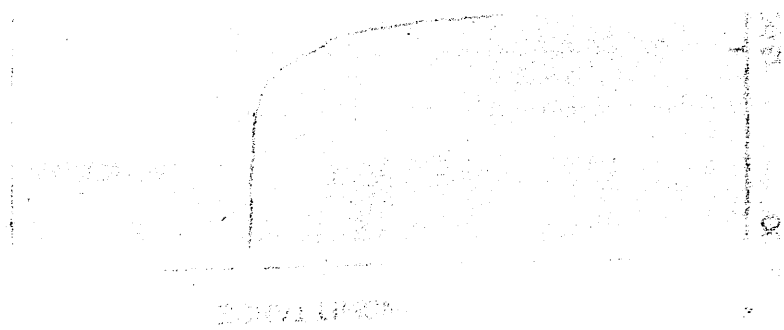


Figure 9.7 UV spectra of 1:50 Co(acac)₃ - PVAc blend before and after degradation to 225°C

EXTENT OF DEGRADATION	VISUAL APPEARANCE	SOLUBILITY IN CH ₂ Cl ₂	SPECTROSCOPIC FEATURES
None	Green, transparent, compatible	Yes	IR and UV spectra show no sign of interaction
225°C	Transparent, tinted light brown	Yes	No chelate absorptions in IR spectrum but 1580cm ⁻¹ absorbance => carboxylate. UV spectrum similar to PVAc but 290nm absorption intensified and broadened.
328°C	Yellow-orange	No	IR spectrum similar to that of PVAc at the same extent of degradation (See Fig. 9.8)
485°C	Brown char	No	IR spectrum featureless

Table 9.2 Structure of 1:50 Co(acac)₃ - PVAc Blend and Changes During Degradation.



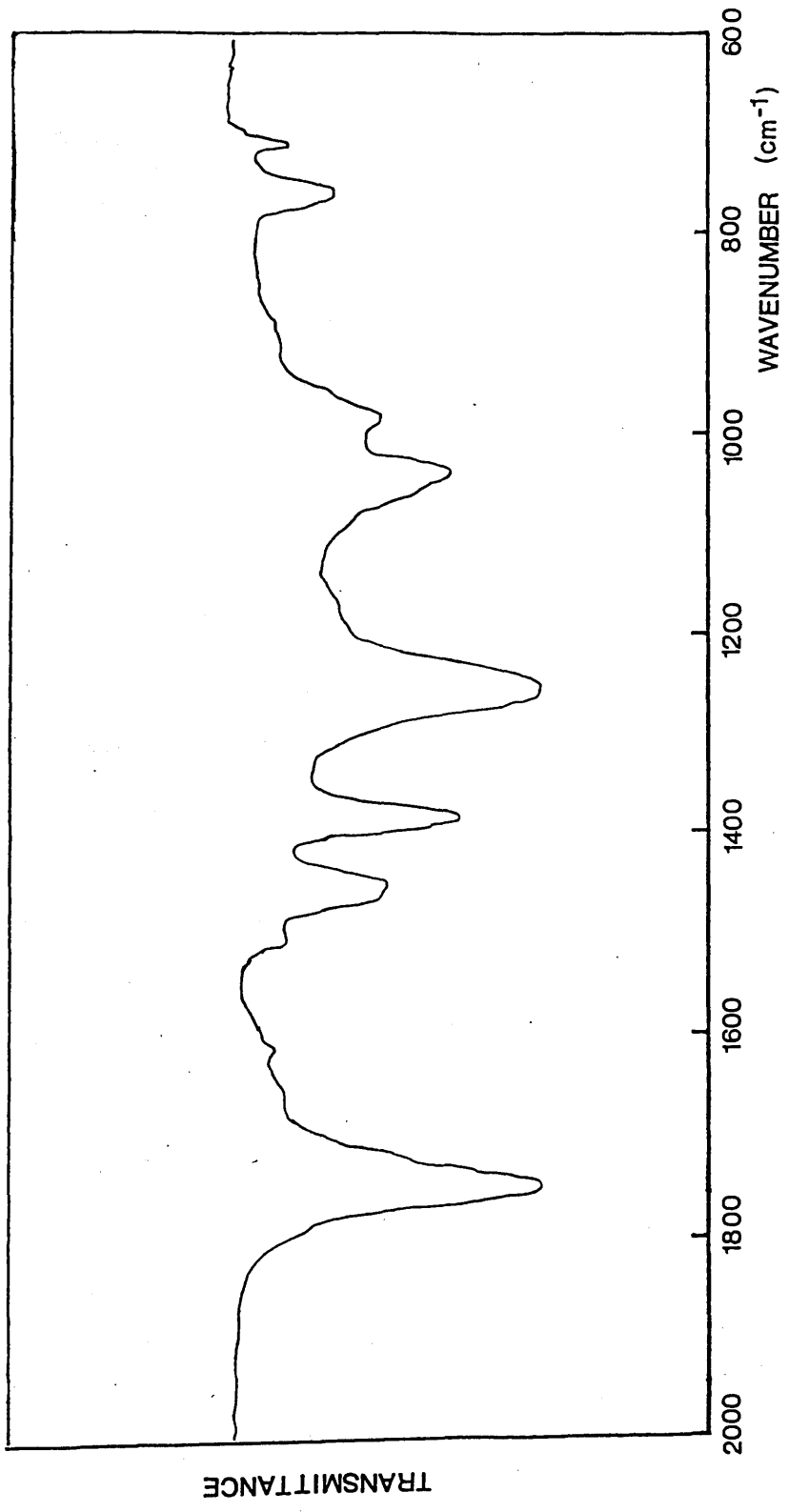


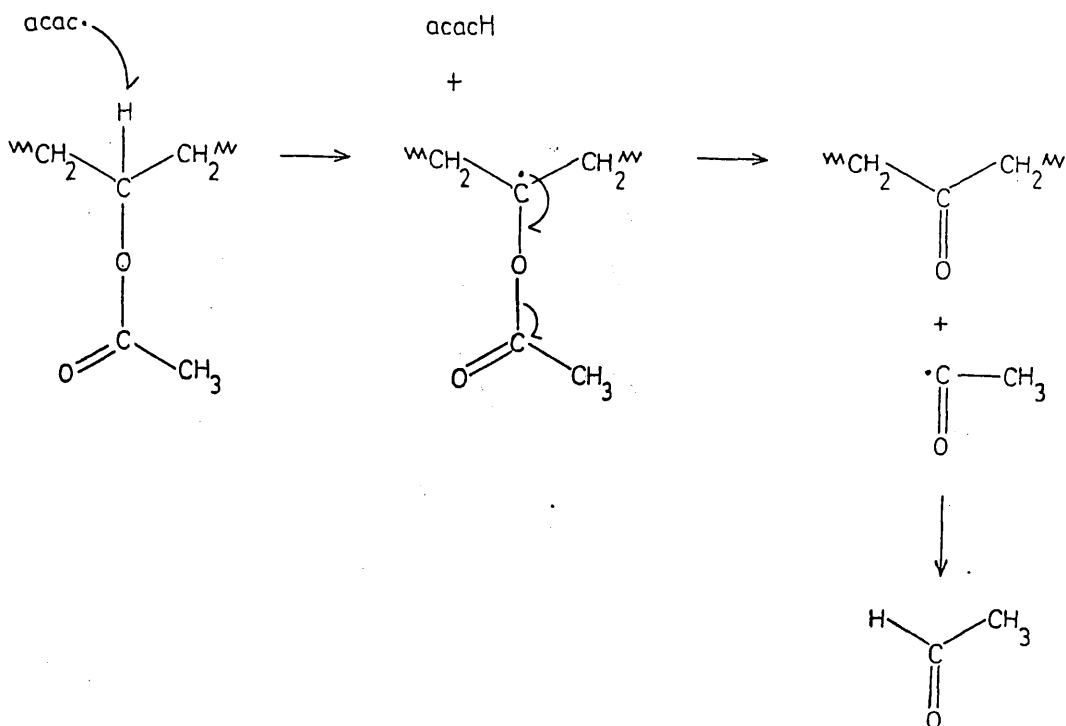
Figure 9.8 IR spectrum of PVAc after degradation to 325°C

and chelate. This was also the case for the $\text{Co}(\text{acac})_3$ - PMMA blends but for these blends there was TVA evidence for a $\text{Co}(\text{acac})_3$ - unsaturated chain end interaction. Such an interaction would also occur at any unsaturated chain ends of PVAc. However, for the same degree of polymerisation there are fewer unsaturated chain ends in PVAc than in PMMA,¹⁵⁵ and due to the different degradation behaviour of PVAc (i.e. no depolymerisation) the decomposition of such a π -complex would have only a minimal effect on the TVA curve.

CHANGES OF STRUCTURE ON DEGRADATION

The detection of acetylacetone as a product of degradation by 225°C (see following section) indicates decomposition of the $\text{Co}(\text{acac})_3$ with the formation of $\text{Co}(\text{acac})_2$. Both $\text{Co}(\text{acac})_3$ and $\text{Co}(\text{acac})_2$ will sublime from the blend and $\text{Co}(\text{acac})_2$ is itself unstable at this temperature, thus it is no surprise to find an absence of chelate absorptions in the IR spectrum of the residue at this point, although there is some carboxylate.

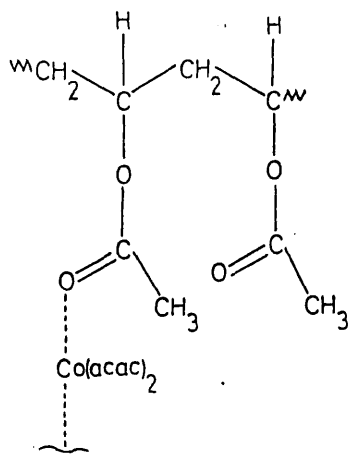
The formation of acetylacetone will involve the abstraction of H atoms by the $\text{acac}\cdot$ radicals produced in the reduction of $\text{Co}(\text{acac})_3$. This is most likely to occur at the labile α -hydrogen on the polymer backbone.



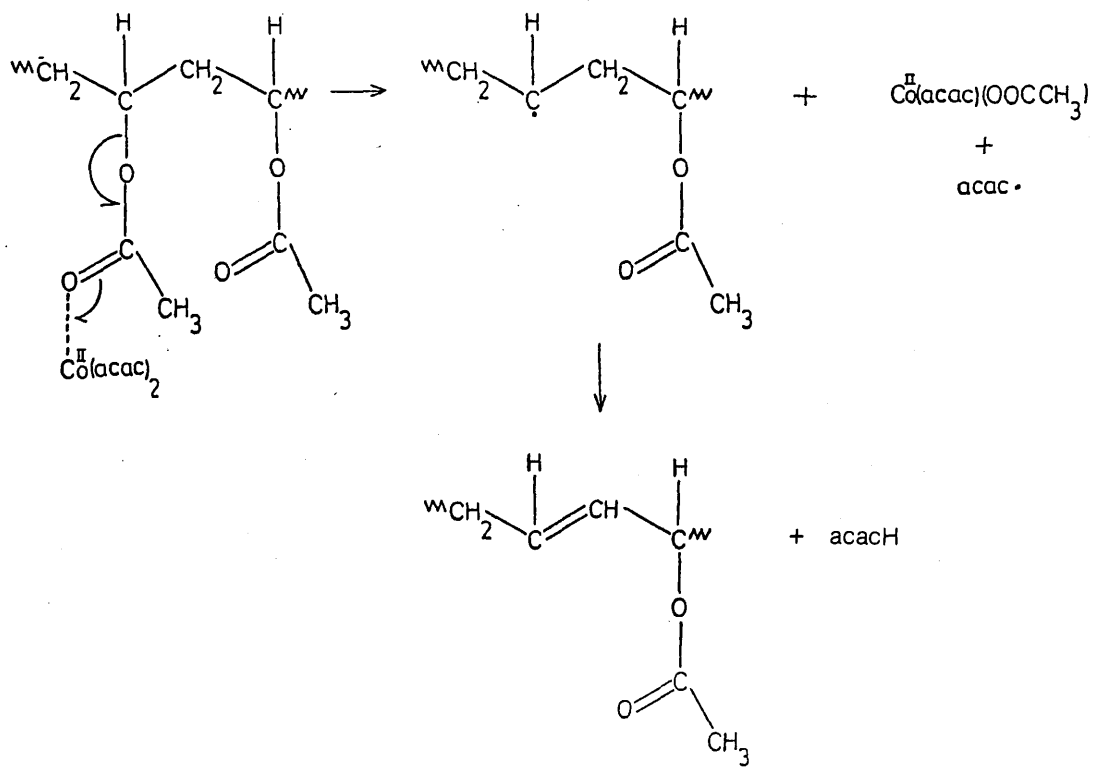
A ketonic absorption is not observed in the IR spectrum of the residue but this could easily be masked, at the expected low concentration of the ketone groups, by the ester absorption. The exaggerated 290nm absorption of the UV spectrum of the residue, which otherwise has the features of a slightly unsaturated PVAc could be due to a saturated ketone as such groups absorb in this region with an extinction coefficient similar to PVAc. However, it is more likely to be due to the presence of a trace amount of $\text{Co}(\text{acac})_2$ which absorbs in this region with an extinction coefficient some 300 times that of PVAc.

When formed, some $\text{Co}(\text{acac})_2$ will associate with the acetate side groups in the same manner as with

the ester groups of PMMA, (see following section on the structure of the $\text{Co}(\text{acac})_2$ - PVAc blend).



However, the bonding of the ester oxygen directly to the polymer backbone in PVAc precludes the formation of a polymer-bound cobalt carboxylate analogous to that formed in the $\text{Co}(\text{acac})_3$ - PMMA blends. Instead, the carboxylate salt is formed via the scission of the acetate group from the main chain, the scission being promoted by the association with the chelate.



This accounts for the presence of the unsaturation found in the blend at 225°C without any concurrent evolution of acetic acid (see following section). The lack of polymer-bound carboxylate structures removes the possibility of the crosslinking observed at this same temperature in the PMMA blends.

The $\text{Co}(\text{acac})(\text{OOCCH}_3)$ is not as stable as the cobalt methacrylate salts (no carboxylate is present at 328°C) and will decompose to cobalt oxide and small radical species such as $\text{CH}_3\overset{\text{O}}{\parallel}\text{C}\cdot$ which would attack the polymer chain in much the same fashion as the acac radicals. However above 225°C the normal deacetylation process predominates and the structure of the residue at 328°C is that typical of the degradation of PVAc - highly unsaturated and cross-linked.

-196°C CONDENSIBLE PRODUCTS AND COLD RING FRACTION
FROM 1:50 Co(acac)₃ - PVAc BLEND

The volatile products from the 1:50 $\text{Co}(\text{acac})_3$ - PVAc blend are listed in Table 9.3. The absence of acetic acid as a product in the early stages of degradation is to be noted. Identification of acetone in the later stages is evidence for the formation of $\text{CH}_3\overset{\text{O}}{\parallel}\text{C}\cdot$ radicals by the decomposition of the cobalt-containing structures within the blend. Acetone could be formed along with carbon dioxide by attack of the $\text{CH}_3\overset{\text{O}}{\parallel}\text{C}\cdot$ radicals on the acetate units:-

	EXTENT OF DEGRADATION	
	225°C	485°C
TOTAL -196°C CONDENSIBLE PRODUCTS IDENTIFIED	Acetylacetone	Carbon dioxide, a ketene, acetone benzene, acetic acid (major product, prevents identification of acetylacetone by SAD/IR)
COLD RING FRACTION	Green, apparently Co(acac) ₃ sub- limate. IR spec. shows chelate absorptions + small carbonyl + alkene absorp- tions. UV spec. very similar to chelate π-complex	Considerable quantity of polymer chain fragments (highly unsaturated)

Table 9.3 -196°C Condensible Products and Cold Ring
Fraction From 1:50 Co(acac)₃ - PVAc Blend

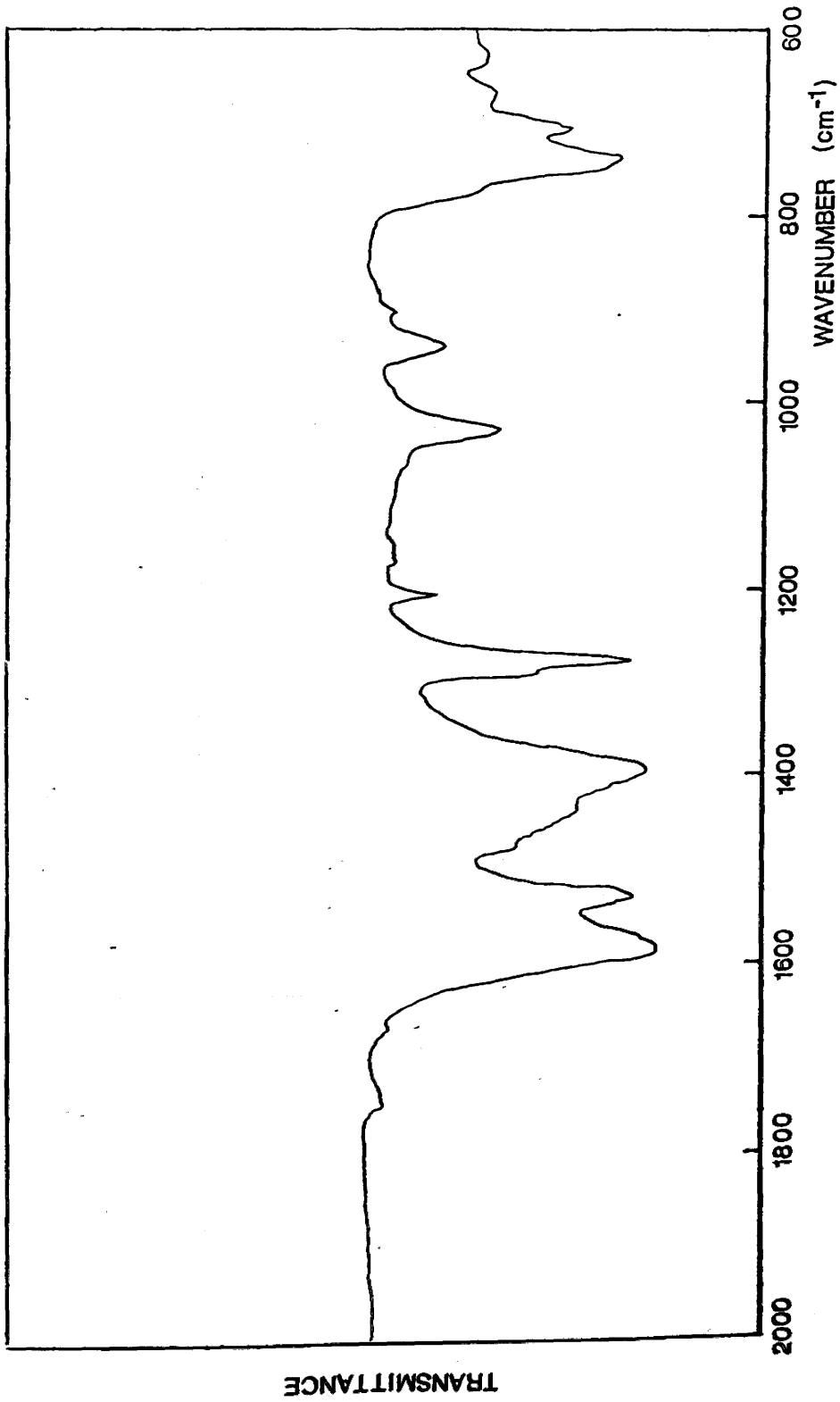


Figure 9.9 IR spectrum of CRF from 1:50 Co(acac)₃ - PVAc blend on degradation to 225°C

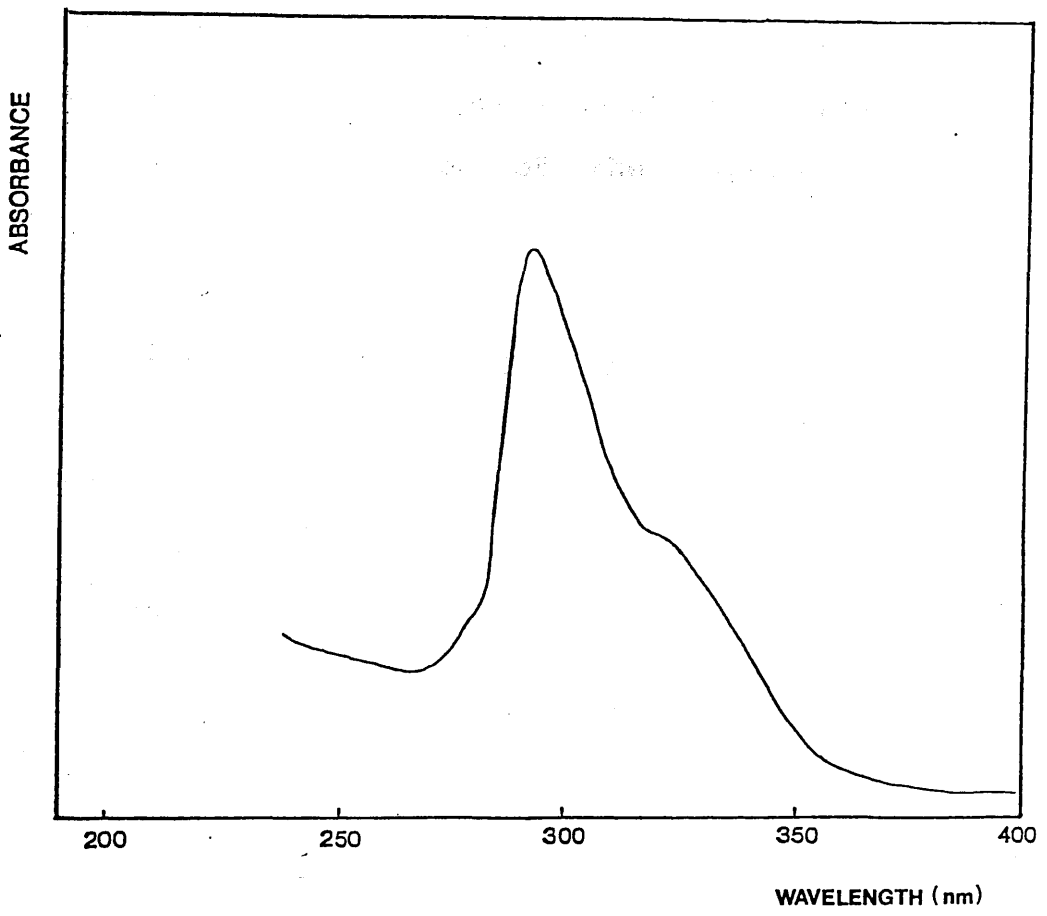


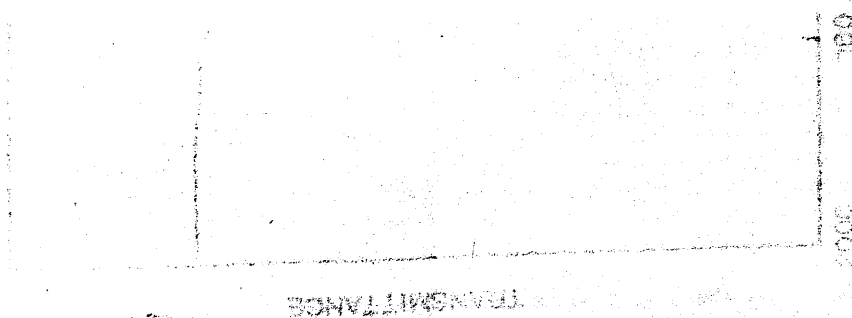
Figure 9.10 UV spectrum of CRF from 1:50 $\text{Co}(\text{acac})_3$ - PVAc blend on degradation to 225°C

1:50 Co(acac)₂ - PVAc BLENDSTRUCTURE OF THE UNDEGRADED BLEND

The IR spectrum of the undegraded 1:50 Co(acac)₂ - PVAc blend is reproduced in Fig. 9.11 and shows simply the sum of the Co(acac)₂ and PVAc spectra. The UV spectrum is shown in Fig. 9.12 and shows a shift in $\lambda(\text{max})$ to 289nm (relative to 291nm in methylene chloride). A similar shift also occurs in the PMMA blends and in the presence of methyl acetate and indicates the coordination of the Co(acac)₂ by the ester groups.

-196°C CONDENSIBLE GASEOUS AND LIQUID PRODUCTS

On degradation to 485°C, the -196°C condensible products were the same as those identified from the Co(acac)₃ - PVAc blend (acetic acid masked any acetylacetone).



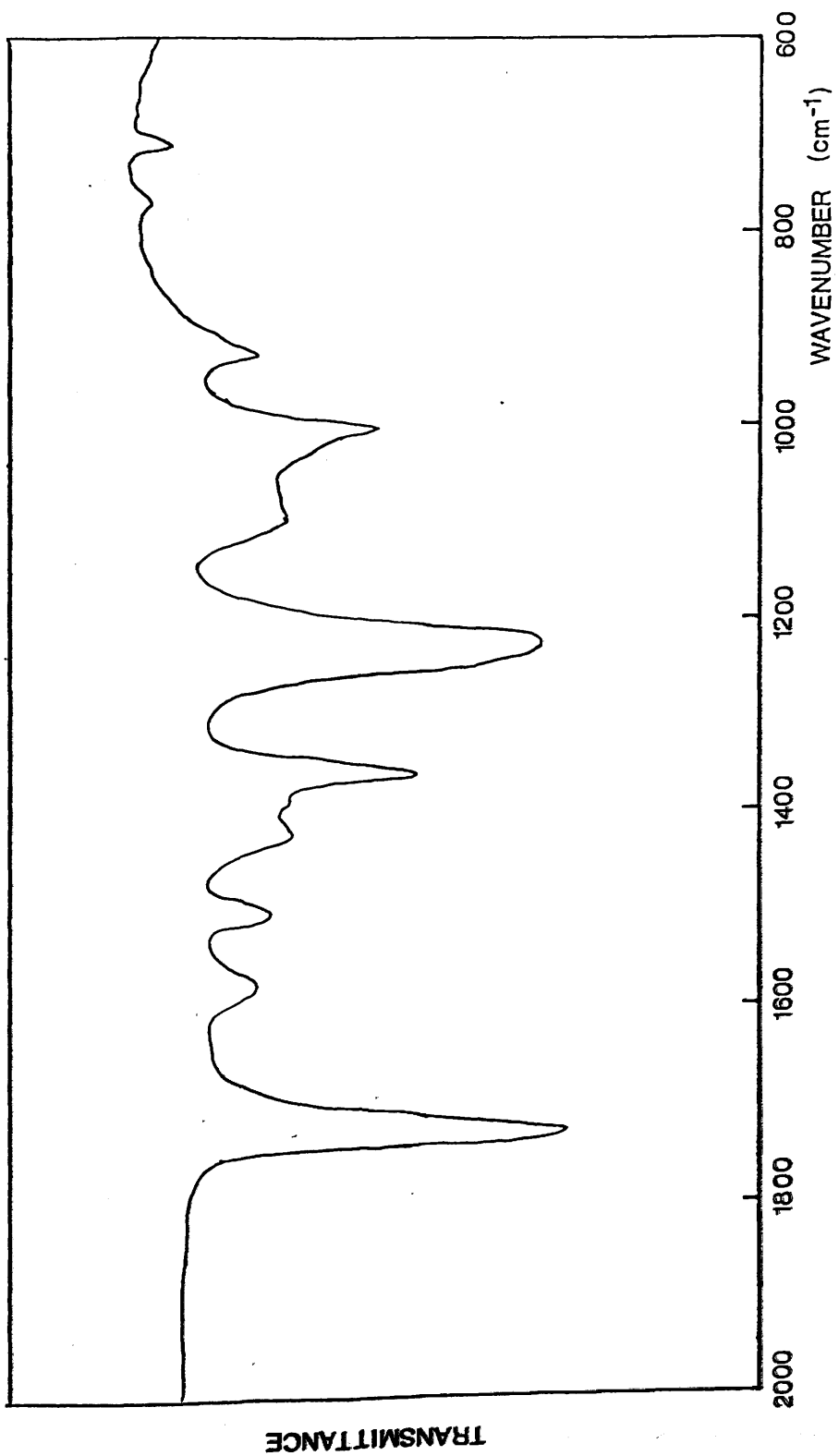


Figure 9.11 IR spectrum of 1:50 Co(acac)₂ - PVAc blend

The UV spectrum of the blend shows a broad absorption band centered at approximately 285 nm, which is characteristic of the Co(acac)₃ complex. The absorbance increases significantly in the 200-250 nm region, indicating the presence of the complex in the blend.

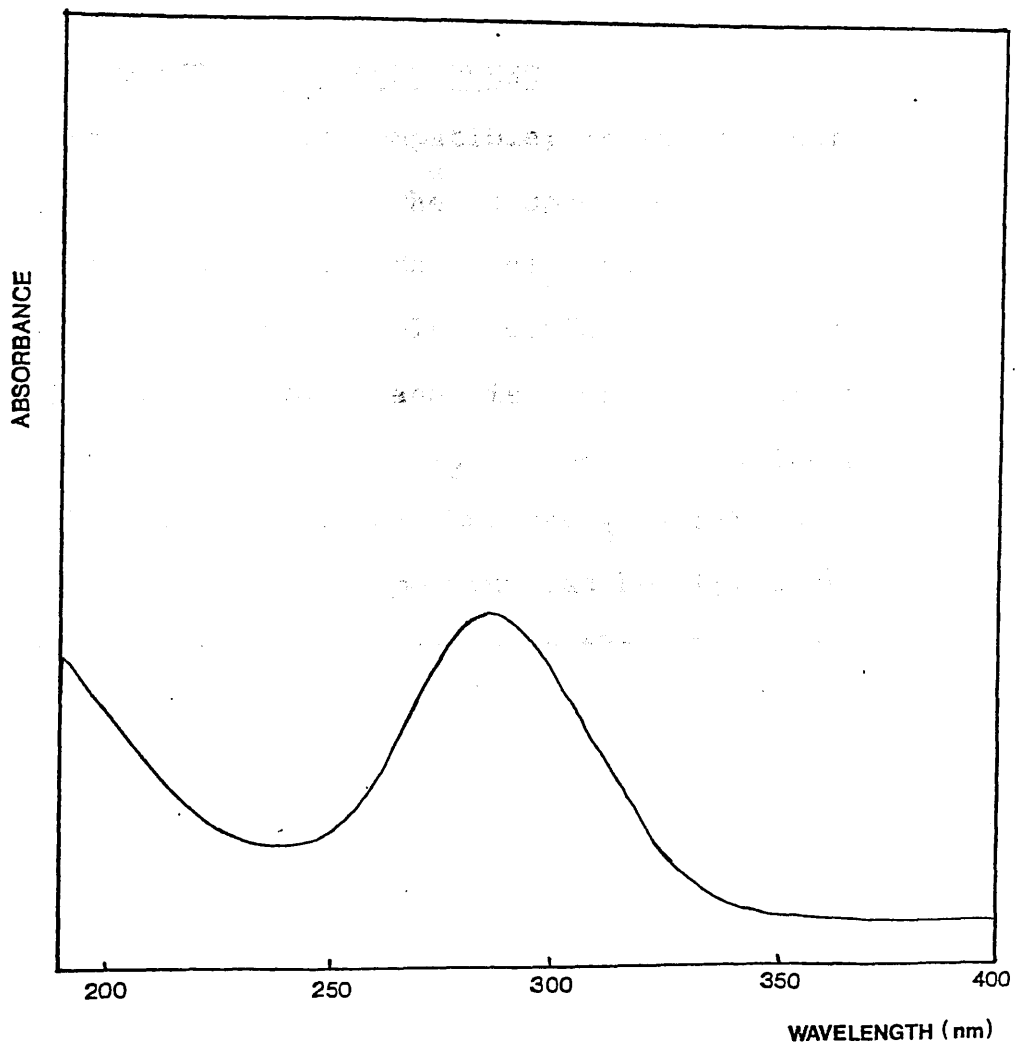


Figure 9.12 UV spectrum of 1:50 Co(acac)₂ - PVAc blend

1:50 Mn(acac)₃ - PVAc BLENDSTRUCTURE AND CHANGES ON DEGRADATION

The IR spectra of the undegraded blends on the residue at 178°C, 328°C and 485°C are shown in Fig. 9.13. The UV spectrum of the undegraded blend and that of the residue at 178°C are reproduced in Fig. 9.14. See Table 9.4.

STRUCTURE OF THE UNDEGRADED BLEND

The blend is compatible; it is transparent with a brown colouration. The IR spectrum shows simply the sum of the PVAc and Mn(acac)₃ absorptions but the UV spectrum is considerably different from those of Mn(acac)₃ and PVAc and is very similar to that obtained for the Mn(acac)₃ - PMMA blends (Chapter 5). As in the case of the Mn(acac)₃ - PMMA blends, the appearance of the UV spectrum can be attributed to the association of the chelate with the ester side groups. However, Mn(acac)₃ sublimes from the compatible PVAc blend unlike the case of the compatible 1:50 Mn(acac)₃ - PMMA blend, and this reflects a weaker interaction with the acetate groups, presumably for steric reasons. The reversibility of the complex formation was demonstrated by dissolving a 1:50 Mn(acac)₃ - PVAc blend in toluene and precipitating the polymer in diethyl ether; the precipitated polymer contained no chelate detectable by UV or IR spectroscopy (Figs. 9.15,

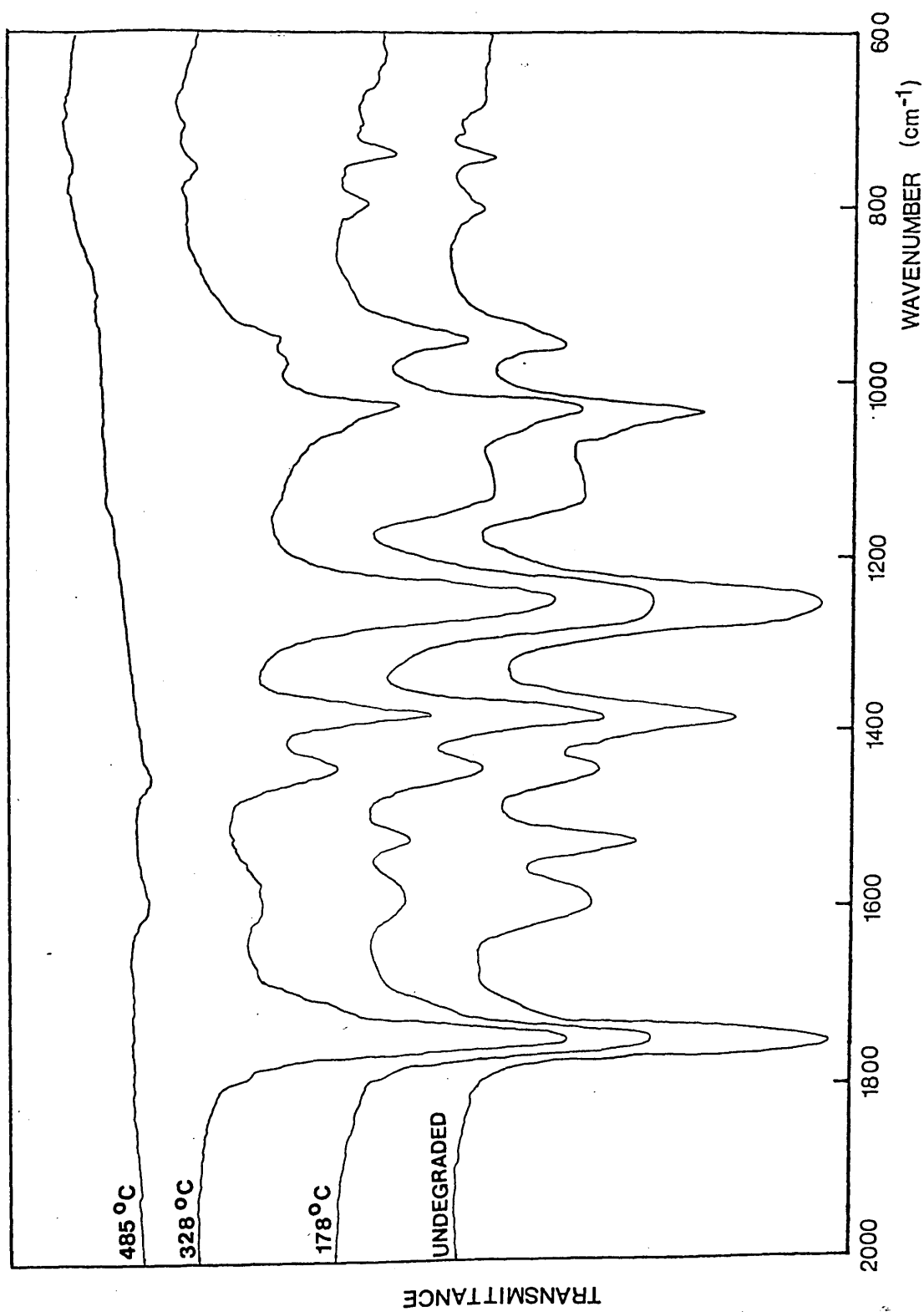


Figure 9.13 IR spectra of 1:50 Mn(acac)₃ - PVAc blend at various stages of the heating programme

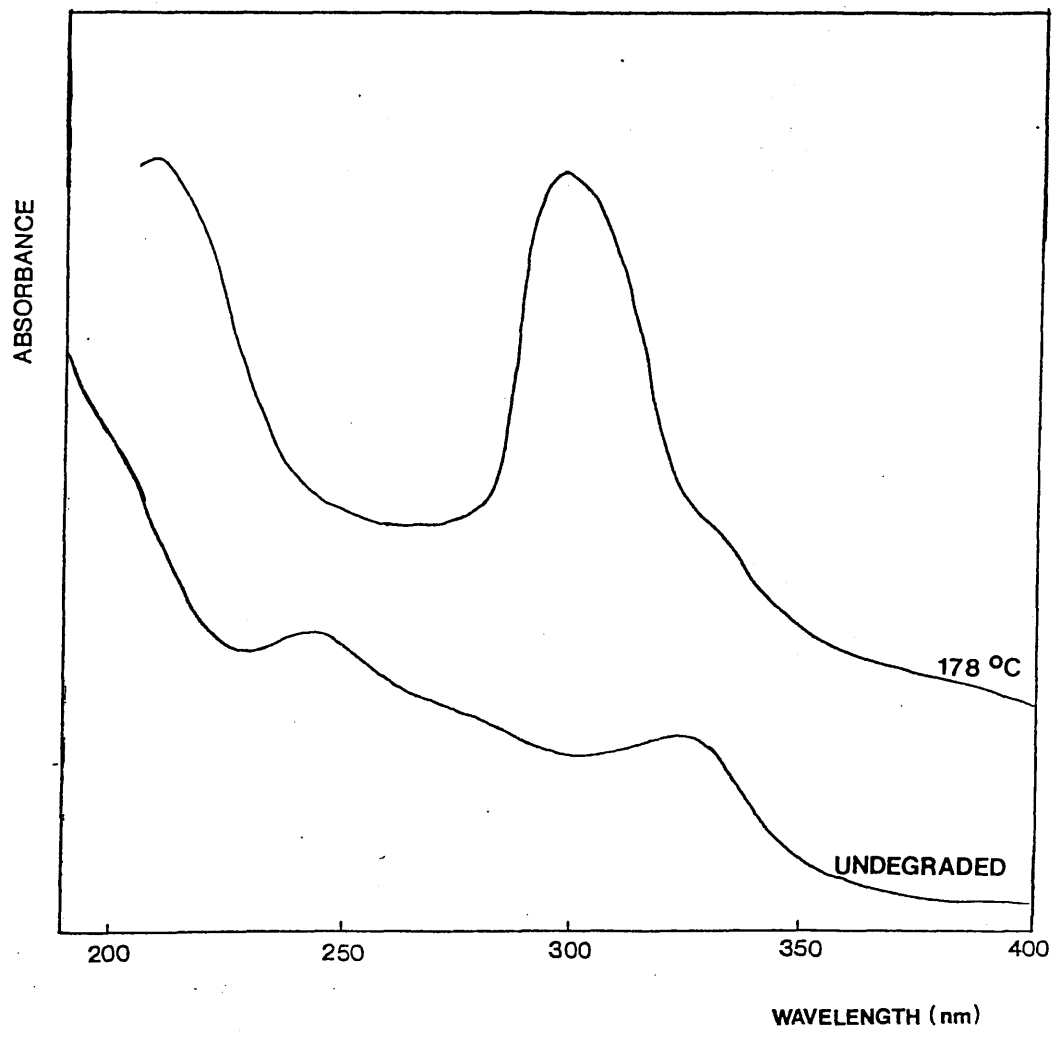


Figure 9.14
UV spectra of 1:50 Mn(acac)₃ - PVAc blend before
and after degradation to 178°C

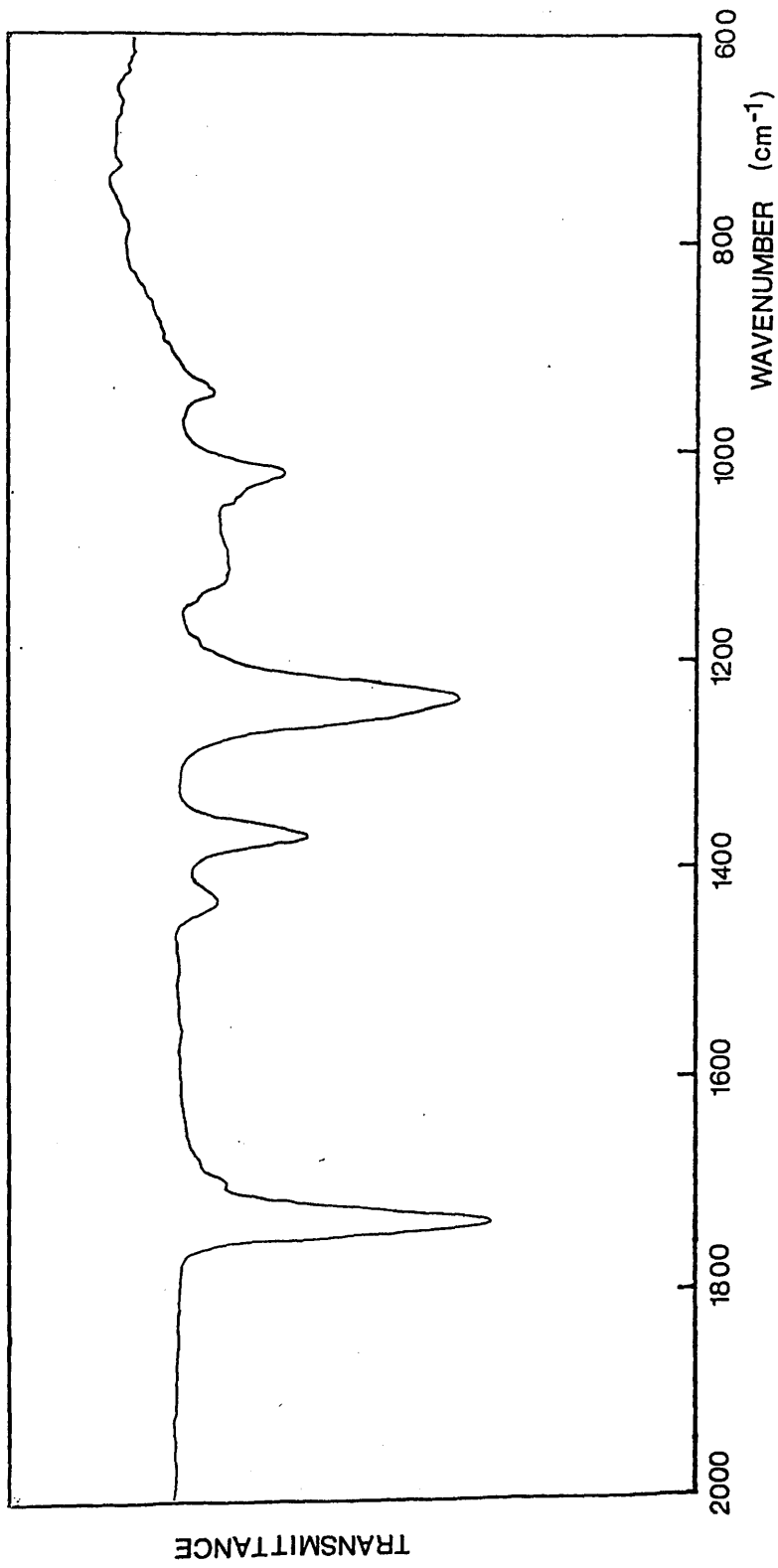


Figure 9.15 IR spectrum of 1:50 Mn(acac)₃ - PVAc blend after precipitation

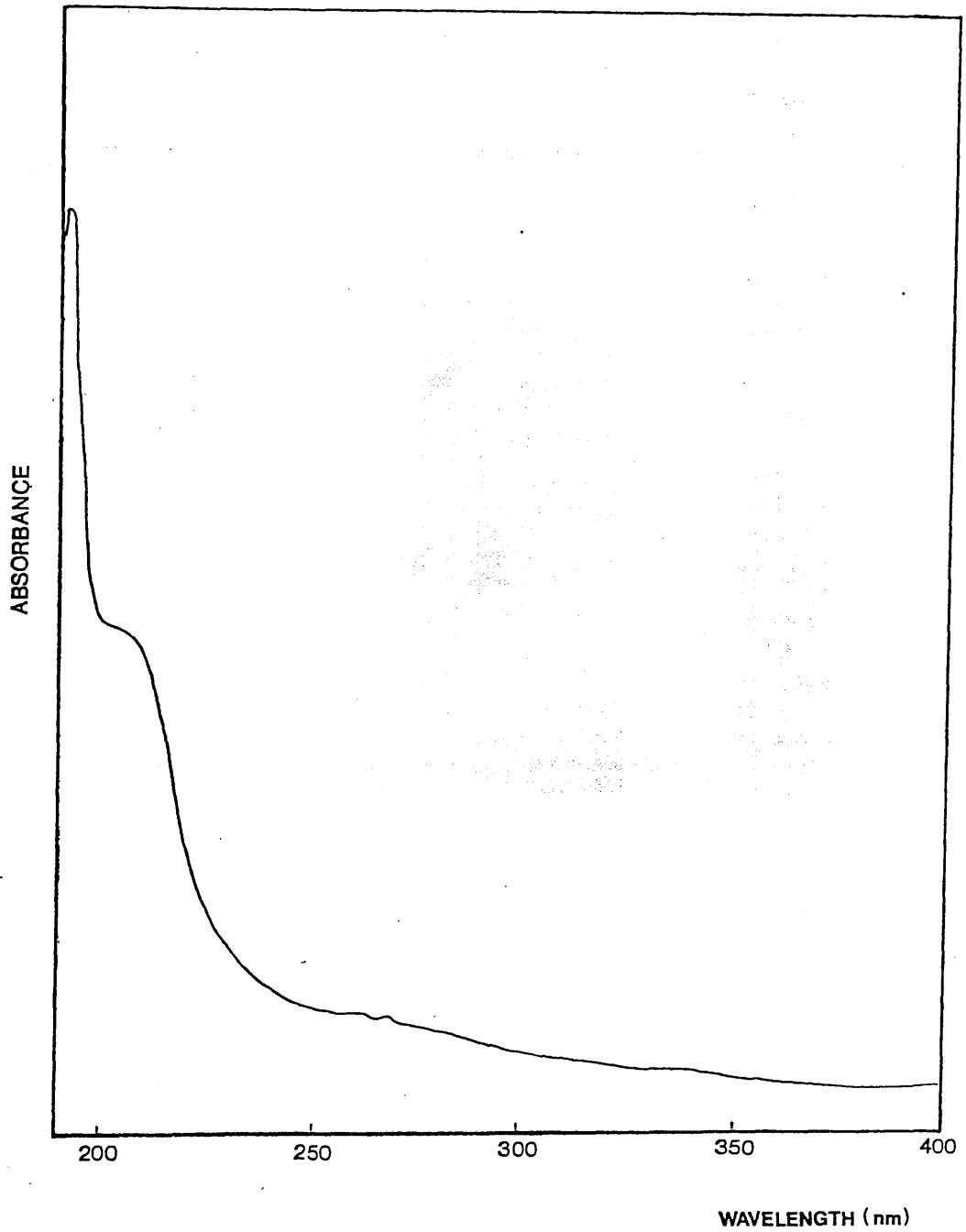


Figure 9.16 UV spectrum of 1:50 Mn(acac)₃ - PVAc blend after precipitation

EXTENT OF DEGRADATION	VISUAL APPEARANCE	SOULBILITY IN CH_2Cl_2	SPECTROSCOPIC FEATURES
None	Brown, transparent, compatible	Yes	IR spectrum - simply chelate + polymer. UV spectrum - complex series of absorptions very similar to $\text{Mn}(\text{acac})_3$ - PMMA or copolymer blends
178°C	Similar to undegraded blend	Yes	IR spectrum shows decrease in chelate concentration. Relative intensification of 1580cm^{-1} band suggests carboxylate structure. UV spectrum shows PVAc (some unsaturation) plus 296nm peak similar to $\text{Mn}(\text{acac})_3$ - PMMA blends at comparable stage of degradation
328°C	Yellow-orange	No	IR spectrum, shows broad absorption centred on 1580cm^{-1} => carboxylate remains. Otherwise comparable to PVAc at the same extent of degradation (Fig. 9.8)
485°C	Brown char	No	No identifiable features

Table 9.4 Structure of 1:50 $\text{Mn}(\text{acac})_3$ - PVAc Blend and Changes During Degradation

9.16).

CHANGES OF STRUCTURE ON DEGRADATION

The structural changes parallel those in the $\text{Co}(\text{acac})_3$ - PVAc blend with the formation of bis chelate, carboxylates and unsaturation. As already noted for the $\text{Co}(\text{acac})_3$ blend, polymer bound carboxylates of the chelate cannot be formed and the carboxylate present will be $\text{Mn}(\text{acac})(\text{OOCCH}_3)$. This manganese carboxylate, like the manganese methacrylates is more stable than its cobalt analogue and persists at 328°C .

Although as with the $\text{Co}(\text{acac})_3$ blend there is no evidence for the chain ketones or acetaldehyde, attack of the acac. radicals on the α -hydrogen is expected to yield backbone ketones.

The UV spectrum of the 178°C residue shows the same features as the 1:50 $\text{Mn}(\text{acac})_3$ - PMMA blend at the same temperature indicating that the association with the ester groups takes much the same form in both PMMA and PVAc blends.

-196°C CONDENSIBLE PRODUCTS AND COLD RING FRACTION
FROM 1:50 Mn(acac)₃ - PVAc BLENDS

The products identified from the degradation from the blend are listed in Table 9.5. The products are the same as those observed from the Co(acac)₃ - PVAc blend. The UV spectrum of the CRF at 178°C (Fig. 9.17) shows the same structure as the Co(acac)₃ - PVAc blend at a similar extent of degradation and can be explained similarly.

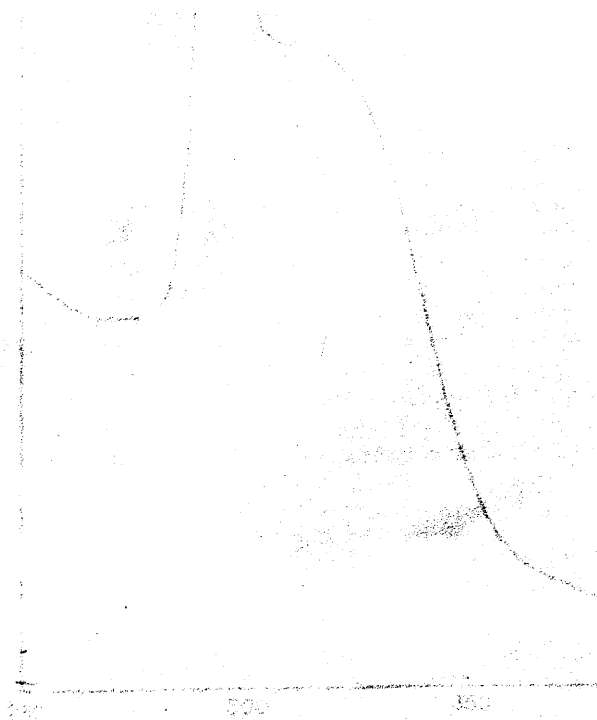


Figure 9.17
 UV spectrum of the cold ring fraction (CRF) from 1:50 Mn(acac)₃ - PVAc blend at degradation temperature of 178°C.

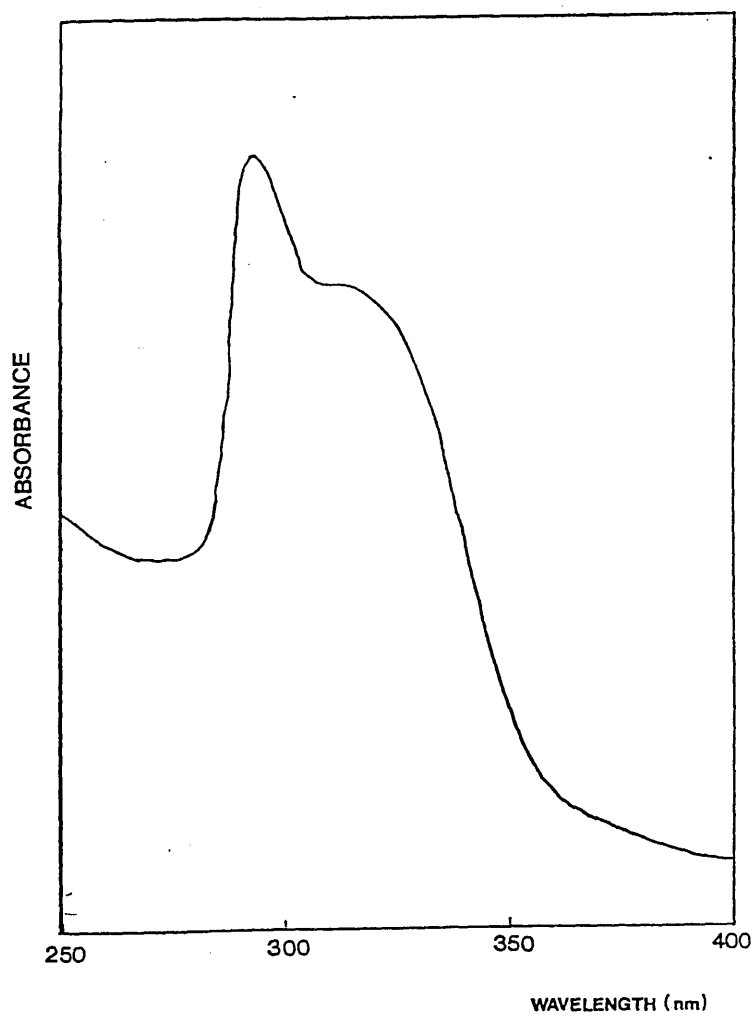


Figure 9.17
UV spectrum of CRF from 1:50 Mn(acac)₃ - PVAc
blend on degradation to 178°C

	EXTENT OF DEGRADATION	
	178°C	485°C
-196°C Condensable Products	Acetylacetone	Carbon dioxide, a ketene, acetone, benzene, acetic acid (major product, masks acetylacetone)
Cold Ring Fraction	Brown, apparently Mn(acac) ₃ sublimate IR spectrum typical of Mn(acac) ₃ . UV spectrum similar to chelate π-complex	Large quantity of highly unsaturated chain fragments

Table 9.5 -196°C Condensable Products and Cold Ring Fraction from 1:50 Mn(acac)₃ - PVAc Blend

EFFECT OF THE CHELATES ON THE THERMAL DEGRADATION OF PVAc - DISCUSSION

The structures of the blends at various stages of degradation and the mechanism of the production of acetylacetone and acetone, the only two products not observed from PVAc alone, have already been discussed and can be considered common to all the chelate-PVAc blends studied except the $\text{Cu}(\text{acac})_2$ blend.

The very small peak below 200°C on the TVA curves of the $\text{Co}(\text{acac})_3$ and $\text{Mn}(\text{acac})_3$ blends is due to the reduction of the chelate, the temperature of the $\text{Mn}(\text{acac})_3$ reduction being lowered by virtue of the ester interaction. As a consequence of this reduction, ketene groups are formed on the polymer backbone. Also occurring in this region is the formation of unsaturated units by side group scission with the associated formation of carboxylate structures.

At the low concentration of chelate employed, lessened still further by sublimation from the blend, neither the ketone groups (which would block deacetylation) nor the double bond structures (which would activate deacetylation) produced by the above reactions have any significant effect on the subsequent deacetylation process. The apparent lowering of the onset of deacetylation for the 1:10 $\text{Mn}(\text{acac})_3$ blend is almost certainly due to overlap with the decomposition of $\text{Mn}(\text{acac})_2$ which occurs above 200°C (such an effect was also observed with the 1:10 $\text{Mn}(\text{acac})_3$ -

PMMA blends). Similarly with the $\text{Co}(\text{acac})_2$ blend.

Of the chelates studied, $\text{Cu}(\text{acac})_2$ is the most thermally stable and will mostly sublime from the blend without decomposition. The effects of the decomposition of any chelate which remains within the polymer matrix would be masked by the normal deacetylation process of the polymer.

THE THERMAL DEGRADATION OF PS AND PVC

The thermal degradation and TGA behavior (Bontrene 161) and PVC (Breon 110) have already been discussed in Chapter 4.

THE THERMAL DEGRADATION OF THE COPOLYESTERS

This has already been discussed in Chapter 4.

PREPARATION OF COPOLYESTERS, $\text{Cu}(\text{acac})_2$ AND $\text{Co}(\text{acac})_2$ WITH PS

Samples of the copolyester blends (a weight ratio of 1:1) were prepared for TGA level studies by casting from chloroform solution. The case of a TGA tube, samples were ground 30-40 mesh and $\text{Cu}(\text{acac})_2$ and $\text{Co}(\text{acac})_2$ blends were combined.

The samples were dried in a "vacuum" oven at 100°C for 24 hours.

CHAPTER 10

BLENDS OF Co(acac)₃, Mn(acac)₃ AND Cu(acac)₂ WITH POLYSTYRENE AND PVC

INTRODUCTION

In view of the activity of Co(acac)_3 , Mn(acac)_3 and Cu(acac)_2 in the polymer blends discussed earlier, a brief TVA survey of the effect of these chelates on two other common polymers, polystyrene (PS) and poly(vinyl chloride) (PVC) was undertaken. The results are detailed in this chapter.

THERMAL DEGRADATION OF PS AND PVC

The thermal degradation and TVA behaviour of PS (Bextrene 161) and PVC (Breon 110) have already been discussed in Chapter 4.

THERMAL DEGRADATION OF THE CHELATES

This has already been discussed in Chapter 3

BLENDS OF Co(acac)₃, Mn(acac)₃, Cu(acac)₂ WITH PS

Samples of the chelate PS blends (chelate: monomer unit ratio of 1:50) were prepared for TVA in the usual manner by casting from chloroform solution onto the base of a TVA tube; samples were around 30 mg. The Co(acac)_3 and Mn(acac)_3 blends were compatible but the Cu(acac)_2 blend had a "frosted" appearance indicative of non-compatibility.

TVA BEHAVIOUR OF THE CHELATE - PS BLENDS

The TVA curves for the three blends are reproduced in Figs. 10.1-10.3. The T(onset) and T(max) values of the major peak are listed in Table 10.1.

Sublimation from the blend was observed in all cases and the cold ring fraction from each blend consisted of chelate and the chain fragments observed from the unblended polymer. The residue from the $\text{Co}(\text{acac})_3$ and $\text{Mn}(\text{acac})_3$ blends consisted merely of a bronzing of the tube base. There was virtually no residue from the $\text{Cu}(\text{acac})_2$ blend which indicates complete sublimation of $\text{Cu}(\text{acac})_2$ from the blend.

The first peak of all the TVA curves is due to solvent (the $\text{Mn}(\text{acac})_3$ - PS blend had been kept in a vacuum oven for several days and show only a very small solvent peak). There are no changes in the TVA curve of the $\text{Cu}(\text{acac})_2$ - PS blend relative to unblended polystyrene but there is an extra, though very small, peak in the TVA curves of the $\text{Co}(\text{acac})_3$ and $\text{Mn}(\text{acac})_3$ blends. In both cases, the T(max) of this small peak (197°C and 162°C respectively) indicates that it is associated with the decomposition of the chelates. The rise is in the 0°C and 45°C traces which suggests that it is due to acetylacetone.

The peak is smaller for the $\text{Co}(\text{acac})_3$ blend as some $\text{Co}(\text{acac})_3$ has sublimed from the film by this point. Sublimation from the $\text{Mn}(\text{acac})_3$ blend is observed only after the peak and thus must be due to the

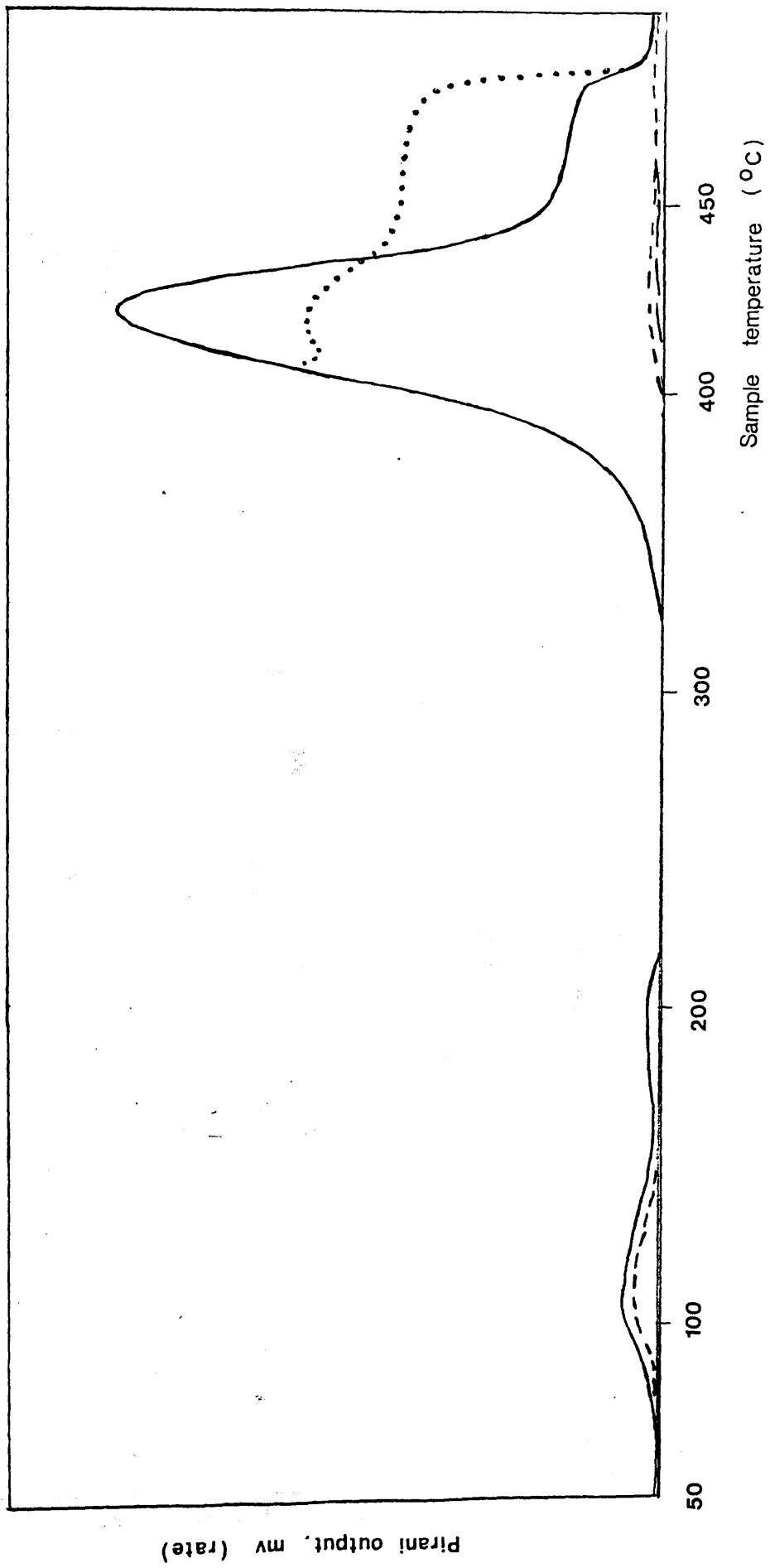


Figure 10.1 TVA curve for 1:50 Co(acac)₃ - PS blend

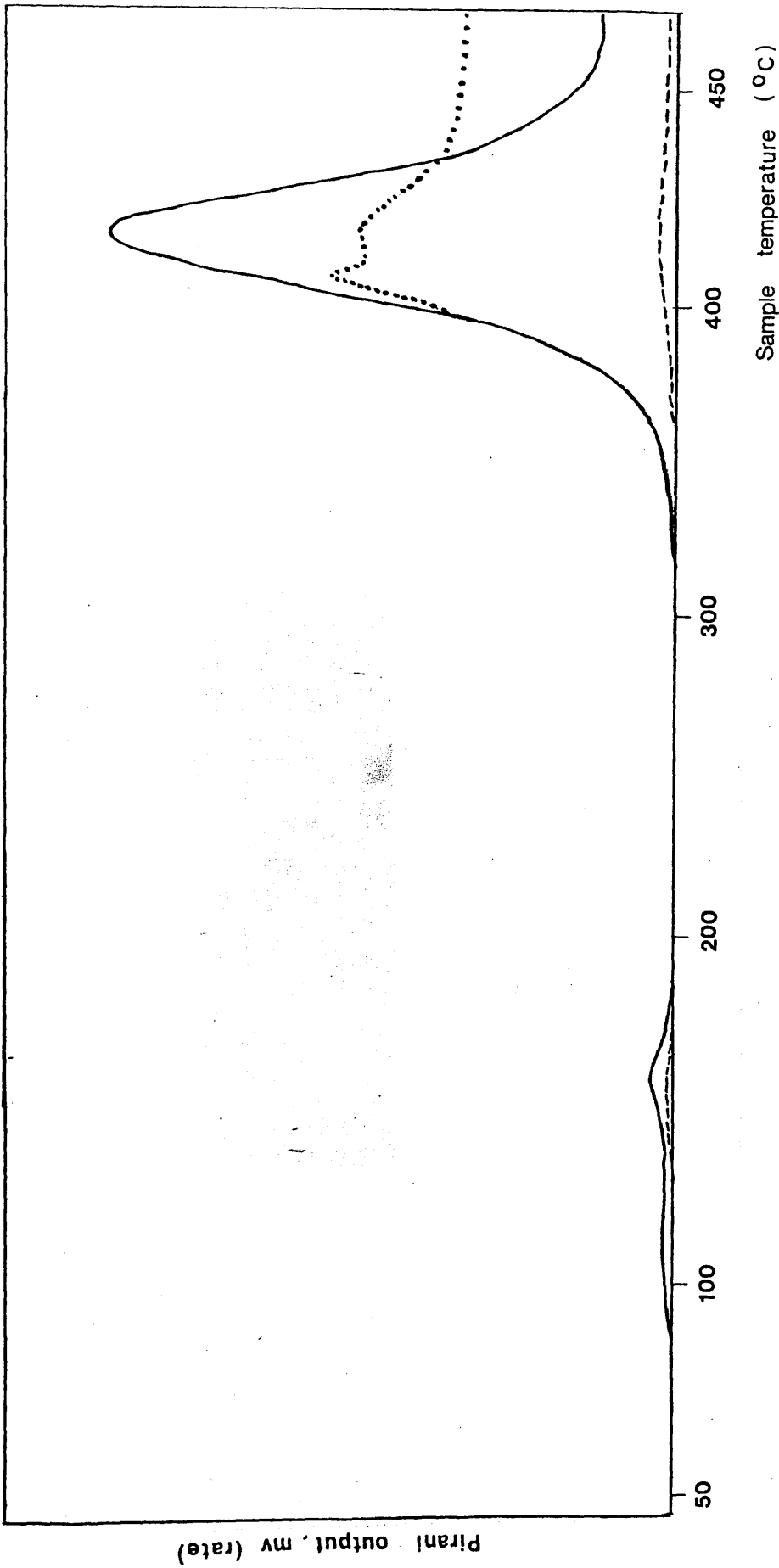


Figure 10.2 TVA curve for 1:50 Mn(acac)₃ - PS blend

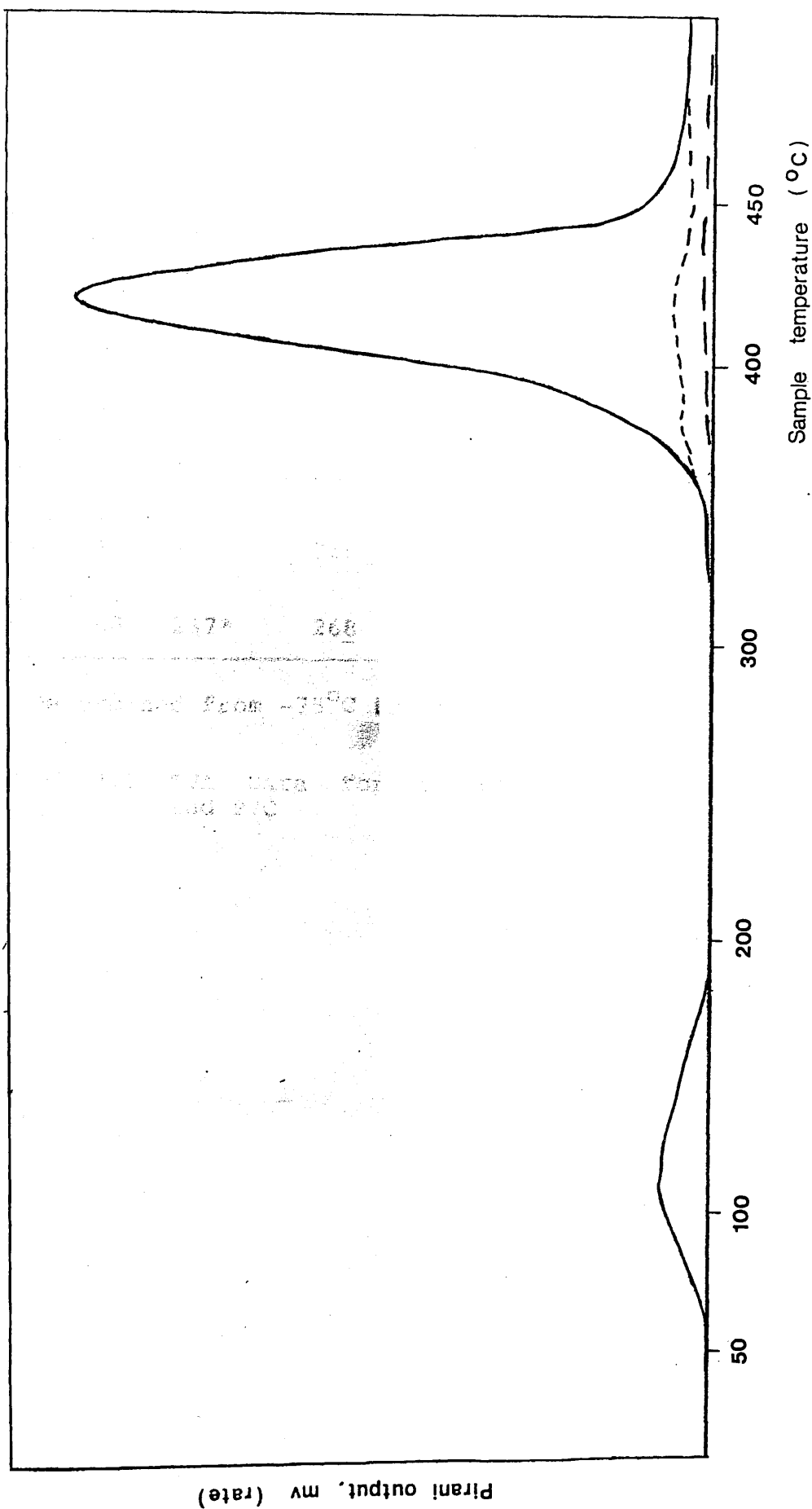


Figure 10.3 TVA curve for 1:50 Cu(acac)₂ - PS blend

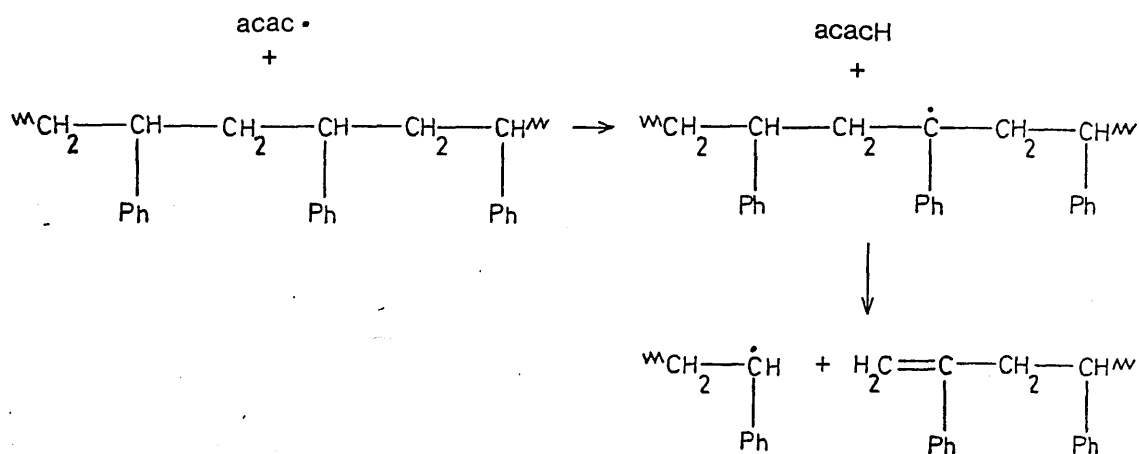
System	Temperature of Major Features ($^{\circ}\text{C}$)				
	T(onset)	T(max)	T(onset)	T(max)	Sublimation
PS	320	423	---	---	---
Co(acac) ₃ -PS 1:50 ³	320	423	---	---	68
Mn(acac) ₃ -PS 1:50 ³	322	423	---	---	178
Cu(acac) ₂ -PS 1:50 ²	328	423	---	---	140
PVC	237*	Variable	374	444	---
Co(acac) ₃ -PVC 1:50	190*	246	338	438	80?-141
Mn(acac) ₃ -PVC 1:50	231*	266	367	447	159
Cu(acac) ₂ -PVC 1:50	237*	268	358	438	122

* Determined from -75°C trace

Table 10.1 TVA Data for Blends of the Chelates with PS and PVC

$Mn(acac)_2$ formed in the decomposition, which is more volatile than $Mn(acac)_3$. It is to be expected that the $Co(acac)_2$ formed by the decomposition of $Co(acac)_3$ would likewise sublime from the $Co(acac)_3$ - PS blend.

Regeneration of acetylacetone from the $acac\cdot$ radicals released in the reduction of the chelates would involve H-abstraction from the polymer matrix but unlike PMMA, PS does not depolymerise below about $300^\circ C$,^{137,138} and thus the H-abstraction will not initiate depolymerisation. Likewise, small radicals produced in the subsequent decomposition of any bis chelate which has not sublimed would also fail to initiate depolymerisation. However, abstraction of the labile α -hydrogen by $acac\cdot$ could lead to chain scission.



CHELATE - POLYSTYRENE BLENDS - CONCLUSIONS

On the basis of the TVA results, $\text{Co}(\text{acac})_3$, $\text{Mn}(\text{acac})_3$ and $\text{Cu}(\text{acac})_2$ have little or no effect on the degradation of polystyrene, although molecular weight studies may show otherwise.

Equally, and just as important to note, polystyrene has no effect on the decomposition of the chelates. Polystyrene terminates almost solely by combination of the growing macroradicals^{156,157} and thus has no unsaturated chain ends with which the chelates could π -complex. Complexation with the aromatic rings is possible, however (see Fig. 3.14), but the expected corresponding decrease in the chelate decomposition temperature is not observed.

BLENDS OF Co(acac)₃, Mn(acac)₃, Cu(acac)₂ WITH PVC

Samples of these blends were prepared, with a chelate:monomer unit ratio of 1:50, by casting directly onto the TVA tube base from tetrahydrofuran solution. Samples were of the order of 30 mg. As with all the other polymer blends studied at 1:50, the Co(acac)₃ and Mn(acac)₃ blends were compatible and the Cu(acac)₂ blend incompatible.

TVA BEHAVIOUR OF THE CHELATE - PVC BLENDS

The TVA curves for the blends of each chelate with PVC are reproduced in Figs. 10.4-10.6 and the values for T(onset) and T(max) of the two major peaks are listed in Table 10.1. As noted in Chapter 4 in relation to the TVA behaviour of PVC, THF is a persistent solvent, difficult to remove from the PVC film without pre-heating. The peak due to the evolution of trapped THF is therefore large and can overlap with the onset of the dehydrochlorination peak. In this situation, the best trace to follow to determine T(onset) is that of the -75°C trap, and T(onset) values for the dehydrochlorination peak are quoted on this basis.

In the presence of Cu(acac)₂, the TVA behaviour of PVC is unchanged. Sublimation of chelate from the blend was observed and the particularly volatile Cu(acac)₂ may sublime completely. However, if chelate did remain in the blend its decomposition (above

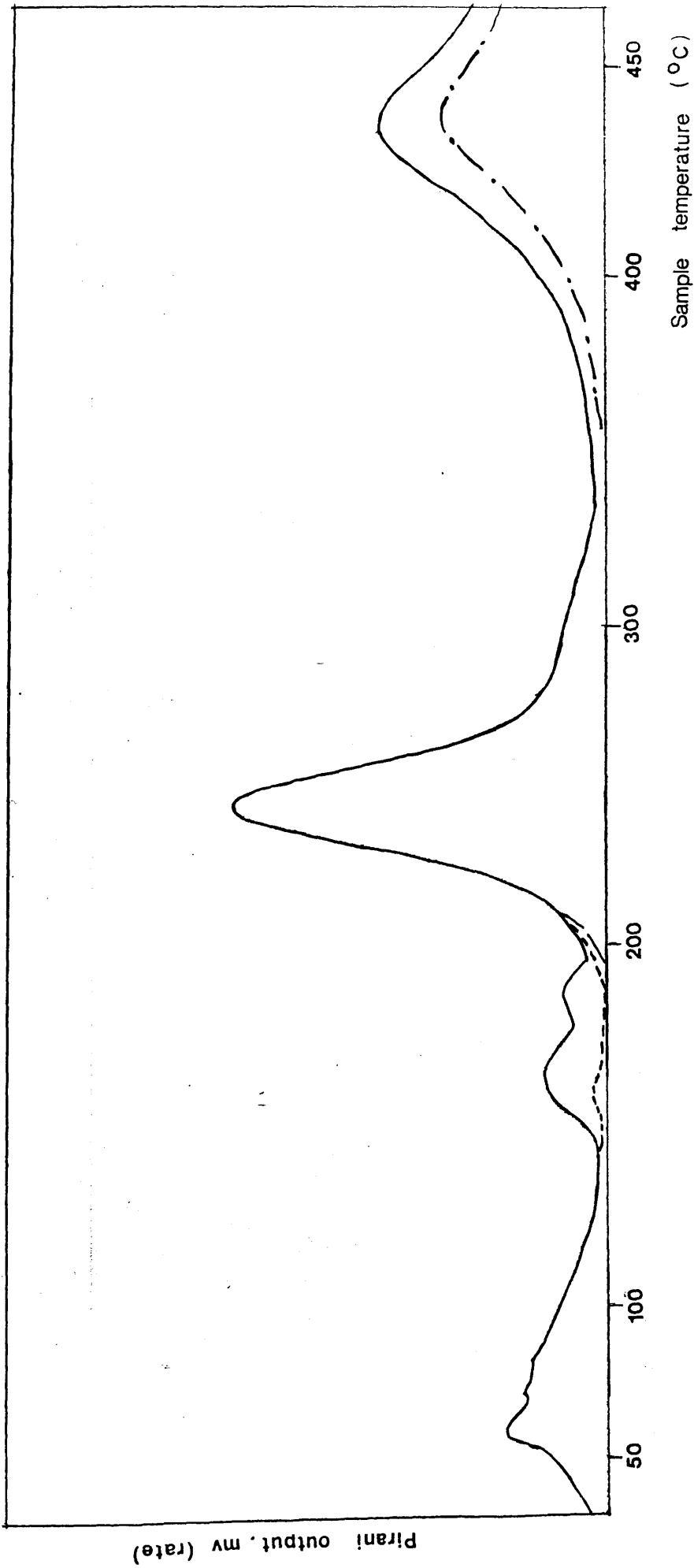


Figure 10.4 TVA curve for 1:50 Co(acac)₃ - PVC blend

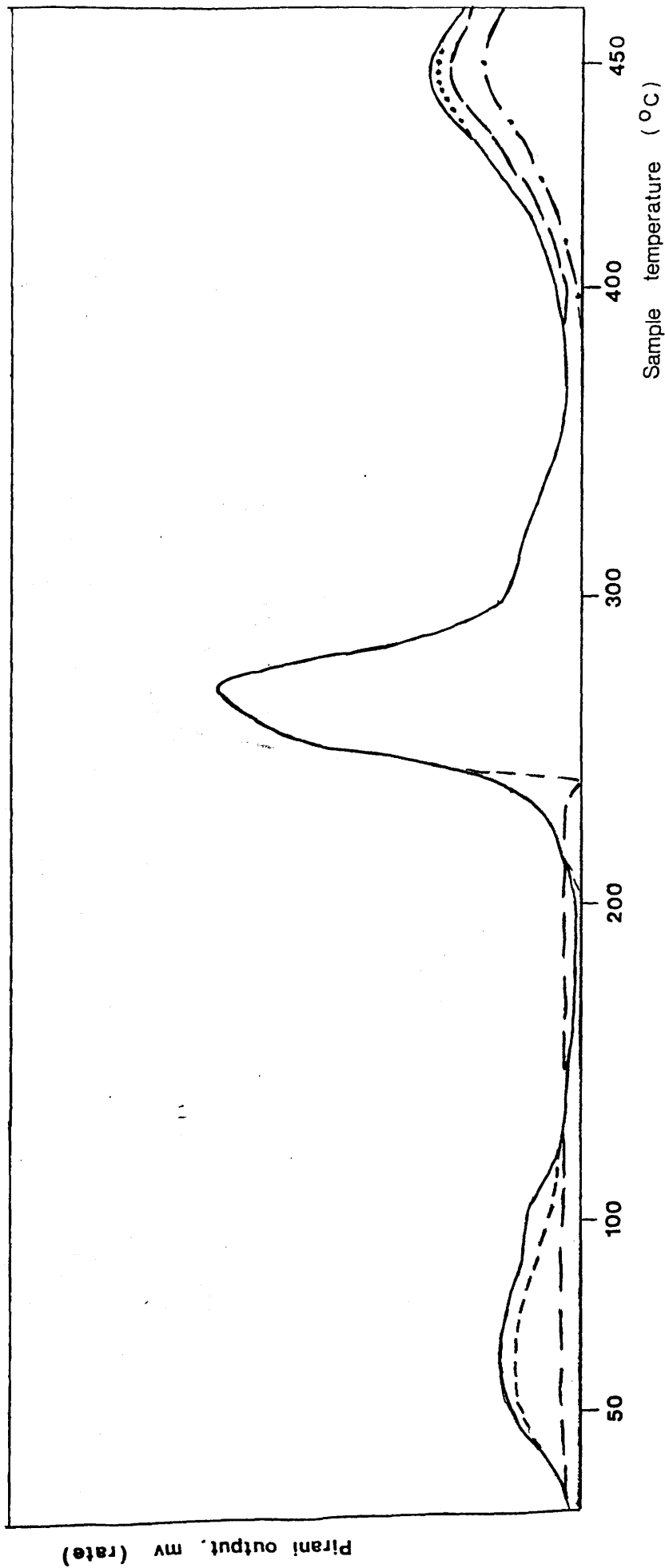


Figure 10.5 TVA curve for 1:50 Mn(acac)₃ - PVC blend

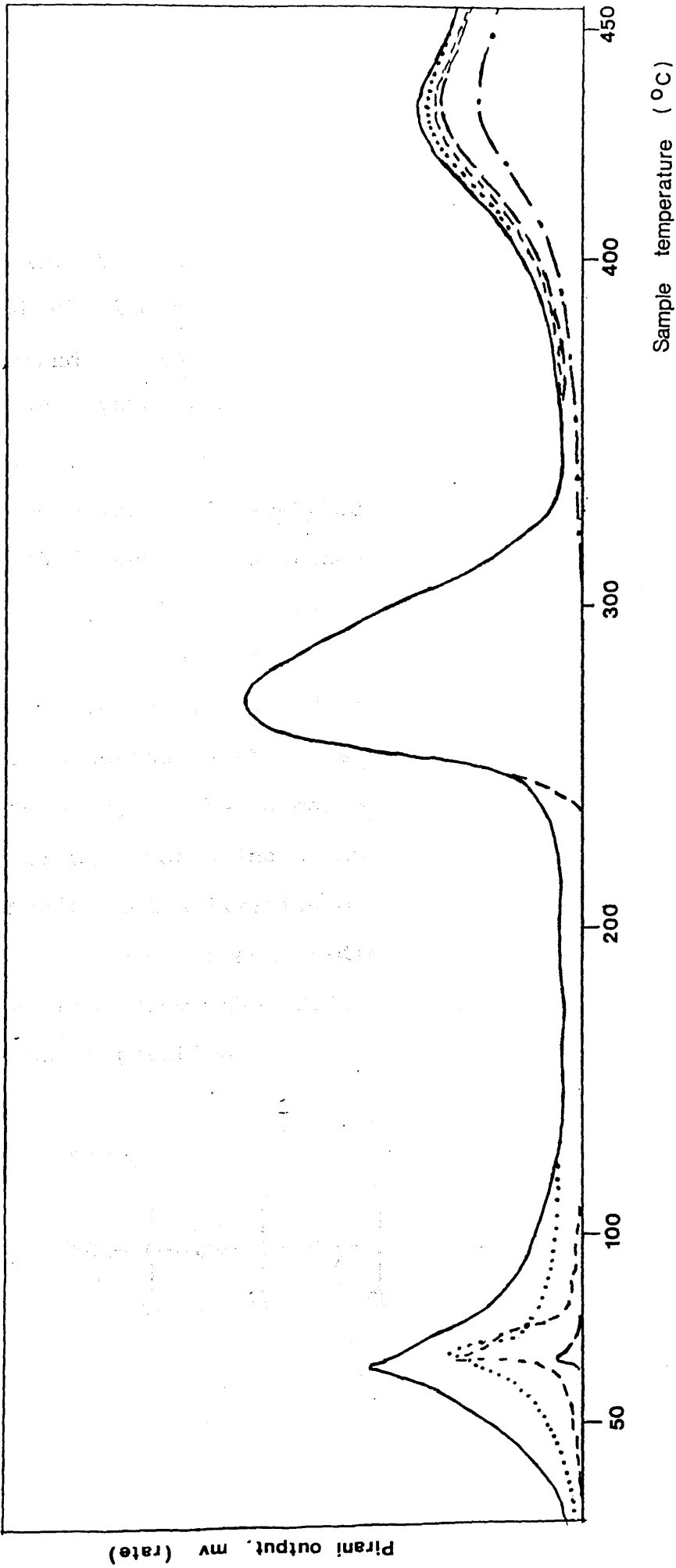
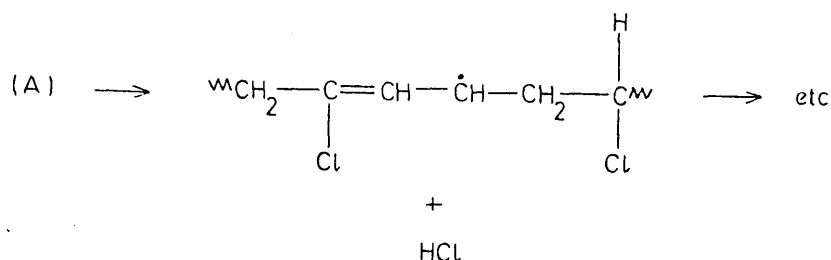


Figure 10.6 TVA curve for 1:50 Cu(acac)₂ - PVC blend

This radical (A) could then serve as an initiation site for the dehydrochlorination process.¹⁵⁸



This would account for the marked reduction in both T(onset) and T(max) observed for the dehydrochlorination reaction in this blend.

The apparent decrease in T(onset) for the fragmentation processes is not significant and merely reflects the earlier cessation of HCl evolution which allows for early detection of the onset of fragmentation.

The Mn(acac)₃ blend, however, does not show the reduction in the temperature of dehydrochlorination which would be expected as this chelate also decomposes by loss of acac· radicals. There is no evidence of TVA peaks due to acetylacetone evolution but an interaction promoted decomposition of Mn(acac)₃ would occur in the region masked by the evolution of solvent and could reduce the amount of Mn(acac)₃ left to decompose normally to the extent that the process is masked by the tail end of the solvent peak. Sublimate was not observed until 159°C, beyond T(onset) for Mn(acac)₃ decomposition, and thus it is almost certain that Mn(acac)₃ is decomposing in situ and not subliming

without decomposition. There are two possibilities for the absence of a change in the temperature of dehydrochlorination such as is observed for the $\text{Co}(\text{acac})_3$ - PVC blend. In the presence of THF, the solvent could compete with the polymer backbone as a source of hydrogen atoms to be abstracted by the acac radical; this would affect the $\text{Mn}(\text{acac})_3$ blend more than the $\text{Co}(\text{acac})_3$ blend due to the acac radicals in the former blend being produced when more THF is present. Alternatively, the dehydrochlorination in the $\text{Co}(\text{acac})_3$ blend could be catalysed by the solid residue of the chelate decomposition. On the evidence available, it is impossible to ascertain the mechanism involved.

CHELATE - PVC BLENDS - CONCLUSIONS

$\text{Cu}(\text{acac})_2$ has no observable effect on PVC, and $\text{Mn}(\text{acac})_3$, although expected to introduce unsaturated sites along the polymer backbone, seems to have little effect on the overall TVA behaviour of the polymer. The effect of $\text{Co}(\text{acac})_3$ is pronounced but the exact mechanism by which it acts remains unclear in the absence of a more detailed study of the degradation.

CHAPTER 11

DEGRADATION OF STYRENE-METHACRYLIC ACID COPOLYMERS

INTRODUCTION

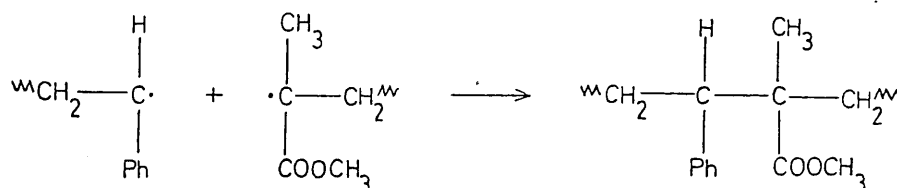
Styrene-methacrylic acid copolymers have a large number of commercial applications in such varied fields as desalination, paper substitutes technology and carpet shampooing.

Despite the industrial uses of these copolymers, little or nothing is known about their thermal degradative behaviour. This alone would justify studying such behaviour. However, the thermal degradation of copolymers is of interest from a purely academic viewpoint as a copolymer may have degradation properties considerably different from those of the corresponding homopolymers. The presence of a comonomer may either stabilise or destabilise the copolymer relative to the homopolymers. For instance the copolymer of styrene with α -chloroacrylonitrile (α -CAN) has its onset of degradation at 140°C, considerably lower than that of polystyrene but the same as that of poly(α -chloroacrylonitrile). The degradation of the copolymer is therefore expected to be initiated by the same mechanism as that of poly(α -CAN).¹⁵⁹

On the other hand, as described in Chapter 3, the presence of methacrylic acid units in MAA-MMA copolymer leads to the production of anhydride structures which effectively stabilise the copolymer by inhibiting the

unzipping of the MMA units.

Similarly, the copolymer of MMA with styrene has a greater thermal stability than PMMA even at low styrene concentrations. This increase in stability is attributed by Grassie and Farish¹⁶⁰ to the inhibition of the disproportionation step which produces in the homopolymerisation of MMA, the unsaturated "weak link" sites (see Chapter 4). In the copolymerising system, most termination occurs by the combination reaction:-



This is the major termination step even at low styrene concentration hence the marked increase in stability even in the low styrene mole fraction copolymer. Alternatively as suggested by McNeill,¹²⁴ the stabilisation could be due to the blocking action of styrene sequences which would not depolymerise below 300°C.

In this study, performed in association with an undergraduate research project, three copolymers of various styrene-methacrylic acid compositions (18, 44, 72 mole % acid) and the respective homopolymers were prepared and their thermal behaviour studied by TVA and TG techniques in addition to product analysis.

PREPARATION OF COPOLYMERS

Copolymers were prepared in bulk in vacuo, using 0.1% w/v benzoyl peroxide as initiator. Monomers had been distilled under vacuum and were degassed immediately prior to use. Polymerisations were performed in a thermostat bath at $60^{\circ}\text{C} \pm 0.01^{\circ}\text{C}$ and the conversions followed by dilatometry. Once the desired conversion had been attained, polymers were isolated by precipitation in petroleum spirit and were further purified by dissolution in toluene or methanol (for the 72% mole fraction MAA copolymer) and precipitation in petroleum spirit. Copolymer compositions were calculated from the monomer feed concentrations using the copolymer composition equation¹⁶¹

$$F_1 = (r_1 f_1^2 + f_1 f_2) / (r_1 f_1^2 + 2f_1 f_2 + r_2 f_2^2)$$

where F_1 is the mole fraction of MAA in the copolymer, f_1 and f_2 the mole fractions in the monomer feed of MAA and styrene respectively, and r_1 and r_2 the respective reactivity ratios for MAA and styrene. Values for r_1 and r_2 were taken from the literature¹⁶²: - $r_1 = 0.7$, $r_2 = 0.15$.

	COPOLYMER 1	COPOLYMER 2	COPOLYMER 3
Mole % MAA in monomer feed	4	25	75
Conversion	3	5	8
Mole % MAA in Copolymer	18	44	72

Table 11.1 Copolymer Composition

PREPARATION OF THE HOMOPOLYMERS

POLYSTYRENE

Polystyrene was prepared by the emulsion polymerisation of styrene under nitrogen with 0.1% w/v potassium persulphate as initiator. The polymer was purified, after separation, by dissolution in chloroform and precipitation in methanol.

POLY(METHACRYLIC ACID)

PMAA was prepared by the polymerisation, in aqueous solution of 51g of methacrylic acid in the presence of 0.75ml of 30% v/v hydrogen peroxide. The polymerisation was performed under nitrogen. The polymer was purified by dissolution in ethanol and precipitation in diethyl ether.

TVA BEHAVIOUR OF THE HOMOPOLYMERS

The degradation behaviour of the homopolymers has been described in Chapter 3, and the TVA curves for

polystyrene and PMAA discussed therein. The TVA curve for the homopolymers and copolymers prepared here were obtained using a different TVA line from that used elsewhere in this research and this is reflected by a slight discrepancy between the degradation temperatures of the polystyrene sample employed for Chapters 3 and 10 and the sample prepared for this project. However, as the same TVA line was used for all the homopolymers and copolymers described here, the conclusions drawn from comparison of T(onset) and T(max) temperatures are unaffected. TVA data for polystyrene and PMAA are included in Table 11.2.

TG-DTG BEHAVIOUR OF THE HOMOPOLYMERS

The TG-DTG curves for polystyrene and PMAA are reproduced in Figs. 11.1 and 11.2. Fig. 11.1 shows clearly the 'one-step' nature of the weight loss due to the depolymerisation of polystyrene.

The TG curve for PMAA shows that the weight loss to 225°C is 19%, nearly twice that calculated for the cyclisation dehydration alone. This phenomenon, also observed by Grant and Grassie,¹⁴² reflects the ease with which PMAA absorbs atmospheric moisture.

THERMAL BEHAVIOUR OR THE COPOLYMERS

THERMAL VOLATILIZATION ANALYSIS

Fig 11.3 - 11.5 show the TVA curves obtained for the copolymers. Samples were of the order of 30mg and

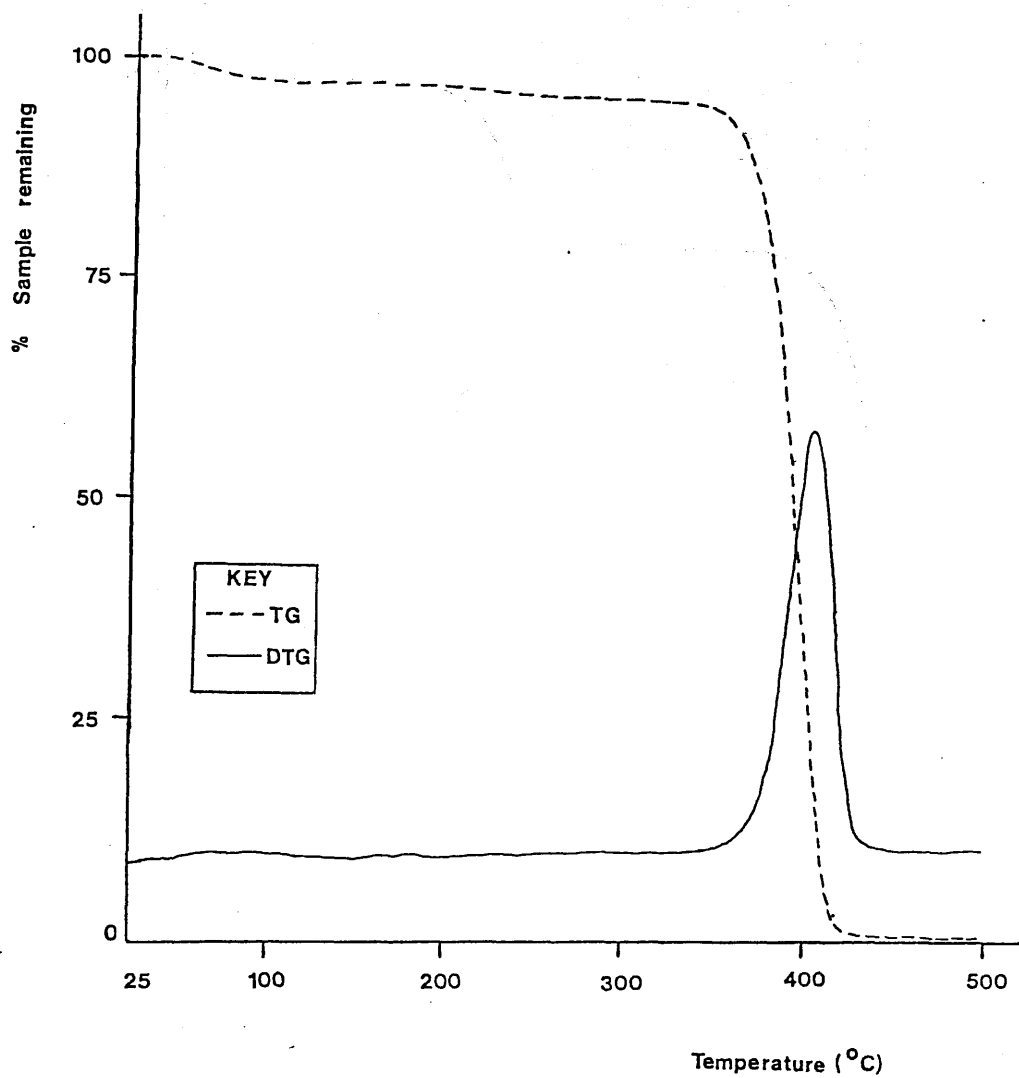


Figure 11.1 TG - DTG curves for "lab-prepared" polystyrene (N₂ atmosphere)

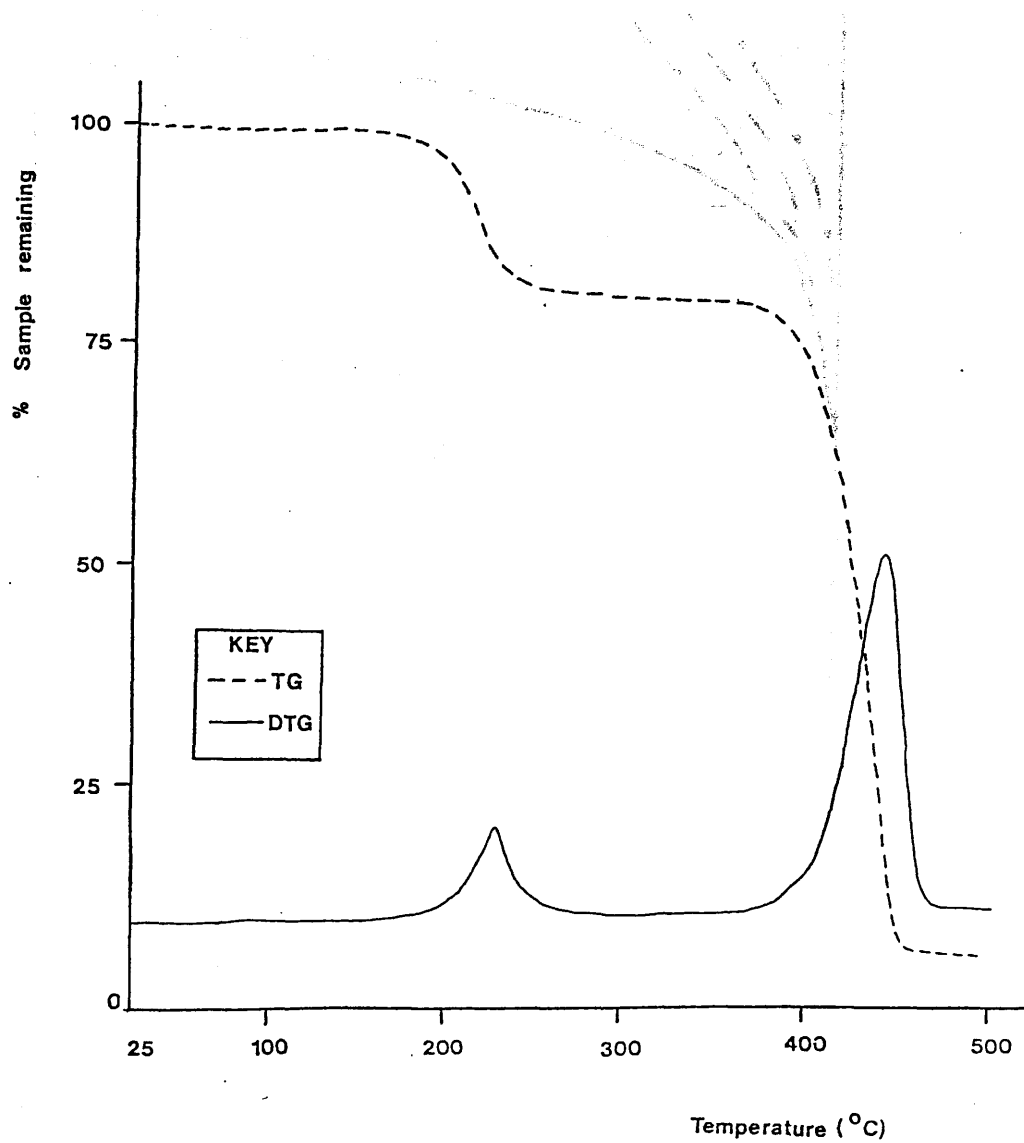


Figure 11.2 TG - DTG curves for "lab-prepared" PMAA (N₂ atmosphere)

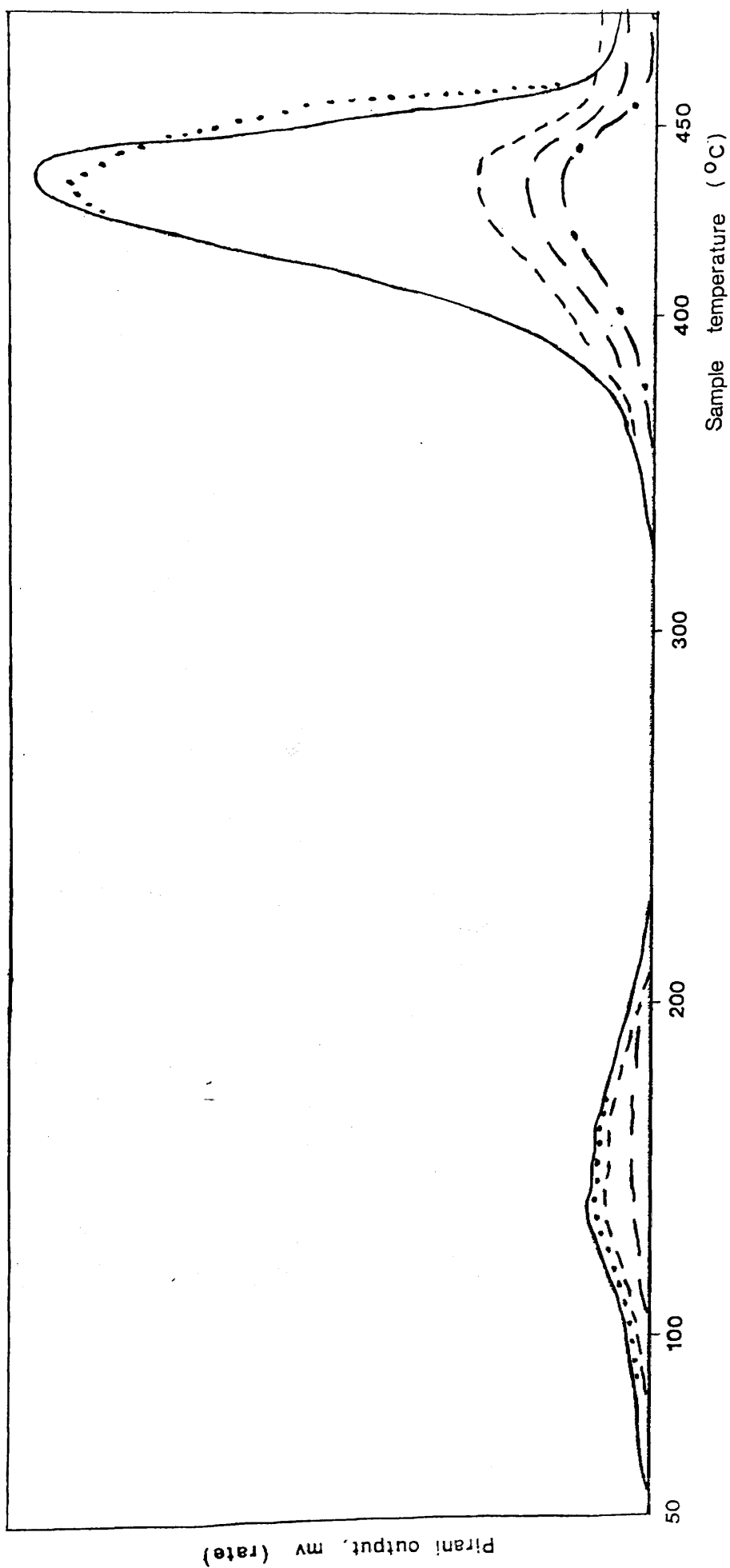


Figure 11.3 TVA curve for 18 mole % MAA copolymer

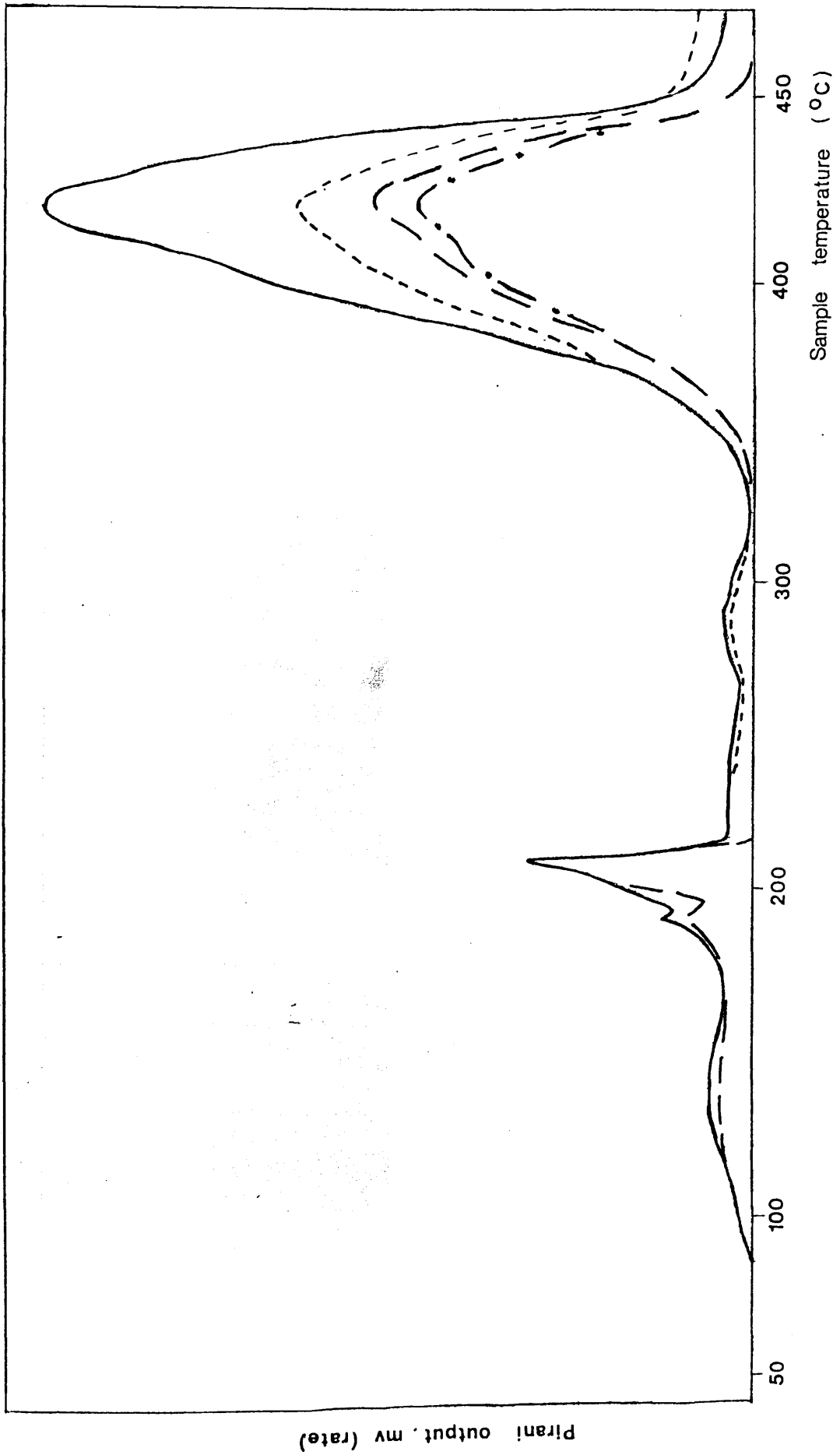


Figure 11.4 TVA curve for 44 mole % MAA copolymer

were in the form of granules. Normal TVA procedure was followed. Table 11.2 lists the T(onset) and T(max) temperatures of the major peak. The T(max) temperatures vary unsystematically within a 15°C range, but this can be attributed to variation in the physical dimensions of the polymer samples, bulk samples being susceptible to the problem of reaction products having to diffuse through the matrix before volatilization. It is to be observed, however, that the T(max) temperature of the major peak for the various samples lies between that of PS and PMAA. In other respects too, the behaviour of the copolymer is intermediate between PS and PMAA. The major peak in the TVA curve of PS is due almost entirely to styrene and has no associated -196°C non-condensable products whilst the major peak of PMAA, due to the fragmentation of the anhydro-polymer is almost entirely due to -196°C non-condensable products. The copolymer series shows a clear trend towards increased formation of -196°C non-condensable products with increasing MAA content. All the copolymers have a peak on their TVA curves below 140°C which is due to the release of precipitant from the purification process. In addition, the 44 and 72 mole % MAA copolymers have peaks which can be ascribed to further loss of precipitant and evolution of water between 150-300°C.

The implication of the evolution of water and -196°C non-condensable gases from those copolymers of

higher MAA content is that these copolymers contain neighbouring MAA units which cyclise exactly as in PMAA to form anhydride ring structures.

POLYMER	T(ONSET) °C	T(MAX) °C
POLYSTYRENE	331	411
POLY(METHACRYLIC ACID)	343	441
COPOLYMERS		
18 mole % MAA	337	426
44 mole % MAA	318	411
72 mole % MAA	307	417

Table 11.2 T(onset) and T(max) of Major Peak of Polystyrene and Poly(Methacrylic Acid) and of the Styrene Methacrylic Acid Copolymers

TG-DTG BEHAVIOUR OF THE COPOLYMERS

The copolymers were examined by thermogravimetry; the curves obtained are shown in Fig. 11.6. Samples were of 2.5-3.5mg and all analyses were performed under a dynamic nitrogen atmosphere.

Unfortunately the presence of trapped precipitant precludes comparison of actual weight losses but of interest is the observed constancy in T(max) of the major weight loss with copolymer composition.

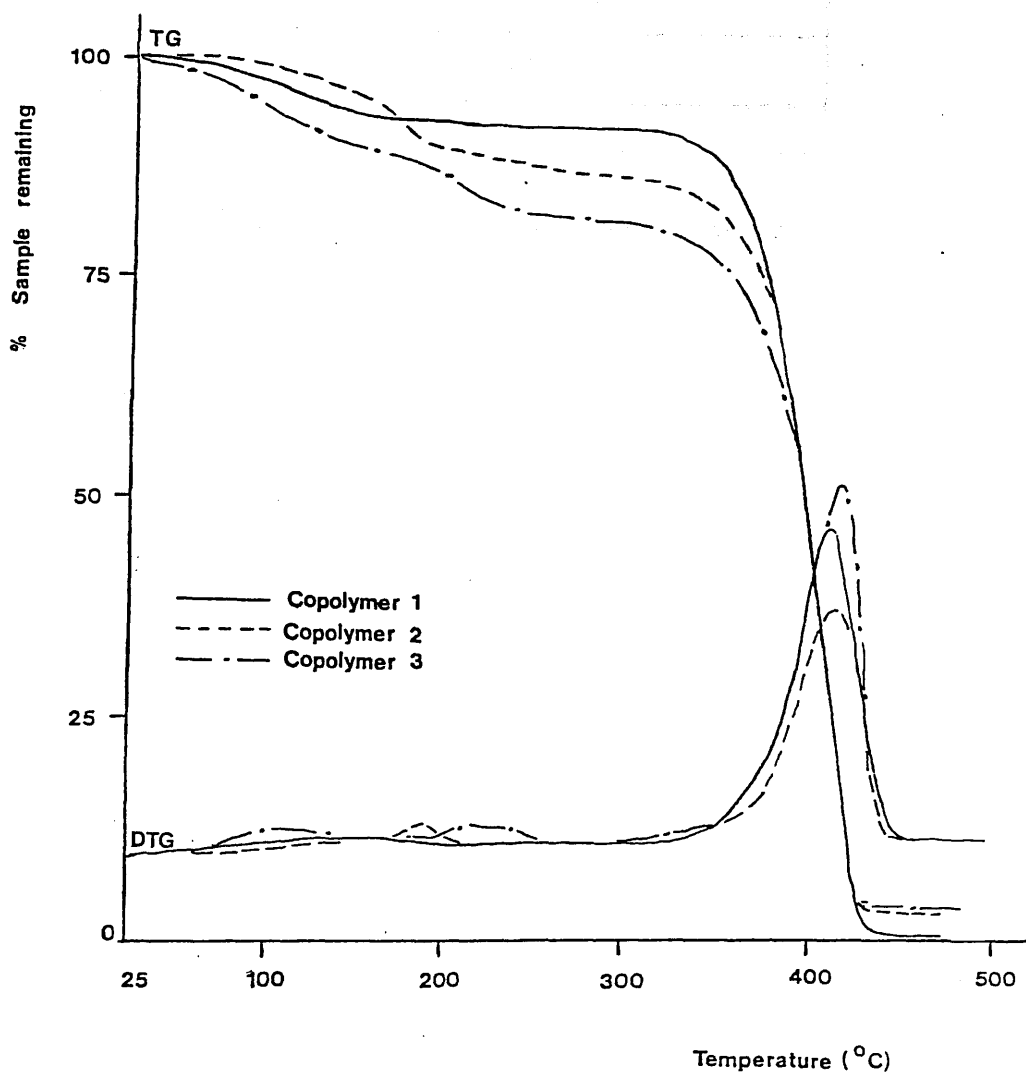


Figure 11.6 TG - DTG curves for the copolymers
(N₂ atmosphere)

POLYMER	T(MAX) OF MAJOR WEIGHT LOSS °C
COPOLYMER 1 18% MAA	410
COPOLYMER 2 44% MAA	412
COPOLYMER 3 72% MAA	413
PS	400
PMAA	440

Table 11.3 Variation of T(max) with Copolymer Composition

The lack of variation in the T(max) temperatures obtained by TG in contrast to the minor variation in the TVA results, is due to the use of samples of similar physical dimensions. The results show clearly that the copolymer is stabilised relative to polystyrene and destabilised relative to PMAA.

... and the PMAA to be grafted ...
 ... by analogy with PMAA, ...
 ... structures were formed within the ...
 ... heating ...

STRUCTURE OF COPOLYMERS AND CHANGES DURING DEGRADATION

The structure of the copolymers was investigated by IR spectroscopy. Fig 11.7 depicts the IR spectra of the undegraded copolymers and, for comparison, those of PMAA and PS. The spectra were of films cast on NaCl discs from THF or methanol solution except those of PMAA and copolymer 2 which were of KBr discs. The spectra of the copolymers contain features of both PS and PMAA with copolymer 1 having principally the characteristics of PS and copolymer 3 having a spectrum closely resembling that of PMAA. As the acid content of the polymer increases going from copolymer 1 to copolymer 3, the 1700cm^{-1} peak due to the acid C=O stretch broadens considerably, indicating increasing dimerisation of the acid groupings.

Fig 11.8 shows the corresponding spectra of the copolymers after degradation under TVA conditions. The temperatures of degradation and important structural changes are noted in Table 11.4. The copolymers were degraded supported on NaCl discs whilst PS and PMAA were degraded in powder form and the residues removed for analysis, the PS by dissolution in THF to be cast as a film on a NaCl disc, and the PMAA to be ground with KBr.

As expected by analogy with PMAA, glutaric-type anhydride structures were formed within the copolymers. However even on heating to approximately 100°C above the temperature at which the anhydrides form in PMAA, free acid groupings remain in the copolymers. This

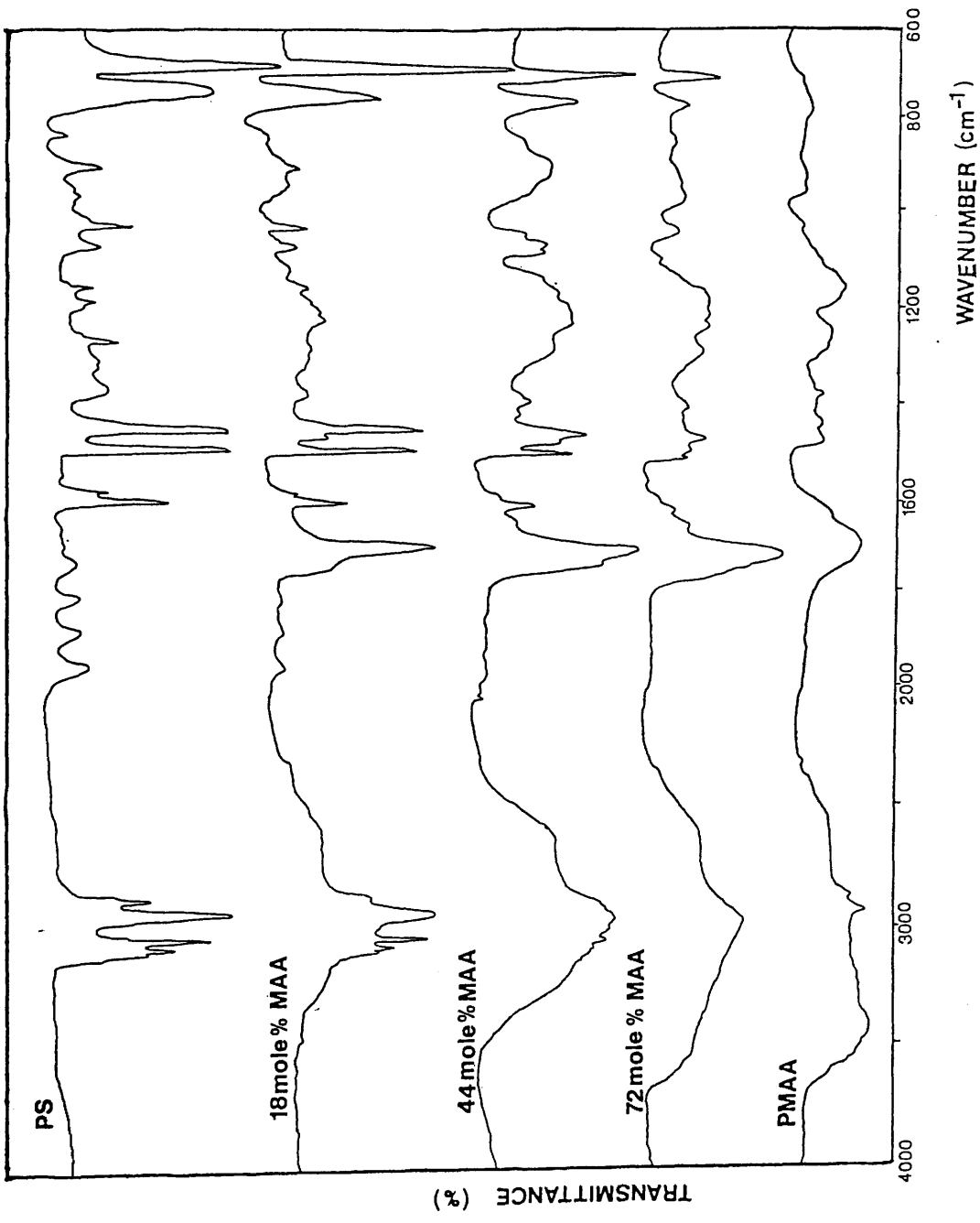


Figure 11.7 IR spectra of the undegraded copolymers and homopolymers

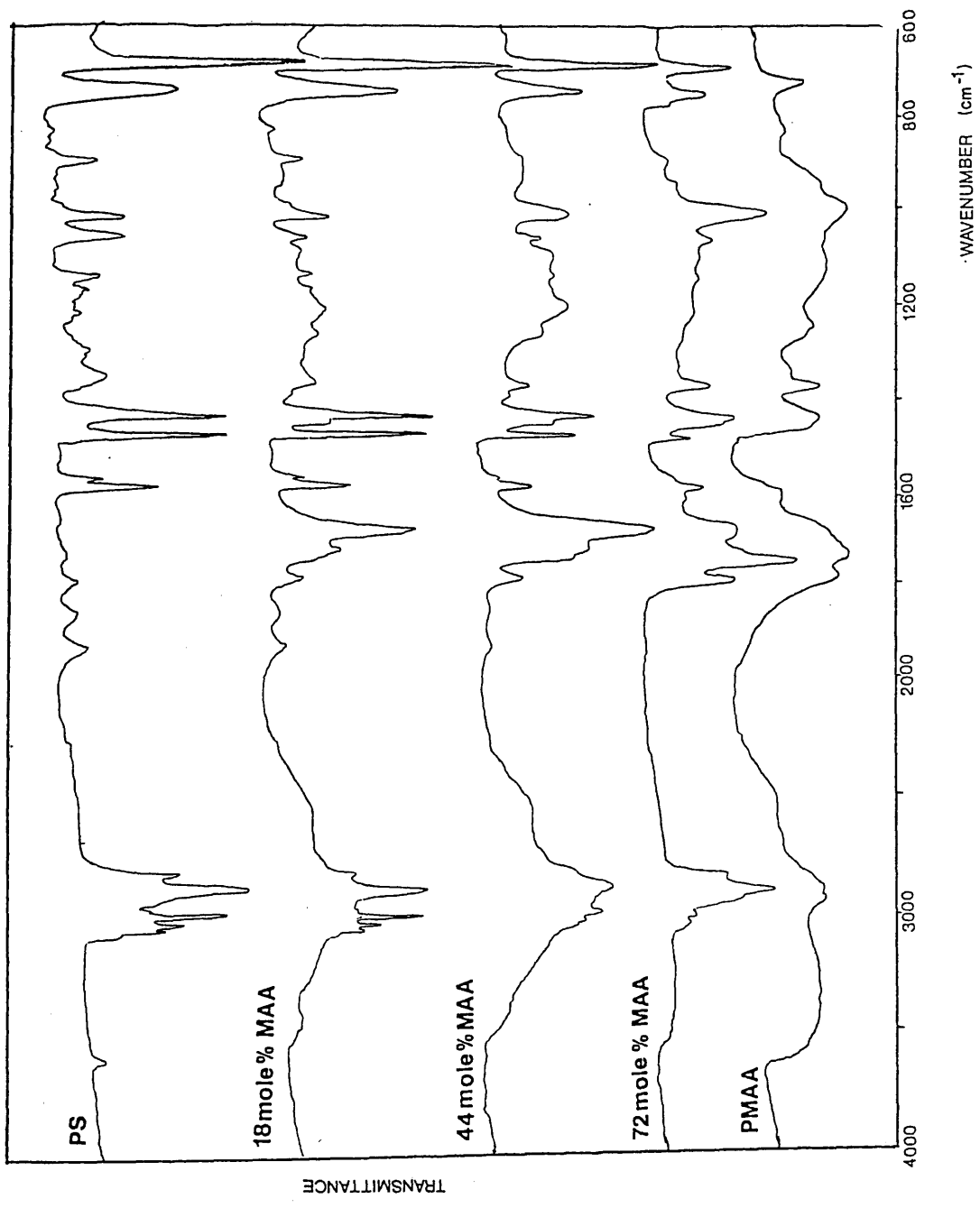


Figure 11.8 IR spectra of the copolymers and homopolymers after partial degradation

reflects the fact that when copolymerised with styrene a number of MAA units become isolated and have no neighbouring MAA unit with which to cyclise. This effect is, of course, most apparent in the 18 mole % MAA copolymer, although since the MAA-styrene system tends towards alternating copolymers, isolated MAA units will also be present in the 72 mole % MAA copolymer.

POLYMER	HEATED TO	FEATURES
PS	356°C	No detectable changes
PMAA	364	Peaks at 1800 and 1760cm ⁻¹ very characteristic of anhydride structures
COPOLYMER 1	367	Characteristic anhydride absorptions, but most of carboxylic groups remain uncombined
COPOLYMER 2	318	As for Copolymer 1
COPOLYMER 3	325	Greater proportion of carboxylic groupings combined relative to Copolymers 1 and 2

Table 11.4 Structural Features of the Styrene-Methacrylic Acid Copolymers and Homopolymers After Degradation

-196°C CONDENSIBLE GAS AND LIQUID PRODUCTS

The -196°C condensible gas and liquid products obtained by degrading 100mg samples of the copolymers to 485°C were collected and fractionated by the SAD technique and identified by IR spectroscopy. The degradation products of the three copolymers and hence their respective SAD curves were found to be broadly similar. The SAD curves of the copolymers, and the products associated with each section of the curves are shown in Figs 11.9 - 11.11.

The major difference in the product composition from each sample is the amount of products such as carbon dioxide, a ketene (most probably dimethyl ketene given the structure of the copolymer) butene and isobutene obtained. As can clearly be seen from the SAD curves, these products are present to the largest extent for the copolymer of highest MAA content. All these products have been identified as fragmentation products of dehydrated poly(methacrylic acid)¹⁴², and the variation in the amounts formed reflects the expected variation in the proportion of anhydride structure within the degrading copolymers.

The IR spectrum of the liquid fraction from the 72 mole % MAA copolymers (Fig 11.12) shows against a background of MAA peaks, the peaks at 1845cm^{-1} and 1775cm^{-1} due to a succinic-type anhydride of the type observed from the degradation of poly(methacrylic acid) (Chapter 3) and other systems in which glutaric-type

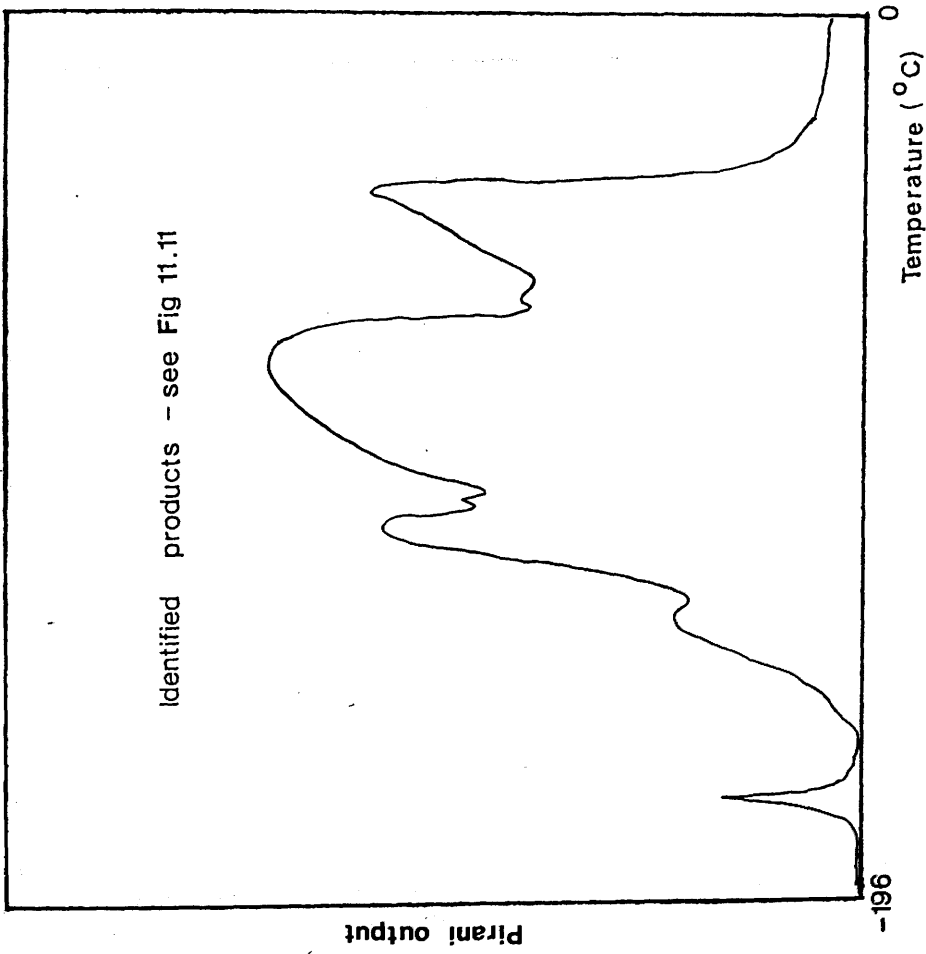


Figure 11.9 SAD curve for 18 mole % MAA copolymer

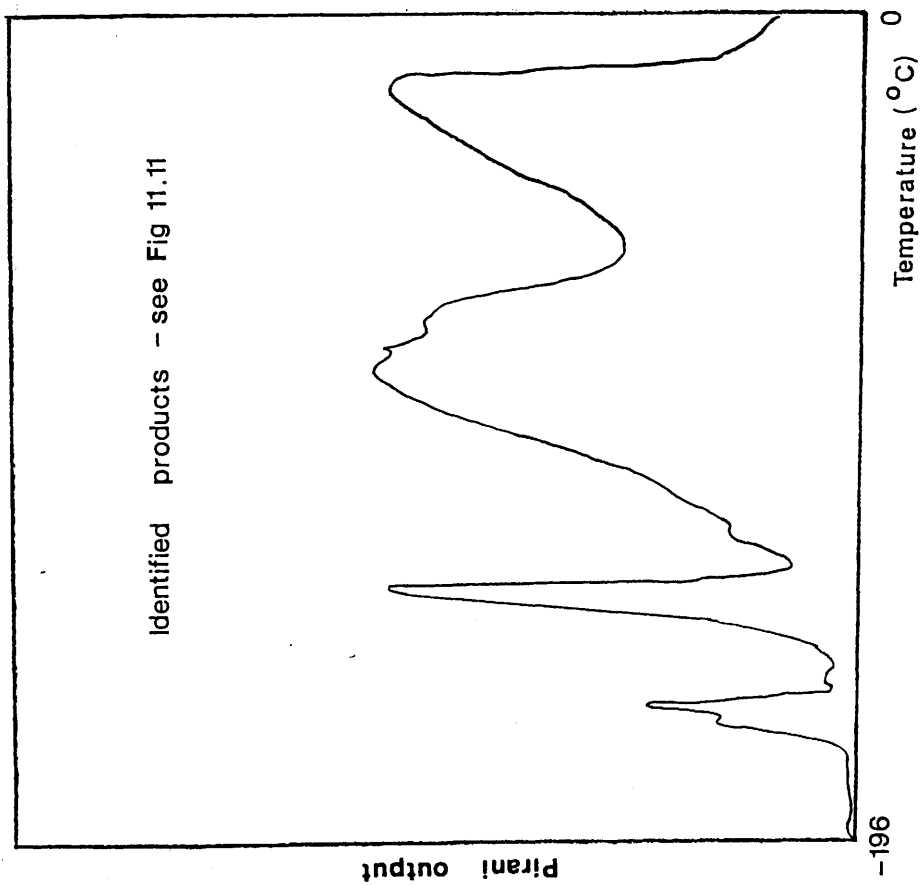


Figure 11.10 SAD curve for 44 mole % MAA copolymer

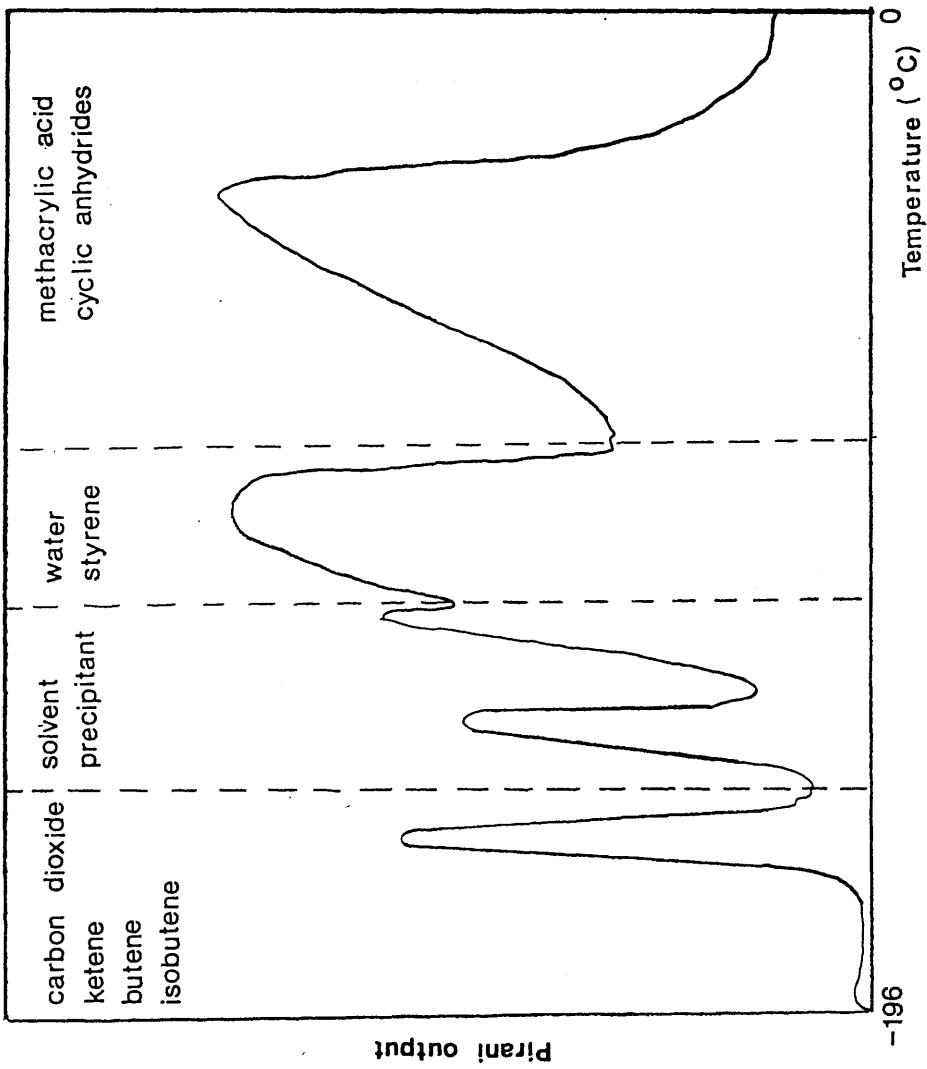


Figure 11.11 SAD curve for 72 mole % MAA copolymer

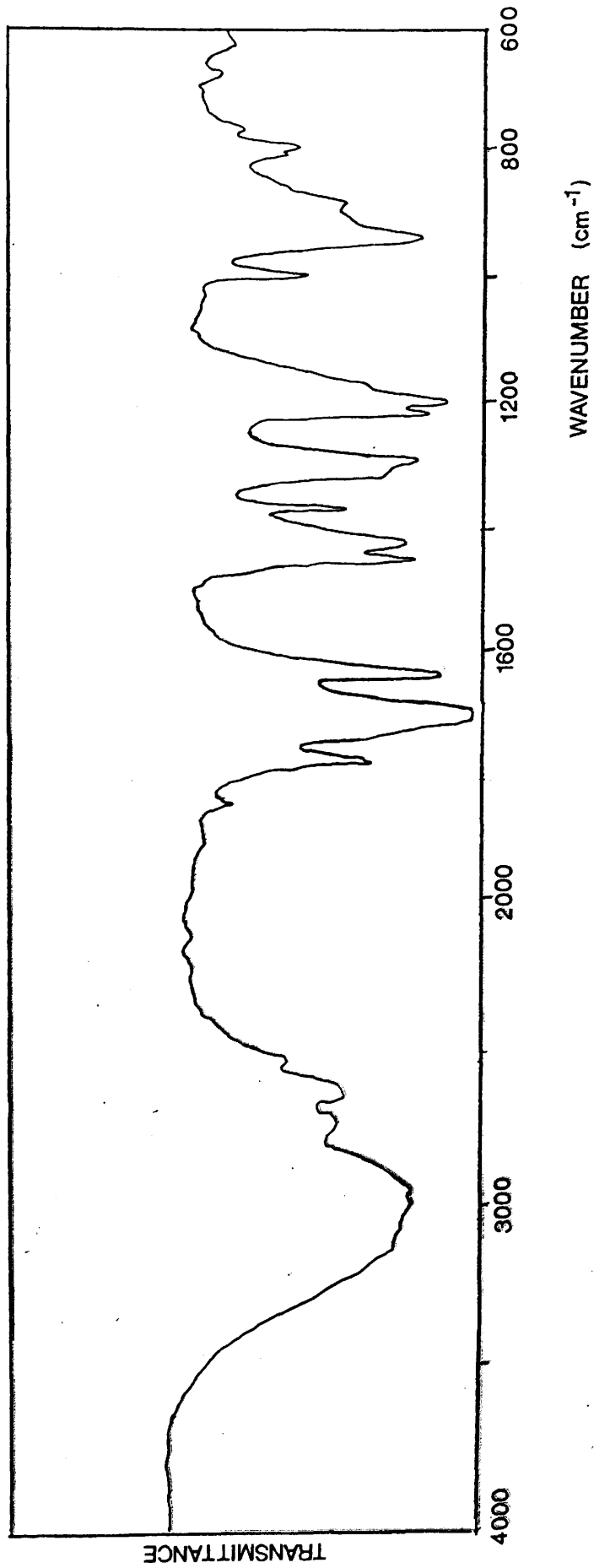


Figure 11.12 IR spectrum of liquid fraction from SAD analysis of products of degradation of 72 mole % MAA copolymer

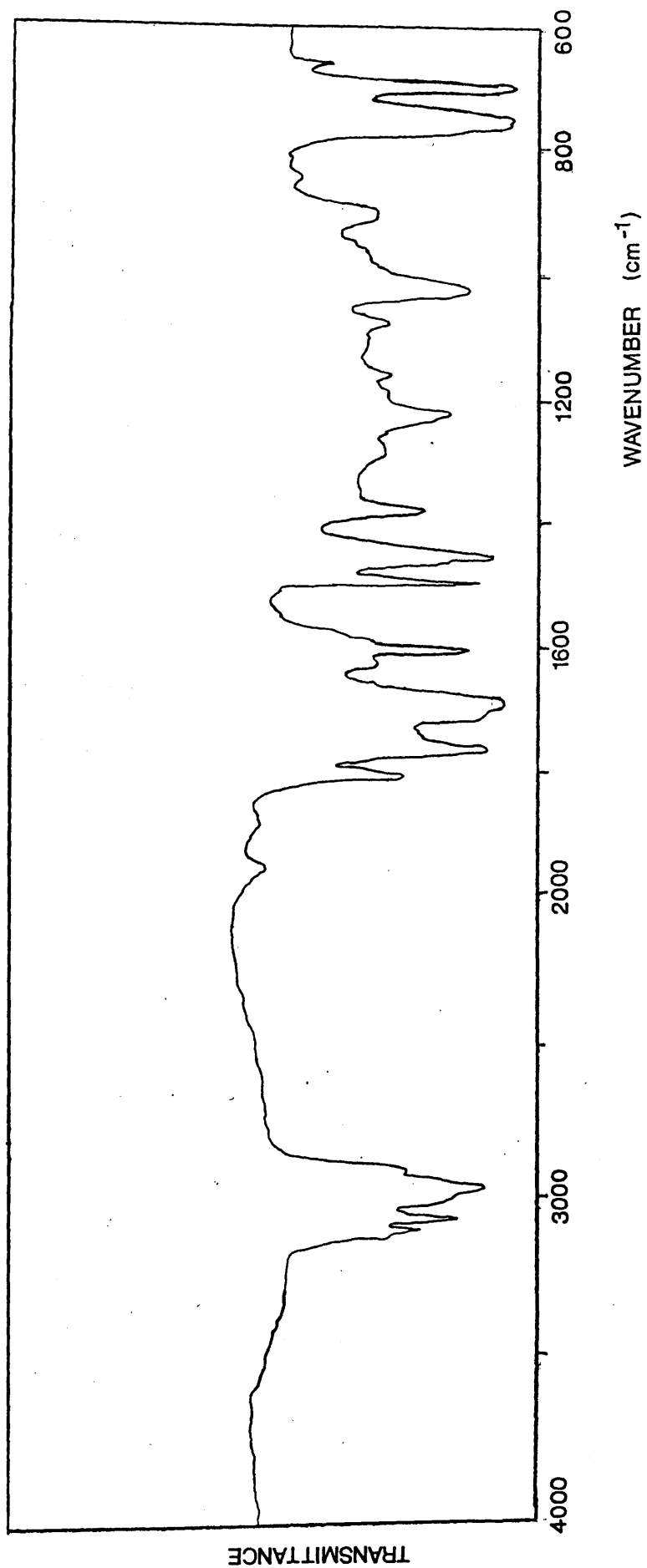


Figure 11.13 IR spectrum of CRF from 44 mole % MAA copolymer

anhydride structures are formed (Chapters 5 - 7).

COLD RING FRACTION

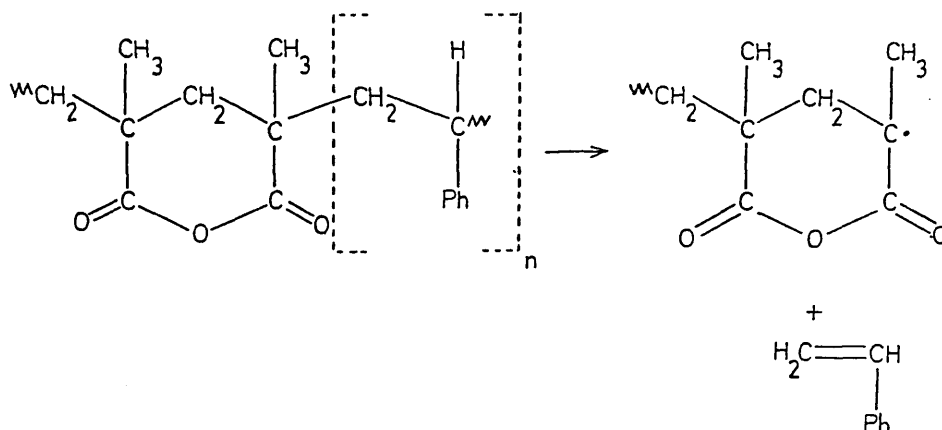
The cold ring fractions obtained on degrading the copolymers to 485°C consist of chain fragments. The IR spectrum of the CRF from the 44 mole % MAA copolymer is representative and shows clearly (Fig 11.13) the presence of chain fragments including some of the glutaric-type anhydride units.

DISCUSSION

The formation of glutaric-type anhydride structures within the copolymers by the cyclisation of neighbouring methacrylic acid groups is apparent from the IR spectra of both the partially degraded polymer and the chain-fragment - containing cold ring fractions. The amount of such structures formed varies with the mole % of MAA in the copolymers and so of course, does the corresponding fragmentation product formation as evidenced by both TVA curves and product analysis.

The temperature of the maximum rate of evolution of volatile products from the major degradation process of the copolymers is markedly higher than that of polystyrene. This increase in stability results from the inhibition of the depolymerisation and inter- and intra- molecular transfer reactions of the styrene sequences within the copolymers. Lacking active

hydrogens, methacrylic acid units, cyclised or not, will lessen the likelihood of inter- and intra- molecular hydrogen abstraction reactions by styrene macroradicals whilst the anhydride ring structures block the depolymerisation of styrene sequences by a mechanism analogous to that in MAA-MMA copolymers.



The anhydride macroradical can then rearrange to a five-membered ring by the mechanism on page 221 or alternatively fragment to give such products as dimethyl ketene and carbon dioxide.

Such macroradicals, can of course, also be produced by random scission of the chain; this will be the major route to their formation in the 72 mole % MAA copolymer.

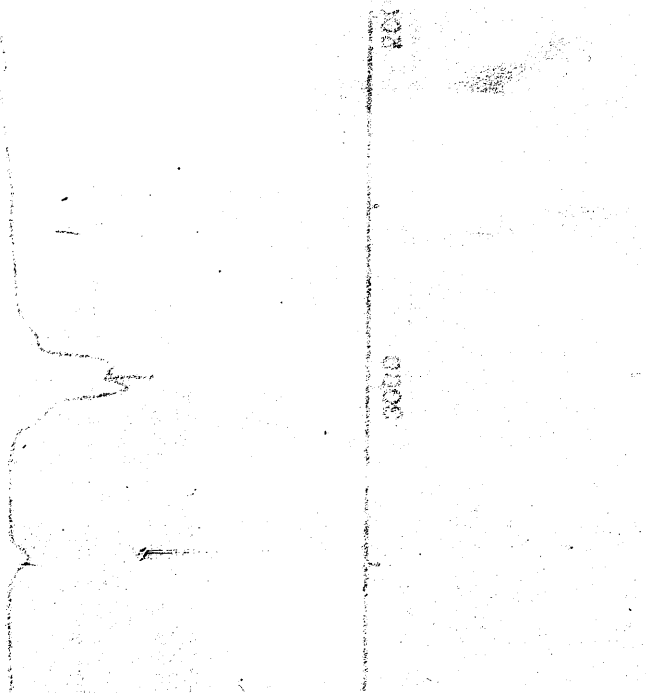
By the very nature of the copolymerisation a proportion of the MAA units are isolated by styrene units and so remain uncyclised. The IR spectra of the partially degraded copolymers all contain in addition to the absorbances of the anhydride structures, the typical 1700cm^{-1} absorbance of isolated methacrylic acid

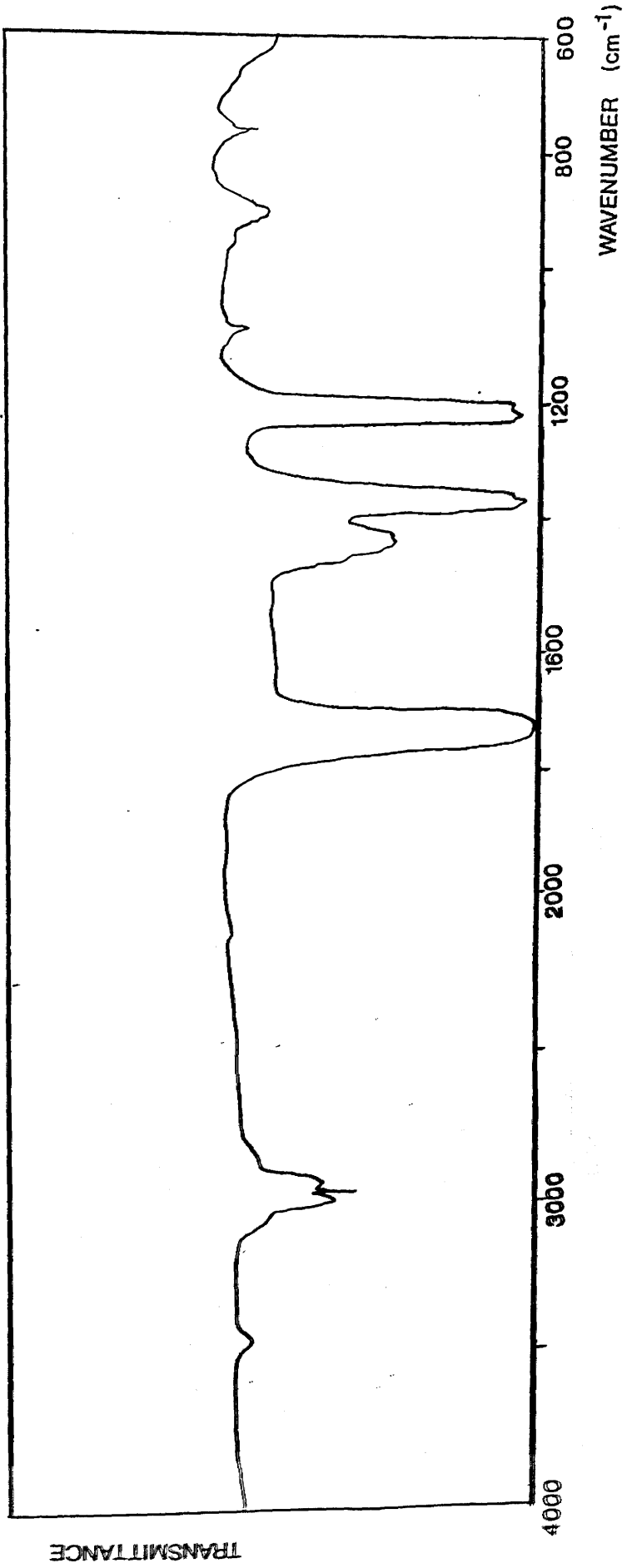
units. There is no evidence of an interaction between these acid units and the neighbouring styrene units and they are expected to depolymerise along with the styrene sequences.

SUMMARY

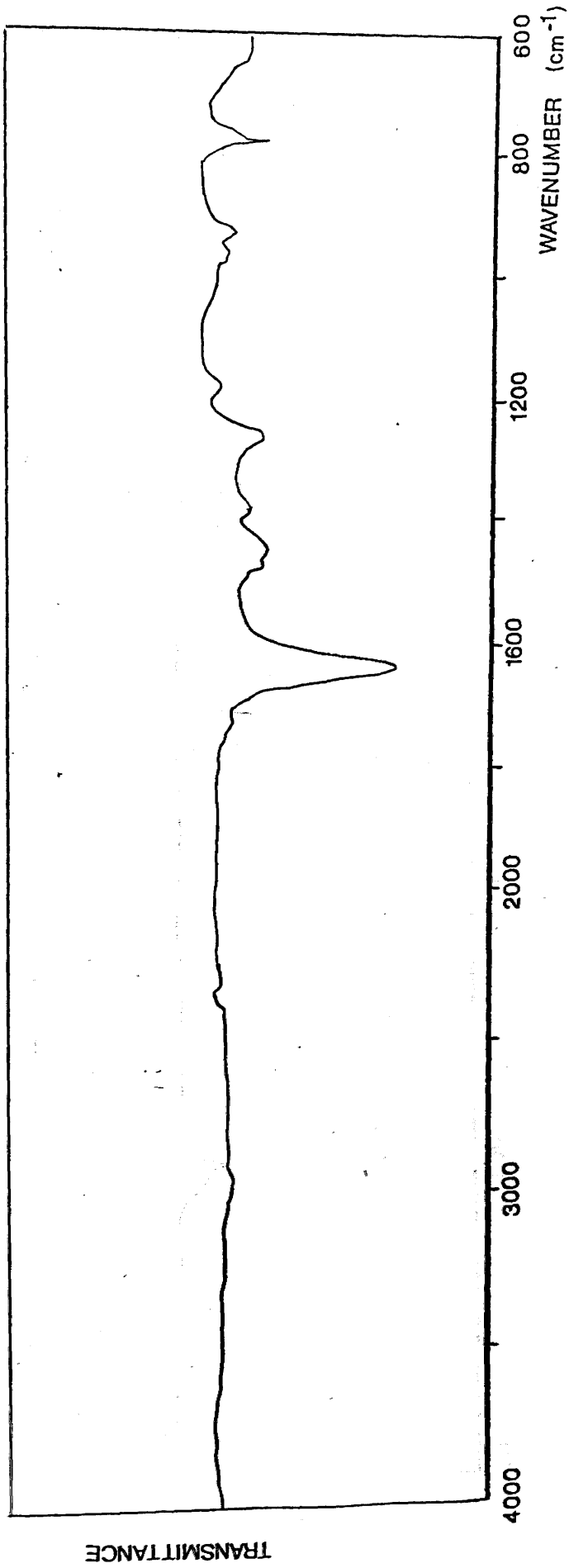
Cyclisation of neighbouring methacrylic acid units in the copolymer forms anhydride ring structures which restrict the depolymerisation of the styrene sequences. This results in a slight increase in the stability of the copolymer relative to polystyrene.

APPENDIX ONE

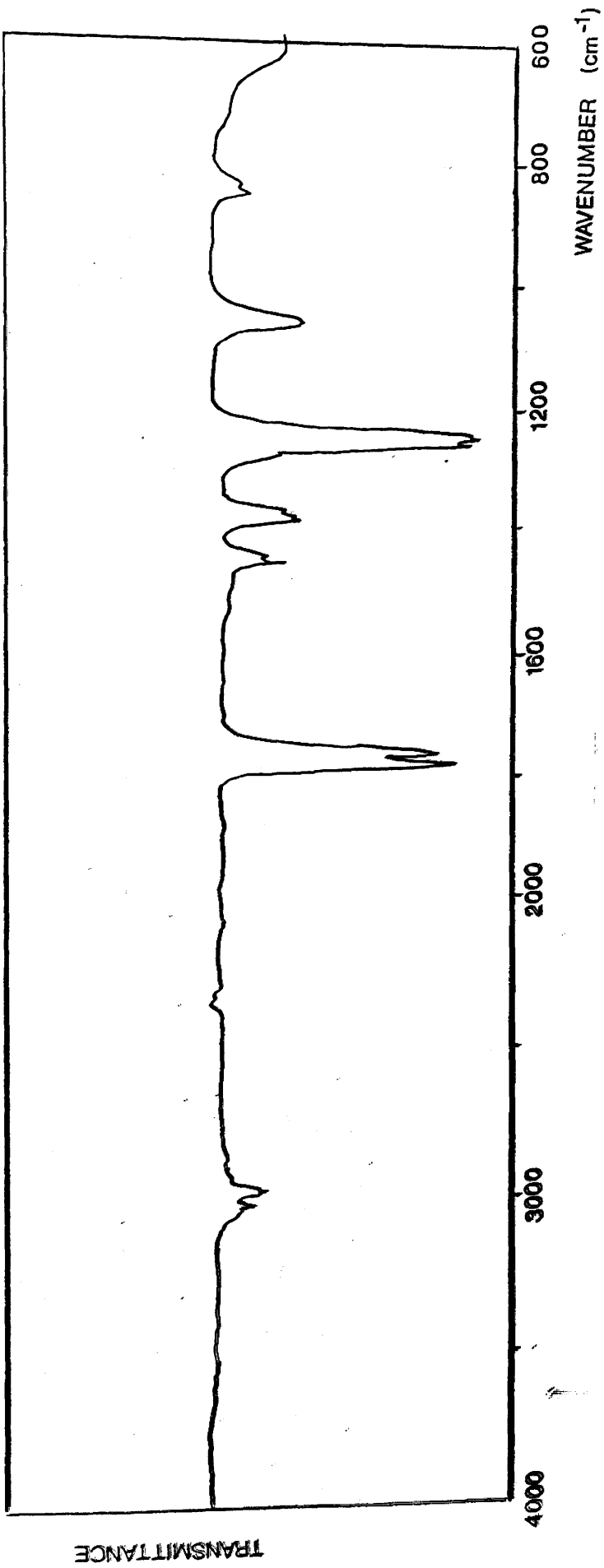
Gas Phase IR Spectra of Several Common
Degradation Products

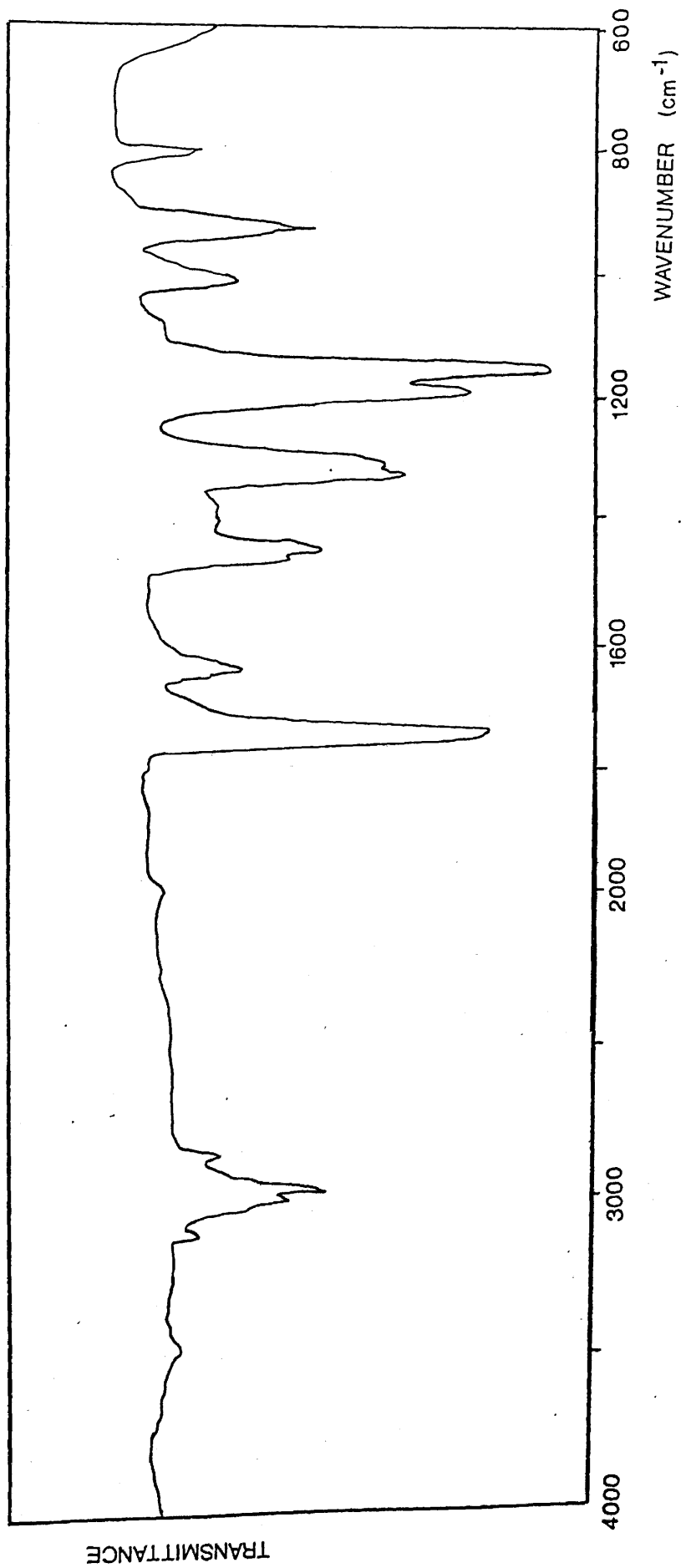


ACETONE



ACETYLACETONE

**METHYL ACRYLATE**

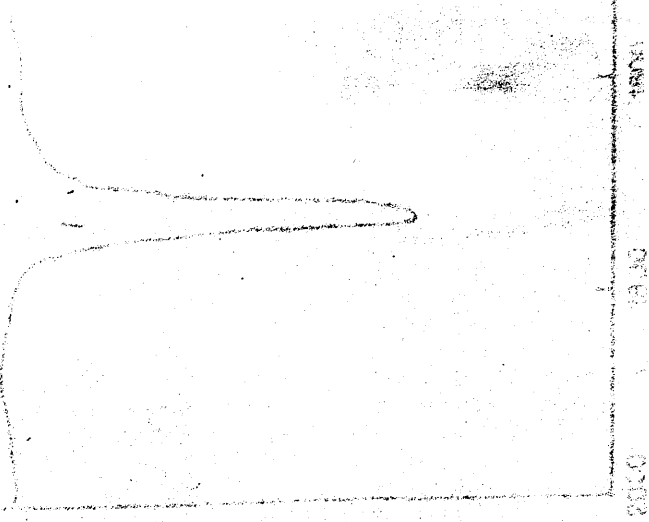


METHYL METHACRYLATE

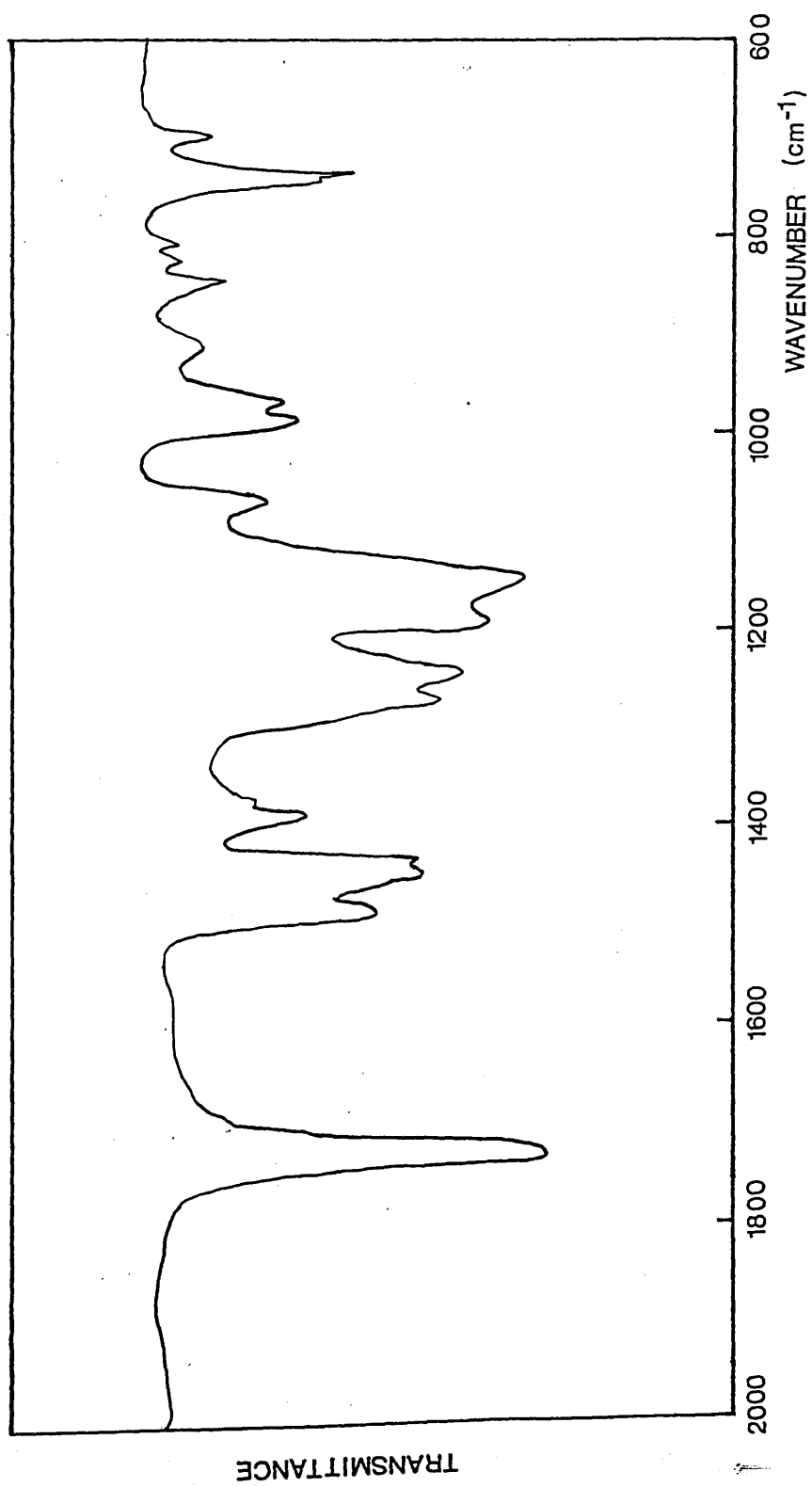
APPENDIX TWO

IR and UV Spectra of PMMA

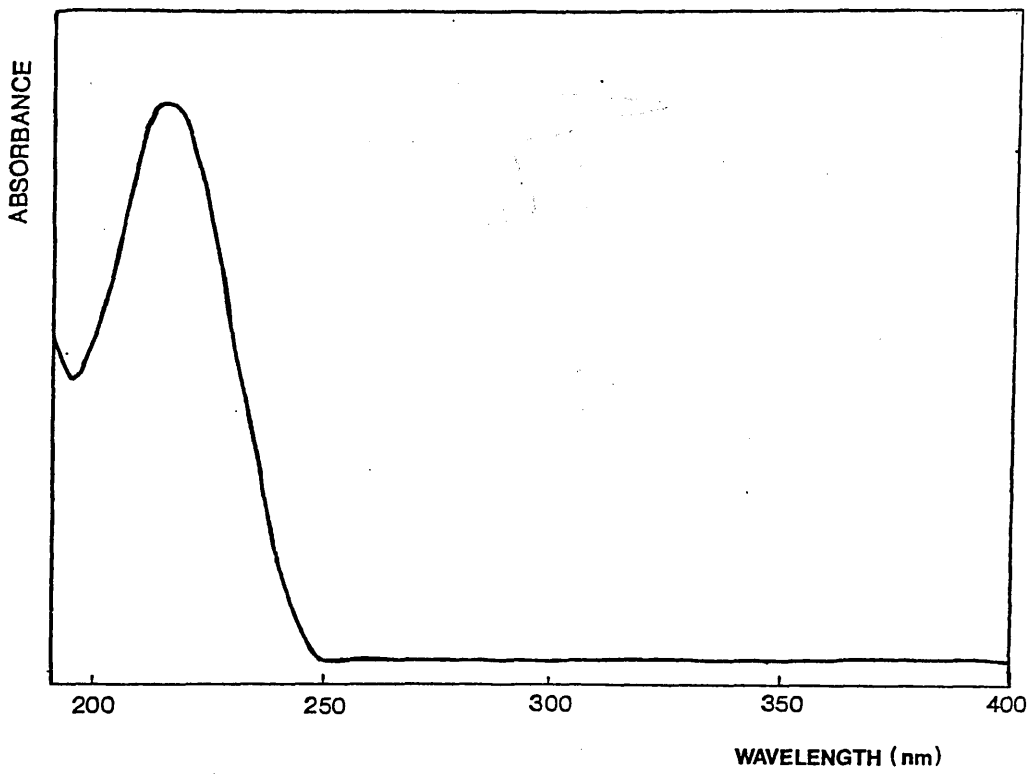
IR and UV Spectra of PVAc



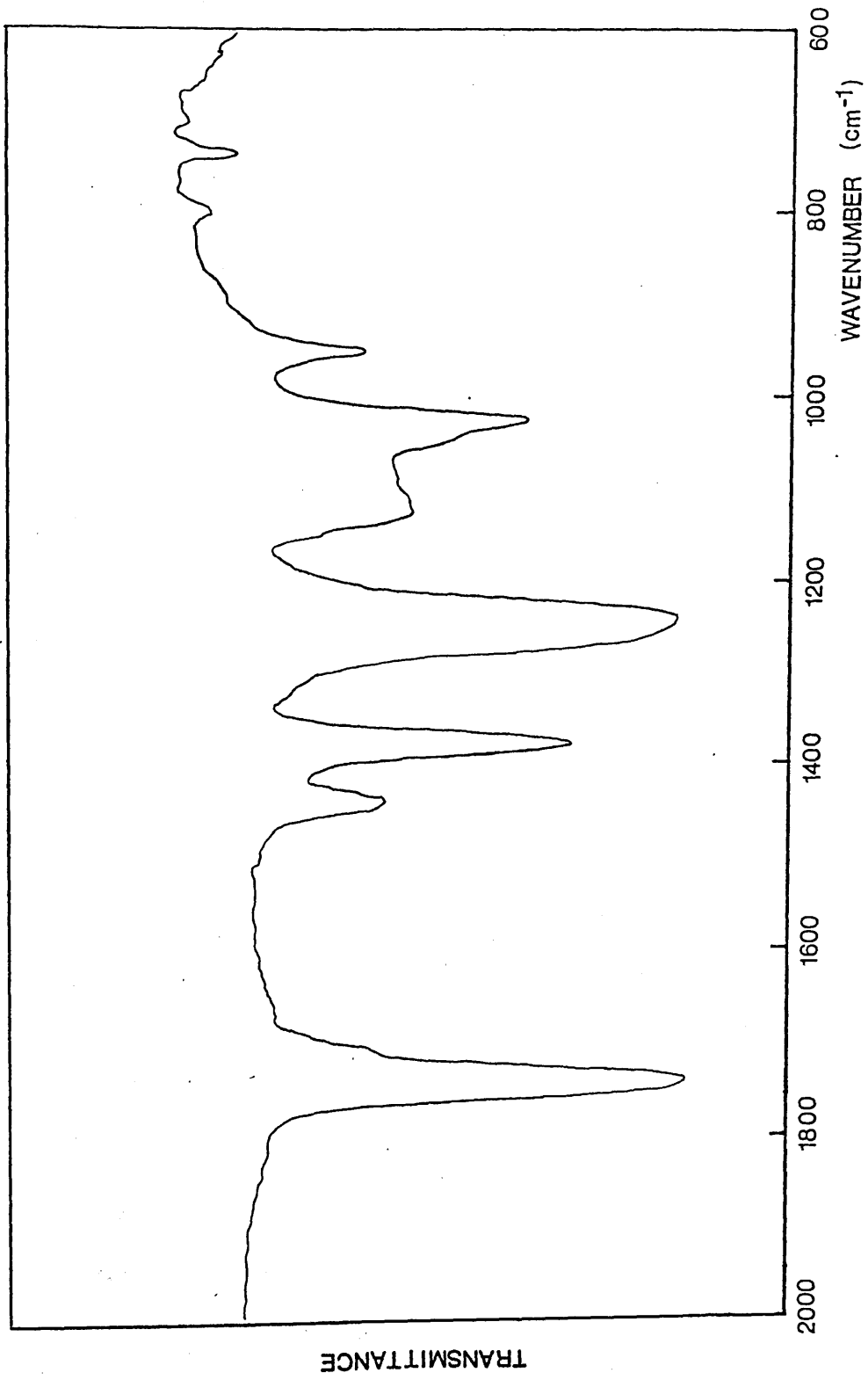
TRANSMITTANCE



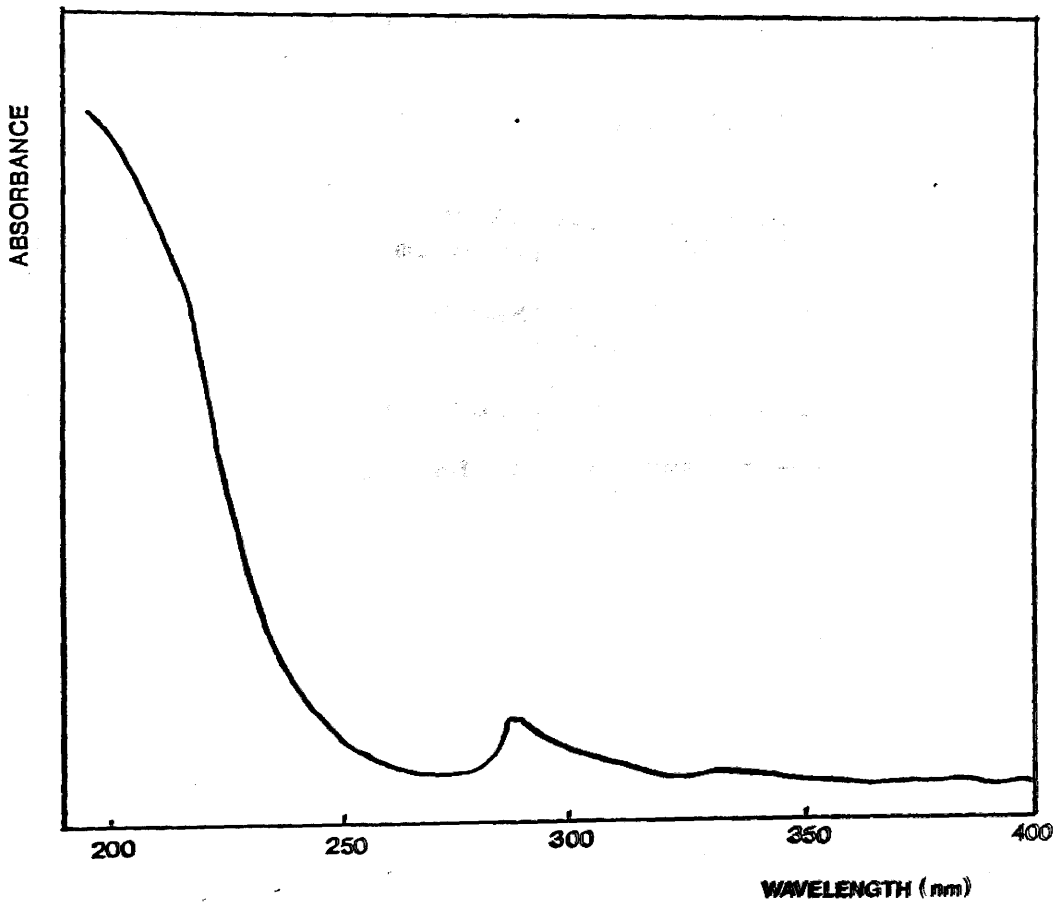
IR spectrum of PMMA



UV spectrum of PMMA



IR spectrum of PVAc



UV spectrum of PVAc

Anal. Calcd. for $C_4H_6O_2$: C, 60.0%; H, 6.67%. Found: C, 59.8%; H, 6.6%. IR (KBr): 1735, 1640, 1450, 1380, 1100, 1050, 1000, 950, 900, 850, 800, 750, 700, 650, 600, 550, 500, 450, 400, 350, 300, 250, 200, 150, 100, 50, 0. *J. Polym. Sci. A-1*, 1963, 1, 1113.

REFERENCES

- 1 J.L. BURDETT and M.T. RODGERS, J. Am. Chem. Soc., 1964, 86, 2105.
- 2 M. CALVIN and K.W. WILSON, J. Am. Chem. Soc., 1945, 67, 2003.
- 3 C. DJORDJEVIC, J. LEWIS and R.S. NYHOLM, Chem. Ind., 1959, 122
- 4 J.P. COLLMAN, R.A. MOSS, S.D. GOLDBY and W.S. TRAHONOVOSKY, Chem. Ind., 1960, 121.
- 5 P.R. SINGH and R. SAHAI, Aust. J. Chem., 1967, 20, 639, 649.
- 6 K. NAKAMOTO and A.E. MARTELL, J. Chem. Phys., 1960, 32, 588.
- 7 K. NAKAMOTO, P.J. MCCARTHY, A. RUBY and A.E. MARTELL, J. Am. Chem. Soc., 1961, 83, 1066.
- 8 K. NAKAMOTO, P.J. MCCARTHY and A.E. MARTELL, J. Am. Chem. Soc., 1961, 83, 1272.
- 9 R.B. ROOF Jr., Acta Cryst., 1956, 1, 781.
- 10 J.P. FAKLER Jr., and A. AVDEFF, Inorg. Chem., 1974, 13, 1864.
- 11 G.J. BULLEN, Acta Cryst., 1959, 12, 703.
- 12 F.A. COTTON and R.C. ELDER, J. Am. Chem. Soc., 1964, 86, 2294.
- 13 F.A. COTTON and R.C. ELDER, Inorg. Chem., 1965, 4, 1145.
- 14 H. KOGAMA, Y. SAITO and H. KUROYA, J. Inst. Polytech. Osaka Univ., 1953, C4, 43. (Chem. Abstr., 1954, 48, 3017).
- 15 N.V. SIDGEWICK, "The Chemical Elements and Their Compounds", Oxford University Press, Oxford, 1950.
- 16 E.W. BERG and J.T. TRUEMPER, J. Phys. Chem., 1960, 64, 487.
- 17 J.F. STEINBACH and H. FREISER, Anal. Chem., 1954, 26, 375.
- 18 R.W. MOSHIER and R.E. SIEVERS, "Gas Chromatography of Metal Chelates", Pergamon Press, Oxford, 1965.

- 19 E.W. BERG and F.R. HARTLEDGE Jr., *Anal. Chim. Acta*, 1965, 33, 173.
- 20 E.W. BERG and A.D. SHENDRIKAR, *Anal. Chim. Acta*, 1969, 44, 159.
- 21 L. REICH and A. SCHINDLER, "Polymer Reviews - 2, Polymerisation by Organometallic Compounds", Wiley Interscience, New York, 1966.
- 22 M.A. MENDELSON, E.M. ARNETT and H. FREISER, *J. Phys. Chem.*, 1960, 64, 660.
- 23 E.M. ARNETT, H. FREISER and M.A. MENDELSON, *J. Am. Chem. Soc.*, 1962, 84, 282.
- 24 E.M. ARNETT and M.A. MENDELSON, *J. Am. Chem. Soc.*, 1962, 84, 3821, 3824.
- 25 E.-G. KASTNING, H. NAARMAN, H. REIS and C. BERDING, *Angew. Chem. Int. Ed. Engl.*, 1965, 4, 322.
- 26 T. OTSU, N. MINIMII and Y. NISHIKAWA, *J. Macromol. Sci.-Chem.*, 1968, A2, 983.
- 27 C.H. BAMFORD and D.H. LIND, *Chem. Ind.*, 1965, 1627.
- 28 C.H. BAMFORD and D.H. LIND, *Proc. Roy. Soc.*, 1968, A302, 145.
- 29 K.M. RICHES, *Makromol. Chem.*, 1967, 103, 175.
- 30 C.H. BAMFORD and A.N. FERRAR, *Proc. Roy. Soc.*, 1971, A321, 425.
- 31 A.F. NIKOLAEV, K.V. BELOGORODSKAYA, J.G. SHIBALOVICH, E.D. ANDREEVA, L.V. BOGDANOVA and M.V. VINOGRADOV, *Zh. Prikl. Khim. (Leningrad)*, 1973, 46, 2718. (*Chem. Abstr.*, 1974, 30, 59381).
- 32 A.F. NIKOLAEV, K.V. BELOGORODSKAYA, V.G. SHIBALOVICH, E.D. ANDREEVA and G.I. IVANOVA, *Zh. Prikl. Khim. (Leningrad)*, 1975, 48, 2028. (*Chem. Abstr.*, 1975, 83, 115042).
- 33 K.V. BELOGORODSKAYA, V.G. SHIBALOVICH, G.I. IVANOVA and A.F. NIKOLAEV, *Vysokomolek Soedin.*, 1975, B17, 370 (*Chem. Abstr.*, 1975, 83, 184195).
- 34 K.V. BELOGORODSKAYA, A.F. NIKOLAEV, V.G. SHIBALOVICH and L.I. PUSHKAREVA, *Vysokomolek. Soedin.*, 1980, B22, 449. (*Chem. Abstr.*, 1980, 93, 221131).

- 35 Yu. V. KORSHAK, T.I. BEVZA and B.D. DOLGOPLOSK, *Vysokomolek. Soedin.*, 1969, B11, 794. (Chem. Abstr. 1970, 72, 55966).
- 36 N.N. DASS, *Progr. Polym. Sci.*, 1983, 10, 51.
- 37 U.S. NANDI, N.D. GUPTA and A.J. BHATTACHARYYA, *J. Polym. Sci. B.*, 1970, 8, 849.
- 38 R. PRABHA and U.S. NANDI, *J. Polym. Sci., Polym. Lett.*, 1976, 14, 19.
- 39 R. PRABHA and U.S. NANDI, *J. Polym. Sci., Polym. Chem. Ed.*, 1977, 15, 1973, 1983.
- 40 S. SAMAL, G. SAHU and P.L. NAYAK, *J. Appl. Polym. Sci.*, 1984, 29, 3283.
- 41 S. LENKA, P.L. NAYAK, I.B. MOHANTY and S.N. MISHRA, *J. Appl. Polym. Sci.*, 1985, 30, 2711.
- 42 S. LENKA and A.K. TRIPATHY, *J. Appl. Polym. Sci.*, 1982, 27, 1859.
- 43 S. LENKA and P.L. NAYAK, *J. Appl. Polym. Sci.*, 1982, 27, 1959.
- 44 D.F. LAWSON, D.F. LOHR, U.S. Patent, 3, 957, 722 (1981). (To Firestone Tyre and Rubber Co.)
- 45 L. MINNEMA and G.N. VAN BOEKEL-MOL, *Eur. Pat. Appl.* 27,300 (1981). (To Philips Gloeilampenfabrieken)
- 46 H. KOBAYASHI, Y. YASUHIRO and I. ENDO, *Ger. Offen.* 2, 702, 227 (1977). (To Canon K.K.)
- 47 ARGUS CHEMICAL N.V., Belgian Patent 875, 960 (1979).
- 48 N. GRASSIE and G. SCOTT, "Polymer Degradation and Stabilisation" Cambridge University Press, Cambridge, 1985.
- 49 R. SASI and U.S. NANDI, *J. Ind. Chem. Soc.*, 1979, 56, 703.
- 50 Y. OGIWARA, H. KUBOTA and Y. KIMURA, *J. Polym. Sci., Polym. Chem. Ed.*, 1978, 16, 2865.
- 51 H.S. LAVER in "Developments in Polymer Stabilisation - 1", p.167, G. Scott (ed.), Applied Science, London, 1977.

- 52 M.U. AMIN and G. SCOTT, Eur. Polym. J., 1974, 10, 1019.
- 53 D.E. DICKENS, U.S. Patent 3,983,086 (1976). (To B.F. Goodrich Co.)
- 54 J. FRITZ, Fr. Demande, 2,393,018 (1978). (To Rhone-Poulenc Ind. S.A.)
- 55 J. FRITZ, Fr. Demande 2,411,857 (1979). (To Rhone-Poulenc Ind., S.A.)
- 56 W.P. WHELAN, U.S. Patent 3,998,783 (1976). (To Uniroyal)
- 57 F. MAYER, German Patent 1,177,816 (1964). (To BASF A.-G.)
- 58 N.J. KROENKE, J. Appl. Polym. Sci., 1981, 26, 1167.
- 59 C.F. CULLIS and M.M. HIRSCHLER, Eur. Polym. J., 1984, 30, 353.
- 60 I.C. McNEILL in "Polymer Yearbook-3", p.141, R.A. Pethrick (ed.), Harwood Scientific, New York, 1986.
- 61 I.C. McNEILL and R.C. McGUINNESS, Polym. Deg. Stab., 1983, 5, 303.
- 62 I.C. McNEILL and R.C. McGUINNESS, Polym. Deg. Stab., 1984, 9, 167.
- 63 I.C. McNEILL and R.C. McGUINNESS, Polym. Deg. Stab., 1984, 9, 209.
- 64 I.C. McNEILL, J. Polym. Sci. A-I, 1966, 4, 2479.
- 65 I.C. McNEILL, Eur. Polym. J., 1967, 3, 409.
- 66 I.C. McNEILL and D. NEIL in "Thermal Analysis", p.353; R.F. Schwenker and P.D. Garn (eds.), Academic Press, New York, 1969.
- 67 I.C. McNEILL in "Thermal Analysis", p.417, R.F. Schwenker and P.D. Garn (eds.), Academic Press, New York, 1969.
- 68 I.C. McNEILL, Eur. Polym. J., 1970, 6, 373.
- 69 I.C. McNEILL, L. ACKERMAN, S.N. GUPTA, M. ZULFIQAR and S. ZULFIQAR, J. Polym. Sci., Polym. Chem. Ed., 1977, 15, 2381.

- 70 L. ACKERMAN and W.J. MCGILL, J. S. Afr. Chem. Inst., 1973, 26, 82.
- 71 W.J. MCGILL, L. PAYNE and J. FOURIE, J. Appl. Polym. Sci., 1978, 22, 2669.
- 72 W.J. MCGILL in "Developments in Polymer Degradation-5", p.1, N. Grassie (ed.), Applied Science, London, 1984.
- 73 M.I. POPE and M.D. JUDD "Differential Thermal Analysis", Heyden, London, 1977.
- 74 R.H. STILL in "Developments in Polymer Degradation-1" p.1, N. Grassie (ed.), Applied Science, London, 1977.
- 75 D. WELTI, "Infrared Vapour Spectra", Heyden, London, 1970.
- 76 R.H. PIERSON, A.N. FLETCHER and E. St. C. GANTZ, Anal. Chem. 1956, 28, 1218.
- 77 "The Aldrich Library of Infrared Spectra", C. J. Pouchert (ed.), Aldrich Chemical Co., Milwaukee, 1981.
- 78 "The Sadtler Handbook of Infrared Spectra", W.W. Simons (ed.), Sadtler-Heyden, London, 1978.
- 79 W.F. ARENDALE and W.H. FLETCHER, J. Chem. Phys., 1957, 26, 793.
- 80 W.H. FLETCHER and W.B. BARISH, Spectrochim. Acta., 1965, 21, 1647.
- 81 B.E. BRYANT and W.C. FERNELIUS, Inorg. Synth., 1957, 5, 188.
- 82- G. URBAIN and A. DEBIERNE, Compt. Rend., 1899, 129, 302.
- 83 F. GACH, Monatsch., 1900, 21, 98.
- 84 A.E. FINN, G.C. HAMPSON and L.E. SUTTON, J. Chem. Soc., 1938, 1254.
- 85 R.G. CHARLES, Inorg. Synth., 1963, 7, 183.
- 86 M.M. JONES, J. Am. Chem. Soc., 1959, 81, 3188.
- 87 A. HAZZARD, B.Sc. Thesis, University of Glasgow, 1985.

- 88 R. LARSSON and O. ESKILSSON, *Acta Chem. Scand.*, 1969, 23, 1765.
- 89 Yu. N. ANISIMOV and G. CHOUDHURI, *J. Gen. Chem. U.S.S.R.*, 1984, 54, 1302.
- 90 L.J. BELLAMY and R.F. BRANCH, *J. Chem. Soc.*, 1954, 4491.
- 91 S. PINCHAS, B.L. SILVER and I. LAULICHT, *J. Chem. Phys.*, 1967, 46, 1506.
- 92 R.H. HOLM and F.A. COTTON, *J. Am. Chem. Soc.*, 1958, 80, 5658.
- 93 A. AUERBACH, N. INDICTOR and J. JOCHSBERGER, *Macromolecules*, 1975, 8, 632.
- 94 D.W. BARNUM, *J. Inorg. Nucl. Chem.*, 1961, 21, 221.
- 95 P.R. SINGH and R. SAHAI, *Inorg. Chim. Acta.*, 1968 2, 102.
- 96 D.W. BARNUM, *J. Inorg. Nucl. Chem.*, 1961, 22, 183.
- 97 R.L. BELFORD, A.E. MARTELL and M. CALVIN, *J. Inorg. Nucl. Chem.*, 1956, 2, 11.
- 98 J.P. FACKLER, F.A. COTTON and D.W. BARNUM, *Inorg. Chem.*, 1963, 2, 97.
- 99 J.P. FACKLER and F.A. COTTON, *Inorg. Chem.*, 1963, 2, 102.
- 100 H.D. GAFNEY and R.L. LINTVEDT, *J. Am. Chem. Soc.*, 1971, 93, 1623.
- 101 H. GRASDALEN, *J.C.S. Faraday II*, 1973, 69, 462.
- 102 C.A. FLEMING and D.A. THORNTON, *J. Mol. Struct.*, 1975, 25, 271.
- 103 Y. OHKATSU, T. OSA and A. MISONO, *Bull. Chem. Soc. Jap.*, 1967, 40, 2111.
- 104 "Stability Constants - Chemical Society Special Publication No. 17", A.E. Martell and L.G. Sillen (Compilers), Chemical Society, London, 1964.
- 105 J. VON HOENE, R.G. CHARLES and W.M. HICKAM, *J. Phys. Chem.*, 1958, 62, 1098.

- 106 R.G. CHARLES, W.M. HICKAM and J. VON HOENE, J. Phys. Chem., 1959, 63, 2084.
- 107 I. YOSHIDA, H. KOBAYASHI and K. UENO, Bull. Chem. Soc. Jap., 1974, 47, 2203.
- 108 J.D.B. SMITH, D.C. PHILLIPS and T.D. KACZMAREK, Microchem. J., 1976, 21, 424.
- 109 M. GLAVAS and T. RIBAR, Glas. Hem. Drus., Beograd, 1967, 32, 229. (Chem. Abstr., 1969, 71, 45285)
- 110 R.G. CHARLES, Inorg. Synth., 1960, 6, 164.
- 111 I. YOSHIDA, K. KOBAYASHI and K. UENO, J. Inorg. Nucl. Chem., 1973, 35, 4061.
- 112 N. FILEPESCU and H. WAY, Inorg. Chem., 1969, 9, 1863.
- 113 G. DOYLE, K.A. ERIKSEN and D. VAN ENGEN, Organometallics, 1985, 4, 830.
- 114 R. NAST and W.-H. LEPEL, Chem. Ber., 1969, 102, 3224.
- 115 T.D.R. NAIR, P. SREEMAN and N. THANKARAJAN, J. Ind. Chem. Soc., 1982, 59, 415.
- 116 C.J. KEATCH and D. DOLLIMORE, "An Introduction to Thermogravimetry", 2nd Edn., Heyden, London, 1975.
- 117 "Diffusion in Polymers", J. Crank and G.S. Park (eds.), Academic Press, London, 1968.
- 118 "Membranes in Gas Separation and Enrichment - Proceedings of the 4th BOC Priestly Conference" Royal Society of Chemistry, London, 1987.
- 119 N.C. BILLINGHAM, P.D. CALVERT and A.S. MANKE, J. Appl. Polym. Sci., 1981, 26, 3543.
- 120 P.J. FLORY "Principles of Polymer Chemistry", Cornell, New York, 1953.
- 121 N. GRASSIE in "Developments in Polymer Degradation-1", p.137, N. Grassie (ed.), Applied Science, London, 1977.
- 122 D.H. GRANT and N. GRASSIE, Polymer, 1960, 1, 445.
- 123 N. GRASSIE and H.W. MELVILLE, Proc. Roy. Soc., 1949, A199, 1, 14, 24.

- 124 I.C. McNEILL, *Eur. Polym. J.*, 1970, 4, 21.
- 125 K. HATADA, T. KITAYAMA and E. MASUDA, *Polym. J.*, 1986, 18, 395.
- 126 T. KASHIWAGI, A. INABA, J.E. BROWN, K. HATADA, T. KITAYAMA and E. MASUDA, *Macromolecules*, 1986, 19, 2160.
- 127 N. GRASSIE, *Trans. Farad. Soc.*, 1952, 48, 379.
- 128 N. GRASSIE, *Trans. Farad. Soc.*, 1953, 49, 385.
- 129 A. SERVOTTE and V. DESRAUX, *J. Polym. Sci. C*, 1968, 22, 367.
- 130 D.L. GARDNER and I.C. McNEILL, *J. Thermal Anal.*, 1969, 1, 389.
- 131 A. JAMIESON, Ph.D. Thesis, University of Glasgow, 1973.
- 132 A. JAMIESON and I.C. McNEILL, *J. Polym. Sci., Polym. Chem. Ed.*, 1976, 14, 1839.
- 133 S.L. MADORSKY, "Thermal Degradation of Organic Polymers" Interscience, New York, 1964.
- 134 H. ZIMMERMAN, *Faserforsch u. Textiltech*, 1966, 17, 228.
- 135 F. CHEVASSUS, R. DE BROUDELLES, "The Stabilisation of Poly(vinyl chloride)", Arnold, London, 1963.
- 136 "Degradation and Stabilisation of PVC", E.D. Owen (ed.), Elsevier, London, 1984.
- 137 G.G. CAMERON and G.P. KERR, *Eur. Polym. J.*, 1968, 4, 709.
- 138 G.G. CAMERON and G.P. KERR, *Eur. Polym. J.*, 1970, 6, 423.
- 139 O. CHIANTORE, M. GUAITA and N. GRASSIE, *Polym. Deg. Stab.*, 1985, 12, 141.
- 140 G.G. CAMERON, *Makromol. Chem.*, 1967, 100, 255.
- 141 G.G. CAMERON, J.M. MEYER and I.T. McWALTER, *Macromolecules*, 1978, 11, 696.
- 142 D.H. GRANT and N. GRASSIE, *Polymer*, 1960, 1, 445.

- 143 A. JAMIESON and I.C. McNEILL, *Eur. Polym. J.*, 1974, 10, 217.
- 144 J.D. FORTUNE, Ph.D. Thesis, University of Glasgow, 1969.
- 145 REFERENCE 125 AND REFERENCES THEREIN.
- 146 J. DABROWSKI and M. TENCER, *Bull. Chem. Soc. Jap.*, 1976, 49, 981.
- 147 I.C. McNEILL and M. ZULFIQAR, *J. Polym. Sci., Polym. Chem. Ed.*, 1978, 16, 3201.
- 148 M. ZULFIQAR, Ph.D. Thesis, University of Glasgow, 1975.
- 149 S. IZAWA, A. SHIMIZU and M. KUBO, *Sci. Rep. Toyo Soda Co.*, 1966, 10, 123.
- 150 P.R.E.J. COWLEY and H.W. MELVILLE, *Proc. Roy. Soc.*, 1951, A210, 461.
- 151 R.H. HANSEN, G.A. RUSSELL, T. DE BENEDICTIS, W.M. MARTIN and J.V. PASCALE, *J. Polym. Sci. A*, 1964, 2, 587.
- 152 P. SABATIER and E.E. REID in "Catalysis Then and Now", Franklin, Engelwood, N.J., 1965.
- 153 H. KWART and K. KING in "The Chemistry of Carboxylic Acids and Esters", S. Patai (ed.), Wiley Interscience, London, 1969.
- 154 A.E. JUKES in "Advances In Organometallic Chemistry-12", F.G.A. Stone and R. West (eds.), Academic Press, New York, 1974.
- 155 H.W. MELVILLE and P.R. SEWELL, *Makromol. Chem.*, 1959, 32, 139.
- 156 J.C. BEVINGTON, H.W. MELVILLE and R.P. TAYLOR, *J. Polym. Sci.*, 1954, 12, 449.
- 157 J.C. BEVINGTON, H.W. MELVILLE and R.P. TAYLOR, *J. Polym. Sci.*, 1954, 14, 463.
- 158 R.T. CONLEY and R. MALLOY in "Thermal Stability of Polymers", Vol. I, p.281, R.T. Conley (ed.), Dekker, New York, 1970.
- 159 N. GRASSIE and E.M. GRANT, *Eur. Polym. J.*, 1966, 2, 255.

- 160 N. GRASSIE and E. FARISH, Eur. Polym. J., 1967, 3, 305.
- 161 F.W. BILLMEYER Jr., "Textbook of Polymer Science", p.313, Wiley Interscience, New York, 1962.
- 162 E.C. CHAPIN, G.E. HAM and C.L. MILLS, J. Polym. Sci., 1949, 4, 597.